DEPARTMENT OF CHEMISTRY
INDIAN INSTITUTE OF TECHNOLOGY MADRAS
CHENNAI – 600 036

Organocatalyzed Enantioselective Domino and One-Pot Synthesis of Heterocyclic Compounds Using Formal 1,3-Dipolar Cycloaddition

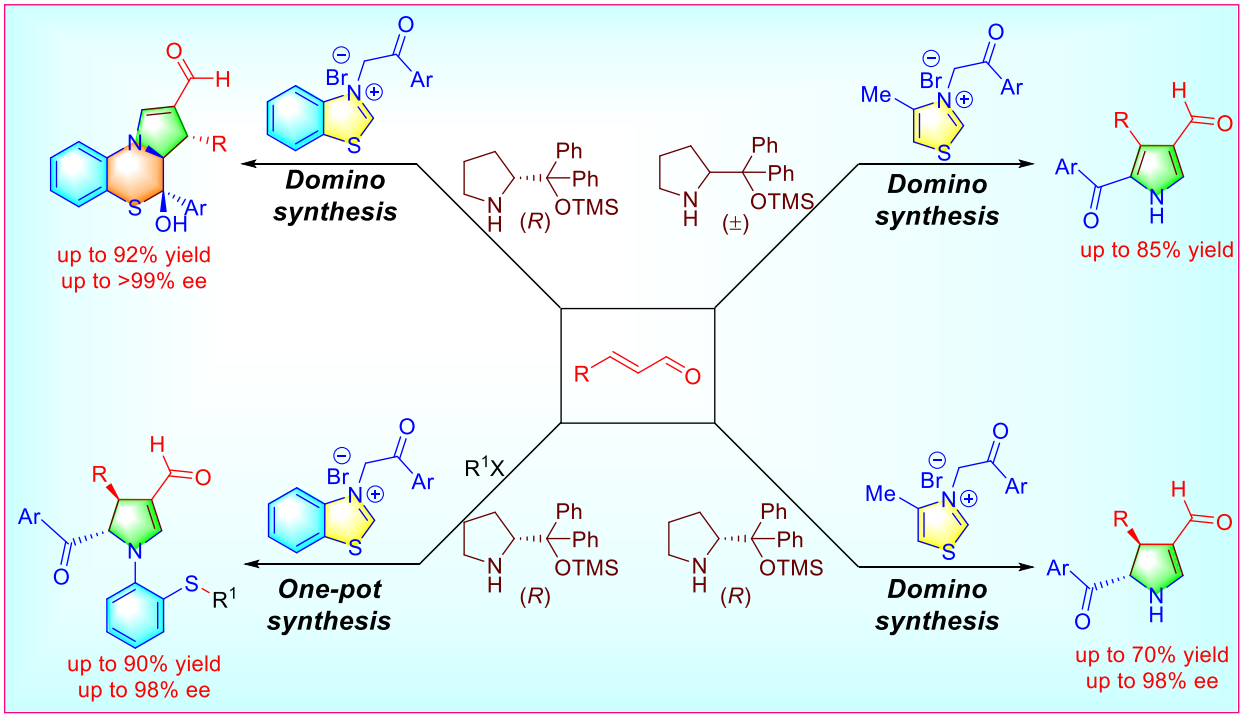

A Thesis

Submitted by

PANDIDURAI S

For the award of the degree

Of

DOCTOR OF PHILOSOPHY

June 2024

Dedicated to my family, teachers, and friends

THESIS CERTIFICATE

This is to certify that the thesis titled "**Organocatalyzed Enantioselective Domino and One-Pot Synthesis of Heterocyclic Compounds Using Formal 1,3-Dipolar Cycloaddition"** submitted by me to the Indian Institute of Technology Madras for the award of the degree of **DOCTOR OF PHILOSOPHY**, is a bona fide record of research work carried out by me under the supervision of **Prof. G. Sekar**. The contents of this thesis, in full or in parts, have not been submitted to any other Institute or University for the award of any degree or diploma.

Place: IIT Madras **Research Scholar**

Date: 16 June 2024

Research Guide

LIST OF PUBLICATIONS

I. REFEREED JOURNALS BASED ON THE THESIS

1. **Pandidurai, S., V. S. Kumar Choutipalli, V. Subramanian, and G. Sekar** (2024) Organocatalyzed Enantio- and Diastereoselective Formal Domino 1,3-Dipolar Cycloaddition/Rearrangement: Synthesis of Chiral Pyrrolo-thiazine-2-carbaldehydes. *Org. Lett.* **26**, 2971-2975.

2. **Pandidurai, S., V. S. Kumar Choutipalli, V. Subramanian, and G. Sekar** (2023) Organocatalyzed Enantio- and Diastereoselective Domino [3+2]-Dipolar Cycloaddition: Synthesis of Chiral Pyrrolothiazine-2-carbaldehydes and Dihydropyrrole carbaldehydes *ChemRxiv*. doi:10.26434/chemrxiv-2023-jx61g.

II. REFEREED JOURNALS BASED ON THE THESIS (YET TO BE PUBLISHED)

1. **Pandidurai, S.,** and **G. Sekar** One-pot Enantioselective Synthesis of *N*-Phenyl Thioether-tethered Tetrasubstituted 4,5-Dihydropyrrole-3-carbaldehydes **(Manuscript under review)**.

2. **Pandidurai, S.,** and **G. Sekar** Formal Domino 1,3-Dipolar Cycloaddition/Ring-Opening/C-S and C-N Bond Cleavage Reaction: Synthesis of Trisubstituted 1H-Pyrrole-3-carbaldehydes (**Manuscript under preparation**).

3. **Pandidurai, S., C. N. Babu,** and **G. Sekar** Asymmetric Domino Synthesis of Trisubstituted 4,5-Dihydro-1*H*-pyrrole-3-carbaldehydes Through Formal Domino 1,3-Dipolar Cycloaddition/C-S and C-N Bond Cleavage Reaction (**Manuscript under preparation**).

IV. PATENT BASED ON THE THESIS

1. **Pandidurai, S.,** and **G. Sekar** (2023) Enantio-and Diastereoselective Process for One-step Synthesis of Enantioenriched Pyrrolo[1,2-d][1,4]thiazine-2-carbaldehydes Core Using Chiral Organocatalyst, Indian Patent Application No.: 202241065630, Grant No.: 454952, 2023.

V. OTHER PUBLICATIONS

1. **Parveen, N., S. Pandidurai, and G. Sekar** (2023) Binaphthyl-Stabilized Palladium Nanoparticle-Catalyzed Stereoselective Synthesis of 3 Arylidene-2-oxindoles via One-Pot Heck-Carbocyclization/Nucleophilic Addition. *J. Org. Chem.* **88**, 1730-1741.

2. **Nair, V. V., D. Arunprasath, S. Pandidurai, and G. Sekar** (2022) Synergistic Dual Amine/Transition Metal Catalysis: Recent Advances, *Eur. J. Org. Chem*. e202200244 1-16.

IV. PRESENTATION IN CONFERENCES

1. **Pandidurai, S.** and **G. Sekar**, Organocatalytic Enantio- and Diastereoselective Construction of Pyrrolo[1,2-*d*][1,4]thiazine-2-Carbaldehydes Core via Consecutive [3+2] Cycloaddition and Rearrangement, *Chemistry in-House Symposium-2022 (CiHS-2022*), Department of Chemistry, Indian Institute of Technology Madras, Chennai, September, 2022 (**Poster Presentation**).

2. **Pandidurai, S.** and **G. Sekar**, Organocatalytic Enantio- and Diastereoselective Construction of Pyrrolo[1,2-*d*][1,4]thiazine-2-Carbaldehydes Core via Consecutive [3+2] Cycloaddition and Rearrangement, *2nd National Conference on Contemporary Facets in Organic Synthesis (CFOS-2022)*, Indian Institute of Technology Roorkee, Uttarakhand, December, 2022 (**Poster Presentation**).

3. **Pandidurai, S.** and **G. Sekar**, Organocatalyzed Enantio- and Diastereoselective Construction of Pyrrolo[1,2-*d*][1,4]thiazine-2-Carbaldehydes Core via Consecutive [3+2] Cycloaddition and Rearrangement, *Chemistry in-House Symposium-2023 (CiHS-2023)*, Department of Chemistry, Indian Institute of Technology Madras, Chennai, September, 2023 (**Oral Presentation**).

4. **Pandidurai, S.** and **G. Sekar**, Organocatalyzed Enantioselective Synthesis of Chiral Heterocyclic Compounds using Domino Cycloaddition/Rearrangement, Conferences for Young Researches *XVIII J-NOST-2023*, Department of Chemistry, Indian Institute of Educational and Research, (IISER Pune), Pune, October, 2023 (**Oral Presentation**).

ACKNOWLEDGEMENTS

This is an important part of my thesis. I was able to reach this stage because of the cooperation of some people who played a pivotal role in my journey. So, it is with tremendous gratitude, I sincerely write this acknowledgment to show my appreciation to those who have helped me throughout the years.

It is indeed a great pleasure to express my overwhelming gratitude to my research advisor **Prof. G. Sekar** for the opportunity to work in his research group and for the constant encouragement, motivation, and valuable suggestions he has provided do asymmetric synthesis and throughout my research career at IIT Madras. I am grateful to him for introducing me to the field of asymmetric synthesis. It is important to mention that this thesis would not be possible without his support during my tough times. Mere words are not sufficient to express my heartfelt thanks for the enthusiastic support extended in all endeavors of both my personal and professional life during my stay at IIT Madras. I would like to express my gratitude for his sincerity, dignity, and decency towards work. The association with my guide will remain memorable throughout my life.

I am grateful to **Prof. Sanjay Kumar** (head of the department) **Prof. Mangala Sunder Krishnan, and Prof. Indrapal Singh Aiden** (former head of the department) for their kind support and the necessary infrastructures to conduct the research.

I express my thanks to all my doctoral committee members, **Prof. S. Sankararaman (CY**), **Prof. S. Baskaran (CY), Prof. P. Venkatakrishnan (CY),** and **Prof. M. Michael Gromiha (BT)** for their valuable feedback and suggestions. I wish to express my gratitude to my course work teachers **Prof. S. Sankararaman**, **Prof. S. Baskaran**, **Prof. G. Sekar**, **Prof. K. M. Muraleedharan, Prof. Anbarasan, Prof. M. Jaganmohan, Prof. Anbarasan, and Prof. Beeraiah Baire.** I also owe my thanks to all faculty members in the department of chemistry for their help and interest evinced by them in the progress of my work.

I express my thanks to my computational collaborator, **Prof. Venkatesan Subramanian (CY**), and his students, **Dr. Surya Venkata Kumar Choutipalli**

(CLRI), Dr. Kannan Sadasivam (CLRI), for their help, valuable feedback, and suggestions.

I wish to thank IIT Madras for the research fellowship and DST, New Delhi, for funding towards the Bruker 400 MHz NMR instrument to the department of chemistry, IIT Madras, and the ESI-MS facility under FIST program. I also thank SAIF and IIT Madras for their support.

I would like to thank all my past and present lab mates for their cooperation, fruitful discussion, and generous help throughout my research period. I extend my thanks to my seniors **Dr. Arun Prasath Lingam**, **Dr. D. Devi Bala, Dr. Arun Prasath, Dr. Rajib Saha, Dr. Imran Kazi, Dr. Naziya Parveen, Dr. N. Sundara Velu, Dr. Golapalli Narashima Rao, Dr. Anuradha Nandy, Mr. Vysakh V. Nair, Mr. Neerathi Ligam,** and my lab mates **Ms. Soundarya Palanisamy, Ms. Shiyana, Mr. R. Selvam, Mr. D. Sathish**, **Mr. R. Gopalakrishnan**, **Mr. Suman Sasmal, Mr. Atanu Mahato, Mr. K. Kathirvel, Mr. G. Sai Kumar, Mr. Harshal Patil, Mr. Kishore, Mr. M. Chinna babu, Mr. Sayan Pahan, and Mr. Rajesh Kumar Bisoyi**, **Mr. Sudip Ray, Mr. Shivam, Ms. Nithiya, Mr. Jagadeesh, and Mr. M. Vinoth Kumar** for their support. I especially thank my seniors and my friends in the department, and all other research scholars of the department who have been very friendly and helped me in various ways.

I thank **Dr. Bhaskar** for helping me record NMR, **Mr. Elias, Mr. Chiranjeevi**, and **Mr. Naveen** for recording HRMS and **Mr. V. Ram Kumar** for single crystal XRD analysis. I also thank all non-teaching staff members of the chemistry department for their timely help.

I thank my beloved UG classmate friends **Mr. A. Pandidurai, Mr. K. Paneer Selvam, Mr. E. Balakrishnan, Mr. Prabu, Mr. Ambalavana, and Mr. Khadar.** I thank my beloved PG senior and classmate friends **Dr. Thangamani, Dr. John Tamilarasan, Mr. Srinath, Mr. Thennarasan, Mr. Ragupathi, Mr. Prabakaran, Mr. Gopinath, Mr. Balakrishnan, Ms. Thangamalar,** I thank my beloved Ph.D friends **Mr. D. Sujeeth Kumar, Mr. K. Kalidass, Dr. Velliyadevan, Mr. Hariprasad Narayanan, Mr. Prabu Kumar, Mr. Bakkiyaraj, Mr. N. Aravindhan, Mr. R. Logeshwaran, Mr. Arjun, Mr. L. Prakash, Mr. Surenthiran,** for their motivation, constant encouragement, and support throughout my research period.

I am happy and proud to express my heartfelt gratitude to my parents **Mr. Solai Manikam** and **Ms. Panjalai Solai** who is responsible for my growth and success in life. Special thanks to my sister and brother, **Ms. Sathiya** and **Mr. Ajith Kumar** for their constant support and help throughout my education (Ph.D.). I would like to thank my uncle and sister **Mr. Sekar, Mr. Thangaraj, and Ms. Navaneetham** for supporting me throughout my education. And I express my gratitude to my beloved sister and uncle cousins **Iniya, Divya Shri, and Punnagai.**

PANDIDURAI S

ABSTRACT

KEYWORDS: Asymmetric synthesis, Enantioselective reaction, Diastereoselective reaction, Organocatalysts, Chiral proline catalyst, Benzothiazole, Benzothiazolium salt, α,β-Unsaturated aldehydes, 1,3-Dipolar cycloaddition, Ring-opening, Rearrangement, DFT study, Fluorescent study, Docking study, Anti-cancer activity, Pyrrolo-thiazine carbaldehydes, C-S bond formation, Dihydropyrroles, Tetrasubstituted pyrrole-3-carbaldehydes, 1,4-Thiazine, 4-Methyl thiazolium salt, Trisubstituted pyrroles, C-S bond cleavage, C-N bond cleavage.

1,3-Dipolar cycloaddition of azomethine ylides and dipolarophiles represents an effective approach to synthesize diverse *N, S*-heterocyclic compounds. Notably, thiazolium and benzothiazolium azomethine ylides are known to exhibit distinct reactivity patterns compared to other azomethine ylides. Over the past decades, thiazolium and benzothiazolium azomethine ylides based 1,3-dipolar cycloadditions have been explored in the synthesis of racemic heterocyclic compounds with multiple stereogenic centers. However, the enantioselective synthesis of optically active heterocyclic compounds is yet to be synthesized within this framework. Thus, this Ph.D thesis aims to address this gap by developing a methodology for the synthesis of enantioenriched heterocyclic compounds containing multiple stereogenic centers by utilizing commercially available α,β-unsaturated aldehydes along with easily accessible thiazolium and benzothiazolium salts in the presence of chiral organocatalysts starting with 1,3-dipolar cycloaddition reactions. This thesis work includes (i) Enantio- and diastereoselective synthesis of pyrrolo-thiazine-2-carbaldehydes through an organocatalyzed domino process utilizing benzothiazolium salts; (ii) One-pot,

organocatalyzed, enantioselective synthesis of tetrasubstituted dihydropyrrole-3-carbaldehydes utilizing benzothiazolium salts; (iii) Synthesis of trisubstituted-1*H*-pyrrole-3-carbaldehydes *via* an organocatalyzed domino process utilizing thiazolium salts; and (iv) Organocatalyzed, domino synthesis of chiral trisubstituted dihydro-1*H*-pyrrole-3-carbaldehydes, utilizing thiazolium salts. This thesis has been divided into four Chapters.

Chapter 1 provides a brief introduction about asymmetric synthesis, organocatalysts, chiral proline catalyst and ylides. Also, this introduction Chapter provides a detailed report about the reactivity and applications of cycloiminium salt-based azomethine ylides, particularly thiazolium and benzo thiazolium salts. This Chapter also offers a detailed account of organo- and metal catalyzed enantio- and diastereoselective organic transformations of azomethine ylides in 1,3-dipolar cycloadditions.

Chapter 2 deals with proline-derived organocatalyzed enantio- and diastereoselective synthesis of novel pyrrolo[1,2-*d*][1,4]thiazine-2-carbaldehyde heterocyclic scaffolds with excellent yield, enantio- and diastereoselectivity (up to >99% ee and up to >20:1 d.r.) *via* intermolecular formal 1,3-dipolar cycloaddition/intramolecular rearrangement using benzothiazolum salt and α,β-unsaturated aldehydes. The synthesized chiral molecules have three contiguous stereogenic centers including one quaternary chiral carbon with fluorescent emissive character. Usage of (*R*)-dipheneylprolinol trimethylsilyl ether as a chiral organocatalyst provides excellent selectivity for the domino transformation. This method works well with electron-donating, electron-withdrawing groups containing benzothiazolium salts and α, β-unsaturated aldehydes. DFT study was performed to understand the stability of reaction intermediates and the

reaction mechanism. A fluorescent study was performed to showcase the molecule's fluorescent activity. In-silico study was achieved which showed that the synthesized chiral molecules have substantial anticancer activity towards selected B-Raf anti-cancer protein targets.

Chapter 3 deals with the development of a one-pot, efficient, and novel protocol for the synthesis of thioether-tethered tetrasubstituted 4,5-dihydropyrrole-3-carbaldehdes using benzothiazolum salt and α, β-unsaturated aldehydes in the presence of (*R*)-diphenylprolinol trimethylsilyl ether as a chiral catalyst. The reaction proceeds *via* 1,3-dipolar cycloaddition/intramolecular rearrangement followed by C-S bond formation and base-promoted ring-opening. The reaction was performed in open-air conditions at room temperature to form chiral scaffolds up to 92% yield with excellent enantio- and diastereoselectivity (up to >98% ee and up to >20:1 d.r.). This protocol disclosed excellent reactivity towards various alkyl, aryl, allyl, and propargyl halides. Particularly, the halides containing electron-donating and electron-withdrawing groups afforded the products in good yields with excellent enantioselectivity. This method worked well with electron-donating and electron-withdrawing groups containing benzothiazolium salts and α, β-unsaturated aldehydes. The synthetic utility of the product was achieved through various organic transformations.

Chapter 4A deals with (±)-diphenylprolinol trimethylsilyl ether catalyzed synthesis of novel trisubstituted-1*H*-pyrrole-3-carbaldehydes using 4-methylthiazolium salt and α,β-unsaturated aldehydes *via* formal 1,3-dipolar cycloaddition/intramolecular ring-opening, C-S and C-N bond-cleavage at room temperature. From the mechanistic study and HRMS analysis, the formation of by-product 1-mercaptopropan-2-one was

confirmed. The product is formed *via* base-promoted C-S bond cleavage, enamine tautomerism, and iminium ion formation followed by hydrolysis of iminium ion to cleave the C-N bond to produce the trisubstituted-1*H*-pyrrole-3-carbaldehyde in good yields up to 85%. It is noted that an unusual reactivity was found with 4-methyl thiazolium salt and α,β-unsaturated aldehydes in the presence of amine organocatalyst to afford trisubstituted pyrroles rather than stopping at hydropyrrolo-thiazine.

Chapter 4B deals with the asymmetric synthesis of enantioenriched dihydropyrrole using enantiopure (*R*)-diphenylprolinol trimethylsilyl ether as a chiral catalyst at 0 °C. The optically active trisubstituted dihydro-1*H*-pyrrole-3-carbaldehydes are synthesized in good yields with excellent enantio- and diastereoselectivity (up to >98% ee, and up to >20:1 d.r.) *via* asymmetric domino formal 1,3-dipolar cycloaddition/intramolecular ring-opening, C-S and C-N bond-cleavage.

Chapter 5 provided the summary of important findings drawn from the thesis work and conclusions.

TABLE OF CONTENTS

LIST OF TABLES

LIST OF FIGURES

LIST OF SCHEMES

ABBREVIATIONS

CCDC	Cambridge Crystallographic Data Centre
Calcd	Calculated
DCM	Dichloromethane
DMF	Dimethyl formamide
DMSO	Dimethyl sulfoxide
DMAP	4-Dimethylaminopyridine
DIPEA	*N, N*-Diisopropylethylamine
DMA	Dimethyl amine
DBA	Dibutyl amine
DABCO	1,4-Diazabicyclo[2,2,2]octane
d	Doublet
dd	Doublet of doublet
dq	Doublet of quartet
d.r.	Diastereomeric ratio
EDG	Electron donating group
EWG	Electron withdrawing group
MCR	Multi-component reaction
Ee/ee	Enantiomeric excess
equiv.	Equivalent
ESI-MS	Electrospray ionization mass spectrometry
g	Gram
HRMS	High resolution mass spectrometry
HPLC	High performance liquid chromatography
h	Hour
^{i}PrOH	Iso-Propyl alcohol

IR	Infrared
m	Multiplet
m/z	Mass/Charge
MHz	Megahertz
min	Minute
mL	Milliliter
mmol	Millimole
mol	Mole
mp	Melting point
NMR	Nuclear magnetic resonance
Ph	Phenyl
ppm	Parts per million
q	Quartet
r_t	Retention time
rt	Room temperature
s	Selectivity factor
s	Singlet
t	Triplet
^{t}Bu	Tertiary butyl
tert	Tertiary
THF	Tetrahydrofuran
TLC	Thin layer chromatography
TMS	Tetramethyl silane
TMSCl	Trimethylsilyl chloride

NOTATION

α	Alpha
β	Beta
γ	Gamma
%	Percentage
J	Coupling constant
δ	Chemical shift
°	Degree
°C	Degree centigrade

INSTRUMENTATION AND GENERAL CONSIDERATIONS

THIN LAYER CHROMATOGRAPHY (TLC)

Thin layer chromatograms were run on silica gel 60 F_{254} plates obtained from Merck with pankal solution, UV light, iodine, alkali $KMnO_4$, 2,4-DNP, and PMA solution as detecting agents.

COLUMN CHROMATOGRAPHY

Column chromatography was performed using silica gel (100-200 mesh). The solvents used for column chromatography were distilled prior to use.

MELTING POINTS

Melting points were measured either on a Toshniwal melting point apparatus or on a Guna melting point apparatus. The melting points were uncorrected.

IR SPECTROSCOPY

IR spectra were recorded on a JASCO FT-IR spectrometer. Band positions are reported in reciprocal centimeters.

NMR SPECTROSCOPY

^{1}H and ^{13}C NMR spectra were recorded on Bruker 400 and 500 MHz spectrometers using TMS as an internal standard. Chemical shifts are reported in parts per million (δ) downfield from the internal tetramethyl silane reference and the coupling constants (*J*) in Hertz.

MASS SPECTROMETRY

The ESI (electron spray ionization) mass spectra were recorded on a Waters/Micro mass Q-TOF mass spectrometer equipped with a Harvard apparatus syringe pump. The measurements were performed in EtOAc, MeOH, and acetonitrile solvents.

HIGH PERFORMANCE LIQUID CHROMATOGRAPHY (HPLC)

The initial reaction rate was determined by Waters 2965 HPLC systems using Luna® 5 µm Silica (2) 100 Å, LC Column 250 x 4.6 mm. HPLC solvents were purchased from SD fine-chem limited, India, and used as such received.

CHAPTER 1

INTRODUCTION

1.1 ASYMMETRIC SYNTHESIS

A molecule is said to be chiral when its mirror counterpart cannot be superimposed with the original. The concept was first proposed by Lord Kelvin, stating that "*if a geometric figure or a set of points is chiral and has chirality, its reflection in a plane mirror, if perfectly realized, cannot be superimposed on itself*."[1] Any molecules with the chiral centre, that is four different substituents attached with the same carbon atom, and its mirror image cannot be superimposed are called "*enantiomers*." The term "*optical activity*" refers to the ability of a solution or solid to rotate plane-polarized light. When plane-polarized light of a particular wavelength passes through a chiral molecule, it undergoes rotation. The term '*asymmetric synthesis'* refers to the achievement of enantioselective synthesis of optically active chiral substances, ideally as a single enantiomer.[2]

1.1.1 Significations of Enantioselectivity

The term chirality and symmetry are prevalence in nature, which substantially affects medicinal and agricultural chemistry. Biological systems often recognize two enantiomers as different substances, and the two enantiomers may result in different behaviours. For instance, naturally occurring *L*-phenylalanine ***L*-1** tastes bitter, whereas the ***D*-1**-phenylalanine tastes sweeter (Figure 1.1).[3]

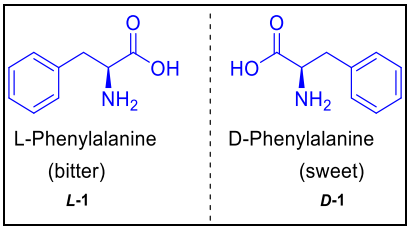

Figure 1.1 Enantiomers of phenylalanine

Particularly, one enantiomer may work as a useful therapeutic drug, while the other is exceptionally harmful. In the mid-19th century, a dreadful medical disaster that was thalidomide's tragedy better be remembered. 1950s and early 1960s, thalidomide was a regularly prescribed medicine for the avoidance of nausea in pregnant women.[4] As a result, hundreds of infants in serious congenital defects in the 1960's. It was realized that enantiomers of a racemic compound can display different biological features and confirmed that only (*S*)-enantiomer of thalidomide is teratogenic and (*R*)-enantiomer of thalidomide is used as a sedative agent (Figure 1.2).[5] Similarly, the isomeric form of (*S*)-ibuprofen is used as a pain killer, whereas (*R*)-ibuprofen is inactive.[6] The (*S*)-isomer of naproxen is teratogenic, whereas (*R*)-naproxen is beneficial for arthralgia pain.[7] Ultimately, (*S*)-ofloxacin is less active against bacterial infection in many different places of the body, whereas (*R*)-ofloxacin is 128 times more potent in bacterial activity than (*S*)-ofloxacin[8] (Figure 1.2).

(*S*)-Enantiomer	**(*R*)-Enantiomer**
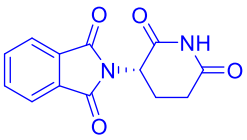	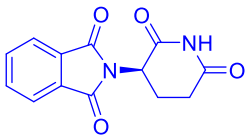
(*S*)-Thalidomide Teratogenic birth defects	(*R*)-Thalidomide Effective sedative agent

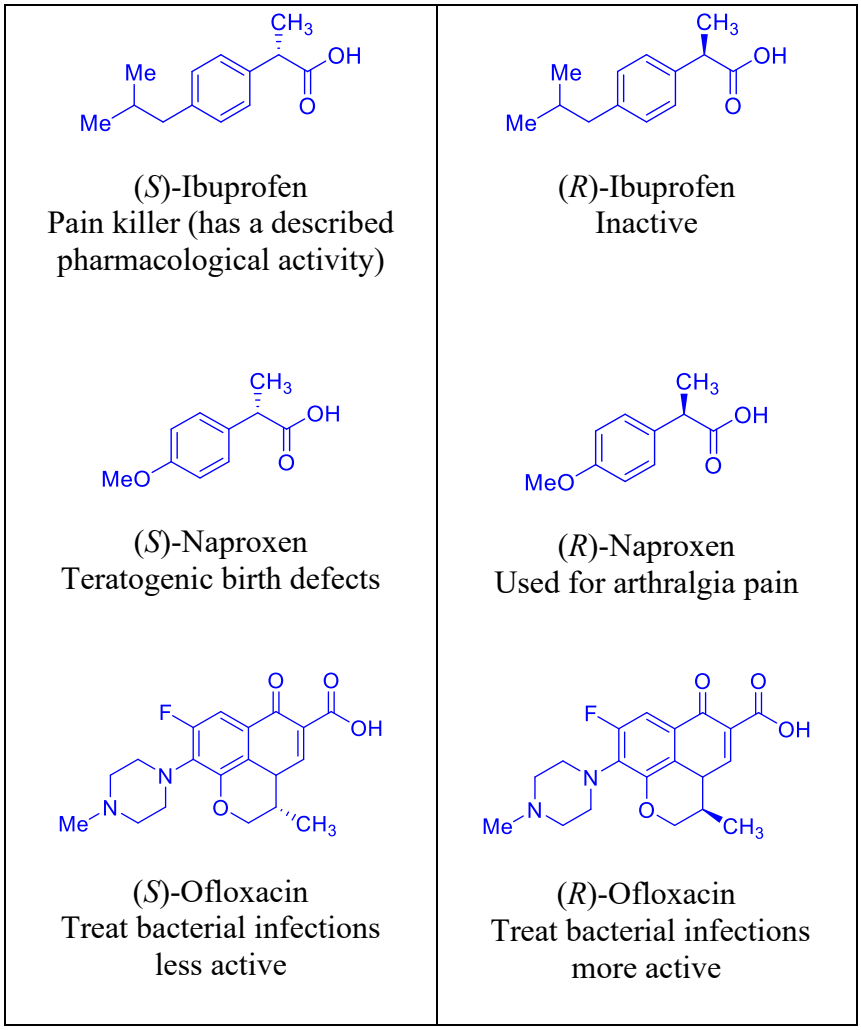

Figure 1.2 Example of the structure of (*S*)-enantiomers and (*R*)-enantiomers of chiral medicines with different activity

1.1.2 Approaches for Enantioselectivity

Enantiomerically pure synthesis of enantiopure organic compound is a main tool for synthetic chemist due to their need in medicinal applications. Various approaches toward enantiomerically pure synthesis include conventional chiral resolution using diastereomers,[9] chiral pool synthesis, chemical kinetic resolutions,[10-12] enzymatic resolution, and [13] and catalytic asymmetric synthesis.[14] Over the past several decades, synthetic organic chemistry has widely acknowledged the importance and usefulness of asymmetric synthesis for producing enantioenriched molecules. There are various techniques known for asymmetric synthesis such as, 1. Chiral pool synthesis refers to

synthesizing chiral chemicals by starting with widely available chiral starting ingredients.[15,16] 2. Enzyme-catalysed reaction involves enzymes promoting chemical reactions, resulting in the synthesis of optically active compounds. [17,18] 3. Chiral auxiliaries are temporary chiral groups attached to a molecule to regulate its stereochemistry during a chemical process.[19] After completion, the reaction can be separated from the starting materials. 4. Kinetic and dynamic kinetic resolution[11-13] refers to techniques that separate enantiomers based on their differing reaction speeds. 5. Crystallization is a method of purifying chemicals by creating solid crystals from a solution or melting.[20] 6. A catalytic asymmetric catalyst is a material that can selectively stimulate a chemical reaction to create a single enantiomer.[21] Among the methods, catalytic asymmetric synthesis is most extensively used, in which a chiral catalyst can create millions of chiral molecules. It offers a significant economic benefit compared to other asymmetric synthetic methods in academic and industrial frameworks.

1.2 CATALYST

A catalyst is a chemical substance that decreases activation energy and thereby increases the course of a reaction under a mild condition, resulting in involve in a cyclic process.[22] Asymmetric or enantioselective catalysis is a fundamental part of asymmetric synthesis, which transforms prochiral and racemic compounds into major enantioenriched synthetic building blocks. Three types of asymmetric catalysis are known as, 1. Biocatalyst,[23] 2. Transition metal catalyst,[24] and 3. Organocatalysis.[25,27]

1.2.1 Biocatalyst

A biocatalyst or enzymatic catalyst, usually employs biologically active components to carry out chemical transformations that lead to one of the enantiomers of the chiral

product formed at the end and another enantiomer of a racemate being unharmed.[28] Steven *et al.* developed a green biocatalytic process for the manufacture of atorvastatin intermediate in 2009. The active ingredient of the cholesterol-lowering drug has been prepared in two steps and through three enzyme processes. This transformation involved the biocatalytic reduction of ethyl-4-chloroaceoacetate using ketoreductase (KRED) in combination with glucose and NADP-dependent glucose dehydrogenase (GDH), afforded ethyl-4-chloro-3-hydroxybutyrate. It was followed by halohydrin dehalogenation (HHDH) with NaCN at natural pH produced ethyl-4-cyano-3-hydroxybutyrate which was further transformed to atorvastatin using a multi-step process (Scheme 1.1).[29, 30]

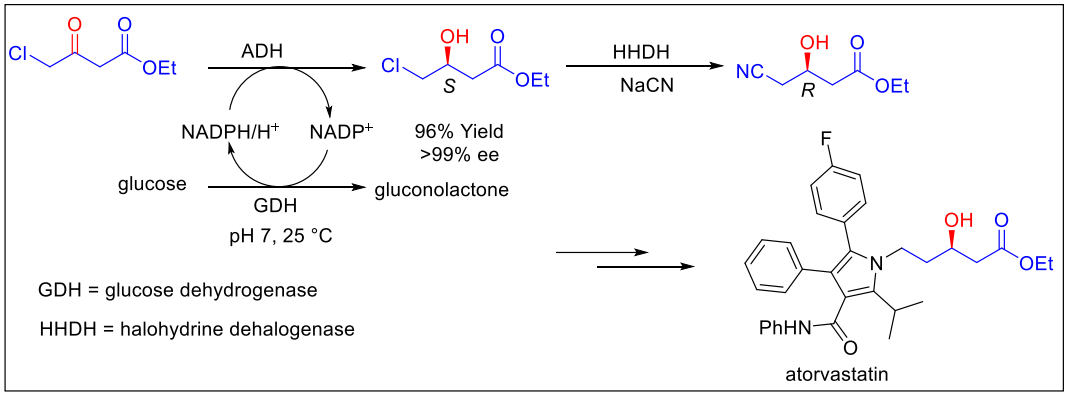

Scheme 1.1 Synthesis of atorvastatin by biocatalysts

1.2.2 Transition metal catalysts

The chiral ligands are complexed with transition metals named transition metal catalysts, which will subsequently be used as catalysts in the reaction precursor to afford a chiral product.

Synthesis of planar chiral oxazole-pyridine *N,N*-ligand has been developed by Yu *et al.* in 2023 for the application of palladium-catalyzed asymmetric acetoxylative cyclization of alkyne-tethered cyclohexadienones. The reaction furnished chiral *cis*-

hydro benzofurans in high yield with excellent enantioselectivity, which belongs to bioactive molecules with potent NF-kB inhibition (Scheme 1.2).[31]

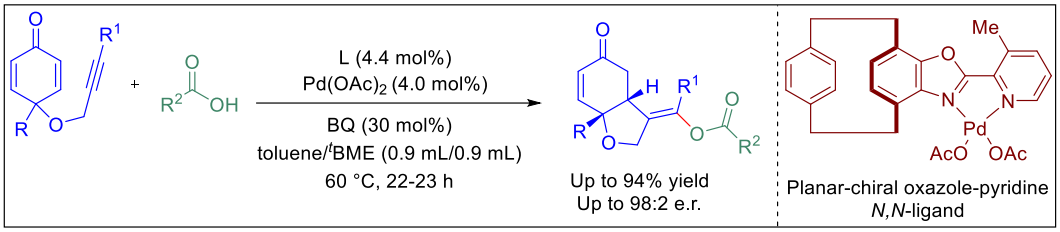

Scheme 1. 2 Example of transition metal complex catalyzed reaction

1.2.3 Chiral Organocatalysts

Chiral organocatalysts are an asymmetric catalyst that catalyzes an asymmetric transformation using small chiral organic molecules without a metal ion.[32] The stimulating substrates are electrophiles or nucleophiles *via* covalent or non-covalent interactions to produce the appropriate chiral product. The major advantages of organocatalysts over transition metal or enzymatic catalysts are as follows: They are oxygen-stable reagents and can be used without anhydrous conditions except for chiral NHC carbene catalysts. It can minimize the cost of synthesis and be compatible with various functional groups that could be sensitive to other processes. In contrast, transition metal catalysts cause environmental issues, including toxicity, harmful metal waste generation, and retaining trace metal contaminants in the end products. Organocatalysts are often cheap and widely available at competitive prize, which is more appropriate for a small-scale reaction into industrial processes. For the above aspects, organocatalysts can be called green catalysts rather than traditional catalysts.

Liebig first discovered that acetaldehyde acts as an organocatalyst in the year of 1860, for the hydrolysis of cyanogen to oxamide. The reaction of dicyanide with water in the presence of acetaldehyde organocatalyst at room temperature provided an oximide

product. Without acetaldehyde, the reaction furnished only a mixture of products. The presence of an acetaldehyde organocatalyst majorly afforded oximide as the product (Scheme 1.4).[33]

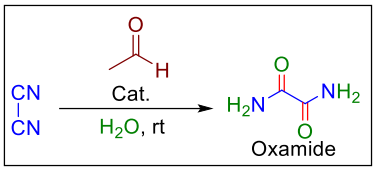

Scheme 1.3 Synthesis of oxamide catalyzed by acetaldehyde organocatalyst

In the first decades of the 1900s, Bredig and Fiske introduced the asymmetric organocatalyst concept. The simple benzaldehyde reacted with hydrogen cyanide utilizing a chiral cinchonine as an asymmetric organocatalyst and achieved chiral 1-hydroxy-1-phenyl acetonitrile with 10% enantioselectivity (Scheme 1.5).[34]

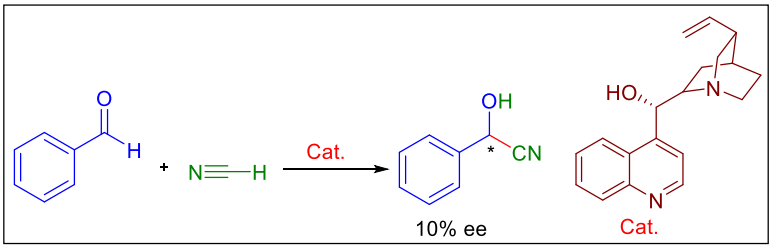

Scheme 1.4 Asymmetric 1,2-addition for the synthesis of benzaldehyde cyanohydrin

In 1971, naturally available amino acid (*L*)-proline as an organocatalysts has been reported by Hajos–Parrish for the intramolecular aldol cyclization, and it is called the "Hajos–Parrish–Eder–Sauer–Wiechert" reaction (Scheme 1.3).[35]

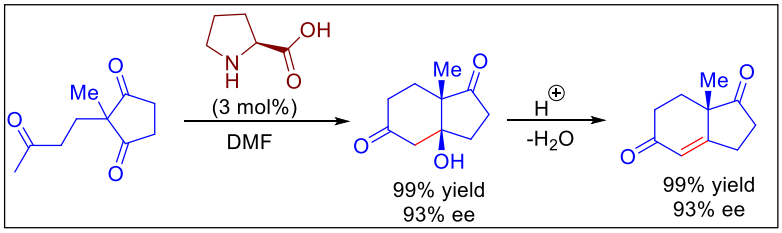

Scheme 1.5 Example of organocatalysts

Subsequently, several asymmetric organocatalysts have been reported, including chiral phase transfer catalysts, chiral hydrogen bonding catalysts, chiral Brønsted acid, and Brønsted base catalysts.[36-44]

In the late 1990s, Benjamin List and David MacMillan independently developed enamine and iminium ion-based chiral amine-based organocatalysts for asymmetric synthesis (Scheme 1.6).[37] The discovery of this catalyst has changed the vision of the asymmetric organocatalytic system to synthesize various chiral organic frameworks in the past two decades. This chiral amine catalyst is more important than other organocatalysts because it mimics the enzyme catalyst, and researchers denoted it as a green catalyst.

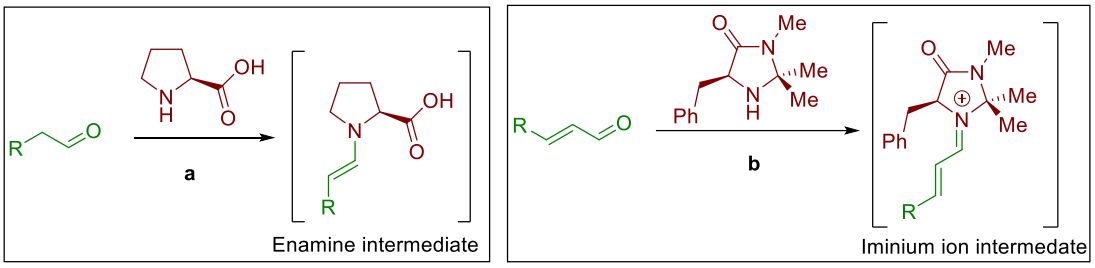

Scheme 1.6 Formation of chiral enamine and iminium ion intermediate

1.2.4 Types of Organocatalysts

Four major types of organocatalysts are known for the asymmetric synthesis. They are categorized into i) chiral Lewis acid,[38] ii) Lewis base,[39,40] iii) Brønsted acid,[41,42] and iv) Brønsted base catalyst.[43,44] Among, chiral boron complex (CBS) reagents and organocatalysts complexes with metal ions (such as Cu, Ti, Al, Rh, and Zn) are considered into Lewis acid catalysts. Chiral proline, imidazoline-derived catalysts, and chiral NHC carbene catalysts are classified into chiral Lewis bases. The chiral thiourea and squaramide chiral phosphoric acid catalysts are characterized as chiral Brønsted acid catalysts. The amines, cinchona alkaloids, and chiral quinine catalysts are

classified as Brønsted base catalysts. Bifunctional organocatalysts such as chiral amine attached with hydrogen bonding catalysts also reported in the literature (Figure 1.3).[45]

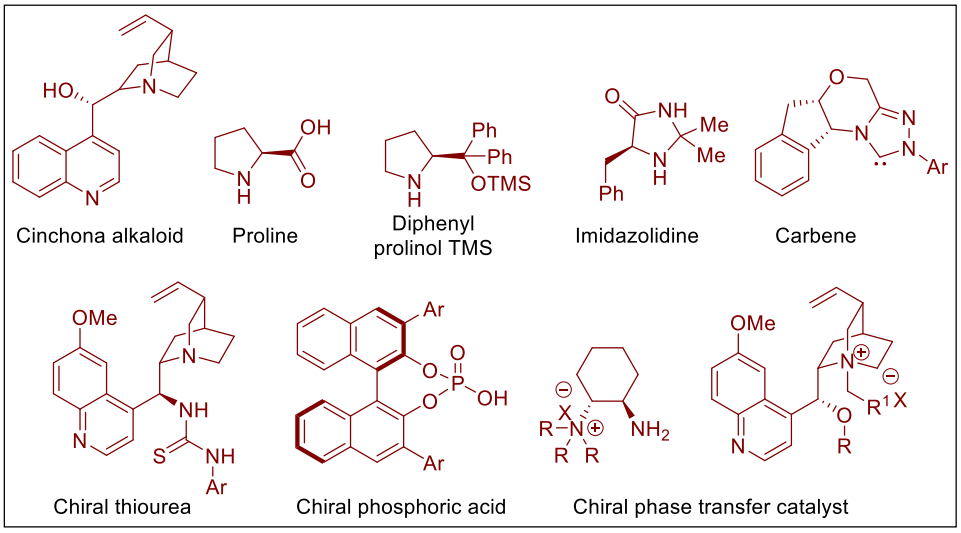

Figure 1.3 Example of organocatalysts

Based on the different activation modes, organocatalysts are further classified into two major types. 1. Covalent bond activation,[46] 2. Non-covalent bond activation.[47] The covalent bond activation can be done when organocatalysts and substrate form a transient covalent bond to create a reactive intermediate. The formed intermediate undergoes further reactions, and eventually organocatalysts are recovered. The most common examples of organocatalysts are amine-[48] and phosphine-based,[49,50] which have led to a wide range of reaction types. Covalent binding of substrate usually requires a high catalyst loading (Figure 1.4).

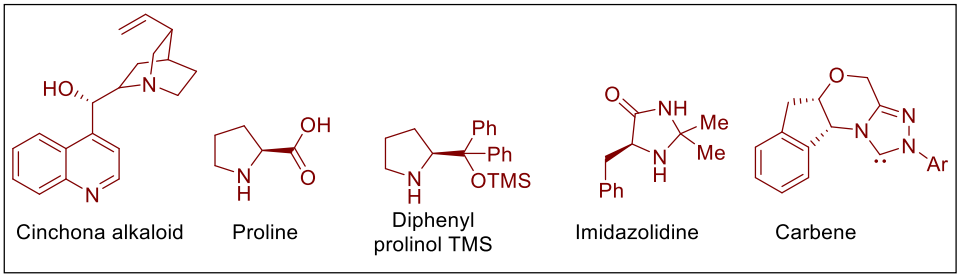

Figure 1.4 Examples of covalent bond activation organocatalysts

Non-covalent bond activation by organocatalysts uses non-covalent interactions between the substrate and organocatalysts to increase the rate of a reaction. Non-covalent interactions or non-bonded interactions are weak interactions between atoms or molecules when electron pairs are not shared, and they do not involve forming or breaking chemical bonds. Non-covalent interactions included ionic bonds, hydrogen bonds, Van der Waals interactions, and hydrophobic interactions. The typical examples of non-covalent organocatalysts are chiral thiourea, squaramide-based hydrogen bonding catalyst, chiral phosphoric acid catalyst, chiral phase transfer catalyst, halonium, chalconium, pnictonium, sulfonium, and selenonium salts (Figure 1.5).[47]

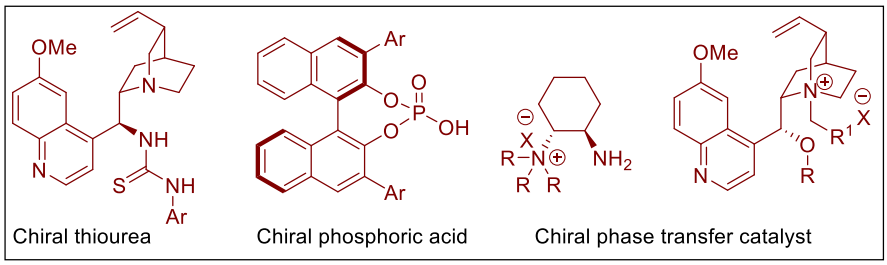

Figure 1.5 Examples of non-covalent organocatalysts

In 2016, Josipa *et al*. reported an enantioselective synthesis of *N*(acyl) *S*-acetals from asymmetric addition of thiols to *N*-acyl ketimines, which was generated *in-situ* from-3-hydroxy isoindolinones using a chiral Brønsted acid catalyst. In this reaction, a chiral ligand non-covalently interacted with ketimines and thiol through hydrogen bonding to achieve a high enantiomeric excess (Scheme 1.7).[51]

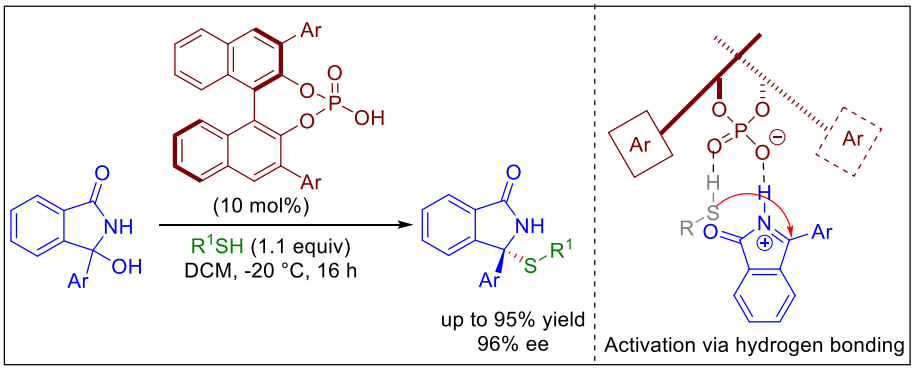

Scheme 1.7 Example of non-covalent bond activation reaction

1.3. CHIRAL AMINE BASED ORGANOCATALYST

Chiral amine-based organocatalysts play a vital role in asymmetric synthesis, and they are versatile and potent catalysts that are useful in a wide range of enantioselective chemical processes.[52,53] They are generated from natural amino acids,[54] such as cinchona alkaloids,[55] and other chiral amines. It is facilitating the creation of chiral compounds with strong enantioselectivity. A significant property of chiral amine organocatalysts is their ability to activate substrates through covalent interactions. By stabilizing reactive intermediates or transition states, these catalysts enhance asymmetric induction, resulting in the preferred synthesis of one enantiomer over the other.

L-Proline is a chiral pool reagent that can react quickly with both enantiomeric forms at a fair cost and is stable under standard conditions. The invention of chiral amine organocatalysts has dramatically enlarged the toolbox of asymmetric synthesis, providing economical and ecologically friendly approaches to a wide range of chiral molecules. Due to their versatility, gentle reaction conditions, and high degrees of enantioselectivity make them indispensable in modern chemical synthesis.[56, 57]

1.3.1 Reactivity of Chiral Proline Organocatalysts

Proline has both pyrrolidine ring and carboxylate in its peculiar structure for the catalytic action. Proline comprises both acidic and basic functional groups, which offers an advantage in its capacity to serve as a bifunctional catalyst and provides simple accessibility to metal complexes. It can operate as an electrophile by forming enamine intermediates *via* rapidly creating iminium ions or as a nucleophile. Because of its cyclic and secondary structure, proline has a larger pKa than other amino acids,

influencing its hydrogen-bonding strength. Additionally, its pyrrolidine component enables it to create enamine and iminium ions more readily than other amines, even cyclic amines like piperidine (Figure 1.6).

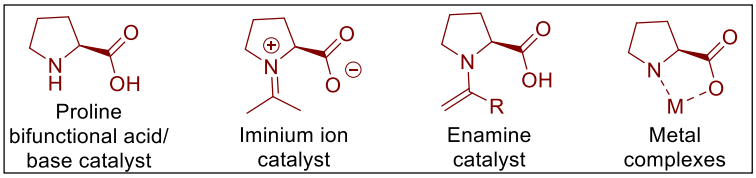

Figure 1.6 Reactivity modes of a proline catalyst

Proline as an organocatalyst finds widespread applications in various asymmetric transformations, including asymmetric aldol reaction, Michael addition, Mannich reaction, Morita-Baylis-Hillman reaction, α-functionalization, and cycloaddition. Most importantly, it is used to synthesize a wide range of bioactive molecules and natural products.[58]

1. Aldol reactions: Chiral amine catalysts facilitate the stereoselective formation of aldol adducts by activating carbonyl compounds and enolizable aldehydes or ketones.[59] A proline-catalyzed asymmetric Robinson annulation reaction (Michael addition followed by intramolecular aldol condensation) for the enantioselective synthesis of Wieland-Miescher ketone has been achieved by Tommy *et al*. in 2000 *via* a single step using methyl vinyl ketone and methyl-substituted cyclohexanedione in aqueous acetic acid. The reaction provided the desired product in good yield and enantioselectivity (Scheme 1.8).[60]

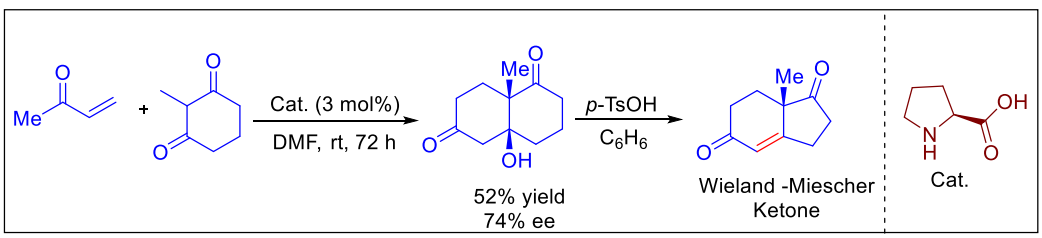

Scheme 1.8 Aldol reaction in Wieland-Miescher ketone synthesis

2. Michael additions: Chiral amine as organocatalysts were used in conjugate addition of α,β-unsaturated carbonyl compounds, and this reaction yielded chiral products with high enantioselectivity.[61] Proline-catalysed Michael addition of ketones with nitro styrene was examined by Dieter *et al*. in 2002. The reaction furnished optically active γ-nitro ketones in good to excellent yield with up to 97% d.r. with *syn*-diastereomers in good enantioselectivity *via* catalytic asymmetric 1,4-addition (Scheme 1.9).[62]

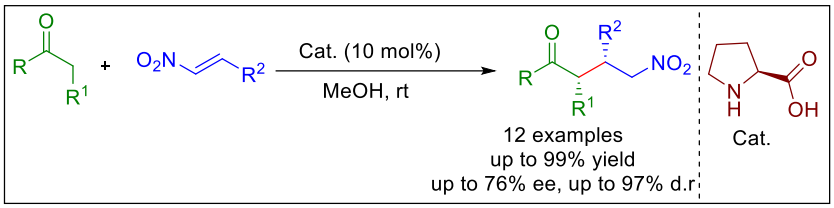

Scheme 1.9 Asymmetric Michael addition reaction

3. Mannich reactions: Asymmetric Mannich reaction is one of the most basic and valuable methods to synthesize chiral β-amino carbonyl compounds. This product can be achieved by chiral amine catalysts *via* the asymmetric addition of nucleophiles (such as amines or enamines) to imines or iminium ions. In 2007, Jung *et al.* developed a catalytic asymmetric Mannich reaction of aldehydes with N-Boc-imines in the presence of a proline catalyst. The reaction provided the chiral β-amino aldehyde or ketone in high diastereo- and enantioselectivities without a need for chromatographic purification (Scheme 1.10)[63]

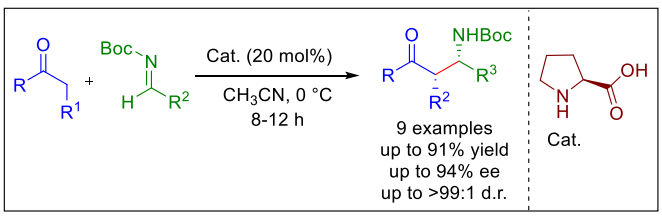

Scheme 1.10 Asymmetric Mannich reaction

4. Morita-Baylis-Hillman (MBH) reaction: In 2007, Naoto and co-workers accomplished a (*L*)-Proline catalyzed asymmetric aza-MBH reaction to synthesize

enantioenriched β-amino carbonyl compounds containing an α-alkylidene group in moderate yield and E/Z isomers with excellent enantioselectivity. The reaction proceeded between β-substituted, unsaturated aldehydes and α-imino esters *via* Mannich-type reaction/isomerization sequence (Scheme 1.11).[64]

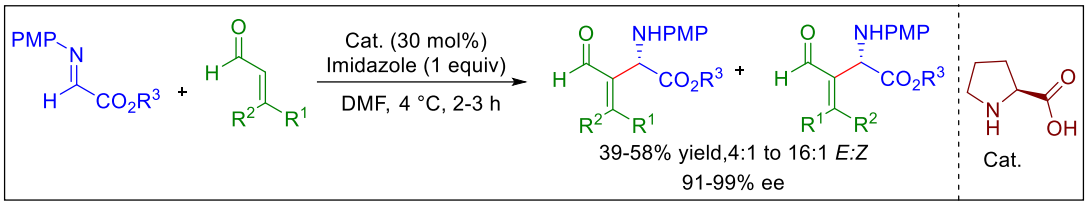

Scheme 1.11 Asymmetric aza-MBH reaction

5. α-Functionalization: (*L*)-proline catalyzed several α-functionalization reactions has been reported in the literature, which offers new technologies to access valuable α-functionalized products in a greener and more sustainable manner. The α-functionalization methods include α-amination of aldehyde and ketones, aminoxylation, alkylation, allylation, and halogenation.[58]

5.1 α-Amination of Aldehyde and Ketones

α-Amination is a highly efficient method for synthesizing chiral compounds that contain *C-N* linkages. Azodicarboxylates are appropriate electrophiles for the enamine-catalyzed addition of aldehydes or ketones. In 2002, Nagaswamy *et al.* developed the first asymmetric α-amination of ketones using azodicarboxylates as a nitrogen source *via* direct *L*-proline-catalysed reaction provided highly valuable optically active α-hydrazino ketones in good yield and high enantioselectivity with good regio isomeric ratio. It is further transformed into optically active compounds like α-aminated ketones and alcohol (Scheme 1.12).[65]

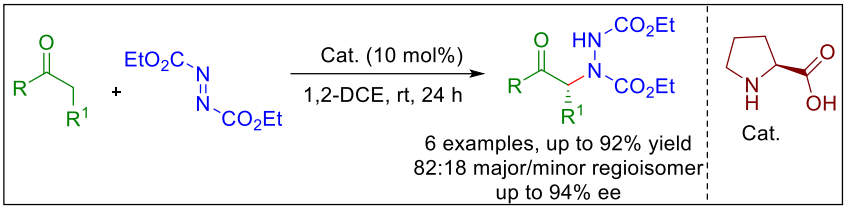

Scheme 1.12 Asymmetric α-amination of ketones

Later in 2002, Benjamin developed the proline-catalyzed direct catalytic asymmetric α-amination of aldehydes with azodicarboxylates followed by sodium borohydride reduction, which provided the 2-hydrazino alcohol in excellent yield and enantioselectivity (Scheme 1.13).[66]

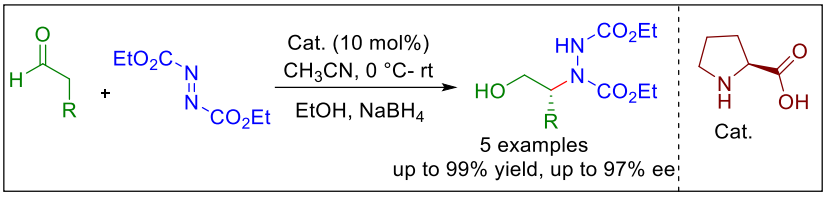

Scheme 1.13 Asymmetric α-amination of aldehyde

5.2 α-Aminoxylation of Cyclic Ketones

Developing a proline-catalyzed enantioselective reaction of cyclic ketone and nitrosobenzene into chiral α-hydroxy ketones is another important transformation to build valuable compounds. In 2004, Anders and co-workers developed a direct catalytic enantioselective α-aminoxylation of cyclic ketones to assess stereoselective synthesis of α-hydroxy and α,α'-hydroxy ketones in high yield and enantioselectivity using proline as a chiral catalyst (Scheme 1.14).[67]

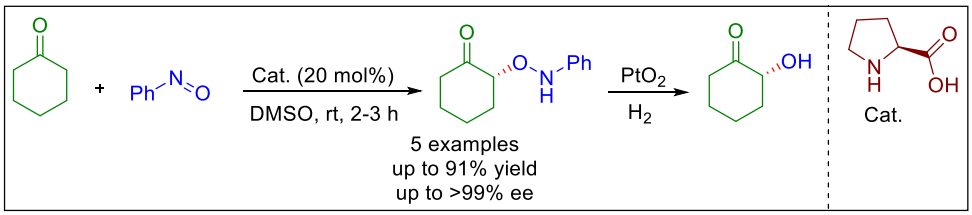

Scheme 1.14 Asymmetric α-aminoxylation of cyclic ketone

5.3 α-Alkylation

The enantioselective α-alkylation of aldehydes is a highly valuable method using simple *L*-proline as a chiral catalyst. In 2008, Rafik *et al.* developed a challenging strategy for asymmetric intermolecular enamine-catalyzed formal α-alkylation of aldehydes *via* vinylogous iminium ion intermediate generated from aryl sulfonyl indoles in good yield and enantio- and diastereoselectivity using *L*-proline chiral catalyst (Scheme 1.15).[68]

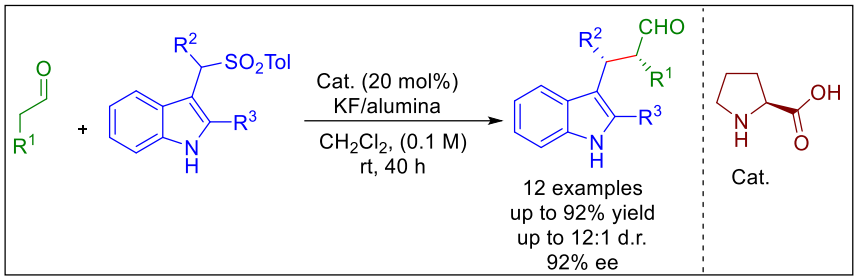

Scheme 1.15 Asymmetric α-alkylation reaction

5.4 α-Halogenation

The asymmetric α-halogenation method of aldehydes and ketones is a highly valuable method for the synthesis of biologically active molecules. Among them, the synthesis of optically pure fluorine compounds is highly important in medicinal and drug delivery systems due to its high lipophilicity character. The first example of direct α-fluorination of 2-phenyl propionaldehyde and fluorination agent in the presence of *L*-proline as a chiral asymmetric catalyst was developed by Derek and co-workers in 2005. The reaction furnished corresponding α-fluoro aldehydes in good yields with excellent enantioselectivity (Scheme 1.16).[69]

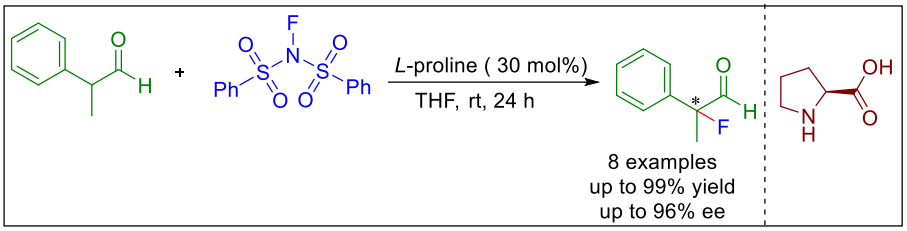

Scheme 1.16 Asymmetric α-fluorination reaction

6. Cycloaddition

Cycloadditions are very effective and commonly employed processes for producing substrates containing carbon-carbon and carbon-heteroatom bonds while achieving precise control over stereochemistry.[70] A first highly enantioselective organocatalyzed carbo [4+2] cascade cycloaddition of two different α,β-unsaturated aldehydes achieved by Bor-Cherng and co-workers, in 2006. This cycloaddition methodology furnished chiral cyclohexadiene carbaldehydes in good yields with excellent enantioselectivity (Scheme 1.17).[71]

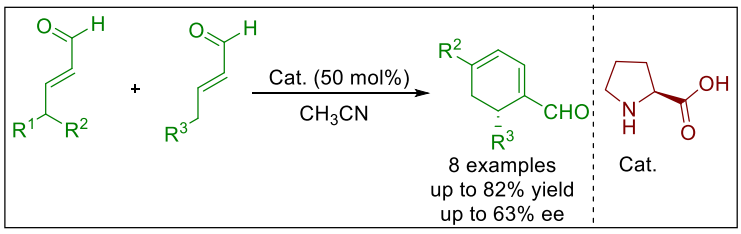

Scheme 1.17 Asymmetric cycloaddition reaction

1.3.2 Modification of Chiral Proline Organocatalyst

The efficacy of simple proline and imidazolidinones was proven in catalytic processes that highly favored organocatalysts during their initial years, which involved enamine and iminium ion intermediates *via* HOMO and LUMO activation modes (Figure 1.7).[48] They are commonly used in straightforward and fundamental reactions to create bonds, but only for a limited number of functional groups. Although a notable advancement in

organocatalytic approaches since the early years, their investigations also uncovered certain limitations and obstacles.

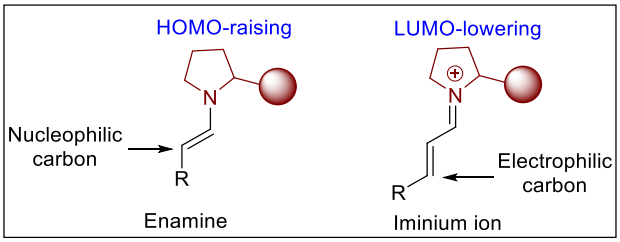

Figure 1.7 Enamine (HOMO activation) and iminium ion (LUMO activation)

Considering those limitations, the researchers modified the simple proline catalyst to substituted proline catalysts by increasing the bulkiness. The motivation for the invention of modification in simple proline was diarylprolinol silyl ethers, which originated from two related compounds they are, diarylmethylpyrrolidine and diarylprolinol.[72] The diarylmethylpyrrolidines generally gave good catalytic turnover at modest selectivity, whereas the diarylprolinols performed well in stereocontrol; however, poor reaction rates were achieved. The lack of stereocontrol for the diarylmethylpyrrolidines was suggested to originate from insufficient steric shielding, the lack of catalytic turnover for the diarylprolinol was more surprising. It was found that a "*parasitic equilibrium"* existed with the development of an oxazolidine species in the case of diarylprolinol catalyst containing a hydroxy group (Figure 1.8). A simple silyl protection overcame this problem, and hence, the diarylprolinol silyl ether catalysts were produced.

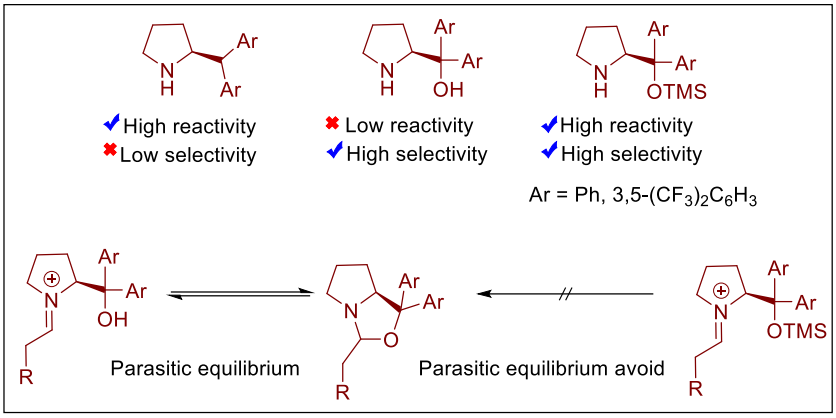

Figure 1.8 Reactivity and parasitic equilibrium of diarylprolinol silyl ether catalysts

They can easily condense with both saturated and unsaturated aldehydes to form enamine and iminium ion intermediate *via* different transition states (Figure 1.9). Among different *E* and *Z* isomers of enamine intermediate, "*E-s-trans"* is said to be a highly stable and more reactive intermediate. In the case of iminium ion intermediate, the "*E*, *E*-trans" transition state is more stable and highly reactive.[73]

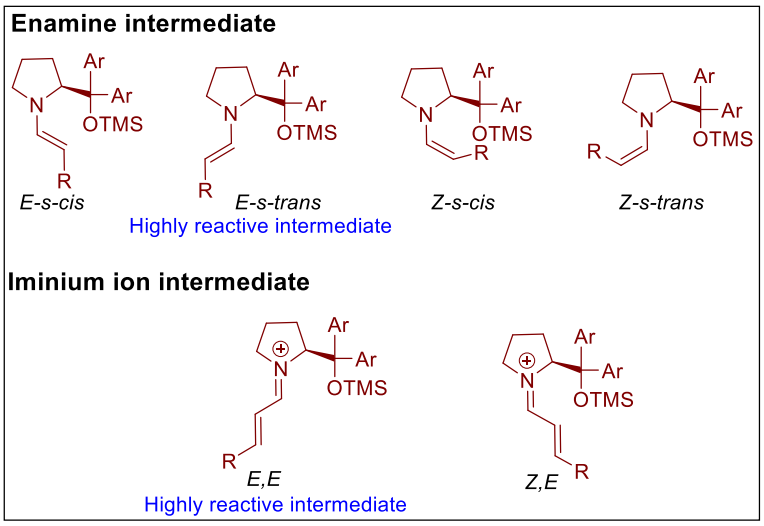

Figure 1.9 Enamine and iminium ion transition states

1.3.3 Applications of Diarylprolinol Silyl Ether Catalyst

Synthesis of pyrrole functionalized cyclobutene derivatives with three contiguous stereocenters with excellent yield and high regio-, enantio-, and diastereocontrol *via*

organocatalytic vinylogous Fridel-Craft alkylation initiated formal [2+2] cycloaddition through iminium-enamine activation of enals has been achieved by Guo *et al.* in 2013 (Scheme 1.18).[74]

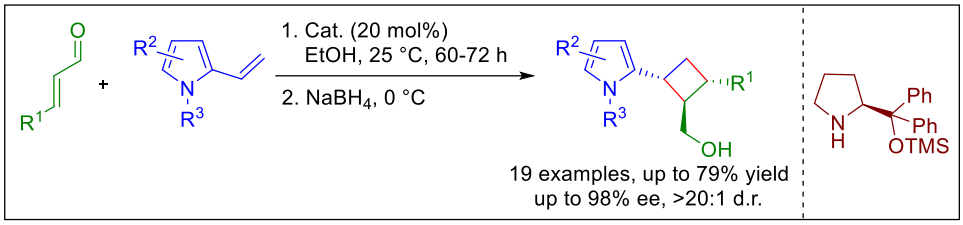

Scheme 1.18 [2+2] Cycloaddition for the synthesis of pyrrole-functionalized cyclobutanes

In 2016, Alex and co-workers developed an organocatalytic stepwise [2+2] cycloaddition for the synthesis of substituted heterodimeric and homochiral cyclobutenes *via* secondary amine-catalyzed hetero-dimerization of two different cinnamic acid derived subunits with high enantio- and diastereoselectivity (Scheme 1.19).[75]

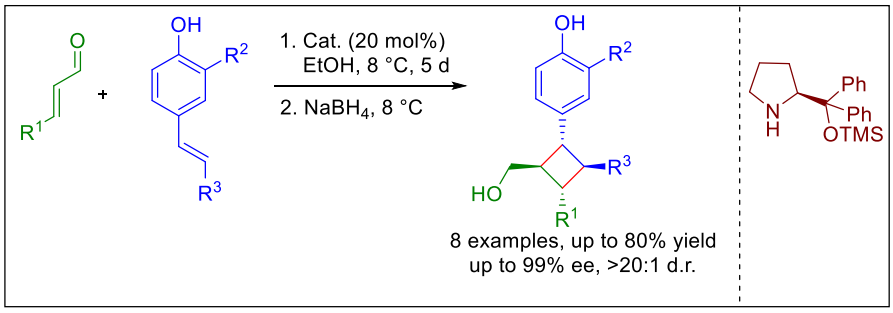

Scheme 1.19 [2+2] Cycloaddition for the synthesis of heterodimeric and homochiral cyclobutenes

Kim *et al.* developed a [3+2] cycloaddition in 2016, between vinyl cyclopropanes and unsaturated aldehydes catalyzed by synergistic palladium and chiral amine organocatalysts for the stereoselective synthesis of highly substituted cyclopentanes with four contiguous stereocenters in high yield, good enantio- and diastereoselectivity (Scheme 1.20).[76]

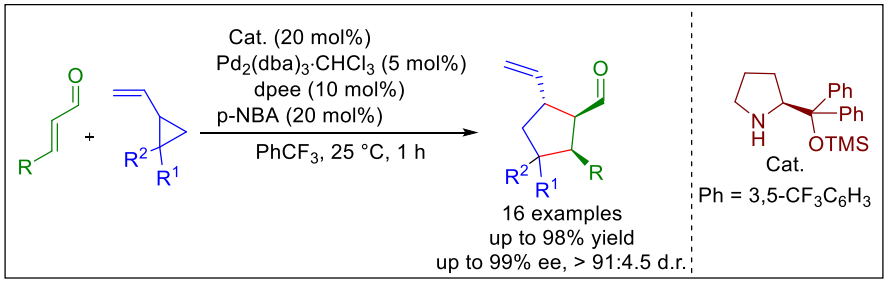

Scheme 1.20 Asymmetric [3+2] cycloaddition for the synthesis of cyclopentanes

The enantioselective Diels-Alder reactions of α,β-unsaturated aldehydes with cyclopentadienones were accomplished in 2007 by Hiroaki and Yujiro *via* chiral amine catalyst and triflic acid combination. They achieved the cycloadduct product in good yields in a highly exo-selective manner (Scheme 1.21).[77]

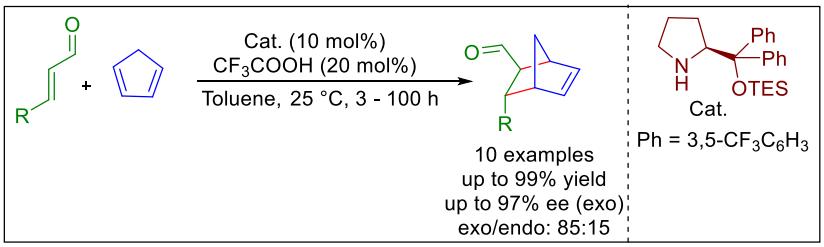

Scheme 1.21 Asymmetric Diels-Alder reaction for the synthesis of exo-cycloadduct products

In 2013, Dieter and co-workers developed a catalytic asymmetric three-component triple cascade of 3-vinyl indoles with unsaturated aldehydes *via* iminium-enamine activation sequence yielded the unsaturated tetracyclic pyrido-carbazole derivatives in high-yield with excellent enantio- and diastereoselectivity (Scheme 1.22).[78]

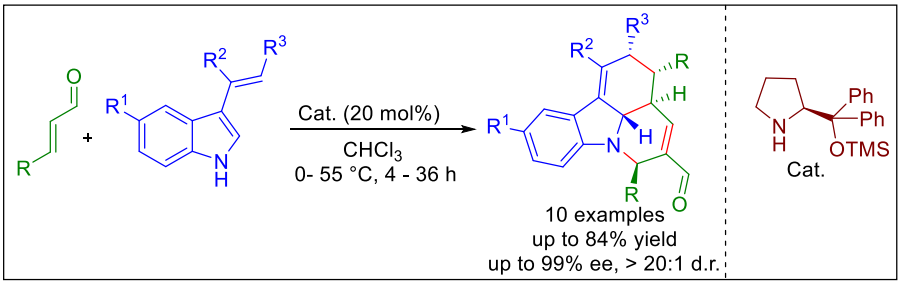

Scheme 1.22 Asymmetric three-component triple cascade reaction for the synthesis of tetracyclic pyrido-carbazoles

In 2015, Iker *et al.* developed a chiral amine catalyzed enantioselective [4+2] cycloaddition using 4-alkynyl-5H-1,2-3oxathiazole 2,2-dioxides and cinnamaldehyde derivatives through iminium-enamine activation, and the reaction afforded trans-decline framework and densely functionalized cyclohexenes in excellent yield with high enantio- and diastereoselectivity (Scheme 1.23).[79]

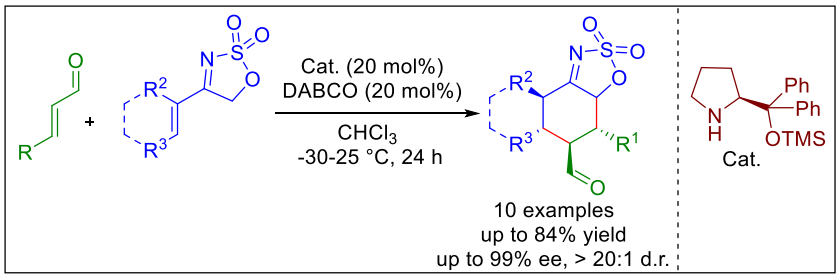

Scheme 1.23 Asymmetric [4+2] cycloaddition for the synthesis of densely functionalized cyclohexenes

Marta and co-workers reported an enantioselective ring opening of vinyl cyclopropanes with conjugated aldehydes *via* a combined transition metal and amine catalyst. The reaction furnished the cyclopentane derivatives with excellent yield with moderate stereoselectivity (Scheme 1.24).[80]

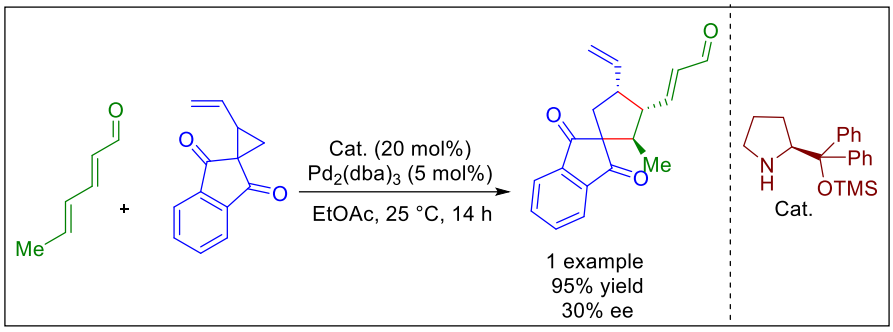

Scheme 1.24 Synergistic catalyst in enantioselective synthesis of cyclopentane derivatives

1.4 YLIDES

Ylide is a neutral dipolar molecule with a formally negatively charged atom (carbanion) directly connected to the positively charged heteroatoms (Nitrogen, phosphorus, and sulfur), in which both atoms have full octets of electrons (Figure 1.10).[81]

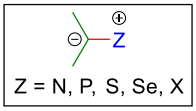

Figure 1.10 General representation of ylides

Ylides are 1,2-dipolar compounds belonging to a subgroup of zwitterions that can act as a reactive intermediate in organic chemistry. Ylides are classified into three types: Nitrogen,[82] phosphorus,[83] and sulfur ylides.[84] Although arsenic, selenium, and halogens ylides are known in the literature. The phosphorus and sulfur ylides have two conical forms, but nitrogen has only one conical form (Figure 1.11).

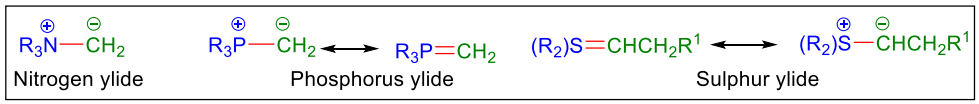

Figure 1.11 Representation of nitrogen, phosphorus, and sulfur ylides

Phosphorus ylide (phosphorane), known as the Wittig reagent, has an essential class of reactive intermediates in organic chemistry. It can be used to synthesize various functionally diverse alkenes and isometric forms of alkenes such as *E*-alkene and *Z*-alkenes from aldehydes and ketones.[85] Sulfur ylides are another important class of reactive intermediates, which are mainly classified into dimethylulfonium methylides and dimethylsulfoxinium methylides. Depending on their stability, they have been widely used in various applications of organic synthesis including epoxidation, cyclopropanation, sigmatropic rearrangements, homologation, ring expansion, and ring contraction reactions. For instance, sulfonyl ylides can be used to synthesize *E* and *Z*-alkenes *via* Julia olefination.[86]

Nitrogen ylides, also known as azomethine ylides or nitrilimines,[82] are fascinating versatile intermediates in organic synthesis. These ylides have nitrogen atom with a positive charge close to a carbanion, rendering them highly reactive species. Nitrogen ylides are known to synthesize functionalized trisubstituted nitrogen-containing

compounds from respective quandary ammonium salts through Sommelet-Hauser[87] and Stevens rearrangement.[88] Generally, phosphorus and sulfur ylides are 1,2-dipolar, but these nitrogen ylides exist in both 1,2-and 1,3-dipolar forms. The 1,2-dipolar nature is called simple nitrogen ylides, and the 1,3-dipolar nature is called "*Azomethine ylides.*"[89]

One of the most notable applications of nitrogen ylides is known for the synthesis of heterocycles, particularly pyrrolidines using 1,3-dipolar cycloaddition (Huisgen cycloaddition). This reaction offers an effective method for the development of complex molecular scaffolds. Nitrogen ylides have attracted in asymmetric synthesis, which enables the generation of chiral compounds with high stereoselectivity. Their utility extends to the production of natural products and physiologically active chemicals. Despite their synthetic value, the handling, and stability of nitrogen ylides pose issues due to their tendency for decomposition and sensitivity to reaction circumstances.

1.4.1 Cycloaddition

Cycloaddition is a key reaction in organic chemistry, where two or more unsaturated molecules join to generate cyclic compounds. These reactions are characterized by their regioselectivity and stereoselectivity, making them a powerful tool for building complex chemical frameworks. The most prevalent types of cycloadditions are [4+2], [2+2], and [3+2] based on the number of participating atoms in the reactants. The [4+2] cycloadditions, known as Diels-Alder reactions, are among the most widely investigated and exploited in organic synthesis due to their diversity and efficiency. In the Diels-Alder reaction, a conjugated diene (conjugate alkene) combines with a dienophile (a double-bond molecule) to generate a six-membered ring. This reaction is

found to have significant use in the synthesis of natural compounds, medicines, and materials.[90]

Other prominent cycloaddition reactions include the Huisgen cycloaddition or 1,3-dipolar cycloaddition,[91] which consists of the reaction between dipolarophile and 1,3-dipole. This [3+2] cycloaddition reaction finally produces heterocyclic frameworks. Orbital symmetry based on cycloaddition reactions, and their methods generally involve the production of cyclic transition states. These responses have been intensively investigated and refined over the years, leading to the development of novel approaches and applications. Due to their synthetic value, handling, and stability of nitrogen ylides pose issues owing to their tendency for decomposition and sensitivity to reaction circumstances. However, their unusual reactivity continues to drive research in organic chemistry.

1.4.2 1,3-Dipolar Cycloaddition

In the 1960s, Rolf Huisgen introduced 1,3-dipolar cycloaddition or Huisgen cycloaddition, which is an essential reaction in organic chemistry wherein a 1,3-dipole 4π system (such as an azide or a nitrile oxide) combines with a dipolarophile 2π systems (typically an alkene or alkyne) to generate a five-membered heterocycle. Huisgen classified the 1,3-dipolar systems into bent type (allyl anion type) and linear type (propargyl allenyl type), as shown in Figure 1.12. The Huisgen cycloaddition offers various advantages, including regioselectivity and efficiently forming complex molecular structures. It is broadly used in medical chemistry, material science, and natural product synthesis.

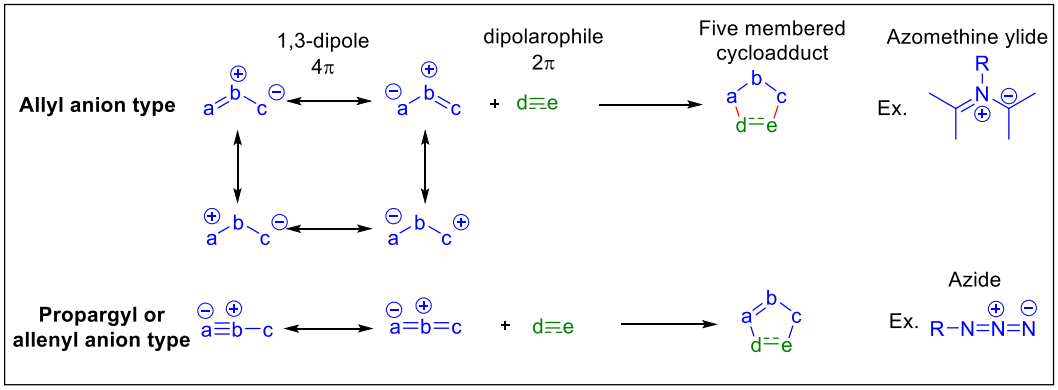

Figure 1.12 General representation of 1,3-dipole and dipolarophile

The mechanism of 1,3-dipolar cycloaddition involves the concerted or stepwise (radical and ionic intermediates) creation of two new bonds, resulting in the stereospecific construction of the heterocyclic rings. The regioselectivity of the reaction can be determined by the frontier molecular orbitals of the dipole and dipolarophile, as well as steric considerations. Notable examples of 1,3-dipolar cycloaddition reactions include the synthesis of triazoles from azides and alkynes and the production of isoxazoles from nitrile oxides and alkenes. Many types of allyl anion and propargyl anion types 1,3-dipolar systems are widely explored in the literature, as shown in Figure 1.13.

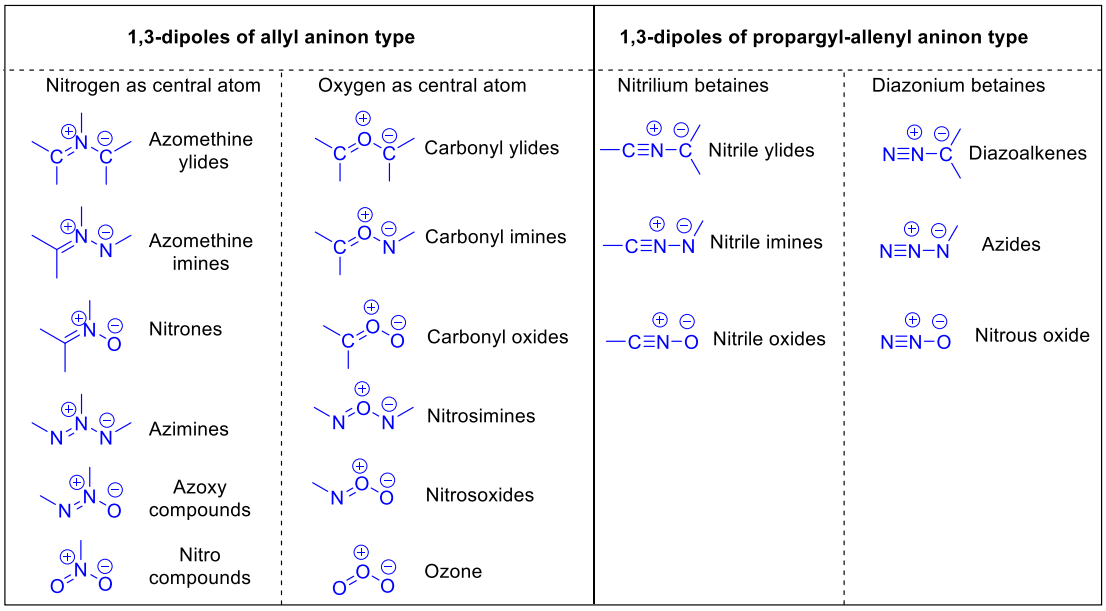

Figure 1.13 Classification of 1,3-dipolar systems

One of the important allyl anion types of the 1,3-dipolar system is "***azomethine ylides,***" widely used in 1,3-dipolar cycloaddition with dipolarophiles to synthesize nitrogen-containing heterocyclic compounds, especially highly substituted pyrrolidine heterocycles. These reactions have been widely explored, leading to new approaches and applications in organic synthesis.[92]

1.5 AZOMETHINE YLIDES

Azomethine ylides are nitrogen-based 1,3-dipoles and consist of three atoms, an iminium ion next to a carbanion. They can easily form five-membered heterocycles, such as pyrrolidines and pyrrolines, exceedingly stereo- and regioselective processes could develop to form four new contiguous stereocenters *via* 1,3-dipolar cycloaddition reactions (Figure 1.15).[93]

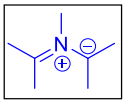

Figure 1.14 General representation of azomethine ylide

Thus, Azomethine ylides are a valuable component in broad synthesis, developing chiral ligands, and manufacturing pharmaceuticals. Azomethine ylides can be produced from simple precursor compounds like aziridines,[94] imines,[95] and iminiums.[96]

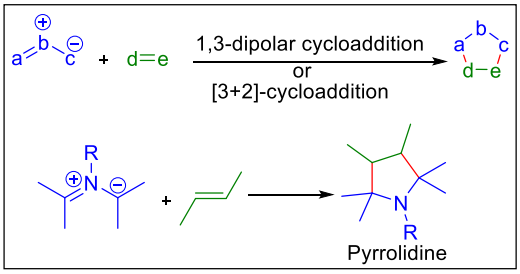

Figure 1.15 General representation of azomethine ylides for 1,3-dipolar cycloaddition

They are typically made by *in-situ* formation in the reaction medium and react right away with dipolarophile. Four electrons are dispersed throughout the three-atom C–N–C unit in azomethine ylides, which are known as 1,3-dipoles of the allyl anion type. Four zwitterionic resonance forms can be employed to explain them (Figure 1.16). The most frequent representation of allyl anion character, the two octets configuration, shows a negative charge dispersed between the two carbon atoms, a positive nitrogen atom, and an iminium center.[97]

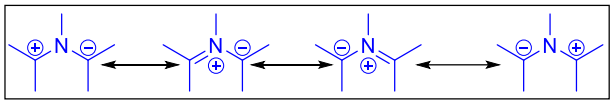

Figure 1.16 Canonical structure of azomethine ylides

According to Woodward–Hoffmann rule,[91,98] the 1,3-dipolar cycloaddition of azomethine ylides with a dipolarophile consists of six electrons [4πs+2πs] and occurs in a thermally viable superficial process. Although such cycloadditions are concerned with both carbon-carbon bonds forming simultaneously, the presence of singlet diradical or zwitterionic intermediates has also been questioned. The concerted process, however, is strongly supported by the stereospecificity of the cycloadditions, in which the relative stereochemistry of the alkene dipolarophile is conserved in the pyrrolidine product. The geometry of the dipoles and the dipolarophiles impacts the stereochemical outcome of the cycloaddition of azomethine ylides.

1.5.1 Classification of Azomethine Ylides

Azomethine ylides are mainly classified into three types depending on the electronic characteristics. i) Non-metallated stabilized ylides, ii) *N*-metallated stabilized ylides, iii) non-stabilized ylides.

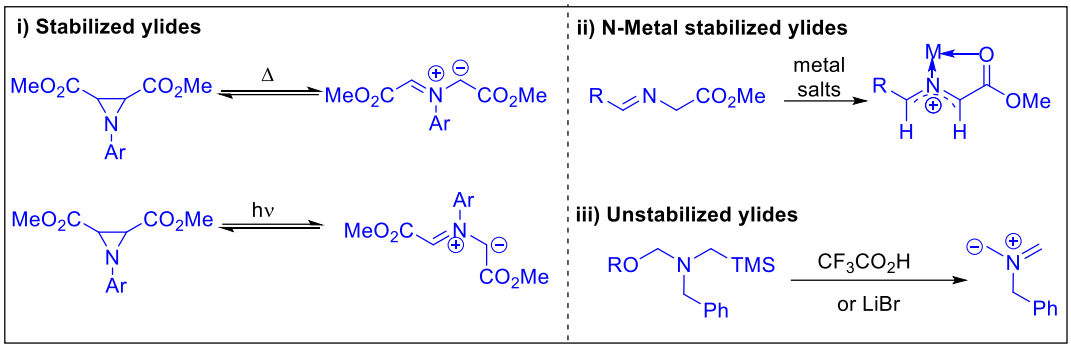

Figure 1.17 Classification of azomethine ylides based on stability.

Stereospecific ring-opening of aziridine under photochemical or thermal conditions can be easily obtained from the stabilized azomethine ylides. In photochemical conditions, it undergoes disrotatory, providing the trans-stabilized azomethine ylides, whereas in thermal conditions, it gives cis-stabilized ylides *via* conrotatory (Figure 1.17-i). The *N*-metal stabilized azomethine ylides can be synthesized from imine when treated with amine/metal salts or alkaline metal salts. This undergoes stabilization *via* nitrogen lone pair or adjacent electron-withdrawing carbonyl oxygen lone pair *in-situ* to produce *N*-metallated azomethine ylides (Figure 1.17-ii). The non-stabilized azomethine ylides can be easily produced from the leaving group comprising trisubstituted amine when treated with acidic condition or Lewis acid condition elimination of leaving group *via in-situ* generation of non-stabilized azomethine ylides (Figure 1.17-iii).

1.5.2 Reactivity of Azomethine Ylides

Azomethine ylides give a concerted process, which is strongly supported by the stereospecificity of the cycloadditions, in which the relative stereochemistry of the alkene dipolarophile is conserved in the pyrrolidine product. The geometry of the dipoles and the dipolarophiles impacts the stereochemical outcome of the cycloaddition of azomethine ylides (Figure 1.18).[97]

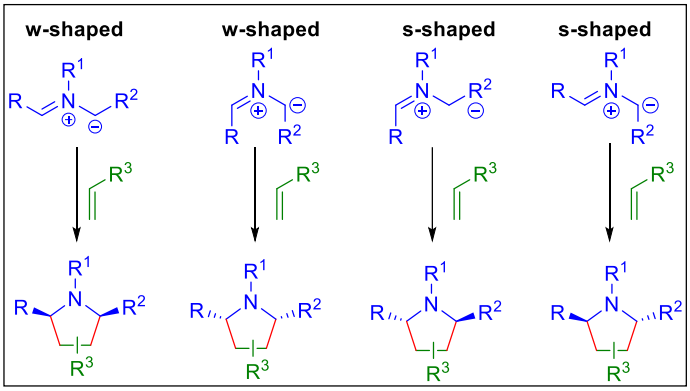

Figure 1.18 Reactivity of azomethine ylides

1.5.3 Synthetic Route for Azomethine Ylides

Azomethine ylides can be synthesized *in-situ* in the reaction medium by several routes, as shown in Figure 1.19.

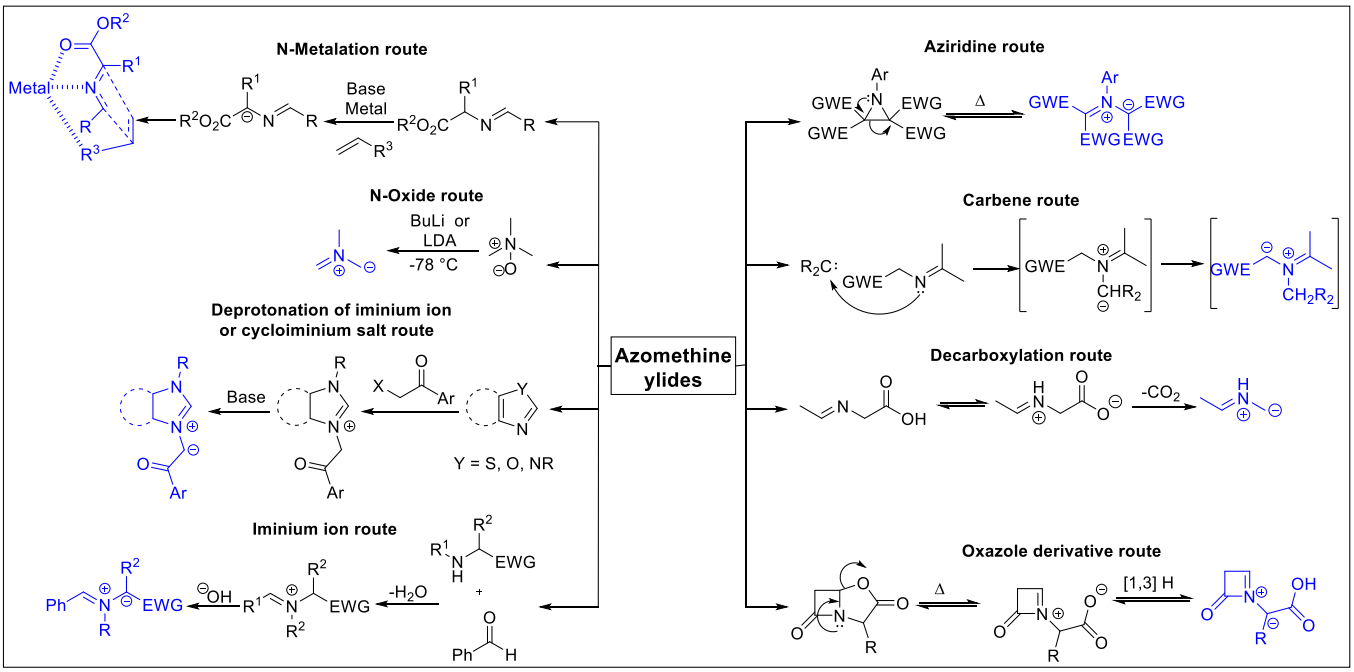

Figure 1.19 Synthetic routes for azomethine ylides

Various synthetic routes of aziridine ring-opening were discussed in Figure 1.17-i, they are the carbene insertion route, decarboxylation route, oxazole derived route, iminium ion route, deprotonation of cycloiminium salt route, *N*-oxide route, and *N*-metalation route. All routes of azomethine ylide (1,3-dipolar system) with dipolarophile majorly produce pyrrolidine or highly substituted pyrrolidine. Only a few of the azomethine

ylides have been used to synthesize other than pyrrolidine heterocyclic products. For example, one of the azomethine ylide precursors is cycloiminium salt, which has an entirely different reactivity compared to all other azomethine ylides, which can be used to synthesize diverse heterocyclic frameworks.[98]

1.5.4 Cycloiminium Salt

Cycloiminium salts are a class of azomethine ylide precursors which can be synthesized i*n-situ* by base-promoted deprotonation. They can be easily synthesized from readily available starting materials like *N*-heterocyclic compounds and react with 2-halo substituted electron withdrawing group compounds *via* S_N2 displacement (Figure 1.20).[99]

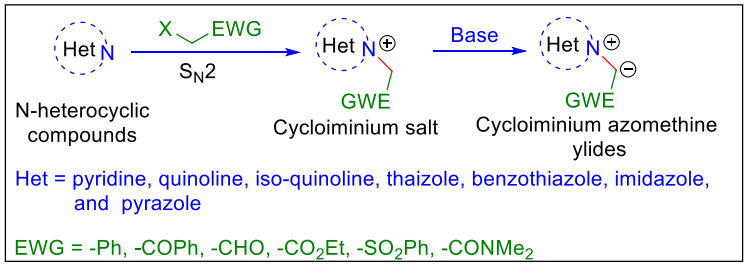

Figure 1.20 General method for the synthesis of cycloiminium salts

1.5.5 Types of Cycloiminium Salt

Different types of cycloiminium salt are reported in the literature, such as thiazolium salt,[100] benzothiazolium salt,[101] pyridinium salt,[102] quinolium salt,[103] iso-quinolium salt,[104] and azomethine imine salt,[105] All can be easily synthesized from corresponding heterocyclic compounds with halogen derivatives, as shown in Figure 1.21.

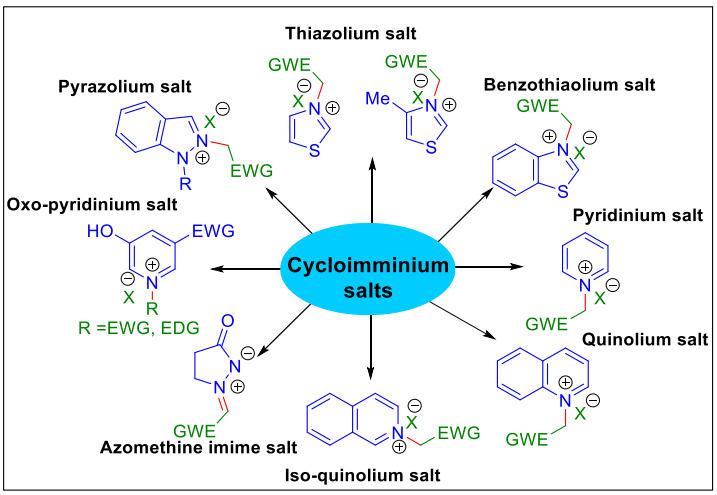

Figure 1.21 Types of cycloiminium salts

1.5.6 Applications of Cycloiminium Salt

Cycloiminium salt of azomethine ylides has been widely used and prevalent to synthesize various heterocyclic compounds *via* 1,3-dipolar- or [3+2]-cycloaddition with various dipolarophiles.

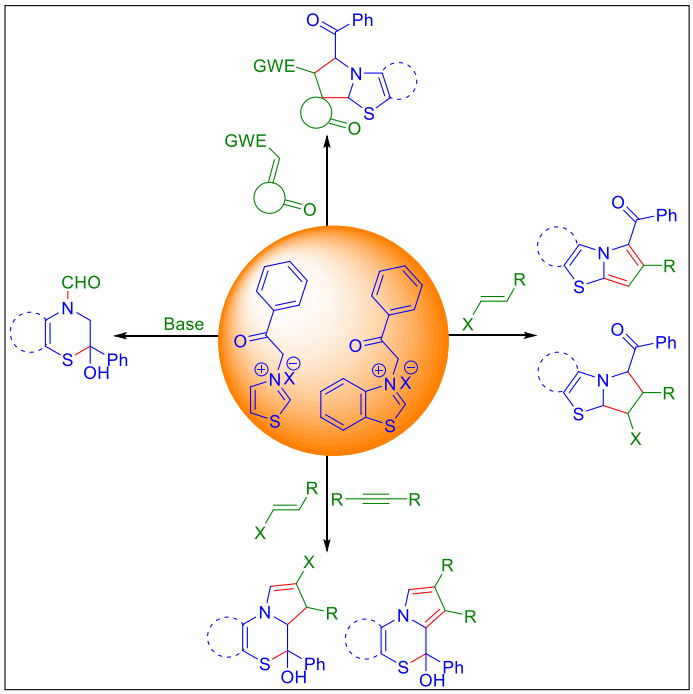

Figure 1.22 Unusual reactivity of thiazolium and benzothiazolium salts

To compare the reactivity and selectivity of thiazolium and benzothiazolium azomethine ylide, it is found that they are entirely different from other cycloiminium

salts. First, it undergoes the usual 1,3-dipolar or [3+2] cycloaddition with various dipholophiles to provide the cycloadduct or spiro cycloadduct and followed by ring opening and/or rearranged to give exclusively new products (Figure 1.22).[106-109]

1.5.7 Thiazolium and Benzothiazolium Salt

The five-membered thiazolium and benzothiazolium cycloiminium salt of azomethine ylides have been known to the synthetic community for many decades. These can be easily synthesized by treating electron withdrawing group attached α-alkyl halides in ethanol under reflux conditions, followed by base at room temperature (Scheme 1.25).[110]

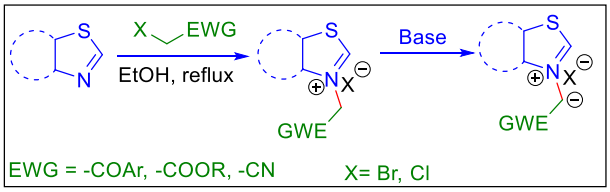

Scheme 1.25. General preparation of thiazolium/benzothiazolium salts

Thiazolium and benzothiazolium ylides have been used to synthesize multiple chiral centers containing functionalized hydro pyrrolo[1,2]thiazine, hydro benzopyrrolo[1,4]thiazine and its polyhydro derivatives *via* diastereoselective manner. They are essential privileged *N, S*-containing heterocyclic cores in many bioactive and pharmacological reagents.[111] Because of this unique and unusual reactivity of thiazolium and benzothiazolium azomethine ylides, it has been used for the synthesis of other than pyrrolidine heterocyclic compounds. Thiazolium salt has more exciting properties such as *in-situ* carbon-sulfur bond cleavage in the presence of an electron-withdrawing group near a sulphur-carbon atom. Then, it undergoes 1,2-addition to the adjacent π-system, eventually generating the rearrangement product of 1,4-thiazine derivatives in the presence of a base.[108] In the presence or absence of an oxidizing agent,

thiazolium and benzothiazolium cycloadduct undergo oxidative aromatization, provided the pyrrolo-thiazine or benzo pyrrolo-thiazines.[112]

1.5.8 Applications of Thiazolium and Benzothiazolium Azomethine Ylides in 1,3-Dipolar Cycloaddition Reactions

In 1985, Otohiko and co-workers reported a 1,3-dipolar cycloaddition of thiazolium azomethine ylide with maleimide in the presence of NEt_3 at room temperature. The reaction afforded the stereospecific endo cycloadduct product in excellent yield (Scheme 1.26).[113]

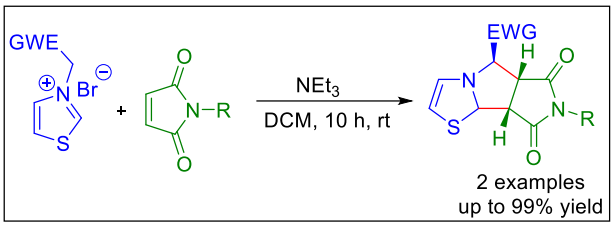

Scheme 1.26 1,3-Dipolar cycloaddition of thiazolium salt for the synthesis of pyrrolo[2,1-*b*][1,3]thiazoles

In 1996, Iwamura *et al.* developed a 1,3-dipolar cycloaddition reaction/rearrangement sequence involving thiazolium cycloiminium azomethine ylide, DMAD as a dipolarophile and NEt_3 base in dry DMF at room temperature. The reaction yielded racemic pyrrole-thiazine derivatives in good yields (Scheme 1.27).[108]

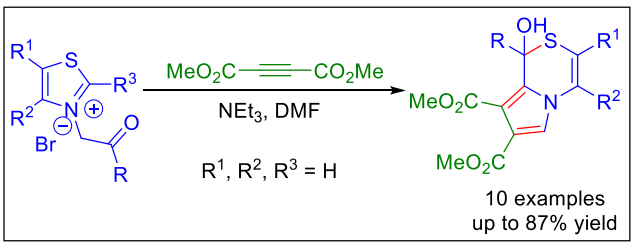

Scheme 1.27 1,3-Dipolar cycloaddition of thiazolium salt for the synthesis of pyrrolo-thiazines

The synthesis of 2-hydroxy-alkyl/aryl-4-formyl-2,3-dihydro-1,4-thiazines has been achieved by Harji Singh *et al*. in 1992, from 4-methyl thiazolium salt treated with 2%-

8% aq. NaOH solution. The reaction undergoes intermolecular ring-opening followed by intramolecular 1,2-addition delivering the ring-expanded product in good yields (Scheme 1.28).[106]

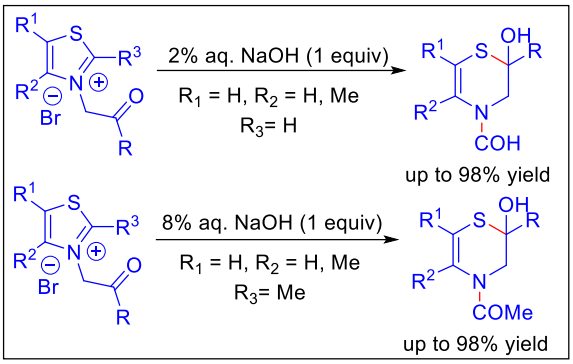

Scheme 1.28 Nucleophile addition/ring-opening of thiazolium salt for the synthesis of formyl-2,3-dihydro-1,4-thiazines

In 2007, Craig and co-workers accomplished a synthesis of pyrrolo[2,1-*b*]thiazoles from the C-2 methane thiol group containing thiazole, acetylene derivatives, and methyl triflate *via in-situ* formation of thiazolium salt, further involved in [3+2] cycloaddition. The reaction furnished the pyrrorlo[2,1-b]thiazole as a product in good yields by elimination of methanethiol (Scheme 1.29)[114]

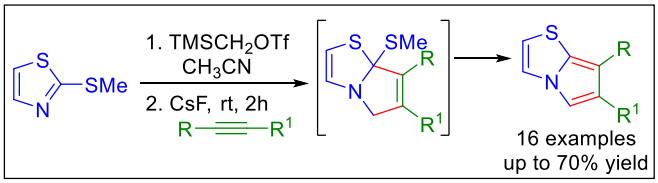

Scheme 1.29 Thiazolium salt [3+2] reaction for the synthesis of pyrrolo[2,1-*b*]thiazoles

An easy method for creating [5,5]-annulated *N*-fused heterocycles, specifically pyrrolo[2,1-*b*]thiazoles, using oxidative [3+2] reactions has been achieved in 2023 by Vladimir *et al*. The process involves the annulation of nitroalkenes and thiazolium ylides in the presence of Cu(II) to produce desired *N*-fused heterocycles with moderate to high yields (Scheme 1.30).[115]

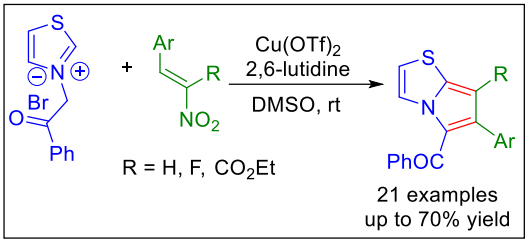

Scheme 1.30 [3+2] Cycloaddition of thiazolium salt for the synthesis of pyrrolo[2,1-*b*]thiazoles

In 2008, Jose *et al*. accomplished the synthesis of polyfunctionalized pyrrolo[2,1-*b*][1,3]thiazoles in moderate yields, with high regio- and stereoselective manner *via* 1,3-dipolar cycloaddition of thiazolium azomethine ylides with enantiopure acyclic and cyclic vinyl sulfoxides (Scheme 1.31).[116]

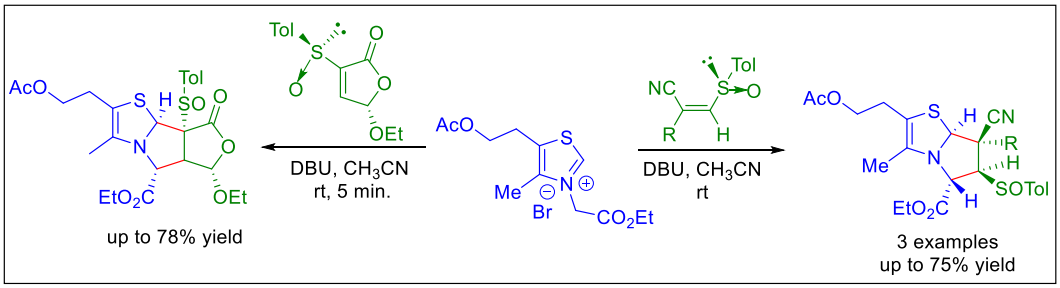

Scheme 1.31 1,3-Dipolar cycloaddition of thiazolium salt for the synthesis of pyrrolo[2,1-*b*][1,3]thiazoles

Otohiko *et al.* in 1985 achieved a 1,3-dipolar cycloaddition with dipolarophile in the presence of NEt_3 at room temperature, and it furnished the stereospecific endo cycloadduct product in excellent yields (Scheme 1.32).[113]

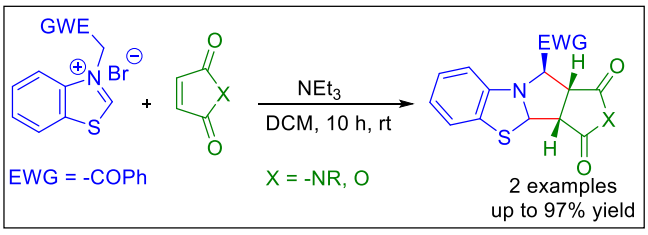

Scheme 1.32 1,3-Dipolar cycloaddition of benzothiazolium salt for the synthesis of benzopyrrolo[2,1-*b*][1,3]thiazoles

Tsuge and co-workers described the synthesis of diverse tetrahydropyrrolo-thiazole derivatives in the year 1981 *via* a 1,3-dipolar cycloaddition of benzothiazolium azomethine ylides with a wide range of methylenecyclopropane dipolarophiles in dry THF and NEt_3 as a base at 0°C to room temperature. When cyclohexane diketone containing cyclopropene dipolarophile was subjected to the same reaction condition, it yielded two distinct products such as ring-cleavages and condensation products, respectively (Scheme 1.33).[117]

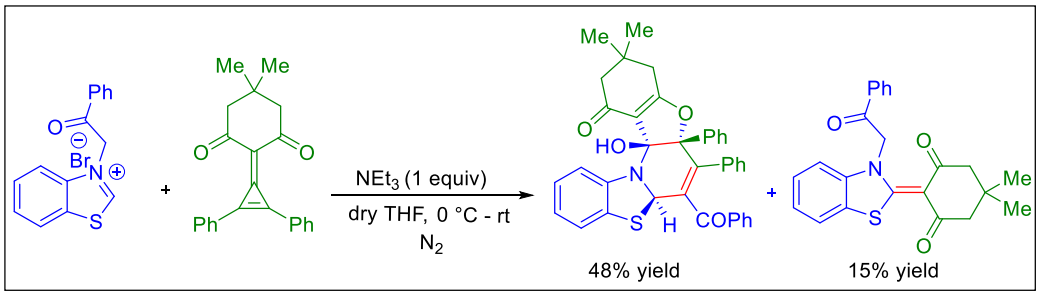

Scheme 1.33 1,3-Dipolar cycloaddition of benzothiazolium salt for the synthesis of benzopyrrolo[2,1-*b*][1,3]thiazoles

The synthesis of benzo[*d*]pyrrolo[2,1-*b*]thiazoles was achieved by the same group in 2017 *via* a 1,3-dipolar cycloaddition reaction of *N*-phenacylbenzothiazolium bromides with nitroalkenes in the presence of DDQ under reflux, resulting the products in excellent yields (Scheme 1.34).[112]

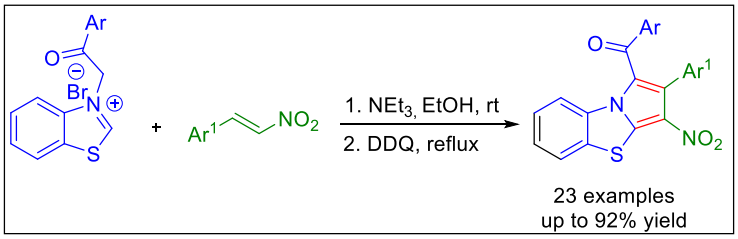

Scheme 1.34 1,3-Dipolar cycloaddition for the synthesis of benzo[*d*] pyrrolo[2,1-*b*]thiazoles

In 2017, Shen and co-workers accomplished a domino cycloaddition reaction involving benzothiazolium azomethine ylides and 3-phenacylideneoxindoles in the presence of NEt_3 in ethanol at room temperature. The reaction furnished the functionalized

spiro[benzo[*d*]pyrrolo[2,1-*b*]thiazole-3,3'-indolines] in high yields with excellent diastereoselectivity (Scheme 1.35).

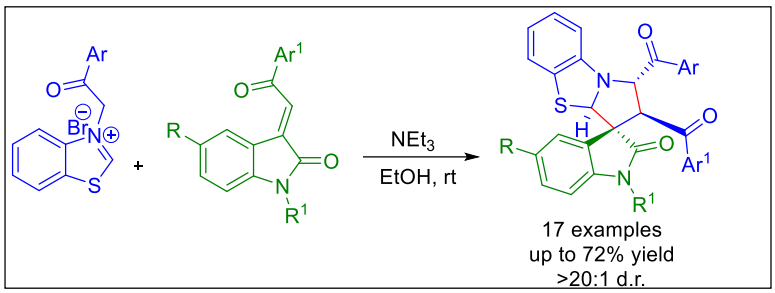

Scheme 1.35 1,3-Dipolar cycloaddition for the synthesis of spiro[benzo[*d*]pyrrolo[2,1-*b*]thiazole-3,3'-indolines]

Similarly, they also described a similar reaction using *N*-phenacylthiazolium bromides with ethyl 2-(2-oxoindolin-3-ylidene) acetates under identical reaction conditions. The reaction provided corresponding functionalized spiro[benzo[*d*]pyrrolo[2,1-b]thiazole-3,3'-indolines] in moderate yields and diastereoselectivity (Scheme 1.36).[118]

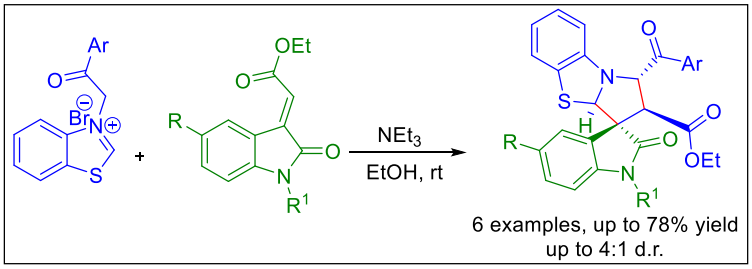

Scheme 1.36 1,3-Dipolar cycloaddition for the synthesis of spiro[benzo[*d*]pyrrolo[2,1-*b*]thiazole-3,3'-indolines] derivatives

A two-step reaction was performed by the same group in 2017, using the ylide and nitrochromenes under NEt_3/EtOH/rt condition, and the reaction provided tetrahydrobenzo[*d*]chromeno[3',4':3,4]pyrrolo[2,1-*b*]thiazoles. Subsequently, the addition of DDQ under reflux conditions facilitated the elimination of the nitro group and yielded the corresponding dehydrogenated benzo[d]chromeno[3',4':3,4]pyrrolo[2,1-b]thiazoles with excellent yields (Scheme 1.37).[119]

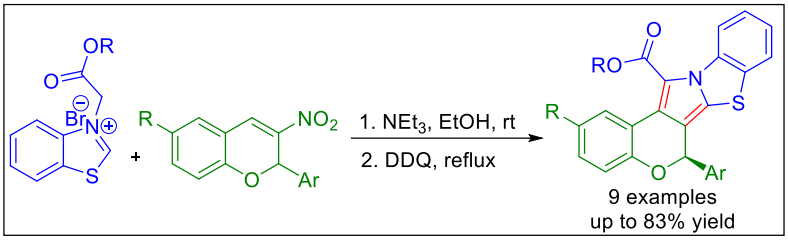

Scheme 1.37 1,3-Dipolar cycloaddition for the synthesis of benzo[*d*]chromeno[3',4':3,4]pyrrolo[2,1-*b*]thiazoles

1.6 ASYMMETRIC TRANSFORMATIONS OF AZOMETHINE YLIDES

The azomethine ylides are versatile intermediates in the synthesis of optically active compounds. They have been used in 1,3-dipolar cycloaddition with dipolarophiles to give multi-substituted chiral frameworks. The enantioselective transformation of acyclic imine azomethine ylides is a powerful tool in the asymmetric synthesis of chiral pyrrolidines. Apart from chiral pyrrolidine heterocyclic frameworks, there are many azomethine ylides have been used to synthesize other heterocyclic frameworks in an enantio- and diastereoselective manner. This enantioselective transformation can be used in various chiral catalytic systems such as chiral organocatalysts (hydrogen-bonding, phase transfer catalysts, chiral NHC, and chiral amine catalyst) and chiral metal complex catalysts (Ag, Au, Cu, Sc, Mg, Zn, Ni, etc.,).[120, 121]

1.6.1 Enantioselective Transformations of Azomethine Ylides

In 2015, Tapas *et al.* demonstrated an enantioselective desymmetrization of prochiral cyclopentene-1,3-dione using silver(I)-ferrophox complex *via* [3+2] cycloaddition of azomethine ylide which afforded the highly functionalized enantioenriched 5,5-fused bicyclic pyrrolidine derivatives in good yield with excellent enantio- and diastereoselectivity (Scheme 1.38).[122]

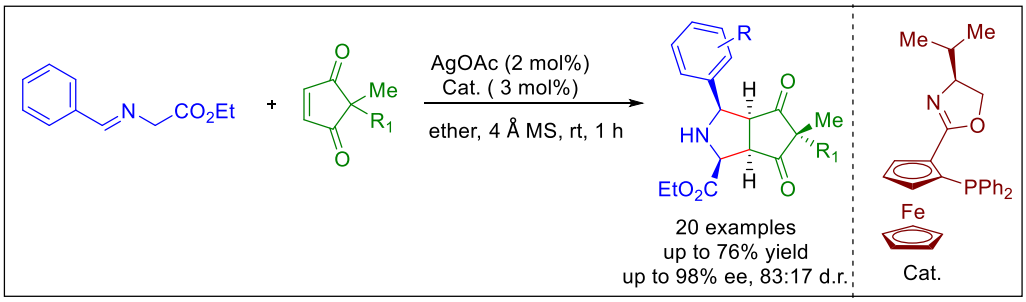

Scheme 1.38 Enantioselective desymmetrization for the synthesis of 5,5'-fused bicyclic pyrrolidine

The organocatalytic synthesis of spiro[pyrrolidine-3,3'-oxindoles] was developed by Xiao and co-workers in 2009, *via* a three-component, 1,3-dipolar cycloaddition of a broad range of methyleneindolinone with aldehydes, and amine ester in the presence of chiral phosphoric acid provided spirooxindoles in high yield with excellent enantio- and diastereoselectivity under mild condition (Scheme 1.39).[123]

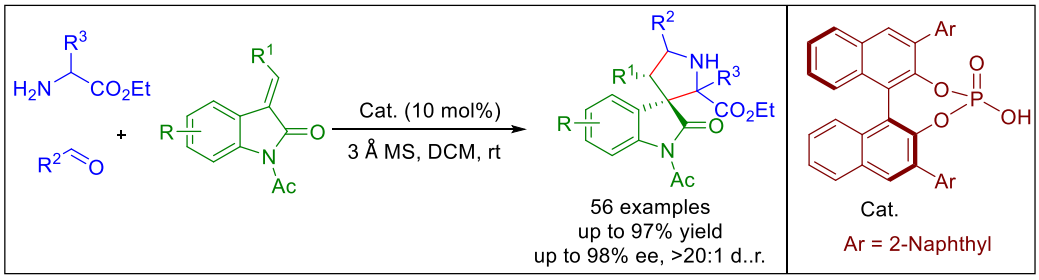

Scheme 1.39 Three-component, 1,3-dipolar cycloaddition for the synthesis of spiro oxindole

In 2009, Andrey *et al.* reported a highly enantioselective synthesis of natural-product inspired 3,3'-pyrrolidine spiro-oxindoles, which contains all-carbon quaternary center and three tertiary stereocentres using a cooperative catalyst with *N, P*-ferrocenyl chiral ligand *via* a 1,3-dipolar cycloaddition of azomethine ylides. The reaction afforded substituted 3-methylene-2-oxindoles in high yields with excellent enantio- and diastereoselectivity (Scheme 1.40).[124]

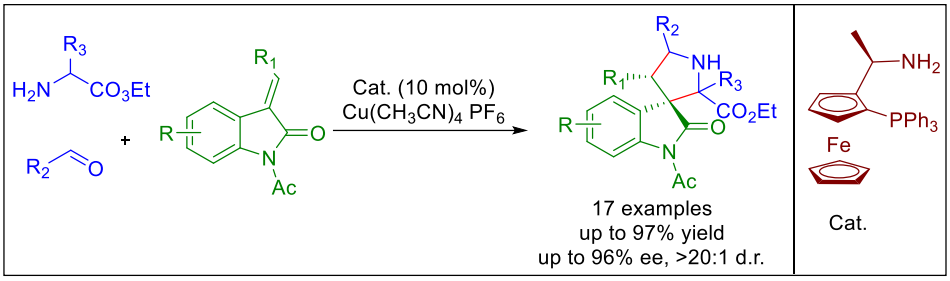

Scheme 1.40 Enantioselective 1,3-dipolar cycloaddition for the synthesis of substituted 3-methylene-2-oxindoles

A catalytic asymmetric double 1,3-dipolar cycloaddition reaction using a chiral silver complex was developed in 2013 by Andrew *et al.* The enantioenriched highly substituted pyrrolizidines with six stereogenic centers were achieved from inexpensive and commercially available starting materials with good yields and high stereoselectivity (Scheme 1.41).[125]

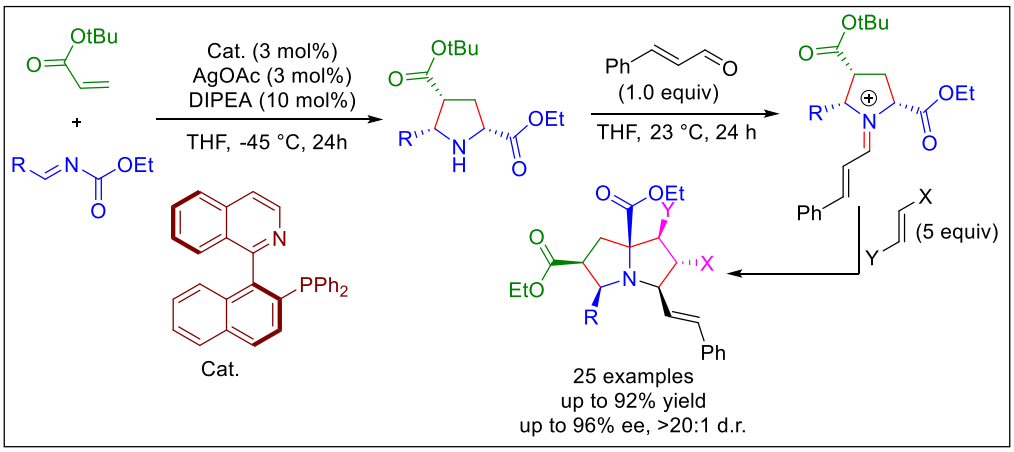

Scheme 1.41 Asymmetric double 1,3-dipolar cycloaddition for the synthesis of highly substituted pyrrolizidines

The biology-oriented synthesis of (BIOS) novel iridoids (cyclopentano[*c*]pyran monoterpenes) was accomplished by Hiroshi and co-workers, in 2013. The design and development of novel iridoid-inspired compound *via* [3+2] cycloaddition of azomethine ylides with racemic 2*H*-pyran-3(6*H*)-ones in good yields with excellent enantio- and diastereoselectivity. This chiral product is used as an inhibitor for Wnt and Hedgehog signaling pathways (Scheme 1.42).[126]

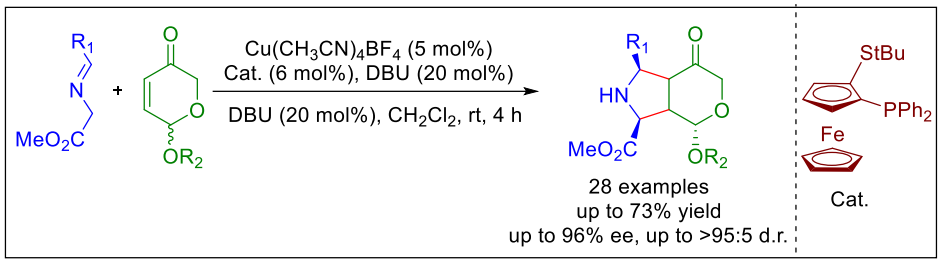

Scheme 1.42 Asymmetric [3+2] cycloaddition for the synthesis of iridoids (cyclopentano[*c*]pyran monoterpenes)

Later, Rishikesh and co-workers 2013 developed a natural product inspired by tropanes 8-azabicyclo[3,2,1]octane *via* a catalytic 1,3-dipolar cycloaddition of 1,3-fused azomethine ylides and nitroolefin. The reaction produced tropane scaffolds with four stereocenters in a single step in good yields and a stereocontrolled manner (Scheme 1.43).[127]

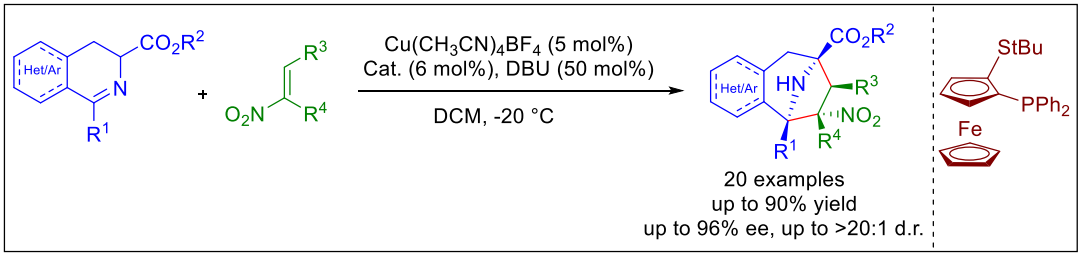

Scheme 1.43 Asymmetric 1,3-dipolar cycloaddition for the synthesis of tropanes 8-azabicyclo[3,2,1]octane

In 2013, Kang *et al.* reported the unprecedented silver(I) catalyzed asymmetric desymmetrization of spiro-cycohexadienone lactones having five contagious stereocenters with one spiro quaternary stereogenic center *via* a 1,3-dipolar cycloaddition of azomethine ylide with cycohexadienone. The reaction provided the optically active spirolactone-pyrrolidines with high yields with excellent enantio- and diastereoselectivity (Scheme 1.44).[128]

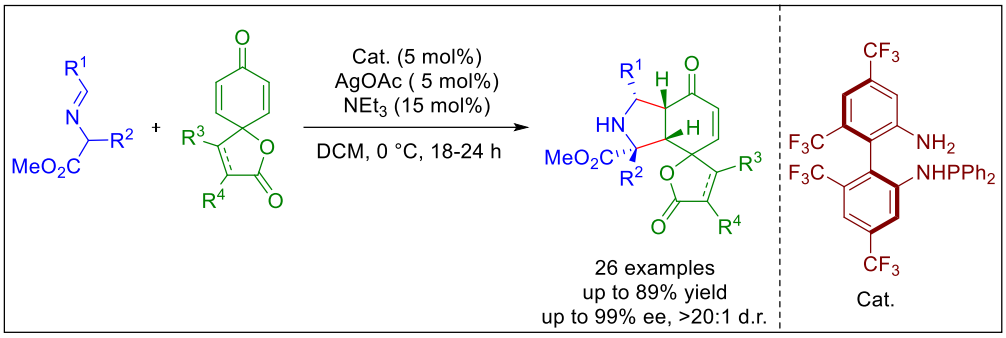

Scheme 1.44 Asymmetric desymmetrization reaction for the synthesis of spironolactone-pyrrolidines

Nickel(II)-catalyzed asymmetric 1,3-dipolar cycloaddition of azomethine betaines with alkylidene malonates using *N,N*-dioxide chiral ligand for the synthesis of numerous trans pyrazolone derivatives with high yield with excellent enantio- and diastereoselectivity was demonstrated by Jiangting *et al.* in 2013 (Scheme 1.45).[129]

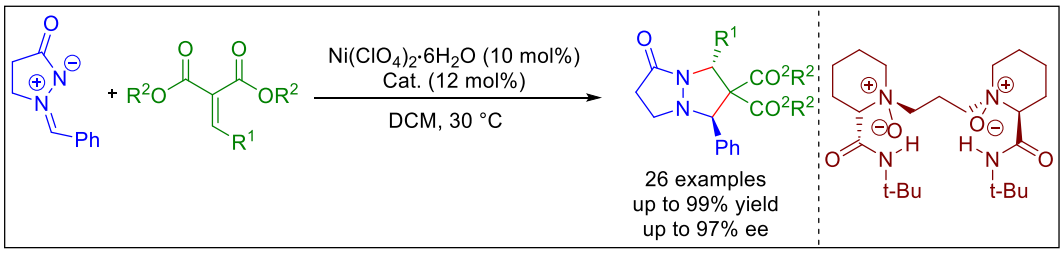

Scheme 1.45 Asymmetric 1,3-dipolar cycloaddition reaction for the synthesis of pyrazolone derivatives

In 2011, Takuya *et al.* developed an asymmetric inverse-electron-demand 1,3-dipolar cycloaddition of C,N-cyclic azomethine imines as a dipolar system with vinyl ether electron-rich dipolarophile utilizing an axially chiral dicarboxylic acid containing chiral Brønsted acid catalyst. They have successfully achieved the C1-chiral tetrahydroisoquinolines with high yields and excellent enantioselectivity (Scheme 1.46).[130]

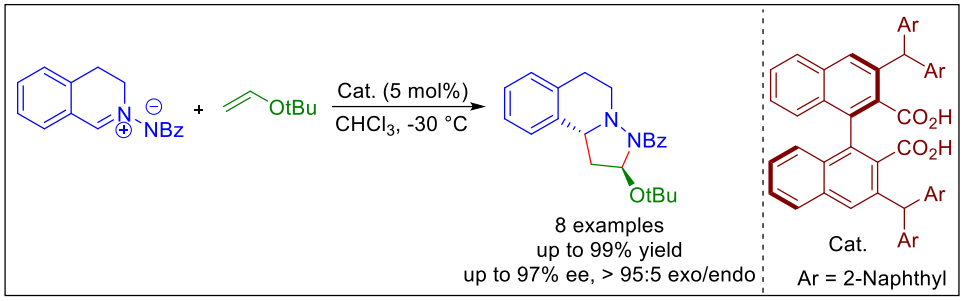

Scheme 1.46 Asymmetric inverse-electron-demand 1,3-dipolar cycloaddition for the synthesis of C1-chiral tetrahydroisoquinolines

The reactions between benzothiazolium salt azomethine ylides and simple chalcones in the presence of a chiral *N,N′*-dioxide ligand and $Mg(OTf)_2$ to form a chiral metal complex, followed by addition of K_3PO_4 as a base in DCM solvent at room temperature, provided the chiral dihydropyrrolo-thiazole derivatives with excellent yields, good enantio- and diastereoselectivity was reported by Zhang *et al*. in 2018 (Scheme 1.47).[109]

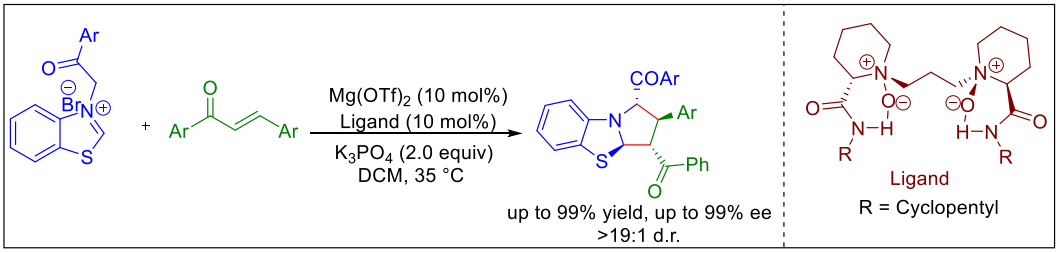

Scheme 1.47 1,3-Dipolar cycloaddition for the synthesis of chiral hydropyrrolo-thiazole derivatives

In 2020, Dong and co-workers developed the diversified transformation of enantio-and diastereoselective [3+2] cycloaddition between pyridinium ylides and enones using chiral *N,N*-dioxide earth metals complexes, which enable *in-situ* generation of optically active key tetrahydroindolizines intermediate. Further, the intermediate involved convenient rearomatic oxidation and light-active aza-Narrish II rearrangement converted into the 3-arylindolizine derivatives and dicarbon-functionalized 1,5-dicarbonyl compounds in high yields with excellent enantio- and diastereoselectivity Scheme (1.48).[131]

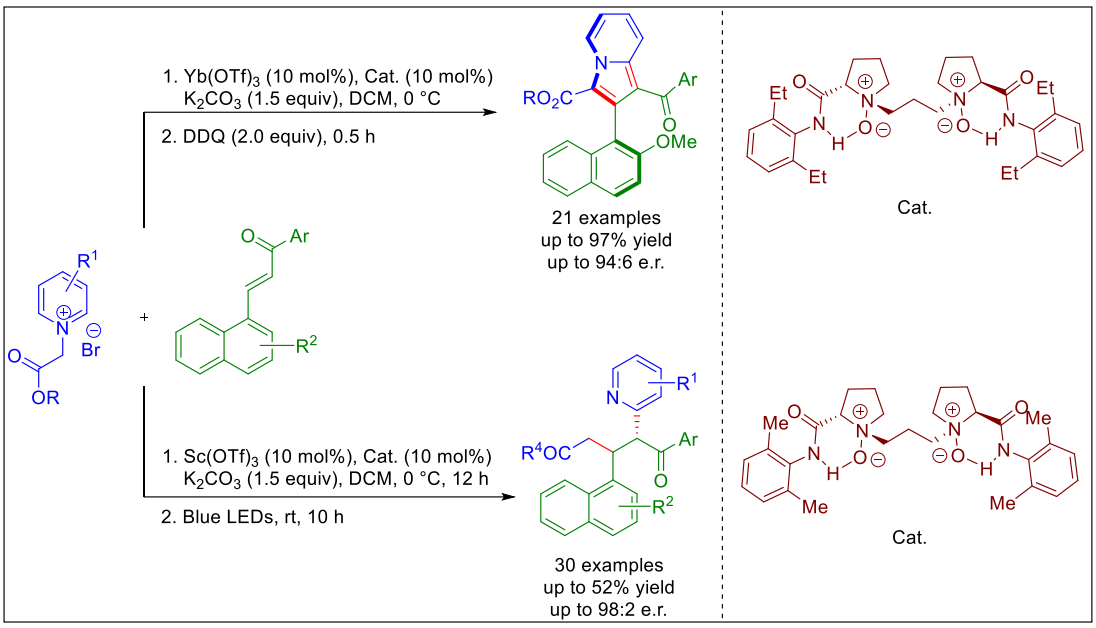

Scheme 1.48 Asymmetric [3+2] cycloaddition of pyridinium azomethine ylide for the synthesis of 3-arylindolizine and dicarbon-functionalized 1,5-dicarbonyls

1.6.2 Chiral Amine Catalyzed Enantioselective Transformations of Azomethine Ylides

In 2007, Ismail *et al.* demonstrated a high chemo-, enantio-, and diastereoselective organocatalytic multi-component [C+NC+CC] coupling process between aldehydes, 2-amino malonates, and α,β-unsaturated aldehydes utilizing a chiral amine catalyst. This protocol furnished the highly functionalized pyrrolidine derivatives in good yields with >10:1 d.r. and up to 98% enantioselectivity (Scheme 1.49).[132]

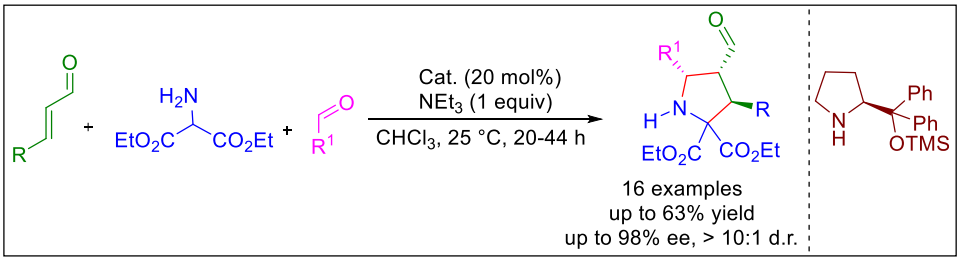

Scheme 1.49 Asymmetric multi-component reaction for the synthesis of pyrrolidines

The enantioselective synthesis of biologically active tropane scaffolds was reported in 2023 by Johannes and co-workers *via* an organocatalyzed 1,3-dipolar cycloaddition of 3-oxidopyridinium betaines with α,β-unsaturated aldehydes using chiral amine as an organocatalyst. This transformation achieved the tropane scaffolds in moderate yield with excellent endo/exo, regio- and enantioselectivity (Scheme 1.50).[133]

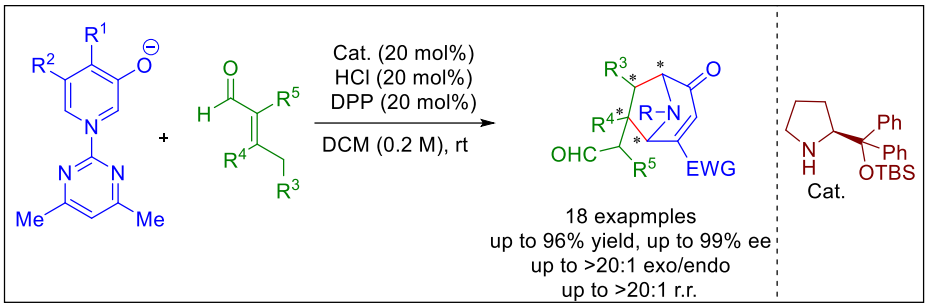

Scheme 1.50 Enantioselective 1,3-dipolar cycloaddition reaction for the synthesis of tropanes

Hiroyuki *et al.* in 2010 accomplished an asymmetric 1,3-dipolar cycloaddition between acrolein and various *N,N'*-cyclic azomethine imines utilizing an *L*-proline catalyst (30 mol%) to synthesize the five-membered pyrazoline cycloadduct product. This reaction only favored the *endo*-cycloadduct product up to 99:1 dr with moderate to good enantioselectivity up to 83% ee (Scheme 1.51).[134]

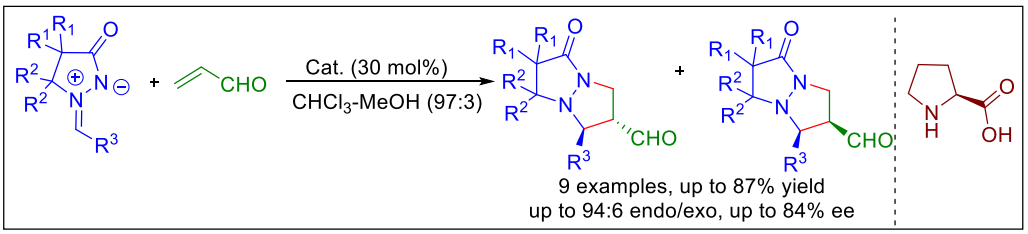

Scheme 1.51 Asymmetric 1,3-dipolar cycloaddition reaction for the synthesis of pyrazoline cycloadduct product

Organocatalytic enantioselective [3+2] cycloaddition of simple imine azomethine ylides with α,β-unsaturated aldehydes to synthesize the densely substituted chiral pyrrolidines as a product with excellent yield, high regio-, enantio- and

diastereoselectivity was reported by Jose and co-workers in 2007. The synthetic utility was exemplified by the synthesis of proline derivatives in which an additional stereogenic center was created in a highly selective manner using sodium borohydride (Scheme 1.52).[135]

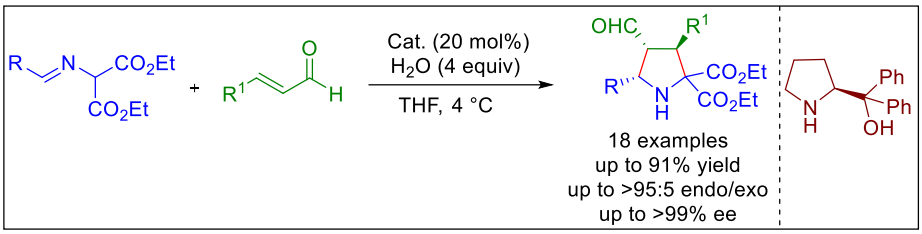

Scheme 1.52 Enantioselective [3+2] cycloaddition reaction for the synthesis of pyrrolidines

Xue and co-workers reported in 2021 synthesis of chiral pyrimido[2,1-*b*]benzothiazoles with excellent yield and excellent enantio- and diastereoselectivity *via* organocatalytic asymmetric [4+2] cycloaddition of 2-benzoyhiazolelimines and α,β-unsaturated aldehydes using a chiral amine as an organocatalyst (Scheme 1.53).[136]

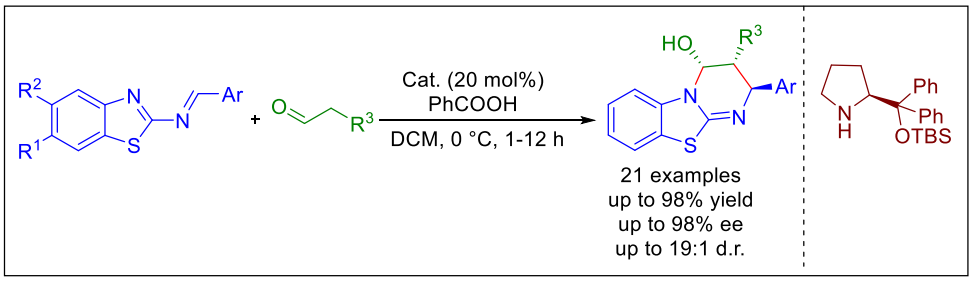

Scheme 1.53 Asymmetric [4+2] cycloaddition reaction for the synthesis of pyrimido[2,1-*b*]benzothiazoles

In 2015, Mingxia *et al.* developed a new strategy for the construction of optically active spiro-[pyrrolidine-3,2'-oxindole] *via* an organocatalytic 1,3-dipolar cycloaddition of ketimines with α,β-unsaturated aldehydes in excellent yields with good enantio- and diastereoselectivity (Scheme 1.54).[137]

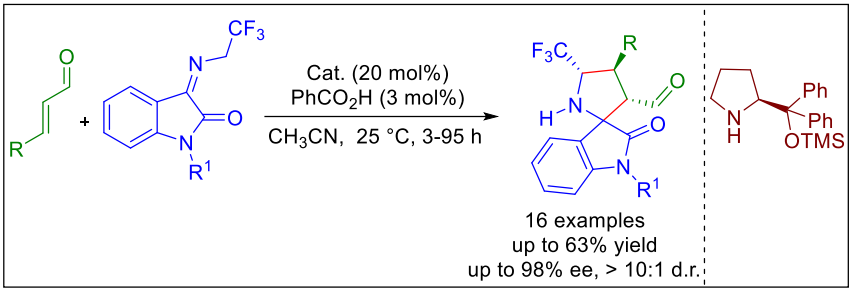

Scheme 1.54 Asymmetric 1,3-dipolar cycloaddition reaction for the synthesis of 5-CF_3 spiro-[pyrrolidine-3,2'-oxindole]

A first [3+2] cycloaddition of nitrones with α,β-unsaturated aldehydes using chiral amine with trimethylsilyl triflate catalyst was reported by San *et al.* in 2007. The reaction afforded the chiral isoxazolidines in high yield with excellent diastereo- and enantioselectivity (Scheme 1.55).[138]

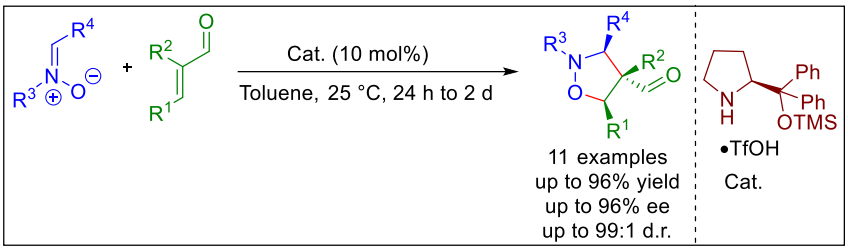

Scheme 1.55 Asymmetric 1,3-dipolar cycloaddition reaction for the synthesis of 5-CF_3 spiro-[pyrrolidine-3,2'-oxindole]

An asymmetric, one-pot, three-component 1,3-dipolar cycloaddition of nitrone, which can be produced *in-situ* from the appropriate hydroxylamine and α,β-unsaturated aldehydes, was reported in 2007 by Ramon *et al.* The reaction resulted in the formation of chiral isoxazolidine adducts in high yield, excellent enantio- and diastereoselectivity, and control over the stereochemistry of the endo-product (Scheme 1.56).[139]

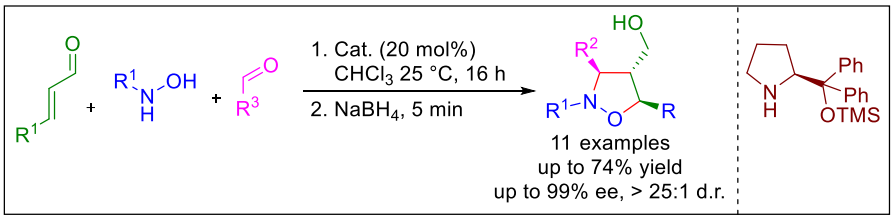

Scheme 1.56 Asymmetric, one-pot, three-component 1,3-dipolar cycloaddition for the synthesis of isoxazolidine

In 2008, Jan group developed a three-component, one-opt catalytic asymmetric synthesis of chiral cycloheptane derivatives with terminal olefin-functionalized α,β-unsaturated aldehydes, hydroxylamine, and aldehydes using a chiral amine organocatalyst. Initially, an intermolecular [3+2] cycloaddition reaction between nitrone and olefin-functionalized α,β-unsaturated aldehydes to produce chiral oxazole derivatives. Introducing an additional hydroxylamine equivalent from a nitrone with the aldehyde part of the initial compound. This is followed by an intramolecular [3+2] cycloaddition with the end olefin, creating tricyclic bis-isoxazolidines. This reaction exhibited good chemo- and regioselectivity with high diastereo- and enantioselectivity. The mechanistic study claimed that a single diastereoisomer was formed through an endo-approach to the *Re*-face of the iminium-ion in the initial phase, followed by an endo-addition that produced a seven-membered ring (Scheme 1.57).[140]

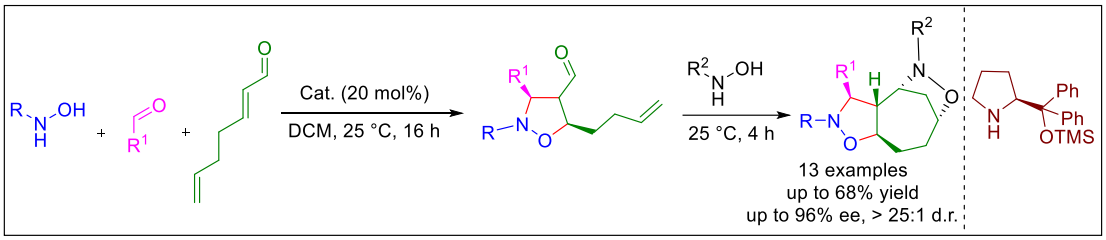

Scheme 1.57 Three-component one-pot 1,3-dipolar cycloaddition reaction for the synthesis of tricyclic bis-isoxazolidine cycloheptanes

In 2016, Pernille *et al.* developed the asymmetric cascade regio- and stereoselective 1,3-dipolar cycloaddition of poly conjugated 2,4-dienals with nitrones in the presence of chiral amine organocatalysts, and they achieved the bis-isoxazolodines products in good yields with excellent enantio- and diastereoselectivity (Scheme 1.58).[141]

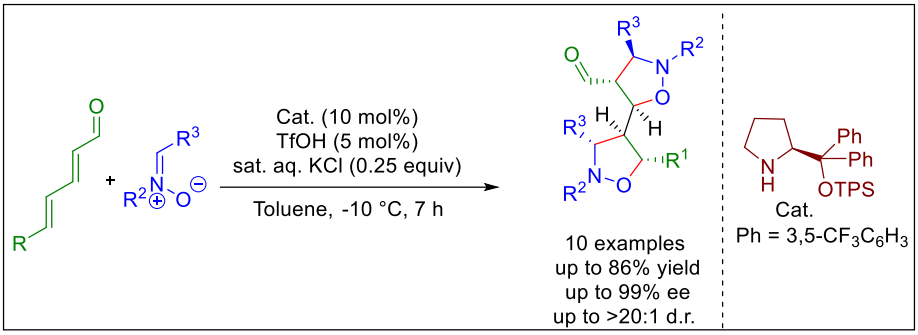

Scheme 1.58 Asymmetric cascade 1,3-dipolar cycloaddition reaction for the synthesis of bis-isoxazolines

An asymmetric synthesis of tetrahydroisoquinoline developed by Wenjun and co-workers in 2014 *via* enantioselective 1,3-dipolar cycloaddition of α,β-unsaturated aldehydes, and *C,N*-cyclic azomethine imines using chiral amine as an organocatalyst. This protocol furnished the chiral tetrahydroquinolines in good yields with excellent diastereo- and enantioselectivity (Scheme 1.59).[142]

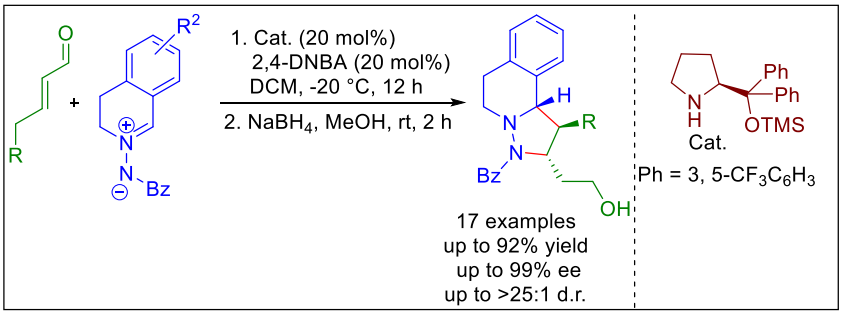

Scheme 1.59 Asymmetric cascade 1,3-dipolar cycloaddition reaction for the synthesis of terahydroisoquinoilnes

Later in 2014, Wenjun *et al.* demonstrated an amine-catalyzed enantioselective 1,3-dipolar cycloaddition of C,*N*-cyclic azomethine imines and substituted α,β-unsaturated aldehydes afforded C-1-substituted tetrahydro iso-quinolines in highly stereoselective manner. Further, this chiral product was efficiently transformed into several other useful polycyclic frameworks (Scheme 1.60).[143]

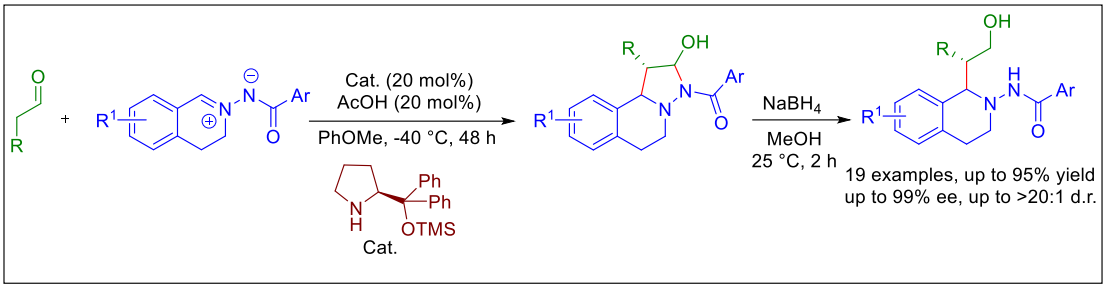

Scheme 1.60 Enantioselective 1,3-dipolar cycloaddition reaction for the synthesis of C-1-substituted tetrahydroisoquinolines

1.7 OBJECTIVE

Azomethine ylides are simple precursors for the synthesis of various important organic molecules. A literature survey reveals that azomethine ylides such as imine, pyridinium, quinolium, iso-quinolium, azomethine imides, thiazolium, and benzothiazolium salts have been used in 1,3-dipolar cycloaddition reaction with various dipolarophiles. The enantioselective transformations of azomethine ylides are well known in the literature with simple imine and azomethine imines azomethine ylides for the synthesis of chiral pyrrolidine and bicyclic pyrazolines heterocycles using various chiral metal complexes and organocatalyst. However, the enantioselective transformations of cycloiminium salts using chiral amine organocatalysts have not been well explored in the synthesis of heterocycles, but very few reports are in perspective. Particularly, the utilization of thiazolium and benzothiazolium salts for the enantioselective transformations is in infancy due to uncontrolled reactivity.

This thesis aims to synthesize various chiral heterocycle frameworks using thiazolium and benzothiazolium salts as a 1,3-dipolar system with α,β-unsaturated aldehydes as a dipolarophile by using chiral amine organocatalysts.

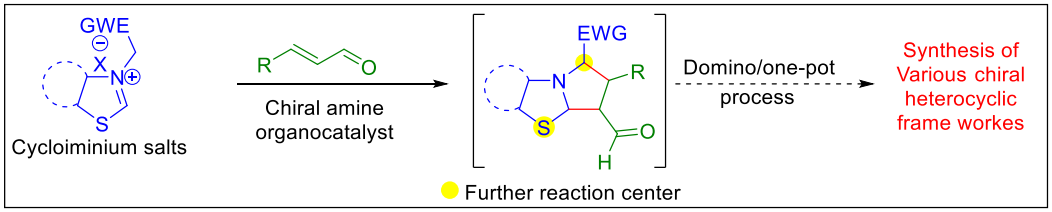

The reaction will be carried out *via* inter or intra-molecular domino and one-pot reaction. The synthesis of various chiral heterocyclic frameworks will be achieved with high enantio- and diastereoselectivity.

CHAPTER 2

ORGANOCATALYZED ENANTIO- AND DIASTEREOSELECTIVE SYNTHESIS OF PYRROLO-THIAZINE-2-CARBALDEHYDES VIA FORMAL DOMINO 1,3-DIPOLAR CYCLOADDITION/REARRANGEMENT

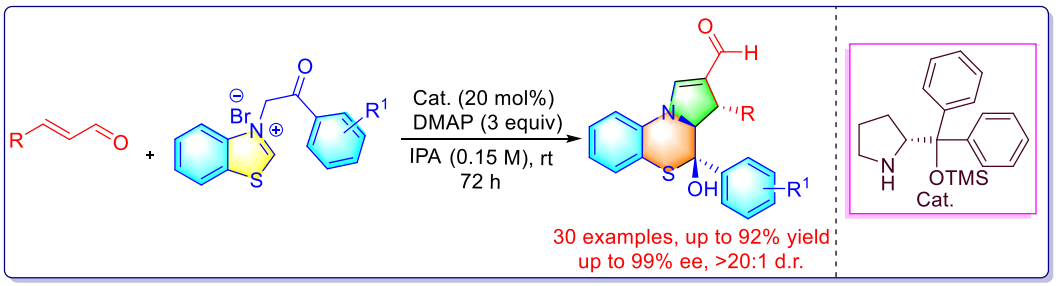

2.1 INTRODUCTION

2.1.1 Importance of Pyrrolo-thiazinens

Pyrrolo-thiazines such as 1,2- and 1,4-pyrrolo-thiazines are significant organic compounds are known to exhibit various biological activities, existence in natural product cores, and functional organic materials.[144] Substituted pyrrolo[1,4]thiazines with multiple chiral centers are the lead compounds for the synthesis of selective HIV-1 reverse transcriptase inhibitors,[145] calcium channel antagonists,[146] and anticonvulsant agents.[147] For instance, 1,4-thiazine derivative **I** with a varying degree of unsaturation is used as a marked calcium entry blocker.[148] In-vitro study of the racemic pyrrolo[1,4]thiazine derivative **II** exhibited antioxidant, anti-inflammatory, SQS inhibitory, and hypolipidemic activities.[149] Additionally, the 1,4-thiazine derivatives **III** and **IV** are employed as selective myocardial calcium channel modulators[150] and β-ribosidases inhibitors, respectively.[151] Similarly, compounds **V** and **VI** are utilized for antitumor properties (Figure 1.1).[152]

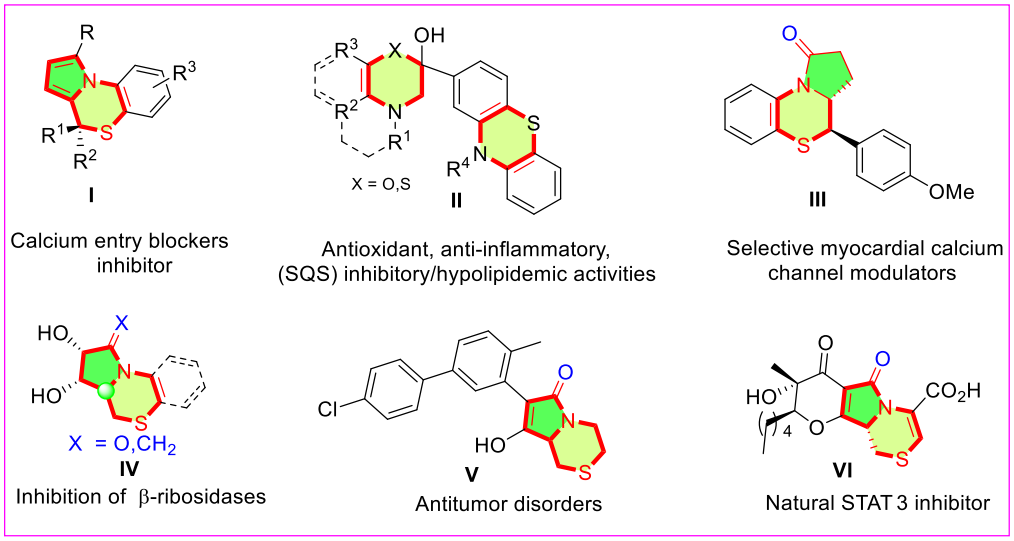

Figure 2.1 Selected examples of biologically active pyrrolo[1,4]thiazine derivatives

In recent years, a significant development for the racemic and the asymmetric synthesis of *N, S*-heterocycles such as thiazoles, 1,4-thiazines, and their polyhydro derivatives with multiple chiral centers have been made *via* one-pot and domino processes.[153, 154]

Cycloaddition is one of the most powerful methods to synthesize complex chiral molecules, particularly with multiple chiral centers.[155] While many cycloaddition reactions are well-known, 1,3-dipolar cycloaddition is a unique method to generate complex heterocycles. The 1,3-dipolar cycloaddition reaction of azomethine ylides and dipolarophiles is a highly effective approach for generating a variety of five-membered heterocycles.[91] Azomethine ylide is an essential nitrogen-containing three-atom component commonly used as 1,3-dipole and utilized for the synthesis of multiple stereogenic centers containing pyrrolidines.[156] Notably, azomethine ylide as part of 5 and 6-membered rings such as quinolinium,[103] isoquinolinium,[104] pyridinium,[157] thiazolium, and benzothiazolium methylides,[158] have been widely utilized in the 1,3-dipolar cycloaddition. Particularly, benzothiazolium ylide has been used in the synthesis of functionalized multiple chiral centers containing thiazoles, pyrrole-thiazoles, pyrrorlo[1,2]thiazine, pyrrorlo[1,4]thiazine and their derivatives.[159, 160]

2.2 LITERATURE BACKGROUND

2.2.1 1,3-Dipolar Cycloaddition Reactions of Benzothiazolium Azomethine Ylides

In 1981, Tsuge and co-workers described a synthesis of diverse tetrahydropyrro-thiazole derivatives *via* 1,3-dipolar cycloaddition of benzothiazolium azomethine ylides with a wide range of methylenecyclopropane dipolarophiles. This synthesis was carried out in dry THF solvent, NEt_3 as a base, and at 0 °C to room temperature, resulting in the observation of various types of products. The reaction of

benzothiazolium salt with nitrile-substituted cyclopropane as a dipolarophile yielded two distinct diastereomeric cycloadduct products with satisfactory yield and high diastereoselectivity (Scheme 2.1a). Similarly, employing dimethyl ester containing dipolarophile in the same reaction condition forms two diastereomeric cycloadduct products in favorable yields (Scheme 2.1b).[113]

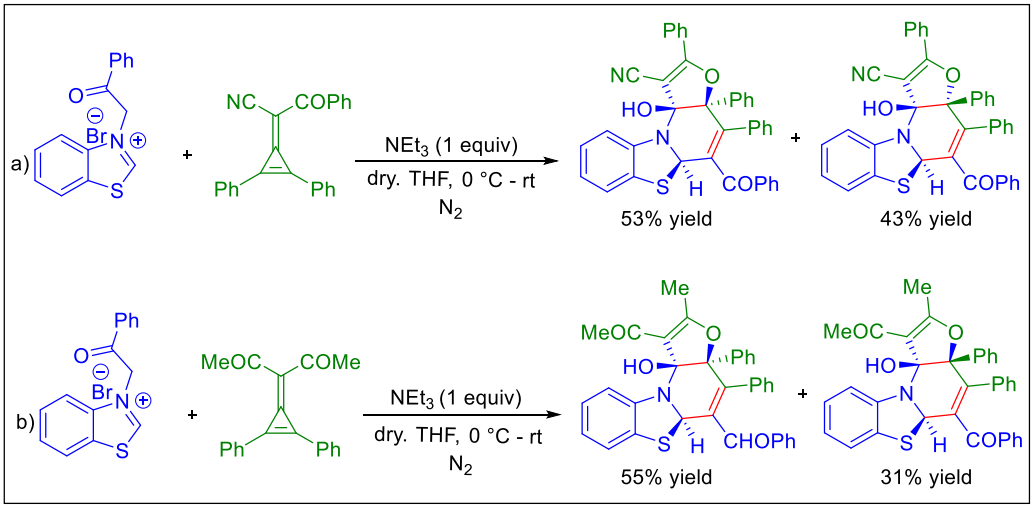

Scheme 2.1 1,3-Dipolar cycloaddition of benzothiazolium azomethine ylide and cyclopropene dipolarophiles

Iwamura and co-workers in 1996 reported the 1,3-dipolar cycloaddition reaction involving benzothiazolium salt of azomethine ylide and DMAD as a dipolarophile. This reaction was facilitated by NEt_3 as a base and dry DMF as a solvent. Under room temperature, the reaction yields racemic pyrrolo-thiazine derivatives through a 1,3-dipolar cycloaddition/rearrangement sequence as shown in Scheme 2.2.[108]

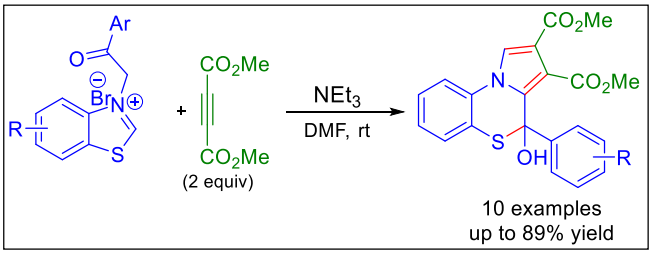

Scheme 2.2 1,3-Dipolar cycloaddition for the synthesis of pyrrolo-[1,4]thiazine

In 2017, Jin and co-workers devised a stepwise 1,3-dipolar cycloaddition reaction involving *N*-phenacylbenzothiazolium bromides and nitroalkenes in the presence of triethylamine and ethanol solvent, which yielded a mixture of two isomeric tetrahydrobenzo[d]pyrrolo[2,1-b]thiazoles. These products exhibited cis/trans configurations, obtained with a good yield and moderate diastereoselectivity (Scheme 2.3).

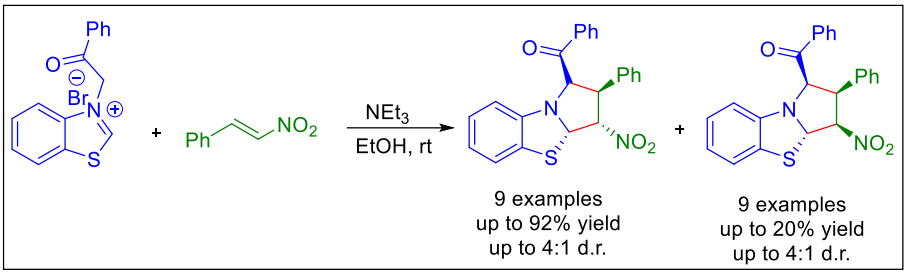

Scheme 2.3 1,3-Dipolar cycloaddition for the synthesis of tetrahydrobenzo[*d*] pyrrolo[2,1-*b*]thiazoles

Moreover, a similar cycloaddition reaction of *N*-phenacylbenzothiazolium bromides with 1-methyl-1-nitroalkenes in ethanol under reflux afforded methylbenzo[d]pyrrolo[2,1-b]thiazoles by the elimination of the nitro group (Scheme 2.4). [112]

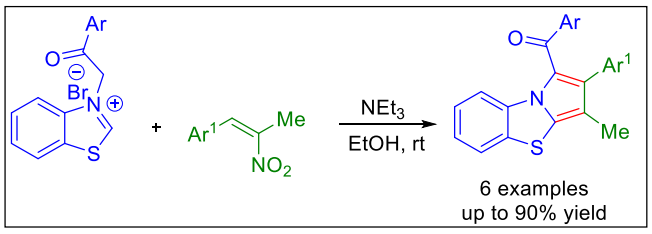

Scheme 2.4 1,3-Dipolar cycloaddition for the synthesis of Methyl benzo[*d*]pyrrolo[2,1-*b*]thiazoles

In 2017, Jiang and co-workers developed a 1,3-dipolar cycloaddition reaction between benzothiazolium azomethine ylides and 3-nitrochromenes in trimethylamine base and ethanol solvent at room temperature. The reaction furnished functionalized

tetrahydrobenzo[d]chromeno[3',4':3,4]pyrrolo[2,1-b]thiazoles with high diastereoselectivity and yielded up to 95% (Scheme 2.5).

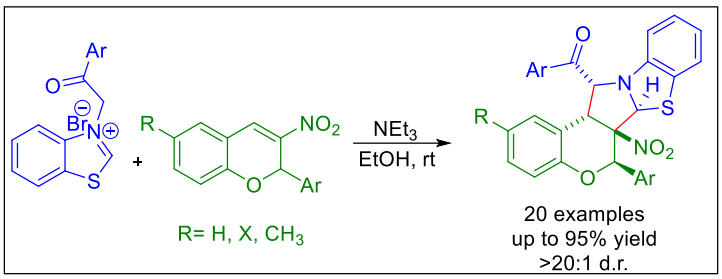

Scheme 2.5 1,3-dipolar cycloaddition for the synthesis of tetrahydrobenzo[*d*]chromeno[3',4':3,4]pyrrolo[2,1-*b*]thiazoles

Similarly, they also reported a comparable reaction using 2-alkoxycarbonylmethylbenzothiazolium azomethine ylides and 3-nitrochromenes under the same conditions provides the desired product in similar yields and diastereoselectivity (Scheme 2.6).[160]

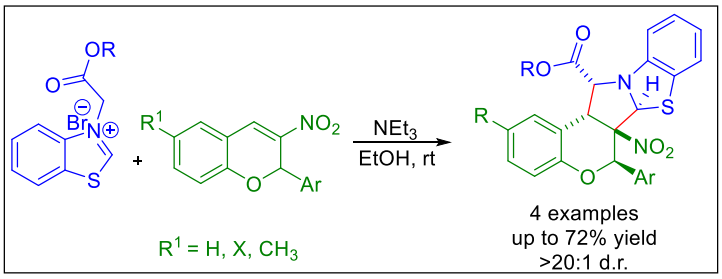

Scheme 2.6 1,3-Dipolar cycloaddition for the synthesis of tetrahydrobenzo[*d*]chromeno[3',4':3,4]pyrrolo[2,1-*b*]thiazoles

Shen and co-workers in 2015 accomplished the domino cycloaddition reaction involving benzothiazolium azomethine ylides and 3-phenacylideneoxindoles in the presence of NEt_3 in ethanol at room temperature. The reaction yielded functionalized spiro[benzo[*d*]pyrrolo[2,1-*b*]thiazole-3,3'-indolines] in high yields with excellent diastereoselectivity (Scheme 2.7).[161]

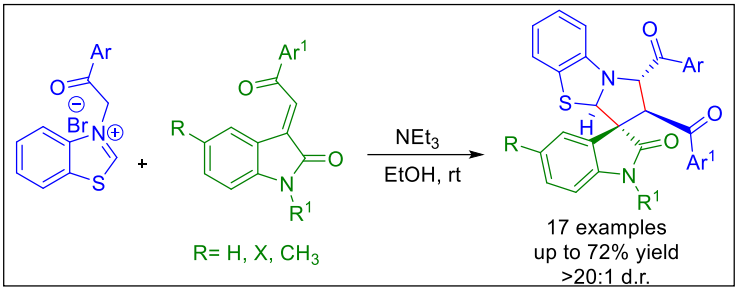

Scheme 2.7 Benzothiazolium azomethine ylide 1,3-dipolar cycloaddition synthesis of spiro[benzo[*d*]pyrrolo[2,1-*b*]thiazole-3,3'-indolines]

In 2018, Zeng and co-workers reported a 1,3-dipolar cycloaddition reaction involving *N*-4-methoxyphenacylbenzothiazolium bromide azomethine ylides with (*Z*)-5-arylidene[1,3]thiazolo[3,2-*b*][1,2,4]triazol-6(5*H*)-one in the presence of triethylamine. The reaction yielded novel 2-(aryl)-1-(4-methoxybenzoyl)-1,2-dihydrospiro[pyrrolo[2,1-*b*][1,3]benzothiazole-3,5′[1,3]thiaol-zolo[3,2*b*][1,2,4] triazol]-6′-ones in moderate yields (Scheme 2.8).[162]

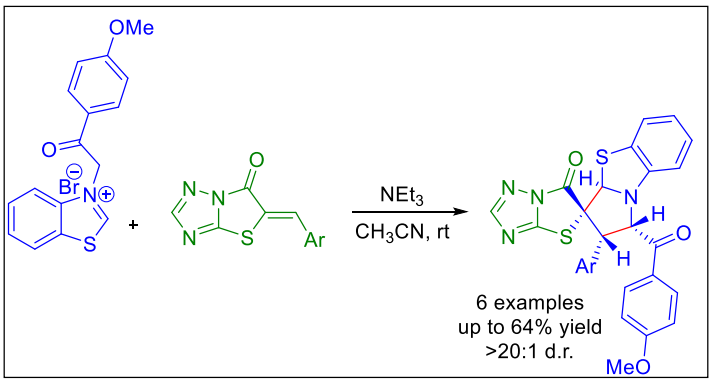

Scheme 2.8 1,3-Dipolar cycloaddition for the synthesis of spiro thiazolo[3,2-*b*][1,2,4]triazole derivatives

The same Zeng research group furnished the synthesis of 6′-ethyl-2-methyl-5′-aryl-1-(4-methoxybenzoyl)-7-methyl-3′-oxo-1,2-dihydro5*H*spiro[pyrrolo[2,1*b*][1,3]benzo thia-zole-3,2′-[1,3]thiazolo[3,2-*a*]pyrimidine]-2,6′-dicarboxylates in 2018 through a 1,3-dipolar cycloaddition reaction. The reaction involves ethyl-5-aryl-2-[(*Z*)-2-methoxy-2-oxoethylidene]-7-methyl-3-oxo-3,5-dihydro-2*H*-thiazolo[3,2-*a*]pyrimidine-6 carboxylates and *N*-4-methoxyphenacylbenzothiazolium azomethine

ylides afforded the desired cycloaddition products in moderate yields with two different diastereomers (Scheme 2.9).[163]

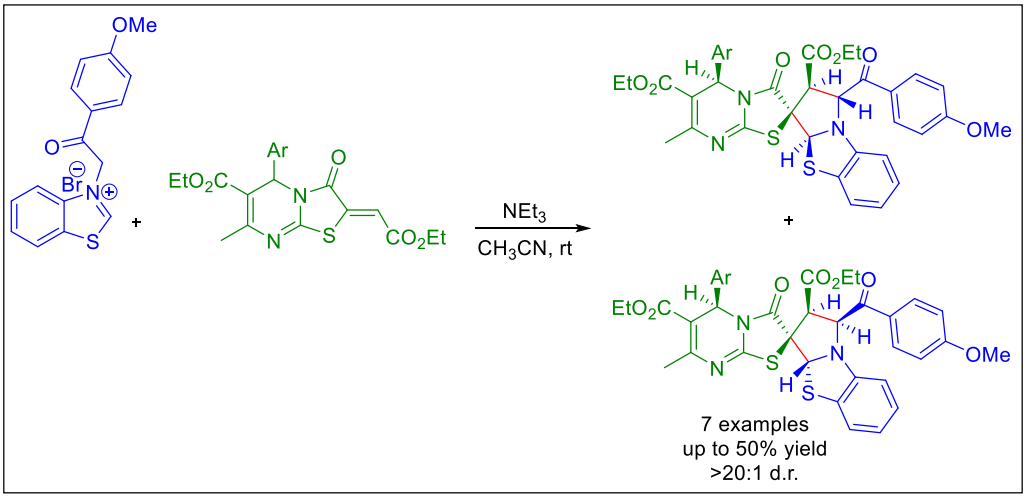

Scheme 2.9 1,3-Dipolar cycloaddition for the synthesis of spiro thiazolo[3,2-*a*]pyrimidine derivatives

Sahoo *et al.* in 2017 devised a method for the metal-free diastereoselective desymmetrization of prochiral cyclopentadienones *via* [3+2] cycloaddition with *N*-phencylbenzothiazolium bromide azomethine ylides generated *in-situ* treatment of DIPEA which provides the tetrahydropyrrolo-thiazole derivatives containing multiple stereogenic centers with excellent diastereoselectivity (Scheme 2.10).[158]

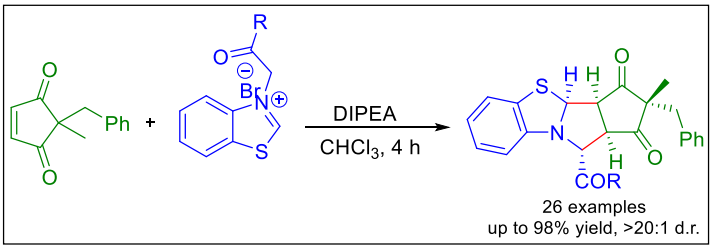

Scheme 2.10 1,3-Dipolar cycloaddition for the synthesis of fused polycyclic derivatives

In 2023, Wang *et al*. reported the 1,3-dipolar cycloaddition reactions of azomethine ylides with various electron-deficient olefinic dipolarophiles.

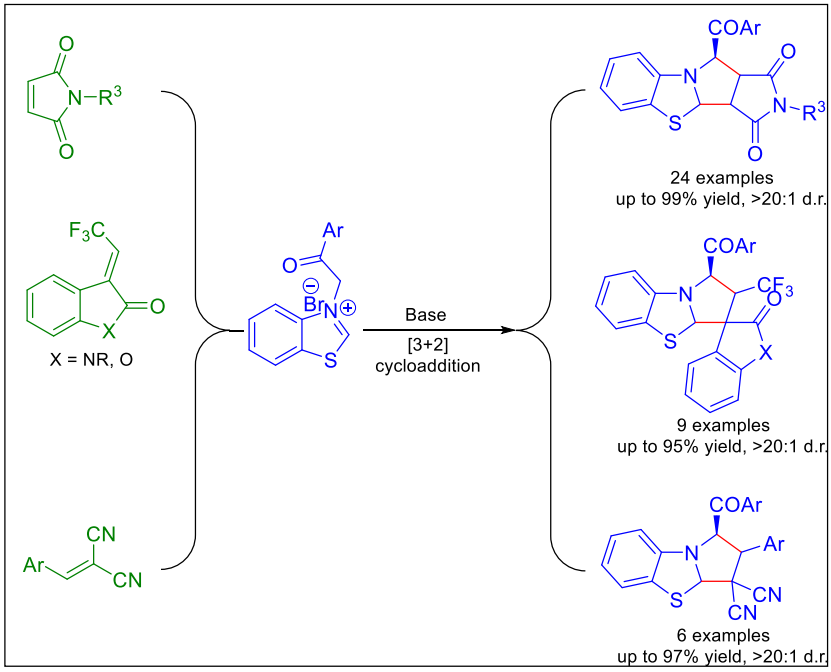

Scheme 2.11 1,3-Dipolar cycloaddition for the synthesis of cycloadduct products

This approach affords diverse heterocyclic compounds including fused polycycles and spirocyclic compounds with excellent yields and diastereoselectivity. The azomethine ylide is generated *in-situ* from N-phenylbenzothiazolium bromide in the presence of different bases (Scheme 2.11).[164]

2.2.2 Enantioselective Transformations of Benzothiazolium Azomethine Ylides

The enantioselective transformations of 1,3-dipolar cycloaddition of benzothiazolium azomethine ylide with dipolarophile for the synthesis of heterocyclic compounds such as chiral pyrrolo-thiazoles and pyrrolo[1,4]thiazine derivatives with multiple stereogenic centers is a challenging task. There are only a very few reports have been documented in the literature.

Sahoo and co-workers 2017 disclosed a solitary instance of an asymmetric variant of 1,3-dipolar cycloaddition of benzothiazolium salt, utilizing hydroquinone-derived thiourea as a chiral catalyst to afford a cycloadduct product that exhibits moderate enantioselectivity (43% ee, 67% yield) as shown in Scheme 2.12.[158]

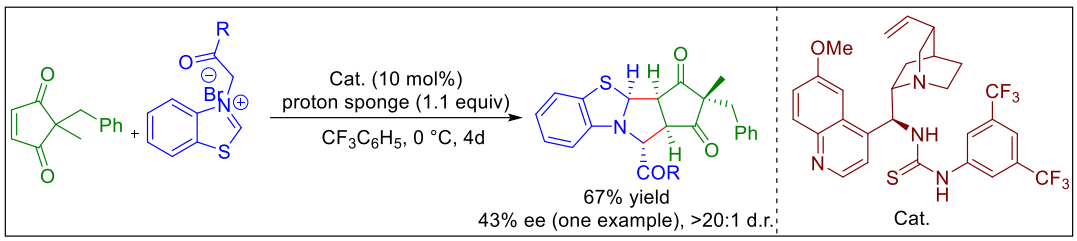

Scheme 2.12 1,3-Dipolar cycloaddition for the synthesis of chiral cycloadduct products

Subsequently, in the year of 2018, Zhang and co-workers reported the synthesis of dihydropyrrolo-thiazoles and [1,4]thiazine derivatives *via* chiral *N, N′*-dioxide-metal salts (Mg and Ni salts) catalyzed asymmetric 1,3-dipolar cycloaddition followed by rearrangement of benzothiazolium salt with various dipolarophiles. The reaction yields various chiral heterocyclic compounds with excellent yields, enantio- and diastereoselectivity.

The reactions between benzothiazolium salt azomethine ylides and simple chalcones in the presence of a chiral *N,N′*-dioxide ligand and $Mg(OTf)_2$ to form a chiral metal complex, followed by addition of K_3PO_4 as a base in DCM solvent at room temperature, provided the chiral dihydropyrrolo-thiazole derivatives with excellent yields, good enantio- and diastereoselectivity (Scheme 2.13).

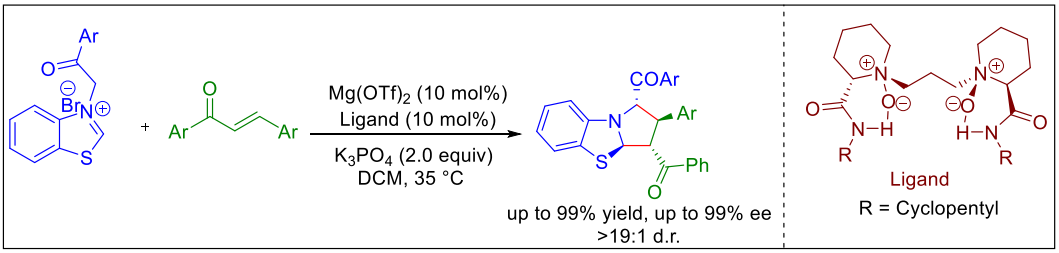

Scheme 2.13 1,3-Dipolar cycloaddition for the synthesis of chiral hydropyrrolo-thiazole derivatives

Similarly, the reactions of benzothiazolium salt azomethine ylides with methyleneindolinone derivatives as dipolarophiles, employing a chiral *N,N′*-dioxide ligand and $Mg(OTf)_2$ to form a chiral metal complex, followed by the addition of

Na_2CO_3 as a base in DCM solvent at room temperature. The reaction furnished the chiral spiro dihydropyrrolo-thiazole derivatives with excellent yields, enantio- and diastereoselectivity (Scheme 2.14).

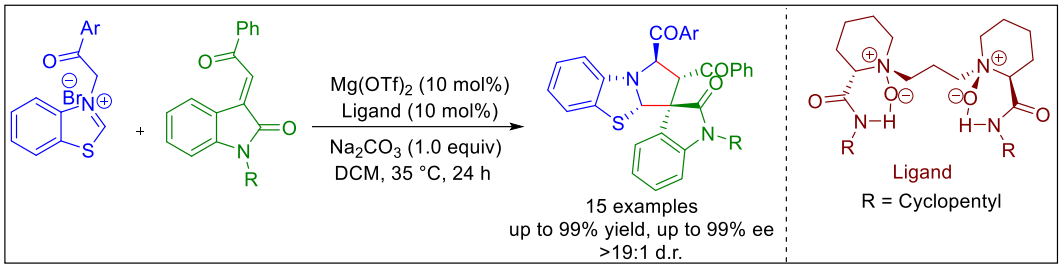

Scheme 2.14 1,3-Dipolar cycloaddition for the synthesis of chiral spiro hydropyrrolo-thiazole derivatives

Similarly, the reactions of benzothiazolium salt azomethine ylides with ester and amide chalcones derivatives as the dipolarophiles, in the presence of chiral *N, N′*-dioxide ligand and $Ni(OTf)_2$ to form chiral metal complex catalyst, followed by addition of Na_2CO_3 as a base, DCM solvent, under 0 °C to room temperature. The reaction provides the cycloaddition/rearrangement product of chiral pyrrorlo[1,4]thiazine derivatives with excellent yield, enantio- and diastereoselectivity (Scheme 2.15).[109]

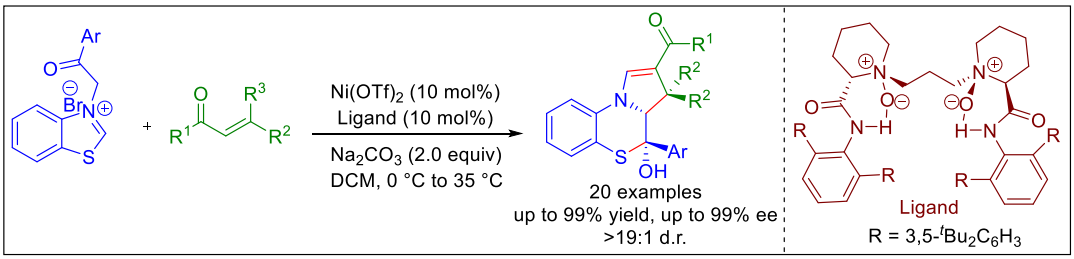

Scheme 2.15 1,3-Dipolar cycloaddition for the synthesis of chiral pyrrolo[1,4]thiazine's derivatives

2.2.3 1,3-Dipolar Cycloaddition Reactions of Azomethine Ylides and α,β-Unsaturated Aldehydes with Chiral Amine Catalysts

In 2007, Vicario *et al.* pioneered the development of the first organocatalytic enantioselective 1,3-Dipolar cycloaddition reactions between imine azomethine ylides and α,β-unsaturated aldehydes, employing chiral diphenylprolinol as an organocatalyst.

The reaction proceeded with complete regioselectivity and exhibited high enantio- and diastereoselectivity, yields highly poly-substituted pyrrolidine products in excellent yield (Scheme 2.16).[165]

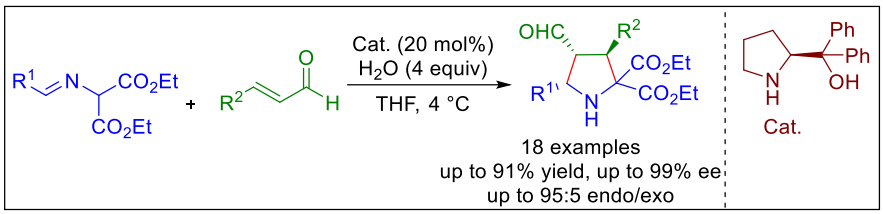

Scheme 2.16 Enantioselective 1,3-dipolar cycloaddition for the synthesis of chiral pyrrolidine

The same research group in 2017 reported an asymmetric 1,3-dipolar cycloaddition of acyclic azomethine ylides with acrolein as a dipolarophile catalyzed by L-proline. The reaction yields C-3 unsubstituted pyrrolidine as a product in good yield, and with high enantio- and diastereoselectivites (Scheme 1.17).[166]

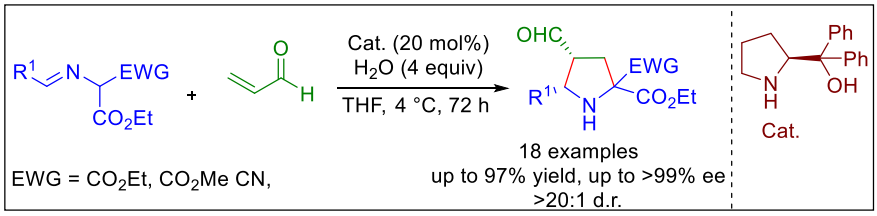

Scheme 2.17 Enantioselective 1,3-dipolar cycloaddition for the synthesis of chiral pyrrolidine

2.3 OBJECTIVE

The asymmetric reactions involving benzothiazolium salts have been limited due to their high reactivity and pose a challenge in controlling their reactivity, selectivity, and other competitive organic transformations. Till now, there are no reports on the proline-derived organocatalytic asymmetric domino 1,3-dipolar cycloaddition/rearrangement of benzothiazolium salts with α,β-unsaturated aldehydes to synthesize enantioenriched polycyclic pyrrolidine derivatives. To overcome the limitations of the mentioned issues, the following is the objective of Chapter 2.

- A new asymmetric domino methodology will be developed for the enantioselective synthesis of chiral pyrrlolo-thiazine-2-carbaldehydes *via* intermolecular 1,3-dipolar cycloaddition followed by intramolecular rearrangement reaction of benzothiazolium azomethine ylides and α,β-unsaturated aldehydes, using a chiral amine as an organocatalyst (Scheme 2.18).

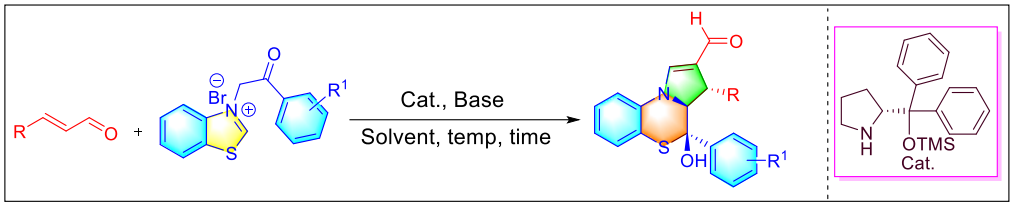

Scheme 2.18 Chiral amine catalyzed enantioselective synthesis of pyrrolo-thiazine-2-carbaldehydes.

- The proposed chiral pyrrlolo-thiazine-2-carbaldehydes will have three contiguous chiral centers along with one quaternary chiral centre.
- The computational study will be performed to understand the reaction mechanism.
- To show the synthetic application of the chiral product, molecular docking will be carried out for anti-cancer activities.

2.4 RESULTS AND DISCUSSION

2.4.1 Optimization Studies

Enantioselective domino synthesis of three contiguous stereogenic centers containing pyrrolo[1,4]thiazine carbaldehyde **3f,** the trail reaction was started by reacting α,β-unsaturated aldehyde **1a** (1.0 equiv), with benzothiazolium salt **2f** (1.0 equiv) in EtOH using *L*-proline **C1** (10 mol%) as an organocatalyst and NEt_3 (1.0 equiv) as a base at room temperature. This domino reaction provided the expected pyrrolo[1,4]thiazine-2carbaldehyde **3f** in 24% yield, 16% ee, and 19:1 d.r. along with the formation of an unexpected rearranged side product **4** in 10% yield (Scheme 2.19). Product **4** might

have formed *via* domino aerobic hydrolysis of benzothiazolium salt **2f**, followed by ring opening/iminium ion formation/ring-closing sequence.[159]

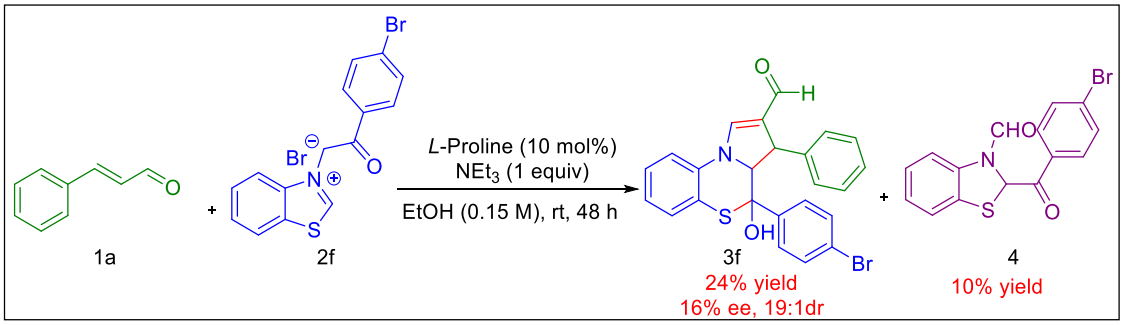

Scheme 2.19 Enantioselective domino synthesis of pyrrolo-thiazine-2-carbaldehyde **3f**

To improve the selectivity of this domino process towards the selective formation of **3f** and minimize the formation of undesired side product **4**, the reaction was optimized the reaction with various catalysts, bases, and solvents, and the results are summarized in Tables 2.1. When the catalyst loading was increased from 10 to 20 mol%, the %ee of the product also increased to 24% (Table 2.1, entry 2). The product yield was improved to 60% by increasing the base to two equivalents and decreasing the yield of the side product by **4** to 5% (Table 2.1, entry 3). Upon further increasing the base to three equivalents, the yield increased to 75% without affecting the %ee, and the yield of side product **4** was reduced to trace quantities (Table 2.1, entry 4). To improve the enantioselectivity of product **3f**, the reaction was screened using several proline-based chiral catalysts. Among them, (*R*)-diphenylprolinol trimethylsilyl ether catalyst **C5** turned out to be the best choice of catalyst, and it provided 90% ee with a moderate yield of 52% (Table 2.1, entry 8). The reaction was then examined with several bases to improve the yield of **3f**. Use of dibutyl amine and diethyl amine bases yielded the product **3f** in 95% yield without formation of the side product **4**, albeit in 15% enantiomeric excess (Table 2.1, entries 9 and 10). The reason may be that the

background reaction was very facile in this condition; the chiral catalyst could not control the reaction. Delightfully, DMAP furnished a maximum yield of 72% with 98% ee (Table 2.1, entry 13). Then, various solvents were screened to improve the yield and enantiomeric excess of product **3f**.

Table 2.1: Optimization of the Domino Reaction[a]

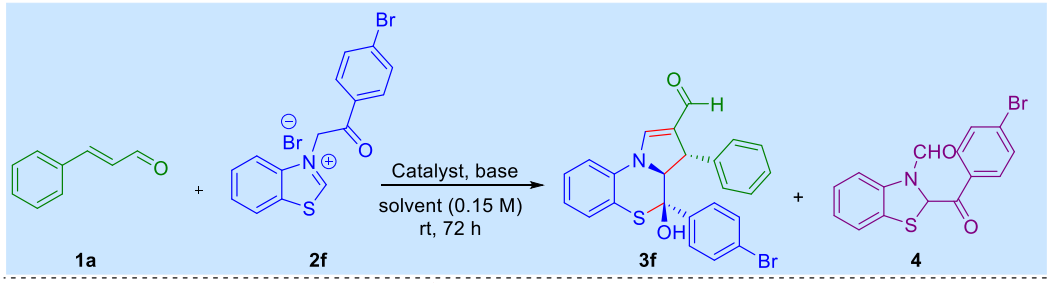

Catalysts

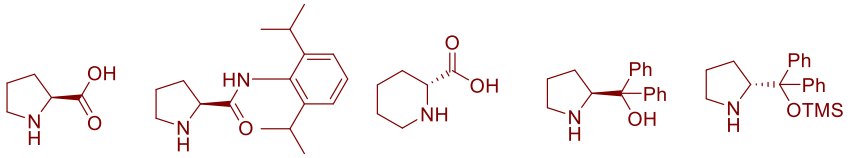

Entry	Base (equiv)	Catalyst (equiv)	Solvent (M)	Yield of 3a (%)[b]	ee (%)[c]	Yield of 4 (%)[d]
1	NEt_3 (1)	**C1** (10)	EtOH	24	16	10
2	NEt_3 (1)	**C1** (20)	EtOH	24	24	10
3	NEt_3 (2)	**C1** (20)	EtOH	60	16	5
4	NEt_3 (3)	**C1** (20)	EtOH	75	16	5
5	NEt_3 (3)	**C2** (20)	EtOH	10	6	10
6	NEt_3 (3)	**C3** (20)	EtOH	41	28	6
7	NEt_3 (3)	**C4** (20)	EtOH	32	38	10
8	NEt_3 (3)	**C5** (20)	EtOH	52	90	5
9	DEA (3)	**C5** (20)	EtOH	90	15	-
10	DBA (3)	**C5** (20)	EtOH	95	10	-
11	K_2CO_3 (3)	**C5** (20)	EtOH	20	60	15

Entry	Base (equiv)	Catalyst (equiv)	Solvent (M)	Yield of 3a (%)[b]	ee (%)[c]	Yield of 4 (%)[d]
12	DABCO (3)	**C5** (20)	EtOH	63	97	8
13	DMAP (3)	**C5** (20)	EtOH	72	98	20
14	DMAP (3)	**C5 (20)**	MeOH	60	74	12
15	DMAP (3)	**C5 (20)**	DCM	65	98	10
16	DMAP (3)	**C5 (20)**	HFIP	20	22	55
17	DMAP (3)	**C5 (20)**	H2O	n.r.	-	-
18	DMAP (3)	**C5 (20)**	IPA	87	98	trace
19	DMAP (3)	**C5 (10)**	IPA	52	38	5
20	DMAP (3)	**C5 (15)**	IPA	35	60	10
21	DMAP (3)	**C5 (25)**	IPA	52	78	5

[a]Reaction conditions: **1a** (0.3 mmol), **2f** (0.3 mmol), base (1 – 3 equiv), chiral catalyst **C1- C5** (x mol%), and solvent (0.15 M) at 72 h. [b&d]Isolated yield. [c]%Ee was determined by HPLC using a Chiralcel OD-H chiral column. The diastereomeric ratio was determined by ^{1}H NMR spectroscopy using the crude reaction mixture. In all cases, we observed a 19:1 d.r ratio.

Where HFIP is used as a solvent, we observed a 50% yield of side product **4** with a trace amount of chiral product (Table 2.1, entry 16). This may be due to the high polarity of HFIP quenching the iminium ion intermediate in the reaction medium. No changes were observed in the reaction medium when H_2O was used as the solvent due to the insolubility of thiazolium salt (Table 2.1, entry 17).

Table 2.2: Base Optimization[a]

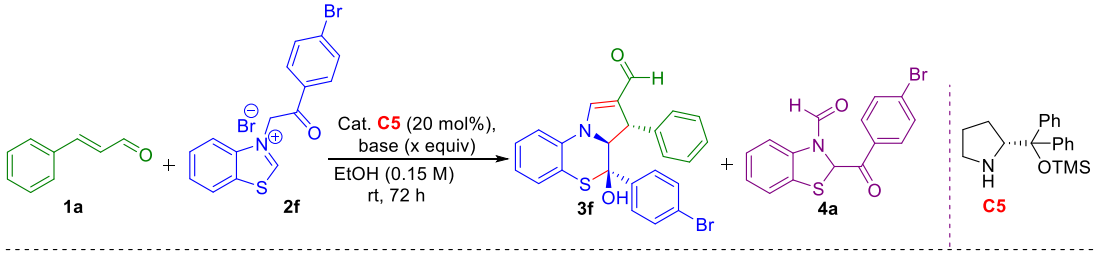

Entry	Base (equiv)	Yield of 3a (%)[b]	ee (%)[c]	d.r.[d]	Yield of 4 (%)[d]
1	NEt_3 (1)	24	90	19:1	10
2	NEt_3 (2)	60	88	19:1	5
3	NEt_3 (3)	52	90	19:1	trace
4	DMAP (3)	72	98	19:1	5
5	DABCO (3)	63	97	19:1	8
6	DIPEA (3)	39	34	19:1	10
7	DIPA (3)	45	54	19:1	15
8	DEA (3)	90	12	19:1	-
9	DBA (3)	95	10	19:1	-
10	Piperidine (3)	95	10	19:1	-
11	K_2CO_3 (3)	20	60	19:1	15
12	NaOAc (3)	24	98	19:1	8
12	DBU (3)	n.r.	-		-
13	2,6-lutidine (3)	n.r.	-		-
14	K_3PO_4 (3)	n.r.	-		-

[a]Reaction conditions: **1a** (0.3 mmol), **2f** (0.3 mmol), base (1 – 3 equiv), chiral catalyst **C1- C5** (x mol%), and solvent (0.15 M) at 72 h. [b&d]Isolated yield. [c]%Ee was determined by HPLC using a Chiralcel OD-H chiral column. The diastereomeric ratio was determined by 1H NMR spectroscopy using the crude reaction mixture in all cases, showing 19:1 d.r.

Table 2.3: Solvent Optimization[a]

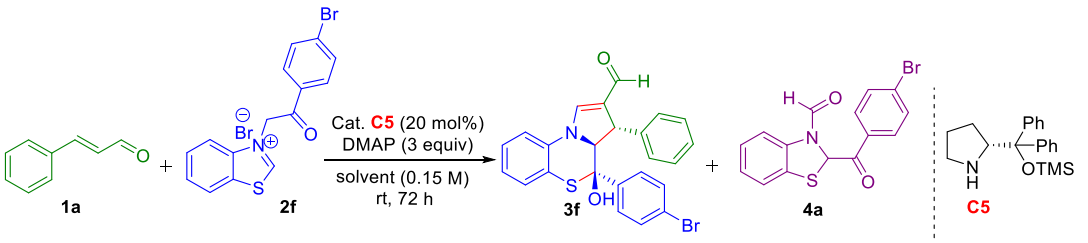

Entry	Solvent (M)	Yield of 3a (%)[b]	ee (%)[c]	d.r.[d]	Yield of 4 (%)[e]
1	EtOH	72	98	19:1	5
2	MEOH	60	74	19:1	12
3	DCM	65	98	19:1	10
4	HFIP	20	22	19:1	55
5	EtOAc	40	80	19:1	15
6	IPA	87	98	19:1	trace
7	1,2-DCE	55	98	19:1	10
8	$CHCl_3$	48	98	19:1	13
9	Toluene	55	96	19:1	16
10	CH_3CN	44	98	19:1	20
11	DMSO	-	-	-	50
12	THF	33	98	19:1	20
12	E_2O	40	98		15
13	1,4-Dioxane	30	92		-
14	H_2O	n.r.	-	-	-

[a]Reaction conditions: **1a** (0.30 mmol), **2f** (0.3 mmol), DMAP (3 equiv) and chiral catalyst **C5** (20 mol%), solvent (0.15 M), [b&e] Isolated yield. [c]*Ee* Determined by HPLC using Chiralcel OD-H chiral column. [d]D.r. ratio was determined by ^1H NMR using a crude reaction mixture, nr = No reaction.

The optimized reaction condition was found when isopropyl alcohol was used as the solvent, benzothiazolium salt (1 equiv), unsaturated aldehyde (1 equiv), (*R*)-diphenylprolinol trimethylsilyl ether (20 mol%), and DMAP (3 equiv) at room temperature. The domino reaction provided **3f** in 87% yield with 98% ee and 19:1 d.r. (Table 2.1, entry 18).

Table 2.4 Combination of Base and Combination of Solvent Screening[a]

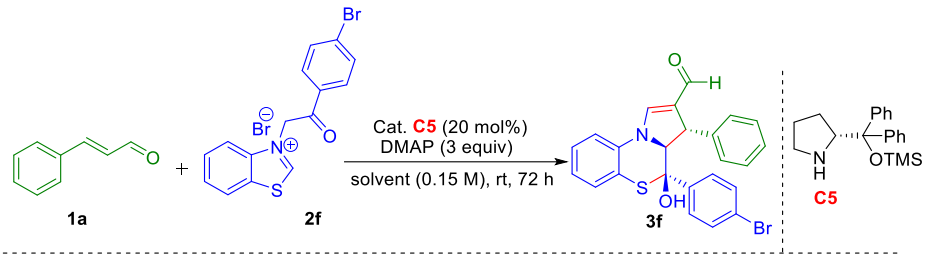

Entry	Base (3 equiv)	Solvent (M)	Yield of 3a (%)[b]	ee (%)[c]	d.r.[d]
1	DMAP	IPA/DCM (1:1)	21	98	19:1
2	DMAP/DABCO (1:1)	MeOH	50	98	19:1
3	DMAP/DBA (1:1)	DCM	75	30	19:1

[a] Reaction conditions: **1a** (0.30 mmol), **2f** (0.3 mmol), mixture of base (1:1, 3 equiv) and chiral catalyst **C5** (20 mol%) in mixture of solvent (1:1, 0.15 M), [b] Isolated yield. [c]Ee was determined by HPLC using the Chiralcel OD-H chiral column. [d]D. r. ratio was determined by ^{1}H NMR using a crude reaction mixture.

Table 2.5: Additive and Inert Condition Screening[a]

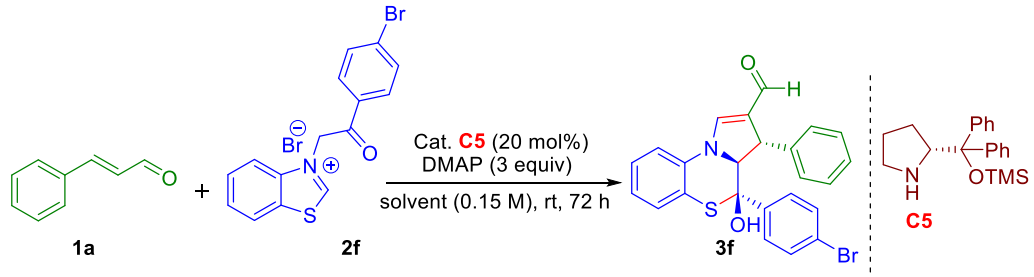

Entry	Solvent (M)	Additive	Yield of 3a (%)[b]	ee (%)[c]	d.r.[d]
1	IPA	$PhCO_2H$ (2 equiv)	55	97	19:1
2	IPA	4 Å M. S	50	98	19:1
3	DCM	$PhCO_2H$ (2 equiv)	60	98	19:1
4	IPA	4 Å M. S	58	98	19:1
5[e]	IPA	-	55	98	19:1
6[e]	DCM	-	45	98	19:1

[a] Reaction conditions: **1a** (0.30 mmol), **2a** (0.3 mmol), DMAP (3 equiv), Additive (2 equiv) and chiral catalyst **C5** (20 mol%) in solvent (0.15 M), [b] Isolated yield. [c] ee was determined by HPLC using Chiralcel OD-H chiral column. [d]D. r ratio was

determined by ^{1}H NMR using a crude reaction mixture. [e]Reaction performed under N_2

Moreover, the yield and enantiomeric excess of the product gradually decreased when the catalyst **C5** loading was varied from 10 – 25 mol% (Table 2.1, entries 19-21). Further, the reaction was screened with various additives, temperatures, a mixture of solvents, bases, and other parameters for better outcomes. Unfortunately, all the attempts failed to get better results (Table 2.4 & 2.5). The absolute configuration of **3f** (3*S*,3*aS*,4*S*) was unambiguously confirmed by single-crystal X-ray diffraction analysis using the flack parameter (Figure 2.2; Flack parameter value: 0.001(5).

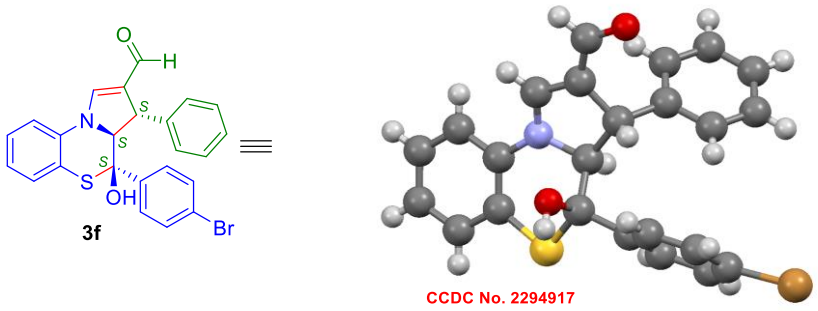

Figure 2.2 X-ray structure of compound **3f** (CCDC: 2294917) with 50% probability ellipsoids

2.5. SUBSTRATE SCOPES FOR PYRROLO-THIAZINE-2-CARBALDEHYDE

With optimized reaction conditions in hand, the generality of the domino process has been investigated with various benzothiazolium salts **2** containing electron-donating, electron-withdrawing, and bulky aryl groups, and the results are summarized in Scheme 2.20. All the domino reactions took place smoothly *via* intermolecular 1,3-dipolar cycloaddition, followed by intramolecular rearrangement to afford the pyrrolo[1,2-*d*][1,4]thiazine-2-carbaldehydes **3a-3n** in good enantioselectivity (96-99.7% ee). Substrates bearing electron-donating groups at the *para* positions exhibited good

reactivity and enantioselectivity **(3a-3c**; 96-98% ee). The halogen substitution at the *para* position provided the desired products **3d–3f** in 71-86% yield with good enantioselectivity (98-99% *ee)*. Then, the electron-donating methoxy group at the *ortho*, *meta*-position, and disubstituted methoxy group delivered the desired chiral products **3g-3i** in 98-99% ee. The electron-withdrawing group at the *para* position **3k-3m** delivered good yield and enantioselectivity (96-99% ee). It is worth mentioning that an electron-withdrawing nitrile group **3l** at the *para* position increased the yield further (92%) with 98% ee. Various aryl substitutions, including phenyl and naphthyl, were well tolerated for this domino strategy to accomplish the desired products **3j** and **3n** with 98-99% ee.

To showcase the functional group tolerance of α,β-unsaturated aldehyde, The reaction was carried out the domino reaction using α,β-unsaturated aldehyde containing electron-donating, electron-withdrawing, halogens, heterocycles, and aliphatic substituents (Scheme 2. 21). Generally, the *meta* and *para* substitutions at the phenyl ring of the cinnamaldehyde underwent the enantioselective 1,3-dipolar cycloaddition/rearrangement and yielded the domino product up to 98% ee. The cinnamaldehyde-bearing electron-donating group at the *para* position delivered the desired products 3o, 3p, and 3t in good yield with 92-98% ee. Notably, the halogen substitution at the *para* position of cinnamaldehyde provided the product 3q, 3r, and 3s in 88-98% ee. Compared with electron-donating and halogen-substituted derivatives, the electron-withdrawing group at the *meta* and *para* positions furnished the desired products 3u-3xin good yields with slightly reduced enantioselectivity (88-94% ee).

Scheme 2.20 Substrate Scope of Benzothiazolium Salts[a]

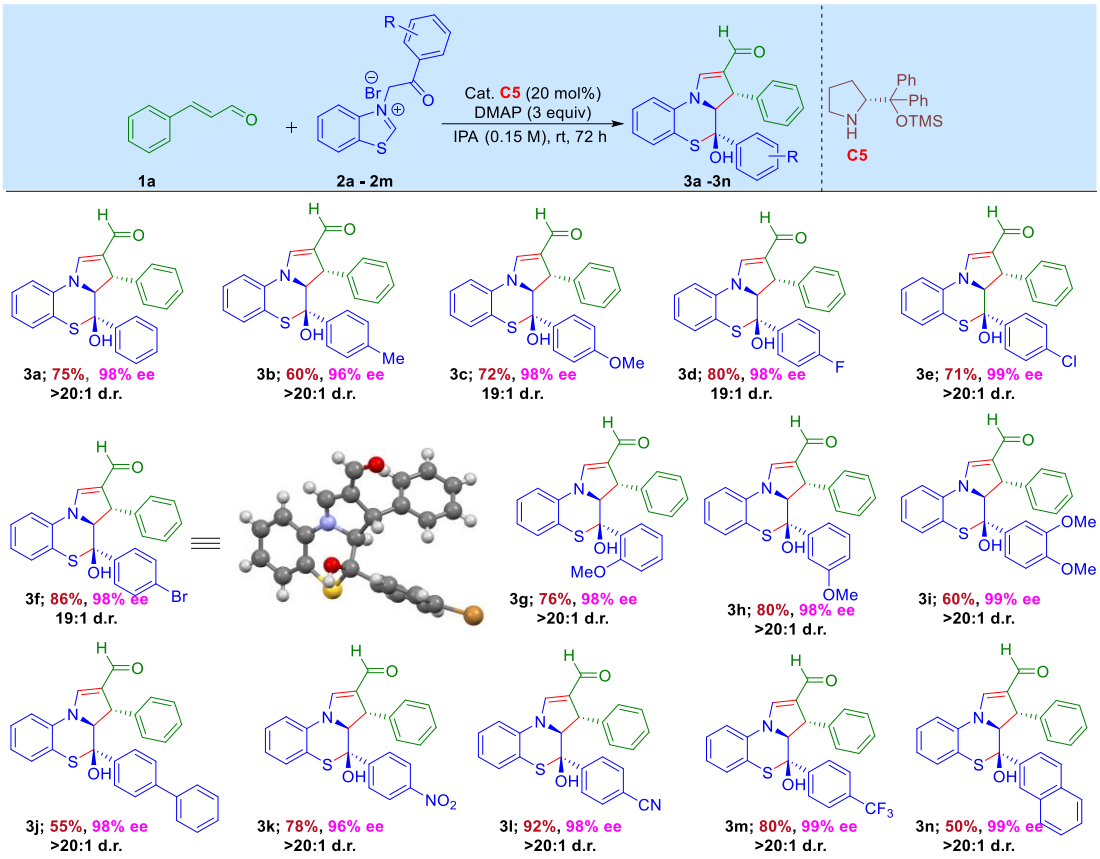

[a]Reaction conditions: **1a** (0.3 mmol), **2a** (0.3 mmol), DMAP (3 equiv), Chiral catalyst (20 mol%), Solvent (0.15 M) at 72 h. [b]Isolated yield. [c]D.r. ratio was determined by ^{1}H NMR using a crude reaction mixture. [d]*Ee* determined by HPLC. The absolute configuration of the product **3f** was determined to be (3*S*,3*aS*,4*S)* by single-crystal XRD analysis. The absolute configurations of other products were assigned to be (3*S*,3*aS*,4*S)* based on same analogy.

The reaction was also suitable for the substitution at the 3-position of *α,β*-unsaturated aldehydes such as furan, anthracene, and biphenyl group instead of phenyl ring, and the domino reaction produced **3y-3aa** in 62 -78% yields with 88-98% ee. Delightfully, the alkyl substitution at the 3-position of α,β-unsaturated aldehydes also delivered the products **3ab-3ad** in moderate to good yields with 80-96% ee.

Scheme 2.21 Substrate Scope of α, β-Unsaturated Aldehydes[a]

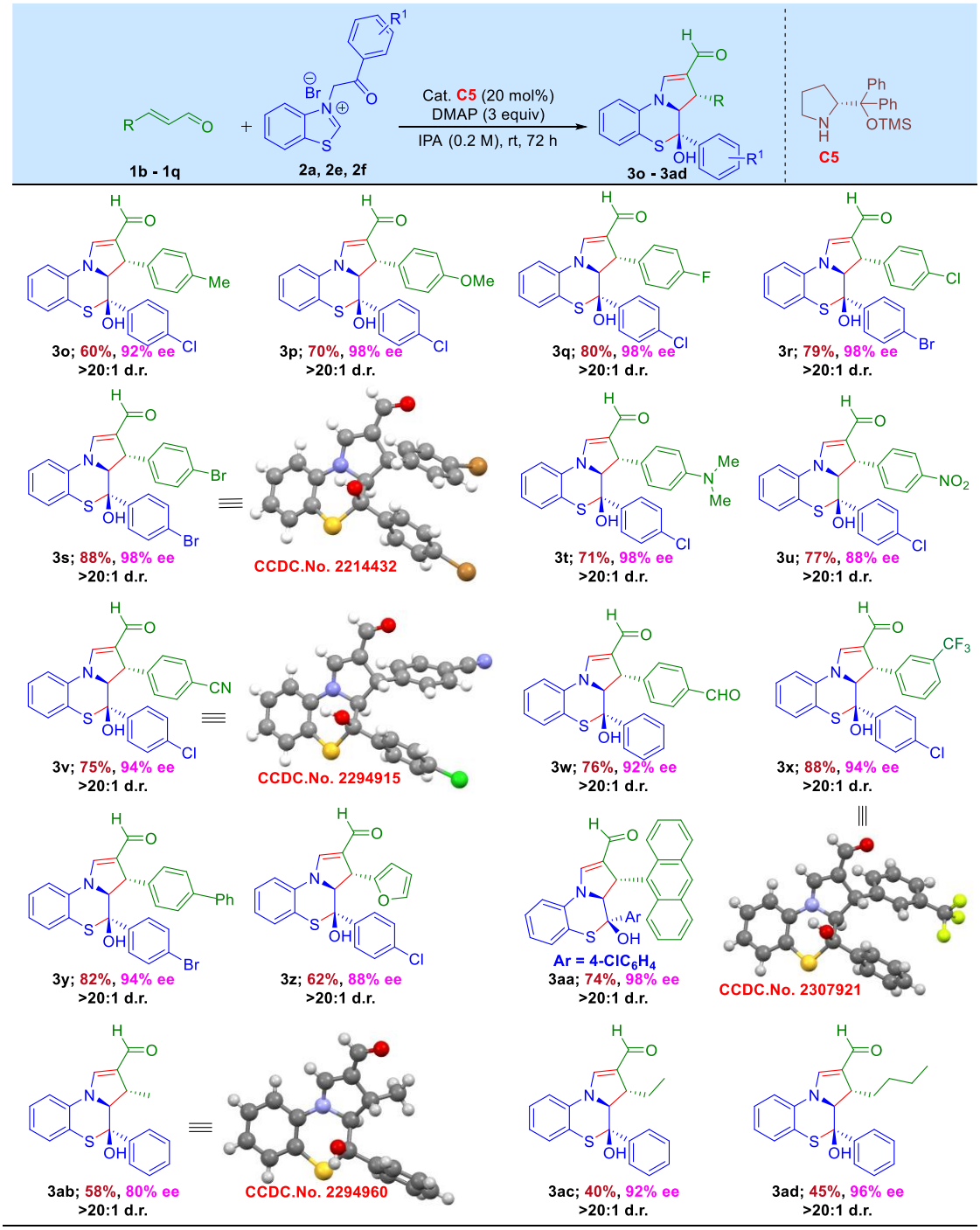

[a]Reaction conditions: **1a** (0.3 mmol), **2a** (0.3 mmol), DMAP (3 equiv), Chiral catalyst (20 mol%), Solvent (0.15 M) at 72 h. [b]Isolated yield. [c]D.r. ratio determined by ^{1}H NMR. [d]*Ee* determined by HPLC. The absolute configuration of the products **3s, 3v, 3x,** and **3ab** were determined to be (3*S*,3*aS*,4*S)* by single-crystal XRD analysis. The absolute configurations of other products were assigned to be (3*S*,3*aS*,4*S)* based on same analogy.

2.6. CONTROL EXPERIMENTS

Several control experiments have been performed to investigate the reaction mechanism. When cinnamaldehyde **1a** reacted with benzothiazolium salt **2f** with **C1**, the reaction gave a 73% yield with 12% ee, along with 19:1 d.r. (Scheme 2.22-i). To investigate the role of the secondary amine (-NH-) in the catalyst, the reaction was performed using *N*-Boc-protected catalysts **C6** and **C7**; however, the reaction yielded only 45% yield of **C6** and 14% yield of **C7**. Notably, both reactions produced only racemic products (Scheme 2.22-ii & iii), which indicates that the free NH group in the catalyst plays a crucial role in producing enantioselective products. When the reaction performed without a base did not progress the reaction which shows that the base plays a major role in the product formation (Scheme 2.22-iv). The background reaction occurs when the reaction is carried out only with the base (Scheme 2.22-v). Particularly, compared with **C1**, **the** bulky phenyl and silyl ether group in **C5** controls the reactivity and drives the enantio- and diastereoselective transformation to afford the products with good yields and high enantioselectivities. This reaction proceeds *via* chiral iminium ion formation rather than a simple base-catalyzed background reaction.

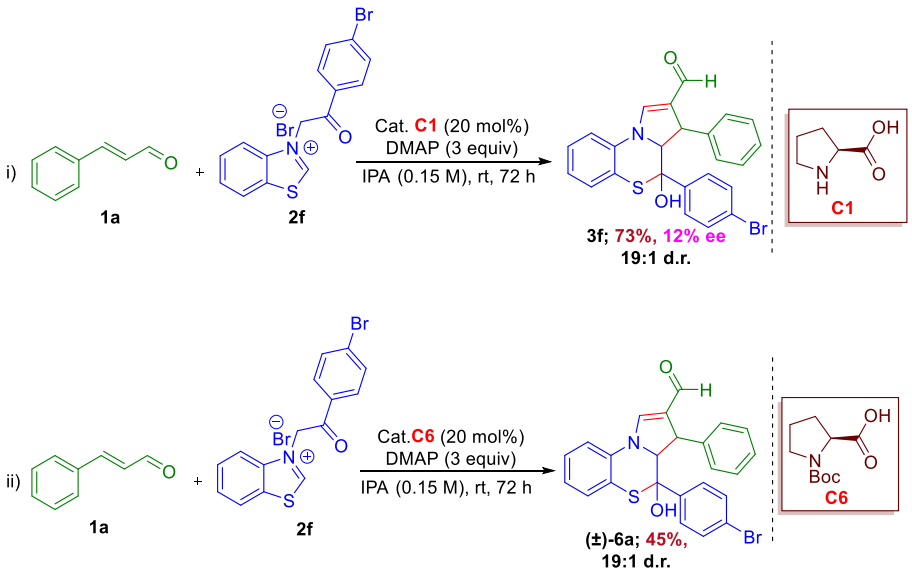

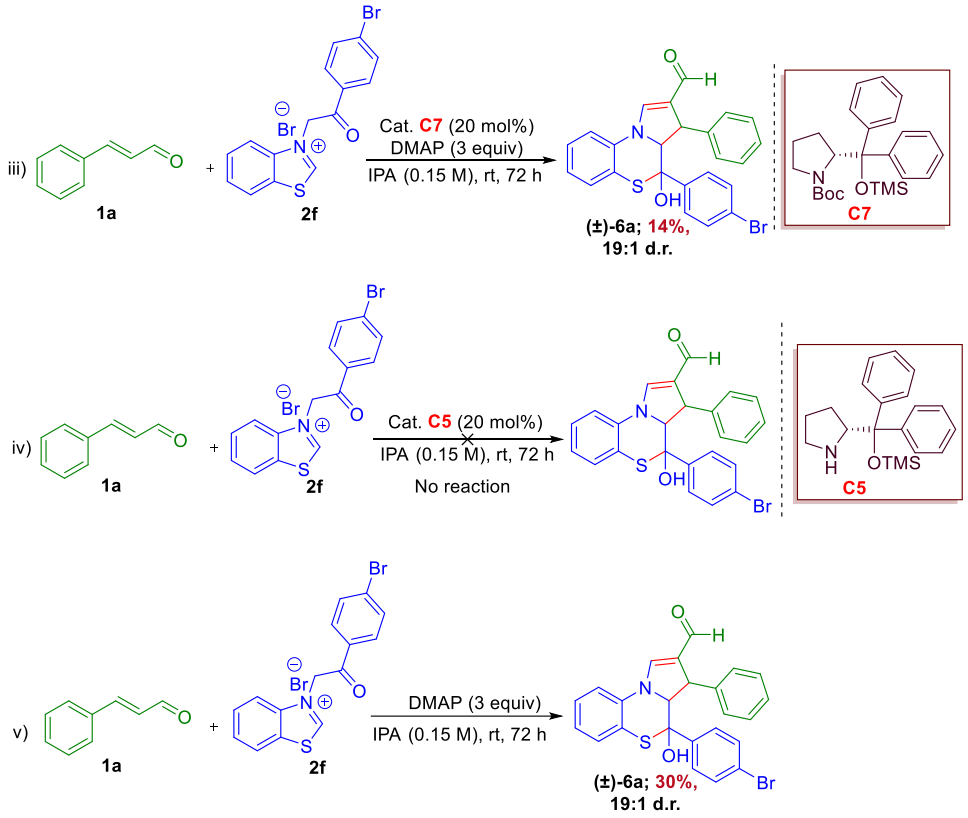

Scheme 2.22 Control experiments for the enantioselective synthesis of pyrrolo-thiazine-2-carbaldehydes.

2.7. DFT CALCULATIONS & MECHANISTIC STUDIES

All the quantum chemical calculations were carried out using the G16 software package.[167] Density Functional Theory (DFT) based M06-2X Minnesota functional[168] in conjunction with LANL2DZ an Effective Core Potentials (ECP) basis[169] set for Br and 6-31G(d,p) basis[170] set for rest of the atoms is used to relax all the geometries to their corresponding global minimum. All geometries are checked as true minima by vibrational analysis (non-imaginary frequencies). Solvent effects are introduced in the polarizable continuum model (PCM) using isopropyl alcohol (2-propanol) as a solvent. Transition state theory has been adopted to trace all the transition states involved in the mechanism, all characterized by a single imaginary frequency criterion. Intrinsic Reaction coordinate (IRC) calculations verify all the transition states.

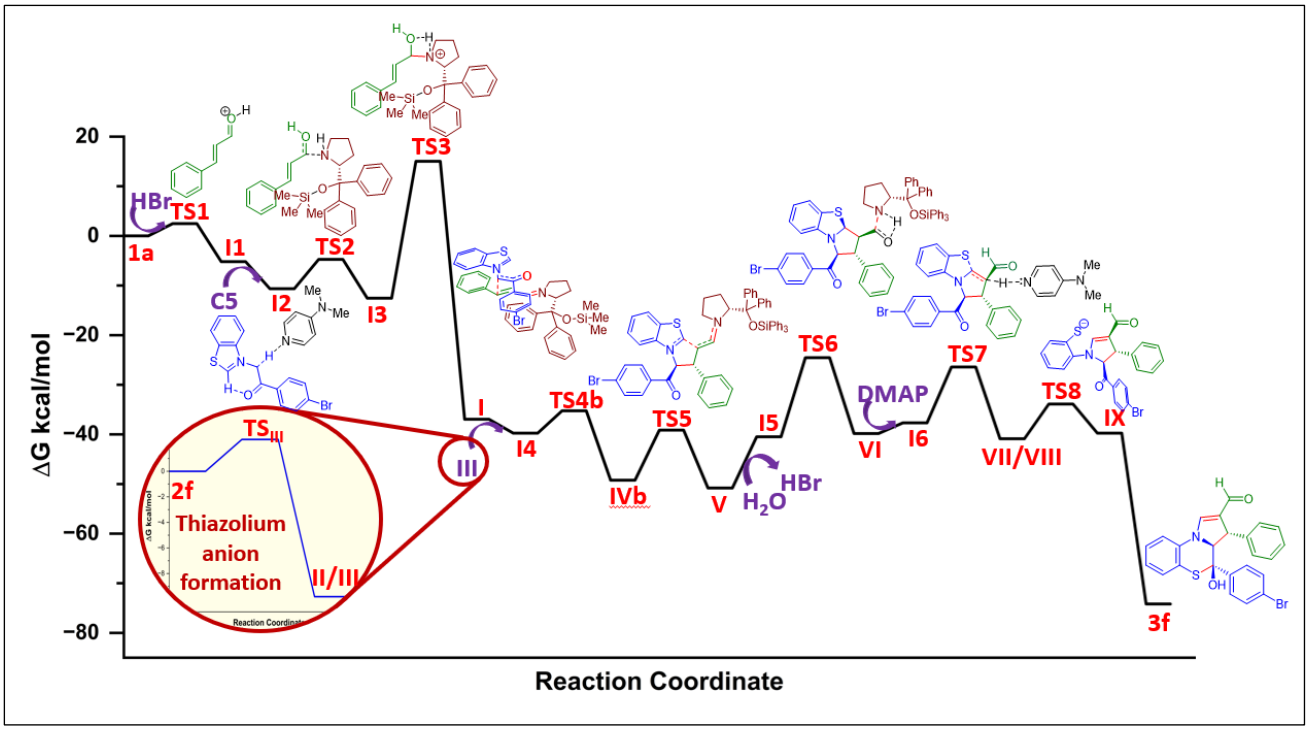

Figure 2.3. Complete reaction profile diagram of the reaction of cinnamaldehyde **1a** and benzothiazolium salt **2f** with *(R)*-diphenylprolinol trimethylsilyl ether **C5** computed at the M06-2X/6-31G(d,p) level of theory using isopropyl alcohol as a solvent.

DFT studies were kick-started by probing the formation of iminium ion intermediate **I** from **1a**. Protonation of **1a** by in situ generated HBr or protonated DMAP proceeds through transition state **TS1** with an activation barrier ($E^{\ddagger}$) 2.46 kcal/mol. Then, the reaction of the protonated **1a** with chiral catalyst **C5** (**TS2**, $E^{\ddagger}$ = -4.74 kcal/mol) and elimination of water (**TS3**, $E^{\ddagger}$ = 15.03 kcal/mol) will lead to the formation of iminium ion intermediate **I**, which is a rate-determining step for the entire reaction cycle. Meanwhile, proton abstraction by DMAP from benzothiazolium salt **2f** gives thiazolium anion **II/III**. This reaction occurred through an activation barrier of 2.49 kcal/mol **TSIII**. The next step proceeds with the reaction between the benzothiazolium salt anions **II/III** and iminium ion **I** to form 1,4-addition intermediate **IV** by forming a new *C-C* bond. The formation of intermediate **IV** is a chiral induction step through the benzothiazolium anion **III** approach from the *Si*-face of iminium ion **I**. This chiral induction step led to the formation of favorable (**TSIVa-d**) and unfavorable (**TSIVe-h**)

diastereomeric transition states (Figure 2.3). Analysis of the transition states of these isomers shows that intermediate **IVb** (red line, Figure 2.4) has a lower activation barrier ($E^{‡}$ = -35.26 kcal/mol), which is a more favorable **TS** than its competing counterparts (Figure 2.4).

Favorable transition states

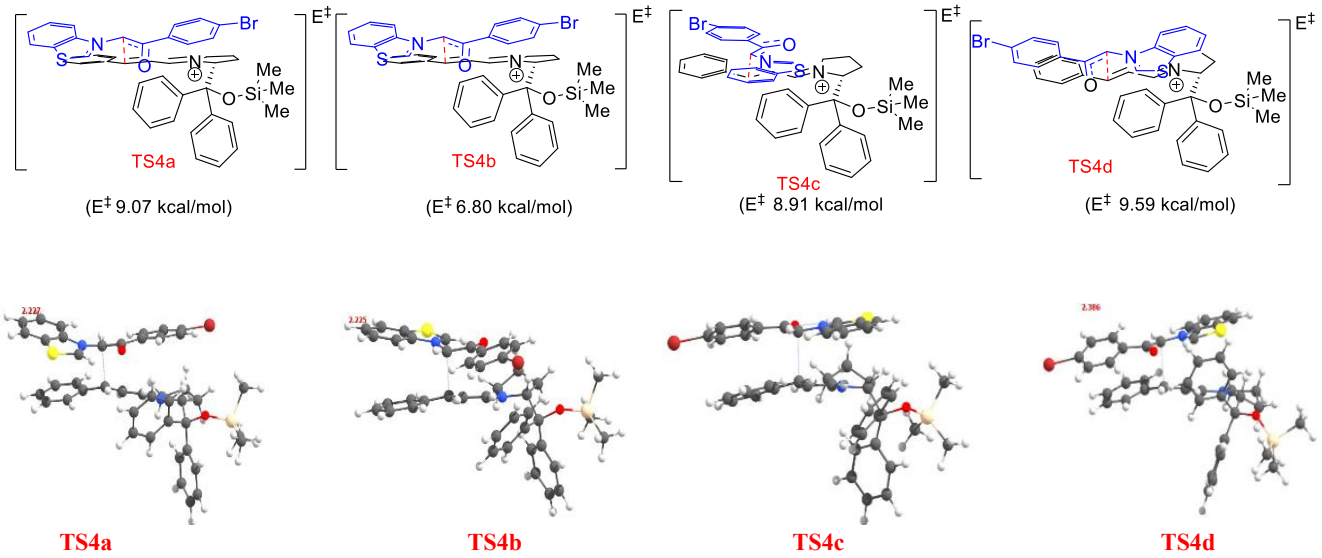

Unfavorable transition states

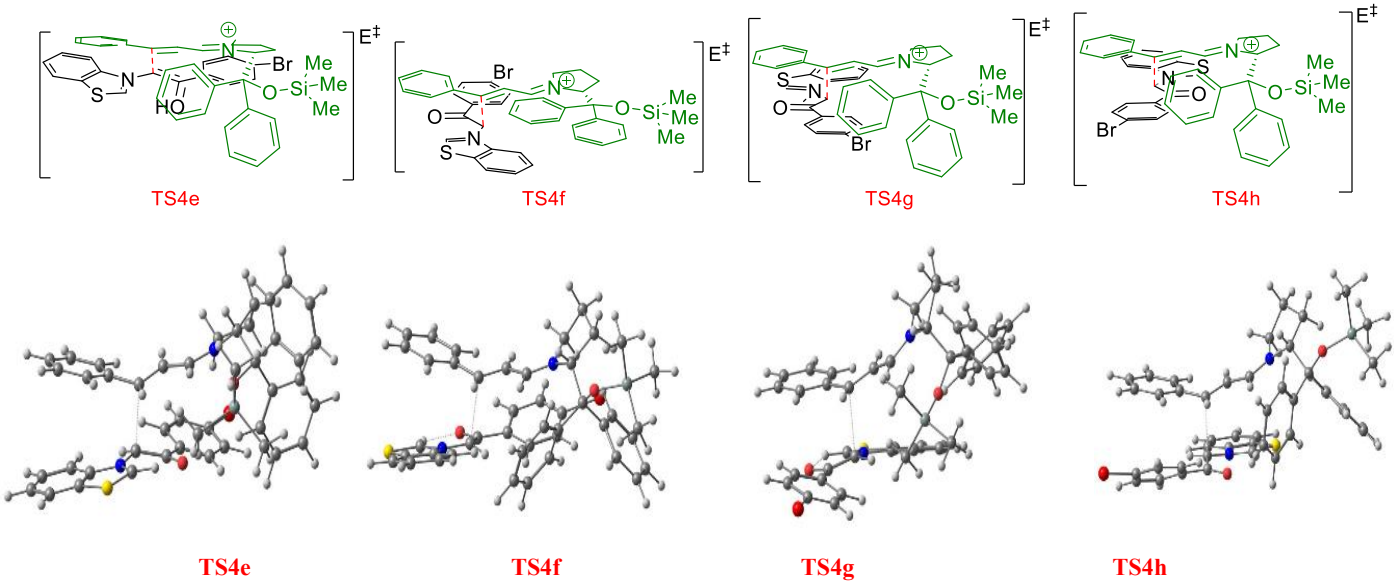

Figure 2.4. 2D and 3D diastereomeric transition state diagrams for various isomers formed during C-C bond formation between **I** and **II/III** computed at the M06-2X/6-31G(d,p) level of theory using isopropyl alcohol as a solvent.

It is clear from the activation barriers that the possibility of reactions to form **IVa, c-h** is very limited compared to the formation of the **IVb** isomer. Furthermore, the benzothiazolium ring's dearomatization leads to forming a five-membered hydropyrrolo-thiazole ring intermediate. This cyclization of **IVb** facilitated the formation of intermediate **V** through **TS5** with $E^{\ddagger}$ = -39.15 kcal/mol.

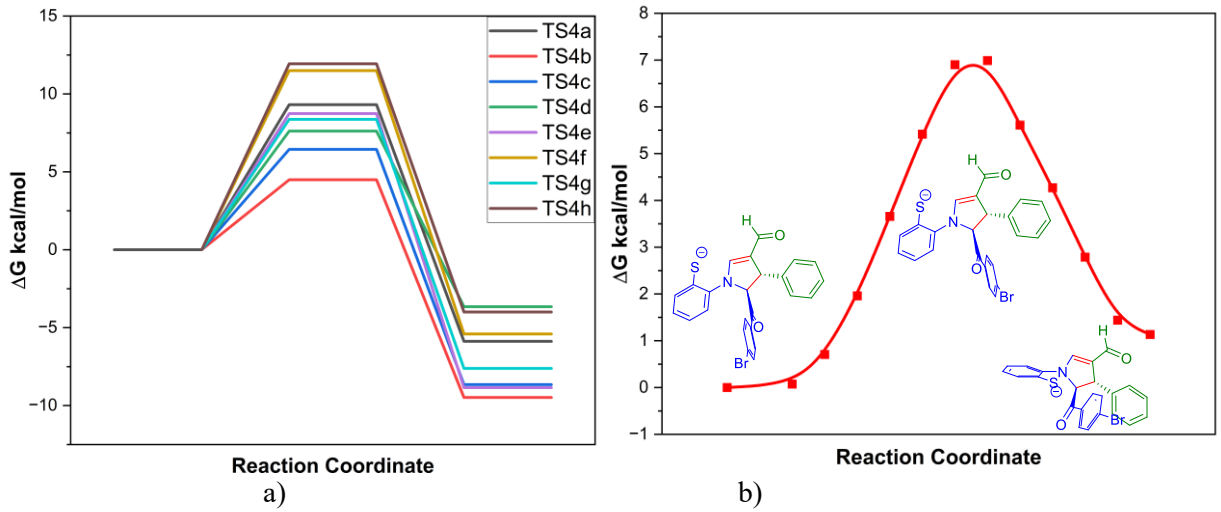

Figure 2.5. a) Reaction profiles of various isomers formed during C-C bond formation between **I** and **II/III** computed at the M06-2X/6-31G(d,p) level of theory; **b**) Rotational barrier for *C*-*N*-bond rotation of intermediate **VIII** to form **IX** computed at the M06-2X/6-31G(d,p) level of theory using isopropyl alcohol as a solvent.

Hereafter, both 1,4-addition and dearomatization steps are referred to as 1,3-dipolar cycloaddition steps. The catalyst regeneration step was followed by water, which was present in the reaction mixture and gave rise to intermediate **VI**. Overall, this step goes through an activation barrier of -24.57 kcal/mol **TS6**. Intermediate **VI** is responsible for the stereoselectivity of the final product. Deprotonation of **VI** with DMAP (**TS7**, $E^{\ddagger}$ = -26.42 kcal/mol) leads to the ring opening at sulfur to form **VII/VIII,** followed by *C*-*N*-bond rotation (**TS8**, $E^{\ddagger}$ = -33.89 kcal/mol) to give intermediate **IX** (Figure 2.5b). The intermediate **IX**'s reaction with in-situ generated HBr or protonated DMAP can form two products. One is the formation of the seven-membered product **IX7** by a 1,2-

addition with aldehyde carbon. The second possibility is the formation of six-membered product **3f** by 1,2-addition of a ketone carbon, which is formed without a transition state or barrier-less pathway (Figure 2.6).

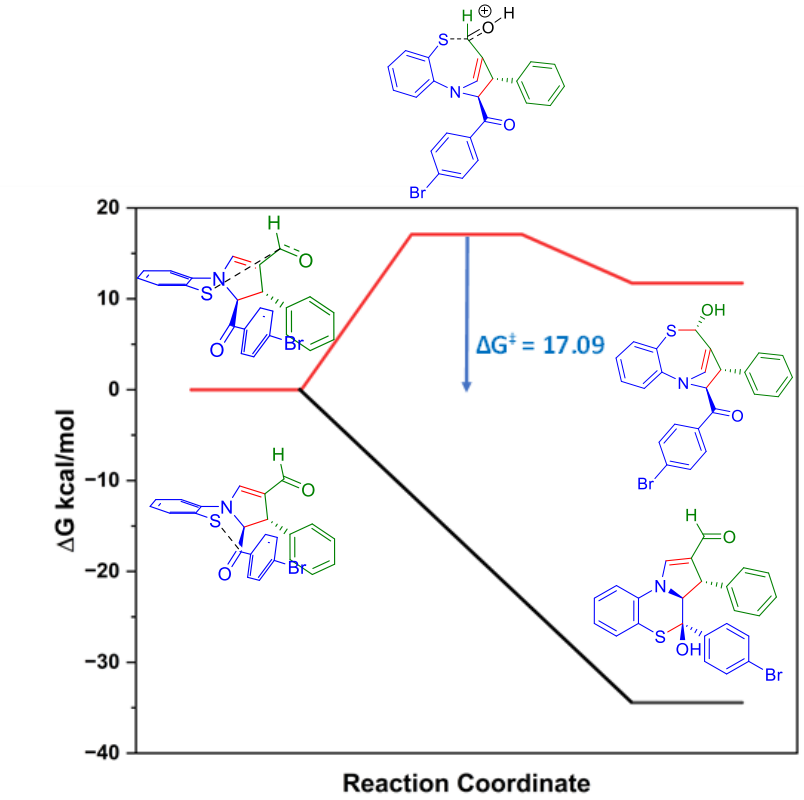

Figure 2.6. The selectivity for **3f** formation (*via* a 6-membered ring) over **IX7** (*via* a 7-membered ring) in the presence of HBr was computed at the M06-2X/6-31G(d,p) level of theory using IPA as a solvent.

In the case of seven-membered ring **IX7** formation, the intermediate requires a high activation energy ($\mathbf{TS_{IX7}}$ $E^{‡}$ = 17.09 kcal/mol), which is much higher than needed for the formation of six-membered product **3f**. The negatively charged sulfur ion attacks the ketone through the *Si*-face to form a six-membered ring, followed by spontaneous protonation to give the final product **3f**. The absence of TS confirmed the spontaneity of these steps despite many trials.

2.8 SYNTHETIC TRANSFORMATIONS OF PYRROLO-THIAZINE

Different functional group transformations were performed to demonstrate the synthetic utility and practicability of **3f**. First, treatment of **3f** with TMSCl in the presence of imidazole afforded **5a** in 94% yield and 96% ee in the experimental procedure (Scheme 2.23). When compound **3f** was treated with DDQ, it provided sequential reactions such as oxidation, ring opening, C-N-bond rotation, and sulfa-Michael addition followed by DDQ oxidation of the benzylic carbon furnished **5b** in 80% yield (Scheme 2.23).

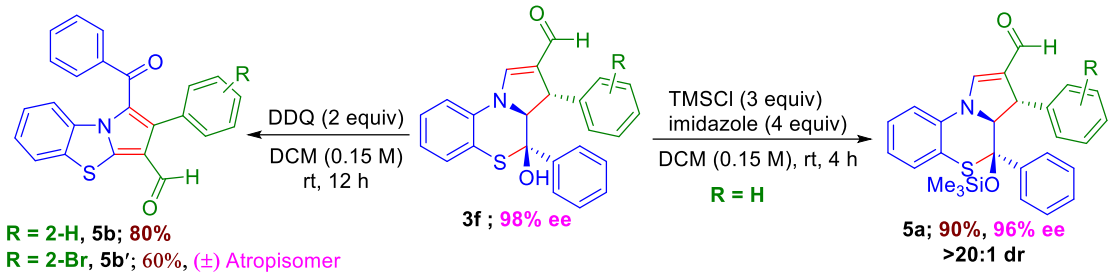

Scheme 2.23 Synthetic transformation of pyrrolo-thiazine-2-carbaldehyde **3f**.

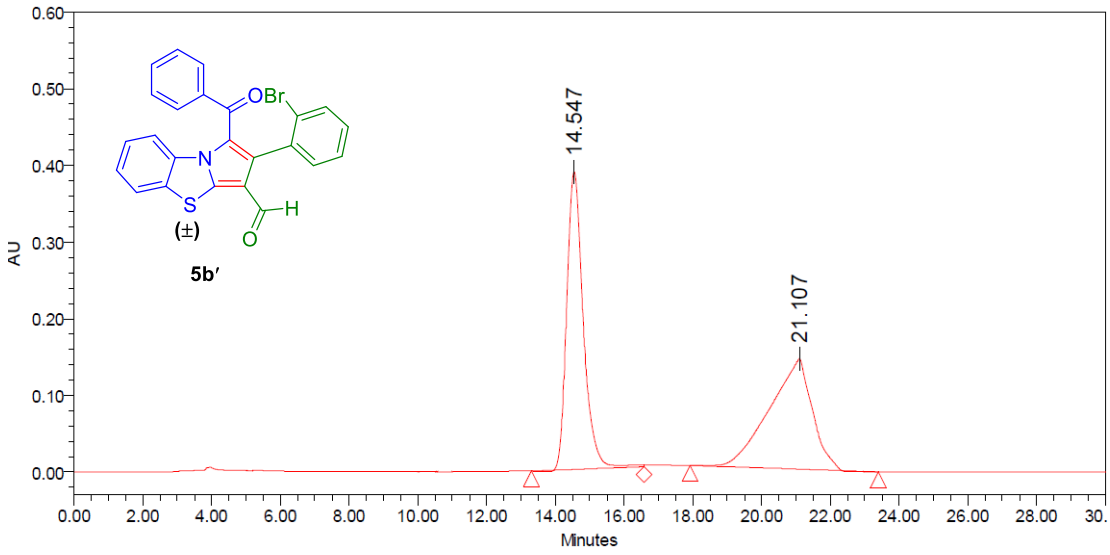

Peak Results

	Name	RT	Area	Height	% Area	% Height
1		14.547	12941155	388529	50.9192	72.9784
2		21.107	12473938	143860	49.0808	27.0216
Sum			25415093.4		100.0000	100.0000

Figure 2.7 HPLC chromatogram for compound (±)-**5b'**

The chiral product **3f** substitution R = 2-Br in DDQ oxidation reaction provides the oxidized product **5b'** surprisingly, gives atropoisomeric product in 60% yield, with a racemic mixture which was successfully confirmed by chiral HPLC using chiralcel OD-H chiral column (Figure 2.7). The plausible reaction mechanism has been proposed in Scheme 2.24.

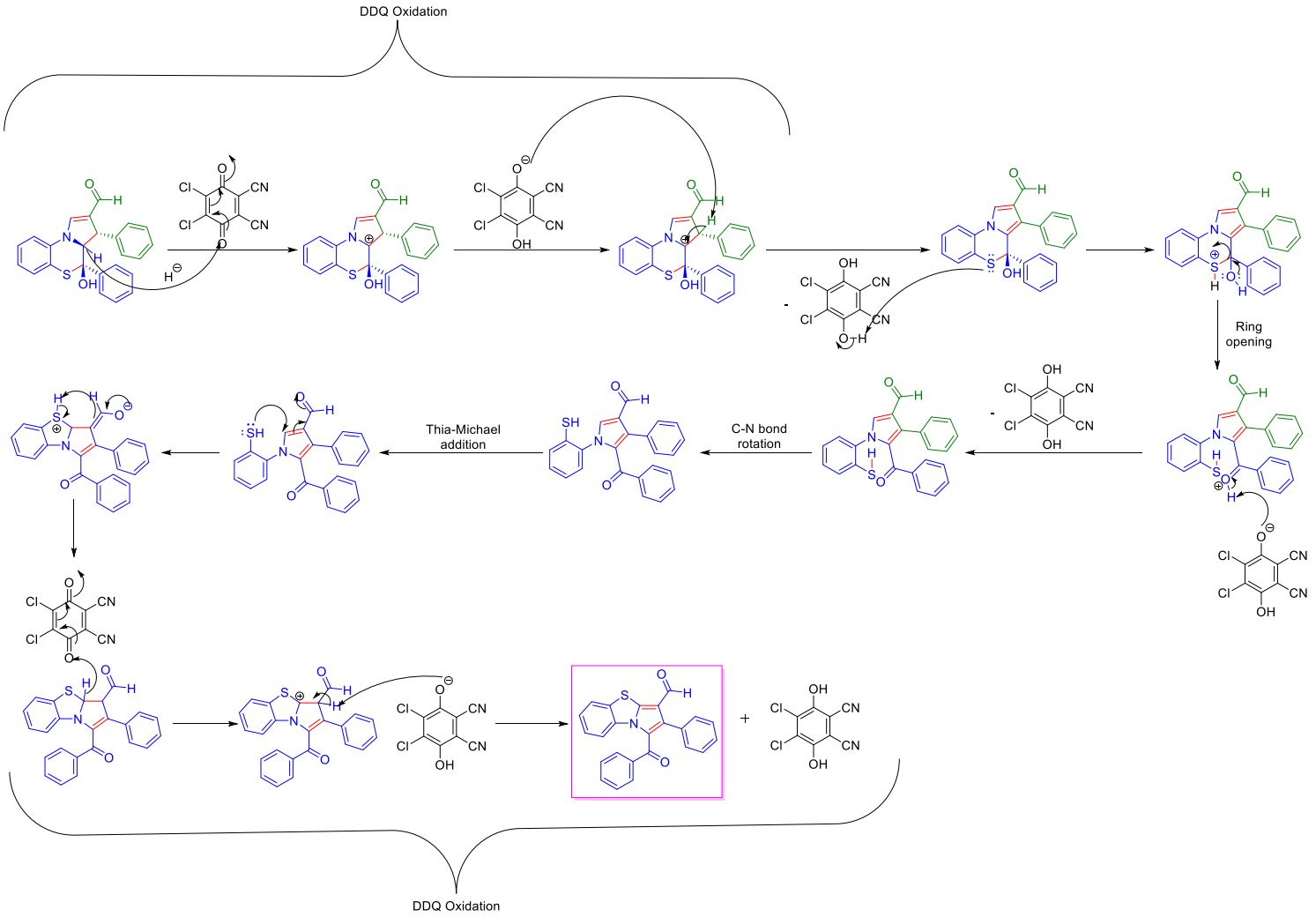

Scheme 2.24 Plausible reaction mechanism for the synthesis of **5b** and **5b'** from **3f**.

2.9 GRAM SCALE SYNTHESIS OF PYRROLO-THIAZINE (3f)

To check the scalability of this domino methodology, a gram-scale reaction was performed using cinnamaldehyde **1a** (3 mmol, 396 mg, 374 μL), benzothiazolium salt

2f (3 mmol, 1.24 g) and DMAP (9 mmol, 1.1 g) under the optimized reaction conditions. The reaction furnished the desired chiral product **3f** in 64% yield (0.9 g) without losing enantio- and diastereoselectivity (Scheme 2.25).

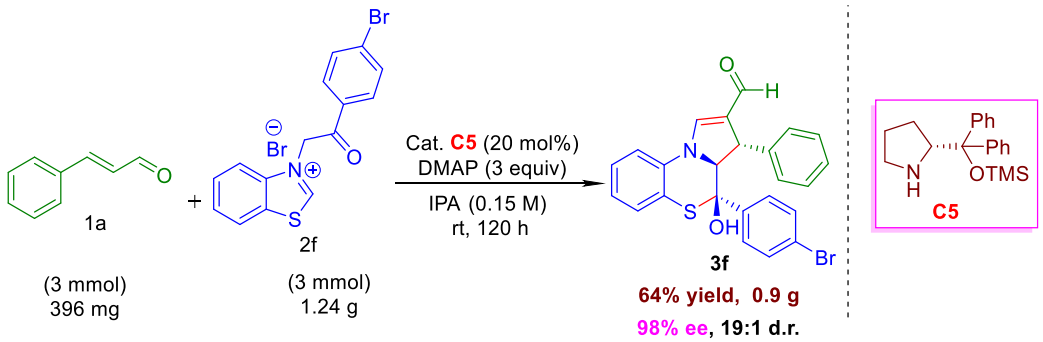

Scheme 2.25 Gram scale synthesis of pyrrolo-thiazine-2-carbaldehyde **3f**.

2.10 PLAUSIBLE REACTION MECHANISM

Based on the control experiments and DFT studies, a plausible reaction mechanism has been proposed which is discussed in section 2.7 and shown in Scheme 2.26.

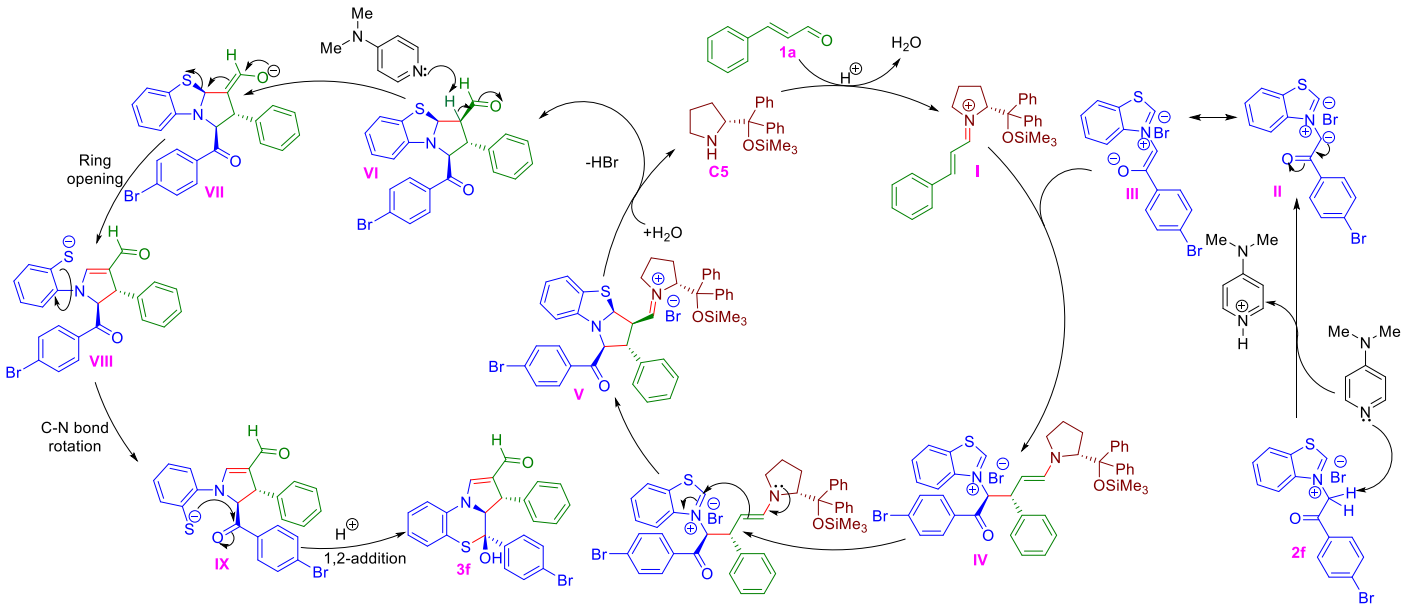

Scheme 2.26 Plausible reaction mechanism for the synthesis of pyrrolo-thiazine-2-carbaldehydes.

2.11 MOLECULAR DOCKING STUDY

The pyrrolo[1,4]thiazine cores show various biological activities (Figure 1.1)[146-152] Inspired by these known molecules, an in-silico approach was investigated for the biological activity of the synthesized chiral pyrrolo[1,2-*d*][1,4]thiazine-2-carbaldehydes **3**. The non-small cell line lung cancer protein (B-Raf kinase) is chosen as the targeted protein retrieved from the protein data bank (PDB), available at https://www.rcsb.org/ with reference ID 6B8U. The active region of the protein is obtained by CASTP[171] and COACH meta servers.[172] The ligands were converted into the 3D format and docked with protein using the Schrodinger software package utilizing Maestro.[173,174] The 3D docking pose and 2D interaction plots are visualized using Discovery Studio.[175]

A total of 23 chiral molecules were studied against RAF kinases protein anticancer; among six chiral molecules showed better interaction with RAF kinases protein. The binding affinities of the 23 ligands for the anticancer protein are presented in Table 2.6. In addition to the previous literature, the amino acid residues in the active region of the anticancer protein are Glu 501, Gln 530, Cys 532, Ser 536, Asp 594, and Phe 595. From (Table 2.6), compounds **3j**, **3n**, **3y**, **3v**, **3g**, and **3z** have numerically more significant interaction energies, with energy values of **-7.9, -7.6, -7.4, -6.4, -6.3** and **-6.0** kcal/mol. The 3D docked pose and 2D interaction plots are shown in (Figure 2.8). Compound **3j** has one hydrogen bonding interaction (Cys 532) and two π–π stacking interactions (Trp 531). Compound **3j** has hydrogen bonding interactions with Ser 536, π-π stacking with Trp 531 and Phe 595, and π-alkyl interactions with ILE 463, Val 471, and Ala 481 (Figure 2.8). Compound **3n** has one hydrogen bonding interaction with Ser 536 and π-π stacking with Trp 531 and Phe 595. Specifically, compound **3n** has a π-sulfur bond

with the Trp 531 residue. Compound **3g** has one π-sulfur bond (Trp 531) and three π-π stacking interactions (Trp 531, Phe 585, and Phe 595). From table 2.6, figure 2.8 out of 23 chiral molecules, six molecules are found to have higher binding affinity against B-Raf kinase proteins, inhibiting the active region of the kinase protein, acting as a suitable RAF inhibitor, and it may exhibit the anticancer activity.

Table 2.6. Docking score for selected compounds

S. No.	Entry	Docking score	S. No.	Entry	Docking score
1	**3a**	-5.76	13	**3o**	-5.26
2	**3b**	-5.92	14	**3p**	-5.77
3	**3c**	-5.22	15	**3q**	-5.71
4	**3d**	-5.38	16	**3r**	-5.62
5	**3e**	-4.76	17	**3s**	-4.94
6	**3f**	-5.44	18	**3t**	-4.86
7	**3g**	**-6.33**	19	**3u**	-4.56
8	**3i**	-4.09	20	**3v**	**-6.40**
9	**3j**	**-7.90**	21	**3x**	-4.58
10	**3k**	-5.94	22	**3y**	**-7.40**
11	**3l**	-5.41	23	**3z**	**-6.09**
12	**3n**	**-7.65**			

a)

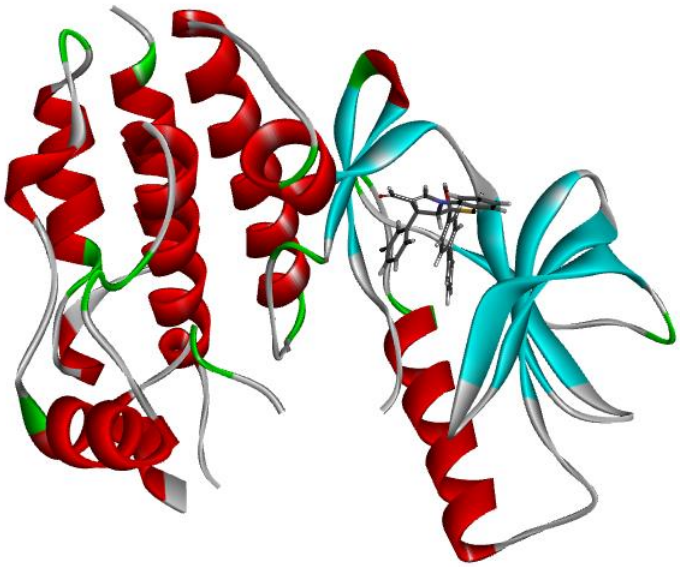

b)

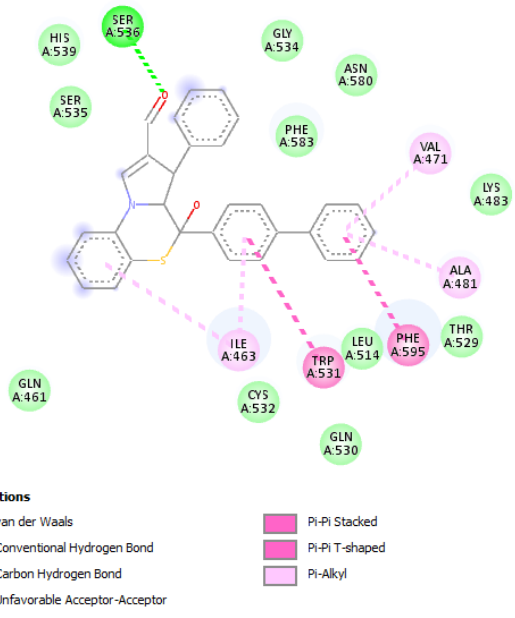
SER A:536
HIS A:539
GLY A:534
ASN A:580
SER A:535
PHE A:583
VAL A:471
LYS A:483
ALA A:481
THR A:529
ILE A:463
LEU A:514
PHE A:595
TRP A:531
GLN A:461
CYS A:532
GLN A:530
Interactions
van der Waals
Conventional Hydrogen Bond
Carbon Hydrogen Bond
Unfavorable Acceptor-Acceptor
Pi-Pi Stacked
Pi-Pi T-shaped
Pi-Alkyl

c)

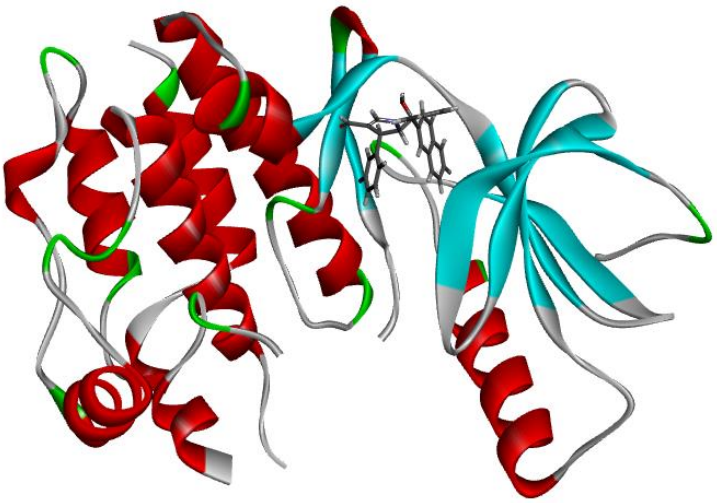

d)

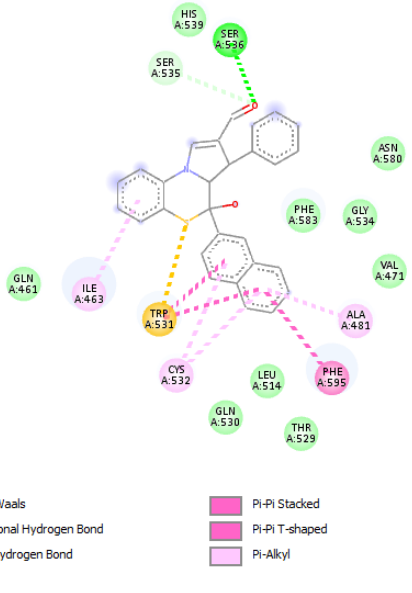
HIS A:539
SER A:536
SER A:535
ASN A:580
PHE A:583
GLY A:534
VAL A:471
GLN A:461
ILE A:463
TRP A:531
ALA A:481
CYS A:532
LEU A:514
PHE A:595
GLN A:530
THR A:529
Interactions
van der Waals
Conventional Hydrogen Bond
Carbon Hydrogen Bond
Pi-Sulfur
Pi-Pi Stacked
Pi-Pi T-shaped
Pi-Alkyl

e)

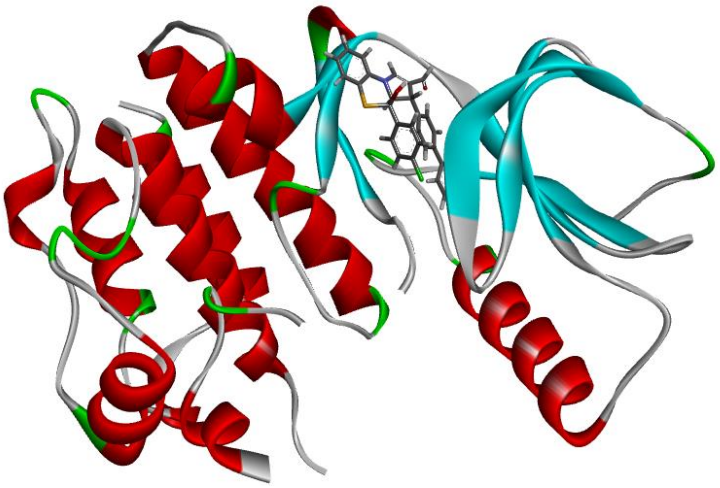

f)

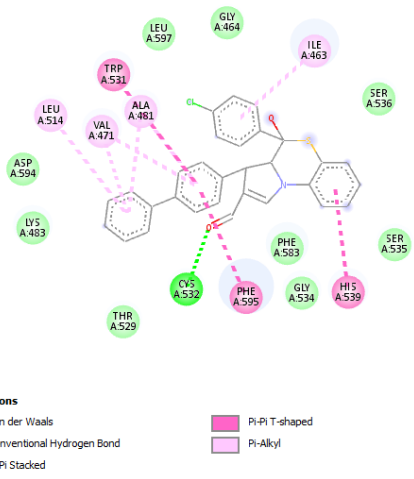
LEU A:597
GLY A:464
ILE A:463
TRP A:531
SER A:536
LEU A:514
ALA A:481
VAL A:471
ASP A:594
LYS A:483
PHE A:583
SER A:535
CYS A:532
PHE A:595
GLY A:534
HIS A:539
THR A:529
Interactions
van der Waals
Conventional Hydrogen Bond
Pi-Pi Stacked
Pi-Pi T-shaped
Pi-Alkyl

g)

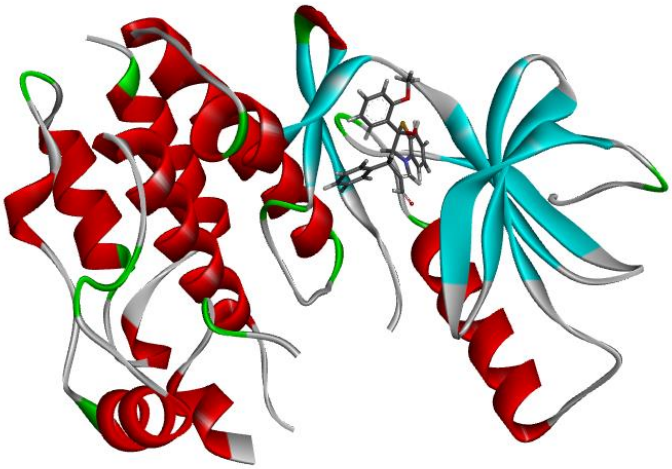

h)

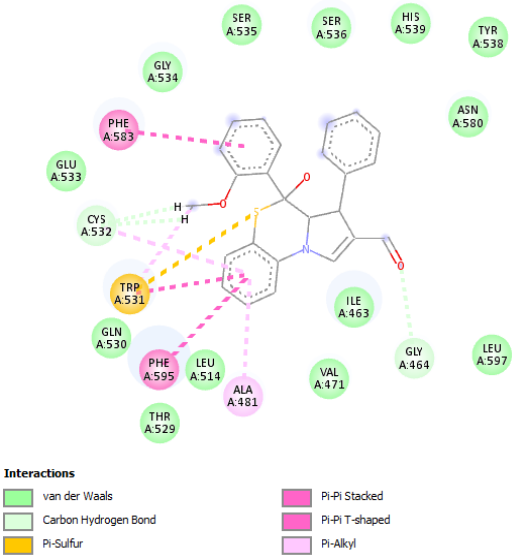
SER A:535
SER A:536
HIS A:539
TYR A:538
GLY A:534
ASN A:580
PHE A:583
GLU A:533
CYS A:532
TRP A:531
ILE A:463
GLN A:530
PHE A:595
LEU A:514
GLY A:464
LEU A:597
VAL A:471
ALA A:481
THR A:529
Interactions
van der Waals
Carbon Hydrogen Bond
Pi-Sulfur
Pi-Pi Stacked
Pi-Pi T-shaped
Pi-Alkyl

i)

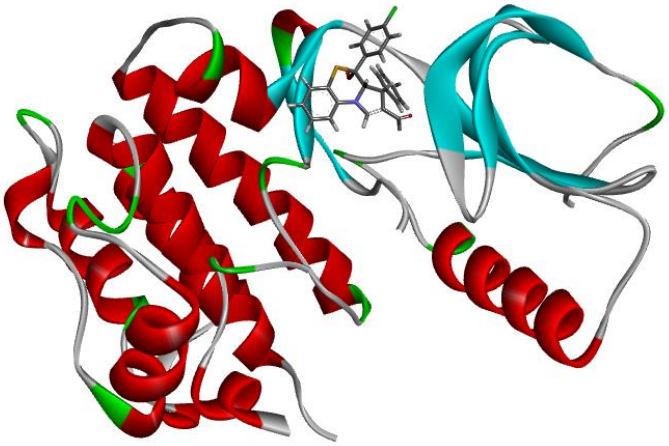

j)

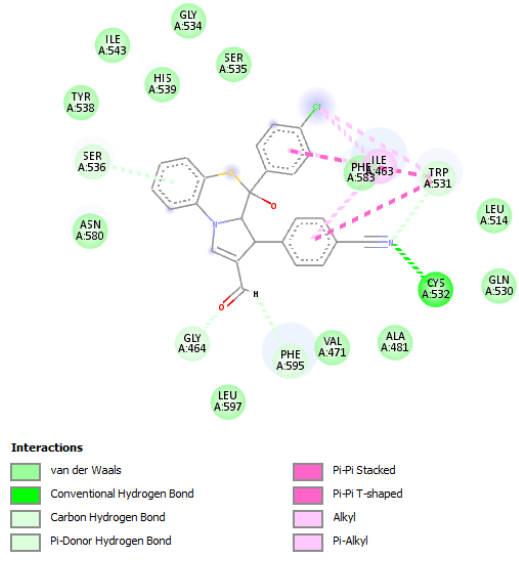
GLY A:534
ILE A:543
SER A:535
HIS A:539
TYR A:538
SER A:536
ASN A:580
PHE A:583
ILE A:463
TRP A:531
LEU A:514
CYS A:532
GLN A:530
GLY A:464
PHE A:595
VAL A:471
ALA A:481
LEU A:597
Interactions
van der Waals
Conventional Hydrogen Bond
Carbon Hydrogen Bond
Pi-Donor Hydrogen Bond
Pi-Pi Stacked
Pi-Pi T-shaped
Alkyl
Pi-Alkyl

k)

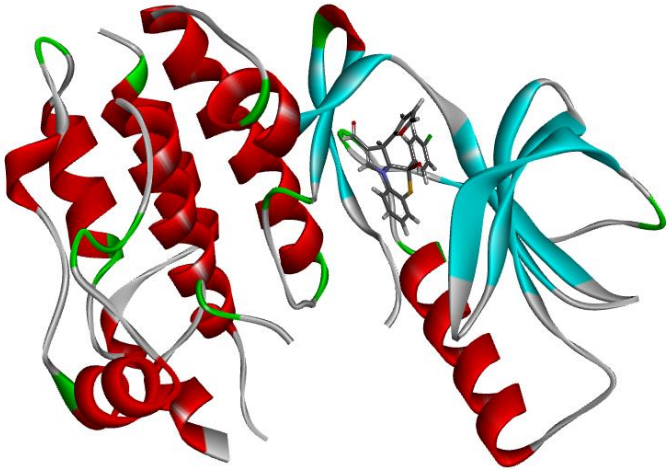

l)

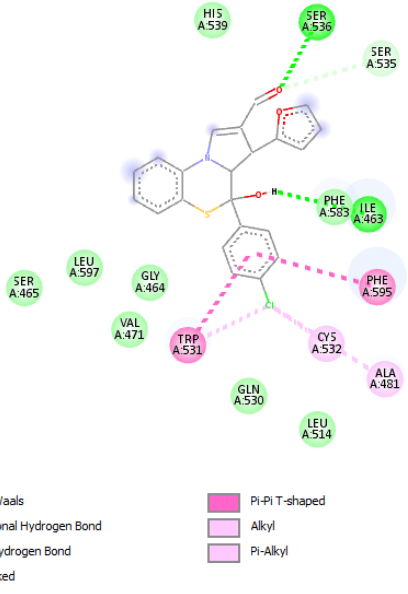
HIS A:539
SER A:536
SER A:535
PHE A:583
ILE A:463
LEU A:597
SER A:465
GLY A:464
PHE A:595
VAL A:471
TRP A:531
CYS A:532
ALA A:481
GLN A:530
LEU A:514
Interactions
van der Waals
Conventional Hydrogen Bond
Carbon Hydrogen Bond
Pi-Pi Stacked
Pi-Pi T-shaped
Alkyl
Pi-Alkyl

Figure 2.8 a) 3D Binding pattern of **3j** within the active site of 6b8u. b) 2D binding interactions of **3j** 6b8u active site. c) 3D Binding pattern of **3n** within the active site of 6b8u. d) 2D binding interactions of **3n** 6b8u active site. e) 3D Binding pattern of **3y** within the active site of 6b8u. f) 2D binding interactions of **3y** 6b8u active site. g) 3D Binding pattern of **3g** within the active site of 6b8u. h) 2D binding interactions of **3g** 6b8u active site. i) 3D Binding pattern of **3v** within the active site of 6b8u. j) 2D binding interactions of **3v** 6b8u active site. k) 3D Binding pattern of **3z** within the active site of 6b8u. l) 2D binding interactions of **3z** 6b8u active site.

2.12 FLUORESCENT STUDIES

To explore the usefulness of pyrrolo[1,2-*d*][1,4]thiazine-2-carbaldehydes **3**, photophysical properties of the selected chiral molecules **3** (**3c, 3f, 3k, 3u, 3w, 3x, 3z** and **3ab**) have been examined (Figure 2.9). Under UV light irradiation (352 nm), molecules show blue fluorescence. The absorption spectra show bands at 352 nm (Figure 2.9a), while the emission spectra exhibited bands with a maximum range of 400-550 nm (Figure 2.9b).

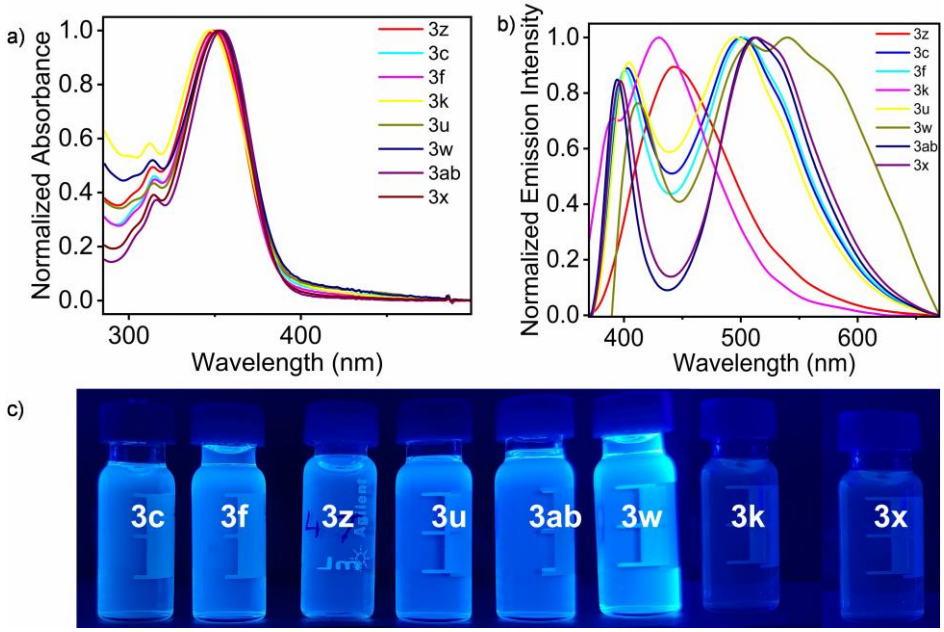

Figure 2.9. (**a**) Absorption spectra in CH_3CN (50 μm) (**b**) Fluorescence spectra in CH_3CN (50 μm) (λ_{ex} = 352 nm). (**c**) Fluorescence image in CH_3CN (λ_{ex} = 365 nm).

The emission of the chiral molecules has been shown fluorescence emission in the presence of an electron-donating group at the *para* position (**3c** and **3ab**), halogen substitution at the *para* position (**3f**), electron-withdrawing substitution at the *meta* and *para* position (**3k, 3u, 3w, 3x**) and 3-furan cinnamaldehyde substitution (**3z**). Due to the fluorescent nature of these chiral molecules, we expect that they may be used for various fluorescent organic materials.

2.13 CONCLUSION

- The first proline-derived organocatalytic asymmetric 1,3-dipolar cycloaddition/rearrangement of α,β-unsaturated aldehydes with benzothiazolium salts was accomplished for the synthesis of enantioenriched pyrrolo[1,2-d][1,4]thiazine-2-carbaldehydes.
- This domino approach yielded fluorescent emissive chiral compounds with three contiguous stereogenic centers and one chiral quaternary carbon center in a single step with high enantioselectivity.
- This strategy works well for a wide range of functional groups, notably aliphatic α,β-unsaturated aldehydes. DFT analysis helped us to understand the stability of the reaction intermediates.
- The formation of hydropyrrolo-thiazine intermediates **VI** (refer to Figure 2.1) is the rate-determining step in the entire catalytic cycle, which is responsible for the formation of pyrrolo[1,2-*d*][1,4]thiazine-2-carbaldehydes.
- An in-silico investigation indicated that pyrrolo[1,2-*d*][1,4]thiazine-2-carbaldehydes might exhibit anticancer activity.

- Owing to its biologically plausible potential, fluorescent activities, ease of operation, and manipulation of this methodology, this asymmetric domino reaction will find broad applications in organic synthesis.

2.14 EXPERIMENTAL SECTION

2.14.1 General information

All reactions were carried out in oven-dried reaction tubes. Benzothiazole, phenacyl bromides, and cinnamaldehydes were purchased from Sigma-Aldrich, Spectrochem, BLD, Carbanio, and Avra Synthesis Pvt. Ltd. The proline and DMAP were purchased from Spectrochem, Avra Synthesis Pvt. Ltd. and used directly as received. All the starting materials were synthesized according to the reported procedures. Reactions were monitored by thin-layer chromatography (TLC) using Merck silica gel 60 F_{254} precoated plates (0.25 mm) and visualized by UV fluorescence quenching using an appropriate mixture of ethyl acetate and hexanes as eluting solvent mixtures. Silica gel for column chromatography (particle size 100-200 mesh) was purchased from Avra Synthesis Pvt. Ltd. and used for column chromatography using hexanes and ethyl acetate mixture as eluent. Using a water bath, organic solutions were concentrated under reduced pressure on a Büchi, Heidolph rotary evaporator. ^{1}H and ^{13}C NMR spectra were recorded on a Bruker 400 or 500 MHz instrument.^{1}H NMR is reported relative to residual $CDCl_3$ (δ 7.26 ppm) or DMSO-d_6 (δ 2.50 ppm). ^{13}C NMR is reported close to residual $CDCl_3$ (δ 77.16 ppm) or DMSO-d_6 (δ 39.52 ppm). Chemical shifts were recorded in parts per million (ppm). Multiplicities are as indicated: s (singlet,) d (doublet,) t (triplet,) q (quartet,) quint (quintet), sext (sextet), sept (septet) dd (doublet

of doublet,) m (multiplet,) tt (triplet of triplet,) td (triplet of doublet). The coupling constant, *J*, is reported in Hertz.

Melting points were recorded on a Guna capillary melting point apparatus and were corrected with benzoic acid as a reference. FTIR spectra were recorded on a JASCO spectrometer and were reported in the frequency of absorption (cm^{-1}) using a dry KBr pellet. The polarimetry was recorded in P-2000 High Accuracy Digital Polarimeter - Jasco Inc. High-resolution mass spectra (HRMS) were recorded on Q-Tof Micro mass spectrometer. All the single crystal X-ray data was collected with a Bruker AXS (Kappa Apex 2) CCD diffractometer equipped with graphite monochromatic Mo (Kα) (λ = 0.7107 A) radiation source. The data were collected with 100% completeness for Θ up to 25º. ω and ϕ scans were employed to collect the data. The frame width for ω for was fixed to 0.5º for data collection. The crystal was solved by direct methods using Bruker SHELXS (Sheldrick, 1997). The Structure was refined using the Bruker SHELXTL (Version 6.12) software package. HPLC spectra were recorded on a Waters Alliance 2695 HPLC and Shimadzu SIL-20ACHT systems using the CHIRALCEL OD-H, AD-H, and CHIRALPACK-IA columns. The cancer protein (B-Raf kinase) was retrieved from the Protein Data Bank (PDB), available at https://www.rcsb.org/ with reference ID 6B8U. The active region of the protein is obtained by CASTp and COACH meta servers in addition to previous literature. The ligands were converted into 3D format and docked with protein using the Schrodinger software package utilizing Maestro. The 3D docking pose and 2D interaction plots are visualized and are taken using Discovery Studio.

2.14.1 General Procedure for the Synthesis of Benzothiazolium Salts and α, β-Unsaturated Aldehydes:

1. General procedure for Synthesis of benzothiazolium salt: Benzothiazolium salts were prepared using benzothiazole and phenacyl bromide with EtOH solvent under reflex conditions by following the reported procedure in Scheme 2.27.[110]

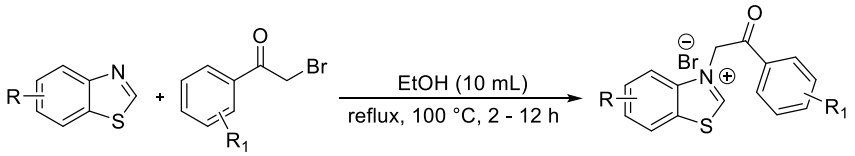

Scheme 2.27 Synthesis of benzothiazolium salts

2. General procedure for Synthesis of α, β-unsaturated aldehydes: The various unsaturated aldehydes were prepared following procedure[176] in Scheme 2.28.

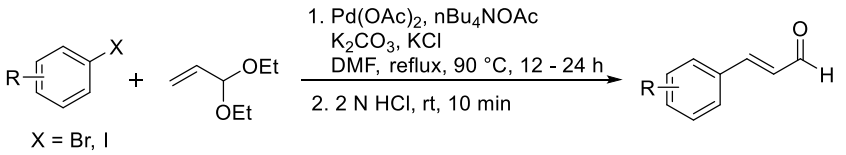

Scheme 2.28 Synthesis of α, β-unsaturated aldehydes

To a stirred solution of substituted halobenzene (0.5 mmol) in 2.0 mL of DMF, were added acrolein diethyl acetal (1.5 mmol), nBu_4NOAc (1.0 mmol), K_2CO_3 (0.75 mmol), KCl (0.5 mmol), and $Pd(OAc)_2$ (0.015 mmol). The mixture was stirred for 12-24 h at 90 °C. After the mixture was cooled, 2 N HCl was slowly added, and the reaction mixture was stirred at room temperature for 10 min. Then, the mixture was diluted with ethyl acetate and washed with water. The organic layer was dried over Na_2SO_4 and concentrated under reduced pressure. The residue was purified by column chromatography using silica gel, 90/10 v/v n-hexane/ethyl acetate to give the described substituted cinnamaldehydes a good yield in Scheme 2.29.

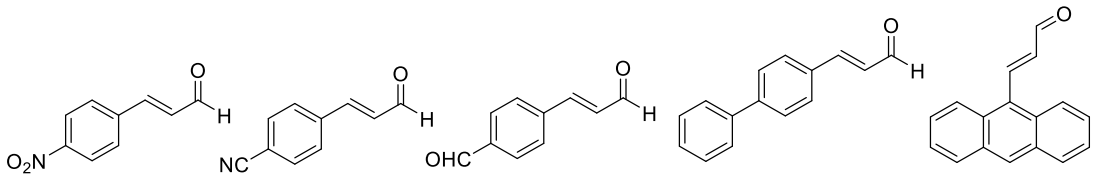

Scheme 2.29 Substrates of α,β-unsaturated aldehydes

2.14.2 Typical Procedure for the Synthesis of Racemic Product of Pyrrolo-thiazine-2-carbaldehydes

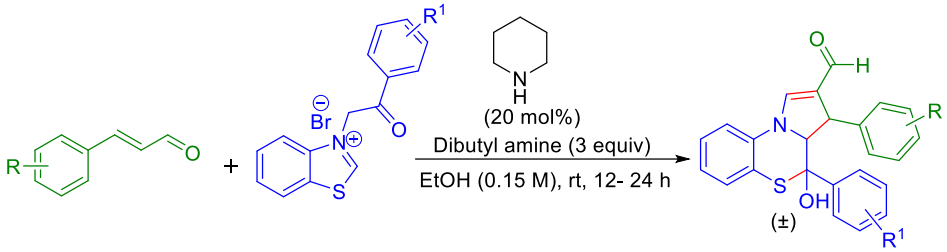

Scheme 2.30 Synthesis of racemic pyrrolo-thiazine-2-carbaldehyde

To a 20 mL oven-dried reaction tube with a magnetic stir bar, piperidine (20 mol%) EtOH (1 mL), followed by cinnamaldehyde (0.3 mmol), was added. The reaction mixture was allowed to stir well at room temperature for one hour. To the stirred reaction mixture, benzothiazolium salt (0.3 mmol), dibutyl amine (3 equiv), and EtOH (1 mL) were added, and the reaction mixture was stirred well for 12 h or until the complete consumption of both starting materials and monitored by TLC. After the reaction was completed, the solvent was removed by rotary evaporation. The residue was added with H_2O (3 x 20 mL), and this aqueous layer was extracted with EtOAc (3 × 20 mL). The combined organic layers were washed with brine (20 mL), the extracted organic layer was dried over Na_2SO_4, and the excess solvent was removed under a vacuum. The residue was purified by column chromatography using silica gel, 70/30 v/v n-hexane/ethyl acetate, to give the desired racemic product with good yield in Scheme 2.30.

2.14.3 Typical Procedure for the Catalytic Enantioselective Synthesis of Chiral Pyrrolo-thiazine-2-carbaldehydes

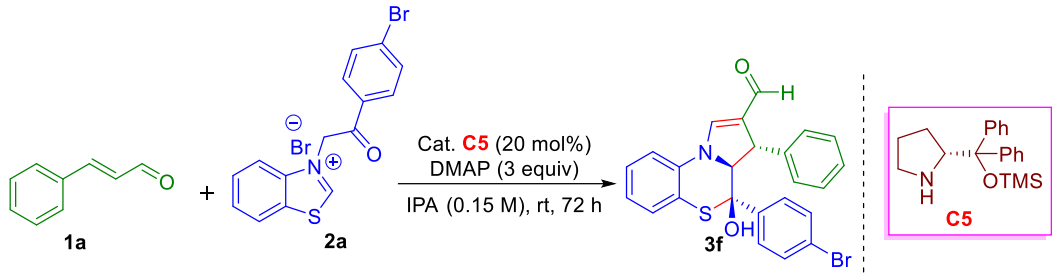

Scheme 2.31 Enantioselective synthesis of chiral pyrrolo-thiazine-2-carbaldehyde

In a 20 mL oven-dried reaction tube with a magnetic stir bar under an open atmosphere, chiral catalyst **C5** (20 mg, 0.06 mmol) and cinnamaldehyde **1a** (40 mg, 38 µL, 0.3 mmol) were dissolved in IPA (0.075 M), closed with glass-stopper, and stirred for 1 hour at room temperature. 4-bromo phenyl thiazolium salt **2a** (126 mg, 0.3 mmol), DMAP (110 mg, 0.9 mmol), and IPA (1 mL) were successively added to the reaction mixture. TLC confirmed the completion of the reaction at 72 h. After the complete formation of the product, the IPA was evaporated from the reaction mixture by a rotary evaporator, and the reaction mixture was extracted with EtOAc (3×5 mL). Brine wash (1×10 mL) was given to the combined organic extractions and dried over anhydrous Na_2SO_4. The residue was purified by column chromatography using silica gel, 70/30 v/v n-hexane/ethyl acetate to give the desired chiral product **3f** as 85% yield, 98% ee with >20:1 diastereoselectivity in Scheme 2.31.

2.14.4 Typical Procedure for the Gram Scale Synthesis of Chiral Pyrrolo-thiazine-2-carbaldehydes

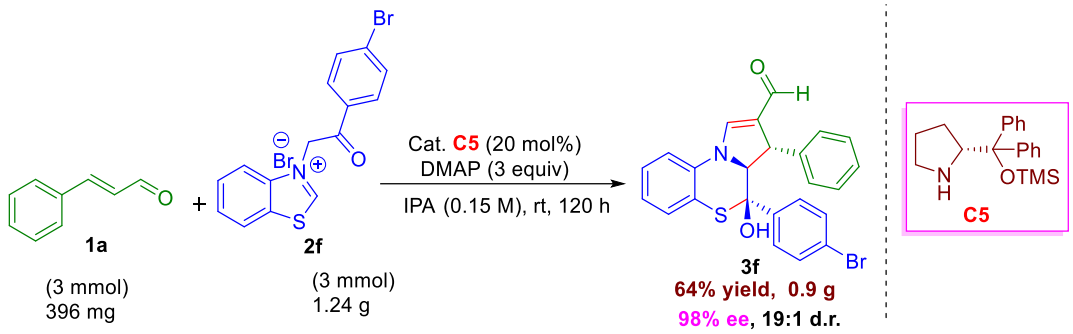

Scheme 2.32 Gram scale synthesis of chiral pyrrolo-thiazine-2-carbaldehyde

In a 50 mL oven-dried round bottom flask with a magnetic stir bar under an open atmosphere, chiral catalyst **C5** (195 mg, 0.6 mmol) and cinnamaldehyde **1a** (396 mg, 374µL, 3 mmol) were dissolved in IPA (10 ml), closed with glass-stopper and stirred for 1 hour at room temperature. 4-bromo phenyl thiazolium salt **2f** (1.24 g, 3 mmol), DMAP (1.1 g, 9 mmol), and IPA (10 mL) were successively added to the reaction mixture. TLC confirmed the completion of the reaction at 120 h. After the complete formation of the product, the IPA was evaporated from the reaction mixture by a rotary evaporator, and the reaction mixture was extracted with EtOAc (3×20 mL). Brine wash (1×30 mL) was given to the combined organic extractions and dried over anhydrous Na_2SO_4. The residue was purified by column chromatography using silica gel, 70/30 v/v n-hexane/ethyl acetate to give the desired chiral product **3f** as 64% yield (0.9 g), 98% ee with >20:1 diastereoselectivity in Scheme 2.32.

2.14.5 Typical Procedure for the Synthetic Transformation of Chiral Pyrrolo-thiazine-2-carbaldehydes to synthesis of 5a

(3*S*,3*aS*,4*S*)-4-(4-bromophenyl)-3-phenyl-4-((trimethylsilyl)oxy)-3*a*,4-dihydro-3*H*-benzo[*b*]pyrrolo[1,2-*d*][1,4]thiazine-2-carbaldehyde 5a:

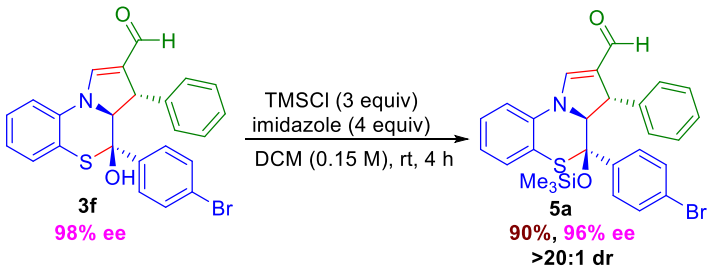

Scheme 2.33 Synthetic transformation for synthesis of **5a**

In a 20 mL oven-dried reaction tube with a magnetic stir bar under an open atmosphere, chiral product **3f** (76 mg, 0.15 mmol) and imidazole (61 mg, 0.9 mmol) were dissolved in DCM (0.15 M) at 0 °C. After 10 minutes, trimethylsilyl chloride (82 mg, 100 µL, 0.75 mmol) was added to the stirred reaction mixture; this reaction mixture was allowed to stir for 30 minutes at the same temperature. After completely consuming the starting material, the reaction mixture was extracted with DCM (3x15 mL) and brine solution (1×10 mL). The combined organic layer was dried over anhydrous Na_2SO_4 and concentrated on the crude product. The residue was purified by column chromatography using silica gel, 80/20 v/v n-hexane/ethyl acetate to give the desired chiral product **5a** as 90% yield, 96% ee with >20:1 diastereoselectivity in Scheme 2.33.

2.14.6 Typical Procedure for the Synthetic Transformation of Chiral Pyrrolo-thiazine-2-carbaldehydes to Synthesis of 5b

(4*S*,5*S*)-5-(4-Bromobenzoyl)-1-(2-(methylthio)phenyl)-4-phenyl-4,5-dihydro-1*H*-pyrrole-3-carbaldehyde 5b

In a 20 mL oven-dried reaction tube with a magnetic stir bar under an open atmosphere, chiral product **3f** (96 mg, 0.2 mmol) was dissolved in DCM (0.15M) and stirred at room temperature. After 5 minutes, DDQ (91 mg, 0.4mmol) was added to the stirred reaction mixture and allowed to stir at the same temperature. TLC monitored the progress of the reaction. After completely consuming the starting material, the reaction mixture was

extracted with DCM (3 x15 mL) and brine solution (1×10 mL). The combined organic layer was dried over anhydrous Na_2SO_4 and concentrated on the crude product. The residue was purified by column chromatography using silica gel, 80/20 v/v n-hexane/ethyl acetate to give the desired product **5b** as 80% yield, **and 5b'** provides 60% yield in Scheme 2.34.

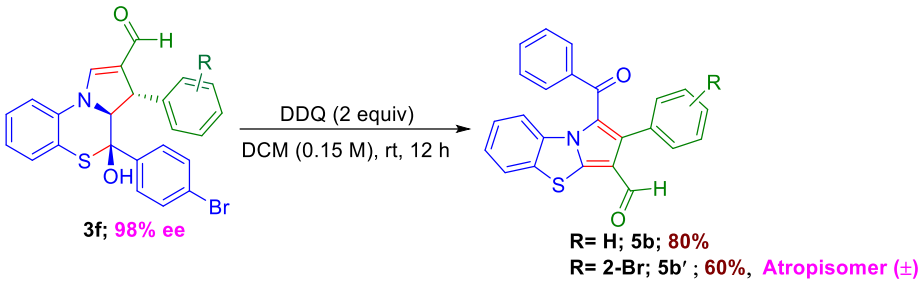

Scheme 2.34 Synthetic transformation for the synthesis of **5b** and **5b'**

2.15 ANALYTICAL AND SPECTRAL DATA:

(3*S*,3*aS*,4*S*)-4-Hydroxy-3,4-diphenyl-3*a*,4-dihydro-3*H*-benzo[*b*]pyrrolo[1,2-*d*][1,4] thiazine-2-carbaldehyde 3a: Prepared according to general procedure D using chiral catalyst **C5**. Purification of crude product was carried out by column chromatography using hexane: EtOAc mixture (70:30) to afford **3a** as a yellow solid (75% yield, 87 mg); R_f = 0.30 (40% ethyl acetate in hexane); mp 100-102 °C; d.r. >20:1(determined by ^{1}H NMR analysis of crude reaction mixture).

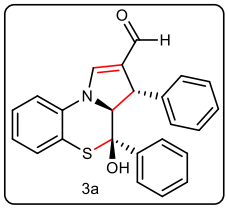

^{1}H NMR (400 MHz, DMSO-d$_6$) δ 9.32 (s, 1H), 8.51 (s, 1H), 7.59 (d, *J* = 8.0 Hz, 1H), 7.56 – 7.48 (m, 2H), 7.46 – 7.36 (m, 4H), 7.25 – 7.12 (m, 2H), 7.08 – 6.95 (m, 4H), 6.37 – 6.25 (m, 2H), 4.31 (d, *J* = 5.6 Hz, 1H), 3.99 (d, *J* = 5.6 Hz, 1H); **^{13}C NMR (100 MHz, DMSO-d$_6$)** δ 182.1, 152.8, 143.2, 139.1, 134.1, 128.5, 128.3, 128.0, 127.3, 126.7, 126.1, 125.5, 123.0, 122.1, 122.0, 117.4, 81.3, 77.3, 46.6; **FTIR (neat)** 3546,

2998, 2628 1710, 1631, 1433, 749 cm^{-1}; **HRMS (ESI)** calculated for $C_{24}H_{20}NO_2S$ $[M+H]^+$: 386.1209; found: 386.1216; **HPLC** conditions: Chiralcel OD-H, hexane/i-PrOH = 80:20 v/v, flow rate = 1.0 mL/min, λ = 350 nm, 25 °C, t_R (major) = 28.70 min, t_R (minor) = 15.82 min, 98% ee, $[\alpha]_D^{20.1}$ = +292.7 (c 1, CH_3CN).

(3*S*,3*aS*,4*S*)-4-Hydroxy-3-phenyl-4-(*p*-tolyl)-3*a*,4-dihydro-3*H*-benzo[*b*]pyrrolo[1,2-*d*][1,4]thiazine-2-carbaldehyde 3b: Prepared according to general procedure D using chiral catalyst **C5**, purification of crude product was carried out by column chromatography using hexane: EtOAc mixture (70:30) to afforded **3b** as a yellow solid; (60% yield, 72 mg); R_f = 0.30 (40% ethyl acetate in hexane); mp 94-96 °C; d.r. 19:1(determined by ^{1}H NMR analysis of crude reaction mixture).

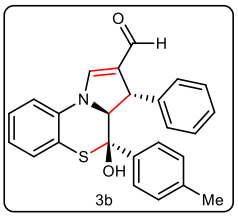

^{1}H NMR (400 MHz, DMSO-d$_6$) δ 9.32 (s, 1H), 8.50 (s, 1H), 7.58 (d, *J* = 8.4 Hz, 1H), 7.43 – 7.31 (m, 3H), 7.26 – 7.11 (m, 4H), 7.07 – 6.95 (m, 4H), 6.41 – 6.30 (m, 2H), 4.28 (d, *J* = 6.0 Hz, 1H), 4.00 (d, *J* = 6.0 Hz, 1H), 2.36 (s, 3H); **^{13}C NMR (100 MHz, DMSO-d$_6$)** δ 182.1, 152.8, 143.2, 137.9, 136.2, 134.1, 128.8, 127.9, 127.2, 126.8, 126.7, 126.1, 125.5, 123.0, 122.3, 122.0, 117.4, 81.3, 77.4, 46.5, 20.7; **FTIR (neat)** 3541, 3004, 2637, 1705, 1636, 1439, 749 cm^{-1}; **HRMS (ESI)**: Calculated for $C_{25}H_{22}NO_2S$ $[M+H]^+$: 400.1366; Found 400.1377; **HPLC** conditions: Chiralcel OD-H, hexane/i-PrOH = 80:20 v/v, flow rate = 1.0 mL/min, λ = 350 nm, 25 °C, t_R (major) = 24.26 min, t_R (minor) = 16.00 min, 96% *ee*, $[\alpha]_D^{20}$ = +233.6 (c 1, CH_3CN).

(3*S*,3*aS*,4*S*)-4-Hydroxy-4-(4-methoxyphenyl)-3-phenyl-3*a*,4-dihydro-3*H*-benzo[*b*]pyrrolo[1,2-*d*][1,4]thiazine-2-carbaldehyde 3c: Prepared according to general procedure D using chiral catalyst **C5**, purification of crude product was carried out by column

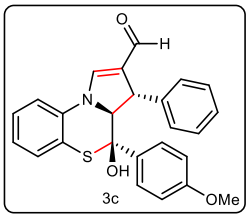

chromatography using hexane: EtOAc mixture (70:30) to afforded **3c** as a pale yellow solid; (72% yield, 90 mg); R_f = 0.30 (50% ethyl acetate in hexane); mp 250-252 °C; d.r. 19:1(determined by ^{1}H NMR analysis of crude reaction mixture).

^{1}H NMR (400 MHz, DMSO-d$_6$) δ 9.31 (s, 1H), 8.49 (s, 1H), 7.57 (d, *J* = 8.4Hz, 1H), 7.40 (d, *J* = 8.4 Hz, 2H), 7.31 (s, 1H), 7.20 – 7.15 (m, 2H), 7.04 – 7.00 (m, 4H), 6.96 (d, *J* = 8.4 Hz, 2H), 6.40 – 6.34 (m, 2H), 4.26 (d, *J* = 5.6 Hz, 1H), 3.99 (d, *J* = 5.6 Hz, 1H), 3.80 (s, 3H); **^{13}C NMR (100 MHz, DMSO-d$_6$)** δ 182.1, 159.4, 152.8, 143.3, 134.1, 131.0 128.6, 128.0, 126.8, 126.7, 126.1, 125.5, 123.0, 122.4, 121.9, 117.4, 113.6, 81.2, 77.5, 55.3, 46.5; **FTIR (neat)** 3572, 2998, 1710, 1642, 1443, 749 cm^{-1}; **HRMS (ESI)** calculated for $C_{25}H_{22}NO_3S$ $[M+H]^+$: 416.1315; found: 416.1320; **HPLC** condition: Chiralcel OD-H, hexane/i-PrOH = 80:20 v/v, flow rate = 1.0 mL/min, λ = 350 nm, 25 °C, t_R (major) = 36.03 min, t_R (minor) = 20.90 min, 98% *ee*, $[\alpha]_D^{20.1}$ = +249.4, (c 1.00, CH_3CN).

(3*S*,3*aS*,4*S*)-4-(4-Fluorophenyl)-4-hydroxy-3-phenyl-3*a*,4-dihydro-3*H*-benzo[b] pyrrolo[1,2-*d*][1,4]thiazine-2-carbaldehyde 3d: Prepared according to general procedure D using chiral catalyst **C5**, purification of crude product was carried out by column chromatography using hexane: EtOAc mixture (70:30) to afforded **3d** as a yellow solid; (80% yield, 96 mg); R_f = 0.30 (40% ethyl acetate in hexane); mp 106-108 °C; d.r. 19:1(determined by ^{1}H NMR analysis of crude reaction mixture).

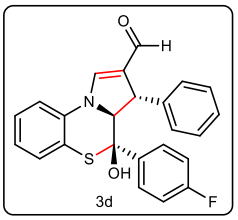

^{1}H NMR (400 MHz, DMSO-d$_6$) δ 9.32 (s, 1H), 8.51 (s, 1H), 7.60 (d, *J* = 8.4 Hz, 1H), 7.57 – 7.51 (m, 2H), 7.50 (s, 1H), 7.26 – 7.13 (m, 4H), 7.08 – 6.97 (m, 4H), 6.46 – 6.40 (m, 2H), 4.36 (d, *J* = 6.0 Hz, 1H), 3.99 (d, *J* = 6.0 Hz, 1H);**^{13}C NMR (100 MHz, DMSO-d$_6$)** δ 182.1, 162.1 (d, *J* = 245.8 Hz), 152.6, 143.2, 135.4 (d, *J* = 2.8 Hz), 134.1,

129.6 (d, J = 8.4 Hz), 128.0, 126.8, 126.7, 126.2, 125.6, 123.0, 122.1, 122.0, 117.3, 115.1 (d, J = 21.6 Hz), 80.8, 77.3, 46.7; **^{19}F NMR (471 MHz, DMSO-d$_6$)** δ -113.74; **FTIR (neat)** 3437, 2930, 1679, 1642, 1480, 703 cm^{-1}; **HRMS (ESI)** calculated for $C_{24}H_{19}FNO_2S$ $[M+H]^+$: 404.1115; found; 404.1119; **HPLC** condition: HPLC Chiralcel OD-H, hexane/i-PrOH = 80:20 v/v, flow rate = 1.0 mL/min, λ = 350 nm, 25 °C, t_R (major) = 27.93 min, t_R (minor) = 16.00 min, 98% *ee*, $[\alpha]_D^{20.1}$ = +236.6 (c 1, CH_3CN).

(3*S*,3*aS*,4*S*)-4-(4-Chlorophenyl)-4-hydroxy-3-phenyl-3*a*,4-dihydro-3*H*-benzo[b] pyrrolo[1,2-*d*][1,4]thiazine-2-carbaldehyde 3e: Prepared according to general procedure D using chiral catalyst **C5**, purification of crude product was carried out by column chromatography using hexane: EtOAc mixture (70:30) to afforded **3e** as a pale yellow solid; (71% yield, 92 mg); Rf = 0.26 (40% ethyl acetate in hexane); mp 238-240 °C; d.r. >20:1(determined by ^{1}H NMR analysis of crude reaction mixture).

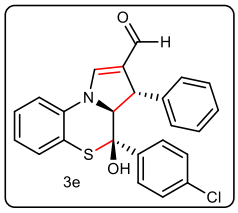

^{1}H NMR (400 MHz, DMSO-d$_6$) δ 9.32 (s, 1H), 8.51 (s, 1H), 7.60 (d, J = 8.4 Hz, 1H), 7.55 – 7.48 (m, 2H), 7.44 (d, J = 8.4 Hz, 2H), 7.25 – 7.14 (m, 2H), 7.06 – 7.00 (m, 4H), 6.43 (dd, J = 3.6, 2.0 Hz, 2H), 4.37 (d, J = 6.0 Hz, 1H), 3.98 (d, J = 6.0 Hz, 1H); **^{13}C NMR (100 MHz, DMSO-d$_6$)** δ 182.1, 152.5, 143.1, 138.2, 134.1, 133.3, 129.2, 128.2, 128.0, 126.8, 126.7, 126.2, 125.6, 123.0, 122.1, 121.8, 117.3, 80.7, 77.1, 46.7; **FTIR** 3541, 3004, 1705, 1642, 1443, 755 cm^{-1}; **HRMS (ESI)** calculated for $C_{24}H_{18}{}^{37}ClNO_2S$ $[M+H]^+$: 422.0790; found: 422.0802; **HPLC** condition: Chiralcel OD-H, hexane/i-PrOH = 80:20 v/v, flow rate = 1.0 mL/min, λ = 350 nm, 25 °C, t_R (major) = 26.60 min, t_R (minor) = 17.10 min, 98% *ee*, $[\alpha]_D^{20.1}$ = +462.9 (c 1, CH_3CN).

(3*S*,3*aS*,4*S*)-4-(4-Bromophenyl)-4-hydroxy-3-phenyl-3*a*,4-dihydro-3*H*-benzo[*b*]pyrrolo[1,2-*d*][1,4]thiazine-2-carbaldehyde 3f: Prepared according to general procedure D using chiral catalyst **C5**, purification of crude product was carried out by column chromatography using hexane: EtOAc mixture (70:30) to afforded **3f** as a yellow solid; (86% yield, 119 mg); R_f = 0.30 (40% ethyl acetate in hexane); mp 214 - 216 °C; d.r. 19:1(determined by ^{1}H NMR analysis of crude reaction mixture).

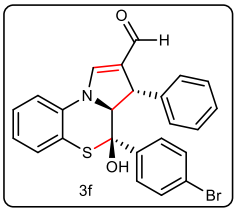

^{1}H NMR (400 MHz, DMSO-d$_6$) δ 9.31 (s, 1H), 8.51 (s, 1H), 7.62 -7.56 (m, 3H), 7.51 (s, 1H), 7.44 (d, *J* = 8.0 Hz, 2H), 7.25 – 7.15 (m, 2H), 7.07 – 6.99 (m, 4H), 6.45 – 6.39 (m, 2H), 4.35 (d, *J* = 6.0 Hz, 1H), 3.96 (d, *J* = 6.0 Hz, 1H); **^{13}C NMR (100 MHz, DMSO-d$_6$)** δ 182.2, 152.6, 143.1, 138.7, 134.1, 131.2, 129.5, 128.0, 126.8, 126.7, 126.2, 125.7, 123.1, 122.1, 122.0, 121.8, 117.3, 80.8, 77.1, 46.8; **FTIR (neat)** 3484, 2925, 2857, 1710, 1642, 1417, 749 cm^{-1}; **HRMS (ESI)** calculated for $C_{24}H_{19}{}^{81}BrNO_2S$ $[M+H]^+$: 466.0294; found: 466.0305; **HPLC** condition: Chiralcel OD-H, hexane/i-PrOH = 80:20 v/v, flow rate = 1.0 mL/min, λ = 350 nm, 25 °C, t_R (major) = 29.26 min, t_R (minor) = 17.90 min, 98% *ee,* $[\alpha]_D^{20.1}$ = +298.7 (c 1, CH_3CN).

(3*S*,3*aS*,4*S*)-4-Hydroxy-4-(2-methoxyphenyl)-3-phenyl-3*a*,4-dihydro-3*H*-benzo[*b*]pyrrolo[1,2-*d*][1,4]thiazine-2-carbaldehyde 3g: Prepared according to general procedure D using chiral catalyst **C5**, purification of crude product was carried out by column chromatography using hexane: EtOAc mixture (60:40) to afforded **3g** as a yellow solid, (76% yield, 95 mg); R_f = 0.30 (50% ethyl acetate in hexanes); mp 96-98 °C; d.r. = >20:1(determined by ^{1}H NMR analysis of crude reaction mixture).

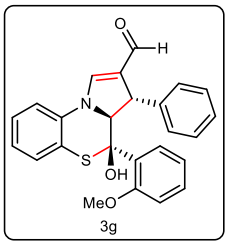

^{1}H NMR (400 MHz, DMSO-d$_6$) δ 9.28 (s, 1H), 8.49 (s, 1H), 7.88 (d, *J* = 7.6 Hz, 1H), 7.46 – 7.7.37 (m, 1H), 7.24 (s, 1H), 7.21 – 7.05 (m, 6H), 7.01 (t, *J* = 7.6 Hz, 1H), 6.79 (d, *J* = 8.0 Hz 1H), 6.47 (dd, *J* = 3.6, 2.4 Hz, 2H), 5.11 (d, *J* = 6.0 Hz, 1H), 3.80 (, *J* = 6.4 Hz, 1H), 3.01(s, 3H); **^{13}C NMR (100 MHz, DMSO-d$_6$)** δ 182.9, 155.8, 152.4, 143.6, 134.2, 130.7, 128.9. 128.0, 126.9, 126.5, 126.1, 126.0, 125.2, 123.1, 122.4, 122.3, 120.1, 117.3, 111.9, 80.1, 72.9, 54.5, 47.3; **FTIR** 3551, 3004, 2628, 1714, 1636, 1448, 755 cm^{-1}; **HRMS (ESI)** calculated for $C_{25}H_{22}NO_3S$ $[M+H]^+$: 416.1315; found: 416.1320; **HPLC** condition: Chiralcel OD-H, hexane/i-PrOH = 80:20 v/v, flow rate = 1.0 mL/min, λ = 350 nm, 25 °C t_R (major) = 28.51 min, t_R (minor) = 18.94 min, 96% *ee*, $[\alpha]_D^{20.1}$ = +338.4 (c 0.1, CH_3CN).

(*3S,3aS,4S*)-4-Hydroxy-4-(3-methoxyphenyl)-3-phenyl-3*a*,4-dihydro-3*H*-benzo[*b*] pyrrolo[1,2-*d*][1,4]thiazine-2-carbaldehy 3h: Prepared according to general procedure D using chiral catalyst **C5**, purification of crude product was carried out by column chromatography using hexane: EtOAc mixture (70:30) to afford **3h** as a pale yellow solid;

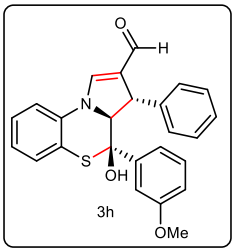

81% yield (100 mg); R_f = 0.30 (60% ethyl acetate in hexane); mp 96-98 °C d.r. >20:1(determined by ^{1}H NMR analysis of crude reaction mixture).

^{1}H NMR (400 MHz, DMSO-d$_6$) δ 9.31(s, 1H), 8.51 (s, 1H), 7.60 (d, *J* = 8.4 Hz, 1H), 7.39 (s, 1H), 7.35 – 7.25 (m, 1H), 7.25 – 7.15 (m, 3H), 7.10 – 6.95 (m, 6H), 6.40 – 6.30 (m, 2H), 4.36 (d, *J* = 5.6 Hz, 1H), 3.98 (d, *J* = 6.0 Hz, 1sH), 3.67 (s, 3H); **^{13}C NMR (100 MHz, DMSO-d$_6$)** δ 182.1, 159.3, 152.5, 143.2, 140.7, 134.1, 129.3, 127.9, 126.8, 126.7, 126.0, 125.5, 122.9, 122.0, 121.0, 119.4, 117.3, 114.2, 112.9, 81.0, 77.2, 55.1, 46.6; **FTIR (neat)** 3436, 2955, 2854, 1622, 1565, 1485, 747 cm^{-1}; **HRMS (ESI)** calculated for $C_{25}H_{22}NO_3S$ $[M+H]^+$: 416.1315; found: 416.1350; **HPLC** condition:

HPLC Chiralcel OD-H, hexane/i-PrOH = 70:30 v/v, flow rate = 1.0 mL/min, λ = 350 nm, 25 °C, t_R (major) = 17.23, t_R (minor) = 11.80 min, 98% *ee*, $[\alpha]_D^{20.1}$ = +338.5 (c 0.1, CH_3CN).

(3*S*,3*aS*,4*S*)-4-(3,4-Dimethoxyphenyl)-4-hydroxy-3-phenyl-3*a*,4-dihydro-3*H*-benzo [*b*]pyrrolo[1,2-*d*][1,4]thiazine-2-carbaldehyde 3i: Prepared according to general procedure D using chiral catalyst **C5**, purification of crude product was carried out by column chromatography using hexane: EtOAc mixture (60:40) to afford **3i** as a orange solid; (60% yield, 80 mg); R_f = 0.40 (60% ethyl acetate in hexane); mp 240-242 ºC; d.r. >20:1 (determined by ^{1}H NMR analysis of crude reaction mixture).

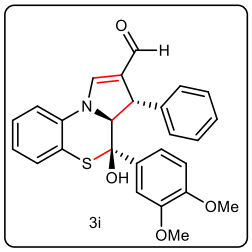

^{1}H NMR (400 MHz, DMSO-d$_6$) δ 9.31 (s, 1H), 8.50 (s, 1H), 7.58 (d, *J* = 8.4 Hz, 1H), 7.34 – 7.29 (m, 1H), 7.23 – 7.17 (m, 1H), 7.17 – 7.12 (m, 1H), 7.09 (d, *J* = 8.4 Hz, 1H), 7.05 – 6.96 (m, 5H), 6.91 (s, 1H), 6.46 – 6.39 (m, 2H), 4.40 (d, *J* = 6.0 Hz, 1H), 3.98 (d, *J* = 6.0 Hz, 1H), 3.79 (s, 3H), 3.52 (s, 3H); **^{13}C NMR (100 MHz, DMSO-d$_6$)** δ 182.2, 152.7, 149.1, 148.6, 143.4, 134.2, 131.4, 127.9, 127.0, 126.7, 126.1, 125.5, 123.1, 122.5, 121.9, 119.8, 117.3, 111.4, 111.1, 81.1, 77.4, 55.8, 55.5, 46.7; **FTIR (neat)** 3525, 2998, 1642, 1485, 1036, 917, 755 cm^{-1}; **HRMS (ESI)** calculated for $C_{26}H_{24}NO_4S$ $[M+H]^+$: 446.1421; found: 446.1427; **HPLC** condition: Chiralcel OD-H hexane/i-PrOH = 80:20 v/v, flow rate = 1.0 mL/min, λ = 350 nm, 25 °C, t_R (major) = 41.52, t_R (minor) = 25.50 min, >99% *ee*, $[\alpha]_D^{20}$ = +299.5 (c 1, CH_3CN).

(3*S*,3*aS*,4*S*)-4-([1,1'-Biphenyl]-4-yl)-4-hydroxy-3-phenyl-3*a*,4-dihydro-3*H*-benzo [b]pyrrolo[1,2-*d*][1,4]thiazine-2-carbaldehyde 3j: Prepared according to general procedure D using chiral catalyst **C5**, purification of crude product was carried out by column chromatography using hexane: EtOAc mixture (60:40) to afford **3j** as a orange solid; (55% yield, 75 mg); R_f = 0.30 (40% ethyl acetate in hexane); mp 202-204 ºC; d.r. >20:1 (determined by ^{1}H NMR analysis of crude reaction mixture).

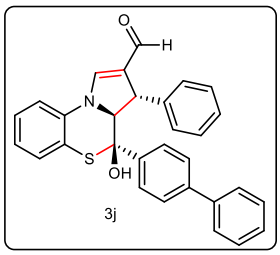

^{1}H NMR (400 MHz, DMSO-d$_6$) δ 9.34 (s, 1H), 8.53 (s, 1H), 7.75 – 6.65 (m, 4H), 7.65 – 6.57 (m, 3H), 7.50 (dd, *J* = 7.2, 4.8 Hz, 3H), 7.41 (t, *J* = 7.6 Hz, 1H), 7.21 (dd, *J* = 8.4, 8.0 Hz, 2H), 7.08 – 6.91 (m, 4H), 6.38 (d, *J* = 7.2 Hz, 2H), 4.35 (d, *J* = 5.6 Hz, 1H), 4.04 (d, *J* = 5.6 Hz, 1H); **^{13}C NMR (100 MHz, DMSO-d$_6$)** δ 182.1, 152.7, 143.2, 140.4, 139.6, 138.2, 134.2, 129.0, 127.9, 127.7, 126.8, 126.8, 126.6, 126.1, 125.6, 123.0, 122.0, 122.0, 117.3, 81.1, 77.5, 46.7; **FTIR(neat)** 3541, 3004, 2628, 1710, 1642, 1439, 744 cm^{-1}; **HRMS (ESI)** calculated for $C_{30}H_{24}NO_2S$ $[M+H]^+$: 462.1522; found: 462.1527; **HPLC** condition: HPLC Chiralcel OD-H, hexane/i-PrOH = 80:20, v/v, flow rate = 1.0 mL/min, λ = 350 nm, 25 °C, t_R (major) = 31.02, t_R (minor) = 23.64 min, 98% *ee*, $[\alpha]_D^{20}$ = +328.4 (c 0.1, CH_3CN).

(3*S*,3*aS*,4*S*)-4-Hydroxy-4-(4-nitrophenyl)-3-phenyl-3*a*,4-dihydro-3*H*-benzo[*b*] pyrrolo[1,2-*d*][1,4]thiazine-2-carbaldehyde 3k: Prepared according to general procedure D using chiral catalyst **C5**, purification of crude product was carried out by column chromatography using hexane: EtOAc mixture (60:40) to afforded **3k** as a yellow solid; (78% yield, 101 mg); R_f = 0.30 (60% ethyl acetate in hexane); mp 246-248 ºC; d.r. >20:1(determined by ^{1}H NMR analysis of crude reaction mixture).

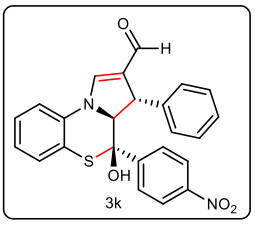

^{1}H NMR (400 MHz, DMSO-d$_6$) δ 9.32 (s, 1H), 8.54 (s, 1H), 8.26 - 8.10 (m, 2H), 7.85 – 7.76 (m, 3H), 7.67 – 7.55 (m, 1H), 7.32 – 7.13 (m, 2H), 7.12 – 6.90 (m, 4H), 6.51 – 6.30 (m, 2H), 4.48 (d, *J* = 6.0 Hz, 1H), 3.97 (d, *J* = 6.0 Hz, 1H); **^{13}C NMR (100 MHz, DMSO-d$_6$)** δ 182.2, 152.4, 147.4, 146.5, 142.8, 134.2, 128.9, 128.1, 126.8, 126.7, 126.2, 125.8, 123.3, 123.1, 122.2, 121.2, 117.3, 80.6, 76.8, 46.9; **FTIR (neat)** 3551, 3004, 2628, 1710, 1636, 1443, 749 cm^{-1}; **HRMS (ESI)** calculated for $C_{24}H_{19}N_2O_4S$ $[M+H]^+$: 431.1060; found: 431.1064; **HPLC** condition: Chiralcel OD-H, hexane/ i-PrOH = 80:20, flow rate = 1.0 mL/min, λ = 350 nm, 25 °C, t_R (major) = 37.51 min, t_R (minor) = 26.63 min, 96% *ee*, $[\alpha]_D^{20.1}$ = +312.6 (c 1, CH_3CN).

(3*S*,3*aS*,4*S*)-2-Formyl-4-hydroxy-3-phenyl-3*a*,4-dihydro-3*H*-benzo[*b*]pyrrolo[1,2-*d*][1,4] thiazinyl) benzonitrile 3l: Prepared according to general procedure D using chiral catalyst **C5**, purification of crude product was carried out by column chromatography using hexane: EtOAc mixture (60:40) to afford **3l** as a yellow solid (92% yield, 113 mg); R_f = 0.30 (50% ethyl acetate in hexanes); mp 114 - 116 °C; d.r. >20:1(determined by ^{1}H NMR analysis of crude reaction mixture).

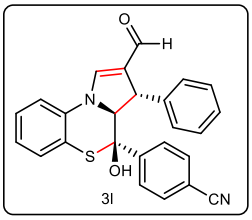

3l

^{1}H NMR (400 MHz, DMSO-d$_6$) δ 9.31 (s, 1H), 8.51 (s, 1H), 7.60 (d, *J* = 8.4 Hz, 1H), 7.54 – 7.48 (m, 3H), 7.45 (d, *J* = 8.4 Hz, 2H), 7.26 – 7.14 (m, 2H), 7.07 – 6.98 (m, 4H), 6.42 (dd, *J* = 4.0, 2.0 Hz, 2H), 4.36 (d, *J* = 6.4 Hz, 1H), 3.96 (d, *J* = 6.0 Hz, 1H); **^{13}C NMR (100 MHz, DMSO-d$_6$)** δ 182.3, 152.4, 144.6, 142.9, 134.2, 132.2, 128.4, 128.1, 126.9, 126.7, 126.3, 125.8, 123.1, 122.2, 121.4, 118.6, 117.3, 111.3, 80.7, 76.8, 46.9; **FTIR (neat)** 3551, 3004, 2623, 1714, 1642, 1433, 744 cm ^{1}; **HRMS (ESI)** calculated for $C_{25}H_{19}N_2O_2S$ $[M+H]^+$: 411.1162; found: 411.1164; **HPLC** condition: Chiralcel OD-H, hexane/ i-PrOH = 80:20 v/v, flow rate = 1.0 mL/min, λ = 350 nm, 25

°C, t_R (major) = 33.80 min, t_R (minor) = 25.80 min, 98% *ee*, $[\alpha]_D^{20.1}$ = +174.1 (c 1, CH_3CN).

(3*S*,3*aS*,4*S*)-4-Hydroxy-3-phenyl-4-(4-(trifluoromethyl)phenyl)-3*a*,4-dihydro-3*H*-benzo[*b*]pyrrolo[1,2-*d*][1,4]thiazine-2-carbaldehyde 3m: Prepared according to general procedure D using chiral catalyst **C5**, purification of crude product was carried out by column chromatography using hexane: EtOAc mixture (60:40) to afford **3m** as an orange solid; (80% yield, 110 mg); R_f = 0.26 (40% ethyl acetate in hexane); mp 94-96 ºC; d.r. >20:1 (determined by ^{1}H NMR analysis of crude reaction mixture).

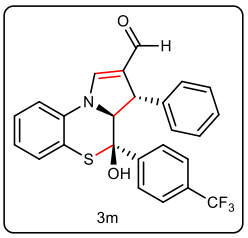

^{1}H NMR (400 MHz, DMSO-d$_6$) δ 9.31 (s, 1H), 8.54 (s, 1H), 7.77 – 7.70 (m, 4H), 7.68 (s, 1H), 7.62 (d, *J* = 8.0 Hz, 1H), 7.27 – 7.15 (m, 3H), 7.05 – 6.90 (m, 4H), 6.34 (d, *J* = 7.6 Hz, 2H), 4.41 (d, *J* = 6.4 Hz, 1H), 3.95 (d, *J* = 6.4 Hz, 1H); **^{13}C NMR (100 MHz, DMSO-d$_6$)** δ 182.3, 152.4, 143.8, 143.0, 134.2, 129.2(q *J* = 32 Hz), 128.3, 127.9, 126.8, 126.8, 126.2, 125.8 124.1 (q, *J* = 270 Hz), 125.2 (q, *J* = 3.4 Hz), 123.1, 122.1, 121.4, 117.3. 80.6, 77.2, 46.9; **^{19}F NMR (471 MHz, CDCl$_3$)** δ -62.7; **FTIR (neat)** 3444, 2924, 2853, 1695, 1474, 1179, 757 cm^{-1}; **HRMS (ESI)** calculated for $C_{25}H_{19}F_3NO_2S$ $[M+H]^+$: 454.1083; found: 454.1087; **HPLC** condition: Chiralcel OD-H, hexane/ i-PrOH = 80:20 v/v, flow rate = 0.7 mL/min, λ = 350 nm, 25 °C, t_R (major) = 28.84, t_R (minor) = 21.82 min, 99% *ee,* $[\alpha]_D^{20.1}$ = +211.80 (c 0.5, CH_3CN).

(3*S*,3*aS*,4*S*)-4-Hydroxy-4-(naphthalen-2-yl)-3-phenyl-3*a*,4-dihydro-3*H*-benzo[*b*]pyrrolo[1,4]thiazine-2-carbaldehyde 3n: Prepared according to general procedure D using chiral catalyst **C5**, purification of crude product was carried out by column chromatography using hexane: EtOAc mixture (60:40) to afford **3n** as a orange solid; (50% yield,

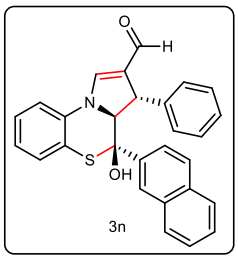

60 mg); R_f = 0.40 (40% ethyl acetate in hexane); mp 226-228 ºC; d.r. >20:1 (determined by ^{1}H NMR analysis of crude reaction mixture).

^{1}H NMR (400 MHz, DMSO-d$_6$) δ 9.31 (s, 1H), 8.52 (s, 1H), 8.20 (s, 1H), 8.05 – 7.95 (m, 2H), 7.86 (d, *J* = 6.8 Hz, 1H) 7.65 – 7.55 (m, 4H), 7.46 (d, *J* = 7.2 Hz, 1H), 7.25 – 7.15 (m, 2H), 6.93 (t, *J* = 6.0 Hz, 1H), 6.82 (t, *J* = 6.0 Hz, 2H), 6.22 (d, *J* = 5.6 Hz, 2H), 4.46 (d, *J* = 4.4 Hz, 1H), 4.04 (d, *J* = 4.4 Hz, 1H); **^{13}C NMR (100 MHz, DMSO-d$_6$)** δ 182.2, 152.9, 143.0, 136.6, 134.3, 132.7, 132.4, 128.4, 128.0, 127.9, 127.5, 126.9, 126.8, 126.7, 126.7, 126.1, 125.6, 124.8, 123.2, 122.3, 122.1, 117.5, 81.7, 77.0, 46.7; **FTIR (neat)** 3577, 3004, 2623, 1710, 1636, 1443, 755 cm^{-1}; **HRMS (ESI)** calculated for $C_{28}H_{22}NO_2S$ $[M+H]^+$: 436.1366; found: 436.1371; **HPLC** condition: Chiralcel OD-H, hexane/ i-PrOH = 50:50 v/v, flow rate = 1.0 mL/min, λ = 350 nm, 25 °C, t_R (major) = 19.42 min, t_R (minor) = 8.54 min, 96% *ee,* $[\alpha]_D^{20.1}$ = +157.4 (c 1, CH_3CN).

(3*S*,3*aS*,4*S*)-4-(4-Chlorophenyl)-4-hydroxy-3-(*p*-tolyl)-3*a*,4-dihydro-3*H*-benzo[*b*]pyrrolo[1,2-*d*][1,4]thiazine-2-carbaldehyde 3o: Prepared according to general procedure D using chiral catalyst **C5**, purification of crude product was carried out by column chromatography using hexane: EtOAc mixture (70:30) to afford **3o** as a yellow solid;

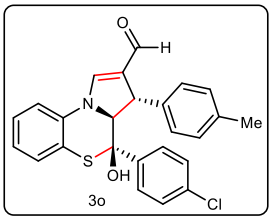

(60% yield, 76 mg); R_f = 0.30 (40% ethyl acetate in hexane); mp 138 – 140 ºC; d.r. >20:1(determined by ^{1}H NMR analysis of crude reaction mixture).

^{1}H NMR (400 MHz, DMSO-d$_6$) δ 9.33 (s, 1H), 8.48 (s, 1H), 7.65 – 7.40 (m, 6H), 7.27 – 7.10 (m, 2H), 7.07 – 6.95 (m,1H), 6.84 (d, *J* = 7.6 Hz, 2H), 6.31 (d, *J* = 7.6 Hz, 2H), 4.31 (d, *J* = 6.0 Hz, 1H), 3.97 (d, *J* = 5.6 Hz, 1H), 2.15 (s, 3H); **^{13}C NMR (100 MHz, DMSO-d$_6$)** δ 182.2, 152.6, 140.2, 138.3, 135.2, 134.2, 133.4, 129.3, 128.7, 128.3, 126.7, 125.7, 123.1, 122.3, 121.9, 117.4, 80.9, 77.2, 46.3, 20.6; **FTIR (neat)** 3441,

2962, 1631, 1558, 1417, 740 cm^{-1}; **HRMS (ESI)** calculated for $C_{25}H_{21}{}^{37}ClNO_2S$ $[M+H]^+$: 436.0947; found: 436.0963; **HPLC** condition: Chiralcel OD-H hexane/i-PrOH = 80:20 v/v, flow rate = 1.0 mL/min, λ = 350 nm, 25 °C, t_R (major) = 24.60, t_R (minor) = 17.24 min, 92% *ee*, $[\alpha]_D^{20}$ = +311.8 (c 1, CH_3CN).

(3*S*,3*aS*,4*S*)-4-(4-Chlorophenyl)-4-hydroxy-3-(4-methoxyphenyl)-3*a*,4-dihydro-3*H*-benzo[*b*]pyrrolo[1,2-*d*][1,4]thiazine-2-carbaldehyde 3p: Prepared according to general procedure D using chiral catalyst **C5**, purification of crude product was carried out by column chromatography using hexane: EtOAc mixture (60:40) to afford **3p** as a pale yellow solid; (70% yield, 94 mg); R_f = 0.30 (40% ethyl acetate in hexane); mp 196 – 198 °C; d.r. = >20:1(determined by ^{1}H NMR analysis of crude reaction mixture).

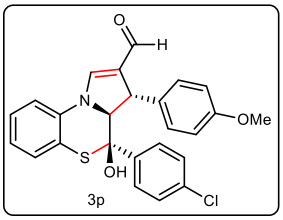

^{1}H NMR (400 MHz, DMSO-d$_6$) δ 9.31 (s, 1H), 8.46 (s, 1H), 7.58 (d, *J* = 8.0 Hz, 1H), 7.55 – 7.45 (m, 6H), 7.25 – 7.15 (m, 2H), 7.02 (t, *J* = 7.6 Hz, 1H), 6.58 (d, *J* = 8.4 Hz, 2H), 6.34 (d, *J* = 8.0 Hz, 2H), 3.92 (d, *J* = 6.0 Hz, 1H), 3. 64 (s, 3H); **^{13}C NMR (100 MHz, DMSO-d$_6$)** δ 182.2, 157.6, 152.4, 138.3, 135.2, 134.2, 133.4, 129.3, 128.3, 127.8, 126.7, 125.7, 123.1, 122.3, 121.8, 117.3, 113.4, 80.8, 77.2, 54.9, 45.9; **FTIR (neat)** 3614, 3008, 2628, 1710, 1636, 1443, 749 cm^{-1}; **HRMS (ESI)** calculated for $C_{25}H_{21}{}^{37}ClNO_3S$ $[M+H]^+$: 452.0896; found: 452.0904; **HPLC** condition: Chiralcel OD-H hexane/i-PrOH = 70:30 v/v, flow rate = 1.0 mL/min, λ = 350 nm, 25 °C, t_R (major) = 26.95, t_R (minor) = 13.0 min, 98% *ee*, $[\alpha]_D^{20.2}$ = +342.5 (c 1, CH_3CN).

(3*S*,3*aS*,4*S*)-4-(4-Chlorophenyl)-3-(4-fluorophenyl)-4-hydroxy-3*a*,4-dihydro-3*H*-benzo[*b*]pyrrolo[1,2-*d*][1,4]thiazine-2-carbaldehyde 3q: Prepared according to general procedure D using chiral catalyst **C5**, purification of crude product was carried out by column

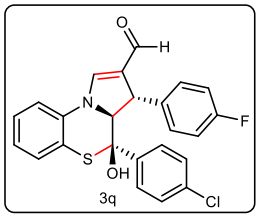

chromatography using hexane: EtOAc mixture (70:30) to afford **3q** as a pale yellow solid; (80% yield, (105 mg); R_f = 0.30 (40% ethyl acetate in hexane); mp 232-234 ºC; d.r. >20:1(determined by ^{1}H NMR analysis of crude reaction mixture).

^{1}H NMR (400 MHz, DMSO-d$_6$) δ 9.30 (s, 1H), 8.52 (s, 1H), 7.33 (d, *J* = 8.4 Hz, 1H), 7.56 – 7.47 (m, 3H), 7.44 d, *J* = 8.4 Hz, 2H), 7.25 – 7.15 (m, 2H), 7.03 (t, *J* = 7.6 Hz, 1H), 6.85 (t, *J* = 8.8 Hz, 2H), 6.50 – 6.45 (m, 2H), 4.42 (d, *J* = 6.4 Hz, 1H), 3.97 (d, *J* = 6.4 Hz, 1H); **^{13}C NMR (100 MHz, DMSO-d$_6$)** δ 182.2, 160.6 (d, *J* = 241.9 Hz), 152.4, 139.2, 138.2, 134.1, 133.4, 129.2, 128.7 (d, *J* = 8.0 Hz), 128.3, 126.7, 125.7, 123.1, 121.9, 121.8, 117.3, 114.7 (d, *J* = 21.3 Hz), 80.6, 77.0, 46.1; **^{19}F NMR (471 MHz DMSO-d$_6$)** δ -116.8; **FTIR (neat)** 3536, 2998, 1710, 1636, 1443, 744 cm^{-1}; **HRMS (ESI)** calculated for $C_{24}H_{18}{}^{37}ClFNO_2S$ $[M+H]^+$: 440.0696; found: 440.0713; **HPLC** condition: Chiralcel OD-H, hexane/i-PrOH = 80:20 v/v, flow rate = 1.0 mL/min, λ = 350 nm, 25 °C t_R (major) = 25.60, t_R (minor) = 17.84 min, 98% *ee*, $[\alpha]_D^{20}$ = +293.3 (c 1, CH_3CN).

(3*S*,3*aS*,4*S*)-4-(4-Bromophenyl)-3-(4-chlorophenyl)-4-hydroxy-3*a*,4-dihydro-3*H*-benzo[b]pyrrolo[1,2-*d*][1,4]thiazine-2-carbaldehyde 3r: Prepared according to general procedure D using chiral catalyst **C5**, purification of crude product was carried out by column chromatography using hexane: EtOAc mixture (70:30) to afford **3r** as a pale yellow solid; (79% yield, 130 mg); R_f = 0.30 (40% ethyl acetate in hexane); mp 234-236 ºC; d.r. >20:1(determined by ^{1}H NMR analysis of crude reaction mixture).

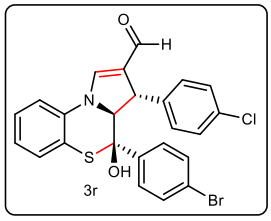

^{1}H NMR (400 MHz, DMSO-d$_6$) δ 9.30 (s, 1H), 8.53 (s, 1H), 7.58 (d, *J* = 7.2 Hz, 4H), 7.44 (d, *J* = 8.4 Hz, 2H), 7.27 – 7.13 (m, 2H), 7.12 – 6.97 (m, 3H), 6.45 (d, *J* = 8.0 Hz, 2H), 4.42 (d, *J* = 6.4 Hz, 1H), 3.96 (d, *J* = 6.4 Hz, 1H); **^{13}C NMR (100 MHz, DMSO-**

d6) δ 182.2, 152.5, 142.1, 138.6, 134.1, 131.2, 130.8, 129.5, 128.8, 127.9, 126.7, 125.7, 123.1, 122.1, 121.8, 121.7, 117.3, 80.6, 76.8, 46.3; **FTIR (ATR)** 3603, 2998, 2628, 1714, 1636, 1443, 749 cm^{-1}; **HRMS (ESI)** calculated for $C_{24}H_{17}{}^{37}Cl^{81}BrNO_2S$ $[M+H]^+$: 501.9875; found: 501.9883; **HPLC** condition: Chiralcel OD-H, hexane/i-PrOH = 80:20 v/v, flow rate = 1.0 mL/min, λ = 350 nm, 25 °C, t_R (major) = 29.41, t_R (minor) = 21.31 min, 98% *ee*, $[\alpha]_D^{20.1}$ = +123.0 (c 1, CH_3CN).

(3*S*,3*aS*,4*S*)-3,4-Bis(4-bromophenyl)-4-hydroxy-3*a*,4-dihydro-3*H*-benzo[b]pyrrolo[1,2-*d*][1,4]thiazine-2 carbaldehyde 3s:

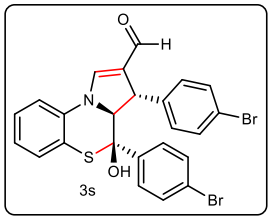

Prepared according to general procedure D using chiral catalyst **C5**, purification of crude product was carried out by column chromatography using hexane: EtOAc mixture (70:30) to afford as a pale yellow solid; (88% yield, (143 mg); R_f = 0.30 (40% ethyl acetate in hexane); mp 234-236 ºC; d.r. >20:1(determined by ^{1}H NMR analysis of crude reaction mixture).

^{1}H NMR (400 MHz, DMSO-d6) δ 9.29 (s, 1H), 8.54 (s, 1H), 7.65 – 7.52 (m, 4H), 7.44 (d, *J* = 8.0 Hz, 1H), 7.27 – 7.12 (m, 4H), 7.03 (t, *J* = 7.6 Hz, 1H), 6.39 (d, *J* = 8.0 Hz, 1H), 4.43 (d, *J* = 6.4 Hz, 1H), 3.94 (d, *J* = 6.4 Hz, 1H); **^{13}C NMR (100 MHz, DMSO-d6)** δ 182.1, 152.5, 142.4, 138.6, 134.1, 131.2, 130.8, 129.5, 129.2, 126.7, 125.7, 123.1, 122.1, 121.8, 121.6, 119.3, 117.3, 80.6, 76.6, 46.3; **FTIR (neat)** 3447, 2925, 1636, 1480, 1224, 814, 740 cm^{-1}; **HRMS (ESI)** calculated for $C_{24}H_{17}{}^{81}Br^{81}BrNO_2S$ $[M+H]^+$: 545.9379; found:545.9387; **HPLC** condition: HPLC Chiralcel OD-H, hexane/i-PrOH = 80:20 v/v, flow rate = 1.0 mL/min, λ = 350 nm, 25 °C, t_R (major) = 34.44, t_R (minor) = 25.50 min, 98% *ee*, $[\alpha]_D^{20.1}$ = +408.3 (c 1, CH_3CN).

(3*S*,3*aS*,4*S*)-4-(4-Chlorophenyl)-3-(4-(dimethylamino)phenyl)-4-hydroxy-3*a*,4-dihydro-3-*H*-benzo[*b*]pyrrolo[1,2-*d*][1,4]thiazine-2-carbaldehyde 3t: Prepared according to general procedure D using chiral catalyst **C5**, purification of crude product was carried out by column chromatography using hexane: EtOAc mixture (60:40) to afford **3t** as a orange solid; (71% yield, 91 mg); R_f = 0.40 (40 % ethyl acetate in hexane); mp 138-140 °C; d.r. > 20:1 (determined by ^{1}H NMR analysis of crude reaction mixture).

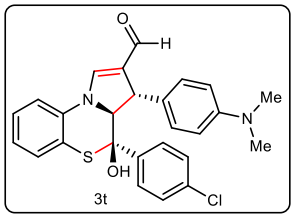

^{1}H NMR (400 MHz, DMSO-d$_6$) δ 9.30 (s, 1H), 8.42 (s, 1H), 7.57 (d, *J* = 8.4 Hz, 1H), 7.54 – 7.42 (m, 5H), 7.24 – 7.12 (m, 2H), 7.02 (t, *J* = 7.6 Hz, 1H), 6.38 (d, *J* = 8.4 Hz, 2H), 6.23 (d, *J* = 8.4 Hz, 1H), 4.26 (d, *J* = 5.6 Hz, 1H), 3.86 (d, *J* = 5.6 Hz, 1H), 2.77 (s, 6H); **^{13}C NMR (100 MHz, DMSO-d$_6$)** δ 182.2, 152.4, 148.9, 138.4, 134.3, 133.3, 130.8, 129.3, 128.2, 127.2, 126.7, 125.7, 123.0, 122.6, 121.9, 117.4, 112.2, 81.0, 77.4, 65.0, 45.7; **FTIR (neat)** 3614, 3004, 2623, 1714, 1631, 1448, 749 cm^{-1}; **HRMS (ESI)** calculated for $C_{26}H_{24}{}^{37}ClN_2O_2S$ $[M+H]^+$: 465.1212; found: 465.1225; **HPLC** condition: Chiralcel OD-H, hexane/i-PrOH = 70:30 v/v, flow rate = 1.0 mL/min, λ = 350 nm, 25 °C, t_R (major) = 21.40, t_R (minor) = 12.54 min, 98% *ee*, $[\alpha]_D^{20.2}$ = +490.1 (c 0.1, CH_3CN).

(3*S*,3*aS*,4*S*)-4-(4-Chlorophenyl)-4-hydroxy-3-(4-nitrophenyl)-3*a*,4-dihydro-3*H*-benzo[*b*]pyrrolo[1,2-*d*][1,4]thiazine-2-carbaldehyde 3u: Prepared according to general procedure D using chiral catalyst **C5**, purification of crude product was carried out by column chromatography using hexane: EtOAc mixture (60:40) to afford **3u** as a yellow solid;

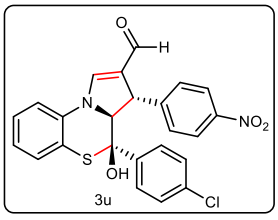

(77% yield, 107 mg); R_f = 0.40 (40% ethyl acetate in hexane); mp 270-272 ºC; d.r. >20:1(determined by ^{1}H NMR analysis of crude reaction mixture).

^{1}H NMR (400 MHz, DMSO-d$_6$) δ 9.29 (s, 1H), 8.61 (s, 1H), 7.90 (d, *J* = 8.0 Hz, 2H), 7.66 – 7.59 (m, 2H), 7.50 (d, *J* = 8.0 Hz, 2H), 7.42 (d, *J* = 8.4 Hz, 2H), 7.26 – 7.16 (m, 2H), 7.04 (t, *J* = 7.6 Hz, 1H), 6.75 (d, *J* = 8.4 Hz, 2H), 4.59 (d, *J* = 6.4 Hz, 1H), 4.10 (d, *J* = 6.8 Hz, 1H); **^{13}C NMR (100 MHz, DMSO-d$_6$)** δ 182.1, 152.6, 150.7, 145.9, 138.1, 134.0, 133.6, 129.1, 128.4, 128.3, 126.8, 125.8, 123.2, 123.1, 121.7, 121.2, 117.3, 80.3, 76.5, 46.9; **FTIR (neat)** 3546, 3004, 2633, 1710, 1642, 1443, 755 cm^{-1}; **HRMS (ESI)** calculated for $C_{24}H_{18}{}^{37}ClN_2O_4S$ $[M+H]^+$: 467.0641; found: 467.0646; **HPLC** condition: HPLC Chiralcel OD-H, hexane/ i-PrOH = 80:20 v/v, flow rate = 1.0 mL/min, λ = 350 nm, 25 °C, t_R (major) = 35.82, t_R (minor) = 18.90 min, 88% *ee,* $[\alpha]_D^{20.2}$ = +78.7 (c 1, CH_3CN).

(*3S,3aS,4S*)-4-(4-Chlorophenyl)-2-formyl-4-hydroxy-3*a*,4-dihydro-3*H*-benzo[*b*] pyrrolo[1,2-*d*][1,4]thiazine-3-yl)benzonitrile 3v: Prepared according to general procedure D using chiral catalyst **C5**, purification of crude product was carried out by column chromatography using hexane: EtOAc mixture (60:40) to afford **3v** as a yellow solid;

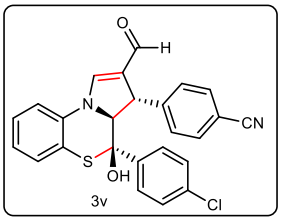

(75% yield, 100 mg); R_f = 0.40 (40% ethyl acetate in hexane); mp 254-256 ºC; d.r. >20:1(determined by ^{1}H NMR analysis of crude reaction mixture).

^{1}H NMR (400 MHz, DMSO-d$_6$) δ 9.29 (s, 1H), 8.59 (s, 1H), 7.08 (d, *J* = 6.0 Hz, 2H), 7.54 – 7.45 (m, 4H), 7.42 (d, *J* = 8.0 Hz, 2H), 7.30 – 7.13 (m, 2H), 7.10 – 6.95 (m, 2H), 6.67 (d, *J* = 7.6 Hz, 2H), 4.54 (d, *J* = 6.8 Hz, 1H), 4.03 (d, *J* = 6.4 Hz, 1H); **^{13}C NMR (100 MHz, DMSO-d$_6$)** δ 182.0, 152.6, 148.6, 138.1, 134.0, 133.5, 131.9, 129.1, 128.3, 128.2, 126.7, 125.7, 123.2, 121.7, 121.2, 118.8, 117.3, 109.0, 80.4, 76.5, 47.1; **FTIR**

(neat) 3541, 3004, 2635, 1736, 1636, 1439, 744 cm^{-1}; **HRMS (ESI)** calculated for $C_{25}H_{18}{}^{37}ClN_2O_2S$ $[M+H]^+$: 447.0743; found: 447.0751; **HPLC** condition: Chiralcel OD-H, hexane/ i-PrOH = 80:20 v/v, flow rate = 1.0 mL/min, λ = 350 nm, 25 °C, t_R (major) = 22.0, t_R (minor) = 15.30 min, 94% *ee*, $[\alpha]_D^{20.1}$ = +599.9 (c 1, CH_3CN).

(*3S,3aS,4S*)-3-(4-Formylphenyl)-4-hydroxy-4-phenyl-3*a*,4-dihydro-3*H*-benzo[*b*] pyrrolo[1,2-*d*][1,4] thiazine-2-carbaldehyde 3w: Prepared according to general procedure D using chiral catalyst **C5**, purification of crude product was carried out by column chromatography using hexane: EtOAc mixture (70:30) to afford **3w** as a pale yellow solid; (76% yield 94 mg); R_f = 0.40 (50% ethyl acetate in hexane); mp 196-198 ºC d.r. >20:1(determined by ^1H NMR analysis of crude reaction mixture).

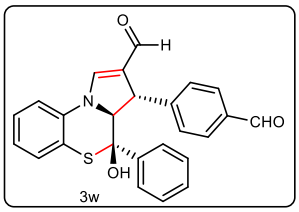

^1H NMR (400 MHz, DMSO-d_6) δ 9.84 (s, 1H), 9.31 (s, 1H), 8.59 (s, 1H), 7.61 (d, *J* = 8.4Hz, 1H), 7.56 – 7.46 (m, 5H), 7.34 (d, *J* = 6.4 Hz, 3H), 7.25 – 7.15 (m, 2H), 7.04 (t, *J* = 6.0 Hz, 1H), 6.55 (d, *J* = 7.6 Hz, 2H), 4.44 (d, *J* = 6.0 Hz, 1H), 5.58 (d, *J* = 6.4 Hz, 1H); **^{13}C NMR (100 MHz, DMSO-d_6)** δ 192.5, 182.0, 152.7, 149.9, 139.0, 134.4, 134.0, 129.2, 128.6, 128.3, 127.7, 127.2, 126.7, 125.5, 123.1, 122.0, 121.4, 117.3, 81.0, 76.8, 46.9; **FTIR (neat)** 3433, 2958, 2851, 1740, 1697, 1583, 1487, 1276, 744 cm^{-1}; **HRMS (ESI)** calculated for $C_{25}H_{20}NO_3S$ $[M+H]^+$: 414.1158; found: 414.1148; **HPLC** condition: HPLC Chiralcel OD-H, hexane/i-PrOH = 70:30 v/v, flow rate = 1.0 mL/min, λ = 350 nm, 25 °C, t_R (major) = 31.85, t_R (minor) = 19.70 min, 92% *ee*, $[\alpha]_D^{20}$ = +243.9 (c 0.1, CH_3CN).

(*3S,3aS,4S*)-4-Hydroxy-4-phenyl-3-(3-(trifluoromethyl)phenyl)-3*a*,4-dihydro-3*H*-benzo[*b*] pyrrolo[1,2-*d*][1,4]thiazine-2-carbaldehyde 3x: Prepared according to general procedure D using chiral catalyst **C5**, purification of crude product was carried out by column chromatography using hexane: EtOAc mixture (70:30) to afford **3x** as a yellow solid; (88% yield 119 mg); R_f = 0.30 (40% ethyl acetate in hexanes); mp 158 -160 ºC; d.r. >20:1 (determined by ^{1}H NMR analysis of crude reaction mixture).

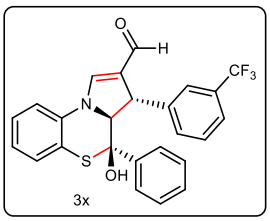

^{1}H NMR (500 MHz, DMSO-d$_6$) δ 9.32 (s, 1H), 8.60 (s, 1H), 7.66 – 7.59 (m, 1H), 7.55 – 7.40 (m, 3H), 7.45 – 7.30 (m, 4H), 7.36 – 7.15 (m, 4H), 7.10 – 7.00 (m, 1H), 7.80 (d, *J* = 8.0 Hz, 1H), 6.34 (s, 1H), 4.13 (d, *J* = 5.0 Hz, 1H), 4.01 (d, *J* = 6.0 Hz, 1H); **^{13}C NMR (125 MHz, DMSO)** δ 182. 6, 153.5, 144.7, 139.4, 134.5, 131.4, 131.2, 129.6, 129.2 (q, *J* = 32 Hz), 129.1, 128.8, 128.4 (q, *J* = 36 Hz), 127.7, 127.2, 126.4, 126.0, 124.4 (q, *J* = 271 Hz), 124.0 (q, J = 3.5 Hz), 123.6, 122.5, 121.4, 117.8, 81.4, 77.4, 47.0; **^{19}F NMR (471 MHz, DMSO-d$_6$)** δ -61.01; **FTIR** 3458, 2953, 2857, 1738, 1622, 1598, 1487, 742 cm^{-1}; **HRMS (ESI)** calculated for $C_{25}H_{19}F_3NO_2S$ $[M+H]^+$: 454.1083; found: 454.1136; **HPLC** condition: HPLC Chiralcel OD-H, hexane/i-PrOH = 80:20 v/v, flow rate = 1.0 mL/min, λ = 350 nm, 25 °C, t_R (major) = 24.12, t_R (minor) = 14.80 min, 98% *ee*, $[\alpha]_D^{20}$ = +227.96 (c 0.1, CH_3CN).

(3*S*,3*aS*,4*S*)-3-([1,1'-Biphenyl]-4-yl)-4-(4-bromophenyl)-4-hydroxy-3*a*,4-dihydro-3*H*-benzo[*b*]pyrrolo [1,2-*d*][1,4]thiazine-2-carbaldehyde 3y: Prepared according to general procedure D using chiral catalyst **C5**, purification of crude product was carried out by column chromatography using hexane: EtOAc (70:30) to afford **3y** as pale yellow

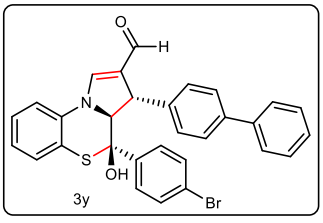

solid; (82% yield 113 mg); R_f = 0.30 (40 % ethyl acetate in hexanes); mp 168 – 170 °C; d.r. >20:1 (determined by ^{1}H NMR analysis of crude reaction mixture).

^{1}H NMR (400 MHz, DMSO) δ 9.35 (s, 1H), 8.54 (s, 1H), 7.66 – 7.52 (m, 6H), 7.50 – 7.35 (m, 5H), 7.36 – 7.28 (m, 3H), 7.25 – 7.15 (m, 2H), 7.04 (t, *J* = 7.6 Hz, 1H), 6.52 (d, *J* = 7.6 Hz, 2H), 4.42 (d, *J* = 6.4 Hz, 1H), 4.04 (d, *J* = 6.0 Hz, 1H); **^{13}C NMR (100 MHz, DMSO)** δ 182.3, 152.6, 142.3, 139.8, 138.7, 138.1, 134.2, 131.2, 129.6, 128.9, 127.5, 127.3, 126.7, 126.5, 126.3, 125.7, 123.1, 122.1, 122.0, 121.8, 117.3, 80.8, 77.0, 46.5; **FTIR** 3440, 2955, 2853, 1633, 1586, 1486, 1218, 1198, 743cm^{-1}; **HRMS (ESI)** calculated for $C_{30}H_{23}{}^{81}BrNO_2S$ $[M+H]^+$: 542.0607; found: 542.0641; **HPLC** condition: HPLC Chiralcel OD-H, hexane/i-PrOH = 70:30 v/v, flow rate = 1.0 mL/min, λ = 350 nm, 25 °C, t_R (major) = 17.95, t_R (minor) = 14.45 min, 94% *ee*, $[\alpha]_D^{20}$ = +625.57 (c 0.1, CH_3CN).

(3*S*,3*aS*,4*S*)-4-(4-Chlorophenyl)-3-(furan-3-yl)-4-hydroxy-3*a*,4-dihydro-3*H*-benzo[*b*]pyrrolo[1,2-*d*][1,4]thiazine-2-carbaldehyde 3z: Prepared according to general procedure D using chiral catalyst **C5**, purification of crude product was carried out by column chromatography using hexane: EtOAc (70:30) to afford **3z** as a brown solid; (62% yield, 76 mg); R_f = 0.35 (40% ethyl acetate in hexanes); mp 210-212 °C; d.r. >20:1 (determined by ^{1}H NMR analysis of crude reaction mixture).

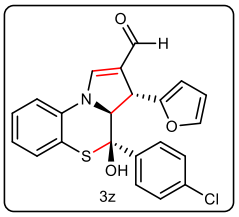

^{1}H NMR (500 MHz, DMSO-d$_6$) δ 9.33 (s, 1H), 8.48 (s, 1H), 7.56 (d, *J* = 7.7 Hz, 4H), 7.46 (d, *J* = 8.1 Hz, 2H), 7.28 (s, 1H), 7.20 (dd, *J* = 18.0, 8.3 Hz, 2H), 7.03 (t, *J* = 7.6 Hz, 1H), 6.13 (d, *J* = 3.2 Hz, 1H), 5.34 (d, *J* = 3.3 Hz, 1H), 4.55 (d, *J* = 6.4 Hz, 1H), 4.11 (d, *J* = 6.5 Hz, 1H); **^{13}C NMR (125 MHz, DMSO-d$_6$)** δ 182.20, 154.06, 152.38, 141.56, 138.16, 133.97, 133.27, 131.17, 129.07, 128.16, 126.73, 125.73, 123.17,

121.74, 119.02, 117.07, 110.23, 105.14, 80.44, 73.71, 40.15; **FTIR (neat)** 3447, 2952, 1636, 1563, 1485, 749 cm^{-1}; **HRMS (ESI)** calculated for $C_{22}H_{17}{}^{37}ClNO_3S$ $[M+H]^+$: 412.0583; found: 412.0591; **HPLC** condition: Chiralcel OD-H, hexane/i-PrOH = 80:20 v/v, flow rate = 1.0 mL/min, λ = 350 nm, 25 °C, t_R (major) = 24.90, t_R (minor) = 15.70 min, 88% *ee*, $[\alpha]_D^{20.1}$ = +99.7 (c 1, CH_3CN).

(3*S*,3*aS*,4*S*)-3-(Anthracen-9-yl)-4-(4-chlorophenyl)-4-hydroxy-3*a*,4-dihydro-3*H*-benzo[*b*]pyrrolo[1,2-*d*][1,4]thiazine-2-carbaldehyde 3aa: Prepared according to general procedure D using chiral catalyst **C5**, purification of crude product was carried out by column chromatography using hexane: EtOAc (70:30) to afford **3aa** as a pale yellow solid; (74% yield (116 mg); R_f = 0.40 (40% ethyl acetate in hexane); mp 244 -246 ºC d.r. >20:1(determined by ^1H NMR analysis of crude reaction mixture).

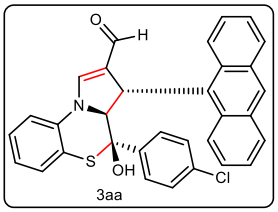

3aa

^1H NMR (400 MHz, DMSO-d_6) δ 9.34 (s, 1H), 8.74 (s, 1H), 8.38 (s, 1H), 8.15 – 8.00 (m, 2H), 7.90 – 7.75 (m, 4H), 7.50 – 7.20 (m, 4H), 7.23 – 7.14 (m, 2H), 7.10 – 6.95 (m, 3H), 6.70 (d, *J* = 7.6 Hz, 2H) 5.65 (d, *J* = 8.0 Hz, 1H), 5.04 (d, *J* = 8.0 Hz, 1H); **^{13}C NMR (100 MHz, DMSO-d_6)** δ 182.5, 151.5, 137.5, 134.4, 133.1, 132.7, 131.3, 130.6, 129.9, 129.7, 129.1, 128.4, 128.1, 127.6, 127.0, 126.9, 126.1, 125.5, 125.1, 124.4, 124.0, 123.6, 123.5, 123.3, 121.9, 117.1, 80.1, 76.4, 41.5; **FTIR (neat)** 3541, 2998, 1705, 1631, 1443, 749 cm^{-1}; **HRMS (ESI)** calculated for $C_{32}H_{23}{}^{37}ClNO_2S$ $[M+Na]^+$: 544.0922; found: 544.0938; **HPLC** condition: HPLC Chiralcel OD-H, hexane/i-PrOH = 50:50 v/v, flow rate = 1.0 mL/min, λ = 350 nm, 25 °C, t_R (major) = 31.50, t_R (minor) = 10.36 min, 98% ee, $[\alpha]_D^{20}$ = +116.9 (c 1, CH_3CN).

(*3S,3aS,4S*)-4-Hydroxy-3-methyl-4-phenyl-3a,4-dihydro-3*H*-benzo[*b*]pyrrolo[1,2-*d*][1,4] thiazine-2-carbaldehyde 3ab: Prepared according to general procedure D using chiral catalyst **C5**, purification of crude product was carried out by column chromatography using hexane: EtOAc (70:30) to afford **3ab** as a pale yellow solid; (58% yield, 56 mg); R_f = 0.30 (40% ethyl acetate in hexane); mp 182 – 184 ºC; d.r. >20:1(determined by ^{1}H NMR analysis of crude reaction mixture).

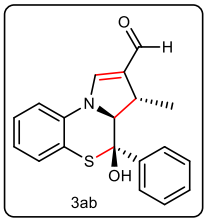

3ab

^{1}H NMR (400 MHz, DMSO-d$_6$) δ 9.30 (s, 1H), 8.30 (s, 1H), 7.63 (d, *J* = 7.6 Hz, 2 H), 7.55 – 7.45 (m, 3H), 7.43 – 7.37 (m, 1H), 7.23 (s, 1H), 7.20 – 7.14 (m, 2H), 7.00 (t, *J* = 7.6 Hz, 1H), 4.24 (d, *J* = 6.4 Hz, 1H), 2.93 (d, *J* = 6.9 Hz, 1H), 0.65 (d, *J* = 6.8 Hz, 1H); **^{13}C NMR (100 MHz, DMSO-d$_6$)** δ 182.5, 151.0, 139.0, 133.9, 128.1, 127.9, 126.7, 126.5, 125.2, 123.0, 122.3, 121.5, 116.2, 80.4, 75.4, 35.7, 19.4; **DEPT-135 (100 MHz, DMSO-d$_6$)** δ 151.8, 128.9, 128.7, 127.5, 127.3, 126.0, 123.1, 117.0, 76.2, 36.5, 20.2; **FTIR (neat)** 3441, 2962, 2925, 1736, 1626, 1491, 1292, 749 cm^{-1}; **HRMS (ESI)** calculated for $C_{19}H_{18}NO_2S$ $[M+H]^+$: 324.1053; found: 324.1048; **HPLC** condition: HPLC Chiralcel OD-H, hexane/i-PrOH = 80:20 v/v, flow rate = 1.0 mL/min, λ = 350 nm, 25 °C, t_R (major) = 28.10, t_R (minor) = 15.34 min, 80% *ee*, $[\alpha]_D^{20}$ = +456.32 (c 0.1, CH_3CN).

(*3S,3aS,4S*)-3-Ethyl-4-hydroxy-4-phenyl-3*a*,4-dihydro-3*H*-benzo[*b*]pyrrolo[1,2-*d*][1,4] thiazine-2-carbaldehyde 3ac; Prepared according to general procedure D using chiral catalyst **C5**, purification of crude product was carried out by column chromatography using hexane: EtOAc (70:30) to afford **3ac** as an orange solid; (40% yield, 40 mg); R_f = 0.30 (30%

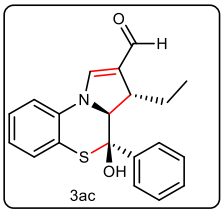

3ac

ethyl acetate in hexane); mp 60 - 62 °C d.r. >20:1(determined by ^{1}H NMR analysis of crude reaction mixture).

^{1}H NMR (400 MHz, DMSO-d$_6$) δ 9.30 (s, 1H), 8.25 (s, 1H), 7.64 (d, *J* = 7.6 Hz, 2H) 7.50 – 7.44 (m, 3H), 7.40 – 7.34 (m, 1H), 7.20 – 7.10 (m, 4H), 7.05 – 6.95 (m, 1H), 4.34 (d, *J* = 5.6 Hz, 1 H), 3.00 – 2.90 (m, 1H), 0.90 – 0.70 (m, 2H), 0.37 (t, *J* = 7.6 Hz, 3H); **^{13}C NMR (100 MHz, DMSO-d$_6$)** δ 182.4, 152.5, 139.1, 134.0, 128.1, 127.9, 127.0, 126.4, 125.1, 122.6, 122.0, 121.0, 116.8, 81.3, 71.9, 41.4, 24.2, 8.4; **DEPT-135 (100 MHZ, DMSO-d$_6$)** δ 153.2, 128.9, 128.7, 127.7, 127.1, 125.9, 123,4, 117.6, 72.7, 42.1, 24.9, 9.2; **FTIR (neat)** 3441, 2955, 2924, 1738, 1620, 1583, 1486, 1217, 751 cm^{-1}; **HRMS (ESI)** calculated for $C_{20}H_{20}NO_2S$ $[M+H]^+$: 338.1209; found: 338.1202; **HPLC** condition: HPLC Chiralcel OD-H, hexane/i-PrOH = 80:20 v/v, flow rate = 1.0 mL/min, λ = 350 nm, 25 °C, t_R (major) = 19.60, t_R (minor) = 13.80 min, 92% *ee*, $[\alpha]_D^{20.1}$ = +201.98 (c 0.1, CH_3CN).

(*3S,3aS,4S*)-3-Butyl-4-hydroxy-4-phenyl-3*a*,4-dihydro-3*H*-benzo[*b*]pyrrolo[1,2-*d*][1,4] thiazine-2-carbaldehyde 3ad: Prepared according to general procedure D using chiral catalyst **C5**, purification of crude product was carried out by column chromatography using hexane: EtOAc (70:30) to afford **3ad** as a pale yellow solid; (45% yield, 50 mg); R_f = 0.40 (30% ethyl acetate in hexane); mp 70 - 72 °C; d.r. >20:1(determined by ^{1}H NMR analysis of crude reaction mixture).

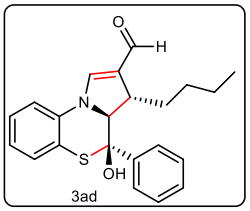

3ad

^{1}H NMR (400 MHz, DMSO-d$_6$) δ 9.29 (s, 1H), 8.22 (s, 1H), 7.64 (d, *J* = 7.6 Hz, 2H), 7.50 (t, *J* = 8.0 Hz, 3H), 7.39 (t, *J* = 7.2 Hz, 1H) 7.20 – 7.15 (m, 3H), 7.01 (t, *J* = 7.6 Hz, 1H), 4.24 (d, *J* = 5.6 Hz, 1H), 3.00 – 2.90 (m, 1H), 2.20 – 2.05 (m, 2H), 1.30 – 1.20 (m, 3H), 1.18 – 1.12 (m, 1H), 0.65 – 0.59 (m, 3H); **^{13}C NMR (100 MHz, DMSO-d$_6$)** δ

182.3, 152.3, 139.1, 134.0, 128.1, 127.9, 127.0, 126.3, 125.1, 122.6, 122.0, 121.8, 116.9, 81.4, 72.7, 40.2, 31.7, 26.1, 21.6, 13.4; **DEPT-135 (100 MHz, DMSO-d$_6$)** δ 153.1, 128.9, 128.7, 127.8, 127.1, 125.9, 123.4, 117.7, 73.5, 41.0, 32.5, 26.9, 22.4, 14.2; **FTIR (neat)** 3437, 2925, 2857, 1740, 1376, 1229, 1047 cm^{-1}; **HRMS (ESI)** calculated for $C_{22}H_{24}NO_2S$ $[M+H]^+$: 366.1522; found: 366.1518; **HPLC** condition: HPLC Chiralcel OD-H, hexane/i-PrOH = 80:20 v/v, flow rate = 1.0 mL/min, λ = 350 nm, 25 °C, t_R (major) = 20.00, t_R (minor) = 12.73 min, 96% *ee*, $[\alpha]_D^{20}$ = +65.98 (c 0.1, CH_3CN).

(3*S*,3*aS*,4*S*)-4-(4-Bromophenyl)-3-phenyl-4-((trimethylsilyl)oxy)-3*a*,4-dihydro-3*H*-benzo[*b*] pyrrolo[1,2-*d*][1,4]thiazine-2-carbaldehyd 5a; Prepared according to general procedure E using chiral compound **3f**, purification of crude product was carried out by column chromatography using hexane: EtOAc (70:30) to afford **5a** as yellow liquid; 94% yield 75 mg); R_f = 0.43 (20% ethyl acetate in hexane); d.r. >20:1(determined by ^{1}H NMR using crude reaction mixture).

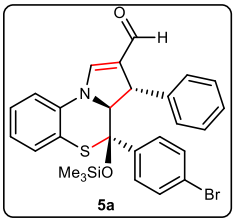

5a

^{1}H NMR (400 MHz, DMSO-d$_6$) δ 9.33 (s, 1H), 8.55 (s, 1H), 7.64 (d, *J* = 8.0 Hz, 2H), 7.59 (d, *J* = 8.0 Hz, 1H), 7.45 (d, *J* = 8.0 Hz, 2H), 7.27 – 7.20 (m, 2H), 7.10 – 7.00 (m, 4H), 6.45 – 6.34 (m, 2H), 4.19 (d, *J* = 5.40 Hz, 1H), 3.99 (d, *J* = 5.0 Hz, 1H), -0.02 (s, 9H); **^{13}C NMR (101 MHz, DMSO-d$_6$)** δ 182.1, 152.3, 142.8, 138.2, 134.0, 131.5, 129.7, 128.1, 126.7, 126.4, 126.3, 126.1, 123.4, 122.6, 122.3, 121.6, 117.5, 83.3, 77.7, 46.4, 1.3; **FTIR (neat)** 3058, 2923, 2852, 1742, 1646, 1417, 757 cm^{-1}; **HRMS (ESI)** calculated for $C_{27}H_{27}{}^{81}BrNO_2SSi$ $[M+H]^+$: 538.0689; found: 538.0669; **HPLC** condition: HPLC Chiralpak-IA, hexane/i-PrOH = 90:10 v/v, flow rate = 1.0 mL/min, λ = 350 nm, 25 °C, t_R (major) = 6.94, t_R (minor) = 9.10 min, 96% *ee*, $[\alpha]_D^{20}$ = +432.90 (c 0.1, CH_3CN).

1-(4-Bromobenzoyl)-2-phenylbenzo[*d*]pyrrolo[2,1-*b*]thiazole-3-carbaldehyde 5b; Prepared according to general procedure F using chiral compound **3f**, Purification of crude product was carried out by column chromatography using hexane: EtOAc (70:30) to afford **5b** as yellow solid; (60% yield, 83 mg); R_f = 0.50 (20% ethyl acetate in hexane); mp: 192 - 194 °C.

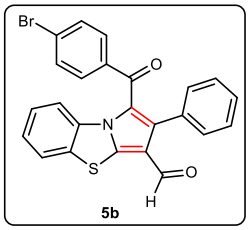

^{1}H NMR (500 MHz, DMSO-d$_6$) δ 9.64 (s, 1H), 8.19 (d, *J* = 7.0 Hz, 1H), 8.11 (d, *J* = 8.0 Hz, 1H), 7.63 (d, *J* = 8.0 Hz, 1H), 7.58 – 7.50 (m, 3H), 7.36 (d, *J* = 8.5 Hz, 1H), 7.28 – 7.17 (m, 6H); **^{13}C NMR (125 MHz, DMSO-d$_6$)** δ 185.7, 184.6, 141.5, 138.9, 138.0, 137.2, 136.9, 134.1, 132.1, 132.1, 131.6, 131.4, 131.3, 128.5, 128.4, 127.2, 126.4, 125.4, 117.3, 114.9; **FTIR (neat)** 3061, 2924, 1635, 1577, 1466, 1222, 794 cm^{-1}; **HRMS (ESI)** calculated for $C_{24}H_{15}{}^{81}BrNO_2S$ $[M+H]^+$: 461.9981; found: 461.9971.

2.16 X-RAY CRYSTALLOGRAPHY DATA:

Figure 2.10 X-ray Crystallographic Data for Racemic Compound 3i':

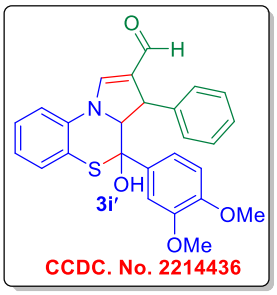

The purified compound **3i' racemic** was dissolved in acetonitrile 0.1 M and placed in a dark cabinet for slow evaporation. Crystals were collected after a few days for X-ray analysis. Thermal ellipsoids are shown at the 50% probability level.

Table 2.7. Crystal data and structure refinement for 3i'

Identification code	123	
Empirical formula	$C_{26}H_{23}NO_4S$	
Formula weight	445.51	
Temperature	296(2) K	
Wavelength	0.71073 Å	
Crystal system	Monoclinic	
Space group	P 2_1/c	
Unit cell dimensions	a = 13.1813(9) Å	α= 90°.
	b = 14.1268(9) Å	β= 115.349(2)°.
	c = 13.3594(9) Å	γ = 90°.
Volume	2248.1(3) $Å^3$	
Z	4	
Density (calculated)	1.316 g cm^{-3}	
Absorption coefficient	0.177 mm^{-1}	
F(000)	936	
Crystal size	0.250 x 0.220 x 0.100 mm^3	
Theta range for data collection	2.219 to 24.819°.	
Index ranges	-15<=h<=14, -16<=k<=16, -11<=l<=15	
Reflections collected	15670	
Independent reflections	3880 [R(int) = 0.0350]	
Completeness to theta = 24.819°	99.9 %	
Refinement method	Full-matrix least-squares on F^2	
Data / restraints / parameters	3880 / 0 / 295	
Goodness-of-fit on F^2	1.129	
Final R indices [I>2sigma(I)]	R1 = 0.0413, wR2 = 0.0944	

R indices (all data)	R1 = 0.0671, wR2 = 0.1057
Extinction coefficient	n/a
Largest diff. peak and hole	0.190 and -0.246 e.Å^{-3}

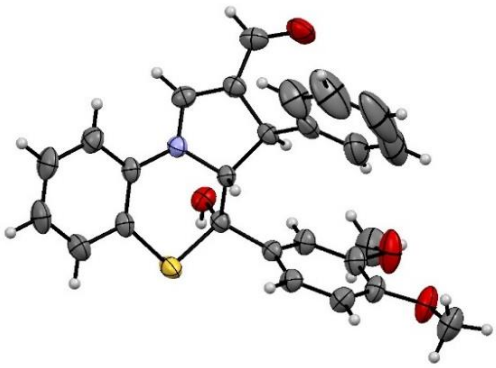

Figure caption: ORTEP diagram of compound **3i'** (47) displacement ellipsoids are drawn at the 50% probability level, and H atoms are shown as small spheres of arbitrary radius. The absolute configuration of the compound was assigned based on the anomalous dispersion method.

Figure 2.11 X-ray Crystallographic Data for Chiral Compound 3f:

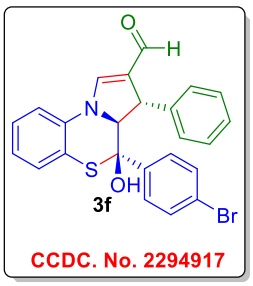

The purified compound **3f chiral** was dissolved in acetonitrile 0.1 M and placed in a dark cabinet for slow evaporation. Crystals were collected after a few days for X-ray analysis. Thermal ellipsoids are shown at the 50% probability level.

Table 2.8. Crystal data and structure refinement for 3f

Identification code	125
Empirical formula	$C_{48}H_{36}Br_2N_2O_4S_2$

Formula weight	928.73	
Temperature	296(2) K	
Wavelength	0.71073 Å	
Crystal system	Orthorhombic	
Space group	$P2_12_12_1$	
Unit cell dimensions	a = 10.1365(3) Å	α= 90°
	b = 10.4504(3) Å	β= 90°
	c = 39.0785(13) Å	γ = 90°
Volume	4139.6(2) $Å^3$	
Z	4	
Density (calculated)	1.490 g cm^{-3}	
Absorption coefficient	2.107 mm^{-1}	
F(000)	1888	
Crystal size	0.180 x 0.160 x 0.120 mm^3	
Theta range for data collection	1.042 to 25.000°.	
Index ranges	-12<=h<=11, -11<=k<=12, -46<=l<=46	
Reflections collected	29301	
Independent reflections	7287 [R(int) = 0.0466]	
Completeness to theta = 25.000°	100.0 %	
Refinement method	Full-matrix least-squares on F^2	
Data / restraints / parameters	7287 / 0 / 531	
Goodness-of-fit on F^2	1.047	
Final R indices [I>2sigma(I)]	R1 = 0.0422, wR2 = 0.0653	
R indices (all data)	R1 = 0.0720, wR2 = 0.0719	
Absolute structure parameter	0.014(5)	
Extinction coefficient	n/a	

Largest diff. peak and hole	0.307 and -0.354 e.Å^{-3}

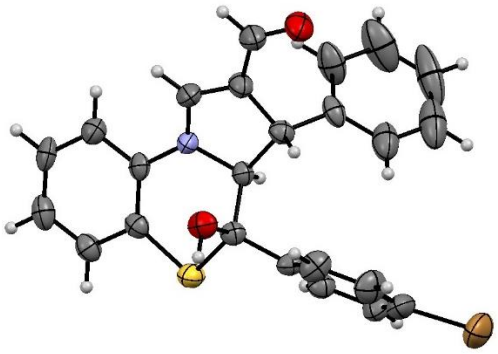

Figure caption: ORTEP diagram of compound **3f** (125) displacement ellipsoids are drawn at the 50% probability level, and H atoms are shown as small spheres of arbitrary radius. The absolute configuration of the compound was assigned based on the anomalous dispersion method.

Figure 2.12 X-ray crystallographic data for chiral compound 3s:

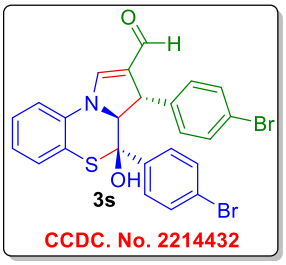

The purified compound **3s chiral** was dissolved in acetonitrile 0.1 M and placed in a dark cabinet for slow evaporation. Crystals were collected after a few days for X-ray analysis. Thermal ellipsoids are shown at the 50% probability level.

Table 2.9. Crystal data and structure refinement for 3s

Identification code	76
Empirical formula	$C_{24}H_{17}Br_2NO_2S$
Formula weight	543.27
Temperature	296(2) K
Wavelength	0.71073 Å

Crystal system	Orthorhombic
Space group	$P2_12_12_1$
Unit cell dimensions	a = 11.5707(4) Å α = 90°
	b = 13.3165(5) Å β = 90°
	c = 13.9154(5) Å γ = 90°
Volume	2144.10(13) $Å^3$
Z	4
Density (calculated)	1.683 g cm^{-3}
Absorption coefficient	3.900 mm^{-1}
F(000)	1080
Crystal size	0.150 x 0.120 x 0.100 mm^3
Theta range for data collection	2.117 to 24.997°.
Index ranges	-13<=h<=13, -15<=k<=14, -16<=l<=16
Reflections collected	18471
Independent reflections	3773 [R(int) = 0.0362]
Completeness to theta = 24.997°	100.0 %
Refinement method	Full-matrix least-squares on F^2
Data / restraints / parameters	3773 / 0 / 275
Goodness-of-fit on F^2	1.096
Final R indices [I>2sigma(I)]	R1 = 0.0248, wR2 = 0.0468
R indices (all data)	R1 = 0.0334, wR2 = 0.0484
Absolute structure parameter	0.001(5)
Extinction coefficient	n/a
Largest diff.peak and hole	0.289 and -0.416 e.$Å^{-3}$

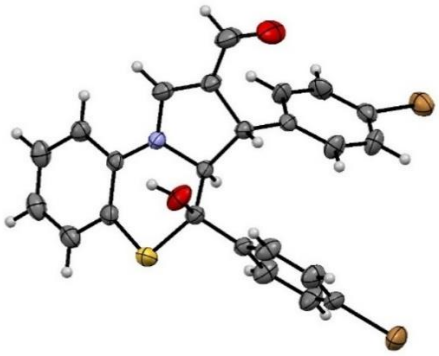

Figure caption: ORTEP diagram of compound **3s** (76) displacement ellipsoids are drawn at the 50% probability level, and H atoms are shown as small spheres of arbitrary radius. The absolute configuration of the compound was assigned based on the anomalous dispersion method.

Figure 2.13 X-ray crystallographic data for chiral compound 3v:

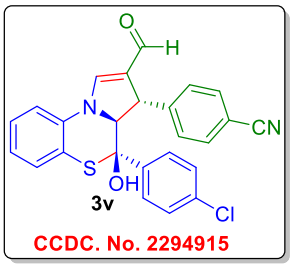

The purified compound **3v chiral** was dissolved in acetonitrile 0.1 M and placed in a dark cabinet for slow evaporation. Crystals were collected after a few days for X-ray analysis. Thermal ellipsoids are shown at the 50% probability level.

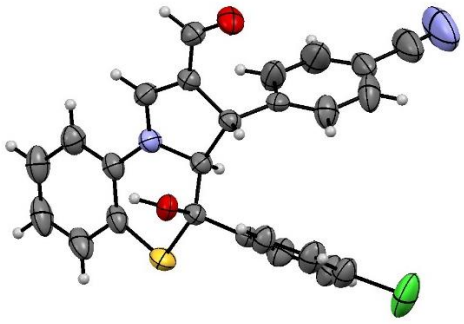

Figure caption: ORTEP diagram of compound **3v** (59) displacement ellipsoids are drawn at the 50% probability level, and H atoms are shown as small spheres of arbitrary radius. The absolute configuration of the compound was assigned based on the anomalous dispersion method.

Table 2.10. Crystal data and structure refinement for 3v

Identification code	59	
Empirical formula	$C_{25}H_{17}ClN_2O_2S$	
Formula weight	444.91	
Temperature	296(2) K	
Wavelength	0.71073 Å	
Crystal system	Orthorhombic	
Space group	P 2_1 2_1 2_1	
Unit cell dimensions	a = 10.3622(6) Å	α = 90°
	b = 11.1598(5) Å	β = 90°
	c = 19.3649(10) Å	γ = 90°
Volume	2239.4(2) $Å^3$	
Z	4	
Density (calculated)	1.320 g cm^3	
Absorption coefficient	0.288 mm^{-1}	
F(000)	920	
Crystal size	0.180 x 0.150 x 0.120 mm^3	
Theta range for data collection	2.103 to 24.998°	
Index ranges	-12<=h<=12, -11<=k<=13, -23<=l<=22	
Reflections collected	17115	
Independent reflections	3939 [R(int) = 0.0278]	
Completeness to theta = 24.998°	100.0 %	

Refinement method	Full-matrix least-squares on F^2
Data / restraints / parameters	3939 / 0 / 284
Goodness-of-fit on F^2	1.032
Final R indices [I>2sigma(I)]	R1 = 0.0387, wR2 = 0.0903
R indices (all data)	R1 = 0.0520, wR2 = 0.0990
Absolute structure parameter	0.02(3)
Extinction coefficient	n/a
Largest diff. peak and hole	0.432 and -0.386 e.Å^{-3}

Figure 2.14 X-ray Crystallographic Data for Chiral Compound 3x:

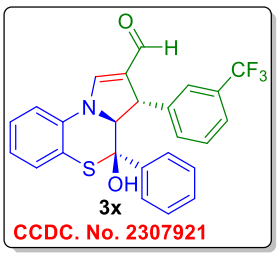

The purified compound **3x chiral** was dissolved in acetonitrile 0.1 M and placed in a dark cabinet for slow evaporation. Crystals were collected after a few days for X-ray analysis. Thermal ellipsoids are shown at the 50% probability level.

Table 2.11. Crystal data and structure refinement for 3x

Identification code	62
Empirical formula	$C_{25}H_{18}F_3NO_2S$
Formula weight	453.46
Temperature	296(2) K
Wavelength	0.71073 Å
Crystal system	Orthorhombic
Space group	$P2_12_12_1$

Unit cell dimensions	a = 11.0417(5) Å	α = 90°
	b = 11.0915(6) Å	β = 90°
	c = 18.2577(10) Å	γ = 90°
Volume	2236.0(2) $Å^3$	
Z	4	
Density (calculated)	1.347 g cm^{-3}	
Absorption coefficient	0.191 mm^{-1}	
F(000)	936	
Crystal size	0.250 x 0.150 x 0.120 mm^3	
Theta range for data collection	2.148 to 24.992°	
Index ranges	-11<=h<=13, -12<=k<=13, -21<=l<=19	
Reflections collected	10074	
Independent reflections	3805 [R(int) = 0.0418]	
Completeness to theta = 24.992°	99.9 %	
Refinement method	Full-matrix least-squares on F^2	
Data / restraints / parameters	3805 / 0 / 294	
Goodness-of-fit on F^2	1.149	
Final R indices [I>2sigma(I)]	R1 = 0.0511, wR2 = 0.1188	
R indices (all data)	R1 = 0.0820, wR2 = 0.1334	
Absolute structure parameter	-0.03(6)	
Extinction coefficient	0.010(2)	
Largest diff. peak and hole	0.460 and -0.277 e.$Å^{-3}$	

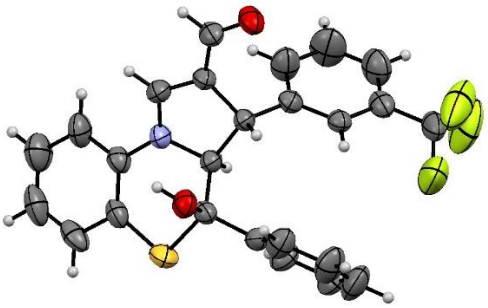

Figure caption: ORTEP diagram of compound **3x** (62) displacement ellipsoids are drawn at the 50% probability level, and H atoms are shown as small spheres of arbitrary radius. The absolute configuration of the compound was assigned based on the anomalous dispersion method.

Figure 2.15 X-ray Crystallographic Data for Chiral Compound 3ab:

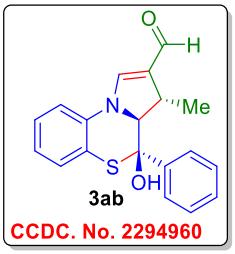

The purified compound **3ab chiral** was dissolved in acetonitrile 0.1 M and placed in a dark cabinet for slow evaporation. Crystals were collected after a few days for X-ray analysis. Thermal ellipsoids are shown at the 50% probability level.

Table 2.12. Crystal data and structure refinement for 3ab

Identification code	203
Empirical formula	$C_{19}H_{17}NO_2S$
Formula weight	323.39
Temperature	296(2) K
Wavelength	0.71073 Å
Crystal system	Orthorhombic

Space group	$P2_12_12_1$	
Unit cell dimensions	a = 8.7669(4) Å	α = 90°
	b = 12.8110(5) Å	β = 90°
	c = 14.5460(4) Å	γ = 90°
Volume	1633.70(11) $Å^3$	
Z	4	
Density (calculated)	1.315 g cm^{-3}	
Absorption coefficient	0.207 mm^{-1}	
F(000)	680	
Crystal size	0.180 x 0.160 x 0.120 mm^3	
Theta range for data collection	2.713 to 25.000°	
Index ranges	-10<=h<=7, -15<=k<=12, -15<=l<=17	
Reflections collected	7172	
Independent reflections	2873 [R(int) = 0.0246]	
Completeness to theta = 25.000°	100.0 %	
Refinement method	Full-matrix least-squares on F^2	
Data / restraints / parameters	2873 / 0 / 213	
Goodness-of-fit on F^2	1.118	
Final R indices [I>2sigma(I)]	R1 = 0.0351, wR2 = 0.0715	
R indices (all data)	R1 = 0.0449, wR2 = 0.0760	
Absolute structure parameter	0.02(4)	
Extinction coefficient	n/a	
Largest diff. peak and hole	0.145 and -0.177 e.$Å^{-3}$	

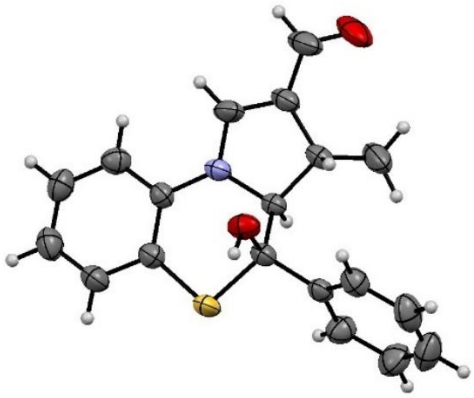

Figure caption: ORTEP diagram of compound **3ab** (203) displacement ellipsoids are drawn at the 50% probability level, and H atoms are shown as small spheres of arbitrary radius. The absolute configuration of the compound was assigned based on the anomalous dispersion method.

2.17 ^{1}H & ^{13}C NMR SPECTRA

(3*S*,3*aS*,4*S*)-4-Hydroxy-3,4-diphenyl-3*a*,4-dihydro-3*H*-benzo[*b*]pyrrolo[1,2-*d*][1,4]thiazine-2-carbaldehyde 3a

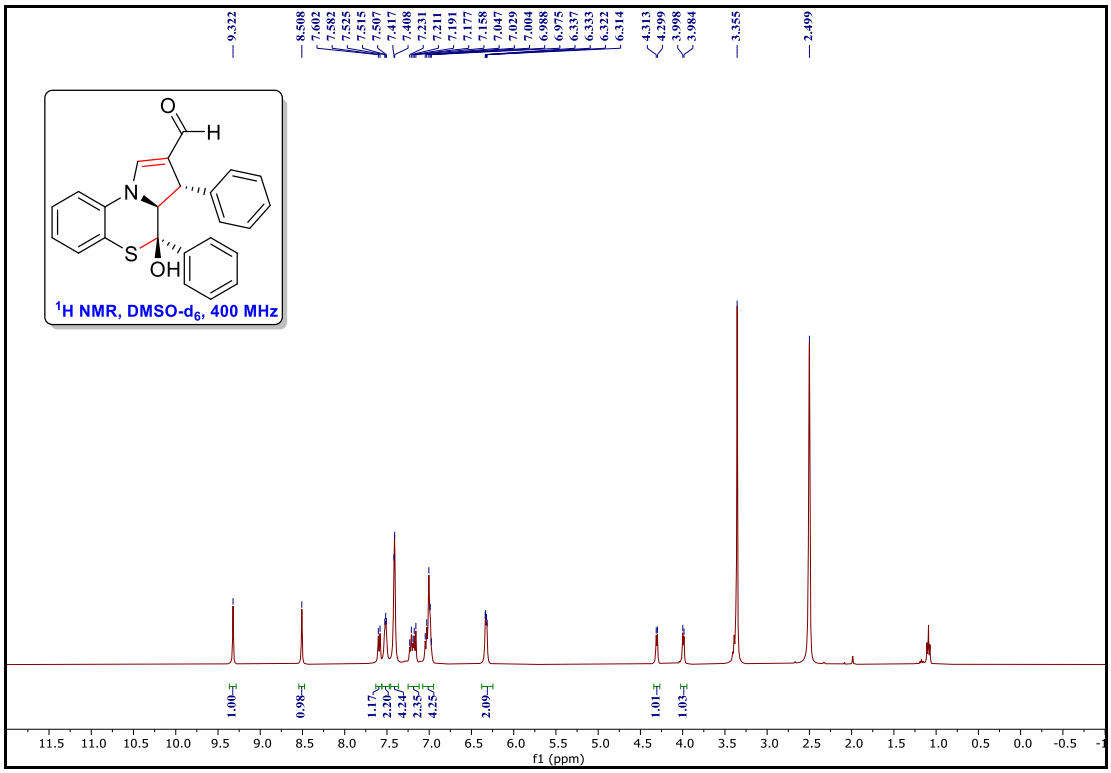

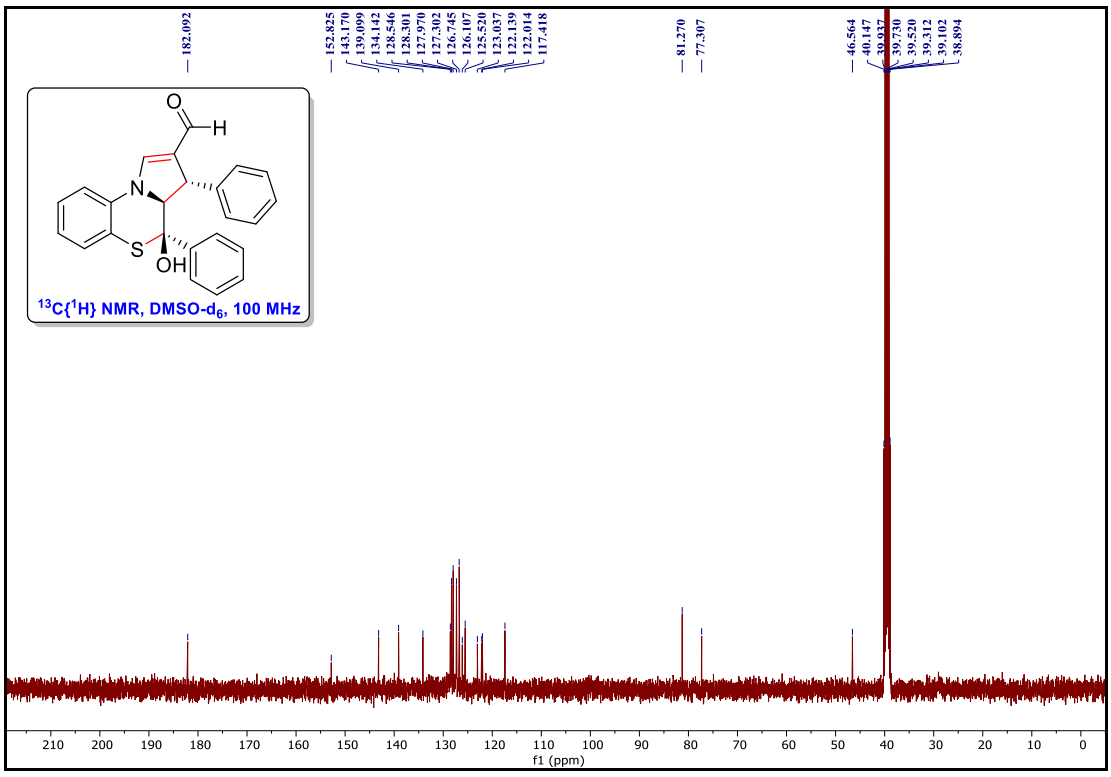

(3*S*,3*aS*,4*S*)-4-Hydroxy-3-phenyl-4-(*p*-tolyl)-3*a*,4-dihydro-3*H*-benzo[*b*]pyrrolo [1,2-*d*][1,4] thiazine-2-carbaldehyde 3b

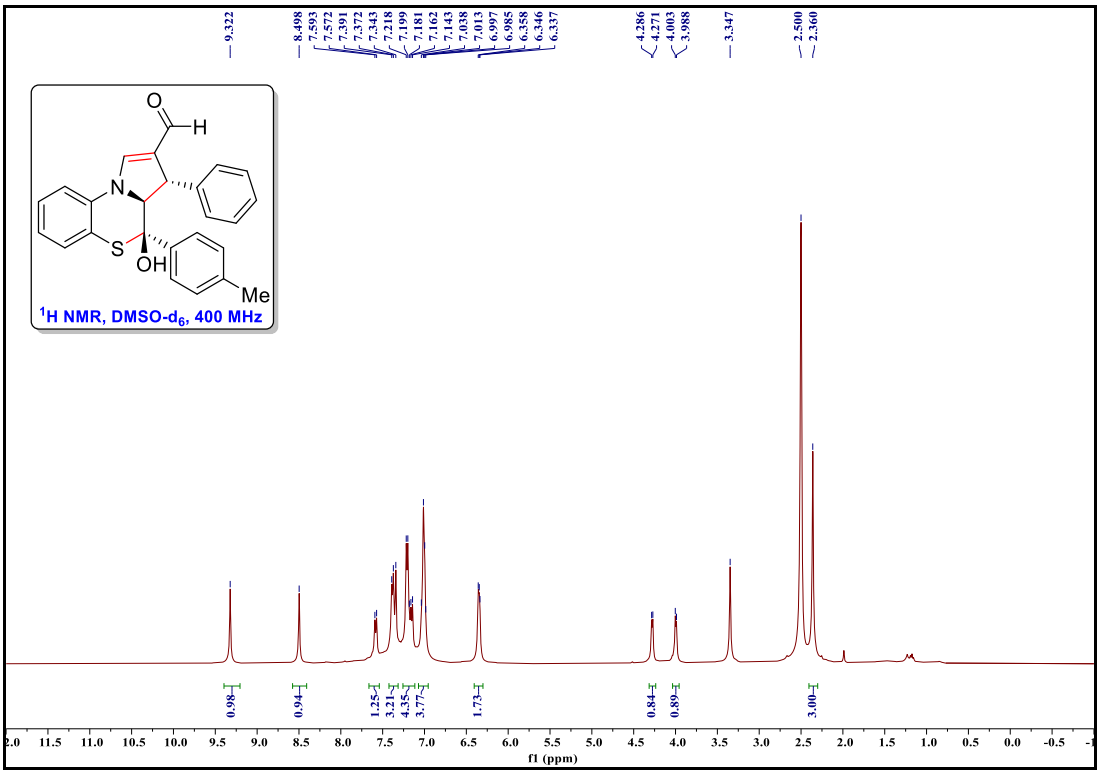

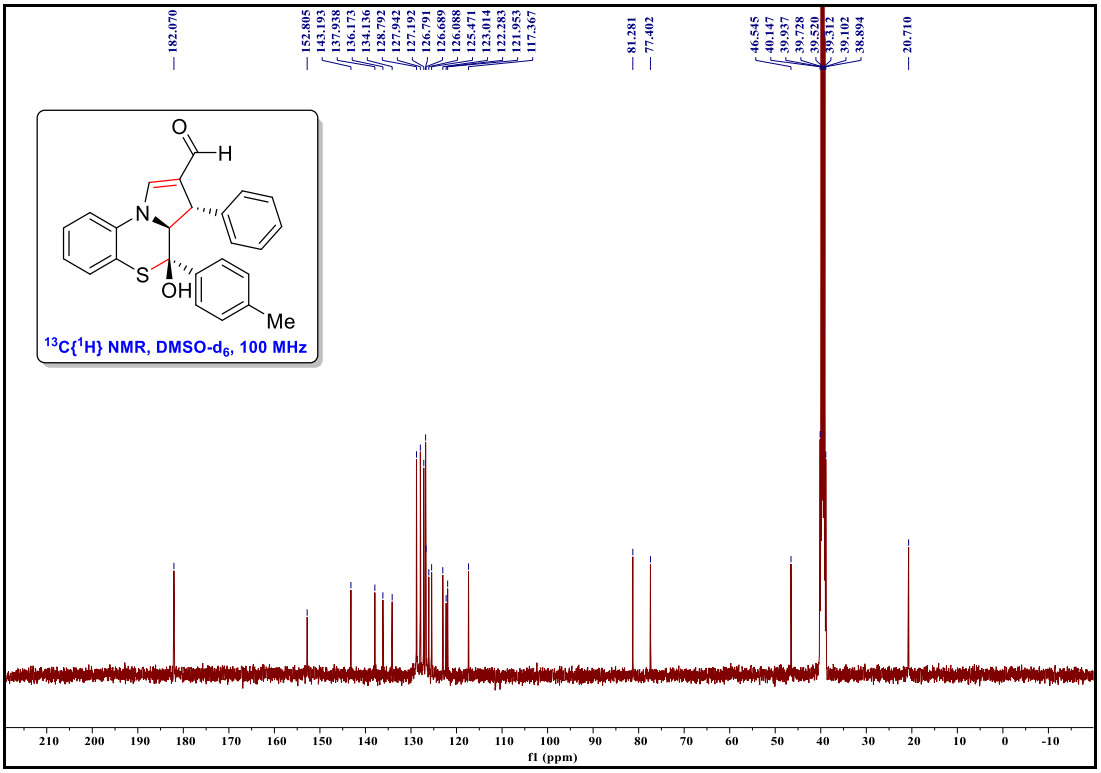

(3*S*,3*aS*,4*S*)-4-(4-Fluorophenyl)-4-hydroxy-3-phenyl-3*a*,4-dihydro-3*H*-benzo[*b*] pyrrolo[1,2-*d*][1,4]thiazine-2-carbaldehyde 3d

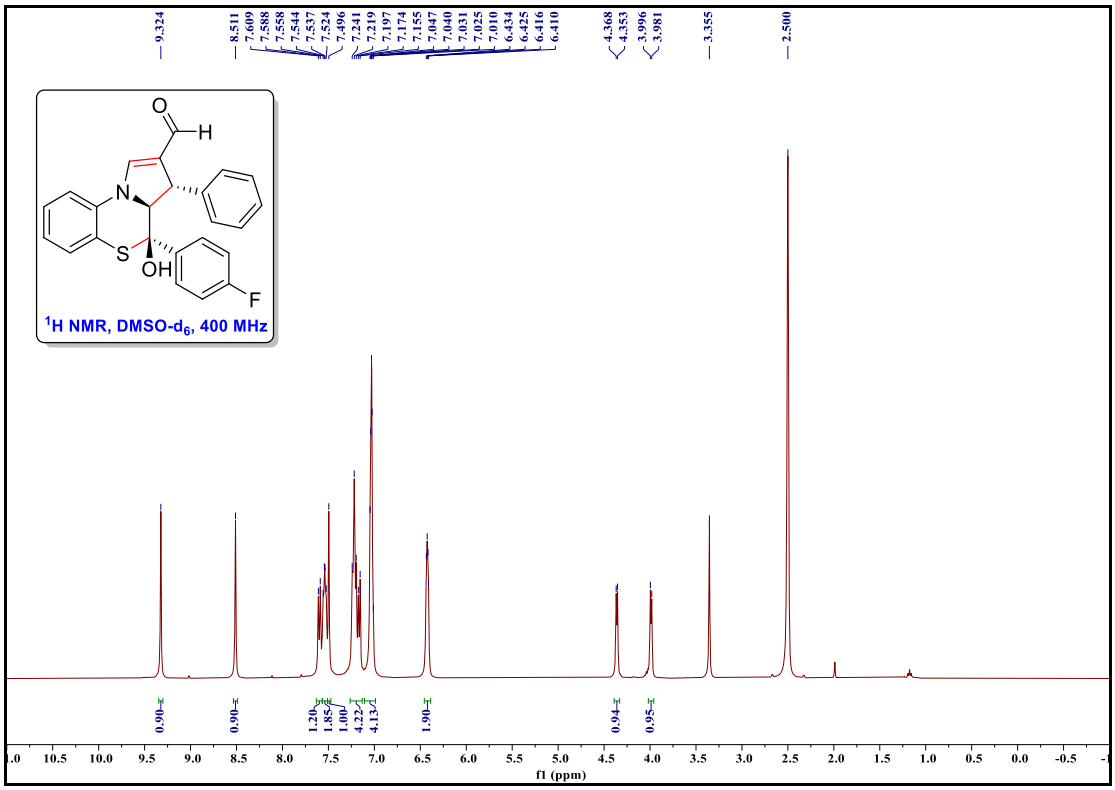

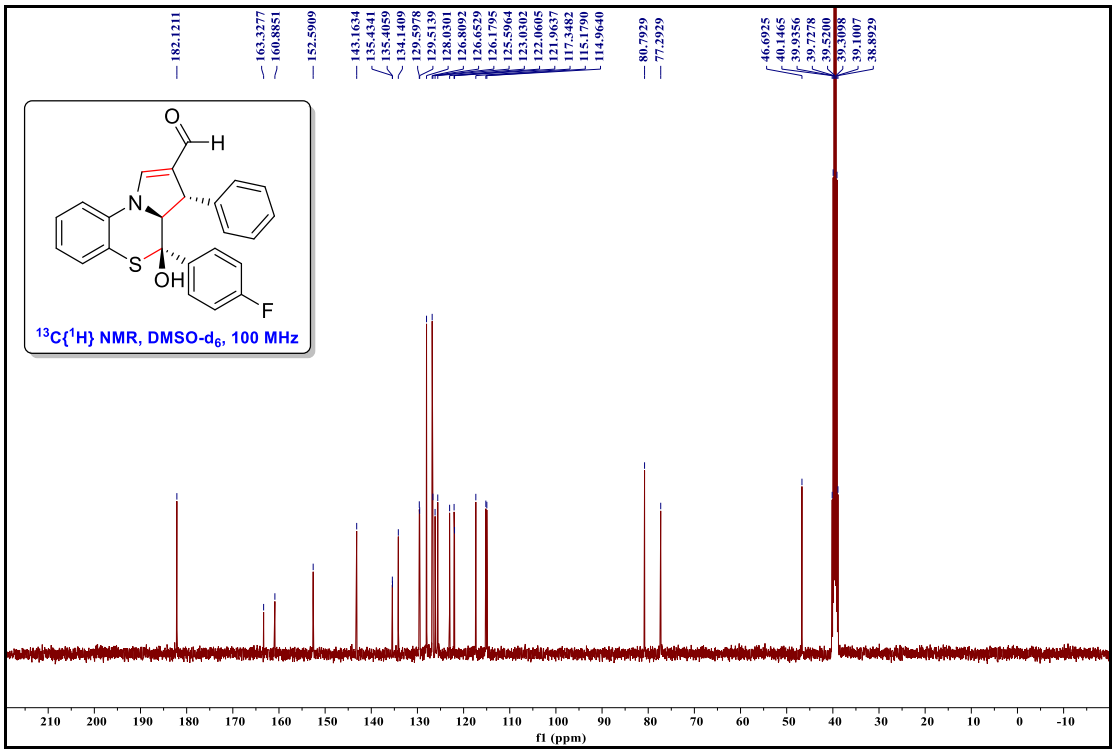

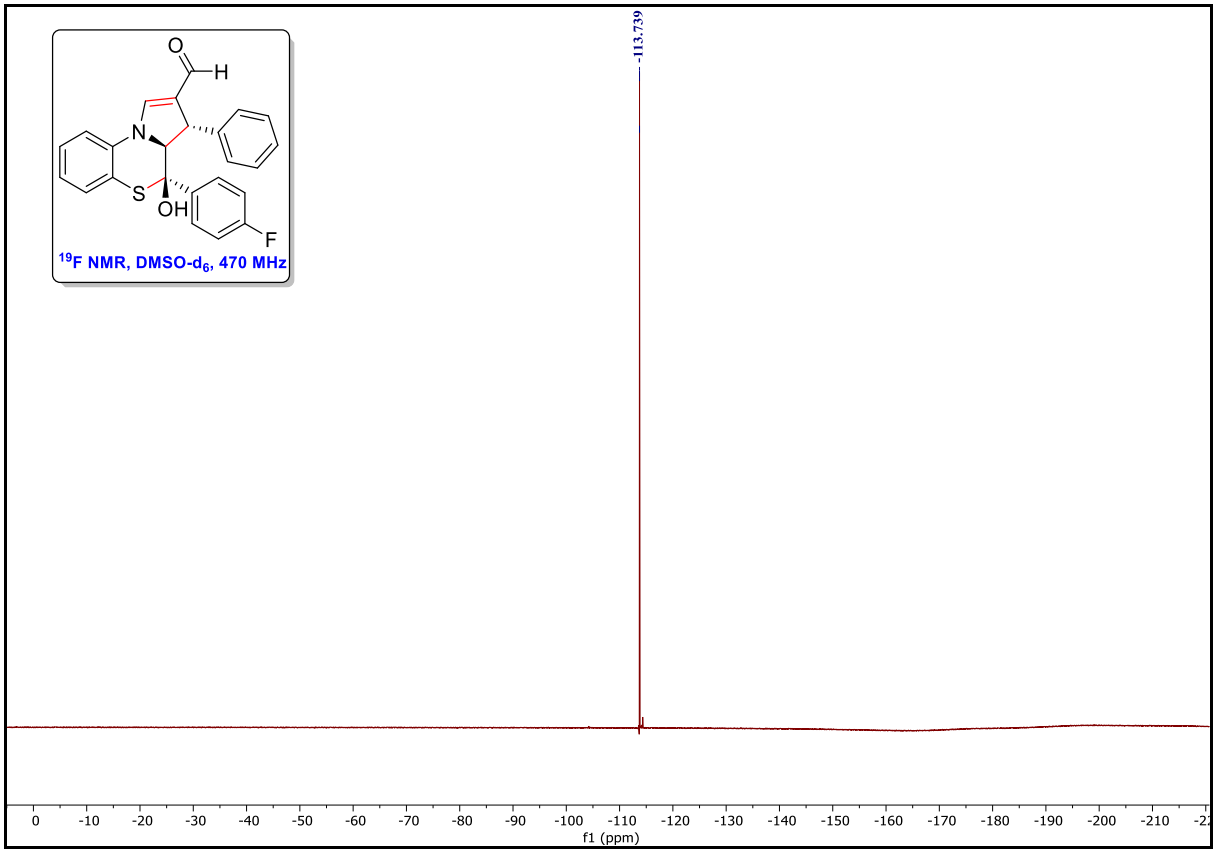
O
H
N
S
OH
F
^{19}F NMR, DMSO-d$_6$, 470 MHz
-113.739
0
-10
-20
-30
-40
-50
-60
-70
-80
-90
-100
-110
-120
-130
-140
-150
-160
-170
-180
-190
-200
-210
f1 (ppm)

(3*S*,3*aS*,4*S*)-4-(4-Chlorophenyl)-4-hydroxy-3-phenyl-3*a*,4-dihydro-3*H*-benzo[*b*] pyrrolo [1,2-*d*][1,4] thiazine-2-carbaldehyde 3e

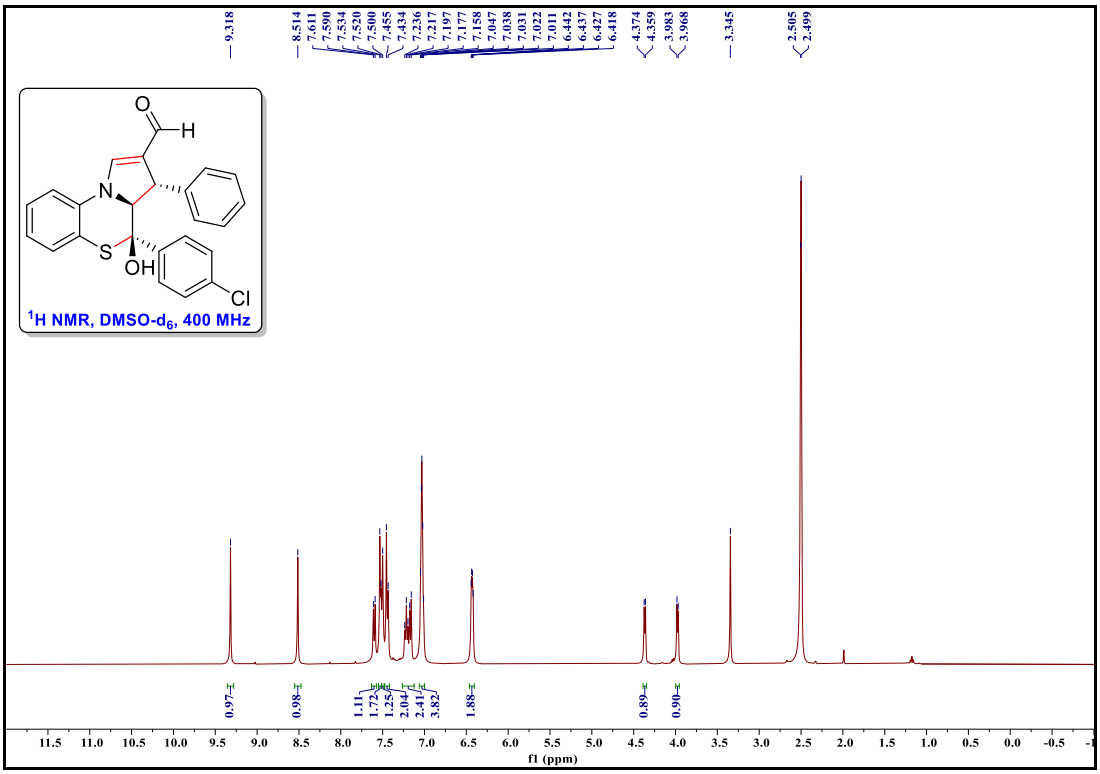

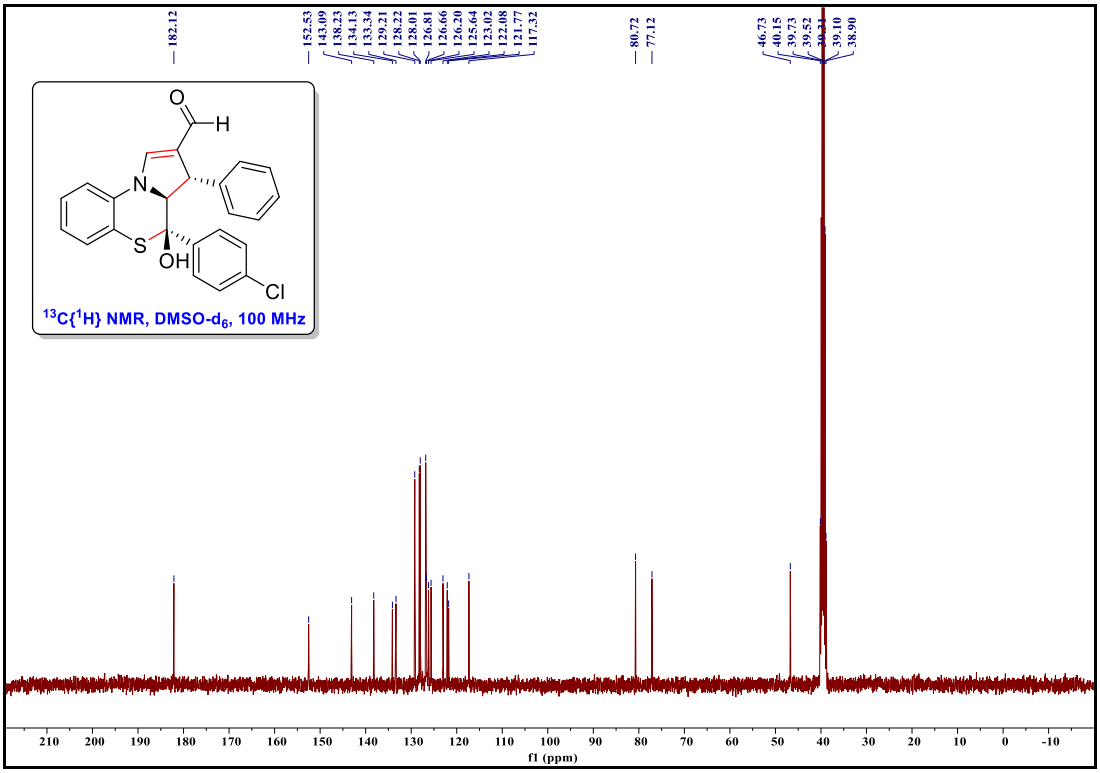

(3*S*,3*aS*,4*S*)-4-(4-Bromophenyl)-4-hydroxy-3-phenyl-3*a*,4-dihydro-3*H*-benzo[*b*] pyrrolo[1,2-*d*][1,4]thi -azine-2-carbaldehyde 3f

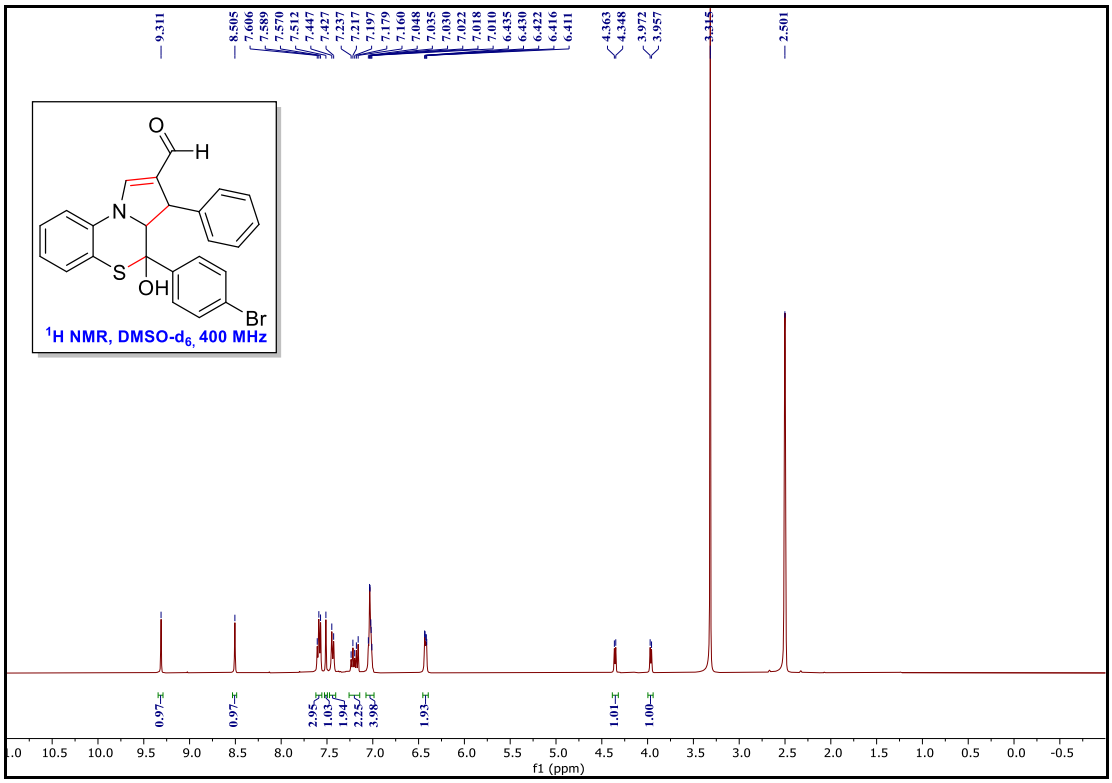

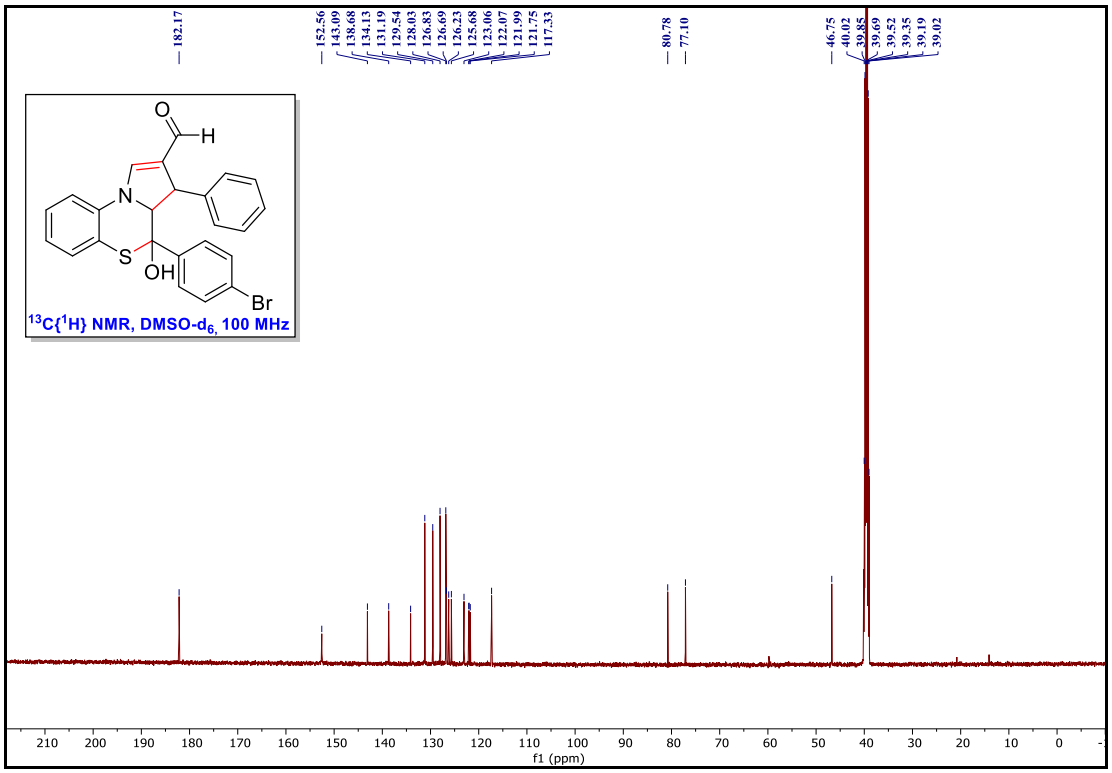

(3*S*,3*aS*,4*S*)-4-Hydroxy-4-(4-nitrophenyl)-3-phenyl-3*a*,4-dihydro-3*H*-benzo[*b*] pyrrolo[1,2-*d*][1,4] thiazine-2-carbaldehyde 3k

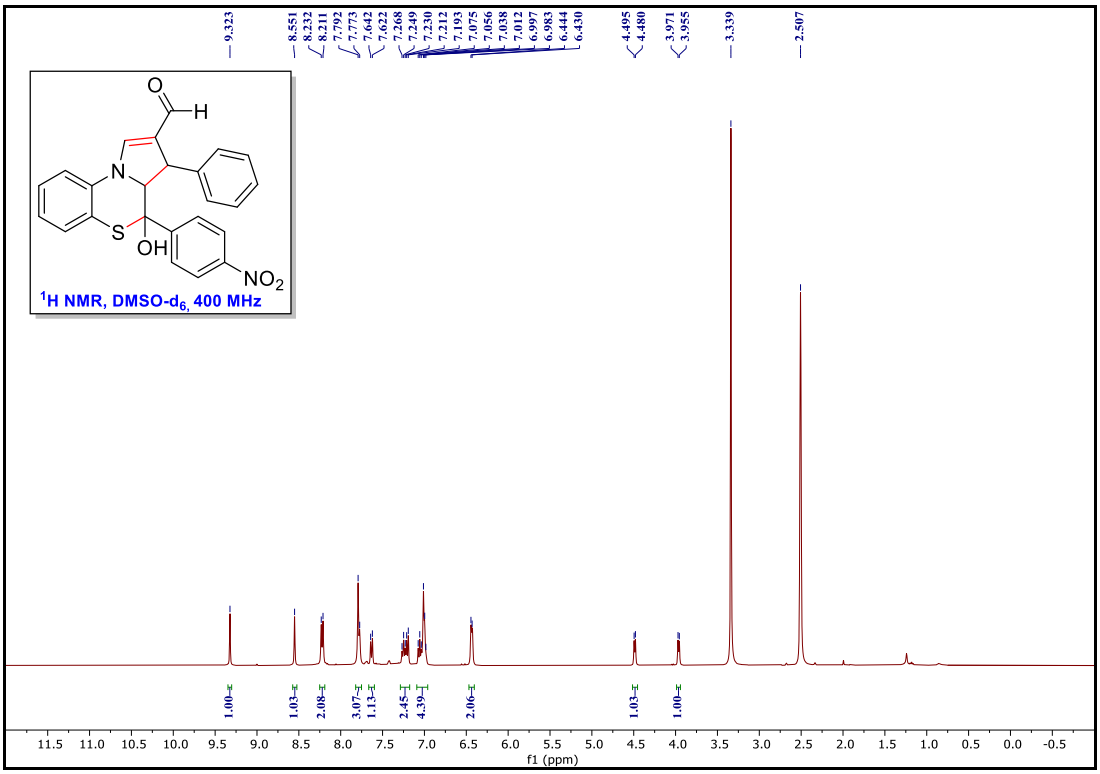

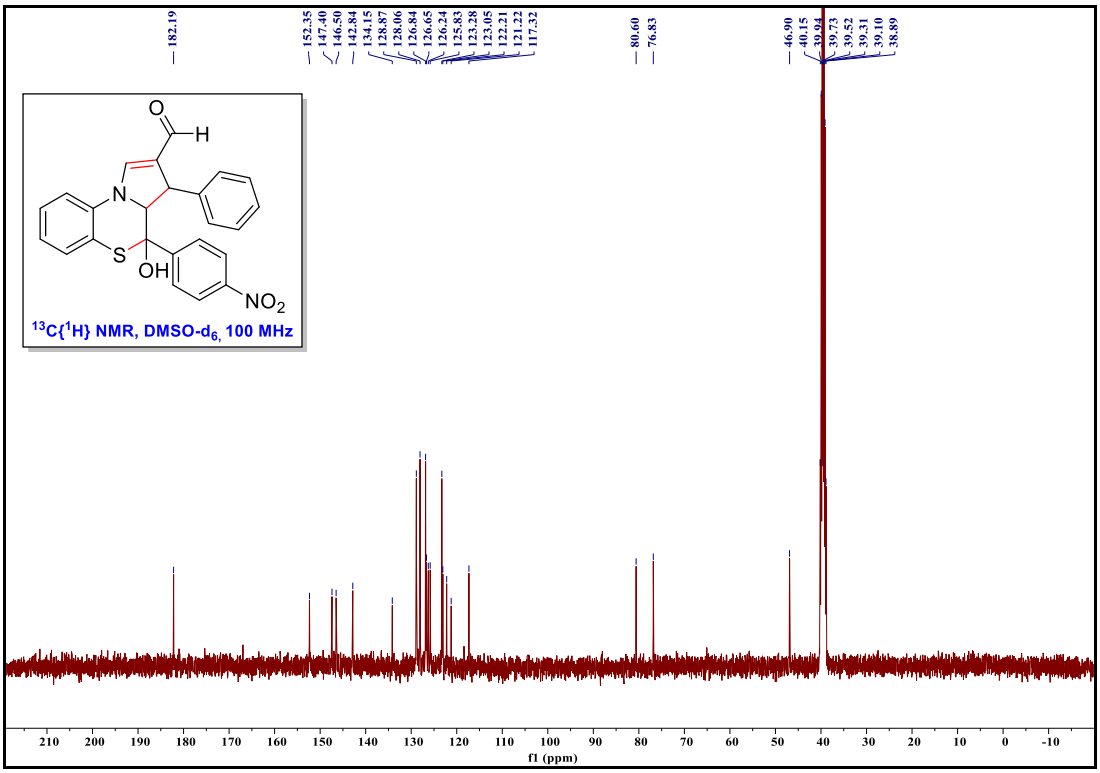

(3*S*,3*aS*,4*S*)-4-(4-Chlorophenyl)-4-hydroxy-3-(4-methoxyphenyl)-3*a*,4-dihydro-3*H*-benzo[*b*] pyrrolo[1,2-*d*][1,4]thiazine-2-carbaldehyde 3p

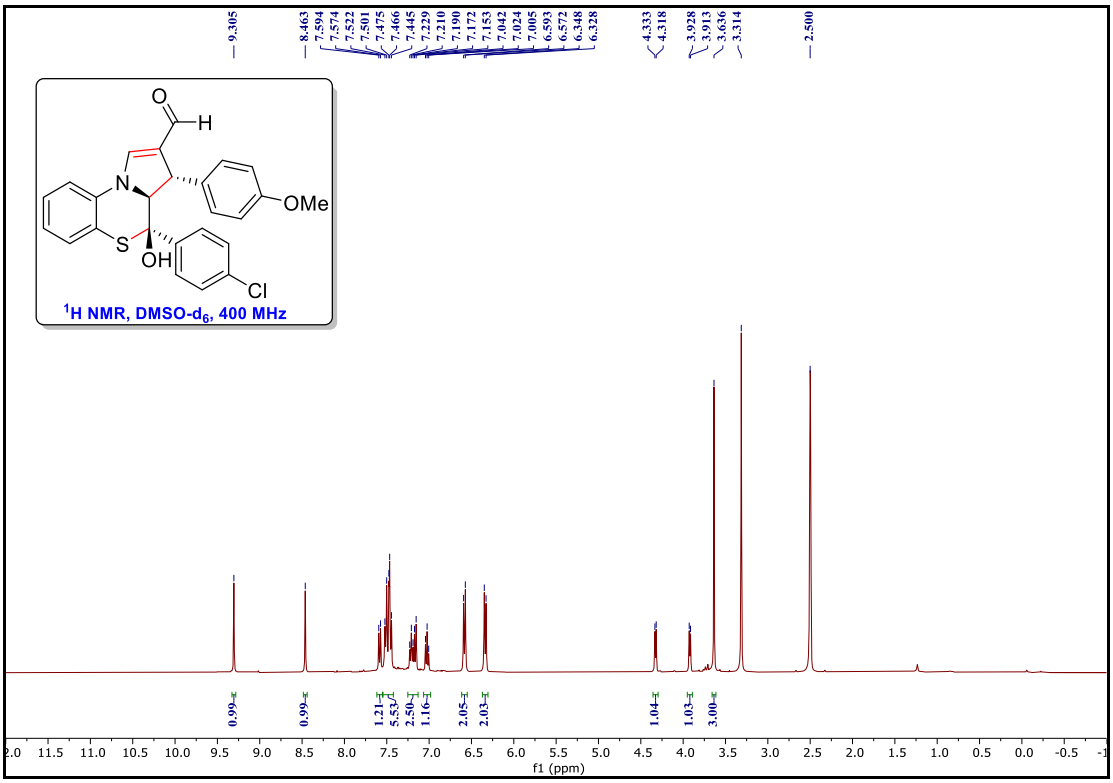

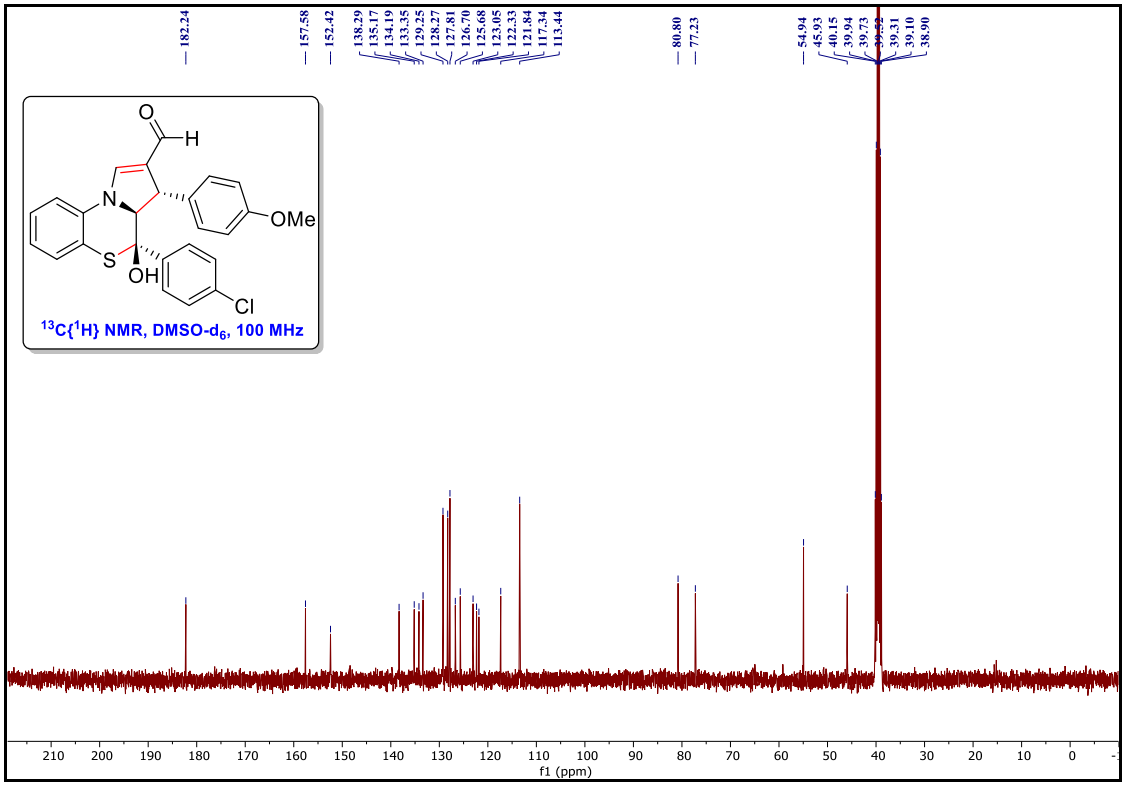

(3*S*,3*aS*,4*S*)-4-(4-Bromophenyl)-3-(4-chlorophenyl)-4-hydroxy-3*a*,4-dihydro-3*H* benzo[b]pyrrolo [1,2-*d*][1,4]thiazine-2-carbaldehyde 3r

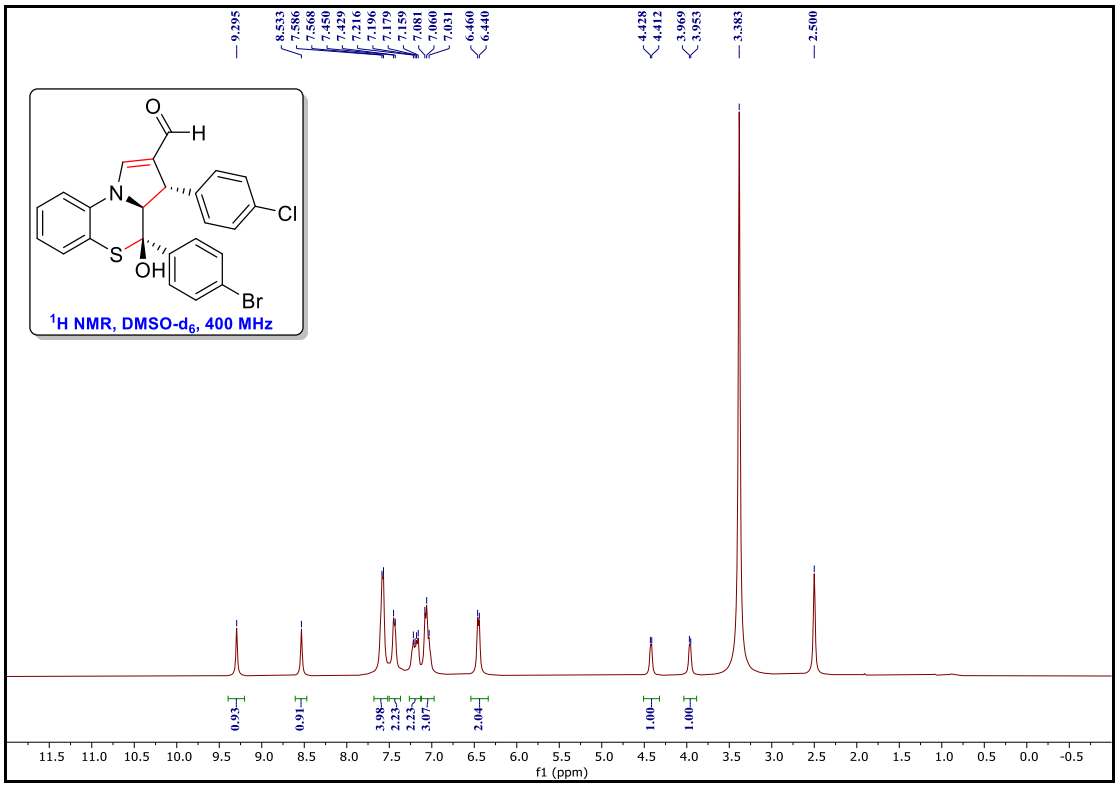

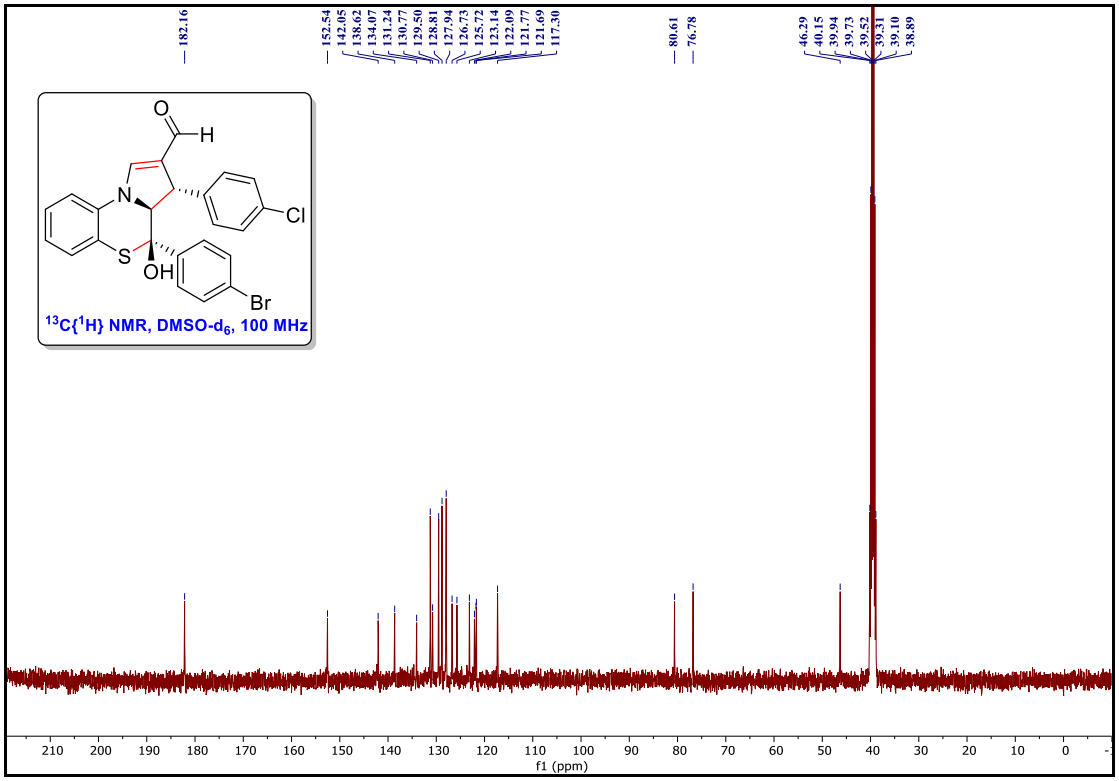

(*3S*,*3aS*,*4S*)-3-(4-Formylphenyl)-4-hydroxy-4-phenyl-3*a*,4-dihydro-3*H*-benzo[*b*] pyrrolo[1,2-*d*][1,4] thiazine-2-carbaldehyde 3w

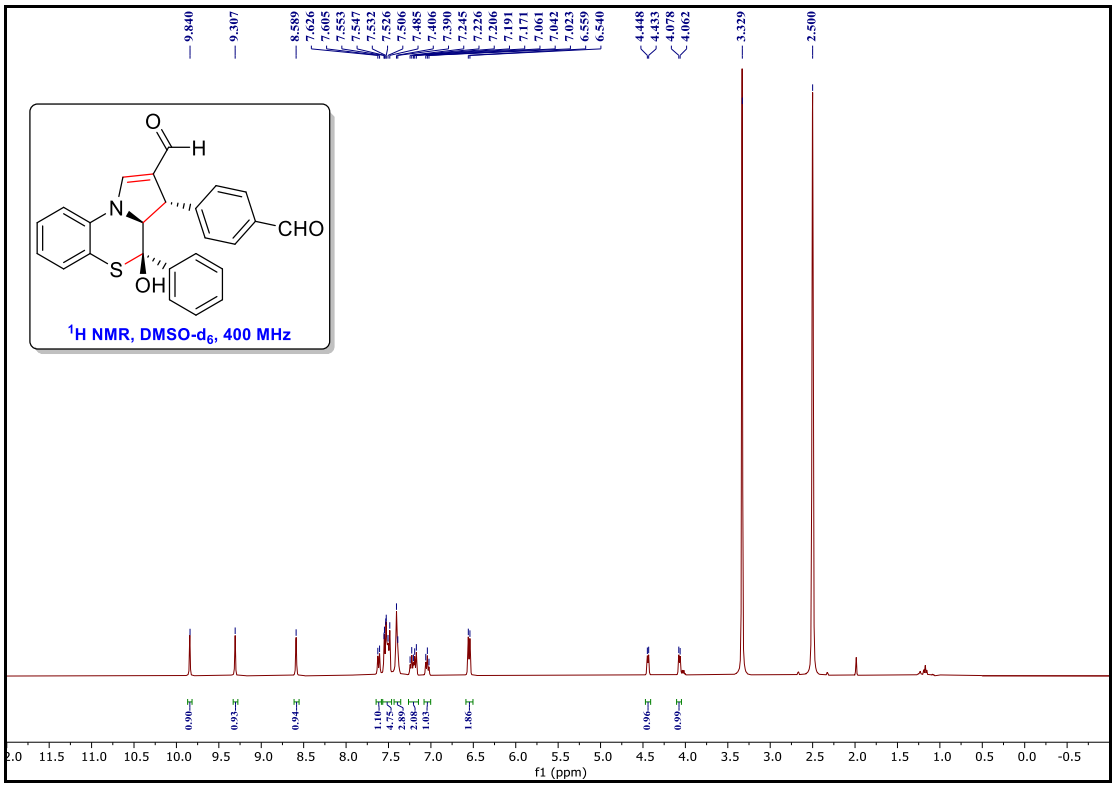

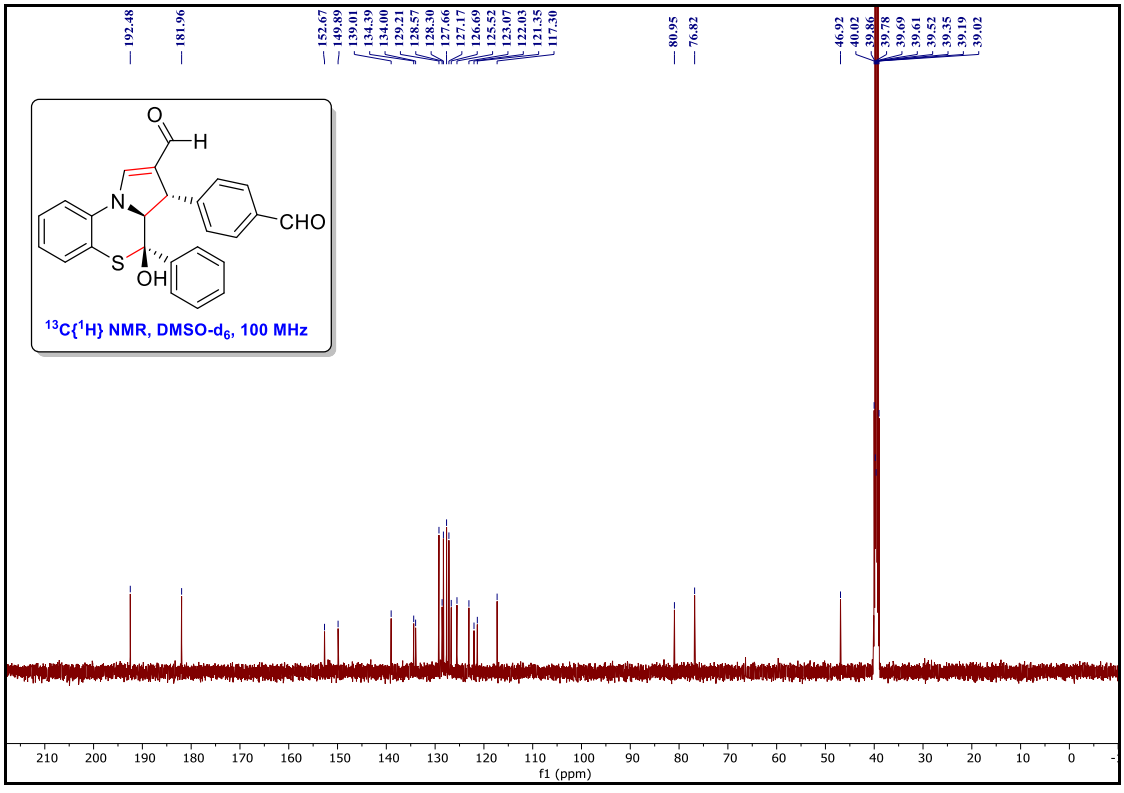

(3*S*,3*aS*,4*S*)-4-(4-Chlorophenyl)-3-(furan-3-yl)-4-hydroxy-3*a*,4-dihydro-3*H*-benzo [*b*]pyrrolo[1,2-*d*][1,4]thiazine-2-carbaldehyde 3z

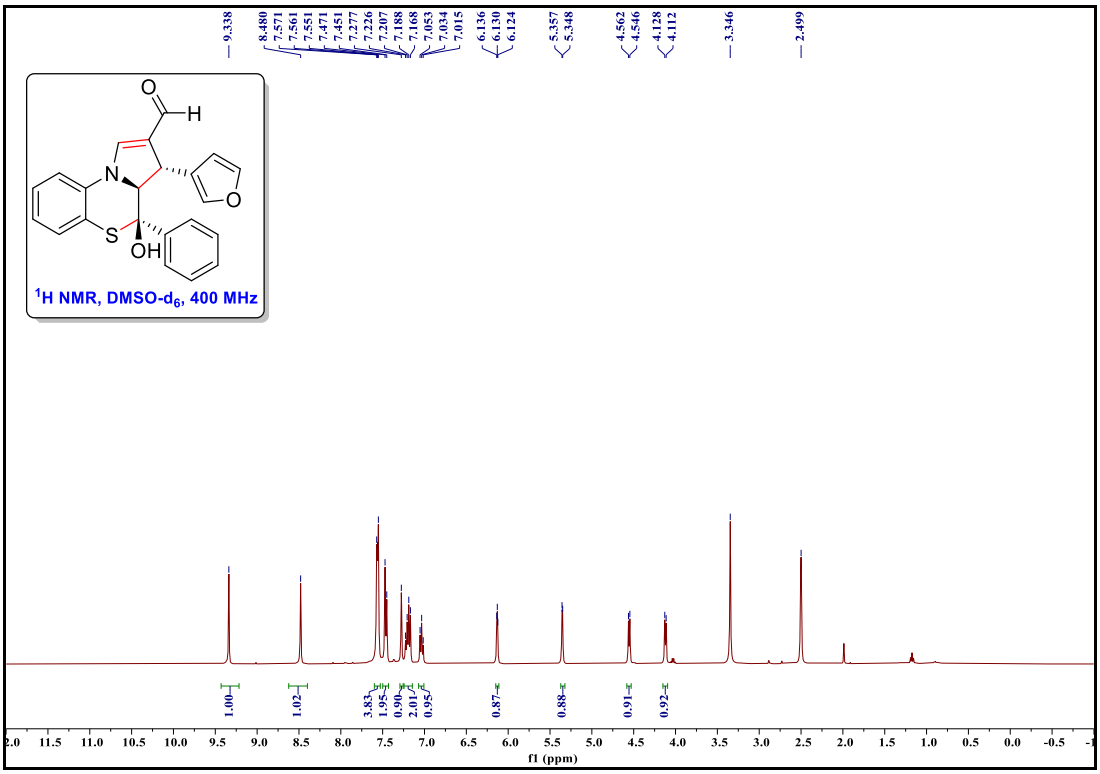

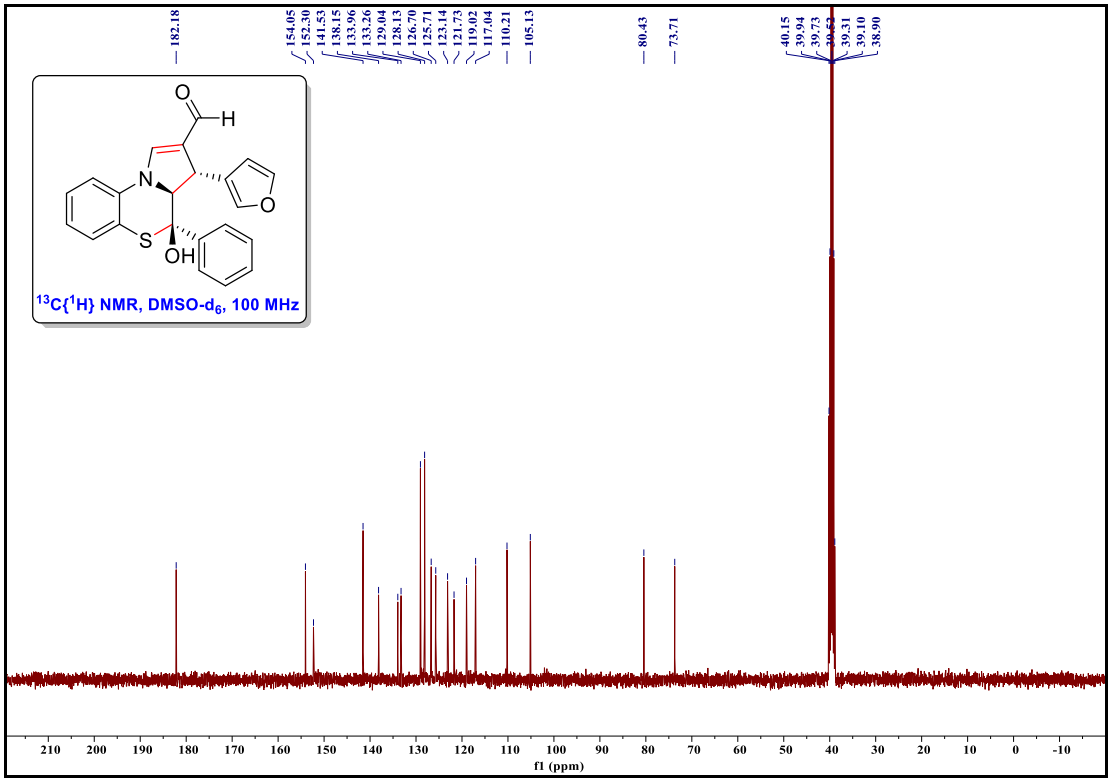

(*3S*,*3aS*,*4S*)-4-Hydroxy-3-methyl-4-phenyl-3a,4-dihydro-3*H*-benzo[*b*]pyrrolo [1,2-*d*][1,4]thiazine-2-carbaldehyde 3ab

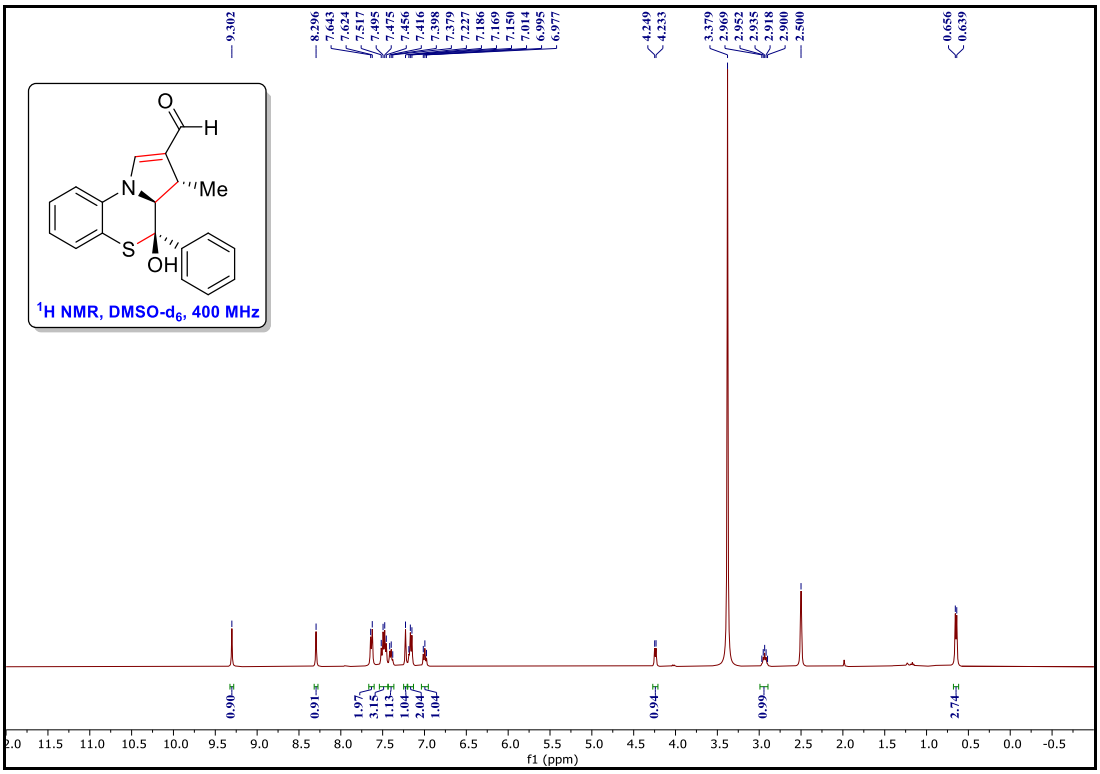

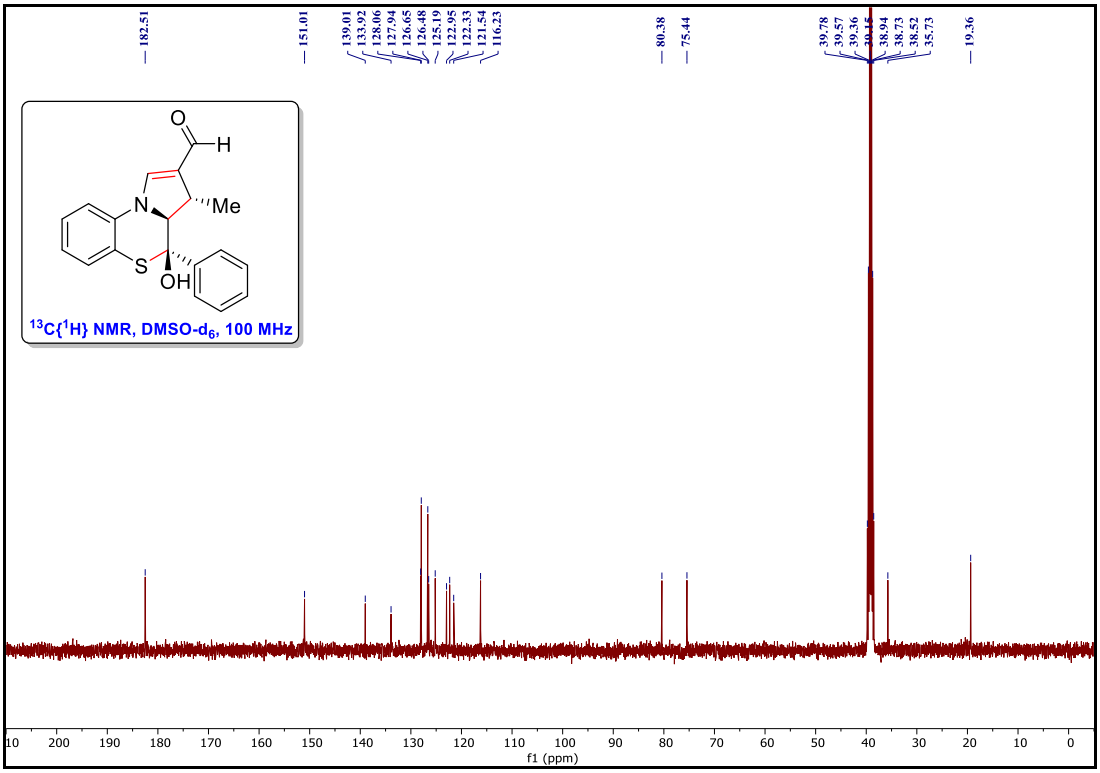

2.18 HPLC CHROMATOGRAMS

(±)-3a

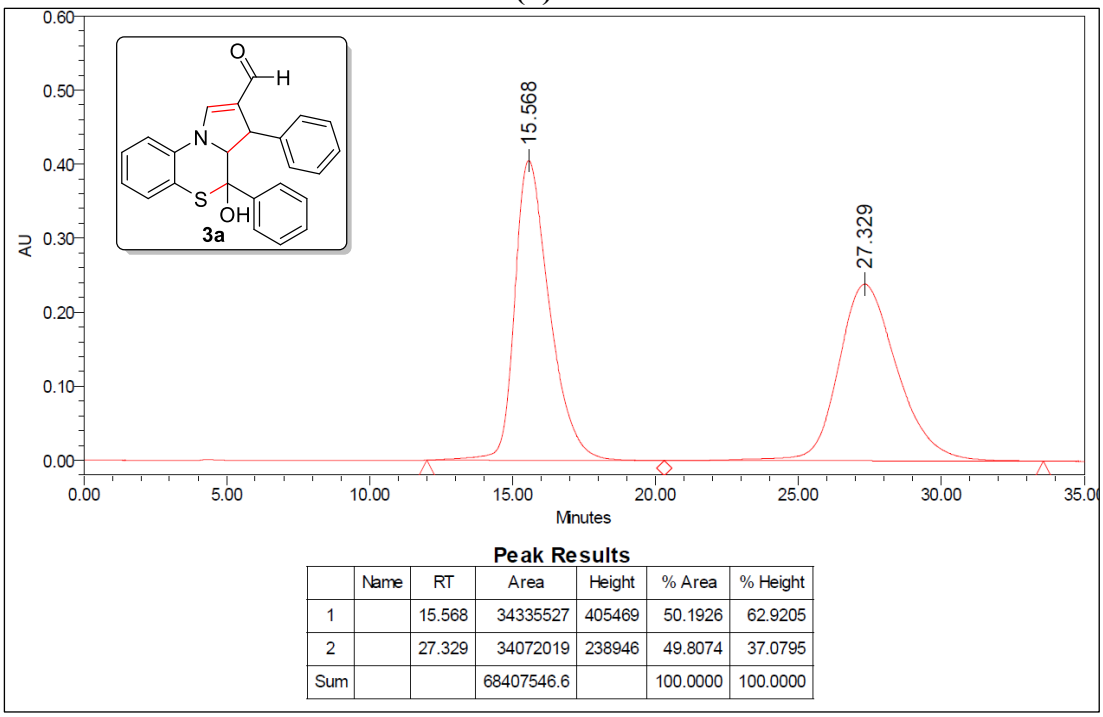

Peak Results

	Name	RT	Area	Height	% Area	% Height
1		15.568	34335527	405469	50.1926	62.9205
2		27.329	34072019	238946	49.8074	37.0795
Sum			68407546.6		100.0000	100.0000

Optical active 3a

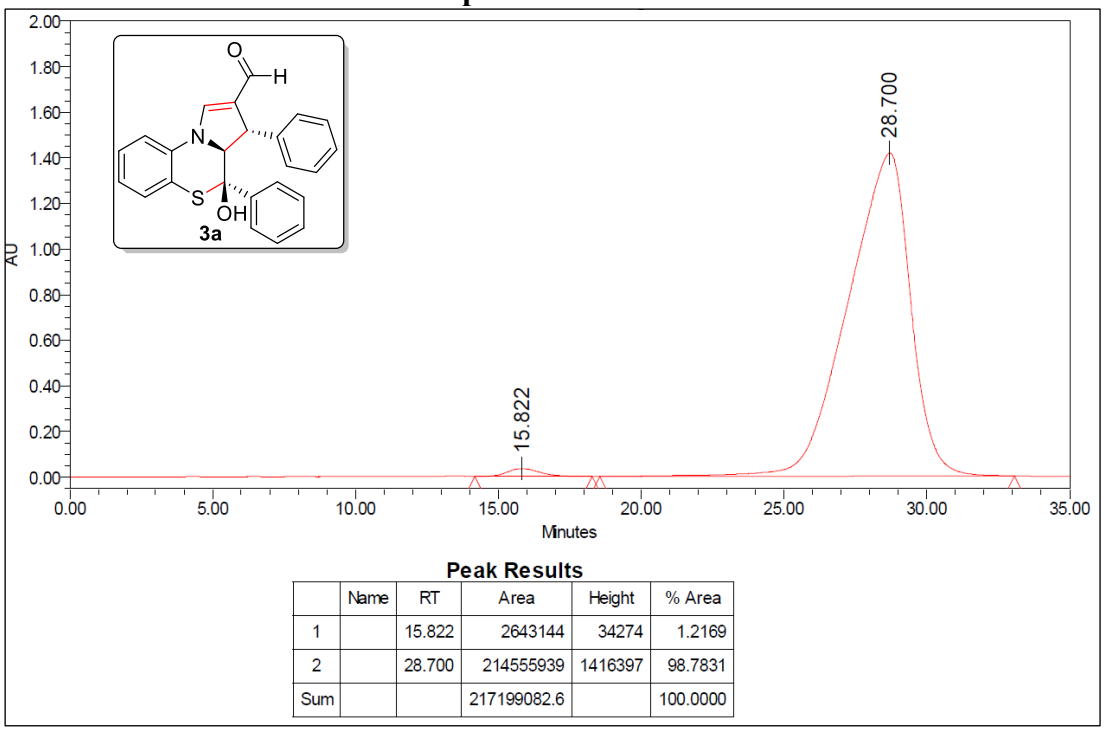

Peak Results

	Name	RT	Area	Height	% Area
1		15.822	2643144	34274	1.2169
2		28.700	214555939	1416397	98.7831
Sum			217199082.6		100.0000

(±)-3b

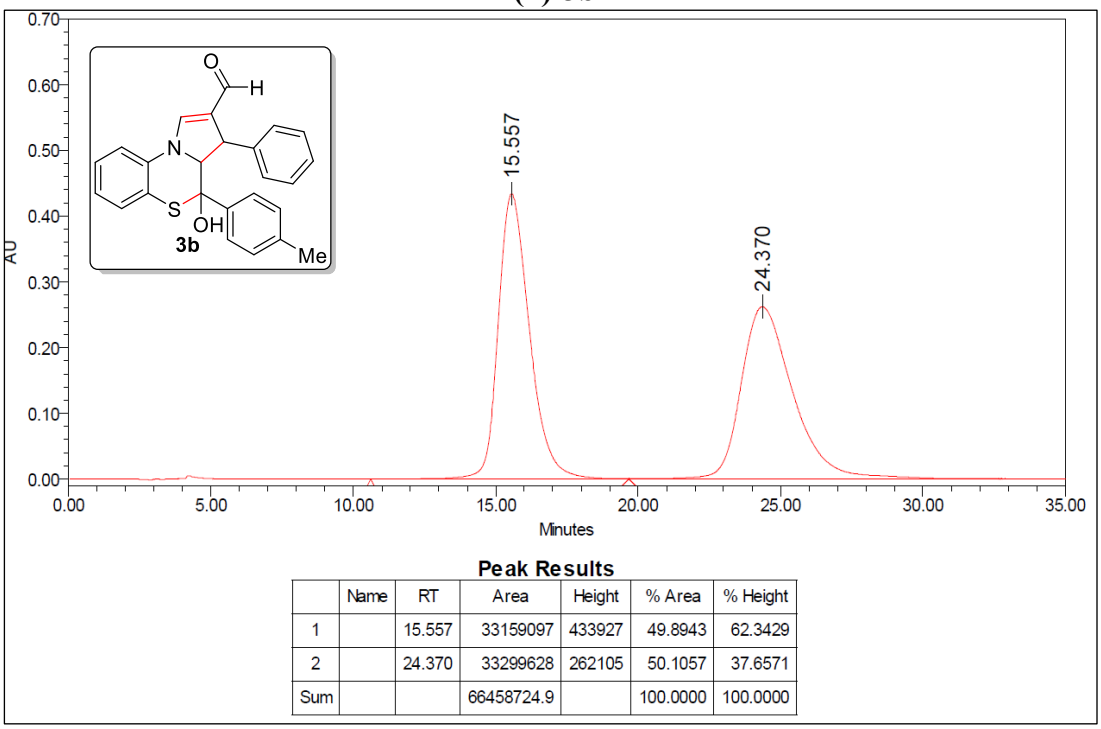

Peak Results

	Name	RT	Area	Height	% Area	% Height
1		15.557	33159097	433927	49.8943	62.3429
2		24.370	33299628	262105	50.1057	37.6571
Sum			66458724.9		100.0000	100.0000

Optical active 3b

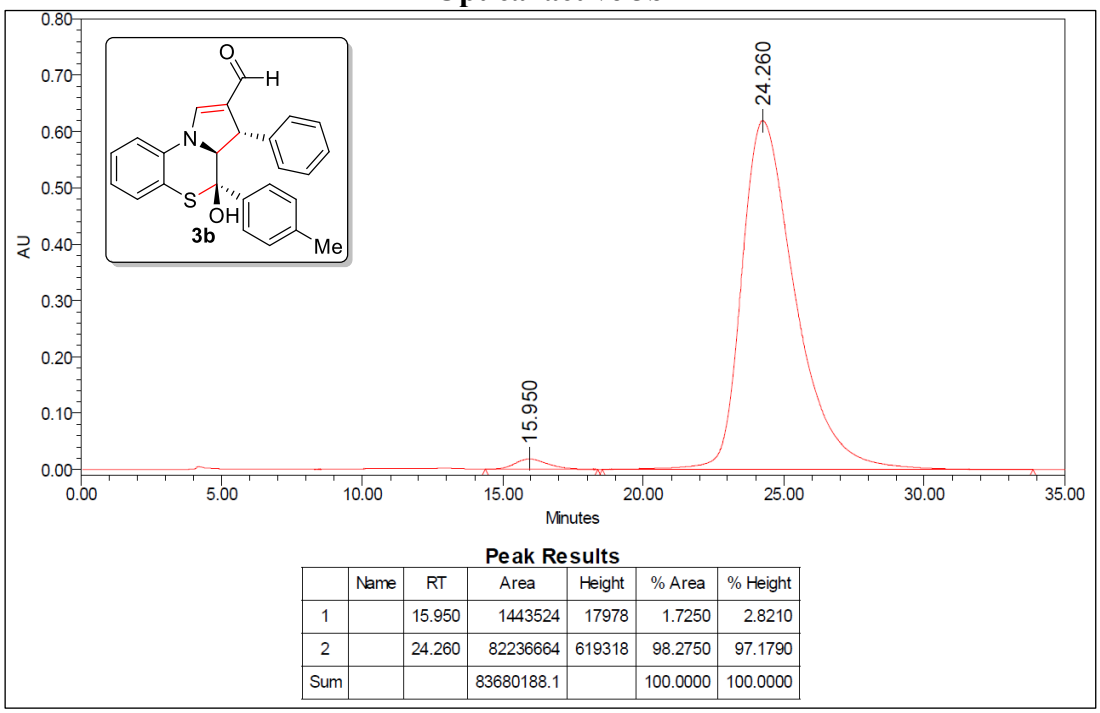

Peak Results

	Name	RT	Area	Height	% Area	% Height
1		15.950	1443524	17978	1.7250	2.8210
2		24.260	82236664	619318	98.2750	97.1790
Sum			83680188.1		100.0000	100.0000

(±)-3c

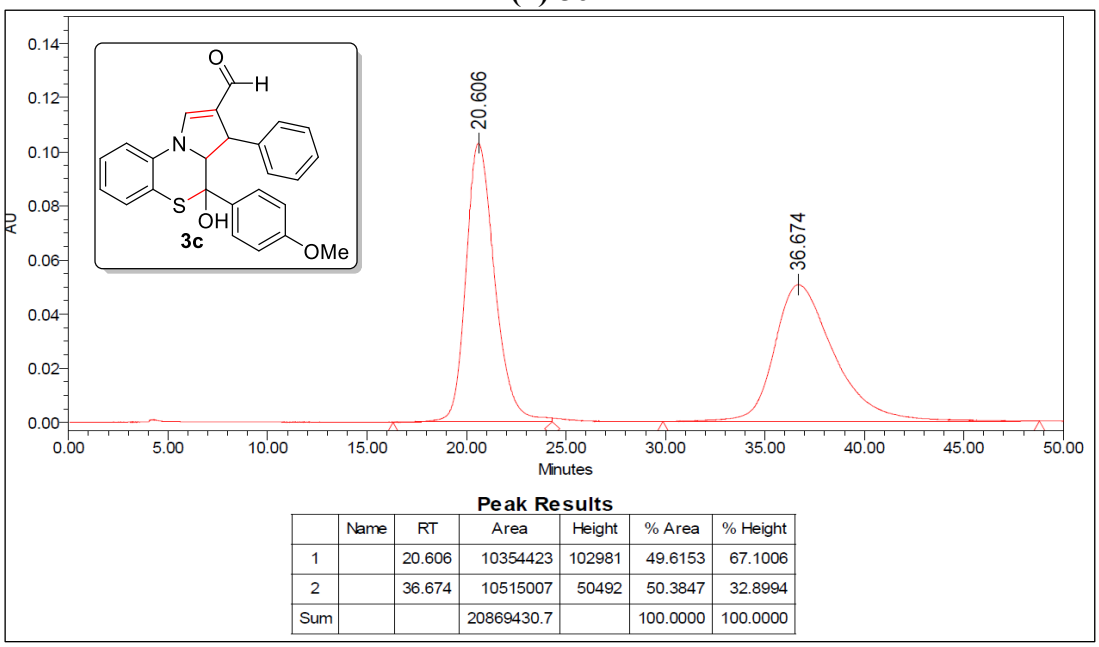

Peak Results

	Name	RT	Area	Height	% Area	% Height
1		20.606	10354423	102981	49.6153	67.1006
2		36.674	10515007	50492	50.3847	32.8994
Sum			20869430.7		100.0000	100.0000

Optical active 3c

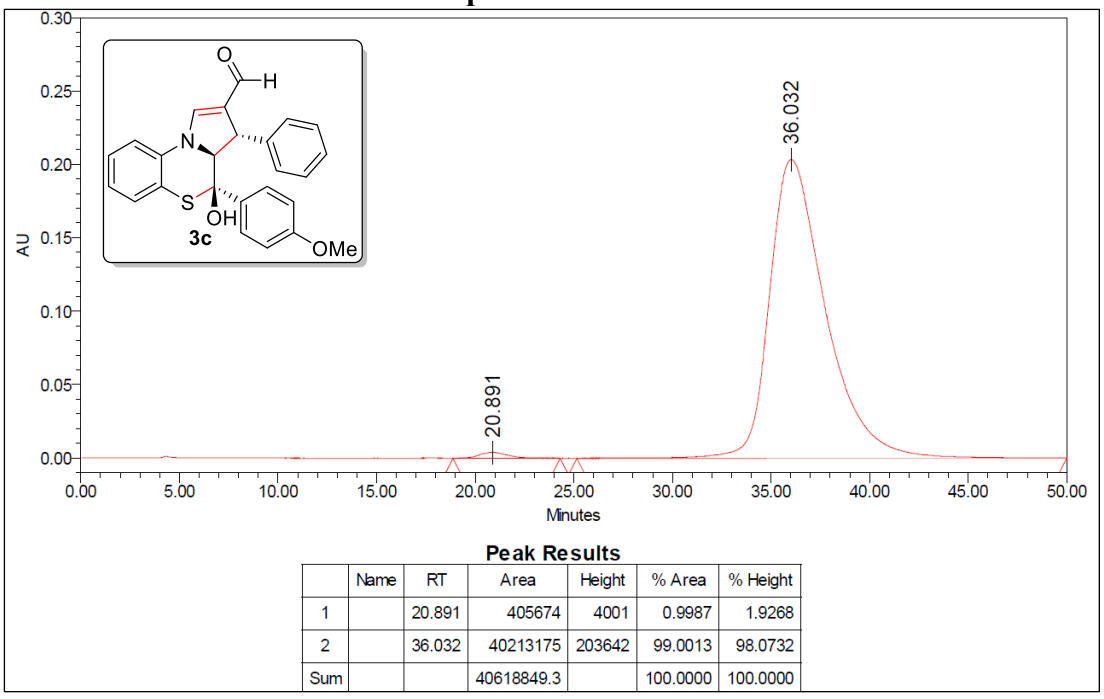

Peak Results

	Name	RT	Area	Height	% Area	% Height
1		20.891	405674	4001	0.9987	1.9268
2		36.032	40213175	203642	99.0013	98.0732
Sum			40618849.3		100.0000	100.0000

(±)-3d

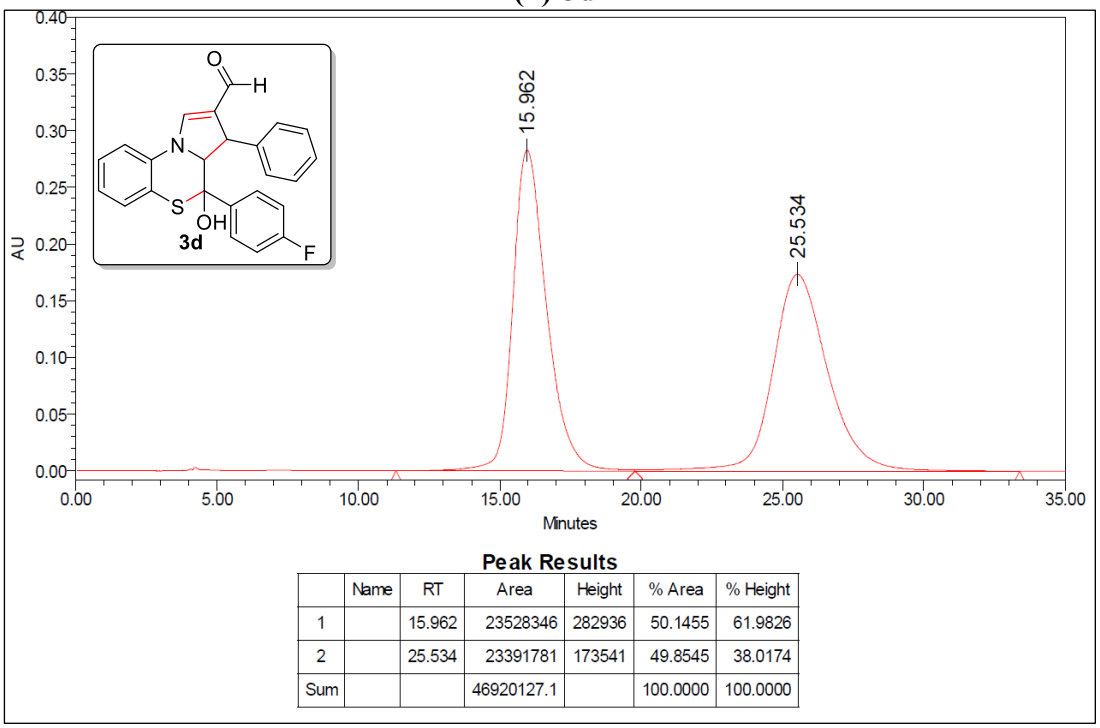

Peak Results

	Name	RT	Area	Height	% Area	% Height
1		15.962	23528346	282936	50.1455	61.9826
2		25.534	23391781	173541	49.8545	38.0174
Sum			46920127.1		100.0000	100.0000

Optical active 3d

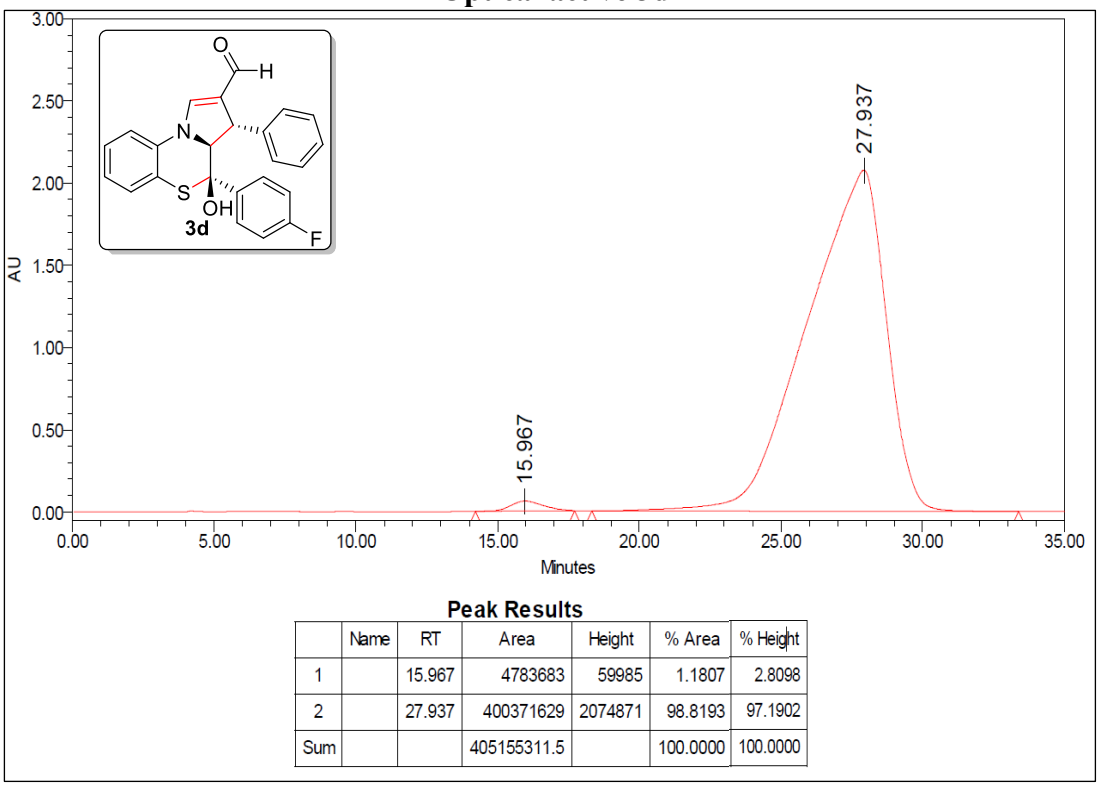

Peak Results

	Name	RT	Area	Height	% Area	% Height
1		15.967	4783683	59985	1.1807	2.8098
2		27.937	400371629	2074871	98.8193	97.1902
Sum			405155311.5		100.0000	100.0000

(±)-3e

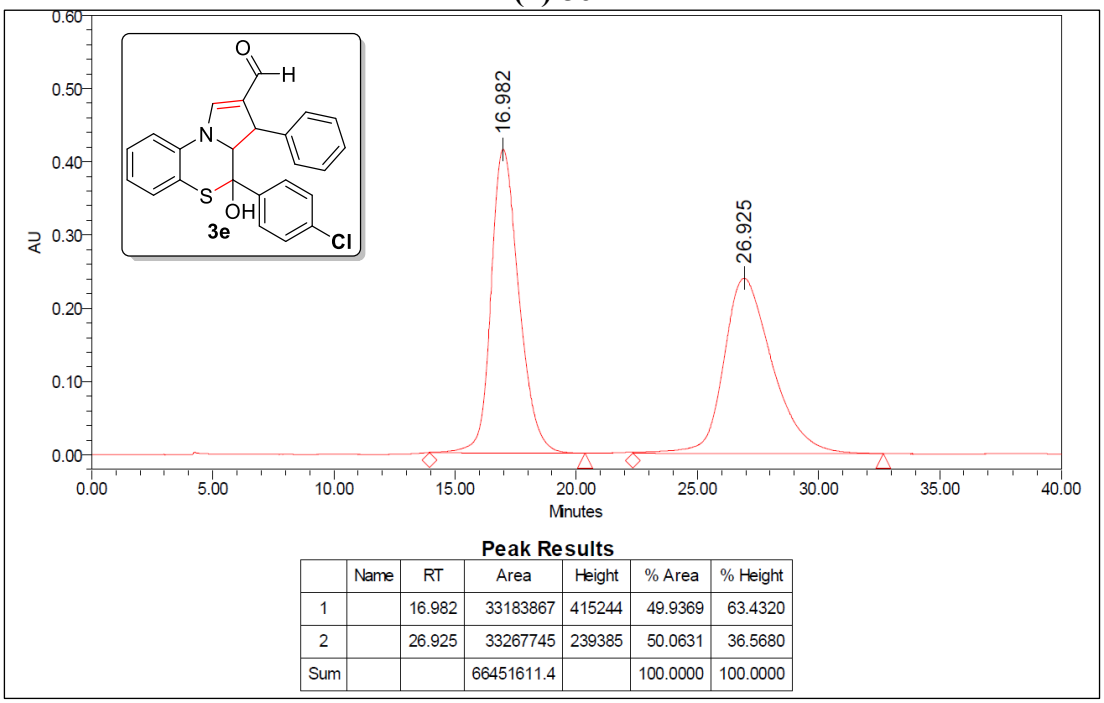

Peak Results

	Name	RT	Area	Height	% Area	% Height
1		16.982	33183867	415244	49.9369	63.4320
2		26.925	33267745	239385	50.0631	36.5680
Sum			66451611.4		100.0000	100.0000

Optical active 3e

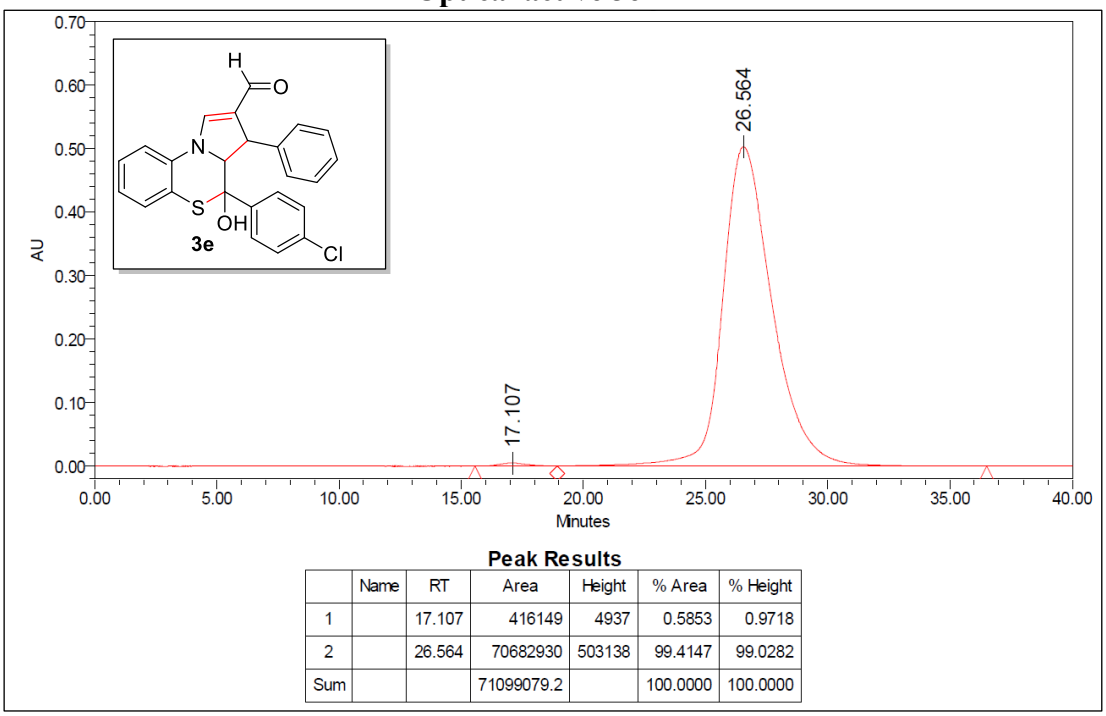

Peak Results

	Name	RT	Area	Height	% Area	% Height
1		17.107	416149	4937	0.5853	0.9718
2		26.564	70682930	503138	99.4147	99.0282
Sum			71099079.2		100.0000	100.0000

(±)-3f

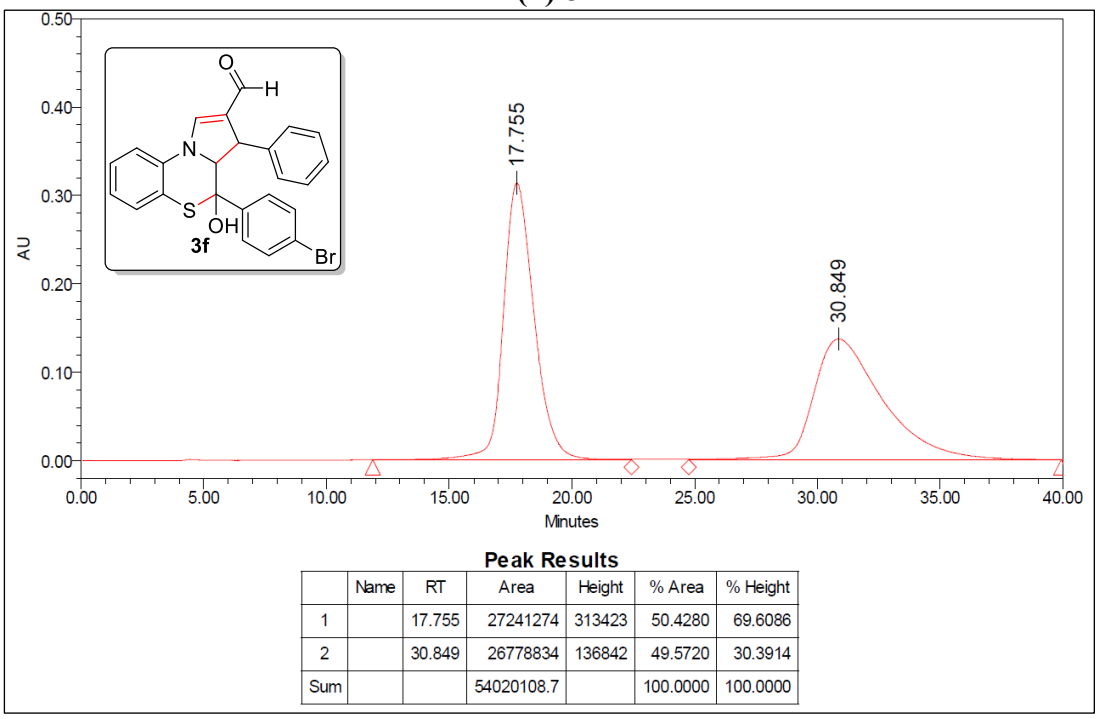

Peak Results

	Name	RT	Area	Height	% Area	% Height
1		17.755	27241274	313423	50.4280	69.6086
2		30.849	26778834	136842	49.5720	30.3914
Sum			54020108.7		100.0000	100.0000

Optical active 3f

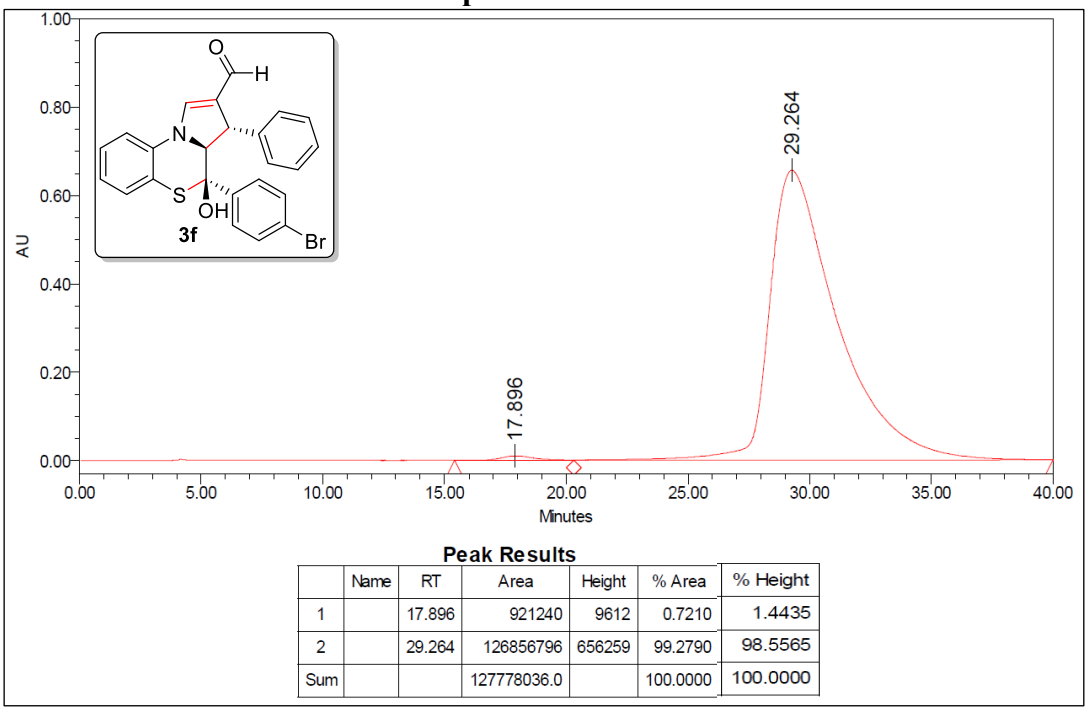

Peak Results

	Name	RT	Area	Height	% Area	% Height
1		17.896	921240	9612	0.7210	1.4435
2		29.264	126856796	656259	99.2790	98.5565
Sum			127778036.0		100.0000	100.0000

(±)-3g

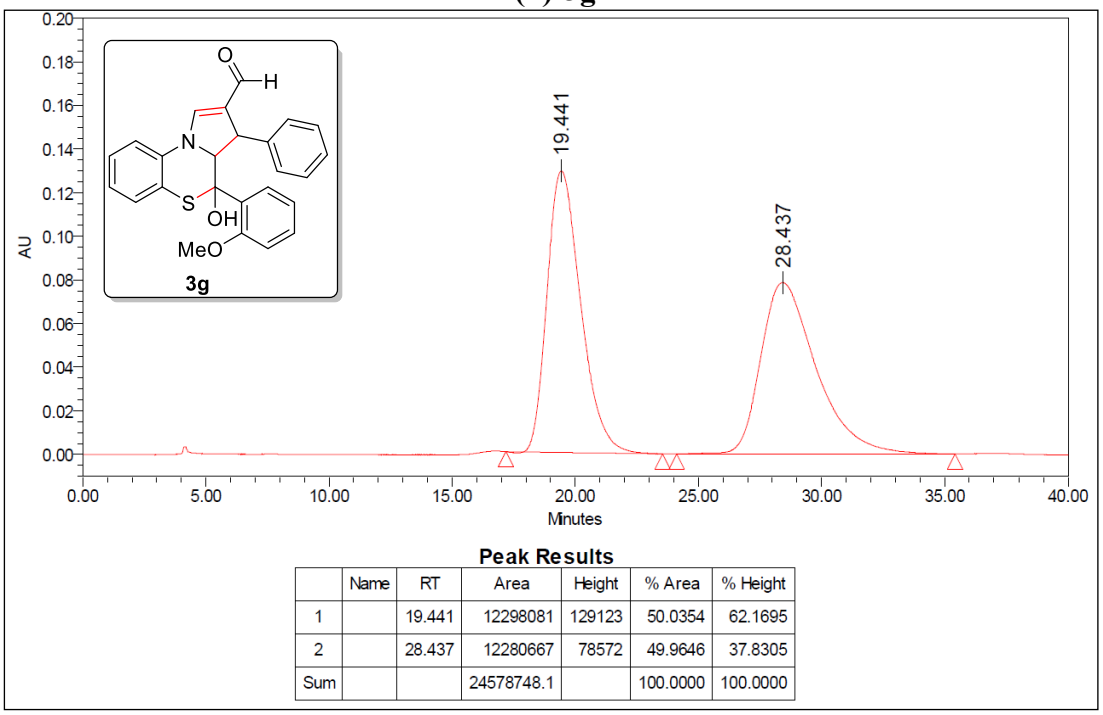

Peak Results

	Name	RT	Area	Height	% Area	% Height
1		19.441	12298081	129123	50.0354	62.1695
2		28.437	12280667	78572	49.9646	37.8305
Sum			24578748.1		100.0000	100.0000

Optical active 3g

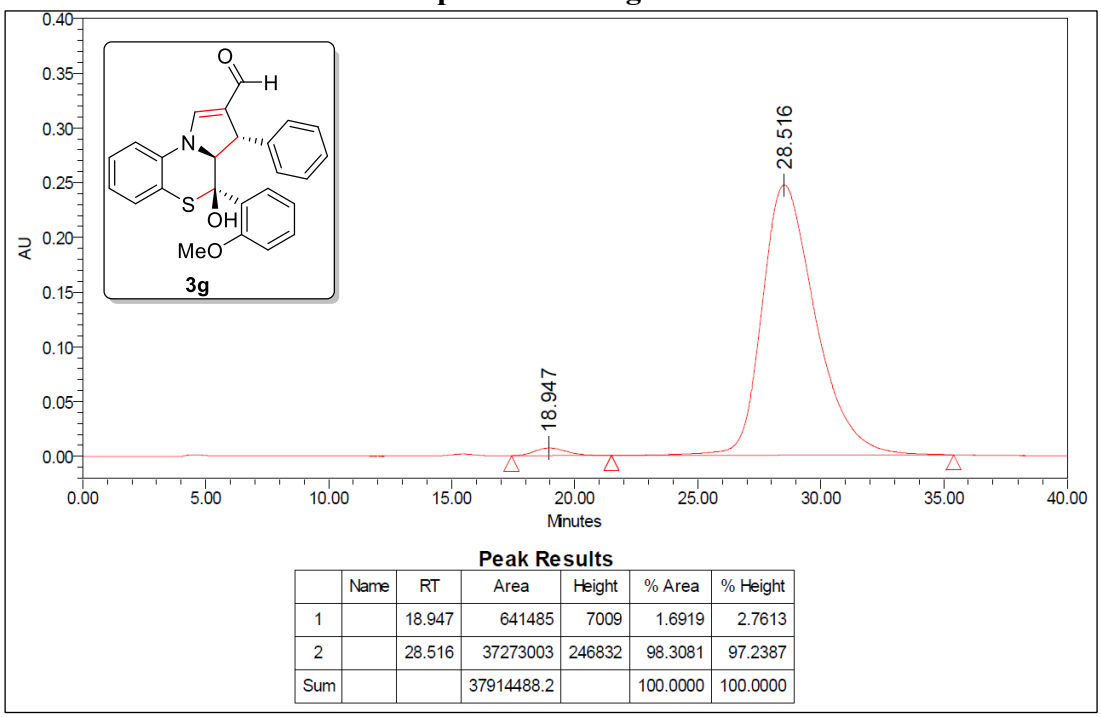

Peak Results

	Name	RT	Area	Height	% Area	% Height
1		18.947	641485	7009	1.6919	2.7613
2		28.516	37273003	246832	98.3081	97.2387
Sum			37914488.2		100.0000	100.0000

(±)-3h

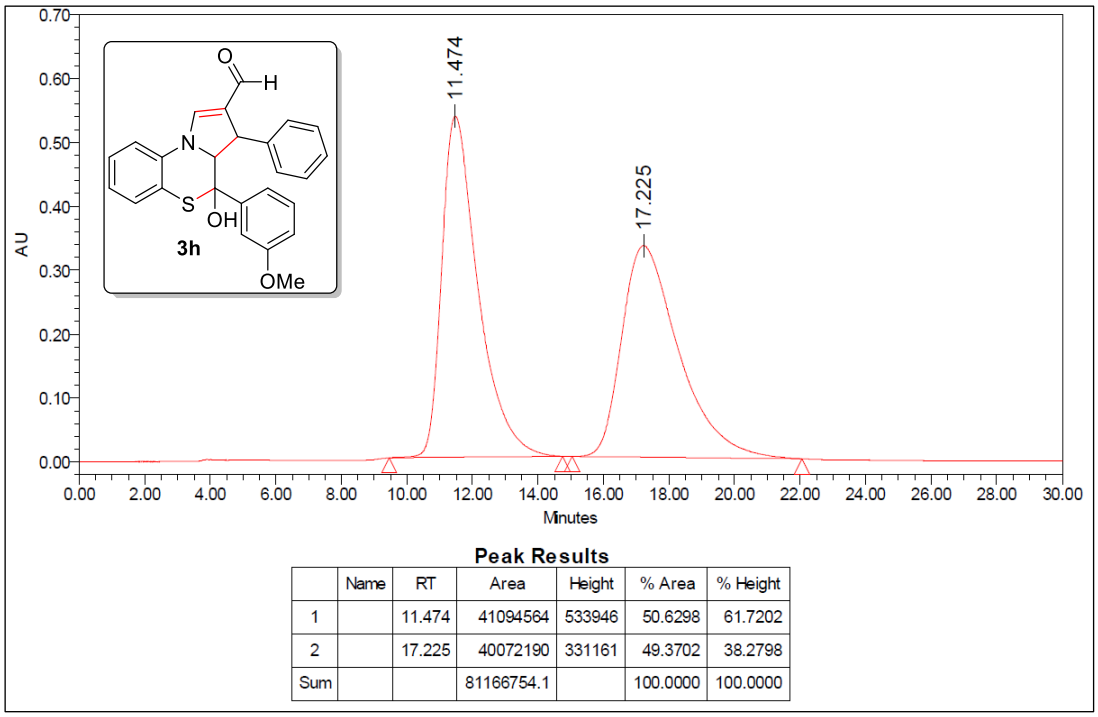

Peak Results

	Name	RT	Area	Height	% Area	% Height
1		11.474	41094564	533946	50.6298	61.7202
2		17.225	40072190	331161	49.3702	38.2798
Sum			81166754.1		100.0000	100.0000

Optical active 3h

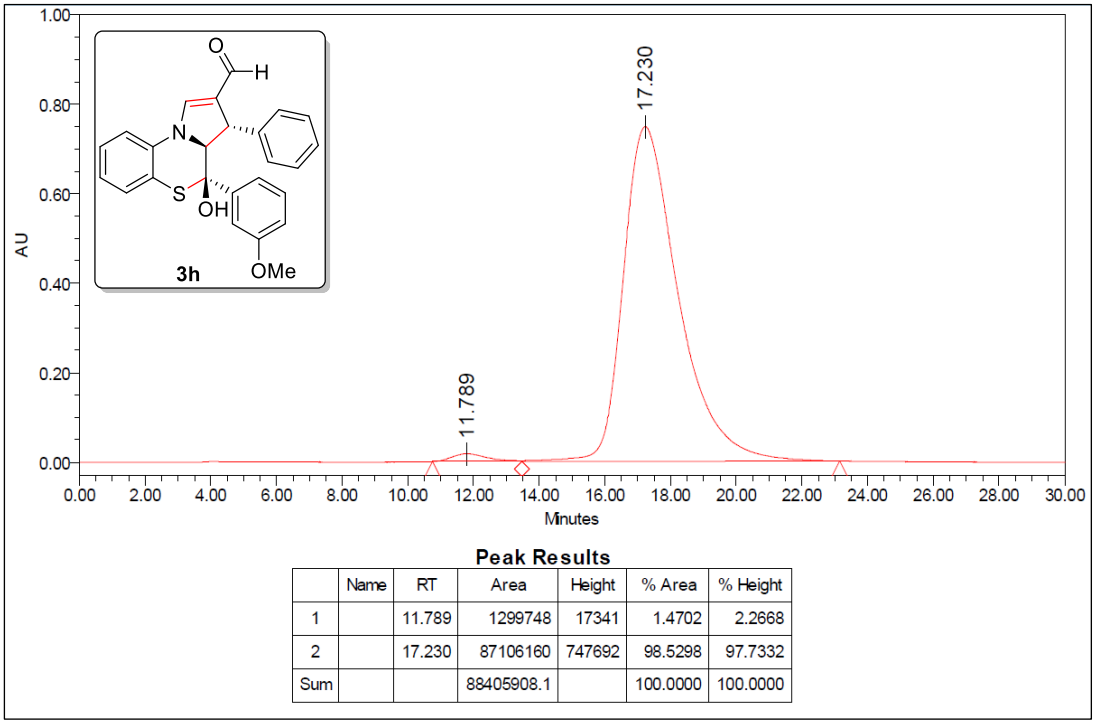

Peak Results

	Name	RT	Area	Height	% Area	% Height
1		11.789	1299748	17341	1.4702	2.2668
2		17.230	87106160	747692	98.5298	97.7332
Sum			88405908.1		100.0000	100.0000

(±)-3i

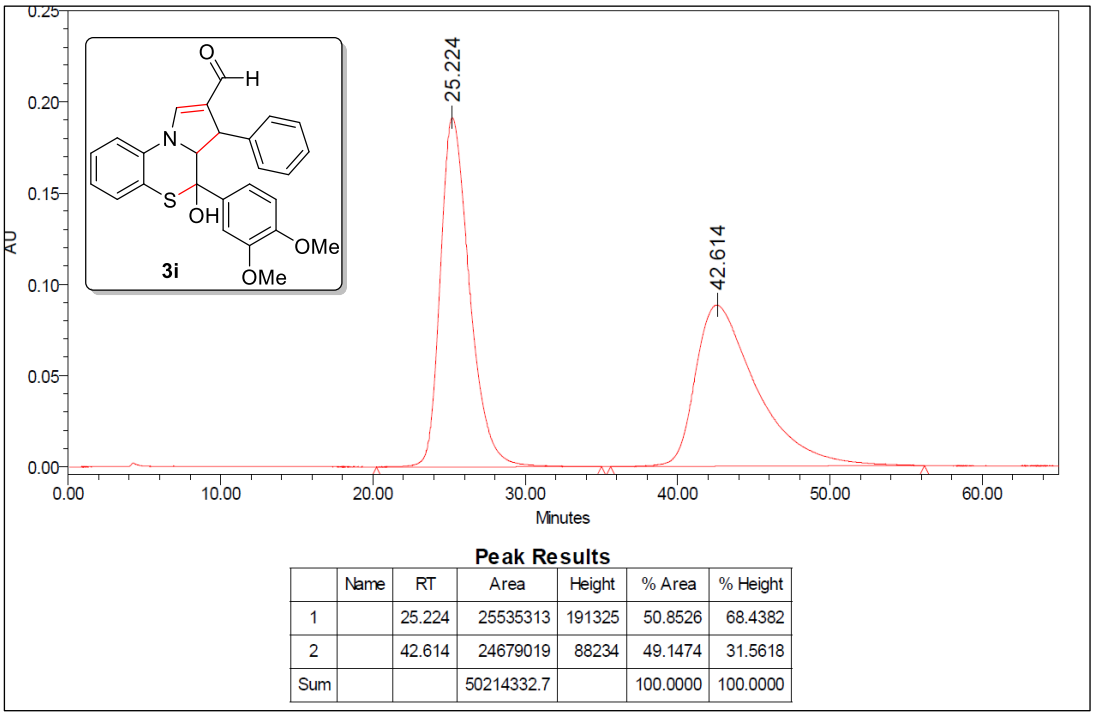

Peak Results

	Name	RT	Area	Height	% Area	% Height
1		25.224	25535313	191325	50.8526	68.4382
2		42.614	24679019	88234	49.1474	31.5618
Sum			50214332.7		100.0000	100.0000

Optical active 3i

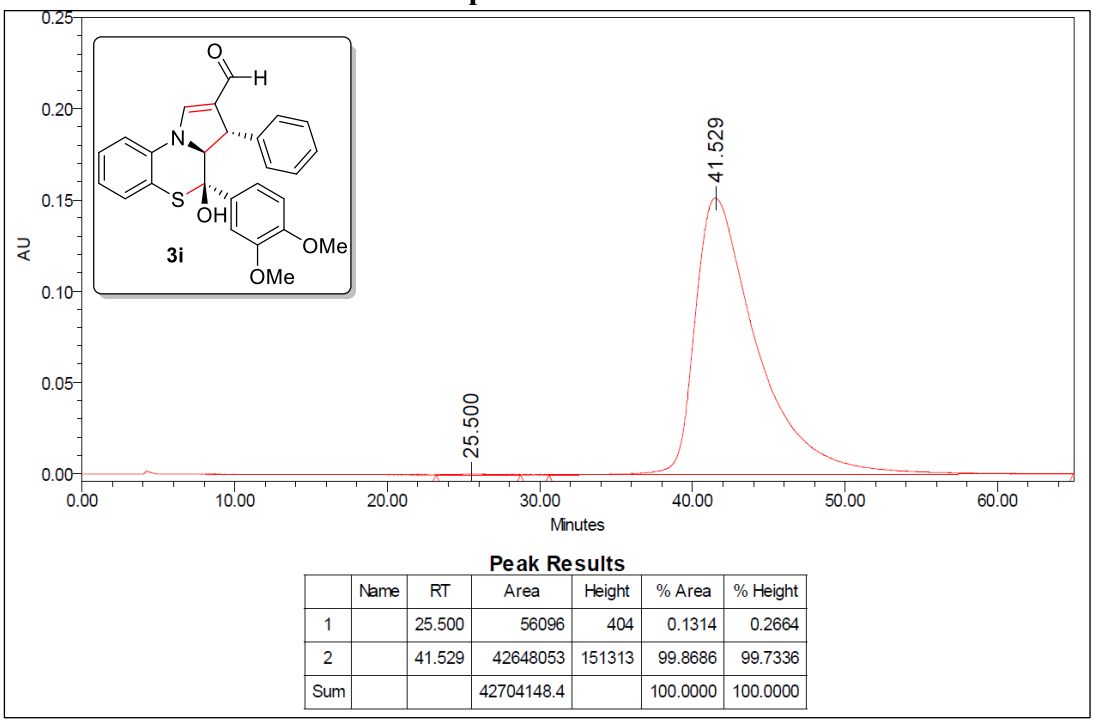

Peak Results

	Name	RT	Area	Height	% Area	% Height
1		25.500	56096	404	0.1314	0.2664
2		41.529	42648053	151313	99.8686	99.7336
Sum			42704148.4		100.0000	100.0000

(±)-3j

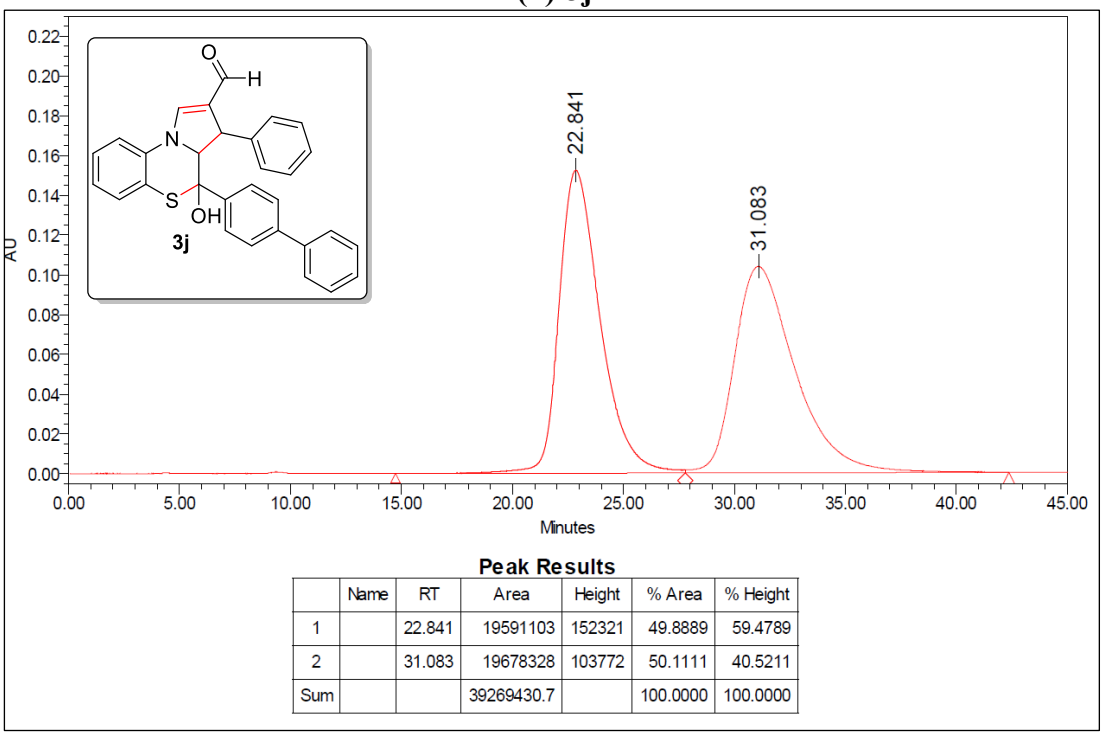

Peak Results

	Name	RT	Area	Height	% Area	% Height
1		22.841	19591103	152321	49.8889	59.4789
2		31.083	19678328	103772	50.1111	40.5211
Sum			39269430.7		100.0000	100.0000

Optical active 3j

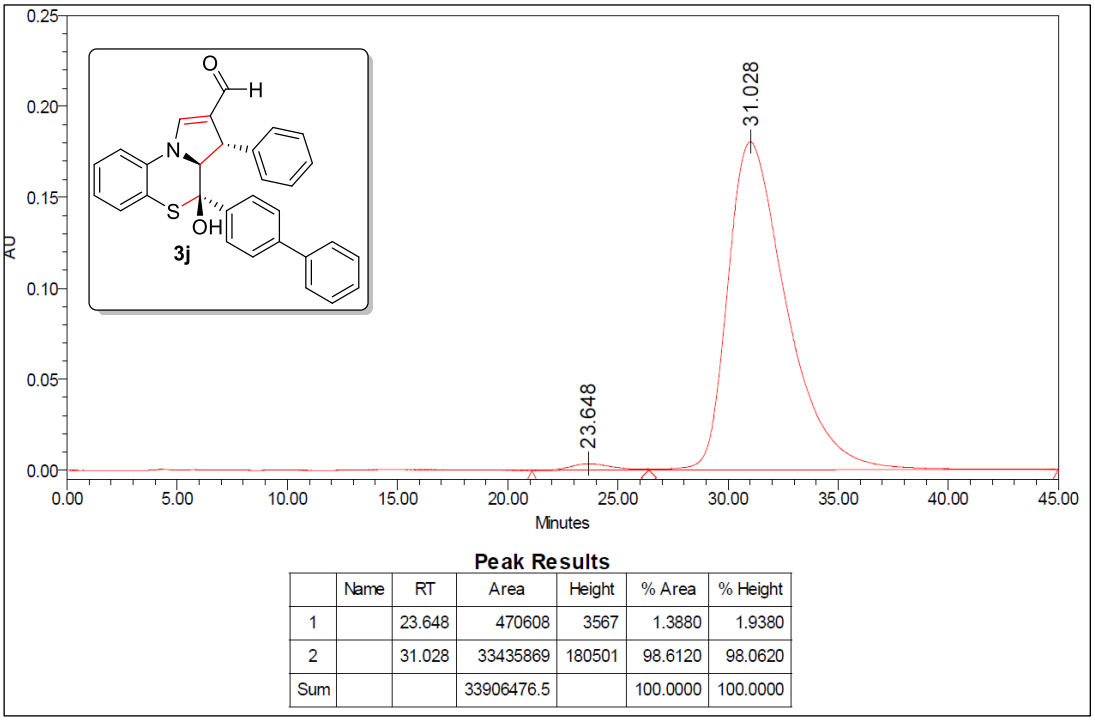

Peak Results

	Name	RT	Area	Height	% Area	% Height
1		23.648	470608	3567	1.3880	1.9380
2		31.028	33435869	180501	98.6120	98.0620
Sum			33906476.5		100.0000	100.0000

(±)-3k

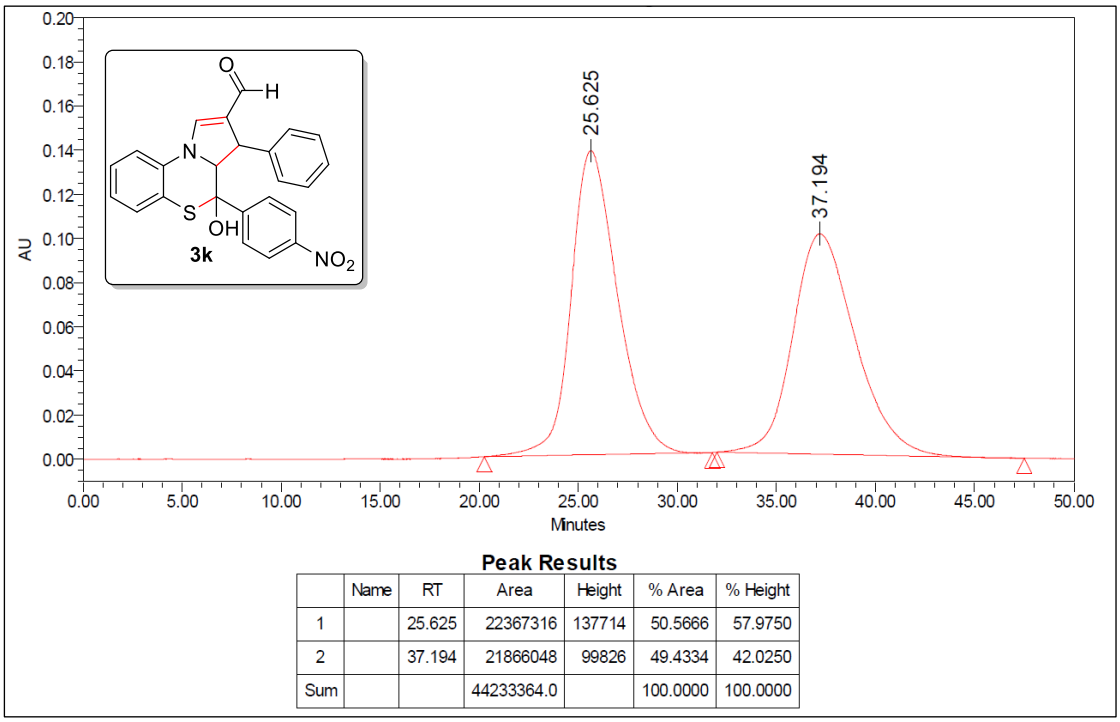

Peak Results

	Name	RT	Area	Height	% Area	% Height
1		25.625	22367316	137714	50.5666	57.9750
2		37.194	21866048	99826	49.4334	42.0250
Sum			44233364.0		100.0000	100.0000

Optical active 3k

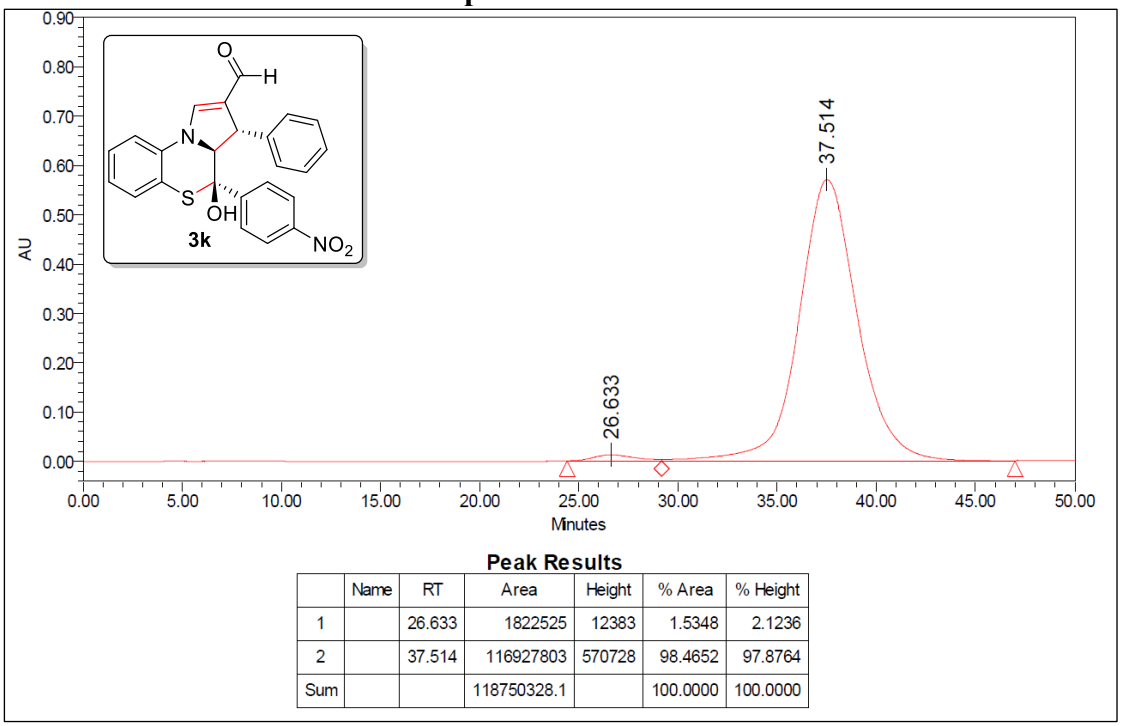

Peak Results

	Name	RT	Area	Height	% Area	% Height
1		26.633	1822525	12383	1.5348	2.1236
2		37.514	116927803	570728	98.4652	97.8764
Sum			118750328.1		100.0000	100.0000

(±)-3l

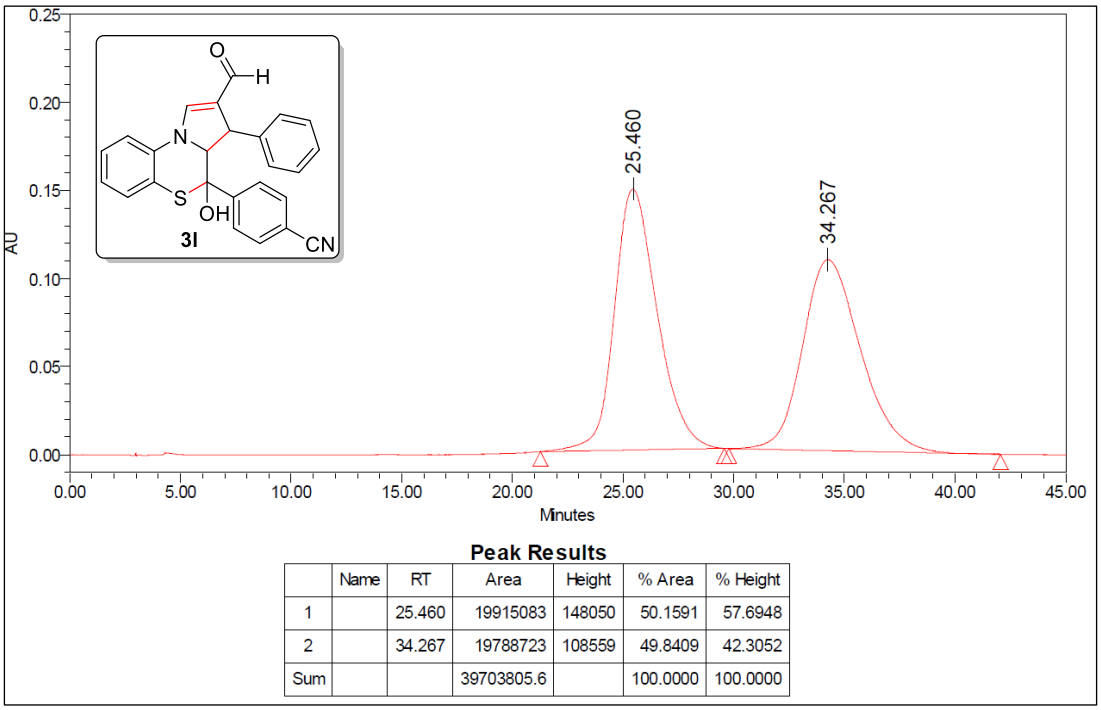

Peak Results

	Name	RT	Area	Height	% Area	% Height
1		25.460	19915083	148050	50.1591	57.6948
2		34.267	19788723	108559	49.8409	42.3052
Sum			39703805.6		100.0000	100.0000

Optical active 3l

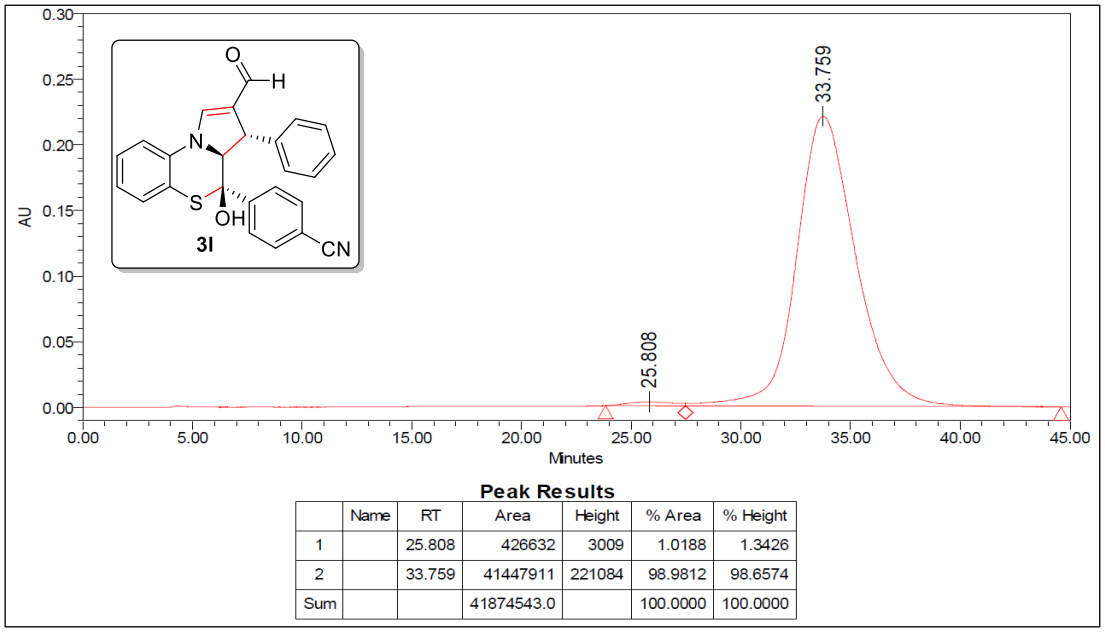

Peak Results

	Name	RT	Area	Height	% Area	% Height
1		25.808	426632	3009	1.0188	1.3426
2		33.759	41447911	221084	98.9812	98.6574
Sum			41874543.0		100.0000	100.0000

(±)-3m

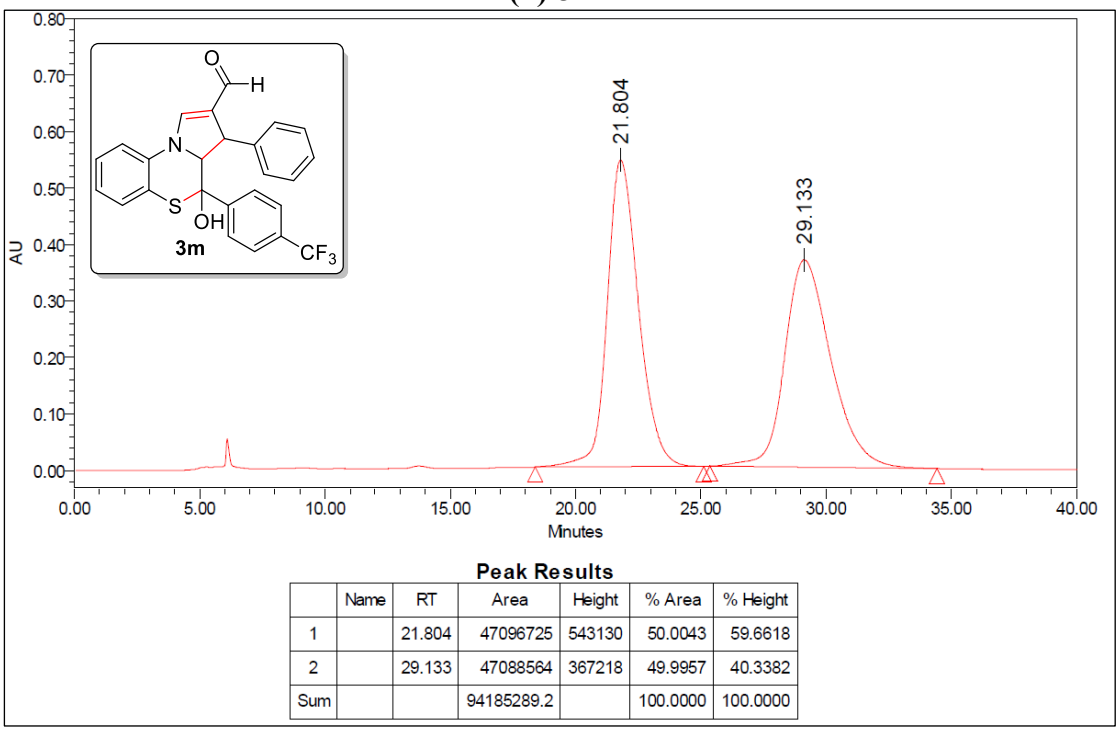

Peak Results

	Name	RT	Area	Height	% Area	% Height
1		21.804	47096725	543130	50.0043	59.6618
2		29.133	47088564	367218	49.9957	40.3382
Sum			94185289.2		100.0000	100.0000

Optical active 3m

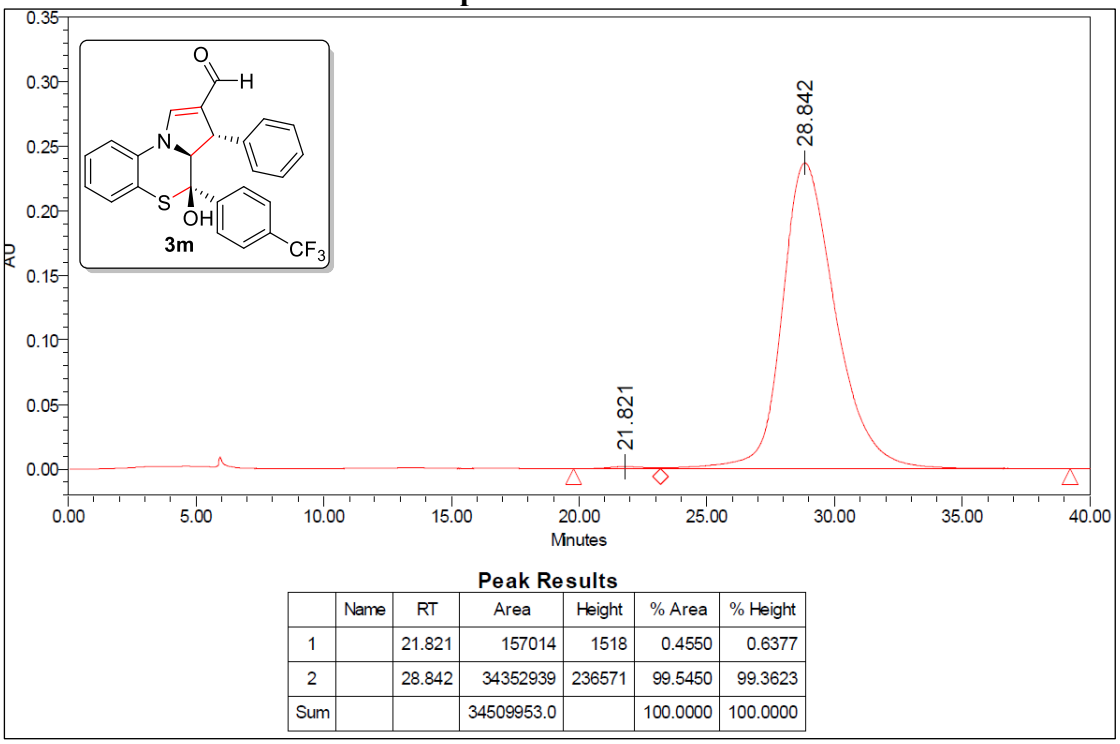

Peak Results

	Name	RT	Area	Height	% Area	% Height
1		21.821	157014	1518	0.4550	0.6377
2		28.842	34352939	236571	99.5450	99.3623
Sum			34509953.0		100.0000	100.0000

(±)-3n

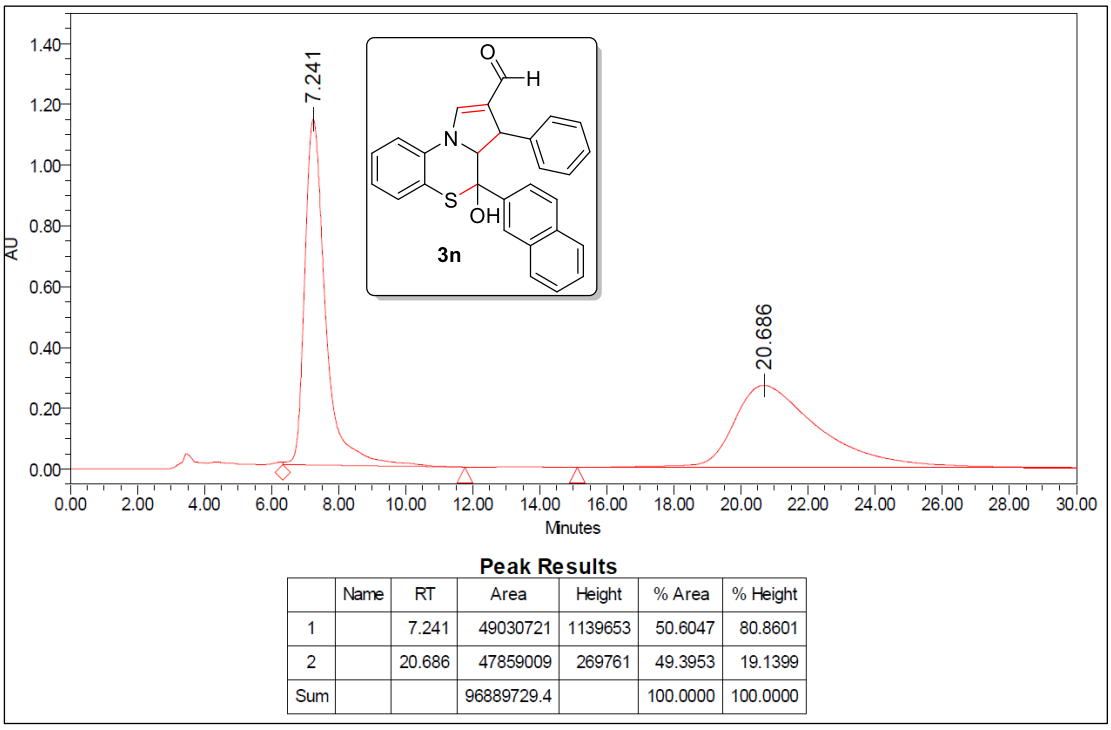

Peak Results

	Name	RT	Area	Height	% Area	% Height
1		7.241	49030721	1139653	50.6047	80.8601
2		20.686	47859009	269761	49.3953	19.1399
Sum			96889729.4		100.0000	100.0000

Optical active 3n

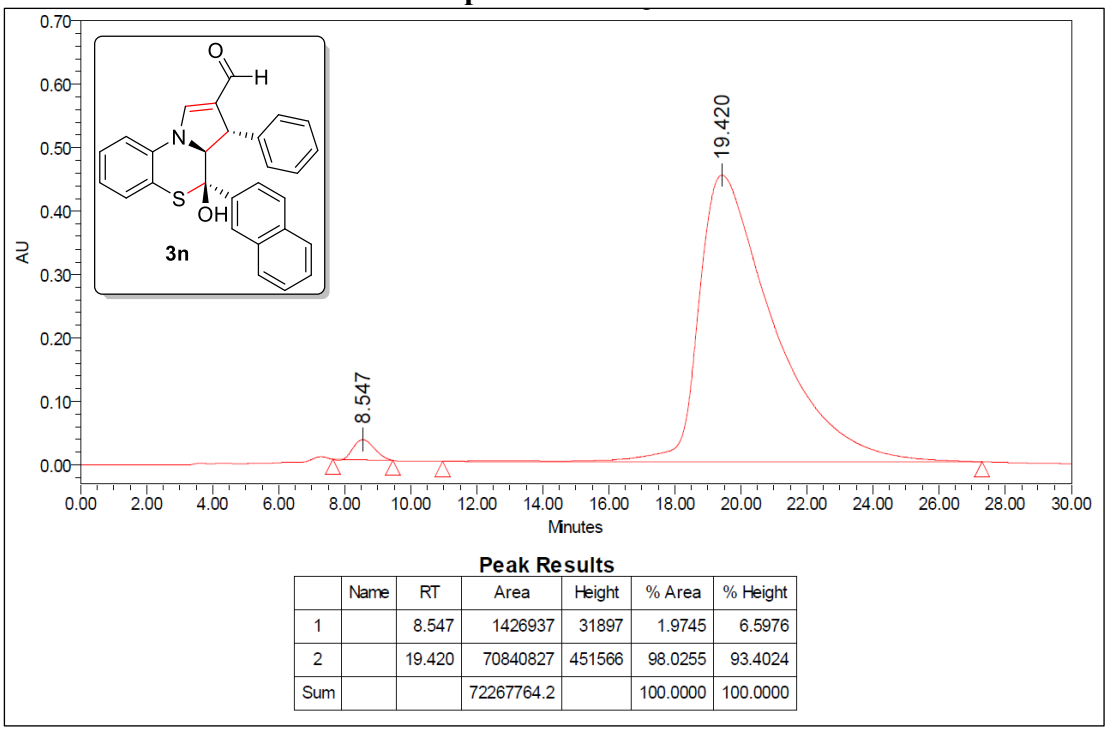

Peak Results

	Name	RT	Area	Height	% Area	% Height
1		8.547	1426937	31897	1.9745	6.5976
2		19.420	70840827	451566	98.0255	93.4024
Sum			72267764.2		100.0000	100.0000

(±)-3o

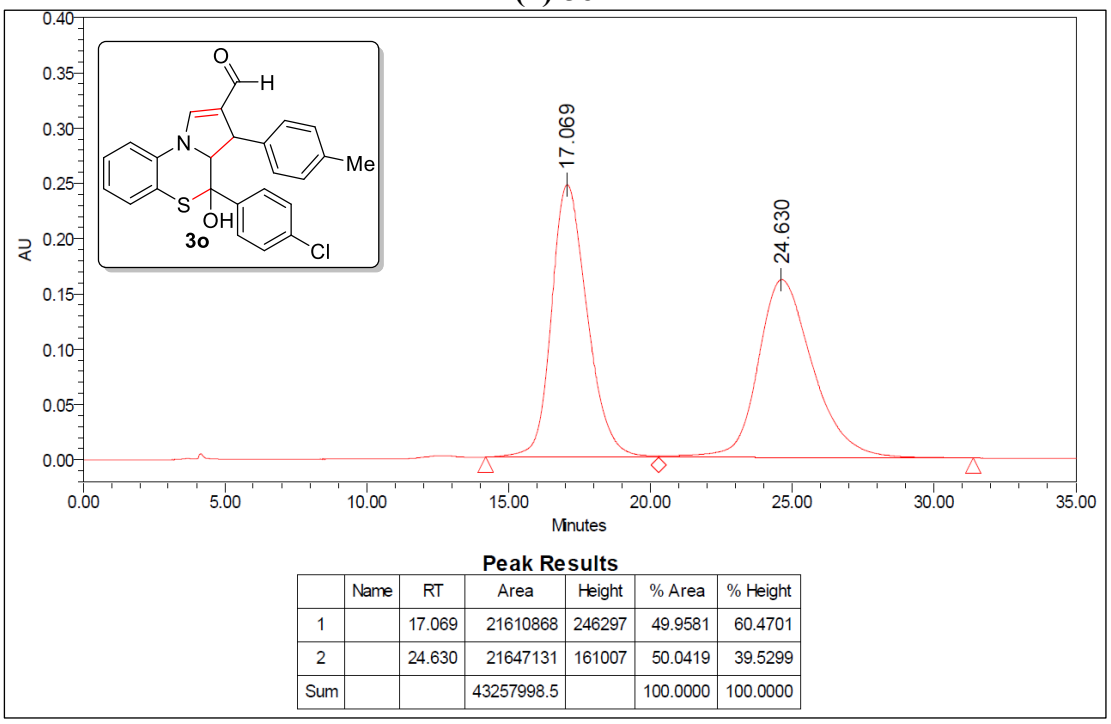

Peak Results

	Name	RT	Area	Height	% Area	% Height
1		17.069	21610868	246297	49.9581	60.4701
2		24.630	21647131	161007	50.0419	39.5299
Sum			43257998.5		100.0000	100.0000

Optical active 3o

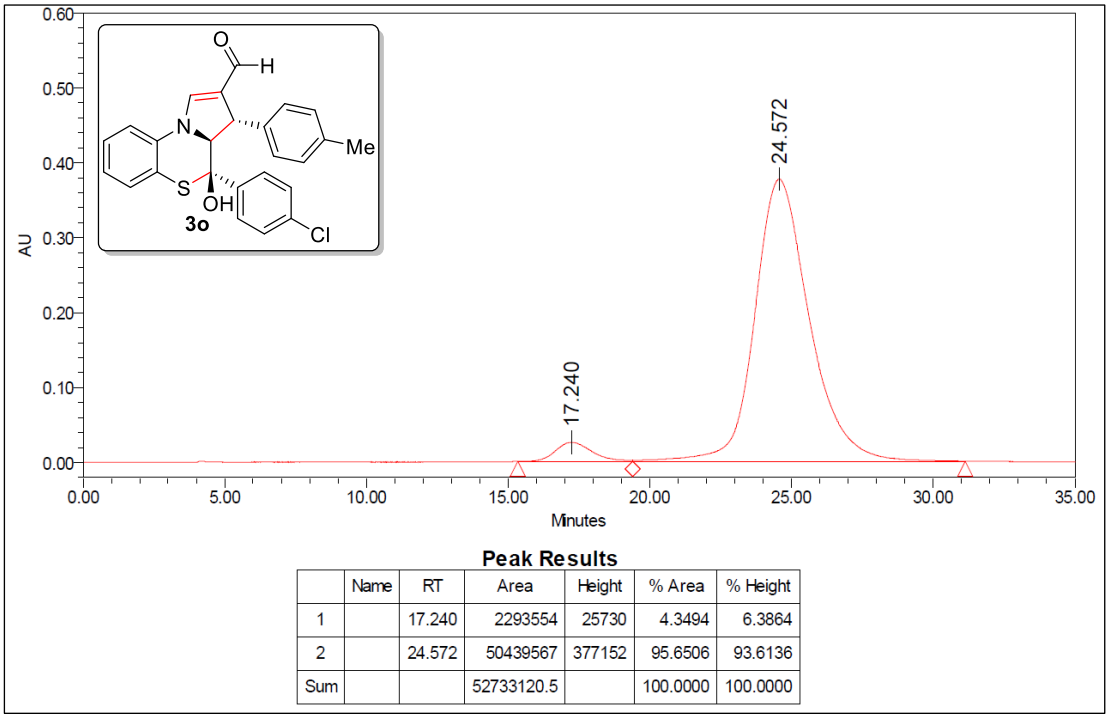

Peak Results

	Name	RT	Area	Height	% Area	% Height
1		17.240	2293554	25730	4.3494	6.3864
2		24.572	50439567	377152	95.6506	93.6136
Sum			52733120.5		100.0000	100.0000

(±)-3p

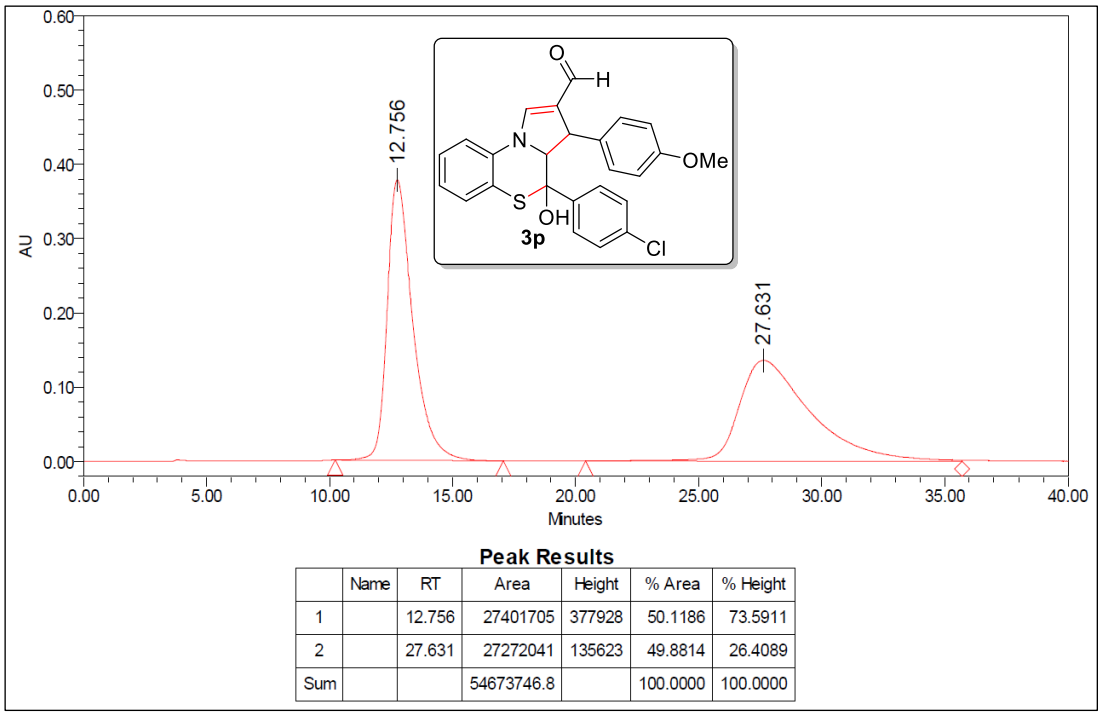

Peak Results

	Name	RT	Area	Height	% Area	% Height
1		12.756	27401705	377928	50.1186	73.5911
2		27.631	27272041	135623	49.8814	26.4089
Sum			54673746.8		100.0000	100.0000

Optical active 3p

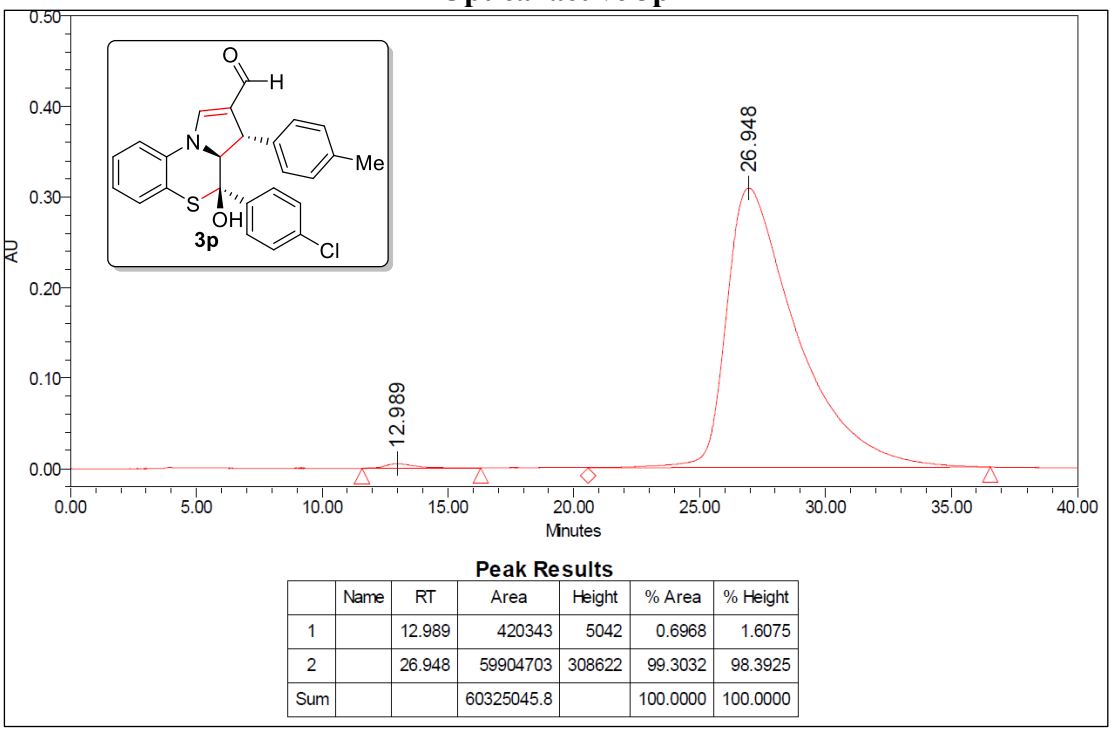

Peak Results

	Name	RT	Area	Height	% Area	% Height
1		12.989	420343	5042	0.6968	1.6075
2		26.948	59904703	308622	99.3032	98.3925
Sum			60325045.8		100.0000	100.0000

(±)-3q

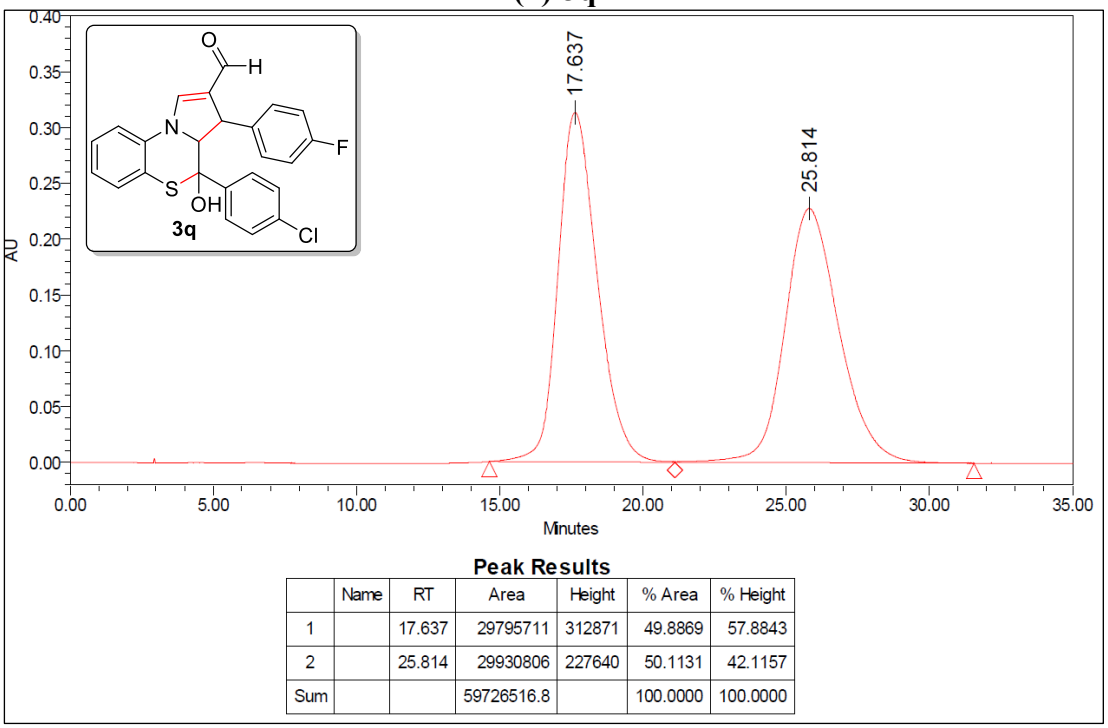

Peak Results

	Name	RT	Area	Height	% Area	% Height
1		17.637	29795711	312871	49.8869	57.8843
2		25.814	29930806	227640	50.1131	42.1157
Sum			59726516.8		100.0000	100.0000

Optical active 3q

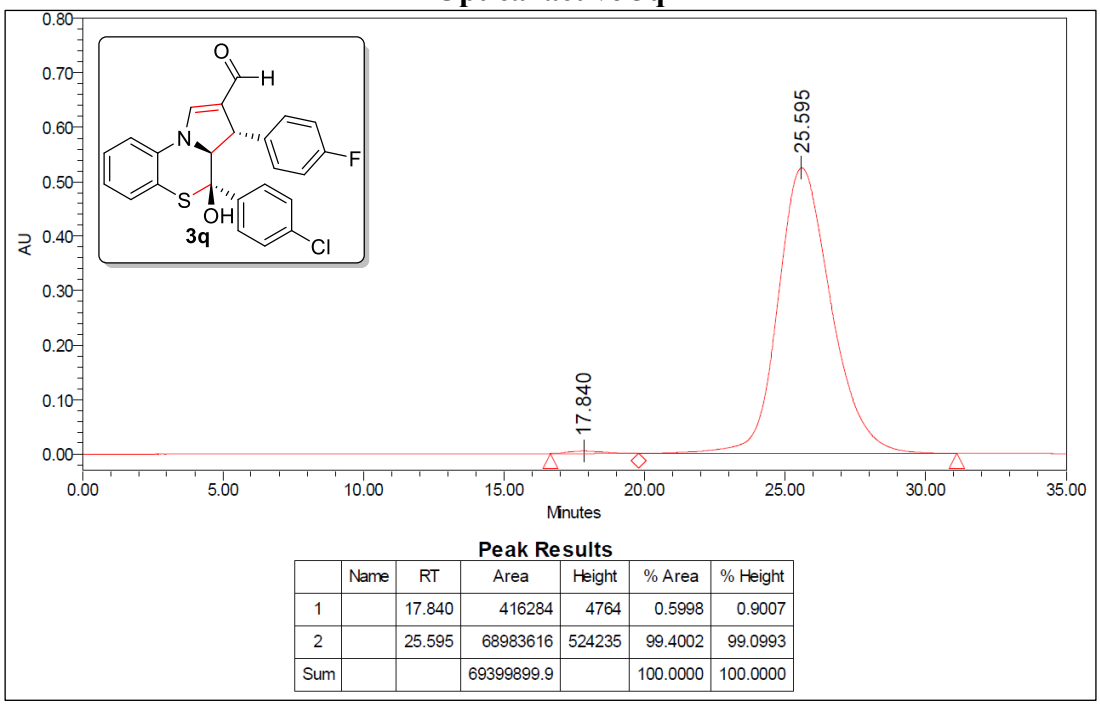

Peak Results

	Name	RT	Area	Height	% Area	% Height
1		17.840	416284	4764	0.5998	0.9007
2		25.595	68983616	524235	99.4002	99.0993
Sum			69399899.9		100.0000	100.0000

(±)-3r

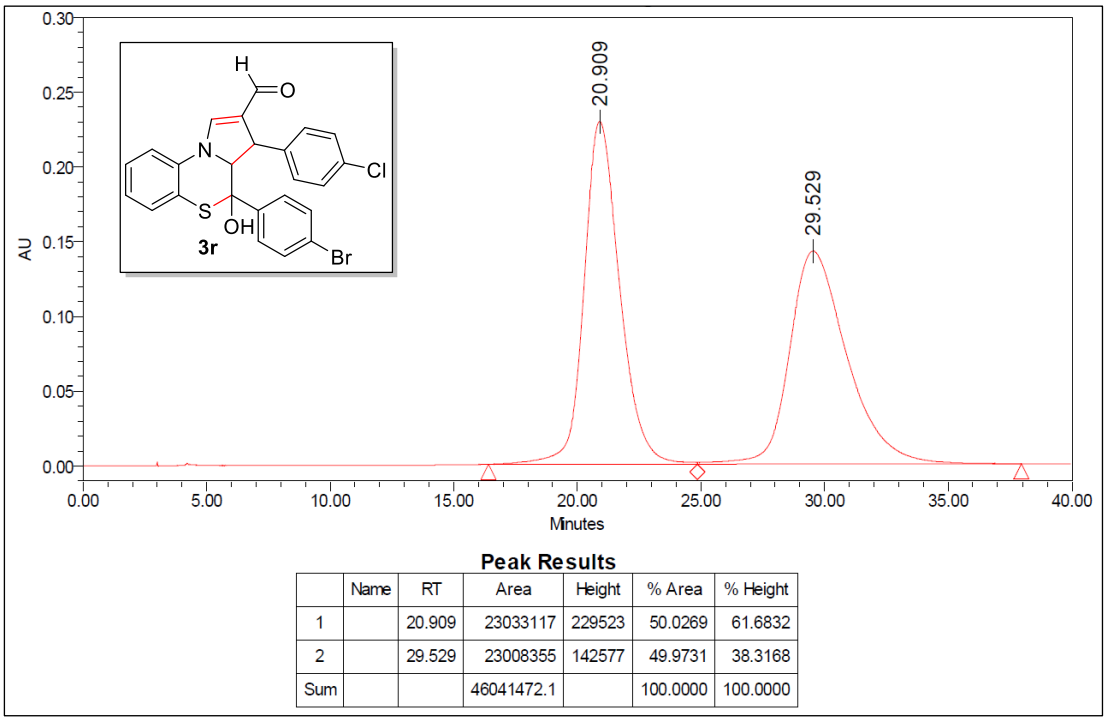

Peak Results

	Name	RT	Area	Height	% Area	% Height
1		20.909	23033117	229523	50.0269	61.6832
2		29.529	23008355	142577	49.9731	38.3168
Sum			46041472.1		100.0000	100.0000

Optical active 3r

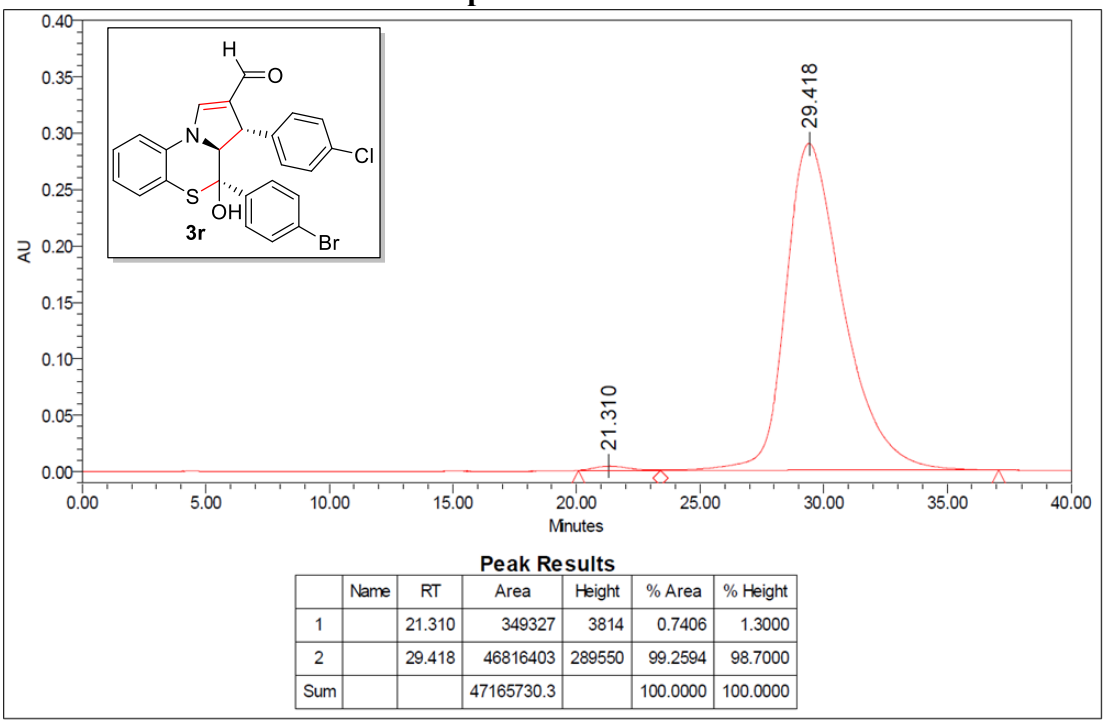

Peak Results

	Name	RT	Area	Height	% Area	% Height
1		21.310	349327	3814	0.7406	1.3000
2		29.418	46816403	289550	99.2594	98.7000
Sum			47165730.3		100.0000	100.0000

(±)-3s

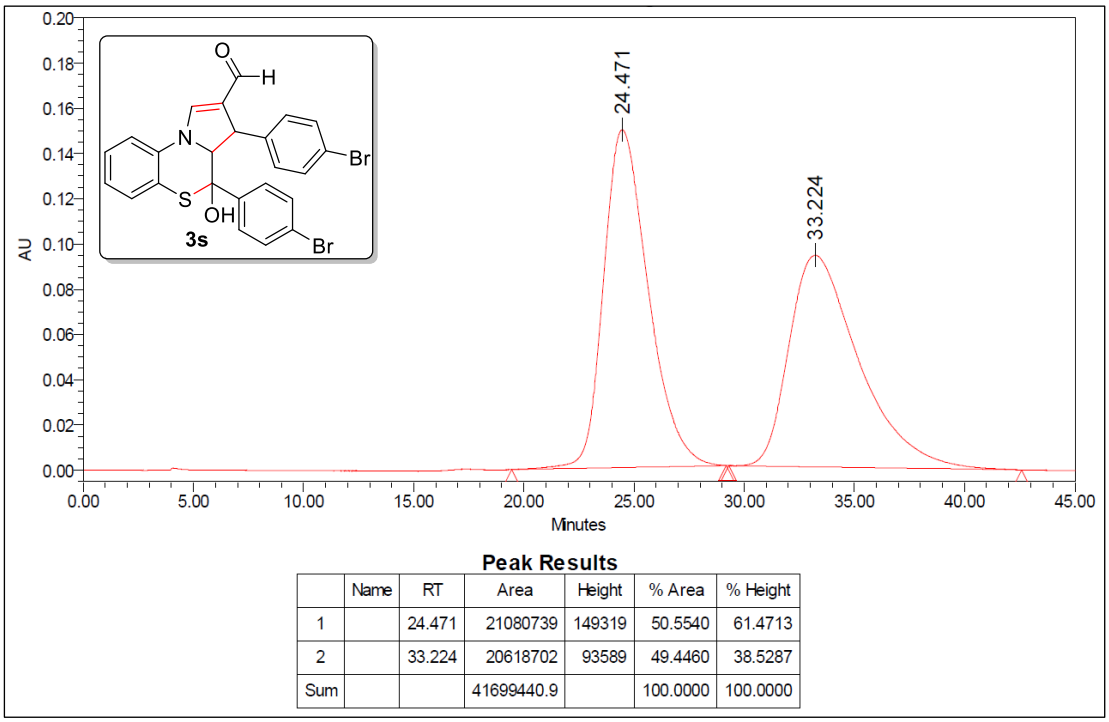

Peak Results

	Name	RT	Area	Height	% Area	% Height
1		24.471	21080739	149319	50.5540	61.4713
2		33.224	20618702	93589	49.4460	38.5287
Sum			41699440.9		100.0000	100.0000

Optical active 3s

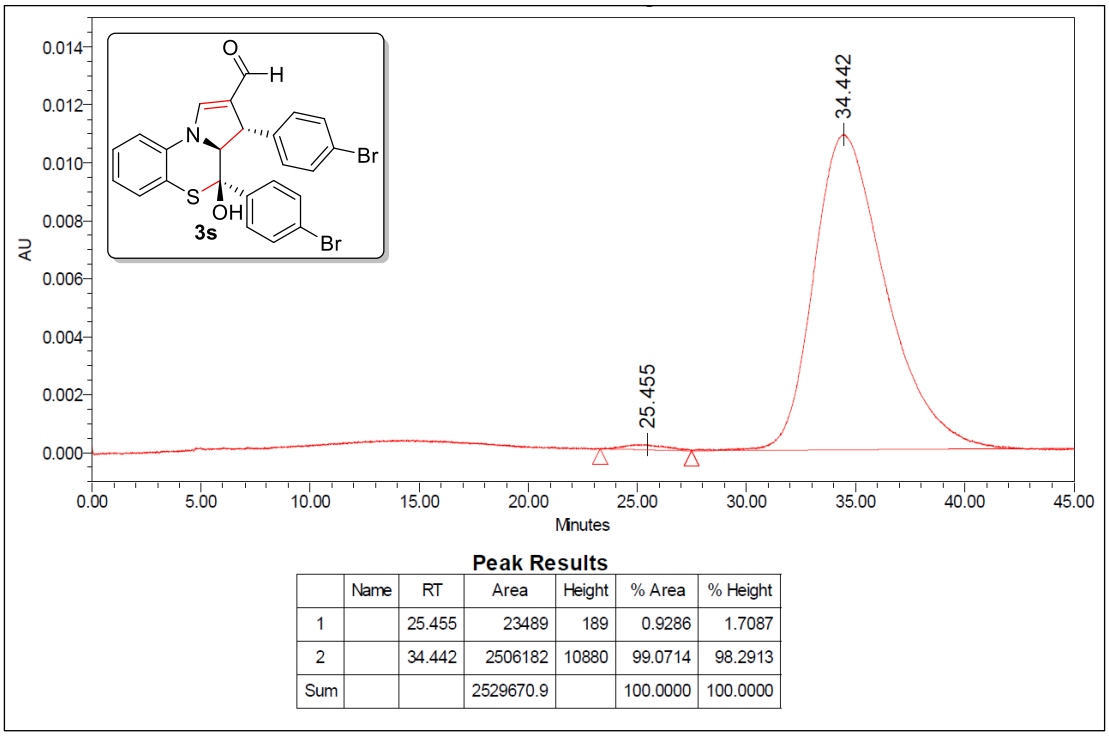

Peak Results

	Name	RT	Area	Height	% Area	% Height
1		25.455	23489	189	0.9286	1.7087
2		34.442	2506182	10880	99.0714	98.2913
Sum			2529670.9		100.0000	100.0000

(±)-3t

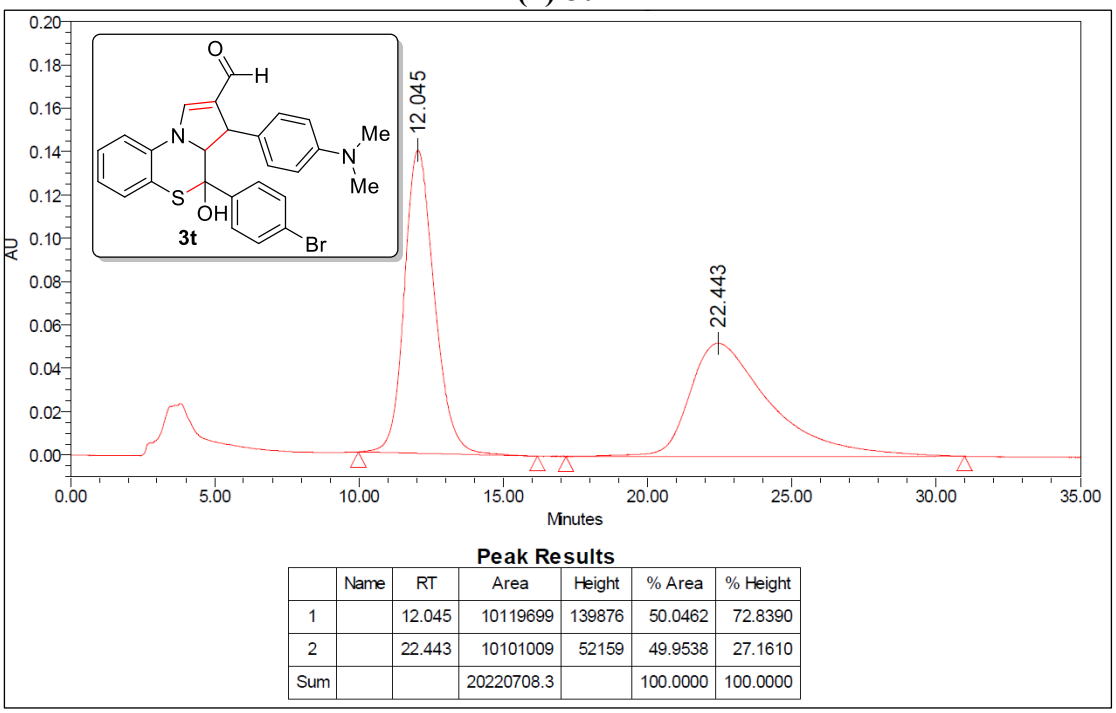

Peak Results

	Name	RT	Area	Height	% Area	% Height
1		12.045	10119699	139876	50.0462	72.8390
2		22.443	10101009	52159	49.9538	27.1610
Sum			20220708.3		100.0000	100.0000

Optical active 3t

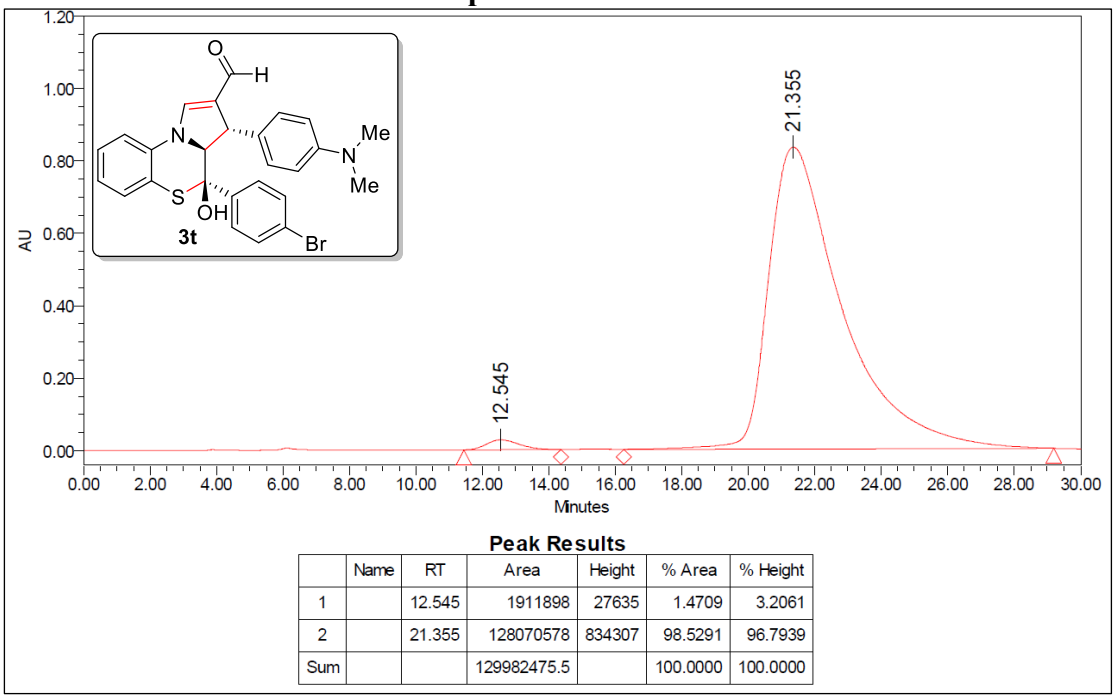

Peak Results

	Name	RT	Area	Height	% Area	% Height
1		12.545	1911898	27635	1.4709	3.2061
2		21.355	128070578	834307	98.5291	96.7939
Sum			129982475.5		100.0000	100.0000

(±)-3u

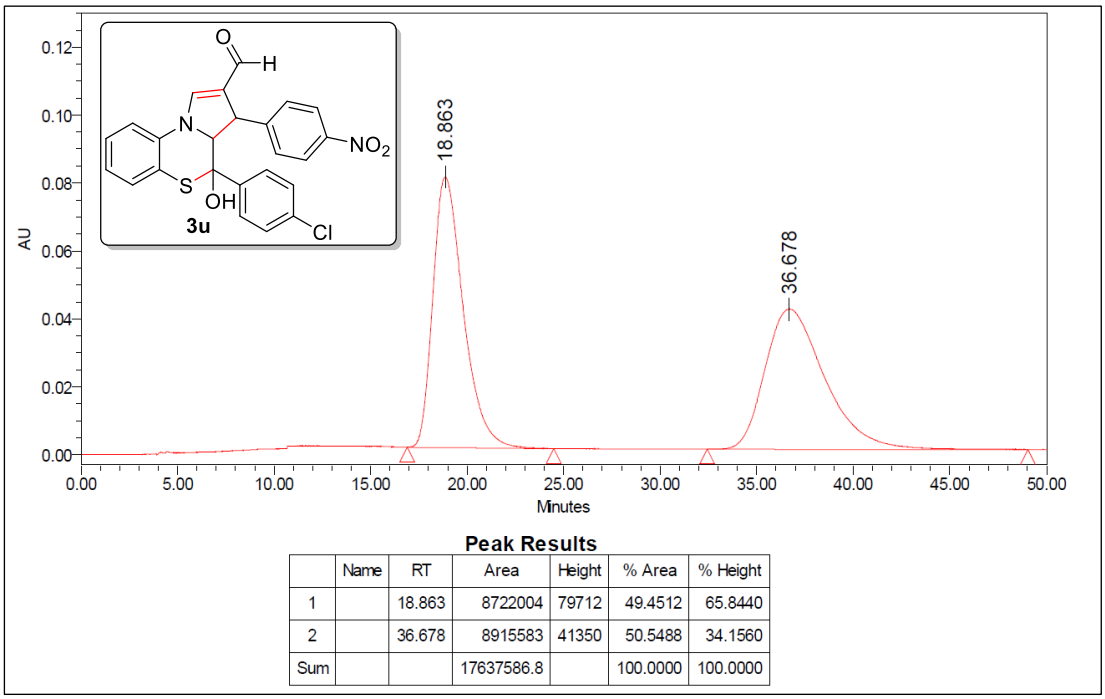

Peak Results

	Name	RT	Area	Height	% Area	% Height
1		18.863	8722004	79712	49.4512	65.8440
2		36.678	8915583	41350	50.5488	34.1560
Sum			17637586.8		100.0000	100.0000

Optical active 3u

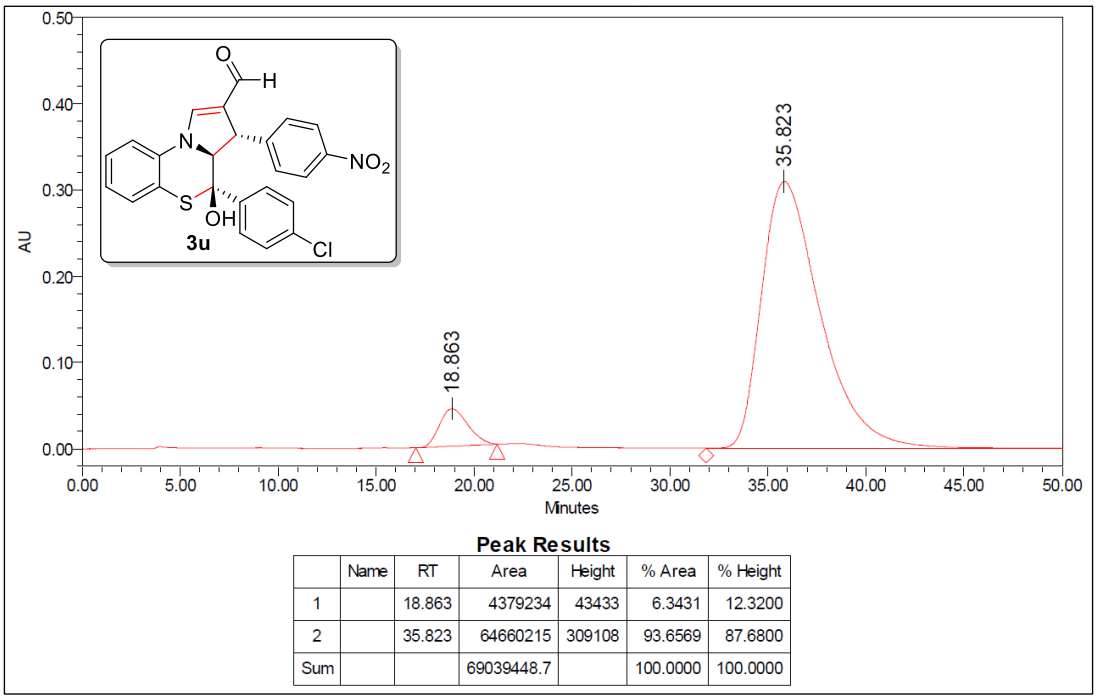

Peak Results

	Name	RT	Area	Height	% Area	% Height
1		18.863	4379234	43433	6.3431	12.3200
2		35.823	64660215	309108	93.6569	87.6800
Sum			69039448.7		100.0000	100.0000

(±)-3v

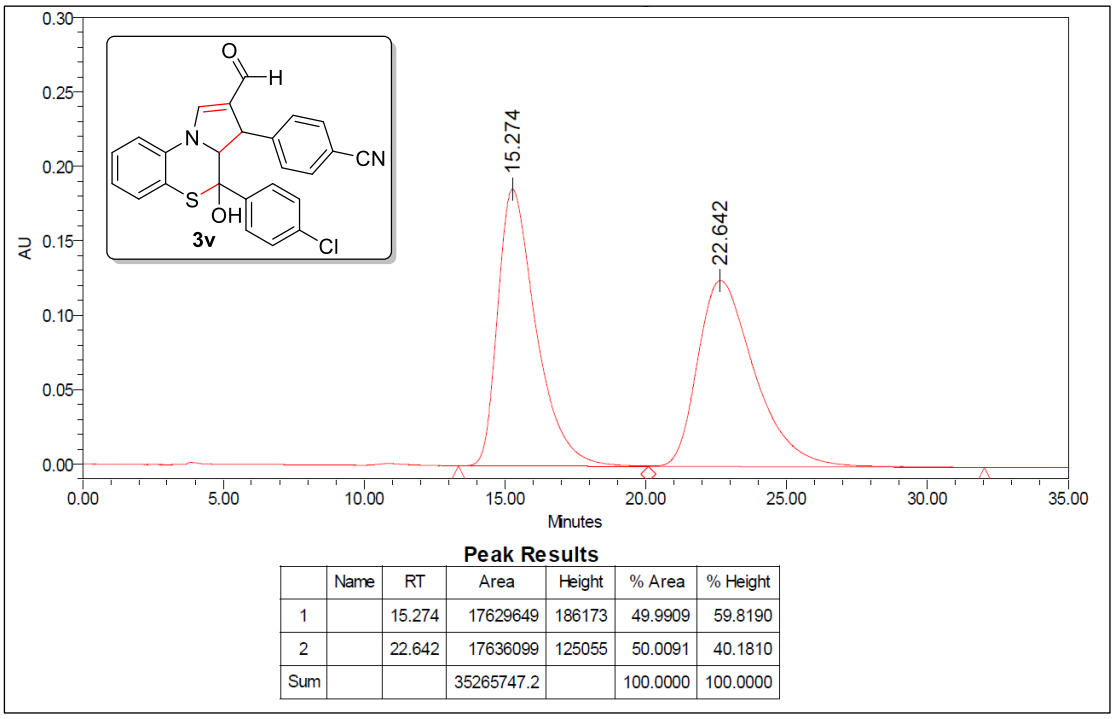

Peak Results

	Name	RT	Area	Height	% Area	% Height
1		15.274	17629649	186173	49.9909	59.8190
2		22.642	17636099	125055	50.0091	40.1810
Sum			35265747.2		100.0000	100.0000

Optical active 3v

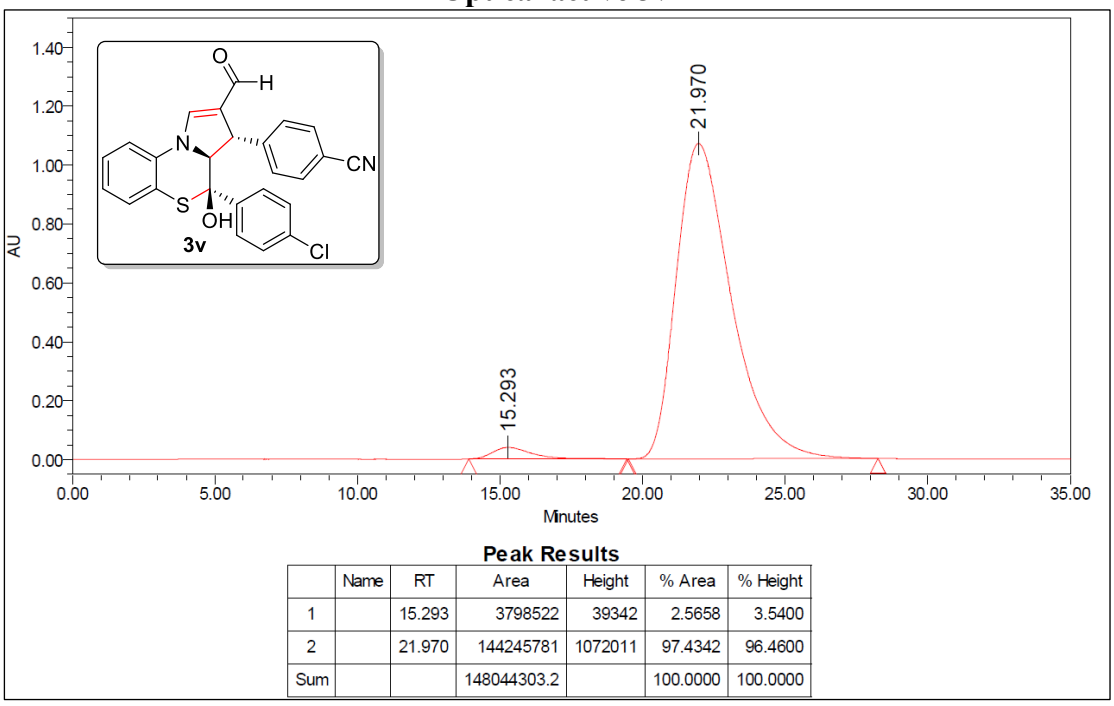

Peak Results

	Name	RT	Area	Height	% Area	% Height
1		15.293	3798522	39342	2.5658	3.5400
2		21.970	144245781	1072011	97.4342	96.4600
Sum			148044303.2		100.0000	100.0000

(±)-3w

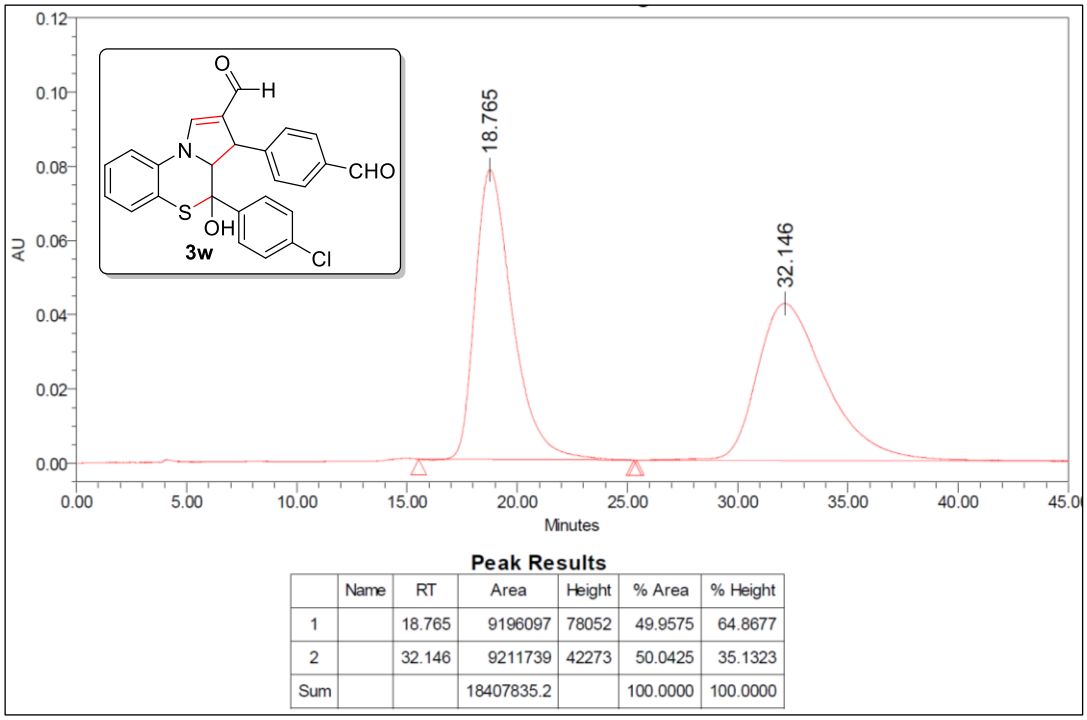

Peak Results

	Name	RT	Area	Height	% Area	% Height
1		18.765	9196097	78052	49.9575	64.8677
2		32.146	9211739	42273	50.0425	35.1323
Sum			18407835.2		100.0000	100.0000

Optical active 3w

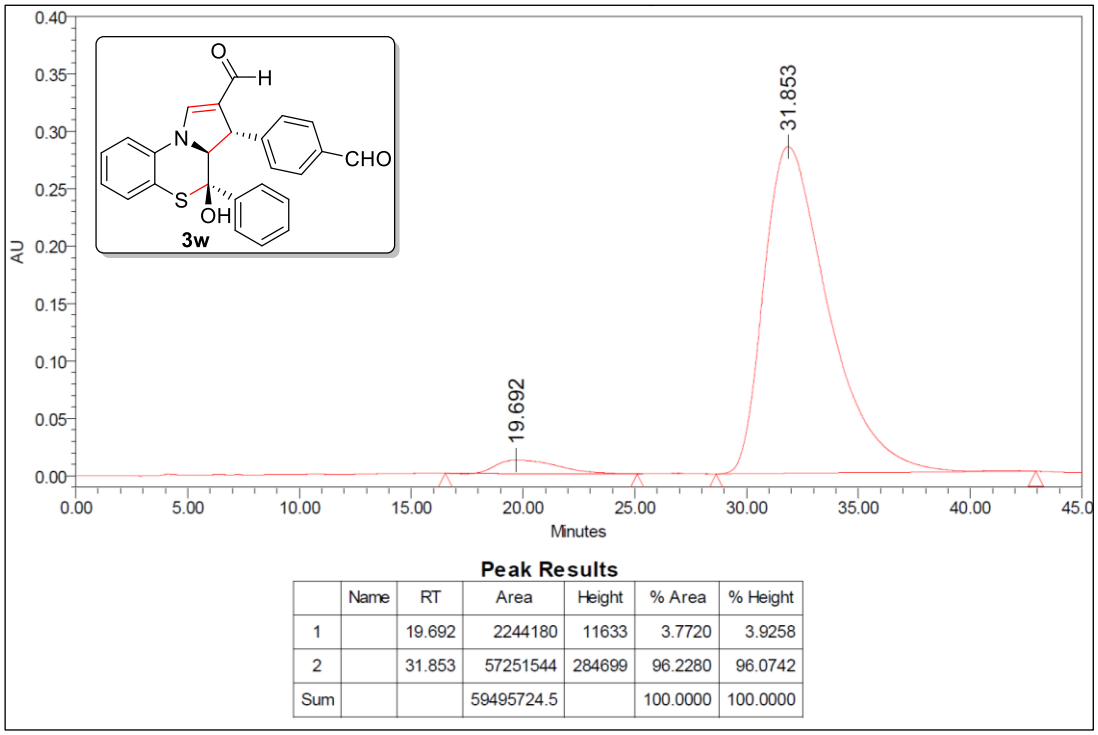

Peak Results

	Name	RT	Area	Height	% Area	% Height
1		19.692	2244180	11633	3.7720	3.9258
2		31.853	57251544	284699	96.2280	96.0742
Sum			59495724.5		100.0000	100.0000

(±)-3x

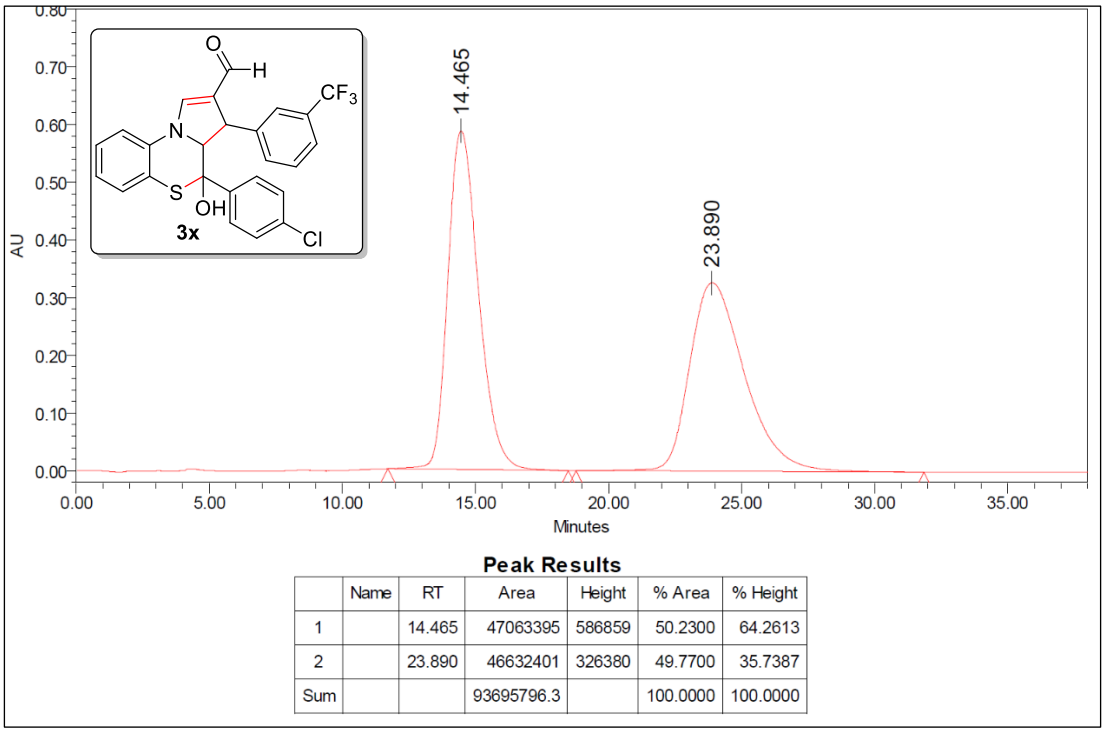

Peak Results

	Name	RT	Area	Height	% Area	% Height
1		14.465	47063395	586859	50.2300	64.2613
2		23.890	46632401	326380	49.7700	35.7387
Sum			93695796.3		100.0000	100.0000

Optical active 3x

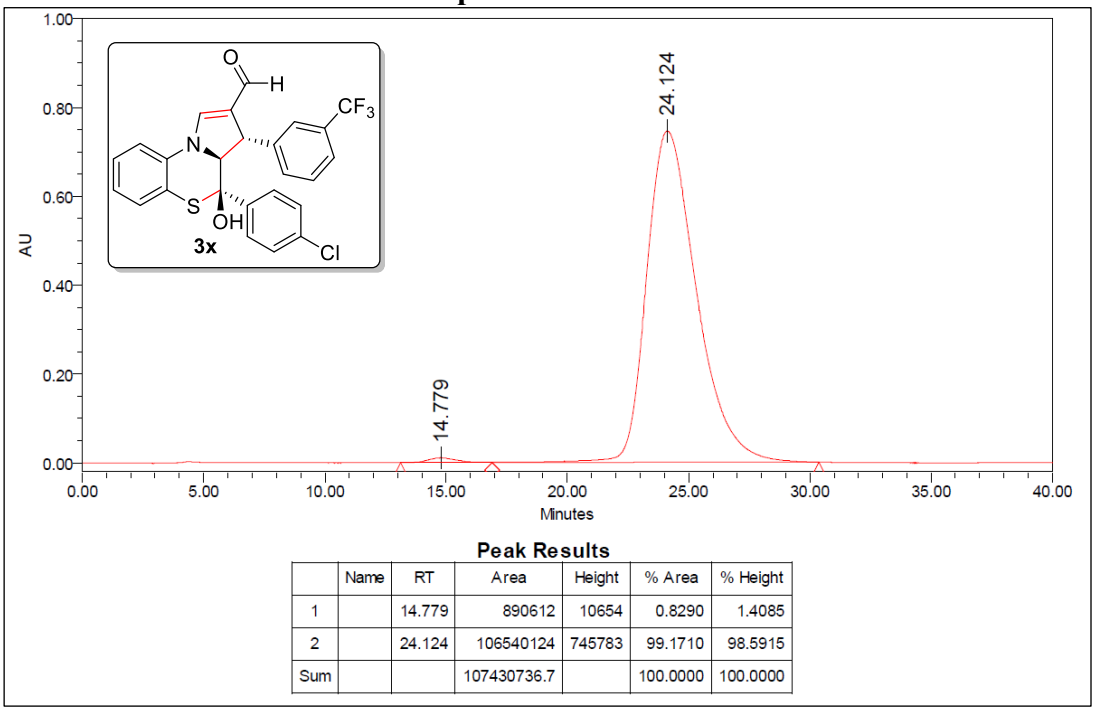

Peak Results

	Name	RT	Area	Height	% Area	% Height
1		14.779	890612	10654	0.8290	1.4085
2		24.124	106540124	745783	99.1710	98.5915
Sum			107430736.7		100.0000	100.0000

(±)-3y

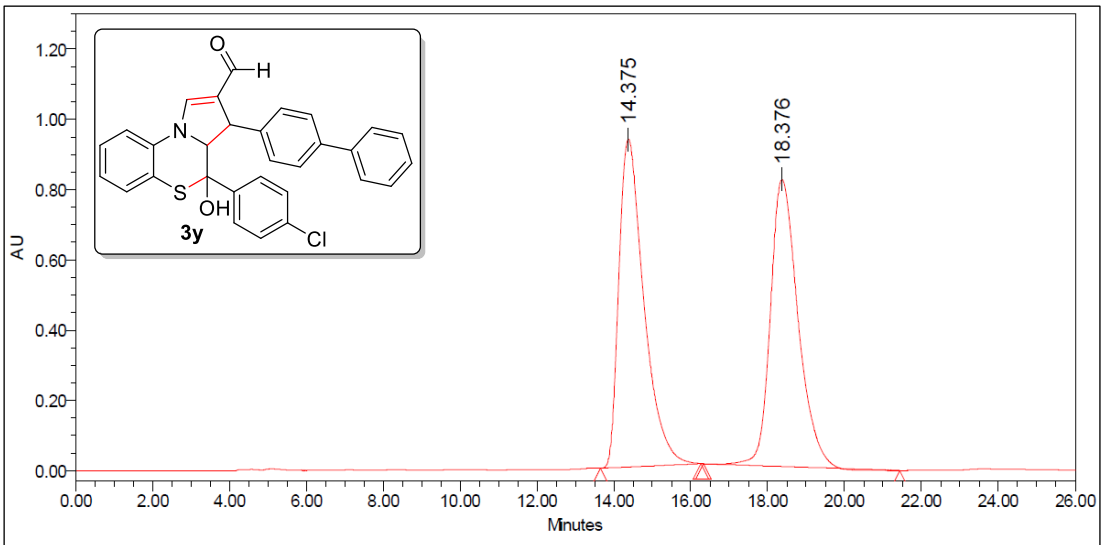

Peak Results

	Name	RT	Area	Height	% Area	% Height
1		14.375	42130706	933303	50.6049	53.3249
2		18.376	41123461	816917	49.3951	46.6751
Sum			83254167.5		100.0000	100.0000

Optical active 3y

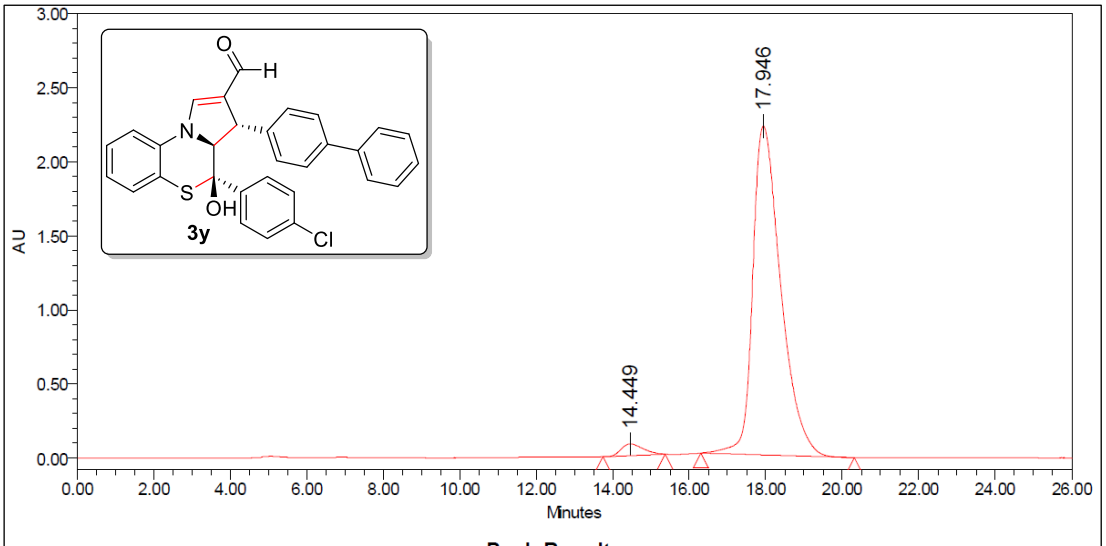

Peak Results

	Name	RT	Area	Height	% Area	% Height
1		14.449	3181938	79877	2.7356	3.4703
2		17.946	113133159	2221875	97.2644	96.5297
Sum			116315097.7		100.0000	100.0000

(±)-3z

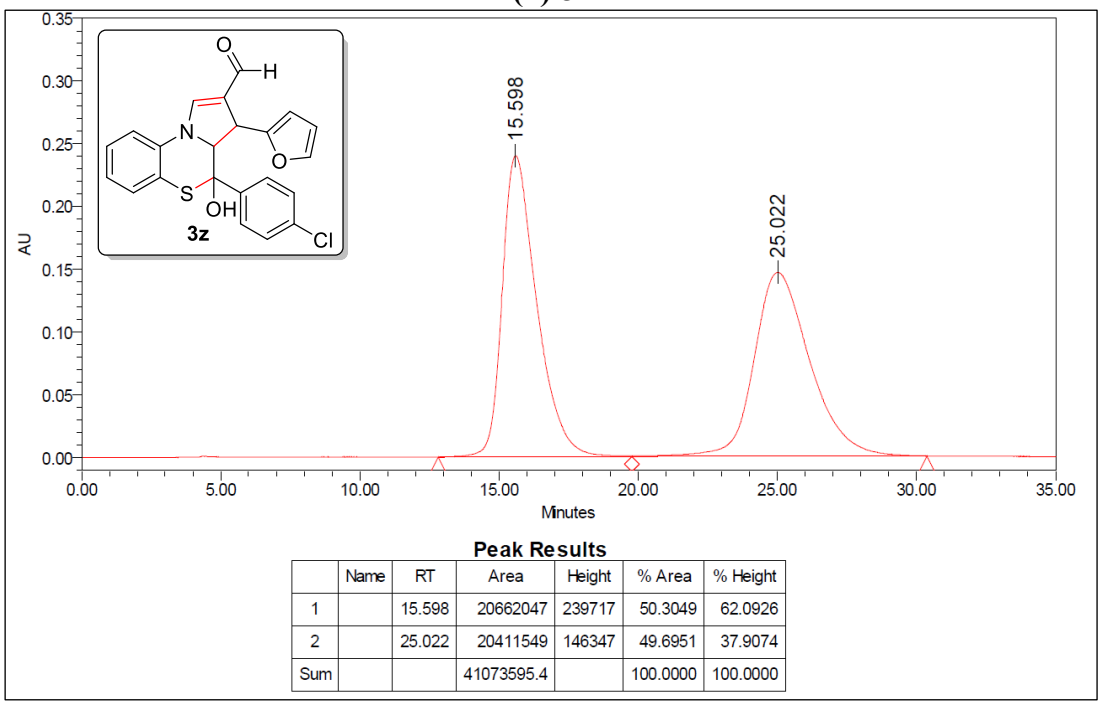

Peak Results

	Name	RT	Area	Height	% Area	% Height
1		15.598	20662047	239717	50.3049	62.0926
2		25.022	20411549	146347	49.6951	37.9074
Sum			41073595.4		100.0000	100.0000

Optical active 3z

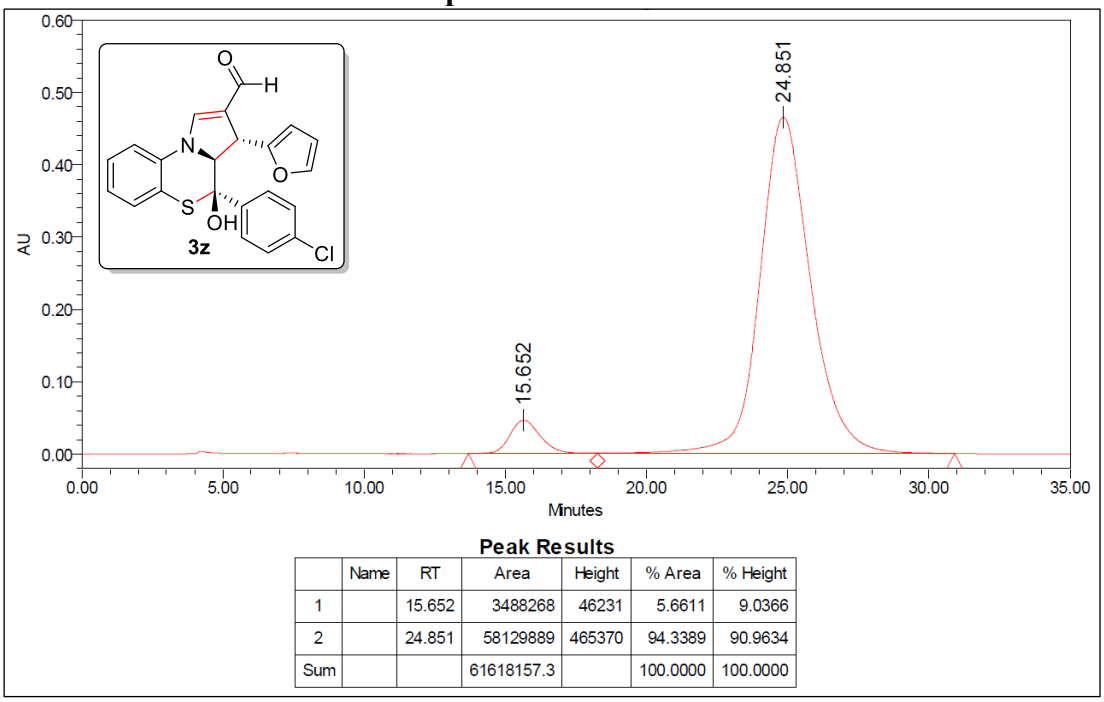

Peak Results

	Name	RT	Area	Height	% Area	% Height
1		15.652	3488268	46231	5.6611	9.0366
2		24.851	58129889	465370	94.3389	90.9634
Sum			61618157.3		100.0000	100.0000

(±)-3aa

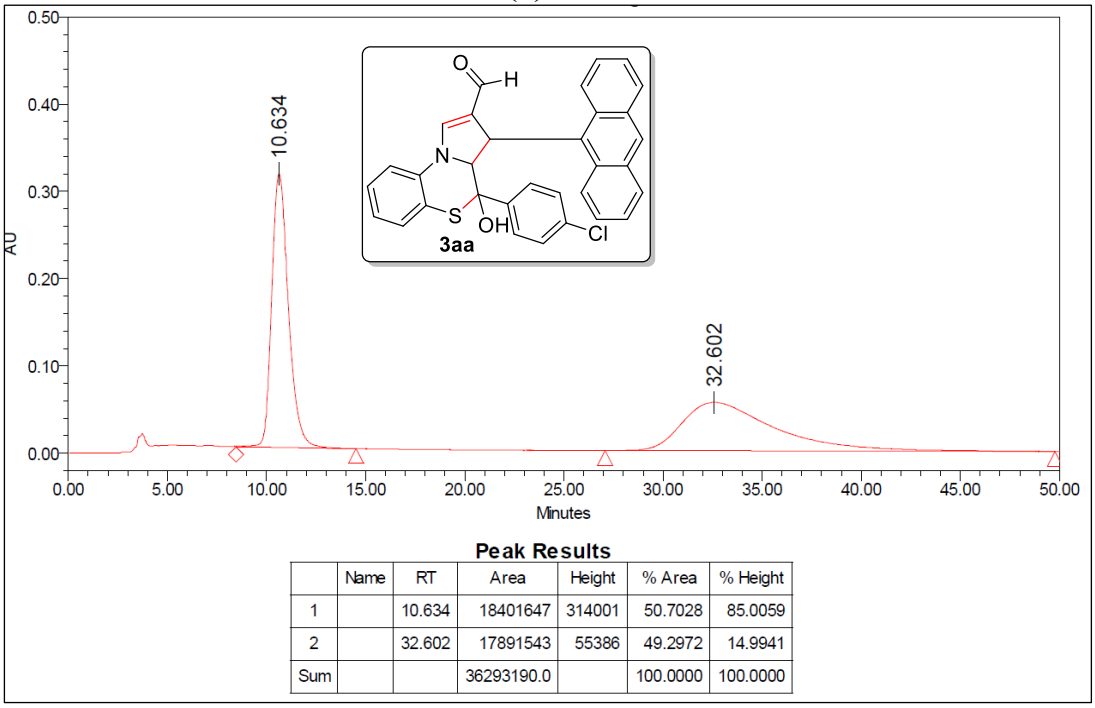

Peak Results

	Name	RT	Area	Height	% Area	% Height
1		10.634	18401647	314001	50.7028	85.0059
2		32.602	17891543	55386	49.2972	14.9941
Sum			36293190.0		100.0000	100.0000

Optical active 3aa

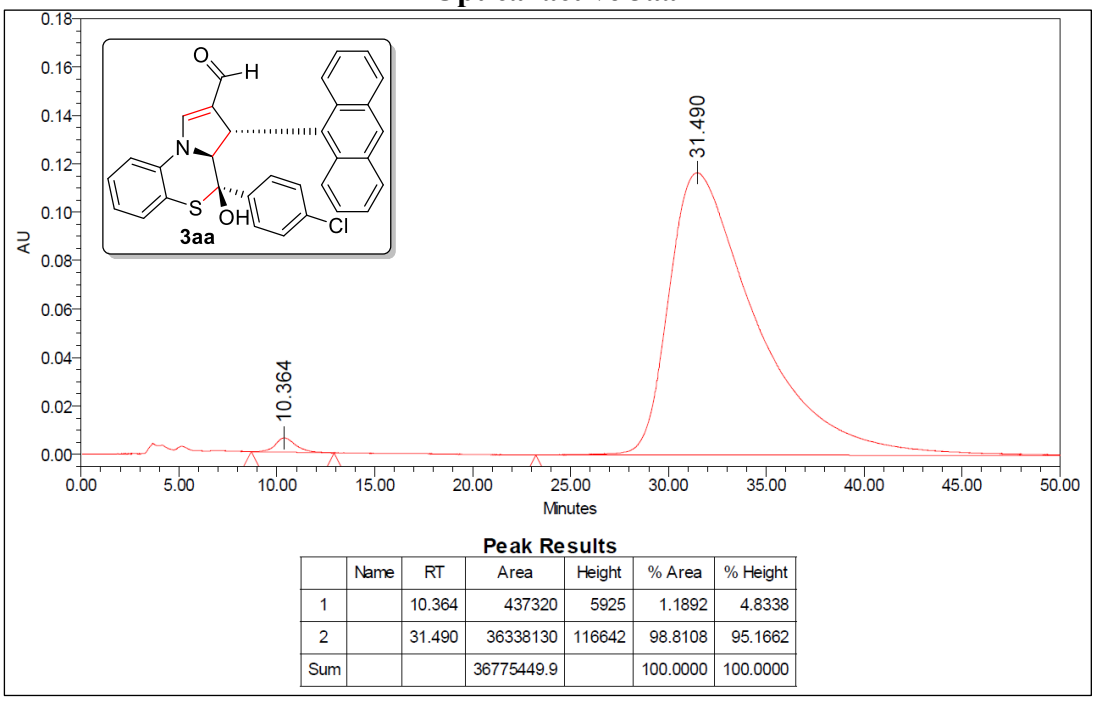

Peak Results

	Name	RT	Area	Height	% Area	% Height
1		10.364	437320	5925	1.1892	4.8338
2		31.490	36338130	116642	98.8108	95.1662
Sum			36775449.9		100.0000	100.0000

(±)-3ab

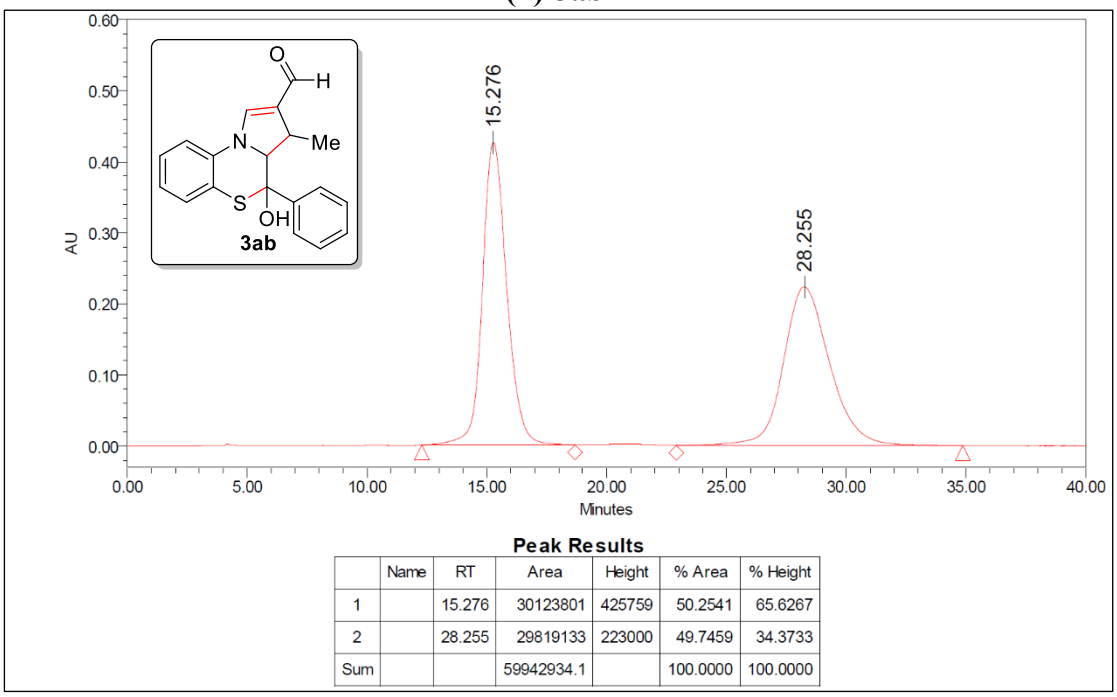

Peak Results

	Name	RT	Area	Height	% Area	% Height
1		15.276	30123801	425759	50.2541	65.6267
2		28.255	29819133	223000	49.7459	34.3733
Sum			59942934.1		100.0000	100.0000

Optical active 3ab

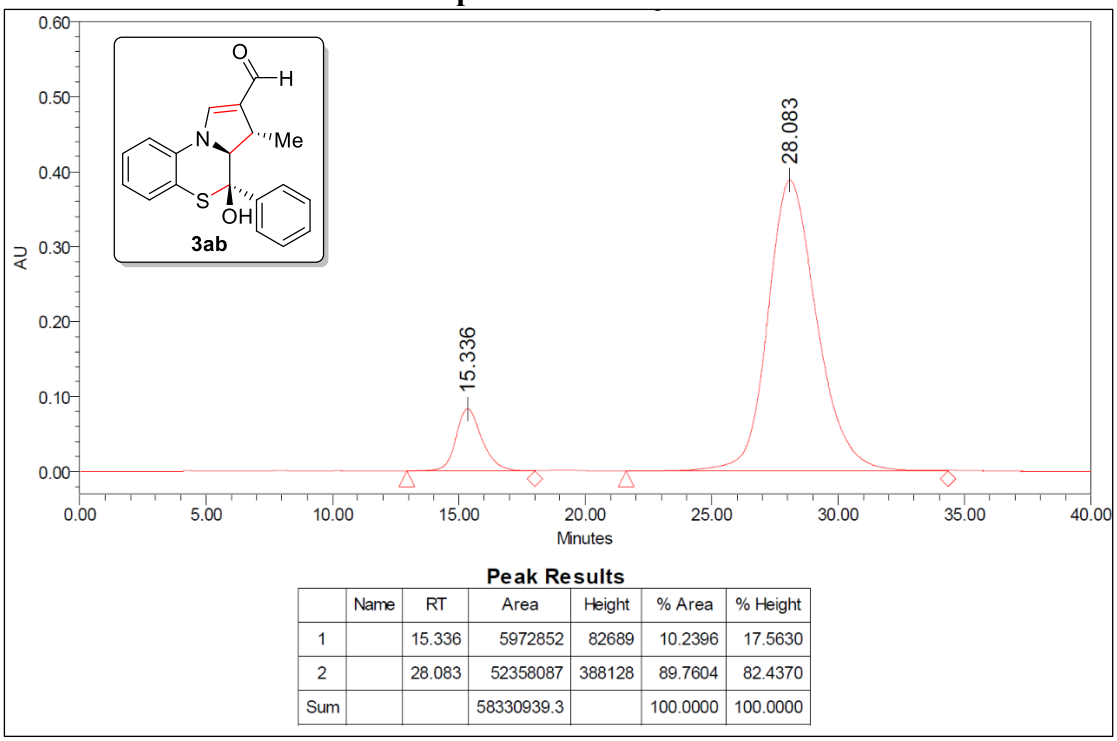

Peak Results

	Name	RT	Area	Height	% Area	% Height
1		15.336	5972852	82689	10.2396	17.5630
2		28.083	52358087	388128	89.7604	82.4370
Sum			58330939.3		100.0000	100.0000

(±)-3ac

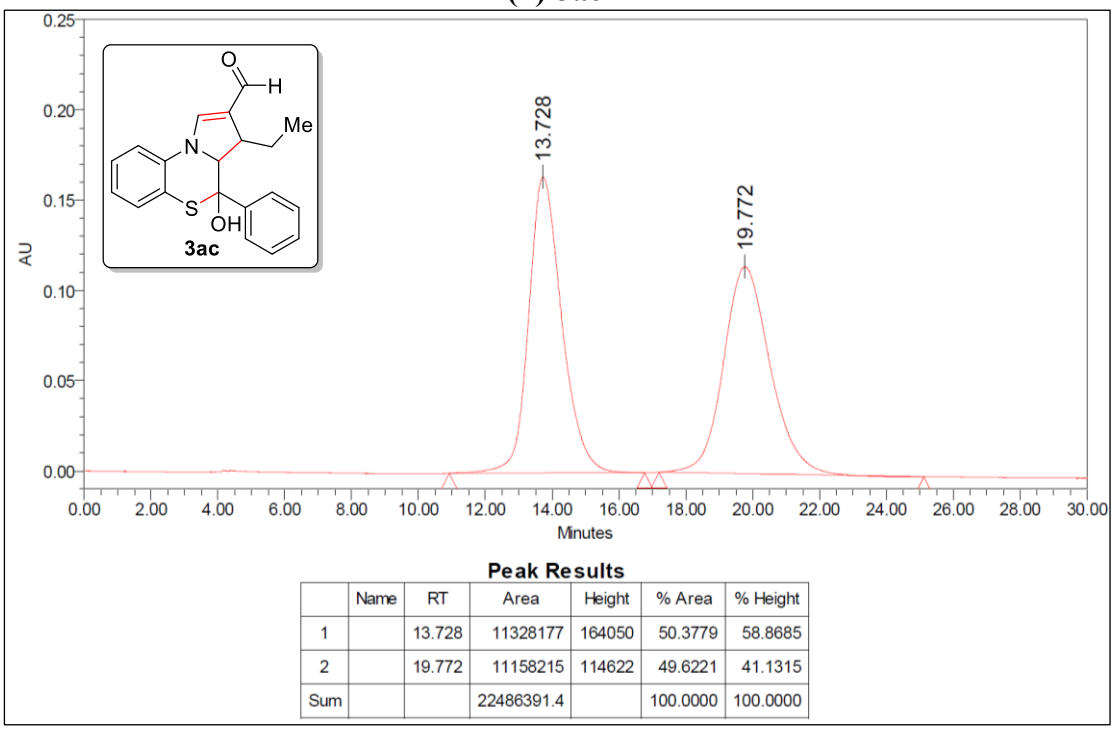

Peak Results

	Name	RT	Area	Height	% Area	% Height
1		13.728	11328177	164050	50.3779	58.8685
2		19.772	11158215	114622	49.6221	41.1315
Sum			22486391.4		100.0000	100.0000

Optical active 3ac

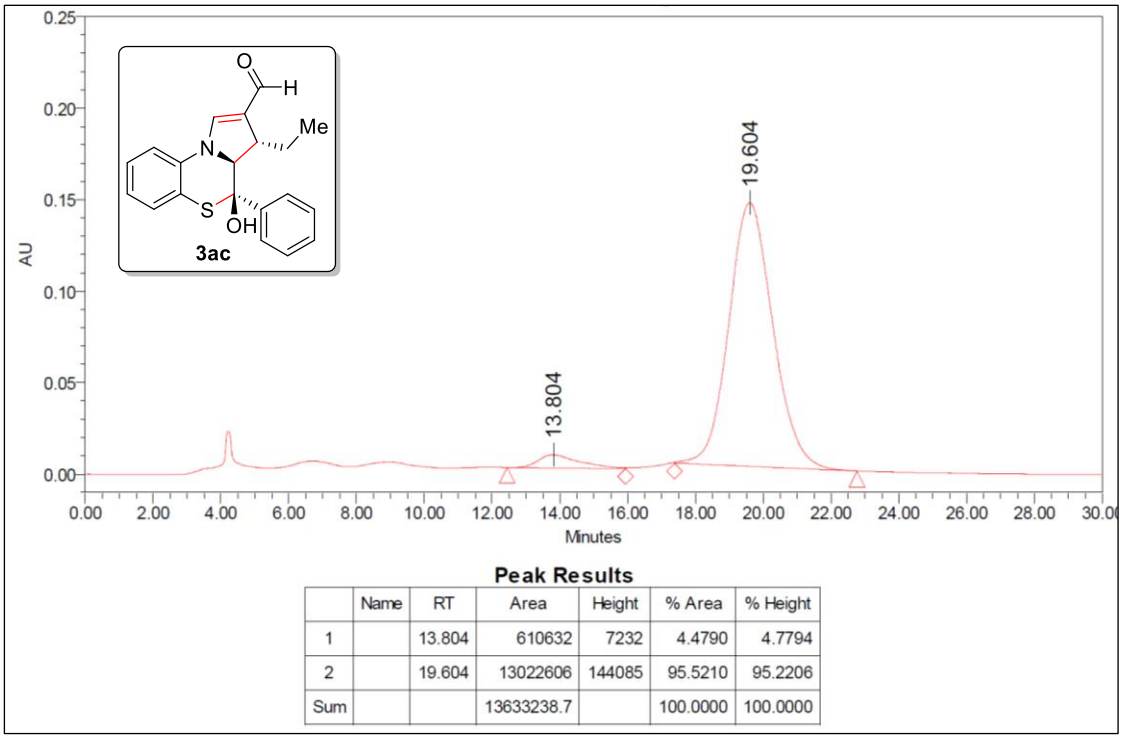

Peak Results

	Name	RT	Area	Height	% Area	% Height
1		13.804	610632	7232	4.4790	4.7794
2		19.604	13022606	144085	95.5210	95.2206
Sum			13633238.7		100.0000	100.0000

(±)-3d

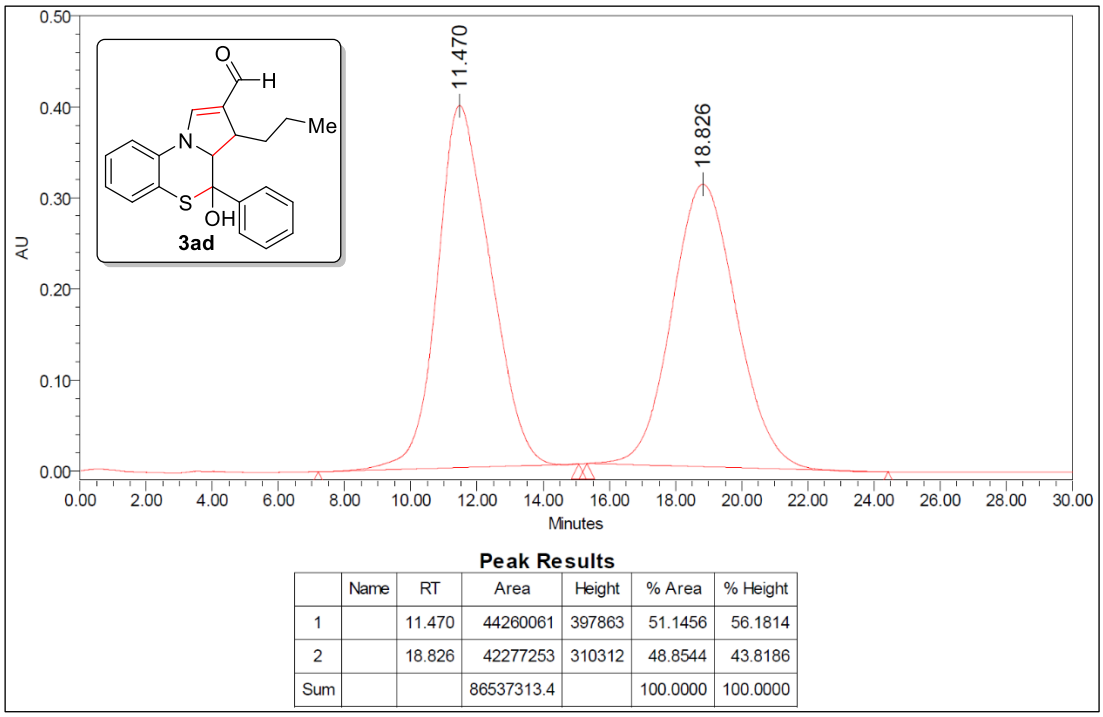

Peak Results

	Name	RT	Area	Height	% Area	% Height
1		11.470	44260061	397863	51.1456	56.1814
2		18.826	42277253	310312	48.8544	43.8186
Sum			86537313.4		100.0000	100.0000

Optical active 3ad

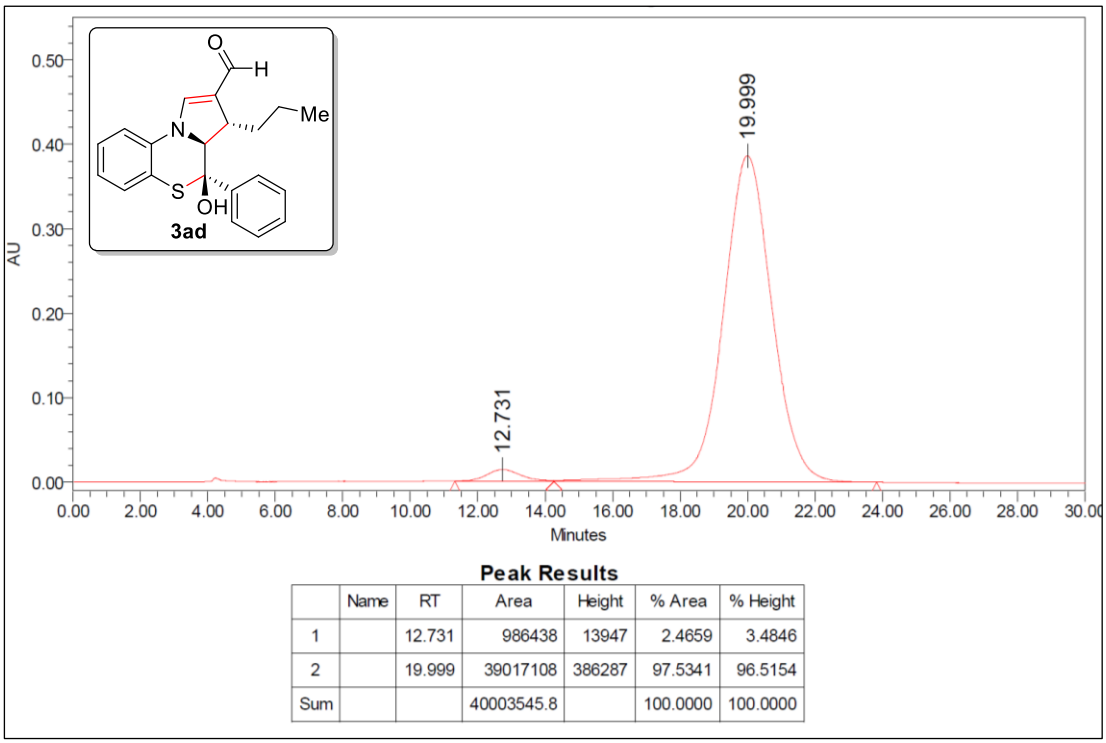

Peak Results

	Name	RT	Area	Height	% Area	% Height
1		12.731	986438	13947	2.4659	3.4846
2		19.999	39017108	386287	97.5341	96.5154
Sum			40003545.8		100.0000	100.0000

CHAPTER 3

ONE-POT ENANTIOSELECTIVE SYNTHESIS OF *N*-PHENYL THIOETHER-TETHERED TETRASUBSTITUTED 4,5-DIHYDROPYRROLE-3-CARBALDEHYDES

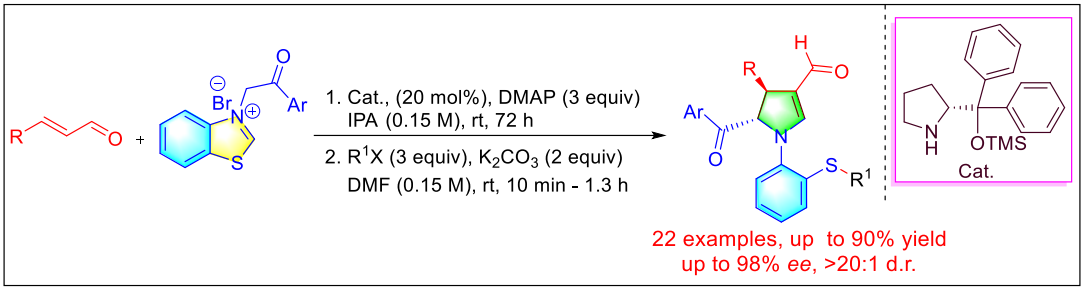

3.1 INTRODUCTION

3.1.1 Importance of Dihydropyrroles

Dihydropyrroles such as (2,3), (2,5), and (4,5)-dihydropyrroles are the important five-membered nitrogen-containing heterocyclic compounds found in various biologically active molecules, natural products, and organic reactive intermediates.[177,178] The dihydropyrrole derivatives are essential building blocks in the organic diverse-orientated synthesis of pyrrole, pyrrolidine, and their complex bioactive analogs.[179,180] Particularly, ploy-substituted dihydropyrrole **I-IV** with multiple stereogenic centers possess various biological active properties such as antifungal, kinesin inhibitory, and antiproliferative properties (Figure 3.1).[181,182] Many methods have been explored in the literature for the synthesis of poly-substituted dihydropyrroles which includes dipolar cycloaddition,[183] metal-mediated cyclization,[184,185] multicomponent and cascade reactions.[186] While significant efforts have been directed towards the synthesis of 2,3- and 2,5-dihydropyrroles,[187,188] synthesis of 4,5-dihydropyrroles remains a very challenging issue. Thus, it is desirable to develop an efficient method for the synthesis of poly-substituted chiral 4,5-dihydropyrroles from readily available starting materials.

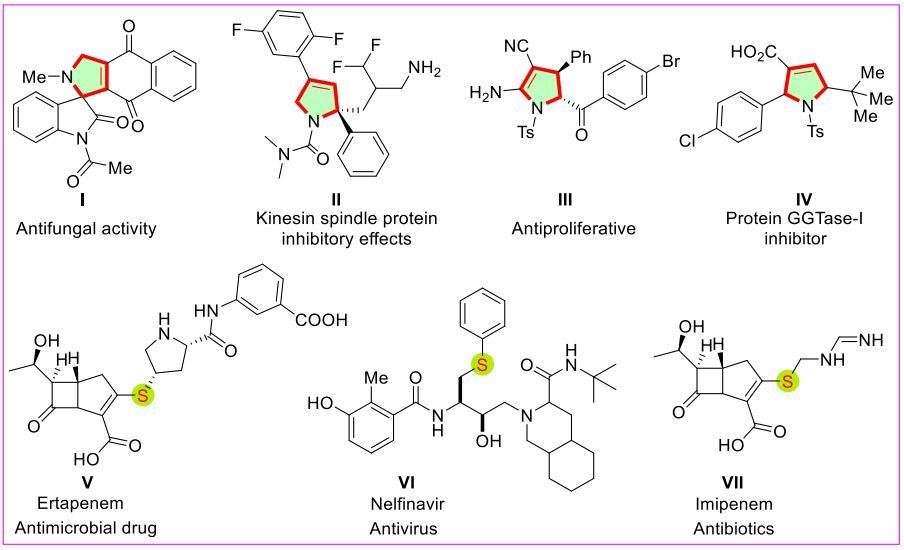

Figure 3.1 Bioactive scaffolds of dihydropyrroles and sulfur containing compounds

Organosulfur compounds are prevalent in many bioactive natural products and pharmaceutical drug molecules.[189,190] For instance, compounds such as thioethers **V-VII** (ertapenem, nelfinavir, and imipenem) exhibit antimicrobial, antiviral, and antibiotic activities, respectively[191,192] (Figure 3.1). The formation of C-S bonds is a potent strategy for generating sulfur-containing compounds such as sulfides, sulfones, and sulfoxides.[193] Traditional methods known for C-S bond formation include nucleophilic substitution reactions between alkyl halides and thiols,[193] transition metal-catalyzed cross-coupling reactions of thiols with aryl halides,[194, 195] and direct sulfenylation of inert C-H bonds using thiols.[196] Among these methods, nucleophilic substitution between thiols and aryl halides is a straightforward approach for the synthesis of organic compounds containing sulfides. The ring-opening reactions of epoxide and aziridine with thiol nucleophiles is a facile method for C-S bond formation.[197-199] However, the ring-opening reaction of 1,4-thiazine and its derivatives is hard and only one report is known in the literature.

In recent years, significant advancements have been made to develop a one-pot cascade and domino processes for the racemic and asymmetric synthesis of ploy-substituted dihydropyrroles.[200-201] Cycloaddition is a highly valuable method to synthesize complex chiral molecules, particularly those with multiple chiral centers.[155] Particularly, the 1,3-dipolar cycloaddition reaction involving azomethine ylide represents a potent method for the synthesis of highly substituted five-membered pyrrolidine heterocycles.[108, 112,] While benzothiazolium azomethine ylides have been recognized for several decades, yet their synthetic applications have received relatively little attention.[164] Only a few reactions have been reported for the synthesis of functionalized pyrroles using thiazolium and benzothiazolium azomethine ylides.[108] Benzothiazolium salt is highly reactive and readily undergoes 1,3-dipolar cycloaddition

reactions with various dipolarophiles. Moreover, they can engage in intramolecular rearrangement reactions in the presence of a base, leading to the formation of diverse heterocyclic compounds.[108, 109, 202]

3.2 LITERATURE BACKGROUND

3.2.1 Synthesis of Dihydropyrroles

In 2005, Shaikh and Zhu groups independently developed an aza-Baylis-Hillman reaction for the synthesis of 2,5-disubstituted dihydropyrroles in good yields with excellent diastereoselectivity *via* phosphine-catalyzed allene-imine [3+2] annulation between substituted allenoates with *N*-sulfonyl imines (Scheme 3.1).[203, 204]

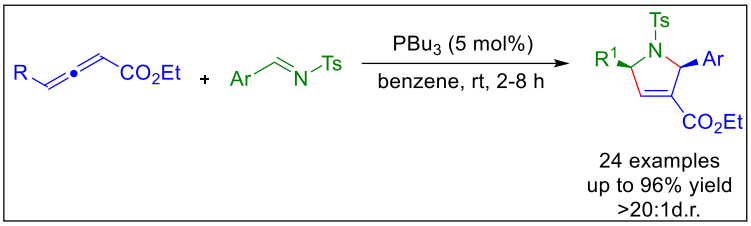

Scheme 3.1 Aza-Baylis-Hillman reaction for the synthesis of 2,5-dihydropyrroles

A novel and efficient method for the regioselective synthesis of dihydropyrroles in moderate to good yields has been described by Li *et al*. in 2011 *via* Lewis acid catalyzed [3+2] cycloaddition of alkyne with azomethine ylides. The azomethine ylides were easily generated from *N*-tosyl aziridines formed by C-C bond heterolysis at room temperature (Scheme 3.2)[205]

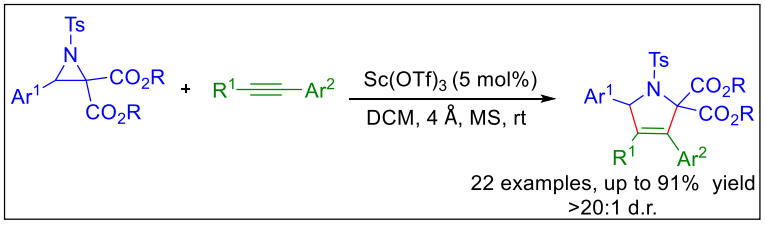

Scheme 3.2 [3+2] cycloaddition for the synthesis of 4,5-dihydropyrroles

In 2012, Ghorai *et al*. accomplished a synthesis of highly functionalized racemic and non-racemic 4,5-dihydropyrroles in an excellent yield and stereoselectivity *via* domino ring opening cyclization (DROC) method of *N*-activated aziridine with malononitrile in the presence of $Sc(OTf)_3$ as a catalyst, and t-BuOK as a base (Scheme 3.3).[206]

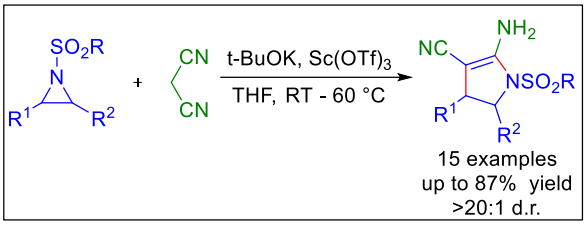

Scheme 3.3 Aziridine ring-opening reaction for the synthesis of 4,5-dihydropyrroles

Since 2013, Miura and co-workers described a stereoselective synthesis of 2,3-dihydropyrrole with excellent yield and diastereoselectivity using *N*-sulfonyl-1,2,3-triazole, alkynes, and α,β-unsaturated aldehydes *via* α-imino rhodium carbene complex generated from alkynes in the presence of rhodium catalyst (Scheme 3.4).

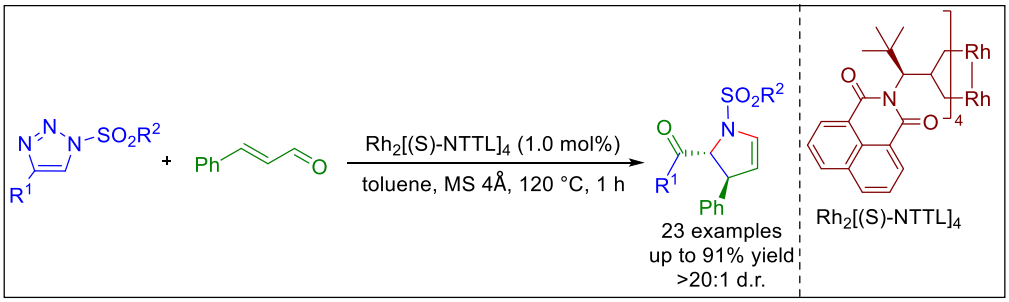

Scheme 3.4 Rhodium catalyzed cyclization reaction for the synthesis of 2,3-dihydropyrroles

The above method was successfully applied to a three-component, one-pot reaction using alkynes, azides, and α,β-unsaturated aldehyde, and CuTC as a co-catalyst. The reaction provided 2,3-dihydropyrroles in good yields and diastereoselectivity (Scheme 3.5).[207]

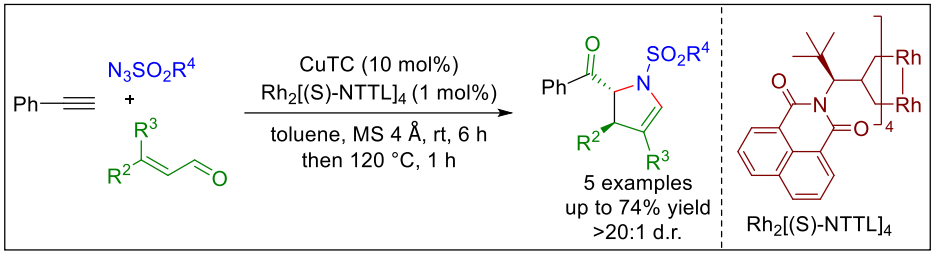

Scheme 3.5 Rhodium catalyzed one-pot cyclization reaction for the synthesis of 2,3-dihydropyrroles

Synthesis of functionalized 4-carboxy and 4-keto-2,3-dihydropyrroles in good to excellent yield under the mild reaction condition was reported in 2014 by Martin *et al. via* $Ni(ClO_4)_2{\cdot}6H_2O$ catalyzed nucleophilic amine ring-opening cyclization of donor-acceptor cyclopropanes (Scheme 3.6).[208]

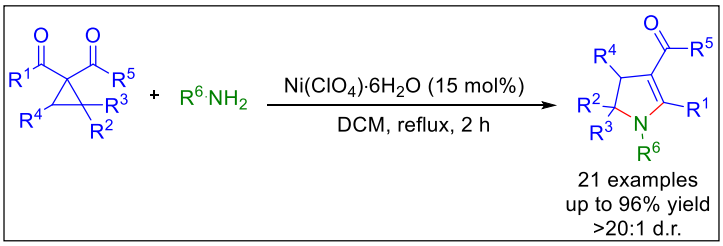

Scheme 3.6 Ring-opening cyclization reaction for the synthesis of 2,3-dihydropyrroles

In 2014, Anaraki-Ardakani *et al.* reported a three-component, one-pot reaction of aryl amides, dialkyl acetylene dicarboxylates, and phenacyl bromides in the presence of PPh_3 and NEt_3. The reaction provided *N*-substituted 2,5-dihydropyrroles in good yields (Scheme 3.7).[209]

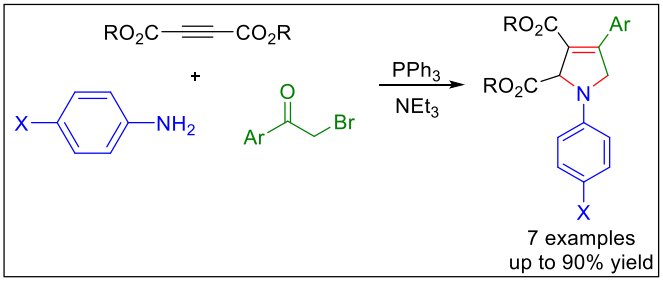

Scheme 3.7 One-pot reaction for the synthesis of 2,5-dihydropyrroles

Li *et al*. in 2015, developed a novel approach for the construction of polysubstituted 2,3-dihydropyrroles in moderate to excellent yields from chalcones and enamine ketones (ester) under mild reaction conditions. The reaction proceeded *via an* iodine-promoted tandem Michael/cyclization sequence (Scheme 3.8).[210]

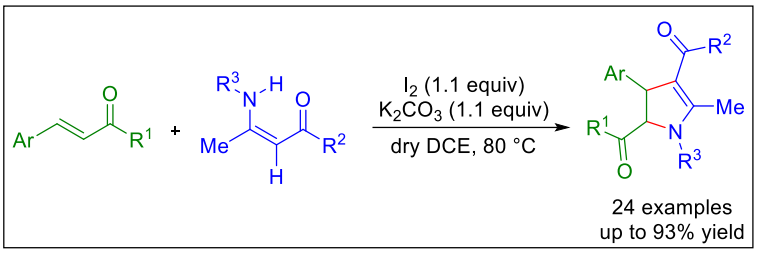

Scheme 3.8 Tandem Michael addition/cyclization reaction for the synthesis of 2,3-dihydropyrroles

In 2015, the phosphine-catalyzed aza-Morita-Baylis-Hillman reaction of vinyl pyridines with protected aromatic imines for the synthesis of 2,3,4-trisubstituted-2,5-dihydropyrroles was reported by Chen *et al*. in good to excellent yields with excellent diastereoselectivity (Scheme 3.9).[211]

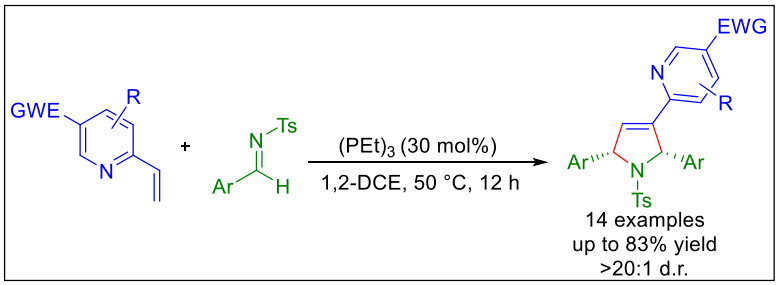

Scheme 3.9 Aza-Morita-Baylis-Hillman reaction for the synthesis of 2,5-dihydropyrroles

In 2015, Xiang and co-workers accomplished a synthesis of 3-carboxy-4,5-dihydropyrroles *via* an intramolecular iminium ion cyclization reaction of readily accessible Baylis-Hillman derivatives with aldehydes. *In-situ* generation of azomethine ylides provided dihydropyrroles in moderate to high yield (Scheme 3.10).[212]

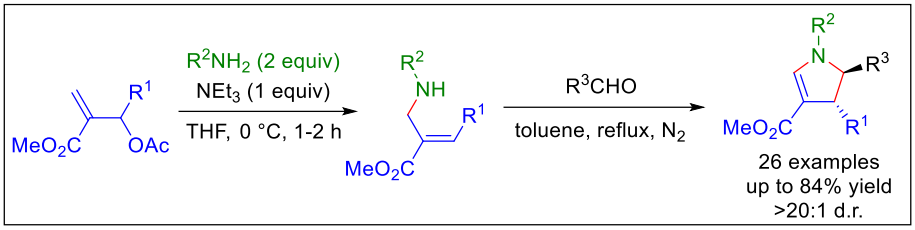

Scheme 3.10 Intramolecular cyclization reaction for the synthesis of 2,3-dihydropyrroles

The synthesis of 2,3-dihydropyrroles in moderate to good yields has been described by Gudmundsson *et al.* in 2018 *via* iron-catalyzed intramolecular nucleophilic cycloisomerization of alleninc sulphonamides. A highly diastereoselective variant of the reaction has also been developed with the use of 1,2-disubstituted allenamides, which affords 2,3-dihydropyrroles with a diastereomeric ratio of > 98:2 (Scheme 3.11).[213]

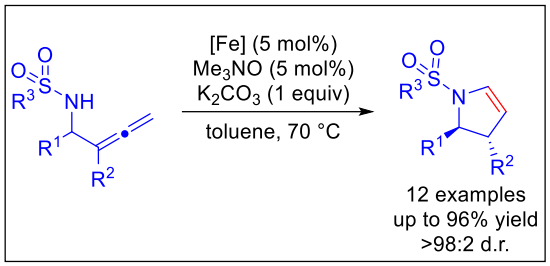

Scheme 3.11 Cycloisomerization reaction for the synthesis of 2,3-dihydropyrroles

Kolos *et al.* in 2019 developed a method for the diastereoselective synthesis of functionalized 4,5-dihydropyrroles through multicomponent reactions of arylglyoxals hydrates, acetylacetone or acetoacetic ester, and aromatic amines in methanol at room temperature (Scheme 3.12).[214]

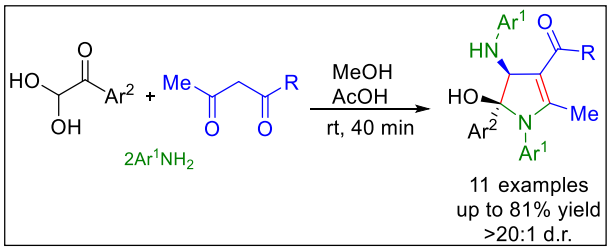

Scheme 3.12 Multicomponent reaction for the synthesis of 4,5-dihydropyrroles

The diastereoselective synthesis of polysubstituted dihydropyrroles in good yield with single diastereomers was reported by Iddmu and co-workers in 2021 *via* three-component reactions of chalcones, benzylamines, and benzaldehydes. This reaction proceeded through 1,3-dipolar cycloaddition between a chalcone and *N*-benzylidene benzylamine (Scheme 3.13).[215]

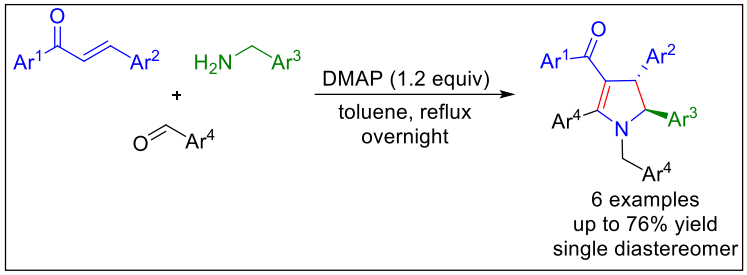

Scheme 3.13 Three-component reaction for the synthesis of 4,5-dihydropyrroles

3.2.2 Enantioselective Synthesis of Dihydropyrroles

In 2006, Yang and co-workers accomplished a synthesis of chiral 2,5-dihydropyrroles in good yields from chiral amino acid-derived *N*-atom substituted terminal alkene and alkynes in the presence of Ru catalyst *via* ring-closing enyne metathesis (RCM) reaction (Scheme 3.14).[216]

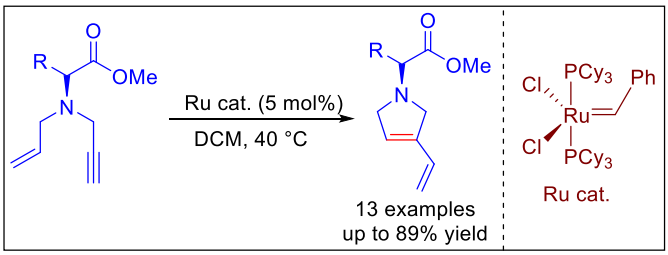

Scheme 3.14 Ring-closing enyne metathesis (RCM) reaction for the synthesis of 2,5-dihydropyrroles

A novel and efficient method for the regioselective synthesis of chiral 2,5-dihydropyrroles in good yields with moderate enantioselectivity (up to 70% ee) was reported in 2011 by Li *et al*. The reaction proceeded *via* Lewis acid-catalyzed [3+2] cycloaddition of alkyne and azomethine ylides with chiral pybox ligand. The

azomethine ylides were easily generated from *N*-tosylaziridines by C-C bond heterolysis at room temperature (Scheme 3.15).[205]

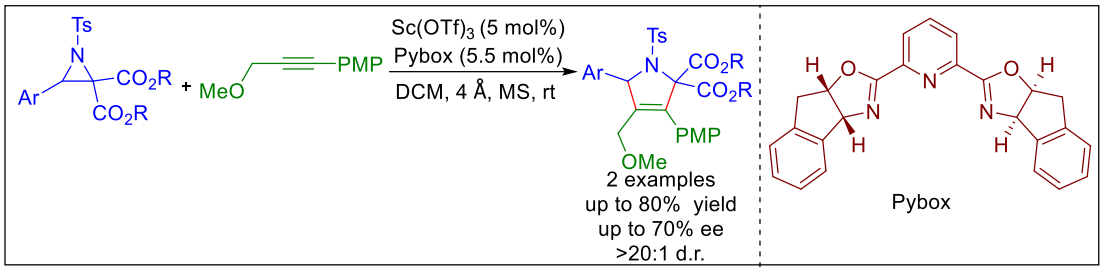

Scheme 3.15 Enantioselective three-component reaction for the synthesis of aryl ketone substituted 2,5-dihydropyrroles

In 2012, The synthesis of highly functionalized chiral 4,5-dihydropyrroles *via* domino ring opening cyclization (DROC) method of chiral *N*-activated aziridine with malononitrile in the presence of $Sc(OTf)_3$ and t-BuOK at room temperature to 60 °C accomplished by Ghorai *et al*. The reaction provided the substituted 4,5-didhydropyrroles in enantiomerically pure form with excellent yields and stereoselectivity (Scheme 3.16).[206]

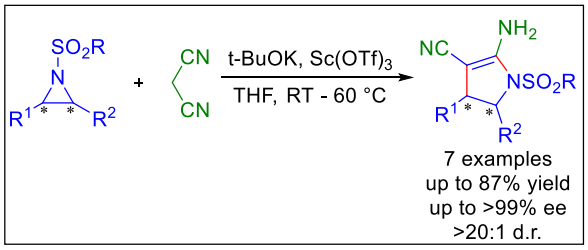

Scheme 3.16 Ring opening cyclization for the synthesis of 5-didhydropyrroles

3.3 OBJECTIVE

From the above-mentioned literature survey, it is understood that numerous azomethine ylides have been utilized for the synthesis of a variety of dihydropyrrole molecules *via* 1,3- dipolar cycloaddition. However, very few reports are known of using benzothiazolium azomethine ylides in the synthesis of poly-substituted pyrrole, pyrrolo-thiazine, and hydropyrrolo-thiazole. But, enantioselective synthesis of poly-

substituted dihydropyrrole using benzothiazolium salt and α,β-unsaturated aldehydes is yet to be developed.

- Inspired by this idea, a new asymmetric one-pot methodology will be developed for the enantioselective synthesis of chiral *N*-phenyl thioether tethered tetrasubstituted dihydropyrrole-3-carbaldehydes.
- The proposed method will use benzothiazolium azomethine ylides, α,β-unsaturated aldehydes as a starting material and a chiral amine as an organocatalyst (Scheme 3.17).

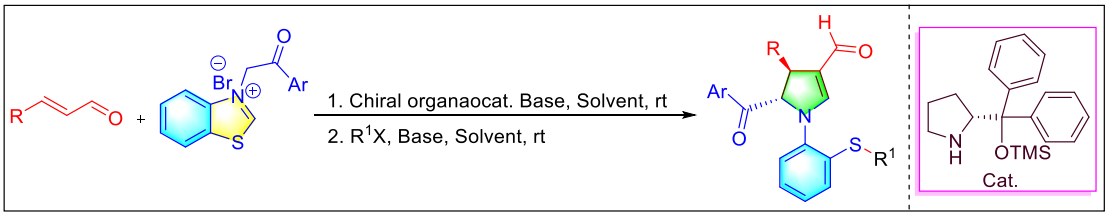

Scheme 3.17 One-pot synthesis of chiral *N*-phenyl thioether-tethered tetrasubstituted dihydropyrrole-3-carbaldehydes

- In this reaction, intermolecular 1,3-dipolar cycloaddition/intramolecular rearrangement will happen, followed by an intermolecular *C-S* bond formation/base-promoted intramolecular ring-opening reaction sequence.
- The method developed will enable the synthesis of novel thioether-tethered chiral dihydropyrrole heterocyclic frameworks using environmentally friendly chiral amines as organocatalysts.

3.4 RESULTS AND DISCUSSION

3.4.1 Optimization Studies

In Chapter 2, the enantioenriched product chiral pyrrolo-thiazine -2-carbaldehyde **3**, which has one quaternary center (hemi thioacetal center), is successfully utilized as a starting material in this Chapter for the synthesis of enantioenriched tetrasubstituted

dihydropyrroles. The cleavage of the C-S bond in 1,4-thiazine ring in **3** is possible by treating it with appropriate electrophile in the presence of a base. In this reaction, the base can easily deprotonate the hemi-thioacetal's -OH proton. To check this hypothesis, the reaction was performed with pyrrolo-thiazine -2-carbaldehyde **3** (1 equiv), K_2CO_3 (2 equiv), and methyl iodide (3 equiv) in DMF (01.5 M) at room temperature. The reaction afforded the expected tetrasubstituted dihydropyrrole carbaldehyde **4o** in 90% yield with 98% ee (Scheme 3.18).

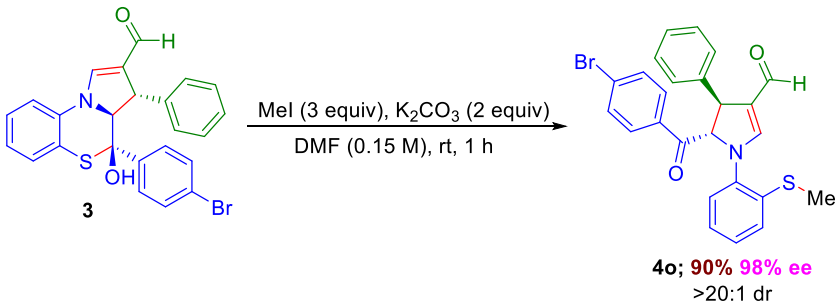

Scheme 3.18 Synthesis of tetrasubstituted dihydropyrrole **4o** from pyrrolo-thiazine -2-carbaldehyde **3**

Considering the importance of chiral dihydropyrroles, to synthesize the tetrasubstituted dihydropyrrole carbaldehydes **4** directly from α,β-unsaturated aldehydes, and benzothiazolium salts adopting a one-pot strategy. Initially, the reaction was started to synthesize the *N*-phenyl thioether-tethered tetrasubstituted dihydropyrrole-3-carbaldehydes **4o** by reacting with α,β-unsaturated aldehyde **1a** (1.0 mmol), benzothiazolium salt **2c** (1.0 equiv), (*L*)-proline **C1** (20 mol%) as an organocatalyst and DMAP (3.0 equiv) as a base in IPA solvent at room temperature. After the reaction was completed by 72 h (monitored by TLC), the solvent evaporated from the reaction mixture, and then benzyl chloride (3 equiv), K_2CO_3 (2 equiv), and DMF added at room temperature. The one-pot reaction provided the expected product **4o** in 78% yield with 24% enantioselectivity and >20:1 d.r. (Table 3.1, entry1).

Table 3.1: Catalyst Screening[a]

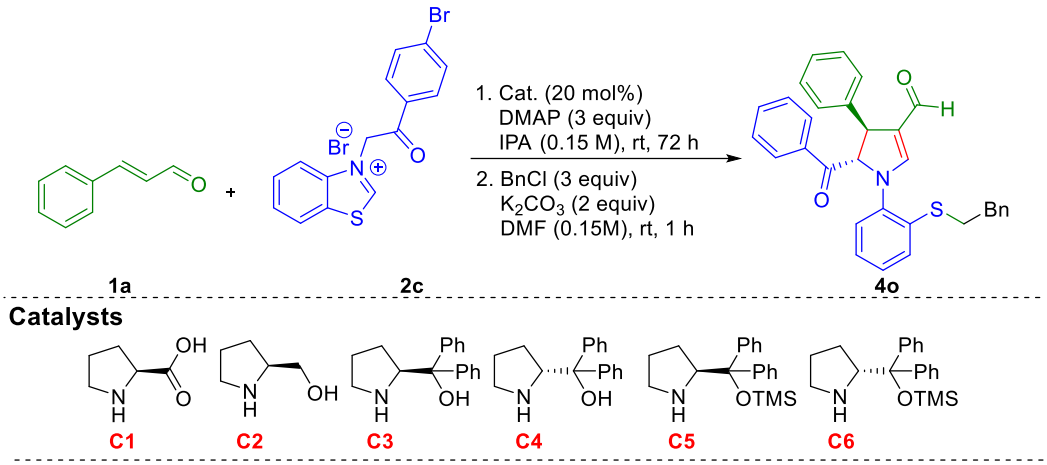

Entry	Catalyst (mol%)	Yield (%) [b]	ee (%) [c]	d.r. [d]
1	**C1** (20 mol%)	78	24	20.1
2	**C2** (20 mol%)	56	10	20.1
3	**C3** (20 mol%)	41	66	20.1
3	**C4** (20 mol%)	50	66	20.1
4	**C5** (20 mol%)	60	85	20.1
5	**C6** (20 mol%)	90	96	20.1

[a]Reaction conditions: Step-1 **1a** (0.3 mmol), **c** (0.3 mmol), DMAP (3 equiv), chiral catalyst **C1-C6** (20 mol%) and solvent (0.15 M) at 72 h. Step-2: BnCl (3 equiv), K_2CO_3 (2 equiv), DMF (0.15 M), [b]Isolated yield. [c]*Ee* was determined by chiralcel AD-H chiral column. [d]D. r. ratio was determined by ^{1}H NMR spectroscopy of the crude reaction mixture.

To improve the enantioselectivity of the one-pot product, the reaction was optimized with various catalysts, bases, and solvents, and the results were summarized in Tables 3.1, 3.2, and 3.3. To improve the enantioselectivity of **4o**, the reaction was screened using several proline-based chiral catalysts (Table 3.1 entries 1-6). The product yield and %ee decreased when the catalyst was changed to **C2** (Table 3.1, entry 2). The reason may be due to the catalyst is less bulky. Upon increasing the bulkiness of

catalysts **C3** and **C4**, the %ee of the product was improved to 66% (Table 3.1, entries 3 and 4). Increasing the bulkiness of the catalyst **C5** further leads to an improvement in %ee to 85% with a 60% yield (Table 3.1, entry 5). The use of *(R)*-diphenylprolinol trimethylsilyl ether catalyst **C6** was the best choice of the catalyst, and it provided 96% ee with a 90% yield of product **4o** (Table 3.1, entry 6). The reaction was further examined with several bases to improve the yield of **4o**.

Table 3.2: Base Screening[a]

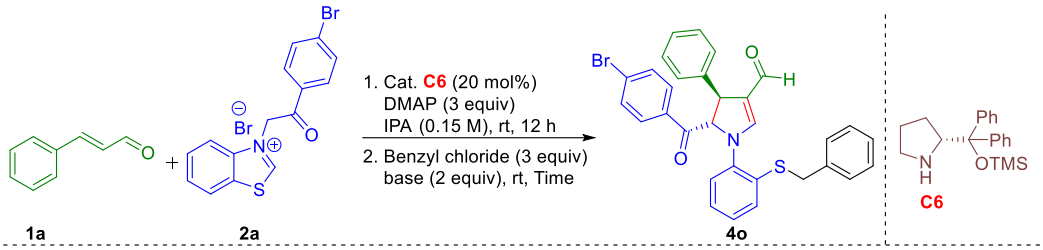

Entry	Base (step-2)	Solvent (M) (step-2)	Time (h)	Yield (%)[b]	ee (%)[c]	d.r.[d]
1	-	IPA	12	30	96	20.1
2	K_2CO_3	DMF	1	60	96	20.1
3	DMAP	DMF	1	24	95	20.1
4	DABCO	DMF	1	10	94	20.1
5	Na_2CO_3	DMF	1	50	96	20.1
6	NEt_3	DMF	1	45	95	20.1
7	NaOAc	DMF	1	30	90	20.1
8	K_3PO_4	DMF	1	52	92	20.1

[a]Reaction conditions: Step-1 **1a** (0.3 mmol), **2c** (0.3 mmol), DMAP (3 equiv), chiral catalyst **C1-C6** (20 mol%) and solvent (0.15 M) at 72 h. Step-2: BnCl (3 equiv), base (2 equiv), DMF (0.15 M), [b]Isolated yield. [c]*Ee* was determined by chiralcel AD-H chiral column. [d]D. r. ratio determined by ^{1}H NMR spectroscopy of crude reaction mixture.

The optimized reaction condition for the first step was taken from previous Chapter 2, and then to optimize step 2, several bases and solvents were screened, and the results were summarized in Tables 3.2 & 3.3. In table 3.2, the reaction was screened with various bases to achieve a better yield of the product **4o** in step-II. The reaction without a base in step II gives only a 30% yield of the product **4o** (Table 3.2, entry 1). When K_2CO_3 is a base, furnished product **4o** has a maximum yield of 60% (Table 3.2, entry 2).

Table 3.3: Solvent Screening[a]

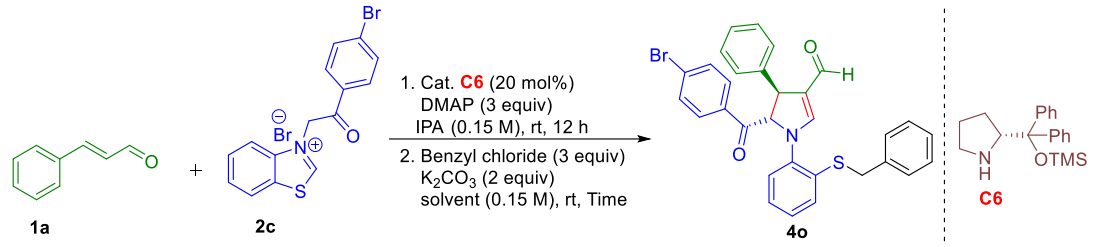

Entry	Base	Solvent (M) (step-2)	Time (h)	Yield (%)[b]	ee (%)[c]	d.r. [d]
1	K_2CO_3	DMF	1	90	96	20.1
2	K_2CO_3	1,4-Dioxane	1	52	96	20.1
3	K_2CO_3	Toluene	1	35	96	20.1
4	K_2CO_3	HFIP	1	20	96	20.1
5	K_2CO_3	DCM	1	30	96	20.1
6	K_2CO_3	IPA	1	20	96	20.1
7	K_2CO_3	EtOH	1	30	96	20.1

[a]Reaction conditions: Step-1 **1a** (0.3 mmol), **2c** (0.3 mmol), DMAP (3 equiv), chiral catalyst **C6** (20 mol%) and solvent (0.15 M) at 72 h. Step-2: BnCl (3 equiv), K_2CO_3 (2 equiv), solvent (0.15 M), [b]Isolated yield. [c]*Ee* was determined by chiralcel AD-H chiral column. [d]D. r. ratio determined by ^{1}H NMR spectroscopy of crude reaction mixture.

By screening various solvents to achieve a better yield, DMF was found to furnish the one-pot reaction in a 90% yield of **4o** with 96% ee and >20:1 d.r. (Table 3.3, entry 1). The absolute configuration of **4q** (4*S*,5*S*) was unambiguously confirmed by single-

crystal X-ray diffraction analysis using the flack parameter (Figure 3.2; Flack parameter value: -0.02(3).

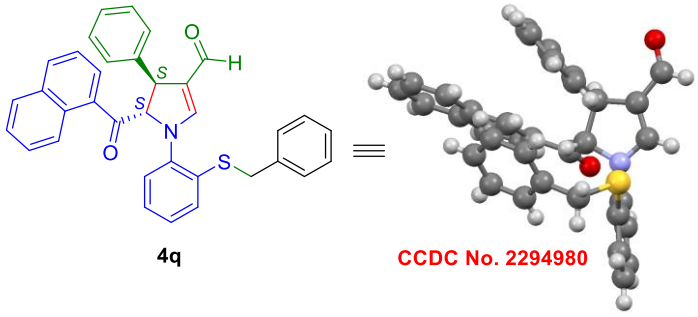

Figure 3.2 X-ray structure of compound **4q** chiral (CCDC: 2294980) with 50% probability ellipsoids

3.5 SUBSTRATE SCOPES

With the optimized reaction condition in hand, the functional group tolerance of the one-pot reaction was investigated with various primary and secondary alkyl halides to furnish the desired products **4a-4l** in good yields with high enantioselectivities (Scheme 3.19). The aliphatic alkyl halides such as methyl, ethyl, isopropyl, allyl, propargyl**,** acetonitrile, and acetate-containing alkyl halides **4a-4g** provided the desired products in good yields with high enantio- and diastereoselectivity (80-96% ee). The aryl group containing various functional groups such as electron-donating group, electron-withdrawing group, and bulky substitutions **4h-4l** also furnished the chiral products in good yield with high enantio-and diastereoselectivity (84-96% ee), as shown in Scheme 3.19.

Scheme 3.19 Substrate scope of alkyl and aryl halides[a,b]

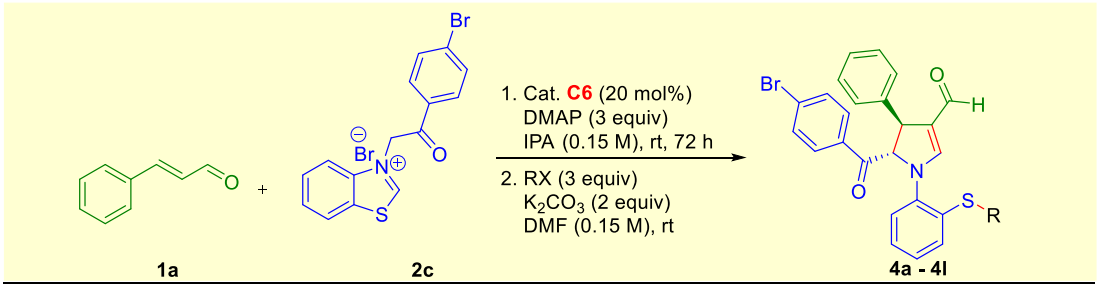

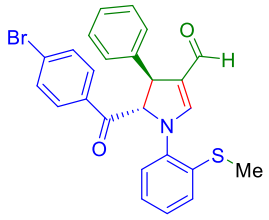

4a; 80%, 96% ee
>20:1 d.r.
72 h + 30 min

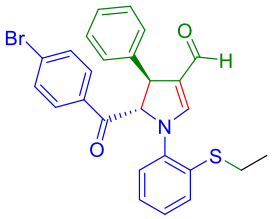

4b; 86%, 88% ee
>20:1 d.r.
72 h + 30 min

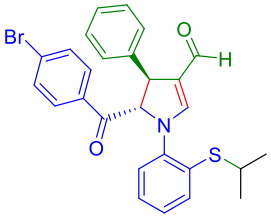

4c; 80%, 86% ee
>20:1 d.r.
72 h + 30 min

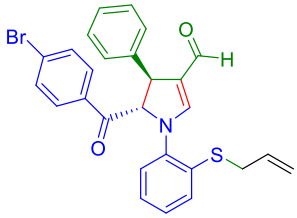

4d; 88%, 80% ee
>20:1 d.r.
72 h + 1 h

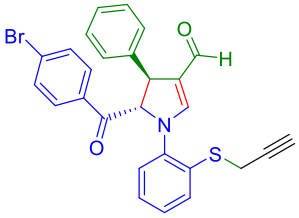

4e; 80%, 82% ee
>20:1 d.r.
72 h + 1 h

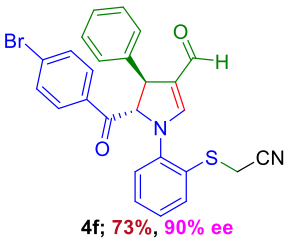

4f; 73%, 90% ee
>20:1 d.r.
72 h +1 h

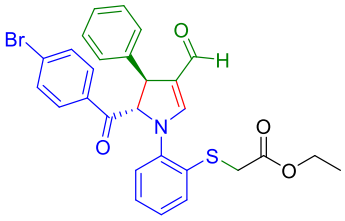

4g; 73%, 98% ee
>20:1 d.r.
72 h + `10 min

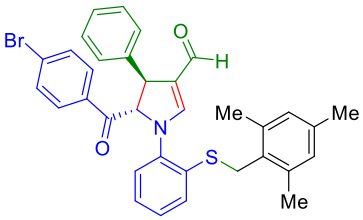

4h; 63%, 88% ee
>20:1 d.r.
72 h + 30 min

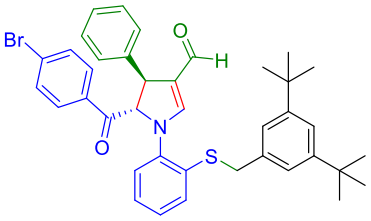

4i; 50%, 84% ee
>20:1 d.r.
72 h + 1.3 h

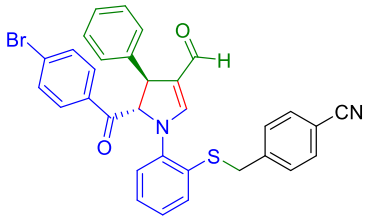

4j; 66%, 96% ee
>20:1 d.r.
72 h +1 h

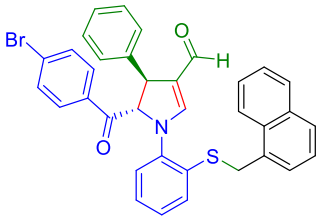

4k; 72%, 96% ee
>20:1 d.r.
72 h + 1 h

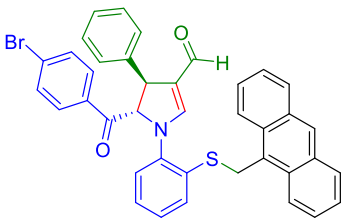

4l; 85%, 90% ee
>20:1 d.r.
72 h + 1 h

[a]Reaction condition: Step-1:**1a** (0.3 mmol), **2c** (0.3 mmol), chiral catalyst **C6** (20 mol %), DMAP (2 equiv) in IPA (0.15 M) at room temperature for 72 h. Step -2: **RX** (3 equiv), K_2CO_3 (2 equiv), and DMF (0.15 M) were added at room temperature. [b]Isolated yield. The absolute configuration of the product **4q** was determined to be

(4*S*,5*S*) by single-crystal XRD analysis. The absolute configurations of other products were assigned to be (4*S*,5*S*) based on same analogy.

Scheme 3.20 The substrate scope of the benzothiazolium salts[a,b]

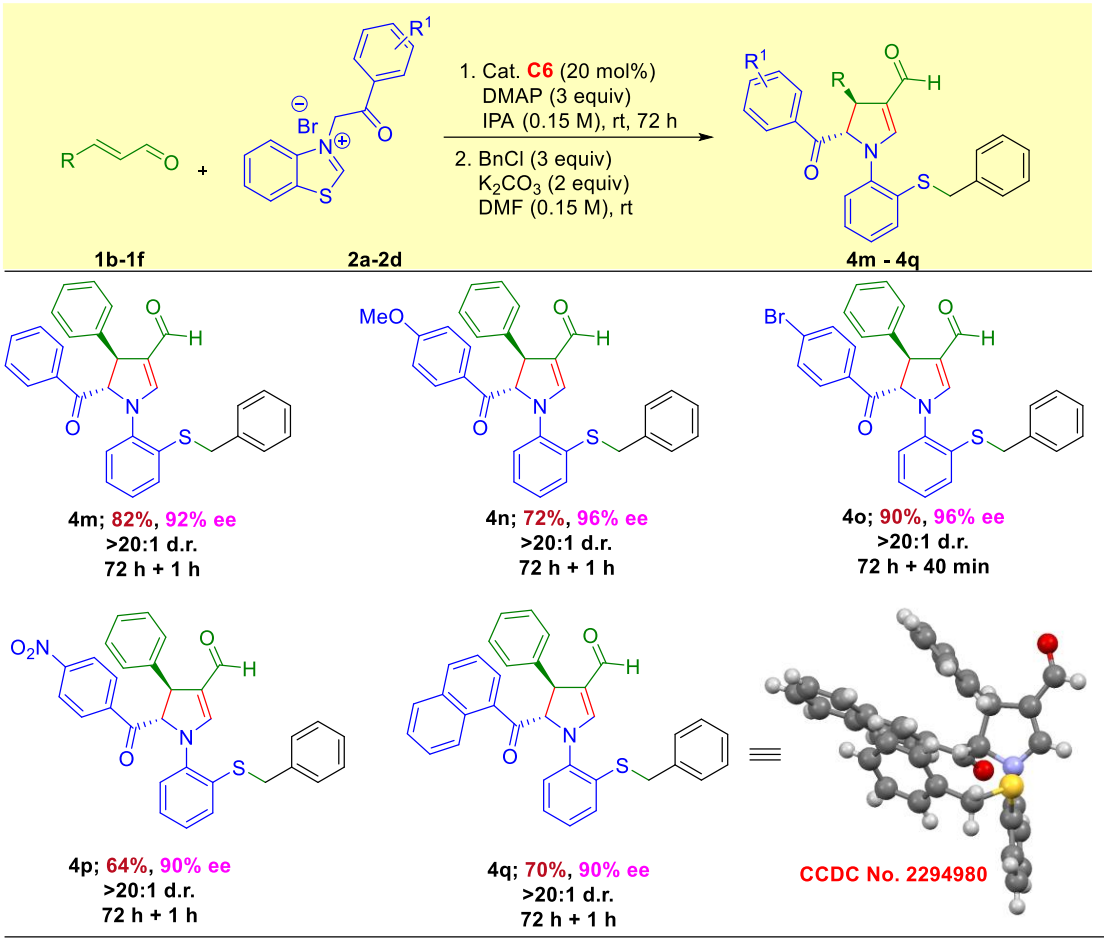

[a]Reaction condition: Step-1; **1a-1f** (0.3 mmol), **2a-2e** (0.3 mmol), chiral catalyst **C6** (20 mol %) and DMAP (3 equiv) in IPA (0.15 M) at rt for 72 h. Step -2: **BnCl** (3 equiv), K_2CO_3 (2 equiv), and DMF (0.15 M) are added at room temperature. [b]Isolated yield. The absolute configuration of the product **4q** was determined to be (4*S*,5*S*) by single-crystal XRD analysis. The absolute configurations of other products were assigned to be (4*S*,5*S*) based on same analogy.

To investigate the generality of benzothiazolium salts **2** in the one-pot reaction, various electron-donating, electron-withdrawing halogens and bulky substitutions bearing benzothiazolium salts were screened. All the reactions furnished the corresponding tetrasubstituted dihydropyrroles (**4m-4q**) in good yield with high enantio- and diastereoselectivity (Scheme 3.20).

Scheme 3. 21 The substrate scope for α,β-unsaturated aldehydes[a,b]

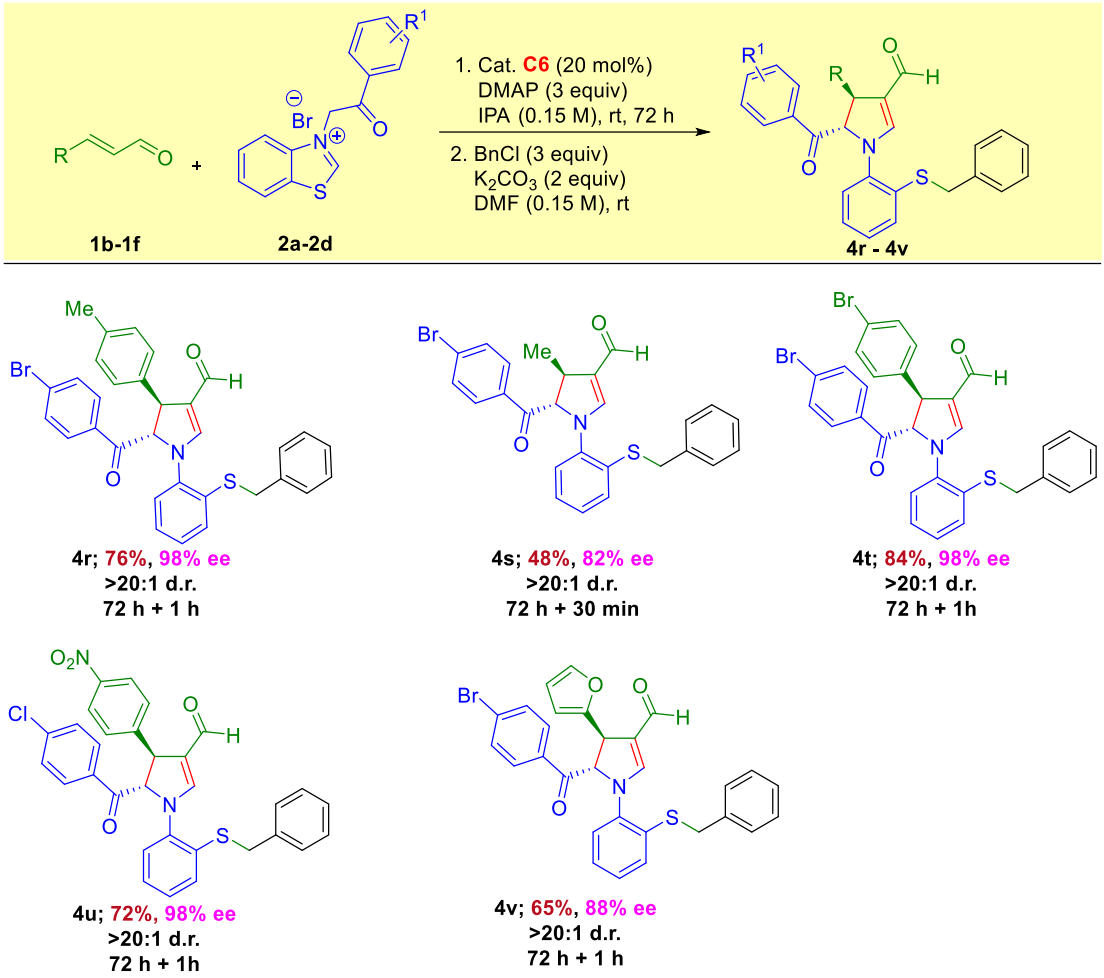

[a]Reaction condition: Step-1; **1a-1f** (0.3 mmol), **2a-2e** (0.3 mmol), chiral catalyst **C6** (20 mol %) and DMAP (3 equiv) in IPA (0.15 M) at rt for 72 h. Step -2: **BnCl** (3 equiv), K_2CO_3 (2 equiv), and DMF (0.15 M) were added at room temperature. [b]Isolated yield. The absolute configuration of the product **4q** was determined to be (4*S,5S)* by single-crystal XRD analysis. The absolute configurations of other products were assigned to be (4*S,5S)* based on same analogy.

Substrates bearing electron-donating groups at the *para* position exhibited good reactivity and enantioselectivity (**4m-4n**; 96-98% ee). The halogen substitution at the *para* position provided the desired product **4o** in 90% yield with good enantioselectivity (96% ee) in Scheme 3.22. An electron-withdrawing NO_2 group at the *para* position **4p** delivered a 64% yield with 90% enantioselectivity. The bulky

substitution naphthyl was well tolerated to obtain the desired products **4q** in 70% yield with 90% ee (Scheme 3.20).

To demonstrate the functional group tolerance of α,β-unsaturated aldehydes **1**, the reaction was carried out as a one-pot reaction using α,β-unsaturated aldehydes containing electron-donating, electron-withdrawing, heterocyclic, and alkyl substituted groups (**4r–4v**). All the reactions furnished the desired products in good yields with high enantio-and diastereoselectivity (Scheme 3.21). The cinnamaldehyde-bearing electron-donating group at the *para*-position delivered the desired product **4r** in good yield with 98% ee. Alkyl substitution at the 3-position of α,β-unsaturated aldehydes afforded the product **4s** in moderate yield with 82% ee. Notably, halogen substitution at the *para*-position of cinnamaldehyde provided product **4t** up to 98% ee. An electron-withdrawing group at the *para* position furnished the desired product **4u** in good yield and 98% ee. The reaction was also suitable for substitution at the 3-position of the α,β-unsaturated aldehyde, for instance, furan afforded **4v** in 65% yield with 88% ee.

3.6 GRAM SCALE SYNTHESIS

To check the scalability one-pot methodology, a gram-scale reaction was performed using cinnamaldehyde **1** (3 mmol, 396 mg, 374 μL), benzothiazolium salt **2c** (3 mmol, 1.24 g), DMAP (9 mmol, 1.1 g), benzyl chloride (6 mmol, 760 mg, 690 μL) and K_2CO_3 (6 mmol, 828 mg) under the optimized reaction conditions. The reaction furnished the desired chiral product **4o** in 75% yield (1.2 g) without loss of enantio- and diastereoselectivity (Scheme 3.22).

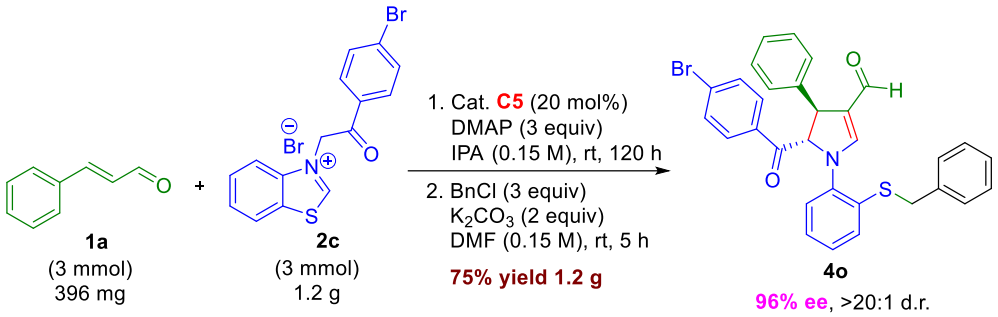

Scheme 3. 22 Gram scale synthesis of **4o**

3.7 SYNTHETIC TRANSFORMATIONS

Different functional group transformations were performed to showcase the synthetic transformations of **4o** (Scheme 3. 23). First, Suzuki coupling reaction of **4o** with $PhB(OH)_2$ in the presence of $Pd(PPh_3)_4$ and K_2CO_3 in THF, and the reaction afforded the corresponding biphenyl-substituted pyrrolo-thiazine-3-carbaldehydes **5a** in 90% yield (Scheme 3.23). When treating **4o** with DDQ, the oxidation reaction provided the aromatized tetrasubstituted pyrrole product **5b** in 90% yield (Scheme 3.23).

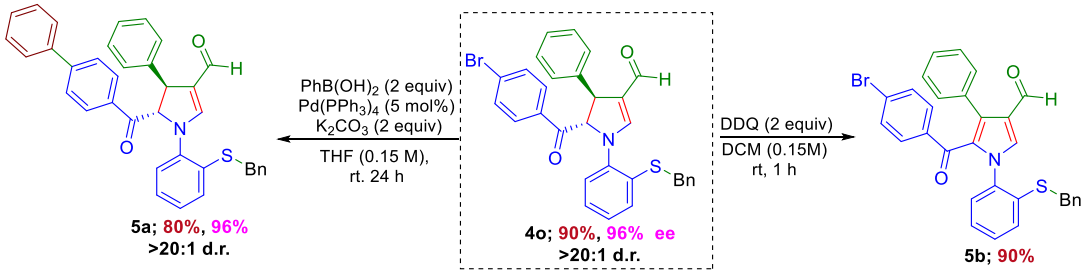

Scheme 3.23 Synthetic transformations of the **4o**

3.8 PLAUSIBLE REACTION MECHANISM

Based on related literature reports[15] and from previous studies,[16] a plausible reaction mechanism is proposed as shown in Scheme 3.24. Initially, the benzothiazolium salt **2c** will react with DMAP to yield azomethine ylide **II/III**. Subsequently, α,β-unsaturated aldehyde **1a** in the presence of chiral catalyst **C6** will provide iminium ion intermediate **I**. The intermediate **I** will react with **III** to form pyrrolo[1,4]thiazine-2-carbaldehyde

intermediate **X** *via* 1,3-dipolar cycloaddition/rearrangement reaction. This intermediate **X** might react with BnCl to form *S*-benzylated intermediate **XI** *via* S_N2 reaction.

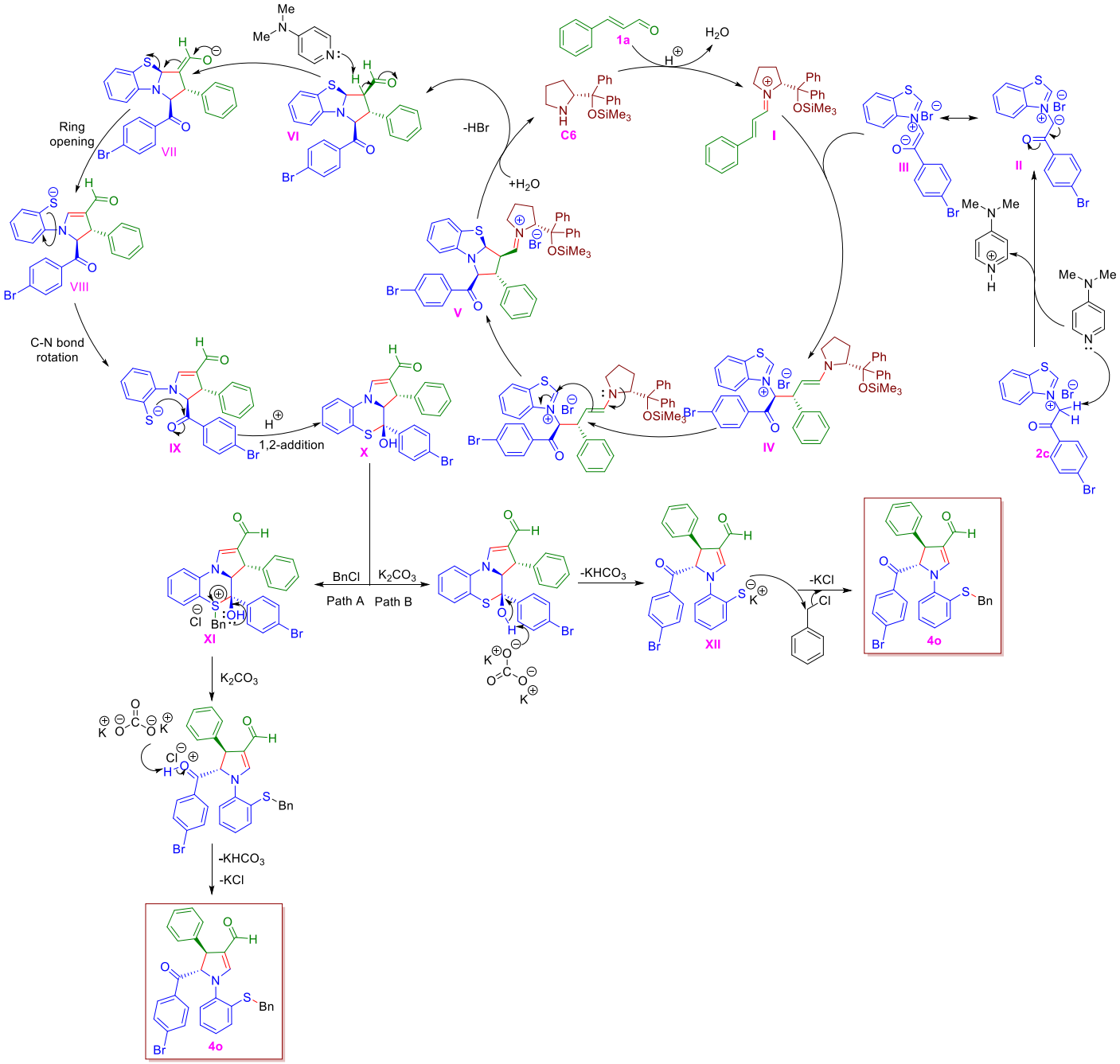

Scheme 3.24 Plausible mechanism for the formation of tetrasubstituted dihydropyrrole-3-carbaldehyde

Then, in the intermediate **XI**, the *C-S* bond cleavage will take place in the presence of the base to yield the desired product **4o** along with $KHCO_3$ and KCl (Path A).

Alternatively, the base K_2CO_3 might deprotonate the hydroxy proton of intermediate **X**, followed by *C*-*S* bond cleavage to form thiolate anion intermediate **XII**. The thiolate anion intermediate **XII** will react with benzyl chloride by a S_N2 reaction to provide the desired product **4o** (Path B).

3.9 CONCLUSION

- An efficient one-pot method for organocatalytic asymmetric synthesis of tetrasubstituted dihydropyrrole-3-carbaldehydes was developed.
- This asymmetric transformation proceeded *via* intermolecular 1,3-dipolar cycloaddition/intramolecular rearrangement followed by an intermolecular C-S bond formation/base-promoted intramolecular ring-opening reaction provided *N*-phenyl thioether-tethered tetrasubstituted chiral dihydropyrrole-3-carbaldehydes with high enantio- and diastereoselectivity.
- The novel method worked well for various functional groups, notably in aliphatic α,β-unsaturated aldehydes.
- The method reported herein is the first report for the synthesis of enantioenriched tetrasubstituted chiral dihydropyrrole-3-carbaldehyde derivatives using benzothiazolium salts reaction with α,β-unsaturated aldehydes *via* one-pot methodology.

3.10 EXPERIMENTAL SECTION

3.10.1 General Information

All reactions were carried out in oven-dried reaction tubes. Benzothiazole, phenacyl bromides, and cinnamaldehydes were purchased from Sigma-Aldrich, Spectrochem,

BLD, Carbanio, and Avra Synthesis Pvt. Ltd. The proline and DMAP were purchased from Spectrochem, Avra Synthesis Pvt. Ltd. and used directly as received. All the starting materials were synthesized according to the reported procedures. Reactions were monitored by thin-layer chromatography (TLC) using Merck silica gel 60 F_{254} precoated plates (0.25 mm) and visualized by UV fluorescence quenching using an appropriate mixture of ethyl acetate and hexanes as eluting solvent mixtures. Silica gel for column chromatography (particle size 100-200 mesh) was purchased from Avra Synthesis Pvt. Ltd. and used for column chromatography using hexanes and ethyl acetate mixture as eluent. Organic solutions were concentrated under reduced pressure on a Büchi, Heidolph rotary evaporator using a water bath. ^{1}H and ^{13}C NMR spectra were recorded on a Bruker 400 or 500 MHz instrument.^{1}H NMR is reported relative to residual $CDCl_3$ (δ 7.26 ppm) or DMSO-d_6 (δ 2.50 ppm). ^{13}C NMR is reported close to residual $CDCl_3$ (δ 77.16 ppm) or DMSO-d_6 (δ 39.52 ppm). Chemical shifts were recorded in parts per million (ppm). Multiplicities are as indicated: s (singlet,) d (doublet,) t (triplet,) q (quartet,) quint (quintet), sext (sextet), sept (septet) dd (doublet of doublet,) m (multiplet,) tt (triplet of triplet,) td (triplet of doublet). The coupling constant, *J*, is reported in Hertz.

Melting points were recorded on a Guna capillary melting point apparatus and were corrected with benzoic acid as a reference. FTIR spectra were recorded on a JASCO spectrometer and were reported in the frequency of absorption (cm^{-1}) using a dry KBr pellet. The polarimetry was recorded in P-2000 High Accuracy Digital Polarimeter - Jasco Inc. High-resolution mass spectra (HRMS) were recorded on Q-Tof Micro mass spectrometer. All the single crystal X-ray data was collected with a Bruker AXS (Kappa Apex 2) CCD diffractometer equipped with graphite monochromatic Mo (Kα) (λ = 0.7107 A) radiation source. The data were collected with 100% completeness for Θ up

to 25º. ω and ϕ scans were employed to collect the data. The frame width for ω for was fixed to 0.5º for data collection. The crystal was solved by direct methods using Bruker SHELXS (Sheldrick, 1997). The Structure was refined using the Bruker SHELXTL (Version 6.12) software package. HPLC spectra were recorded on a Waters Alliance 2695 HPLC and Shimadzu SIL-20ACHT systems using the CHIRALCEL OD-H, AD-H, and CHIRALPACK-AI columns.

3.10.2 Typical procedure for the one-pot synthesis of racemic tetrasubstituted dihydropyrrole-3-carbaldehyde

General procedure A: To a 20 mL oven-dried reaction tube with a magnetic stir bar under an open atmosphere piperidine (20 mg, 0.06 mmol), cinnamaldehyde (**1a**) (38 µL, 0.3 mmol) were dissolved in (0.075 M) EtOH and closed with glass-stopper stirring for 1 hour at room temperature. 4-Bromo phenyl thiazolium salt (**2c**) (126 mg, 0.3 mmol) and Dibutyl amine (150 µL, 0.9 mmol) and 0.075 M) EtOH were successively added to the reaction mixture. Reaction progress monitored by TLC. After completely consuming both starting materials, the EtOH was evaporated from the reaction mixture by a rotary evaporator. After evaporation of the solvent, the reaction mixture dissolved with DMF (0.15 M) followed by adding K_2CO_3 (2 equiv), the reaction mixture was stirred for 10 minutes at room temperature. After the benzyl chloride (105 µL, 3 equiv) was added to the stirred reaction mixture, the reaction was monitored by TLC. After complete consumption of the starting material reaction mixture was poured into ice-cold water extracted with EtOAc (3 x15 mL), brine wash (1×10 mL) was given to the combined organic extractions and dried over anhydrous Na_2SO_4, evaporation of the organic layer to get the crude product. This crude product was purified by column

chromatography on silica gel (eluent: Hexane/Ethyl acetate = 70/30) to get the desired chiral product **4o** as 90% yield, with >20:1 diastereoselectivity (Scheme 3.25).

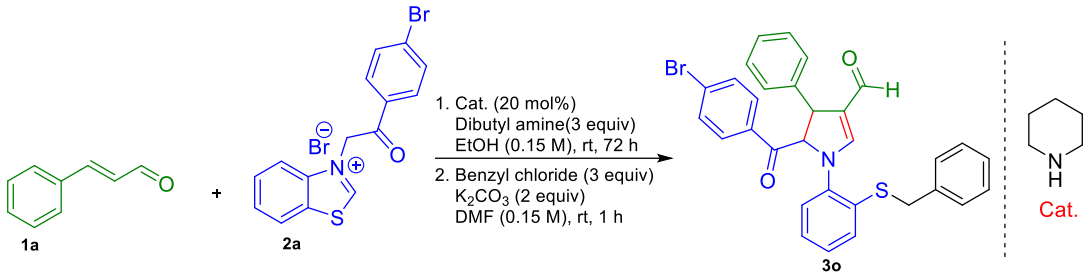

Scheme 3.25 Preparation of racemic compound of tetrasubstituted dihydropyrrole-3-carbaldehyde

3.10.3 Typical procedure for the one-pot synthesis of chiral tetrasubstituted dihydropyrrole-3-carbaldehyde

General procedure B: To a 20 mL oven-dried reaction tube with a magnetic stir bar under open atmosphere (*R*)-diphenylprolinol trimethylsilyl ether (20 mg, 0.06 mmol), cinnamaldehyde (**1a**) (38 µL, 0.3 mmol) were dissolved in (0.075 M) IPA and closed with glass-stopper stirring for 1 hour at room temperature. 4-Bromo phenyl thiazolium salt (**2c**) (126 mg, 0.3 mmol), DMAP (110 mg, 0.9 mmol), and (0.075 M) IPA were successively added to the reaction mixture. Reaction progress monitored by TLC. After completely consuming both starting materials, the IPA was evaporated from the reaction mixture by a rotary evaporator.

After evaporation of the solvent, the reaction mixture dissolved with DMF (0.15 M) followed by adding K_2CO_3 (2 equiv), the reaction mixture was stirred for 10 minutes at room temperature. After the benzyl chloride (105 µ*L*, 3 equiv) was added to the stirred reaction mixture, the reaction was monitored by TLC. After complete consumption of the starting material reaction mixture was poured into ice-cold water extracted with EtOAc (3 x15 mL), brine wash (1×10 mL) was given to the combined organic

extractions and dried over anhydrous Na_2SO_4, evaporation of organic layer to get crude product. This crude product was purified by column chromatography on silica gel (eluent: Hexane/Ethyl acetate = 70/30) to get the desired chiral product **4o** as 90% yield, 96% ee with >20:1 diastereoselectivity (3.26).

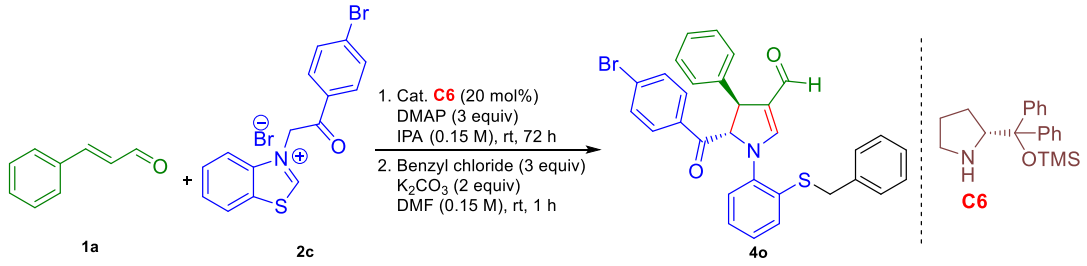

Scheme 3.26 Preparation of chiral compound of tetrasubstituted dihydropyrroles-3-carbaldehyde

3.10.4. Typical procedure for gram-scale synthesis

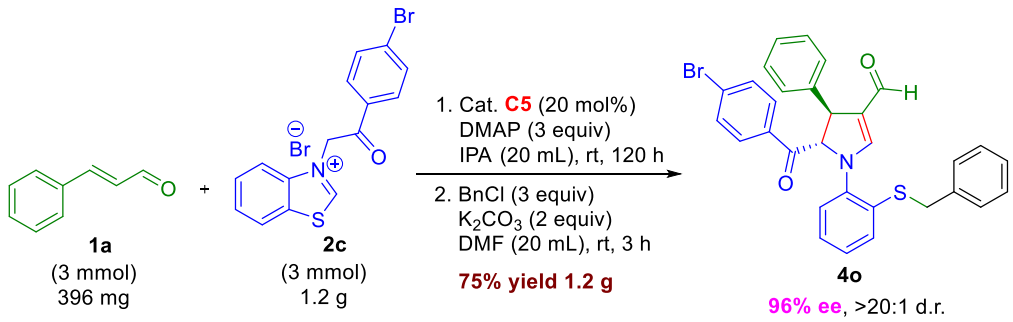

Scheme 3.27 Gram scale synthesis of chiral tetrasubstituted dihydropyrrole-3-carbaldehyde **4o**

General procedure C: To a 20 mL oven-dried reaction tube with a magnetic stir bar under open atmosphere (*R*)-diphenylprolinol trimethylsilyl ether (195 mg, 0.6 mmol), cinnamaldehyde **1a** (396 mg, 374 µL, 3 mmol) were dissolved in (0.075 M) IPA and closed with glass-stopper stirring for 1 hour at room temperature. 4-Bromo phenyl thiazolium salt **2c** (1.2 g, 3 mmol), DMAP (1.1 g, 9 mmol), and (0.075 M) IPA were successively added to the reaction mixture. Completion of the reaction was confirmed by TLC at 120 h. After the complete formation of the product, the IPA was evaporated

from the reaction mixture by a rotary evaporator. After evaporation of the solvent, the reaction mixture dissolved with DMF (0.15 M) followed by adding K_2CO_3 (2 equiv), the reaction mixture was stirred for 10 minutes at room temperature. After the benzyl chloride (1.0 mL, 9 mmol, 3 equiv) was added to the stirred reaction mixture, the reaction was monitored by TLC after complete consumption of starting material reaction mixture poured into ice cold water extracted with EtOAc (3 x15 mL), brine wash (1×10 mL) was given to the combined organic extractions and dried over anhydrous Na_2SO_4, evaporation of organic layer to get crude product. This crude product was purified by column chromatography on silica gel (eluent: Hexane/Ethyl acetate = 70/30) to get the desired chiral product **4o** as 90% yield, 96% ee with >20:1 diastereoselectivity in Scheme 3.27.

3.10.5. Typical procedure for synthetic utility of chiral products

Different functional group transformations were performed to showcase the synthetic transformation of **4o**. First, **4o** was reacted under Suzuki coupling reaction conditions, $PhB(OH)_2$ in the presence of $Pd(PPh_3)_4$ and K_2CO_3 in THF, and the reaction provided the corresponding biphenyl-substituted pyrrolo-thiazine-3-carbaldehydes **5a** 90% yield with 96% ee in Scheme 3.31. When chiral product **4o** was treated with DDQ, the oxidation reaction provided the aromatized tetrasubstituted pyrrole product **5b** with a 90% yield in Scheme 3.28.

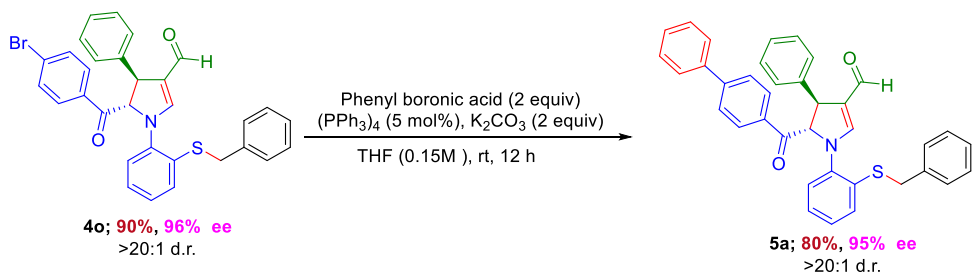

Scheme 3.28 Suzuki coupling reaction for chiral product **4o** to synthesis of **5b**

1. General procedure D: To a 20 mL oven-dried reaction tube with a magnetic stir bar under an open atmosphere, add chiral product **4o** (110 mg, 0.2 mmol), Phenyl boronic acid (2 equiv), $Pd(PPh_3)_4$ (5 mol%), K_2CO_3 (2 equiv), and THF (0.15 M). This reaction was stirred at 80 °C, and the reaction progress was monitored by TLC. After complete consumption of the starting material, the reaction mixture was cooled to room temperature, and the reaction mixture evaporation of THF to get the crude product. This crude product was extracted with DCM (3 x15mL), brine wash (1×10 mL) was given to the combined organic extractions and dried over anhydrous Na_2SO_4, evaporation of the organic layer to get the crude product. This crude product was purified by column chromatography on silica gel (eluent: Hexane/Ethyl acetate = 80/20) to get the desired chiral product **5a** as 80% yield, 96% ee with >20:1 diastereoselectivity in Scheme 3.29.

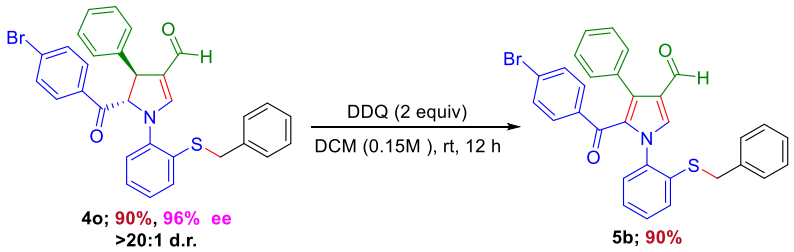

Scheme 3.29 DDQ oxidation reaction for chiral product **4o** to synthesis of **5b**

2. General procedure E: To a 20 mL oven-dried reaction tube with a magnetic stir bar under an open atmosphere chiral product **4o** (96 mg, 0.2 mmol) was dissolved in (0.15M) DCM stirred at room temperature. After 5 minutes, DDQ (0.4mmol) was added to the stirred reaction mixture, this reaction was allowed to stir at the same temperature where the reaction progress was monitored by TLC. After complete consumption of the starting material reaction mixture extracted with DCM (3 x15mL), brine wash (1×10 mL) was given to the combined organic extractions and dried over anhydrous Na_2SO_4, evaporation of organic layer to get the crude product. This crude

product was purified by column chromatography on silica gel (eluent: Hexane/Ethyl acetate = 80/20) to get the desired racemic product **5b** as 90% yield in Scheme 3.31.

3.11. THE ANALYTICAL AND SPECTRAL CHARACTERIZATION DATA'S

4*S*,5*S*)-5-(4-Bromobenzoyl)-1-(2-(methylthio)phenyl)-4-phenyl-4,5-dihydro-1*H*-pyrrole-3-carbaldehyde 4a; Prepared according to general procedure B using (*R*)-diphenylprolinol trimethylsilyl ether **C6**, purification of crude product by column chromatography using (HX/EA) mixture (70:30) to afford the title compound as pale yellow viscous liquid, (80% yield, 115 mg); R_f = 0.36 (30 % ethyl acetate in hexane); d.r. = >20:1(determined by ^{1}H NMR using crude reaction mixture); **^{1}H NMR (400 MHz, CDCl$_3$)** δ 9.41 (s, 1H), 7.67 – 7.62 (m, 3H), 7.59 – 7.52 (m, 2H), 7.51 – 7.45 (m, 1H), 7.45 – 7.35 (m, 4H), 7.35 – 7.29 (m, 1H), 7.25 – 7.16 (m, 3H), 6.15 (d, *J* = 3.6 Hz, 1H), 4.35 (d, *J* = 4.0 Hz, 1H), 2.45 (d, *J* = 1.6 Hz, 3H); **^{13}C NMR (101 MHz, CDCl$_3$)** δ 192.3, 182.7, 156.5, 141.6, 138.2, 134.4, 132.4, 132.3, 130.6, 129.6, 129.1, 127.9, 127.8, 127.5, 126.9, 126.1, 75.4, 50.5, 15.9; **FTIR (neat)** 3058, 3026, 2928, 1672, 1602, 1456, 746 cm^{-1}; **HRMS (ESI)** calculated for $C_{25}H_{20}BrNO_2S$ $[M+H]^+$: 480.0451; found: 480.0433. **HPLC** condition: HPLC Chiralcel AD-H, hexane/i-PrOH = 60:40 v/v, flow rate = 1.0 mL/min, λ = 300 nm, 25 °C, t_R (major) = 13.00, t_R (minor) = 7.41 min, 96% *ee*, $[\alpha]_D^{20}$ = +65.98 (c 0.1, CH_2Cl_2).

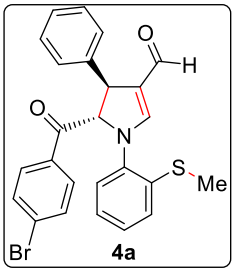

(4*S*,5*S*)-5-(4-Bromobenzoyl)-1-(2-(ethylthio)phenyl)-4-phenyl-4,5-dihydro-1*H*-pyrrole-3-carbaldehyde 4b; Prepared according to general procedure B using (*R*)-diphenylprolinol trimethylsilyl ether **C6**, purification of crude product by column chromatography using (HX/EA) mixture (70:30) to afford the title compound as orange

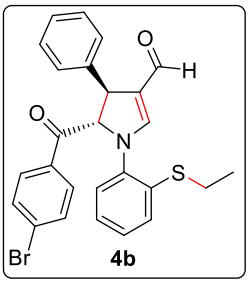

viscous liquid, (86% yield, 128 mg); R_f = 0.46 (30 % ethyl acetate in hexane); d.r. = >20:1(determined by ^{1}H NMR using crude reaction mixture); **^{1}H NMR (400 MHz, CDCl$_3$)** δ 9.42 (s, 1H), 7.68 – 7.62 (m, 3H), 7.57 – 7.53 (m, 2H), 7.46 – 7.41 (m, 3H), 7.40 – 7.34 (m, 2H), 7.33 – 7.29 (m, 2H), 7.24 – 7.18 (m, 2H), 6.18 (d, *J* = 3.6 Hz, 1H), 4.35 (d, *J* = 3.2 Hz, 1H), 2.94 – 2.88 (m, 2H), 1.27 (t, *J* = 6.0 Hz, 3H); **^{13}C NMR (100 MHz, CDCl$_3$)** δ 192.3, 182.7, 156.4, 141.6, 139.7, 132.4, 132.3, 132.1, 130.6, 130.0, 129.52, 129.0, 127.8, 127.7, 127.6, 127.2, 127.0, 121.4, 50.4, 27.8, 14.1; **FTIR (neat)** 2960, 2923, 26852, 1736, 1646, 1476, 701 m^{-1}; **HRMS (ESI)** calculated for $C_{26}H_{22}BrNO_2S$ $[M+H]^+$: 494.0607; found: 494.0619; **HPLC** condition: Chiralcel-AD-H, hexane/i-PrOH = 60:40 v/v, flow rate = 1.0 mL/min, λ = 310 nm, 25 °C, t_R (major) = 10.23, t_R (minor) = 6.01 min, 88% *ee*, $[\alpha]_D^{20}$ = +120.98 (c 0.5, CH_2Cl_2).

(4*S*,5*S*)-5-(4-Bromobenzoyl)-1-(2-(isopropylthio)phenyl)-4-phenyl-4,5-dihydro-1*H*-pyrrole-3-carbaldehyde 4c; Prepared according to general procedure B using (*R*)-diphenylprolinol trimethylsilyl ether **C6**, purification of the crude product by column chromatography using (HX/EA) mixture (70:30) to afford the title compound as orange

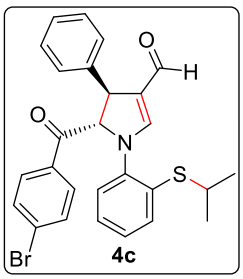

4c

viscous liquid, (80% yield, 120 mg); R_f = 0.50 (30 % ethyl acetate in hexane); d.r. = >20:1(determined by ^{1}H NMR using crude reaction mixture); **^{1}H NMR (400 MHz, CDCl$_3$)** δ 9.43 (s, 1H), 7.70 (s, 1H), 7.67 – 7.63 (m, 2H), 7.58 – 7.54 (m, 2H), 7.46 – 7.40 (m, 3H), 7.39 – 7.35 (m, 3H), 7.32 – 7.28 (m, 2H), 7.22 – 7.17 (m, 1H), 6.26 (d, *J* = 3.2 Hz, 1H), 4.35 (d, *J* = 3.2 Hz, 1H), 3.38 (Sep, *J* = 5.2 Hz, 1H), 1.27 (d, *J* = 5.2 Hz, 3H), 1.20 (d, *J* = 5.2 Hz, 3H); **^{13}C NMR (100 MHz, CDCl$_3$)** δ 192.4, 182.7, 156.2, 141.6, 141.5, 133.9, 132.4, 132.3, 130.6, 129.5, 129.1, 128.2, 127.8, 127.3, 126.9, 121.4, 76.4, 50.4, 38.8, 23.2, 22.8; **FTIR (neat)** 3028, 2970, 2852, 1741, 1636, 1474, 755 cm^{-1}; **HRMS (ESI)** calculated for $C_{27}H_{24}BrNO_2S$ $[M+H]^+$: 508.0764; found:

508.0774; **HPLC** condition: HPLC Chiralcel- AD-H, hexane/i-PrOH = 60:40 v/v, flow rate = 1.0 mL/min, λ = 350 nm, 25 °C, t_R (major) = 8.00, t_R (minor) = 5.17 min, 86% *ee*, $[\alpha]_D^{20}$ = +152.51 (c 0.5, CH_2Cl_2).

(4*S*,5*S*)-5-(4-Bromobenzoyl)-4-phenyl-1-(2-(prop-2-yn-1-ylthio)phenyl)-4,5-dihydro-1*H*-pyrrole-3-carbaldehyde 4d; Prepared according to general procedure B using (*R*)-diphenylprolinol trimethylsilyl ether **C6**, purification of crude product by column chromatography using (HX/EA) mixture (70:30) to afford the

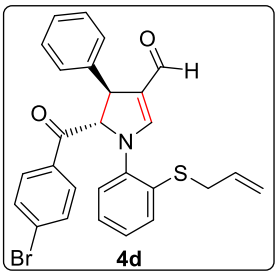

title compound as orange viscous liquid, (88% yield, (133 mg); R_f = 0.59 (30 % ethyl acetate in hexane); d.r. = >20:1(determined by ^{1}H NMR using crude reaction mixture); **^{1}H NMR (500 MHz, $CDCl_3$)** δ 9.34 (s, 1H), 7.63 (s, 1H), 7.60 – 7.56 (m, 2H), 7.52 – 7.47 (m, 2H), 7.39 – 7.34 (m, 3H), 7.32 – 7.28 (m, 2H), 7.27 – 7.24 (m, 2H), 7.16 – 7.10 (m, 2H), 6.13 (d, *J* = 4.0 Hz, 1H), 5.76 – 5.65 (m, 1H), 5.04 – 4.96 (m, 2H), 4.29 (d, *J* = 4.0 Hz, 1H), 3.50 – 3.40 (m, 2H); **^{13}C NMR (125 MHz, $CDCl_3$)** δ 192.3, 182.6, 156.3, 141.6, 140.5, 132.7, 132.5, 132.4, 131.8, 131.1, 130.6, 129.6, 129.1, 127.8, 127.7, 127.5, 127.0, 121.6, 118.6, 76.3, 50.5, 37.4; **FTIR (neat)** 2958, 2923, 1694, 1645, 1578, 1487, 758 cm^{-1}; **HRMS (ESI)** calculated for $C_{27}H_{22}BrNO_2S$ $[M+H]^+$: 504.0627; found: 504.0638; **HPLC** condition: HPLC Chiralcel AD-H, hexane/i-PrOH = 60:40 v/v, flow rate = 1.0 mL/min, λ = 254 nm, 25 °C, t_R (major) = 14.02 min, t_R (minor) = 7.10 min, 80% *ee*, $[\alpha]_D^{20}$ = +137.22 (c 0.5, CH_2Cl_2).

(4*S*,5*S*)-1-(2-(Allylthio)phenyl)-5-(4-bromobenzoyl)-4-phenyl-4,5-dihydro-1*H*-pyrrole-3-carbaldehyde 4e; Prepared according to general procedure B using (*R*)-diphenylprolinol trimethylsilyl ether **C6**, purification of crude product by column chromatography using (HX/EA) mixture (70:30) to afford the title compound as orange viscous liquid, (80% yield, (120 mg); R_f = 0.45 (30 % ethyl acetate in hexane); d.r. = >20:1(determined by ^{1}H NMR using crude reaction mixture); **^{1}H NMR (500 MHz, CDCl$_3$)** δ 9.48 (s, 1H), 7.77 (s, 1H), 7.73 – 7.68 (m, 2H), 7.64 – 7.60 (m, 2H), 7.57 – 7.52 (m, 2H), 7.47 – 7.42 (m, 4H), 7.39 – 7.34 (m, 2H), 7.32 – 7.29 (m, 2H), 6.20 (d, *J* = 4.0 Hz, 1H), 4.40(d, *J* = 4.0 Hz, 1H), 3.72 – 3.59 (m, 2H); **^{13}C NMR (126 MHz, CDCl$_3$)** δ 192.3, 182.6, 156.3, 141.6, 140.5, 132.7, 132.5, 132.4, 131.8, 131.1, 130.6, 129.6, 129.1, 127.8, 127.8, 127.7, 127.5, 127.0, 1216, 118.6, 76.3, 50.5, 37.4; **FTIR (neat)** 2956, 2924, 1696, 1644, 1567, 1474, 761cm^{-1}; **HRMS (ESI)** calculated for $C_{27}H_{20}BrNO_2S$ $[M+H]^+$: 502.0471; found: 502.0482; **HPLC** condition: HPLC Chiralcel AD-H, hexane/i-PrOH = 60:40 v/v, flow rate = 1.0 mL/min, λ = 254 nm, 25 °C, t_R (major) = 17.20, t_R (minor) = 9.15 min, 82% *ee*, $[\alpha]_D^{20}$ = +171.25 (c 0.5, CH_2Cl_2).

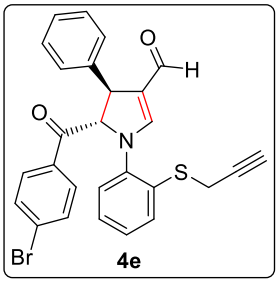

2-(2-(2*S*,3*S*)-2-(4-Bromobenzoyl)-4-formyl-3-phenyl-2,3-dihydro-1*H*-pyrrol-1-yl)phenyl)thio)acetonitrile 4f; Prepared according to general procedure B using (R)-diphenylprolinol trimethylsilyl ether **C6**, purification of crude product by column chromatography using (HX/EA) mixture (70:30) to afford the title compound as yellow viscous liquid, (73% yield, (110 mg); R_f = 0.29 (30 % ethyl acetate in hexane); d.r. = >20:1(determined by ^{1}H NMR using crude reaction mixture); **^{1}H NMR (500 MHz, CDCl$_3$)** δ 9.52 (s, 1H), 7.89 (s, 1H), 7.74 – 7.67 (m, 3H), 7.66 – 7.62 (m, 2H), 7.50 – 7.46 (m, 2H), 7.46 – 7.44 (m, 2H), 7.42 – 7.37 (m, 3H), 7.36 – 7.32 (m, 2H), 6.15 (d, *J*

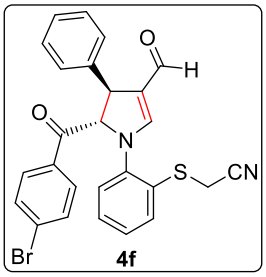

= 4.5 Hz, 1H), 4.41 (d, *J* = 4.5 Hz, 1H), 3.71 (dd, *J* = 17.0, 17.0 Hz, 2H); **^{13}C NMR (126 MHz, $CDCl_3$)** δ 192.3, 183.0, 155.4, 142.5, 141.3, 135.6, 132.4, 132.3, 130.7, 130.5, 129.8, 129.2, 128.0, 127.6, 127.4, 126.0, 125.8, 122.3, 116.0, 77.0, 50.3, 20.8; **FTIR (neat)** 3063, 2955, 2853, 1746, 1694, 1475, 1208, 759 cm^{-1}; **HRMS (ESI)** calculated for $C_{26}H_{19}BrN_2O_2S$ $[M+H]^+$: 505.0403; found: 505.0384; **HPLC** condition: HPLC Chiralcel AD-H, hexane/i-PrOH = 70:30 v/v, flow rate = 1.0 mL/min, λ = 300 nm, 25 °C, t_R (major) = 25.54, t_R (minor) = 11.42 min, 90% *ee*, $[\alpha]_D^{20}$ = +107.25 (c 0.5, CH_2Cl_2).

Ethyl 2-(2-(2*S*,3*S*)-2-(4-bromobenzoyl)-4-formyl-3-phenyl-2,3-dihydro-1*H*-pyrrol-1-yl)phenyl)thio)acetate 4g; Prepared according to general procedure B using (R)-diphenylprolinol trimethylsilyl ether **C6**, purification of crude product by column chromatography using (HX/EA) mixture (70:30) to afford the title compound as orange viscous liquid, (73% yield, 120 mg); R_f = 0.44 (40 % ethyl acetate in hexane); d.r. = >20:1(determined by ^{1}H NMR using crude reaction mixture); **^{1}H NMR (400 MHz, $CDCl_3$)** δ 9.30 (s, 1H), 7.62 (s, 1H), 7.55 – 7.51 (m, 2H), 7.45 – 7.41 (m, 2H), 7.33 (dd, *J* = 1.6, 1.6 Hz, 1H), 7.28 – 7.22 (m, 5H), 7.20 – 7.16 (m, 1H), 7.15 – 7.12 (m, 1H), 7.07 (td, *J* = 1.6, 1.5 Hz, 1H), 6.06 (d, *J* = 4.0 Hz, 1H), 4.22 (d, *J* = 4.0 Hz, 1H), 4.03 – 3.90 (m, 2H), 3.60 – 3.42 (m, 2H), 1.02 (t, *J* = 7.2 Hz, 3H); **^{13}C NMR (101 MHz, $CDCl_3$)** δ 192.4, 182.9, 168.9, 156.3, 141.5, 140.5, 132.4, 132.3, 131.7, 130.6, 130.3, 129.6, 129.1, 128.4, 127.8, 127.7, 127.2, 121.8, 76.2, 61.9, 50.4, 36.3, 14.2; **FTIR (neat)** 3193, 2958, 2852, 1733, 1715, 1696, 1474, 752 cm^{-1}; **HRMS (ESI)** calculated for $C_{28}H_{24}BrNO_4S$ $[M+H]^+$: 552.0662; found: 552,0635; **HPLC** condition: HPLC Chiralcel AD-H, hexane/i-PrOH = 60:40 v/v, flow rate = 1.0

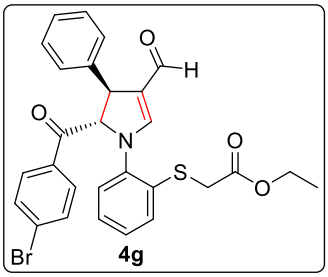

mL/min, λ = 320 nm, 25 °C, t_R (major) = 14.29, t_R (minor) = 7.11 min, 98% *ee*, $[\alpha]_D^{19.9}$ = +258.87 (c 0.5, CH_2Cl_2).

(4*S*,5*S*)-5-(4-Bromobenzoyl)-4-phenyl-1-(2-((2,4,6-trimethylbenzyl)thio)phenyl)-4,5-dihydro-1*H*-pyrrole-3-carbaldehyde 4h; Prepared according to general procedure B using (R)-diphenylprolinol trimethylsilyl ether **C6**, purification of crude product by column chromatography using (HX/EA) mixture (70:30) to afford the title compound as orange brown viscous liquid (63% yield, 113 mg); R_f = 0.29 (20 % ethyl acetate in hexane); d.r. = >20:1(determined by ^{1}H NMR using crude reaction mixture); **^{1}H NMR (500 MHz, $CDCl_3$)** δ 9.26 (s, 1H), 7.63 (s, 1H), 7.58 (d, *J* = 8.5 Hz, 2H), 7.54 (d, *J* = 8.5 Hz, 2H), 7.47 – 7.42 (m, 1H), 7.40 (d, *J* = 7.5 Hz, 1H), 7.36 – 7.31 (m, 2H), 7.30 – 7.20 (m, 6H), 6.85 (s, 2H), 6.03 (d, *J* = 4.0 Hz, 1H), 4.31 (d, *J* = 4.5 Hz, 1H), 4.20 – 4.10 (m, 2H), 2.28 (s, 3H), 2.24 (s, 6H); **^{13}C NMR (126 MHz, $CDCl_3$)** δ 192.5, 182.7, 156.1, 141.6, 140.5, 137.5, 137.3, 132.6, 132.5, 132.4, 132.3, 130.6, 129.6, 129.5, 129.4, 129.0, 127.8, 127.7, 127.5, 126.4, 121.4, 77.0, 50.6, 34.6, 21.1, 19.7; **FTIR (neat)** 3058, 2923, 2852, 1742, 1646, 1417, 757 cm^{-1}; **HRMS (ESI)** calculated for $C_{34}H_{30}BrNO_2S$ $[M+H]^+$: 598.1233; found: 598.1207; **HPLC** condition: HPLC Chiralcel OD-H, hexane/i-PrOH = 70:30 v/v, flow rate = 1.0 mL/min, λ = 254 nm, 25 °C, t_R (major) = 18.42, t_R (minor) = 10.32 min, 96% *ee*, $[\alpha]_D^{20}$ = +89.64 (c 0.1, CH_3CN).

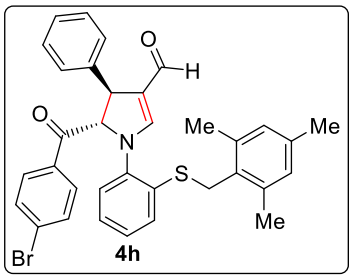

(4*S*,5*S*)-5-(4-Bromobenzoyl)-1-(2-((3,5-di-tert-butylbenzyl)thio)phenyl)-4-phenyl-4,5-dihydro-1*H*-pyrrole-3-carbaldehyde 4i; Prepared according to general procedure B using (R)-diphenylprolinol trimethylsilyl ether **C6**, purification of the crude product by column chromatography using (HX/EA) mixture (70:30) to afford the title compound as orange viscous liquid, (50% yield, 100 mg); R_f = 0.44 (20 % ethyl acetate in hexane); d.r. = >20:1(determined by ^{1}H NMR using crude reaction mixture); **(500 MHz, $CDCl_3$)** δ 9.20 (s, 1H), 7.48 – 7.44 (m, 2H), 7.40 – 7.36 (m, 2H), 7.32 (s, 1H), 7.25 – 7.05 (m, 9H), 7.01 (t, *J* = 7.5 Hz, 1H), 6.84 – 6.80 (m, 2H), 5.93 (d, *J* = 4.0 Hz, 1H), 4.17 (d, *J* = 5.5 Hz, 1H), 3.95 – 3.90 (m, 2H), 1.10 (s, 18H); **^{13}C NMR (126 MHz, $CDCl_3$)** δ 192.4, 182.6, 156.0, 151.3, 141.7, 140.9, 135.68, 133.0, 132.5, 132.3, 131.5, 130.6, 129.5, 129.1, 128.1, 127.8, 127.7, 127.4, 126.8, 123.1, 121.7, 121.5, 76.7, 50.5, 40.4, 34.9, 31.5; **FTIR (neat)** 2961, 2924, 2852, 1742, 1699, 1471, 752 cm^{-1}; **HRMS (ESI)** calculated for $C_{39}H_{40}BrNO_2S$ $[M+H]^+$: 666.2036; found: 666.2009; **HPLC** condition: HPLC Chiralpack- IA, hexane/i-PrOH = 80:20 v/v, flow rate = 1.0 mL/min, λ = 254 nm, 25 °C, t_R (major) = 10.70, t_R (minor) = 6.80 min, 84% *ee*, $[\alpha]_D^{20}$ = +114.84 (c 0.5, CH_2Cl_2).

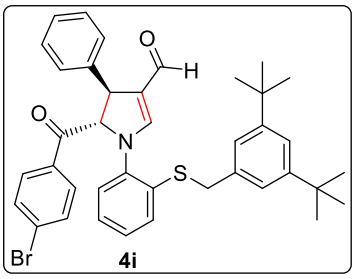

4-(2-(2S,3S)-2-(4-Bromobenzoyl)-4-formyl-3-phenyl-2,3-dihydro-1*H*-pyrrol-1 yl)phenyl)thio)methyl)benzonitrile 4j; Prepared according to general procedure B using (R)-diphenylprolinol trimethylsilyl ether **C6**, purification of crude product by column chromatography using (HX/EA) mixture (70:30) to afford the title compound as orange viscous liquid, (66% yield, 115 mg); R_f = 0.47 (40 % ethyl acetate in hexane); d.r. = >20:1(determined by ^{1}H NMR using crude reaction mixture); **^{1}H NMR (400 MHz, $CDCl_3$)** δ 9.34 (s, 1H), 7.59 (s,

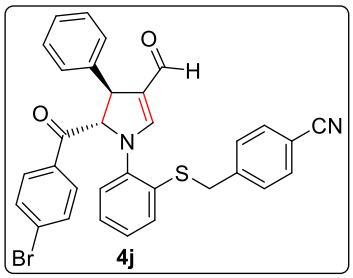

1H), 7.55 – 7.45 (m, 4H), 7.41 (d, J = 8.0 Hz, 2H), 7.33 – 7.23 (m, 6H), 7.20 – 7.13 (m, 5H), 7.04 (t, J = 7.6 Hz, 1H), 5.99 (d, J = 4.4 Hz, 1H), 4.25 (d, J = 4.4 Hz, 1H), 4.07 – 3.93 (m, 2H); **^{13}C NMR (101 MHz, $CDCl_3$)** δ 192.2, 182.8, 155.5, 142.4, 141.5, 141.4, 133.5, 132.4, 132.3, 130.5, 129.8, 129.6, 129.2, 129.0, 128.9, 127.9, 127.7, 127.2, 126.2, 121.8, 118.6, 111.5, 76.6, 50.3, 39.1; **FTIR (neat)** 2955, 2924, 2852, 1742, 1694, 1477, 1206, 752 cm^{-1}; **HRMS (ESI)** calculated for $C_{32}H_{23}BrN_2O_2S$ $[M+H]^+$: 581.0716; found: 581.0686; **HPLC** condition: HPLC Chiralcel AD-H, hexane/i-PrOH = 60:40 v/v, flow rate = 1.0 mL/min, λ = 320 nm, 25 °C, t_R (major) = 2-.90 t_R (minor) = 12.67 min, 96% *ee*, $[\alpha]_D^{20}$ = +93.60 (c 0.1, CH_2Cl_2).

(4*S*,5*S*)-5-(4-Bromobenzoyl)-1-(2-((naphthalen-1-ylmethyl)thio)phenyl)-4-phenyl-4,5-dihydro-1*H*-pyrrole-3-carbaldehyde 4k; Prepared according to general procedure B using (R)-diphenylprolinol trimethylsilyl ether **C6**, purification of the crude product by column chromatography using (HX/EA) mixture (70:30) to afford the title compound as orange viscous liquid, (72% yield, 137 mg); R_f = 0.44 (30 % ethyl acetate in hexane); d.r. = >20:1(determined by ^{1}H NMR using crude reaction mixture); **^{1}H NMR (500 MHz, $CDCl_3$)** δ 8.94 (s, 1H), 7.78 (d, J = 8.5 Hz, 1H), 7.64 (d, J = 8.0 Hz, 1H), 7.53 (d, J = 8.5 Hz, 1H), 7.30 – 7.20 (m, 7H), 7.17 (d, J = 8.0 Hz, 1H), 7.08 – 6.96 (m, 9H), 6.93 (d, J = 7.0 Hz, 1H), 5.72 (d, J = 4.5 Hz, 1H), 4.32 (s, 2H), 4.01 (d, J = 4.5 Hz, 1H); **^{13}C NMR (126 MHz, $CDCl_3$)** δ 192.5, 182.7, 155.9, 141.5, 141.2, 134.2, 133.3, 132.5, 132.4, 132.3, 131.7, 131.4, 130.5, 129.5, 129.1, 129.0, 128.8 128.3, 127.9, 127.7, 127.6, 127.4, 126.9, 126.6, 126.2, 125.3, 123.7, 121.3, 76.8, 50.6, 37.9; **FTIR (neat)** 2954, 2924, 2852, 1715, 1697, 1635, 1488, 779 cm^{-1}; **HRMS (ESI)** calculated for $C_{35}H_{26}BrNO_2S$ $[M+H]^+$: 606.0920; found: 606.0916; **HPLC** condition: HPLC Chiralcel AD-H, hexane/i-PrOH = 60:40 v/v, flow rate = 1.0

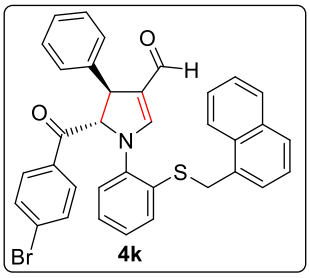

4k

mL/min, λ = 310 nm, 25 °C, t_R (major) = 18.51, t_R (minor) = 10.71 min, 96% *ee*, $[\alpha]_D^{19.9}$ = +103.22 (c 0.5, CH_2Cl_2).

(4*S*,5*S*)-1-(2-(Anthracen-9-ylmethyl)thio)phenyl)-5-(4-bromobenzoyl)-4-phenyl-4,5-dihydro-1*H*-pyrrole-3-carbaldehyde 4l; Prepared according to general procedure B using (R)-diphenylprolinol trimethylsilyl ether **C6**, purification of the crude product by column chromatography using (HX/EA) mixture (70:30) to afford the title compound as pale orange viscous liquid, (85% yield, 166 mg); R_f = 0.50 (30 % ethyl acetate in hexane); d.r. = >20:1(determined by ^{1}H NMR using crude reaction mixture); **^{1}H NMR (500 MHz, $CDCl_3$)** δ 9.42 (s, 1H), 7.82 – 7.79 (m, 2H), 7.64 – 7.60 (m, 1H), 7.52 (s, 1H), 7.49 – 7.46 (m, 2H), 7.46 – 7.42 (m, 5H), 7.43 – 7.34 (m, 4H), 7.32 – 7.30(m, 1H), 7.30 – 7.26 (m, 4H), 7.23 – 7.18 (m, 3H), 6.17 (d, *J* = 4.5 Hz, 1H), 4.41 (d, *J* = 4.0 Hz, 1H), 4.13 (d, *J* = 3.0 Hz, 2H); **^{13}C NMR (125 MHz, $CDCl_3$)** δ 192.5, 182.6, 155.7, 141.2, 141.1, 133.3, 132.4, 132.1, 132.1, 131.6, 130.4, 130.1, 129.4, 128.7, 128.4, 128.3, 128.1, 127.9, 127.5, 127.42, 126.4, 126.4, 125.9, 125.2, 123.8, 121.4, 76.9, 50.6, 33.2; **FTIR (neat)** 3029, 2957, 2852, 1694, 1670, 1569, 1496, 1473, 1417, 754 cm^{-1}; **HRMS (ESI)** calculated for $C_{39}H_{28}BrNO_2S$ $[M+H]^+$: 654.1097; found: 654.1067; **HPLC** condition: HPLC Chiralcel AD-H, hexane/i-PrOH = 70:30 v/v, flow rate = 1.0 mL/min, λ = 254 nm, 25 °C, t_R (major) = 28.44 min, t_R (minor) = 16.80 min, 90% *ee*, $[\alpha]_D^{20.3}$ = +73.18 (c 0.1, CH_2Cl_2).

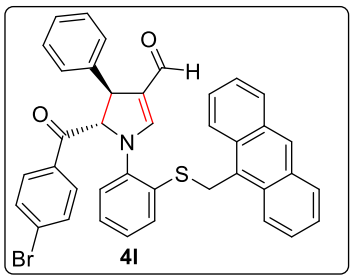

(4*S*,5*S*)-5-Benzoyl-1-(2-(benzylthio)phenyl)-4-phenyl-4,5-dihydro-1*H*-pyrrole-3-carbaldehyde 4m; Prepared according to general procedure B using (R)-diphenylprolinol trimethylsilyl ether **C6**, purification of crude product by column chromatography using (HX/EA) mixture (70:30) to afford the title compound as orange viscous liquid, (82% yield, (117 mg); R_f = 0.41 (30 % ethyl acetate in hexane); d.r. = >20:1(determined by ^{1}H NMR using crude reaction mixture); **^{1}H NMR (500 MHz, CDCl$_3$)** δ 9.34 (s, 1H), 7.75 (d, *J* = 7.6 Hz, 2H), 7.58 (t, *J* = 7.6 Hz, 1H), 7.46 – 7.30 (m, 11H), 7.26 – 7.20 (m, 3H), 7.20 – 7.13 (m, 3H), 6.11 (d, *J* = 4.0 Hz, 1H), 4.34 (d, *J* = 4.0 Hz, 1H), 4.10 (s, 2H); **^{13}C NMR (100 MHz, CDCl$_3$)** 193.4, 182.7 156.3, 141.8, 141.1, 136.9, 134.1, 133.8, 132.9, 131.3, 129.2, 129.0, 128.9, 128.7, 128.1, 127.9, 127.6, 127.5, 127.0, 121.4, 76.8, 50.5, 39.6; **FTIR (neat)** 3061, 3030, 2852, 1739, 1696, 1474, 766 cm^{-1}; **HRMS (ESI)** calculated for $C_{31}H_{25}NO_2S$ $[M+H]^+$: 476.1679; found: 476.1685; **HPLC** condition: HPLC Chiralcel-OD-H, hexane/i-PrOH = 60:40 v/v, flow rate = 1.0 mL/min, λ = 254 nm, 25 °C, t_R (major) = 11.18, t_R (minor) = 7.02 min, 92% *ee*, $[\alpha]_D^{19.9}$ = +109.94 (c 0.5, CH_2Cl_2).

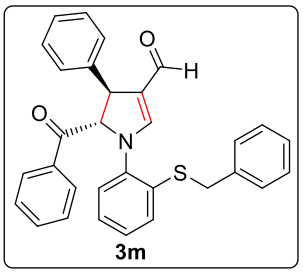

(4*S*,5*S*)-1-(2-(Benzylthio)phenyl)-5-(4-methoxybenzoyl)-4-phenyl-4,5-dihydro-1*H*-pyrrole-3-carbaldehyde 4n; Prepared according to general procedure B using (R)-diphenylprolinol trimethylsilyl ether **C6**, purification of crude product by column chromatography using (HX/EA) mixture (70:30) to afford the title compound as Orange semi-solid, (72% yield, 110 mg); R_f = 0.29 (30 % ethyl acetate in hexane); d.r. = >20:1(determined by ^{1}H NMR using crude reaction mixture); **^{1}H NMR (500 MHz, CDCl$_3$)** δ 9.36 (s, 1H), 7.73 (d, *J* = 9.0 Hz, 2H), 7.46 (s, 1H), 7.42 – 7.39 (m, 3H), 7.38 – 7.34 (m, 2H), 7.34 – 7.31 (m, 2H), 7.31 – 7.27 (m,

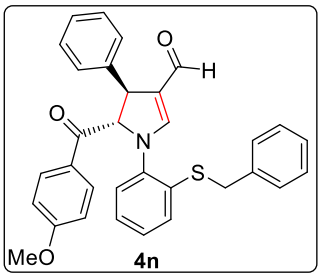

1H), 7.25 – 7.21 (m, 4H), 7.18 – 7.12 (m, 3H), 6.85 (d, J = 9.0 Hz, 2H), 6.10 (d, J = 4.0 Hz, 1H), 4.35 (d, J = 4.5 Hz, 1H), 4.12 – 4.06 (m, 2H), 3.85 (s, 3H); **^{13}C NMR (126 MHz, $CDCl_3$)** δ 192.0, 182.7, 164.4, 156.4, 142.0, 141.2, 136.9, 132.8, 131.5, 131.3, 128.9, 128.9, 128.7, 128.1, 127.9, 127.6, 127.6, 127.4, 126.9, 126.7, 121.4, 114.2, 76.6, 55.7, 50.8, 39.9; **FTIR (neat)** 3060, 2923, 2852, 1736, 1682, 1475, 761 cm^{-1}; **HRMS (ESI)** calculated for $C_{32}H_{27}NO_3S$ $[M+H]^+$: 506. 1784; found: 506.1803; **HPLC** condition: HPLC Chiralcel-AD-H, hexane/i-PrOH = 60:40 v/v, flow rate = 1.0 mL/min, λ = 254 nm, 25 °C, t_R (major) = 18.52, t_R (minor) = 7.98 min, 96% *ee*, $[\alpha]_D^{20}$ = +77.54 (c 0.5, CH_2Cl_2).

(4S,5S)-1-(2-(Benzylthio)phenyl)-5-(4-bromobenzoyl)-4-phenyl-4,5-dihydro-1*H*-pyrrole-3-carbaldehyde 4o; Prepared according to general procedure B using (R)-diphenylprolinol trimethylsilyl ether **C6**, purification of the crude product by column chromatography using (HX/EA) mixture (70:30) to afford the

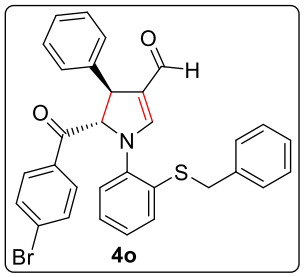

4o

title compound as orange viscous liquid, (90% yield, (150 mg); R_f = 0.46 (30 % ethyl acetate in hexane); d.r. = >20:1(determined by ^{1}H NMR using crude reaction mixtures); **^{1}H NMR (500 MHz, $CDCl_3$)** δ 9.30 (s, 1H), 7.61 – 7.50 (m, 4H), 7.41 – 7.29 (m, 7H), 7.25 – 7.19 (m, 4H), 7.14 – 7.09 (m, 2H), 6.00 (d, J = 4.0 Hz, 1H), 4.32 (d, J = 4.0 Hz, 1H), 4.12 – 4.04 (m, 2H); **^{13}C NMR (125 MHz, $CDCl_3$)** δ 192.4, 182.5, 156.1, 141.5, 140.8, 136.7, 132.7, 132.4, 132.2, 131.2, 130.5, 129.4, 128.9, 128.7, 128.6, 128.0, 127.7, 127.6, 127.5, 127.5, 126.9, 121.2, 76.6, 50.5, 39.7; **FTIR (neat)** 2923, 2852, 1694, 1645, 1473, 784 cm^{-1}; **HRMS (ESI)** calculated for $C_{31}H_{24}BrNO_2S$ $[M+H]^+$: 554.0784; found: 554.0795; **HPLC** condition: HPLC Chiralcel-AD-H, hexane/i-PrOH = 60:40 v/v, flow rate = 1.0 mL/min, λ = 254 nm, 25 °C, t_R (major) = 13.20, t_R (minor) = 7.38 min, 96% *ee*, $[\alpha]_D^{20}$ = +281.65 (c 0.1, CH_2Cl_2).

(4*S*,5*S*)-1-(2-(Benzylthio)phenyl)-5-(4-nitrobenzoyl)-4-phenyl-4,5-dihydro-1*H*-pyrrole-3-carbaldehyde 4p; Prepared according to general procedure B using (R)-diphenylprolinol trimethylsilyl ether **C6**, purification of the crude product by column chromatography using (HX/EA) mixture (70:30) to afford the title compound as red viscous liquid, (64% yield, 100 mg); R_f = 0.46 (30 % ethyl acetate in hexane); d.r. = >20:1(determined by ^{1}H NMR using crude reaction mixture); **^{1}H NMR (500 MHz, $CDCl_3$)** δ 9.44 (s, 1H), 8.30 – 8.27 (m, 2H), 7.95 – 7.92 (m, 2H), 7.53 – 7.45 (m, 4H), 7.44 – 7.41 (m, 4H), 7.36 – 7.32 (m, 2H), 7.30 – 7.26 (m, 4H), 7.21 – 7.17 (m, 2H), 6.12 (d, *J* = 4.0 Hz, 1H), 4.40 (d, *J* = 4.5 Hz, 1H), 4.15 (d, *J* = 4.0 Hz, 2H); **^{13}C NMR (126 MHz, $CDCl_3$)** δ 191.7, 182.6, 155.7, 150.8, 141.2, 140.7, 138.3, 136.6, 132.7, 131.2, 130.1, 129.0, 128.7, 128.6, 128.1, 127.9, 127.7, 127.6, 127.5, 126.9 123.9, 121.2, 6.8, 50.4, 39.7; **FTIR (neat)** 2929, 2860, 1746, 1641, 1593, 1402, 1344, 755 cm^{-1}; **HRMS (ESI)** calculated for $C_{31}H_{24}N_2O_4S$ $[M+H]^+$: 521.1530; found: 521.1522; **HPLC** condition: HPLC Chiralcel AD-H, hexane/i-PrOH = 60:40 v/v, flow rate = 1.0 mL/min, λ = 320 nm, 25 °C, t_R (major) = 13.89, t_R (minor) = 8.55 min, 90% *ee*, $[\alpha]_D^{20}$ = +83.37 (c 0.5, CH_2Cl_2).

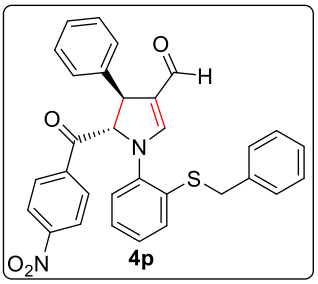

4p

(4*S*,5*S*)-5-(1-Naphthoyl)-1-(2-(benzylthio)phenyl)-4-phenyl-4,5-dihydro-1*H*-pyrrole-3-carbaldehyde 4q; Prepared according to general procedure B using (*R*)-diphenylprolinol trimethylsilyl ether **C6**, purification of the crude product by column chromatography using (HX/EA) mixture (70:30) to afford the title compound as orange solid, (70% yield, 110 mg); R_f = 0.25 (30 % ethyl acetate in hexane); mp 126 – 128 °C; d.r. = >20:1(determined by ^{1}H NMR using crude reaction mixture); **^{1}H NMR (500 MHz, $CDCl_3$)** δ 9.33 (s, 1H), 8.08 (s,

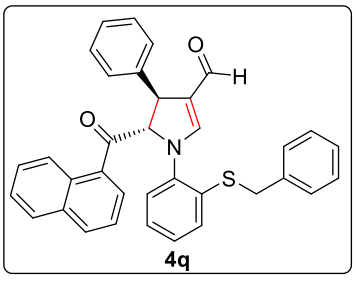

4q

1H), 7.85 – 7.82 (m, 1H), 7.80 (d, J = 8.5 Hz, 2H), 7.64 (d, J = 8.5 Hz, 1H), 7.57 – 7.55 (m, 1H), 7.48 – 7.45 (m, 1H), 7.44 – 7.40 (m, 2H), 7.37 – 7.34 (m, 2H), 7.33 – 7.28 (m, 4H), 7.21 – 7.19 (m, 1H), 7.18 – 7.12 (m, 4H), 7.10 – 7.08 (m, 3H), 6.20 (d, J = 4.5 Hz, 1H), 4.38 (d, J = 4.5 Hz, 1H), 4.05 – 4.03 (m, 2H); **^{13}C NMR (126 MHz, $CDCl_3$)** δ 193.3, 182.6, 156.3, 141.9, 141.1, 136.8, 135.9, 132.8, 132.3, 131.3, 131.2, 130.9, 129.6, 129.1, 128.9, 128.8, 128.8, 128.7, 128.7, 128.6, 128.0, 127.9, 127.8, 127.6, 127.5, 127.4, 127.0, 126.8, 124.2, 121.2, 77.1, 50.8, 39.8; **FTIR (neat)** 3030, 2924, 2855, 1741, 1635, 1476, 761 cm^{-1}; **HRMS (ESI)** calculated for $C_{35}H_{27}NO_2S$ $[M+H]^+$: 526.1835; found: 526.1827; **HPLC** condition: HPLC Chiralcel OD-H, hexane/i-PrOH = 60:40 v/v, flow rate = 1.0 mL/min, λ = 310 nm, 25 °C, t_R (major) = 19.77, t_R (minor) = 8.14 min, 90% *ee*, $[\alpha]_D^{19.9}$ = +30. 25 (c 0.5, CH_2Cl_2).

(4*S*,5*S*)-1-(2-(Benzylthio)phenyl)-5-(4-bromobenzoyl)-4-(p-tolyl)-4,5-dihydro-1*H*-pyrrole-3-carbaldehyde 4r; Prepared according to general procedure B using (R)-diphenylprolinol trimethylsilyl ether **C6**, purification of crude product by column chromatography using (HX/EA) mixture (70:30) to afford the title compound as orange viscous liquid, (76% yield, 130 mg); R_f = 0.46 (30 % ethyl acetate in hexane); d.r. = >20:1(determined by ^{1}H NMR using crude reaction mixture); **^{1}H NMR (400 MHz, $CDCl_3$)** δ 9.50 (s, 1H), 7.74 (d, J = 8.4 Hz, 2H), 7.68 (d, J = 8.4 Hz, 2H), 7.56 (d, J = 7.6 Hz, 1H), 7.51 (d, J = 7.6 Hz, 1H), 7.44 – 7.34 (m, 7H), 7.30 – 7.25 (m, 4H), 6.20 (d, J = 4.4 Hz, 1H), 4.24 (d, J = 4.0 Hz, 1H), 4.21 (s, 2H), 2.50 (s, 3H); **^{13}C NMR (101 MHz, $CDCl_3$)** δ 192.5, 182.9, 156.2, 141.0 138.6, 137.4, 136.8, 132.7, 132.4, 132.3, 131.2, 130.6, 129.7, 129.5, 128.8, 128.7, 128.1, 127.7, 127.6, 127.6, 127.0, 121.5, 76.7, 50.1, 39.8, 21.3; **FTIR (neat)** 2970, 2924, 2853, 1739, 1696, 1364, 697 cm^{-1}; **HRMS (ESI)** calculated for $C_{32}H_{26}BrNO_2S$ $[M+H]^+$: 570.0920; found:

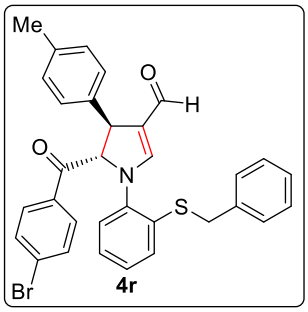

570.0934; **HPLC** condition: HPLC Chiralcel OD-H, hexane/i-PrOH = 60:40 v/v, flow rate = 1.0 mL/min, λ = 310 nm, 25 °C, t_R (major) = 18.05, t_R (minor) = 11.27 min, 98% *ee*, $[\alpha]_D^{19.9}$ = +133.70 (c 0.5, CH_2Cl_2).

(4*S*,5*S*)-1-(2-(Benzylthio)phenyl)-5-(4-bromobenzoyl)-4-(4-bromophenyl)-4,5-dihydro-1*H*-pyrrole-3-carbaldehyde 4s; Prepared according to general procedure B using (R)-diphenylprolinol trimethylsilyl ether **C6**, purification of crude product by column chromatography using (HX/EA) mixture (70:30) to afford the title compound as orange viscous liquid, (84% yield, 90 mg); R_f = 0.43 (30 % ethyl acetate in hexane); d.r. = >20:1(determined by ^{1}H NMR using crude reaction mixture); **^{1}H NMR (400 MHz, $CDCl_3$)** δ 9.29 (s, 1H), 7.56 – 7.48 (m, 4H), 7.41 (d, *J* = 8.0 Hz, 1H), 7.38 – 7.30 (m, 3H), 7.25 – 7.14 (m, 8H), 7.12 – 7.05 (m, 2H), 5.94 (d, *J* = 4.4 Hz, 1H), 4.24 (d, *J* = 4.0 Hz, 1H), 4.10 – 4.00 (m, 2H); **^{13}C NMR (101 MHz, $CDCl_3$)** δ 192.5, 182.9, 156.2, 141.0 138.6, 137.4, 136.8, 132.7, 132.4, 132.3, 131.2, 130.6, 129.7, 129.5, 128.8, 128.7, 128.1, 127.7, 127.6, 127.6, 127.0, 121.5, 76.7, 50.1, 39.8, 21.3; **FTIR (neat)** 2970, 2924, 2852, 1734, 1645, 1471, 750 cm^{-1}; **HRMS (ESI)** calculated for $C_{31}H_{23}Br_2NO_2S$ $[M+H]^+$: 633.9869; found: 633.9854; **HPLC** condition: HPLC Chiralcel AD-H, hexane/i-PrOH = 60:40 v/v, flow rate = 1.0 mL/min, λ = 320 nm, 25 °C, t_R (major) = 15.51, t_R (minor) = 7.46 min, 98% *ee*, $[\alpha]_D^{20}$ = +143.00 (c 0.5, CH_2Cl_2).

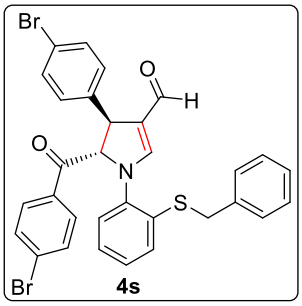

(4*S*,5*S*)-1-(2-(Benzylthio)phenyl)-5-(4-chlorobenzoyl)-4-(4-nitrophenyl)-4,5-dihydro-1*H*-pyrrole-3-carbaldehyde 4t; Prepared according to general procedure B using (R)-diphenylprolinol trimethylsilyl ether **C6**, purification of crude product by column chromatography using (HX/EA) mixture (70:30) to afford the title compound as orange viscous liquid, (72% yield, 118mg); R_f = 0.30 (30 % ethyl acetate in hexane); d.r. = >20:1(determined by ^{1}H NMR using crude reaction mixture); **^{1}H NMR (400 MHz, CDCl$_3$)** δ 9.32 (s, 1H), 8.16 (d, *J* = 8.1 Hz, 2H), 7.58 – 7.51 (m, 6H), 7.50 – 7.45 (m, 1H), 7.44 – 7.40 (m, 1H), 7.39 – 7.35 (m, 1H), 7.30 – 7.22 (m, 5H), 7.26 – 7.09 (m, 2H), 5.98 (d, *J* = 7.6 Hz, 1H), 4.39 (d, *J* = 8.4 Hz, 1H), 4.11 (s, 2H); **^{13}C NMR (101 MHz, CDCl$_3$)** δ 191.7, 182.3, 156.7, 148.6, 147.4, 139.8, 136.4, 132.4, 132.3, 132.0, 131.6, 130.3, 129.9, 128.8, 128.8, 128.6, 128.4, 128.0, 127.9, 127.8, 124.2, 120.0, 75.4, 50.0, 39.5; **FTIR (neat)** 3027, 2970, 2853, 1736, 1635, 1474, 1365, 757 cm^{-1}; **HRMS (ESI)** calculated for $C_{31}H_{23}ClN_2O_4S$ $[M+H]^+$: 555.1140; found: 555.1120; **HPLC** condition: HPLC Chiralcel AD-H, hexane/i-PrOH = 60:40 v/v, flow rate = 1.0 mL/min, λ = 254 nm, 25 °C, t_R (major) = 20.74, t_R (minor) = 9.94 min, 98% *ee*, $[\alpha]_D^{20}$ = +139.00 (c 0.5, CH_2Cl_2).

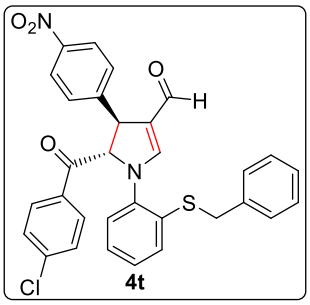

(4*S*,5*S*)-1-(2-(Benzylthio)phenyl)-5-(4-bromobenzoyl)-4-(furan-3-yl)-4,5-dihydro-1*H*-pyrrole-3-carbaldehyde 4u; Prepared according to general procedure B using (R)-diphenylprolinol trimethylsilyl ether **C6**, purification of crude product by column chromatography using (HX/EA) mixture (70:30) to afford the title compound as brown semi-solid, (65% yield, 103 mg); R_f = 0.56 (30 % ethyl acetate in hexane); d.r. = >20:1(determined by ^{1}H NMR using crude reaction mixture); **^{1}H NMR (500 MHz, CDCl$_3$)** δ 9.45 (s, 1H), 7.88 – 7.84 (m, 2H), 7.67 – 7.62 (m, 2H),

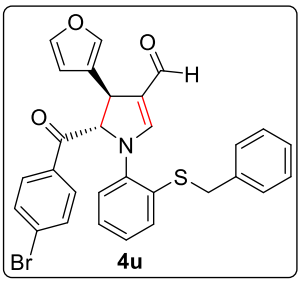

7.50 (s, 1H), 7.45 – 7.40 (m, 2H), 7.38 – 7.35 (m, 1H), 7.30 – 7.24 (m, 5H), 7.20 – 7.16 (m, 1H), 7.12 – 7.08 (m, 2H), 6.39 – 6.37 (m, 1H), 6.33 (d, *J* = 3.5 Hz, 1H), 6. 26 (d, *J* = 3.0 Hz, 1H), 4.56 (d, *J* = 3.5 Hz, 1H), 4.04 – 3.96 (m, 2H); **^{13}C NMR (126 MHz, $CDCl_3$)** δ 192.3, 182.6, 156.9, 153.1, 142.2, 141.0, 136.9, 133.5, 132.4, 132.3, 131.2, 130.7, 129.6, 128.9, 128.6, 128.4, 127.6, 127.5, 126.9, 117.8, 110.9, 107.8, 73.7, 43.4, 39.5; **FTIR (neat)** 3025, 2970, 2853, 1741, 1641, 1475, 782 cm^{-1}; **HRMS (ESI)** calculated for $C_{29}H_{22}BrNO_3S$ $[M+H]^+$: 546.0557; found: 546.0547; **HPLC** condition: HPLC Chiralcel AD-H, hexane/i-PrOH = 60:40 v/v, flow rate = 1.0 mL/min, λ = 254 nm, 25 °C, t_R (major) = 23.59, t_R (minor) = 9.68 min, 88% *ee*, $[\alpha]_D^{20}$ = -40.42 (c 0.5, CH_2Cl_2).

(4*S*,5*S*)-1-(2-(Benzylthio)phenyl)-5-(4-bromobenzoyl)-4-methyl-4,5-dihydro-1*H*-pyrrole-3-carbaldehyde 4v; Prepared according to general procedure B using (R)-diphenylprolinol trimethylsilyl ether **C6**, purification of crude product by column chromatography using (HX/EA) mixture (70:30) to afford the title compound as orange viscous liquid, (48% yield, 60 mg); R_f = 0.30 (30 % ethyl acetate in hexane); d.r. = >20:1(determined by ^{1}H NMR using crude reaction mixture); **^{1}H NMR (400 MHz, $CDCl_3$)** δ 9.49 (s, 1H), 7.75 (d, *J* = 8.1 Hz, 2H), 7.68 (d, *J* = 8.3 Hz, 2H), 7.56 (d, *J* = 3.8 Hz, 2H), 7.51 (d, *J* = 7.6 Hz, 1H), 7.39 (dd, *J* = 13.5, 6.3 Hz, 7H), 7.28 (d, *J* = 7.7 Hz, 4H), 6.19 (d, *J* = 4.3 Hz, 1H), 4.42 (d, *J* = 4.1 Hz, 1H), 4.21 (s, 2H), 2.50 (s, 3H); **^{13}C NMR (101 MHz, $CDCl_3$)** δ 192.5, 182.9, 156.2, 141.0 138.6, 137.4, 136.8, 132.7, 132.4, 132.3, 131.2, 130.6, 129.7, 129.5, 128.8, 128.7, 128.1, 127.7, 127.6, 127.6, 127.0, 121.5, 76.7, 50.1, 39.8, 21.3; **FTIR (neat)** 2929, 2855, 1700, 1631, 1476, 750 cm^{-1}; **HRMS (ESI)** calculated for $C_{26}H_{22}BrNO_2S$ $[M+H]^+$: 494.0607; found: 494.0623; **HPLC** condition: HPLC Chiralpak-IB, hexane/i-PrOH = 60:40 v/v, flow rate

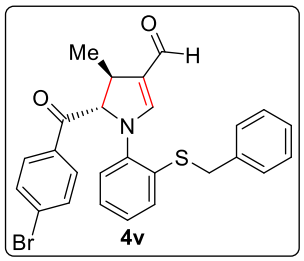

= 1.0 mL/min, λ = 254 nm, 25 °C, t_R (major) = 21.90, t_R (minor) = 25.27 min, 82% *ee*, $[\alpha]_D^{20}$ = -84.84 (c 0.5, CH_2Cl_2).

(4*S*,5*S*)-5-([1,1'-Biphenyl]-4-carbonyl)-1-(2-(benzylthio)phenyl)-4-phenyl-4,5-dihydro-1*H*-pyrrole-3-carbaldehyde 5a; P Prepared according to general procedure D using chiral product **4o**, purification of crude product by column chromatography using (HX/EA) mixture (70:30) to afford the title compound as orange viscous liquid, (66% yield, 100 mg); R_f = 0.40 (30 % ethyl acetate in hexane); d.r. = >20:1(determined by ^{1}H NMR using crude reaction mixture); **^{1}H NMR (500 MHz, $CDCl_3$)** δ 9.37 (s, 1H), 7.85 – 7.80 (m, 2H), 7.64 – 7.58 (m, 4H), 7.49 – 7.39 (m, 7H), 7.39 – 7.28 (m, 5H), 7.26 – 7.20 (m, 4H), 6.14 (d, *J* = 4.0 Hz, 1H), 4.39 (d, *J* = 4.0 Hz, 1H), 4.14 – 4.04 (m, 2H); **^{13}C NMR (100 MHz, $CDCl_3$)** δ 192.9, 182.7, 156.5, 146.7, 141.8, 141.0, 139.7, 136.8, 132.7, 132.3, 131.3, 129.8, 129.1, 129.0, 128.8, 128.7, 128.7, 128.6, 128.1, 127.9, 127.6, 127.6, 127.5, 127.4, 127.0, 121.4, 76.8, 50.5, 39.8.; **FTIR (neat)** 3061, 2923, 2852, 1693, 1642, 1495, 754 cm^{-1}; **HRMS (ESI)** calculated for $C_{37}H_{29}NO_2S$ $[M+H]^+$: 552.1994; found: 552.1974; **HPLC** condition: HPLC Chiralpak -IA, Hexane/i-PrOH = 80:20 v/v, flow rate = 1.0 mL/min, λ = 310 nm, 25 °C, t_R (major) = 8.02, t_R (minor) = 16.00 min, >99% *ee*, $[\alpha]_D^{20}$ = +125.23 (c 0.5, CH_2Cl_2).

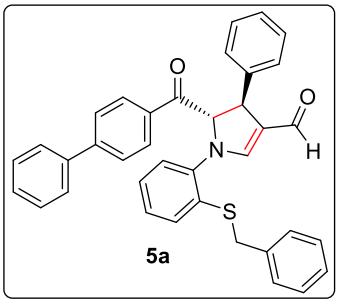

5-Benzoyl-1-(2-(benzylthio)phenyl)-4-phenyl-1*H*-pyrrole-3-carbaldehyde 5b; Prepared according to general procedure E using chiral product**4o**, purification of the crude product by column chromatography using (HX/EA) mixture (70:30) to afford the title compound as pale yellow solid, (95% yield, 105mg); R_f

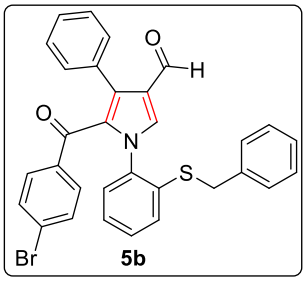

= 0.51 (20 % ethyl acetate in hexane); mp: 110 - 112 °C; **^{1}H NMR (500 MHz, $CDCl_3$)** δ 9.80 (m, 2H), 7.43 – 7.34 (m, 7H), 7.24 – 7.17 (m, 3H), 7.17 – 7.10 (m, 7H), 7.00 (d, *J* = 6.5 Hz, 2H), 3.99 – 3.83 (m, 2H); **^{13}C NMR (125 MHz, $CDCl_3$)** δ 186.5, 185.9, 138.9, 136.1, 135.9, 134.2, 133.0, 132.1, 131.5, 131.5, 131.0, 130.8, 130.3, 129.5, 128.8, 128.6, 128.0, 127.8, 127.7, 127.5, 127.2, 127.1, 125.8, 123.3, 38.5.; **FTIR (neat)** 3061, 2929, 1683, 1641, 1471, 1413, 1285, 771 cm^{-1}; **HRMS (ESI)** calculated for $C_{31}H_{22}BrNO_2S$ $[M+H]^+$: 552.0627; found: 552.0604.

3.12. X-RAY CRYSTALLOGRAPHY DATA

Figure 3.3 X-ray crystallographic data for compound 4o':

All the single crystals X-ray data was collected with a Bruker AXS (Kappa Apex 2) CCD diffractometer equipped with graphite monochromatic Mo (Kα) (λ = 0.7107 A) radiation source. The data were collected with 100% completeness for Θ up to 25º. ω and ϕ scans were employed to collect the data. The frame width for ω for was fixed to 0.5º for data collection. The crystals were solved by direct methods using Bruker SHELXS (Sheldrick, 1997). The Structure was refined using the Bruker SHELXTL (Version 6.12) software package.

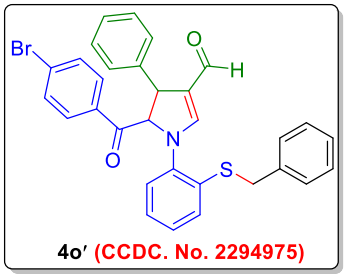

The purified compound **4o' racemic** was dissolved in acetonitrile 0.1 M and placed in a dark cabinet for slow evaporation. Crystals were collected after a few days for X-ray analysis. Thermal ellipsoids are shown at the 50% probability level.

Table 3.4. Crystal data and structure refinement for 4o' racemic

Identification code	88	
Empirical formula	$C_{31}H_{24}BrNO_2S$	
Formula weight	554.48	
Temperature	296(2) K	
Wavelength	0.71073 Å	
Crystal system	Triclinic	
Space group	P -1	
Unit cell dimensions	a = 8.2477(2) Å	α = 80.6827(13)°
	b = 10.7805(3) Å	β = 78.5517(12)°
	c = 15.3993(4) Å	γ = 76.5102(12)°
Volume	1295.32(6) $Å^3$	
Z	2	
Density (calculated)	1.422 g cm^{-3}	
Absorption coefficient	1.697 mm^{-1}	
F(000)	568	
Crystal size	0.250 x 0.220 x 0.130 mm^3	
Theta range for data collection	1.957 to 24.996°	
Index ranges	-8<=h<=9, -12<=k<=12, -18<=l<=18	
Reflections collected	18359	
Independent reflections	4552 [R(int) = 0.0253]	
Completeness to theta = 24.996°	100.0 %	
Refinement method	Full-matrix least-squares on F^2	
Data / restraints / parameters	4552 / 0 / 325	

Goodness-of-fit on F^2	1.272
Final R indices [I>2sigma(I)]	R1 = 0.0296, wR2 = 0.0706
R indices (all data)	R1 = 0.0419, wR2 = 0.0736
Extinction coefficient	n/a
Largest diff. peak and hole	0.284 and -0.432 e.$Å^{-3}$

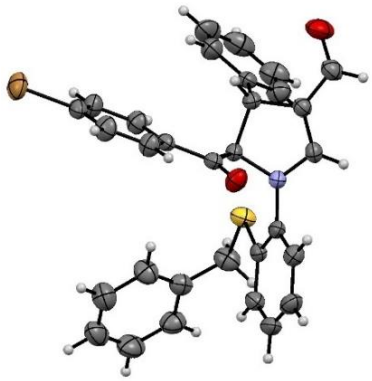

Figure caption: ORTEP diagram of compound **4o'** (88) displacement ellipsoids are drawn at the 50% probability level, and H atoms are shown as small spheres of arbitrary radius. The absolute configuration of the compound was assigned based on the anomalous dispersion method.

Figure 3.4 X-ray crystallographic data for compound 4q:

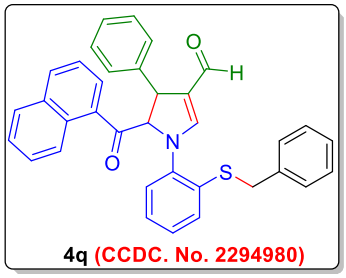

The purified compound **4q chiral** was dissolved in acetonitrile 0.1 M and placed in a dark cabinet for slow evaporation. Crystals were collected after a few days for X-ray analysis. Thermal ellipsoids are shown at the 50% probability level.

Table 3.5. Crystal data and structure refinement for 4q chiral

Identification code	47	
Empirical formula	$C_{35}H_{27}NO_2S$	
Formula weight	525.63	
Temperature	296(2) K	
Wavelength	0.71073 Å	
Crystal system	Orthorhombic	
Space group	$P2_12_12_1$	
Unit cell dimensions	a = 8.8836(16) Å	α = 90°
	b = 11.1569(18) Å	β = 90°
	c = 27.770(4) Å	γ = 90°
Volume	2752.4(8) $Å^3$	
Z	4	
Density (calculated)	1.268 g cm^{-3}	
Absorption coefficient	0.151 mm^{-1}	
F(000)	1104	
Crystal size	0.180 x 0.160 x 0.120 mm^3	
Theta range for data collection	1.467 to 24.997°	
Index ranges	-10<=h<=9, -13<=k<=13, -33<=l<=28	
Reflections collected	15955	
Independent reflections	4847 [R(int) = 0.0243]	
Completeness to theta = 24.997°	100.0 %	
Refinement method	Full-matrix least-squares on F^2	

Data / restraints / parameters	4847 / 0 / 352
Goodness-of-fit on F^2	1.264
Final R indices [I>2sigma(I)]	R1 = 0.0398, wR2 = 0.0980
R indices (all data)	R1 = 0.0489, wR2 = 0.1020
Absolute structure parameter	-0.02(3)
Extinction coefficient	n/a
Largest diff. peak and hole	0.287 and -0.283 e.Å^{-3}

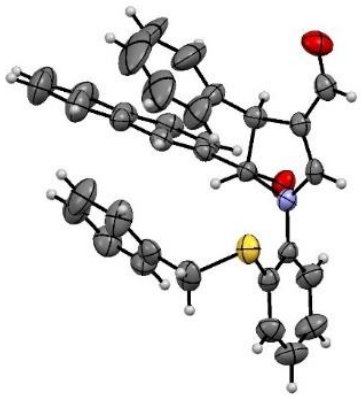

Figure caption: ORTEP diagram of compound **4q** (47) displacement ellipsoids are drawn at the 50% probability level, and H atoms are shown as small spheres of arbitrary radius. The absolute configuration of the compound was assigned based on the anomalous dispersion method.

3.13 ^{1}H and ^{13}C NMR SPECTRA

(4*S*,5*S*)-5-(4-Bromobenzoyl)-1-(2-(methylthio)phenyl)-4-phenyl-4,5-dihydro-1*H*-pyrrole-3-carbaldehyde 4a

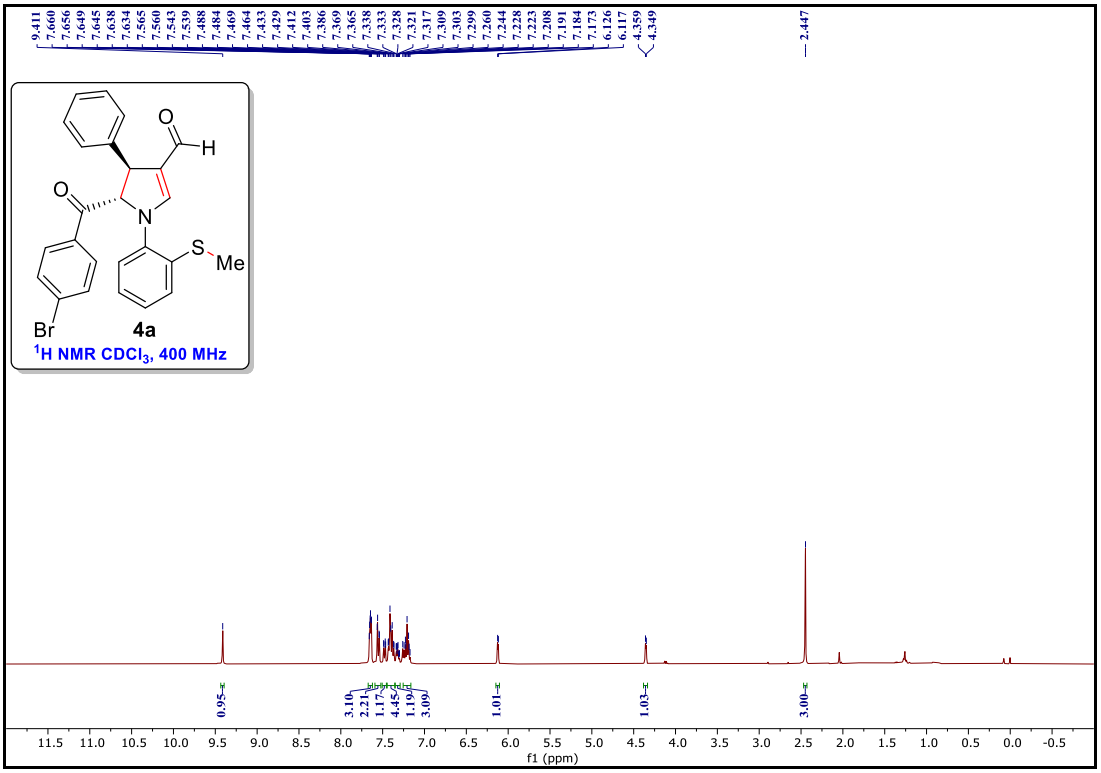

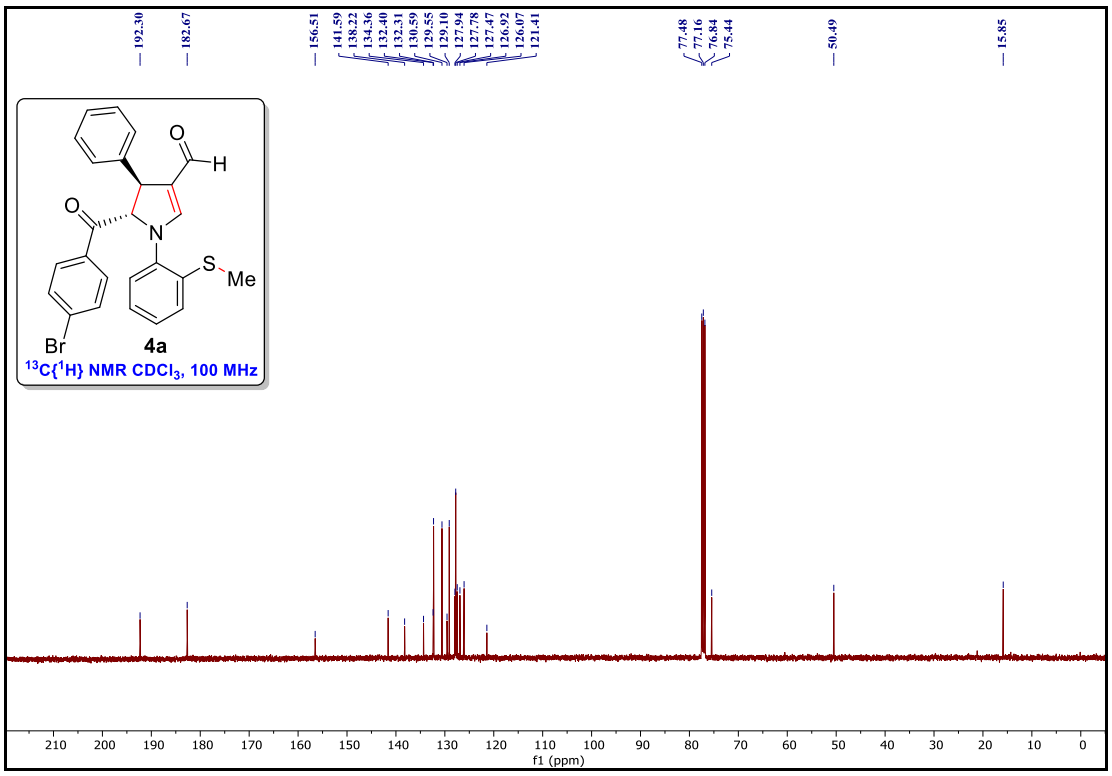

(4*S*,5*S*)-5-(4-Bromobenzoyl)-1-(2-(ethylthio)phenyl)-4-phenyl-4,5-dihydro-1*H*-pyrrole-3-carbaldehyde 4b

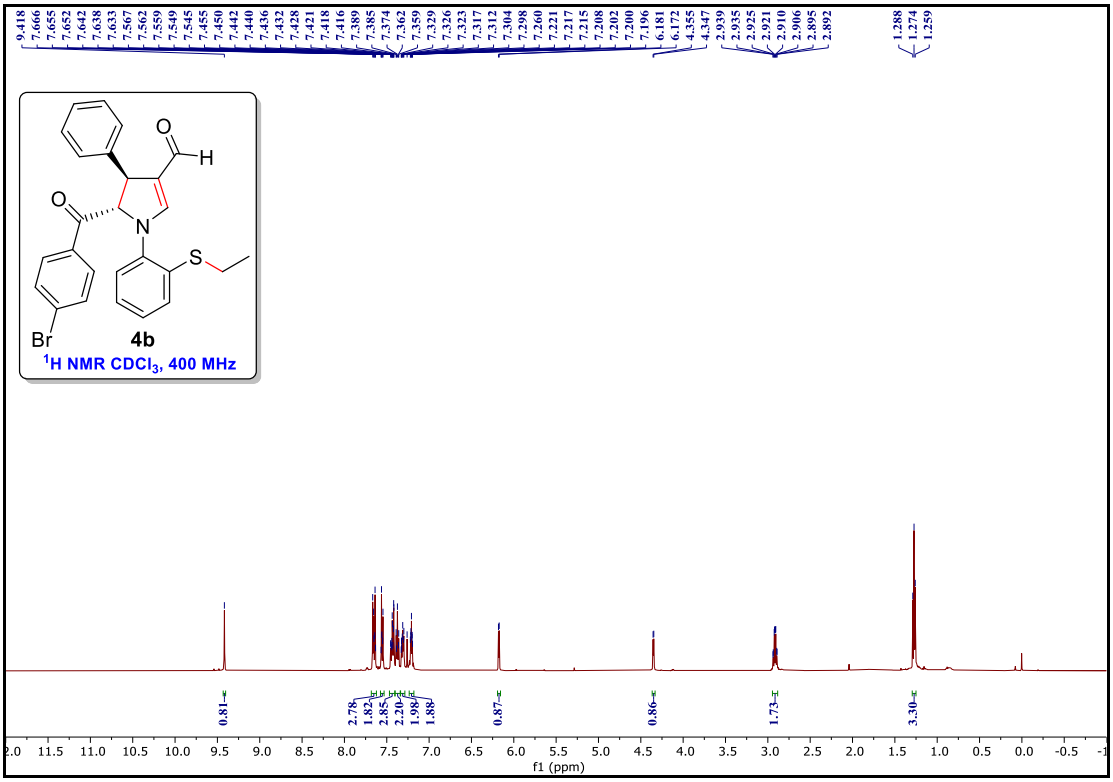

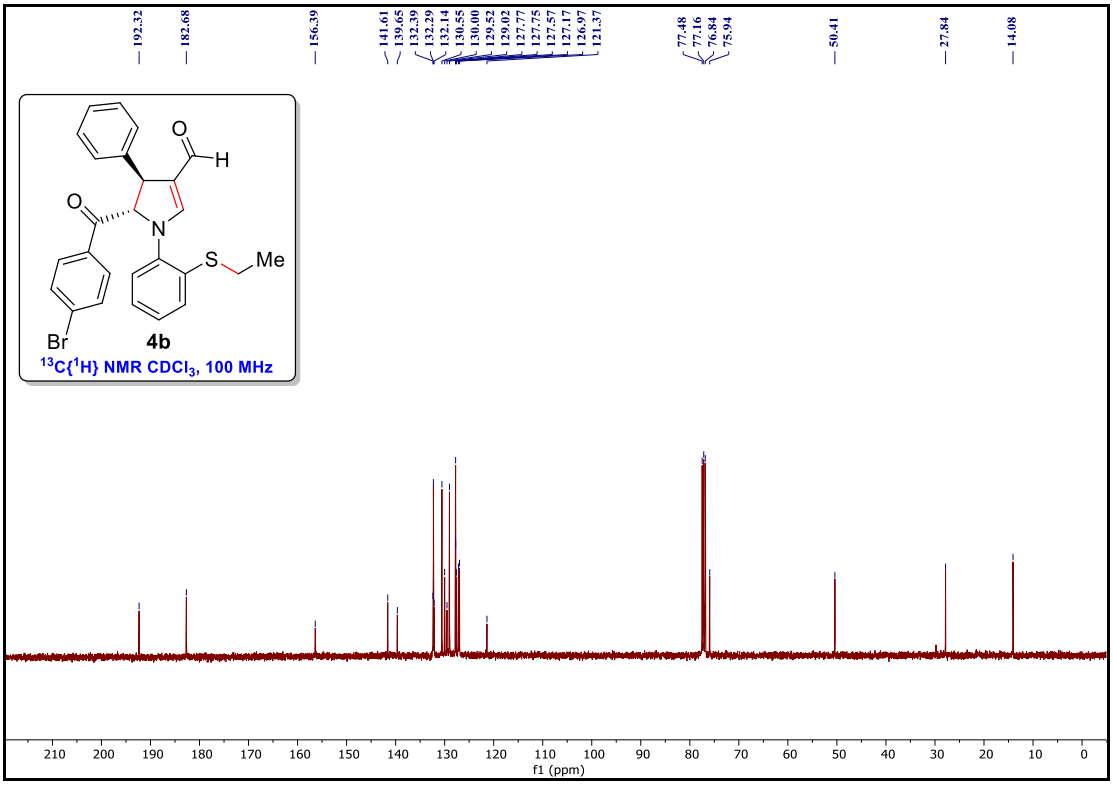

(4*S*,5*S*)-5-(4-Bromobenzoyl)-1-(2-(isopropylthio)phenyl)-4-phenyl-4,5-dihydro-1*H*-pyrrole-3-carbaldehyde 4c

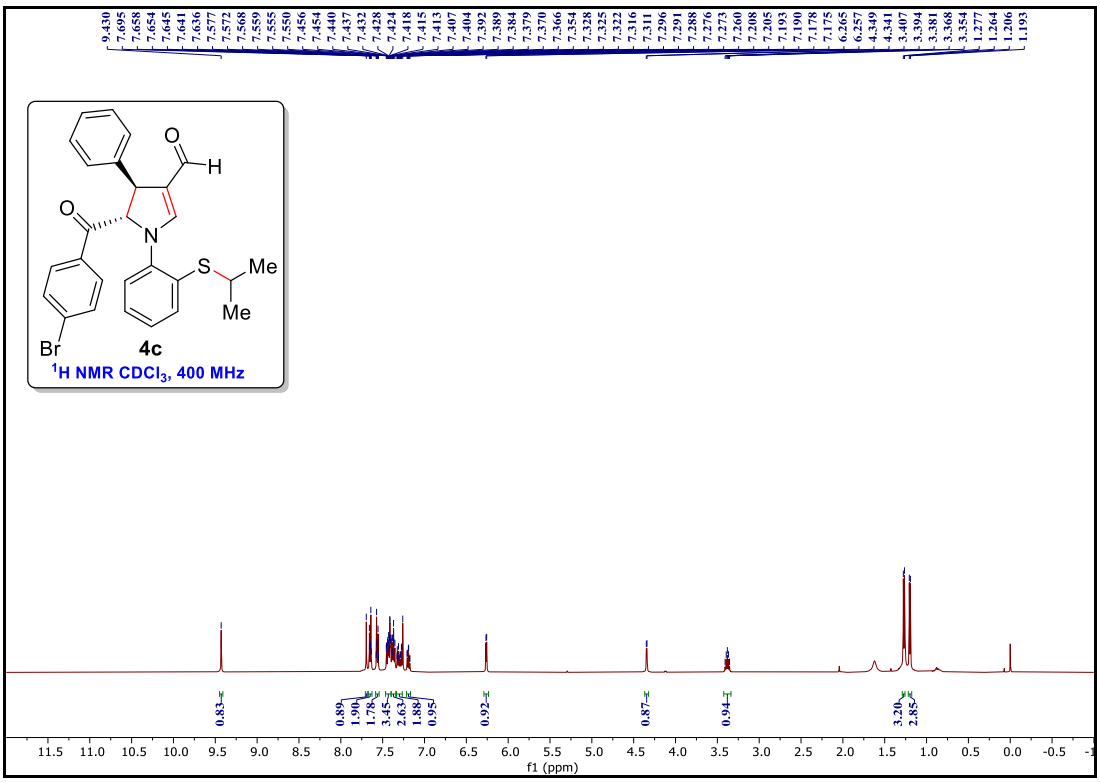

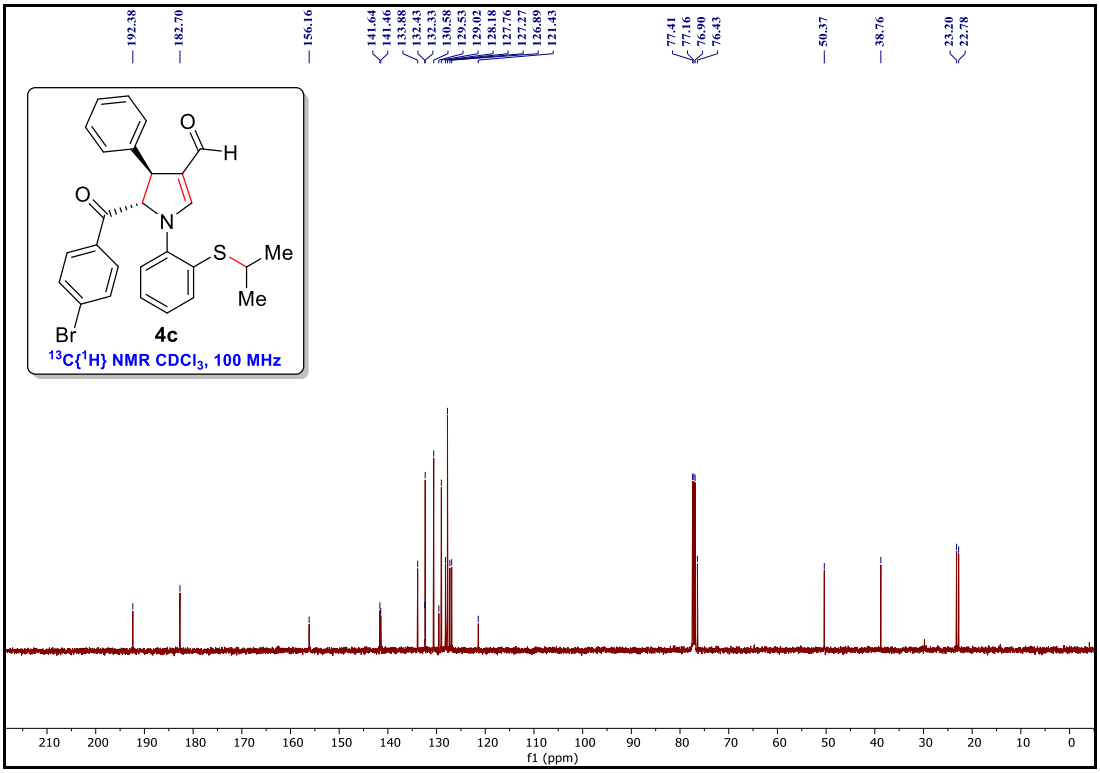

(4*S*,5*S*)-1-(2-(Allylthio)phenyl)-5-(4-bromobenzoyl)-4-phenyl-4,5-dihydro-1*H*-pyrrole-3-carbaldehyde 4d

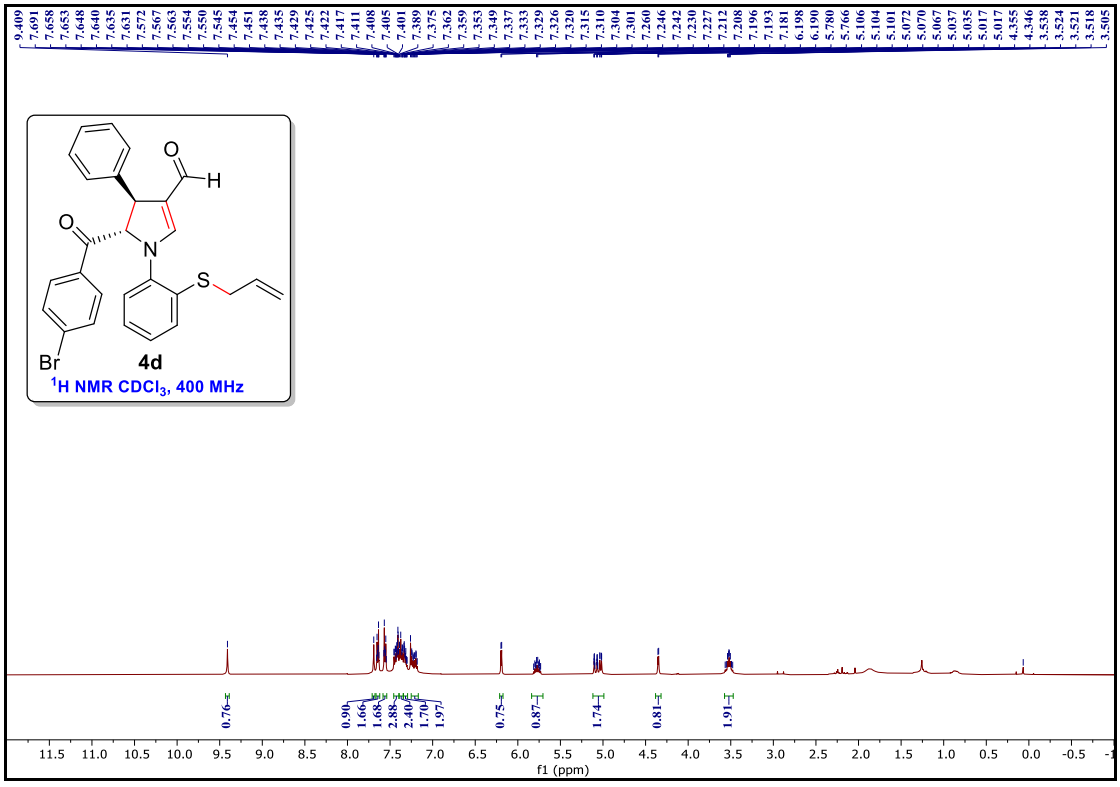

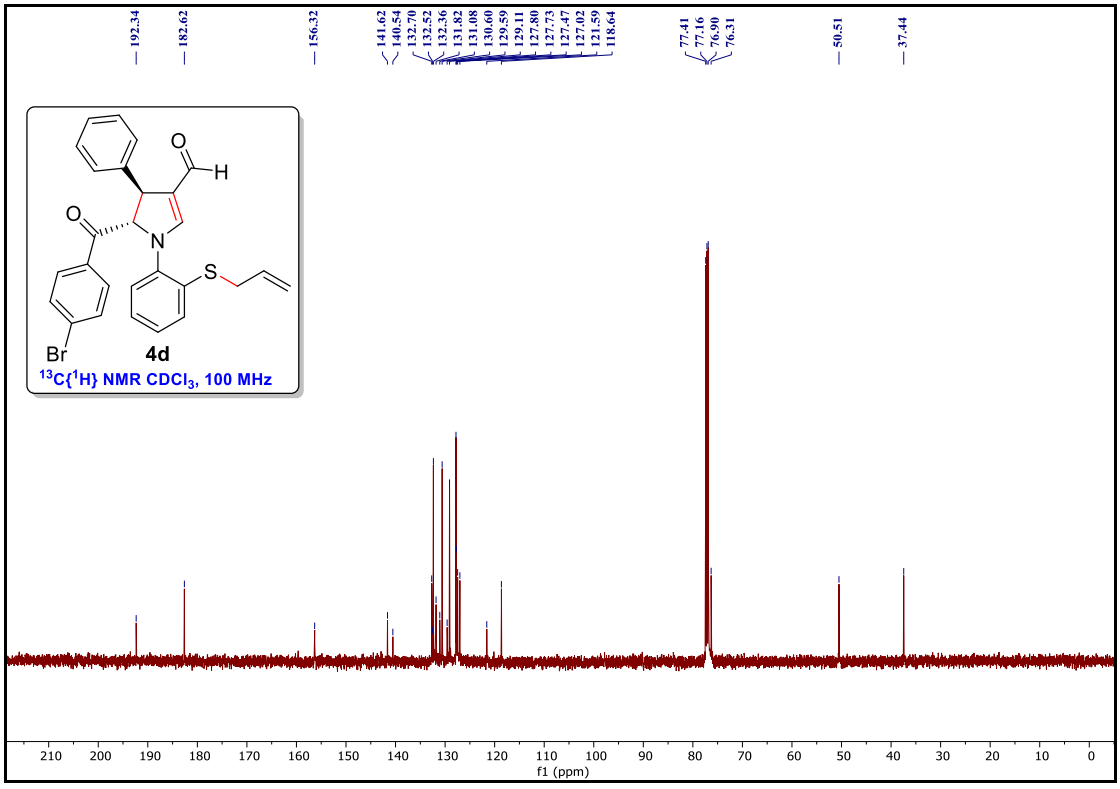

(4*S*,5*S*)-1-(2-(Benzylthio)phenyl)-5-(4-methoxybenzoyl)-4-phenyl-4,5-dihydro-1*H*-pyrrole-3-carbaldehyde 4n

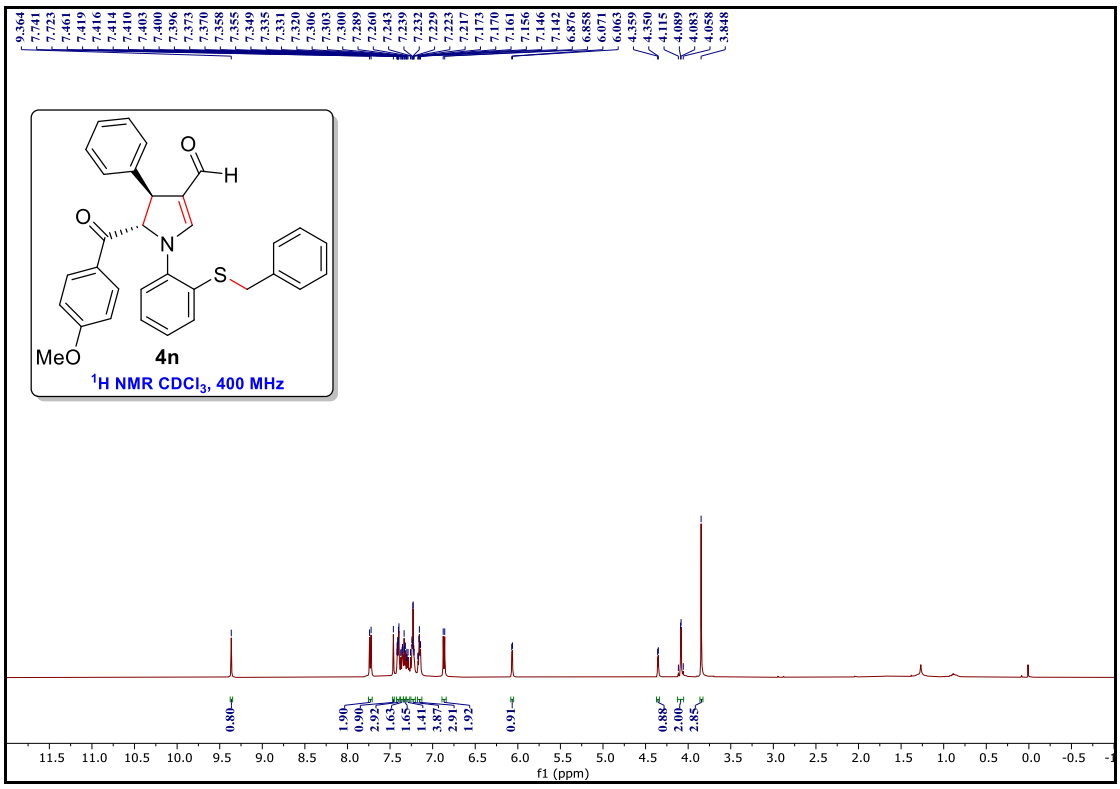

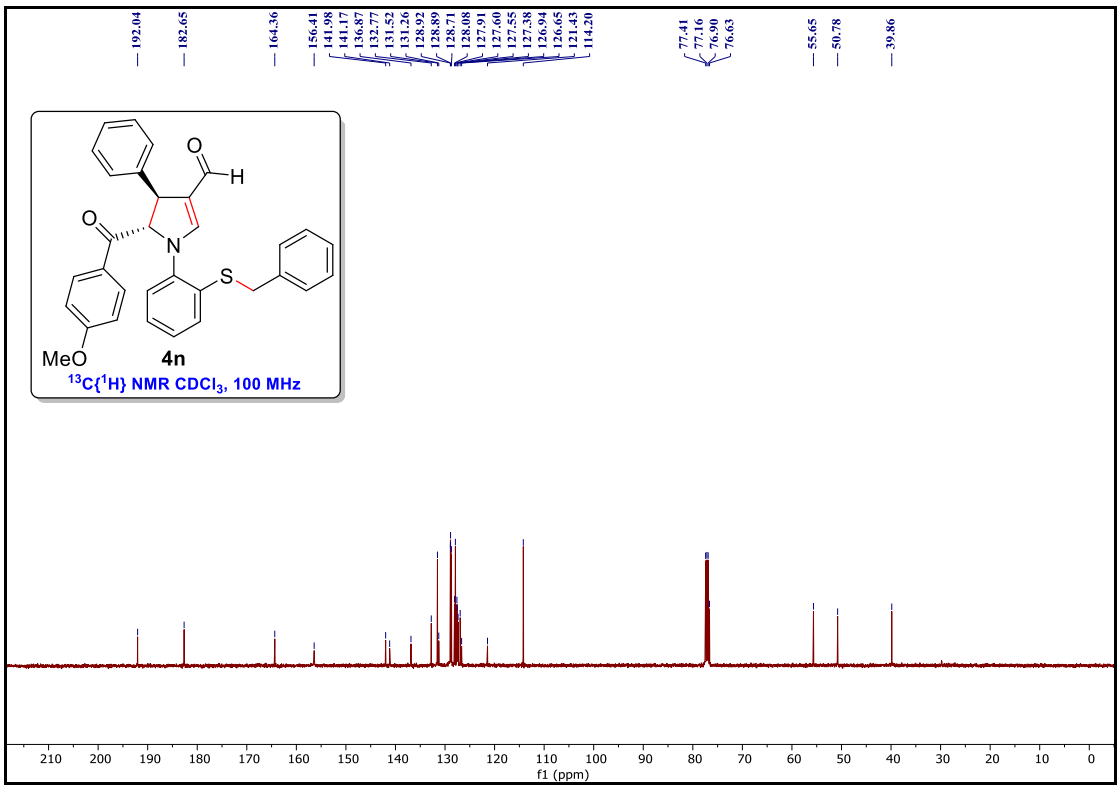

(4*S*,5*S*)-1-(2-(Benzylthio)phenyl)-5-(4-bromobenzoyl)-4-phenyl-4,5-dihydro-1*H*-pyrrole-3-carbaldehyde 4o

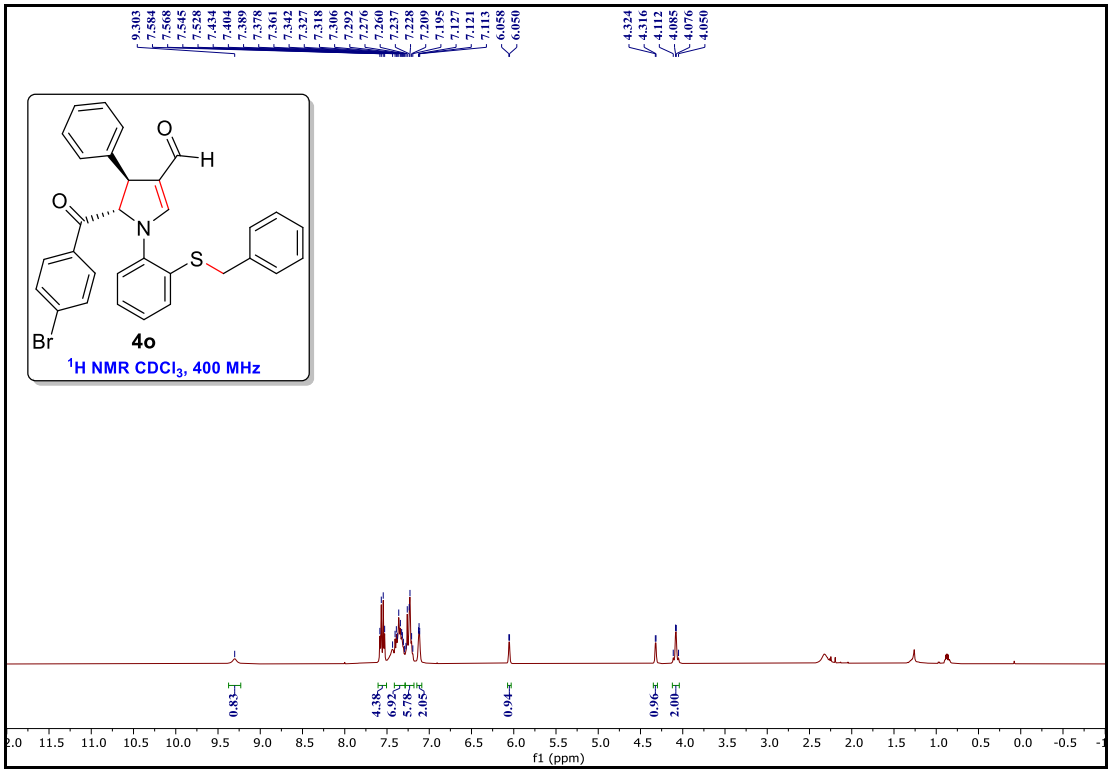

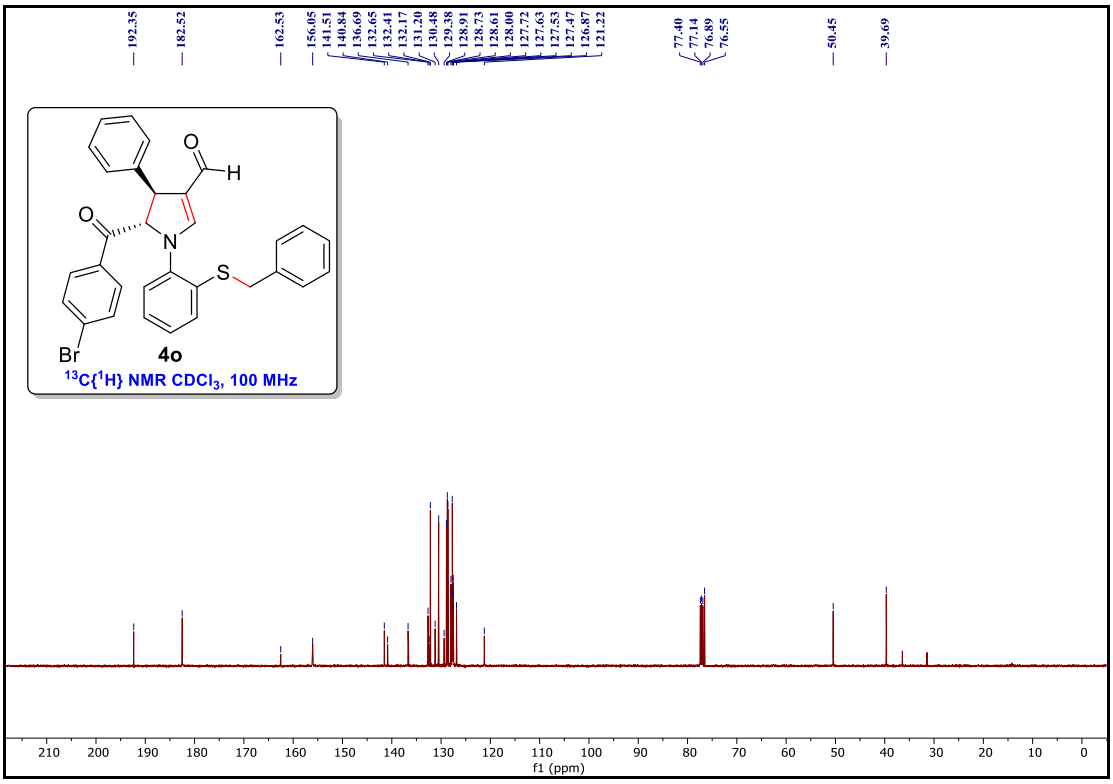

(4*S*,5*S*)-5-(1-Naphthoyl)-1-(2-(benzylthio)phenyl)-4-phenyl-4,5-dihydro-1*H*-pyrrole-3-carbaldehyde 4q

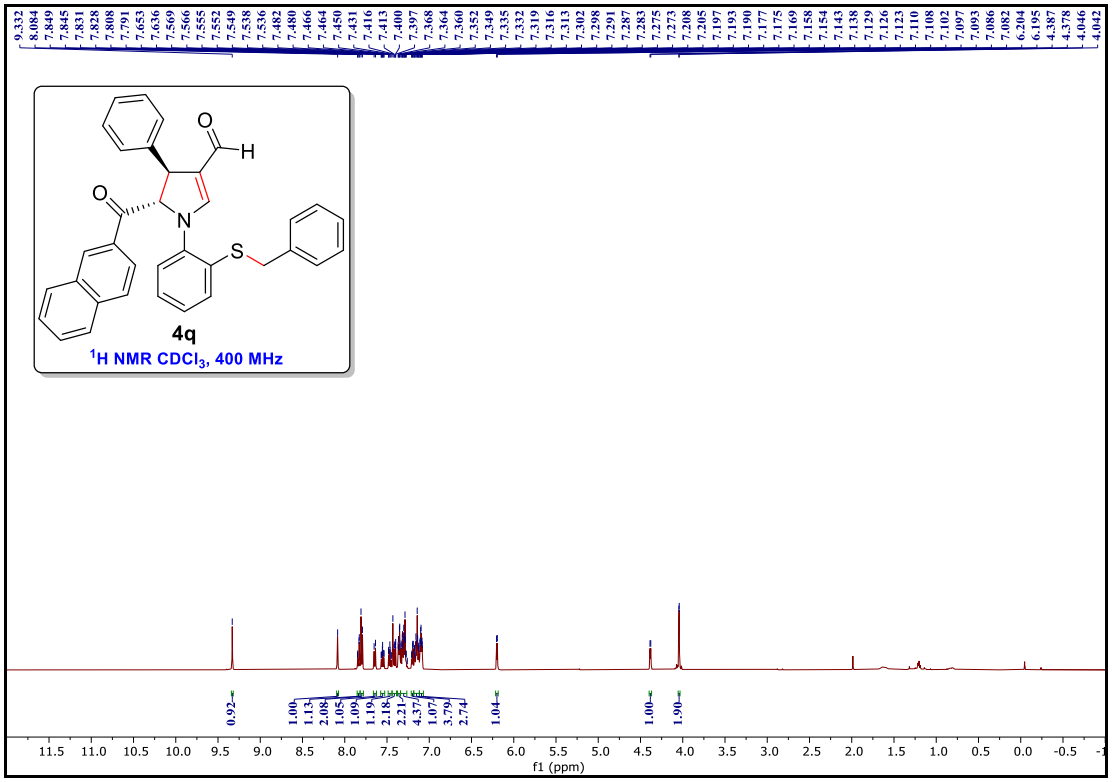

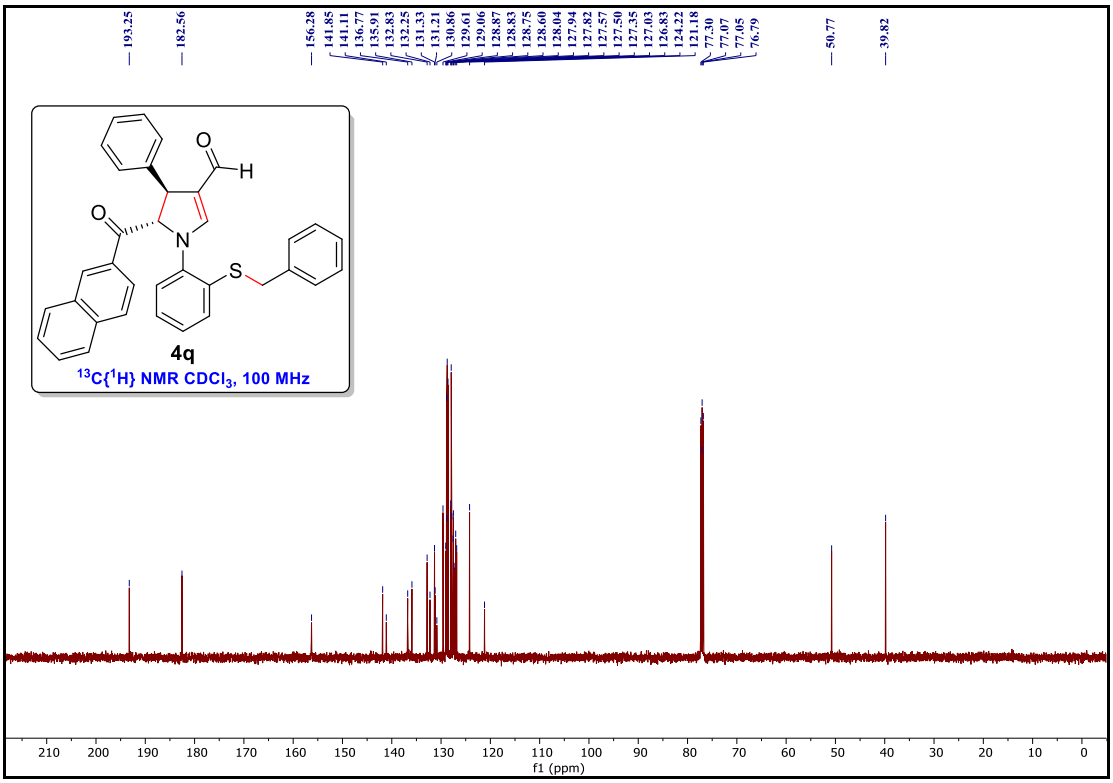

(4*S*,5*S*)-1-(2-(Benzylthio)phenyl)-5-(4-bromobenzoyl)-4-(*p*-tolyl)-4,5-dihydro-1*H*-pyrrole-3-carbaldehyde 4r

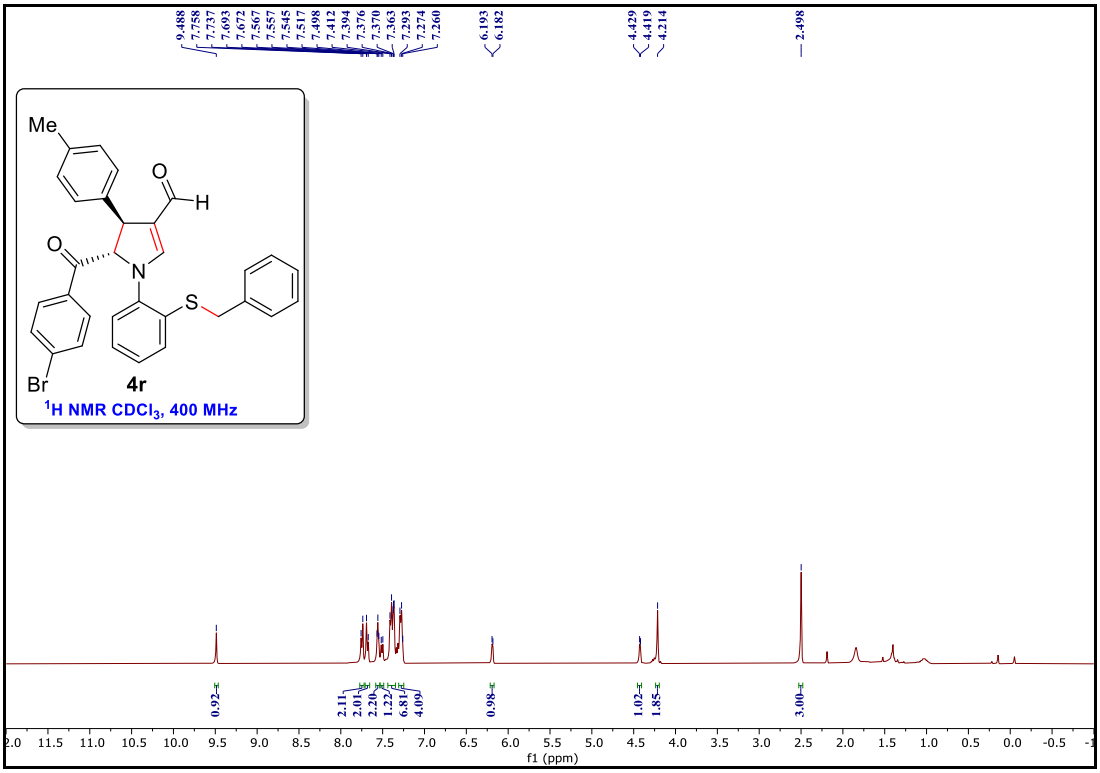

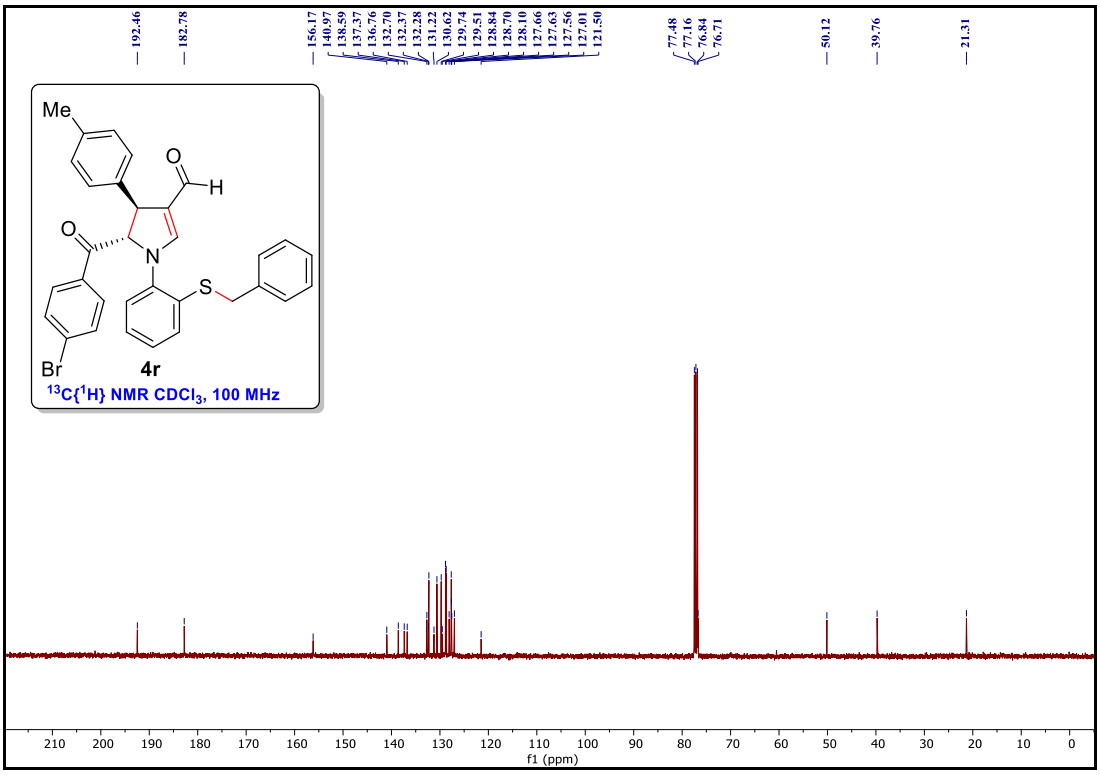

(4*S*,5*S*)-1-(2-(Benzylthio)phenyl)-5-(4-bromobenzoyl)-4-methyl-4,5-dihydro-1*H*-pyrrole-3-carbaldehyde 4s

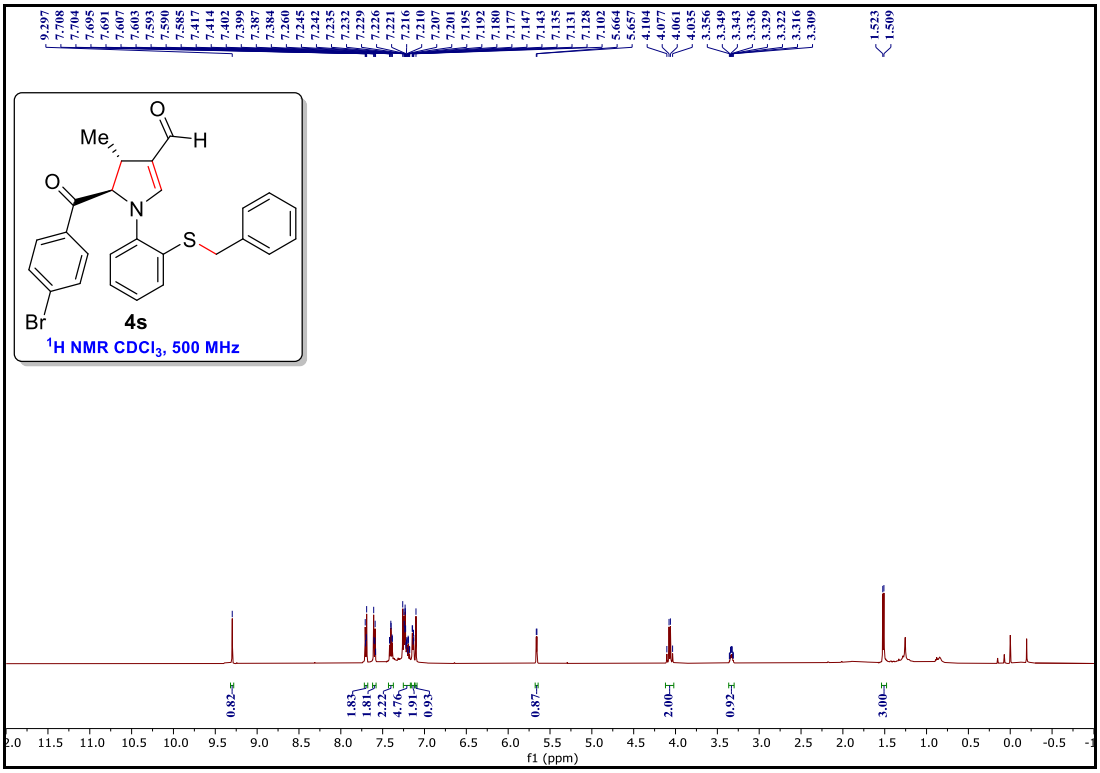

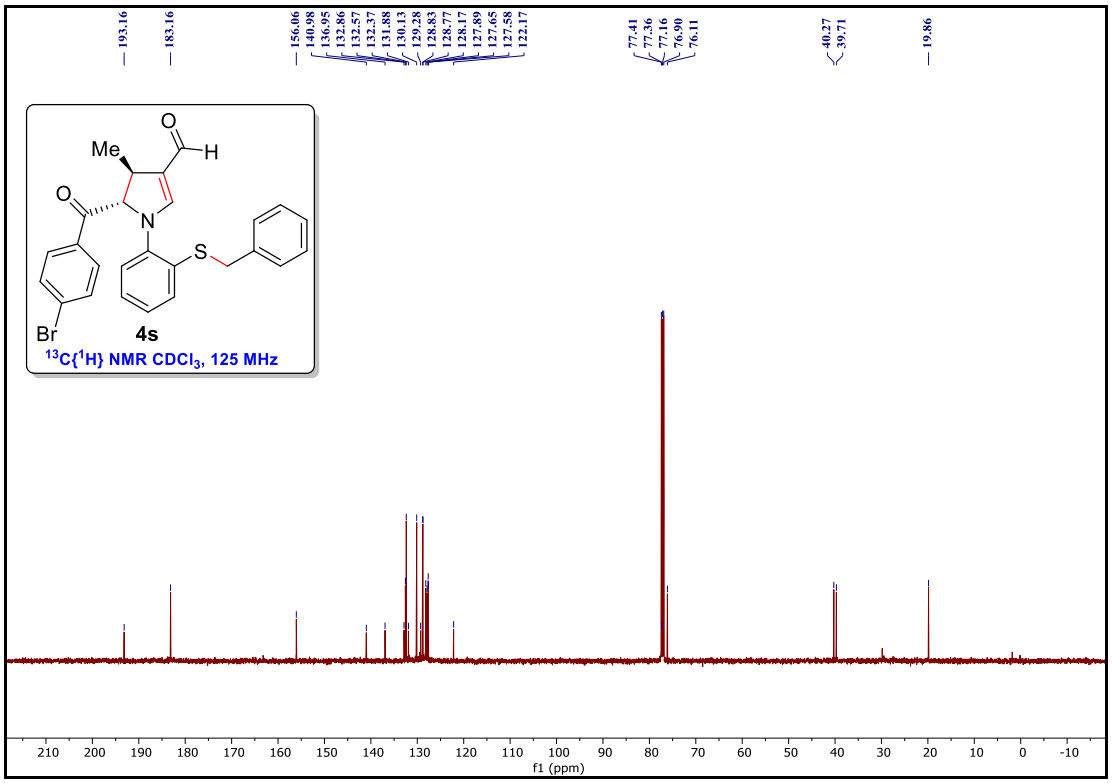

(4*S*,5*S*)-1-(2-(Benzylthio)phenyl)-5-(4-chlorobenzoyl)-4-(4-nitrophenyl)-4,5-dihydro-1*H*-pyrrole-3-carbaldehyde 4u

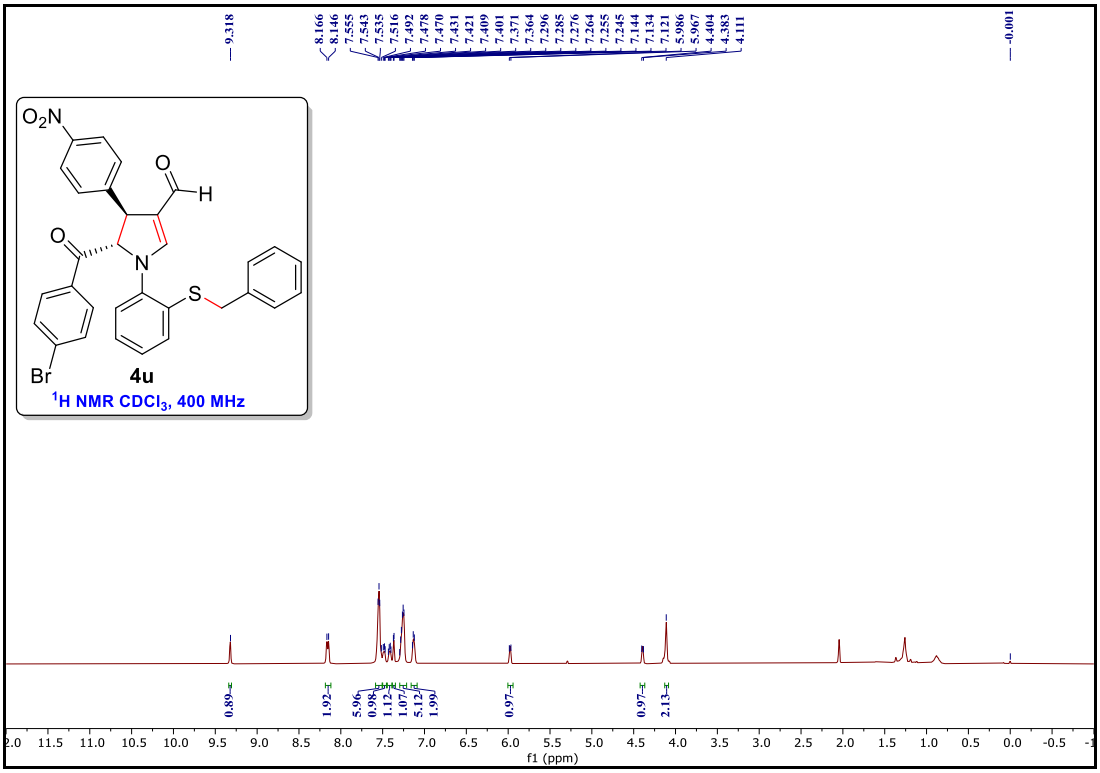

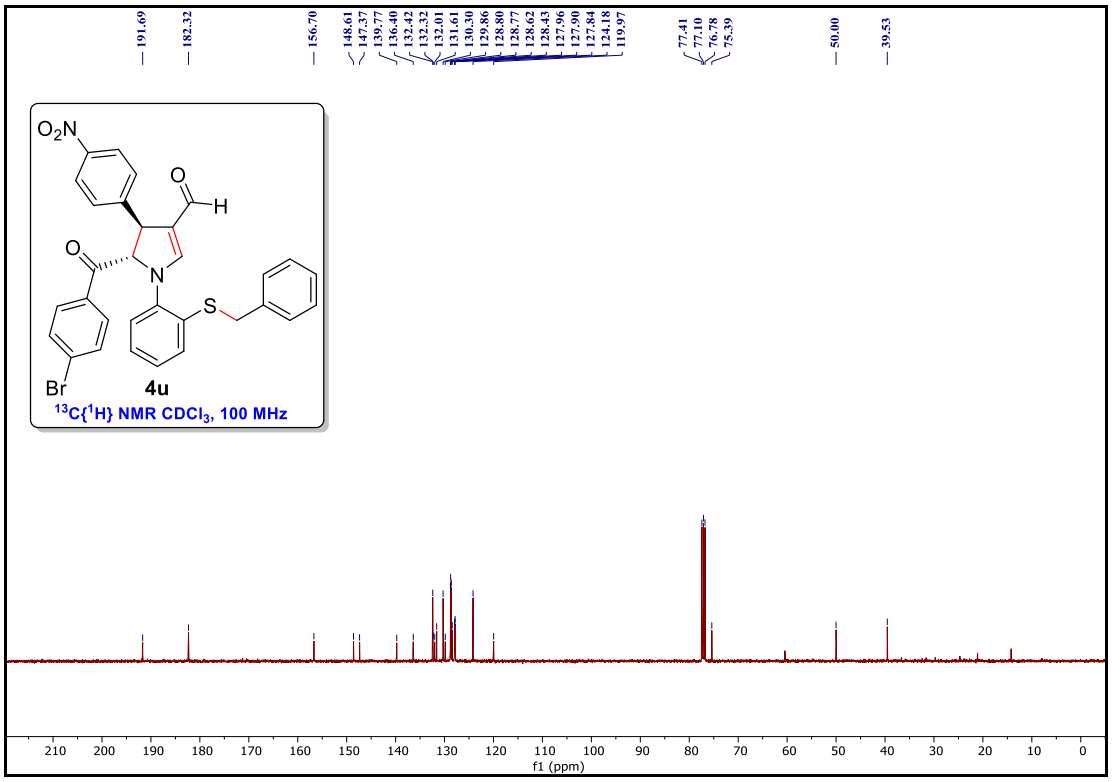

(4*S*,5*S*)-5-(4-Bromobenzoyl)-1-(2-(methylthio)phenyl)-4-phenyl-4,5-dihydro-1*H*-pyrrole-3-carbaldehyde 4v

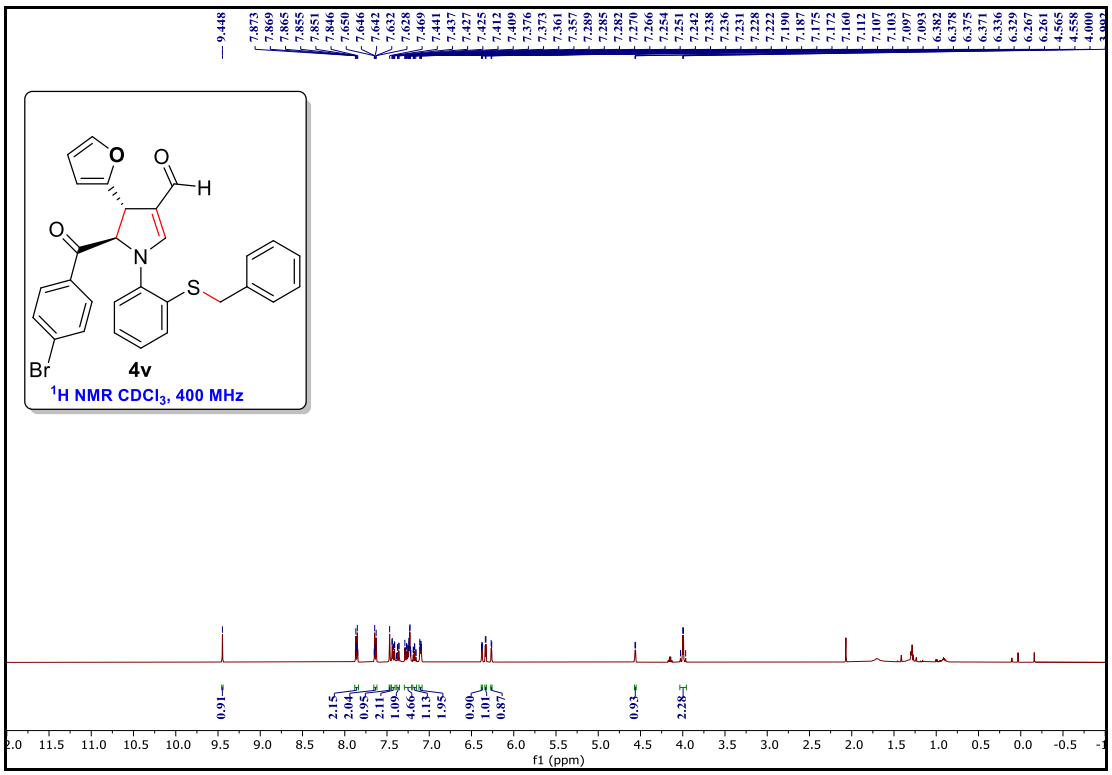

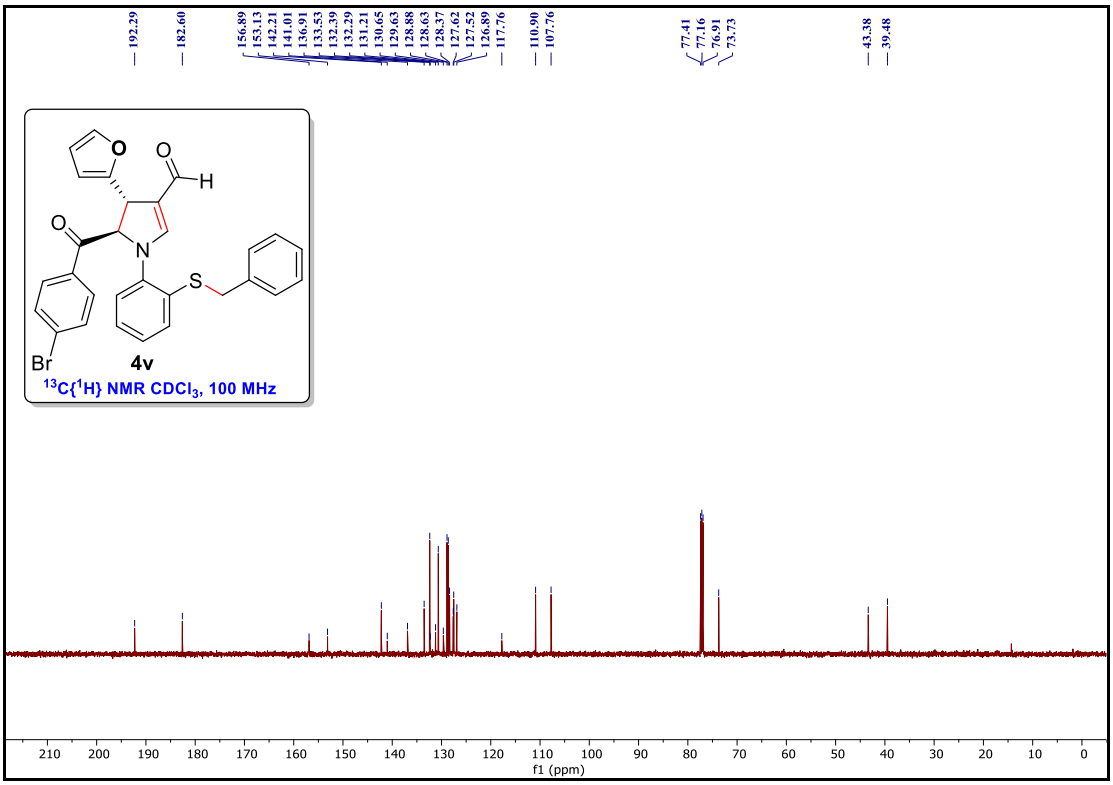

(4*S*,5*S*)-5-([1,1'-Biphenyl]-4-carbonyl)-1-(2-(benzylthio)phenyl)-4-phenyl-4,5-dihydro-1*H*-pyrrole-3-carbaldehyde 5a

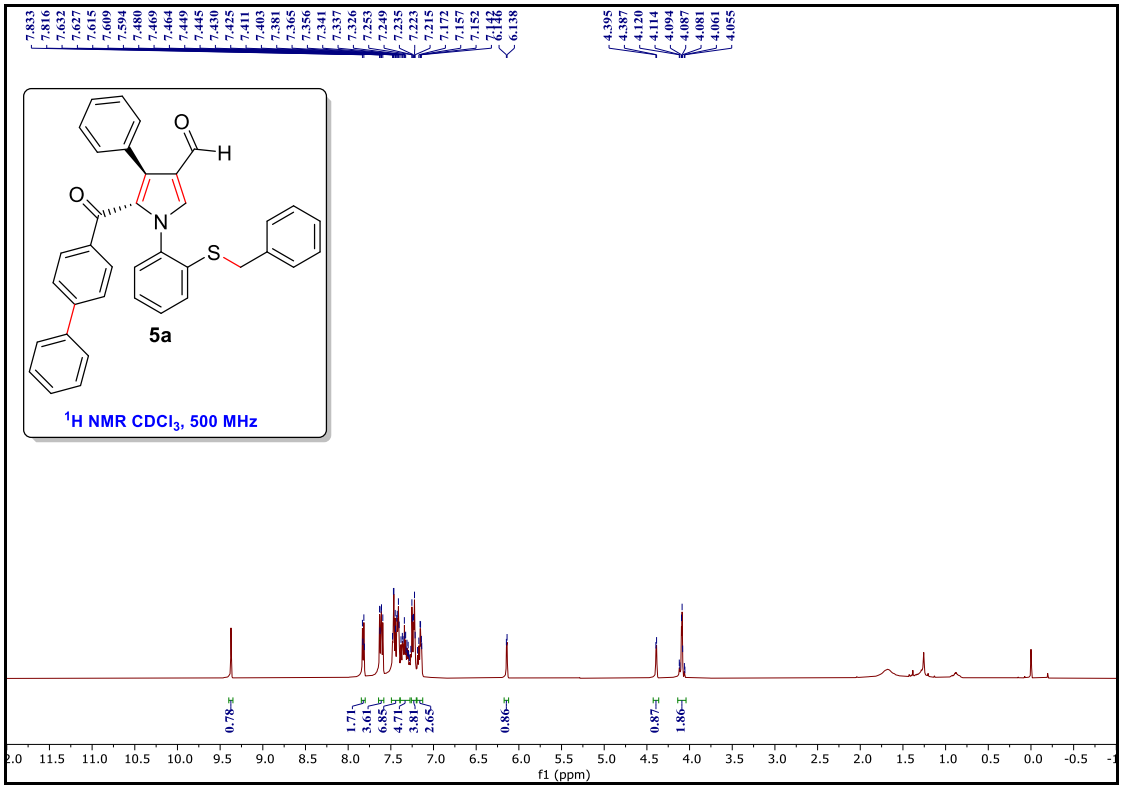

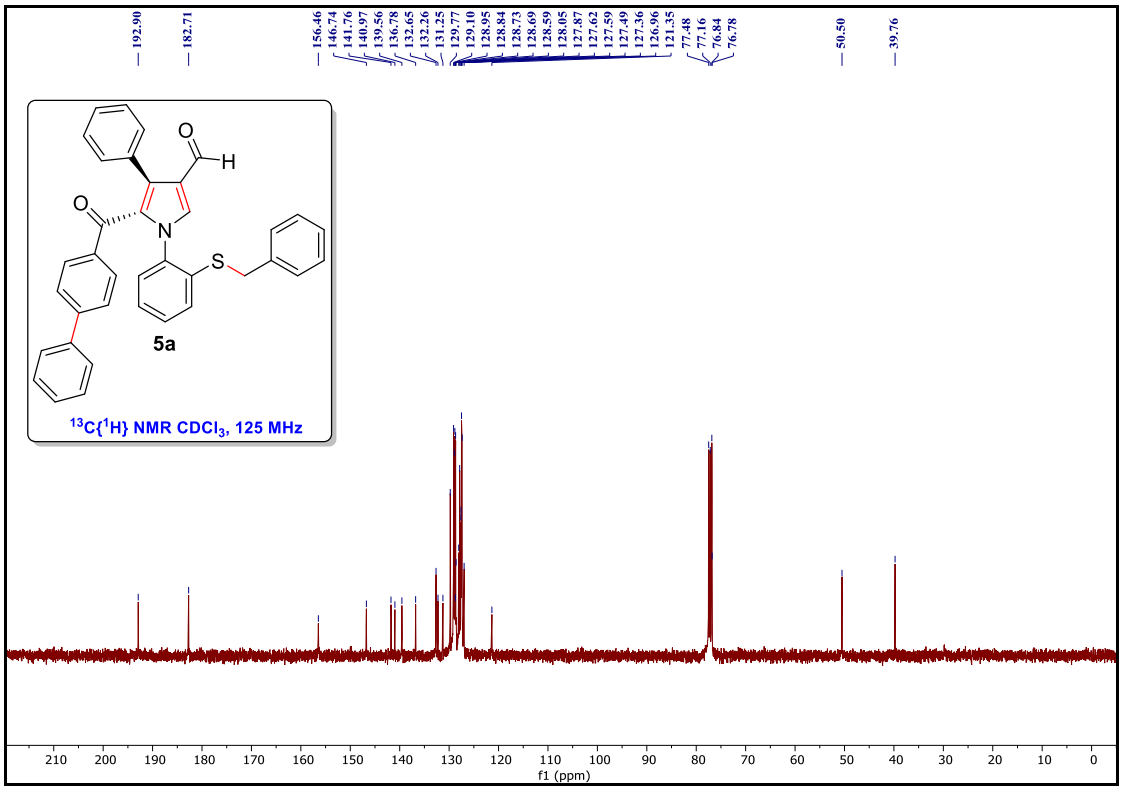

5-Benzoyl-1-(2-(benzylthio)phenyl)-4-phenyl-1H-pyrrole-3-carbaldehyde 5b

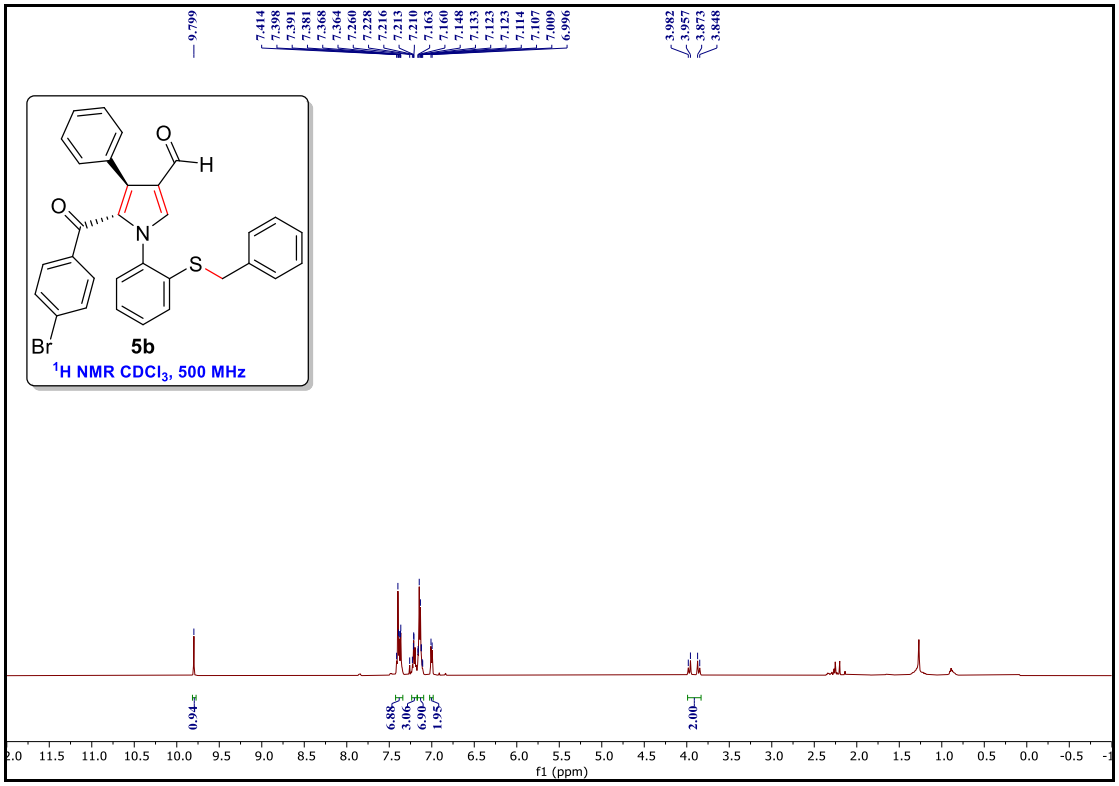

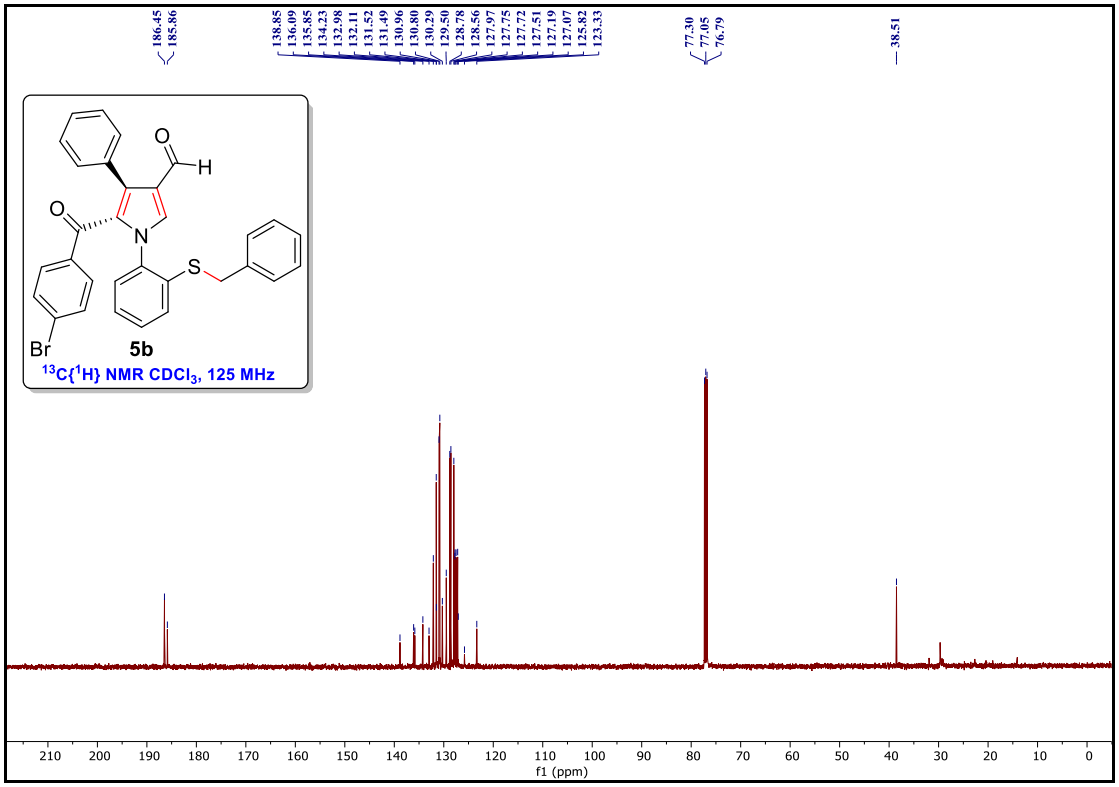

3.14 HPLC CHROMATOGRAMS

(±)-4a

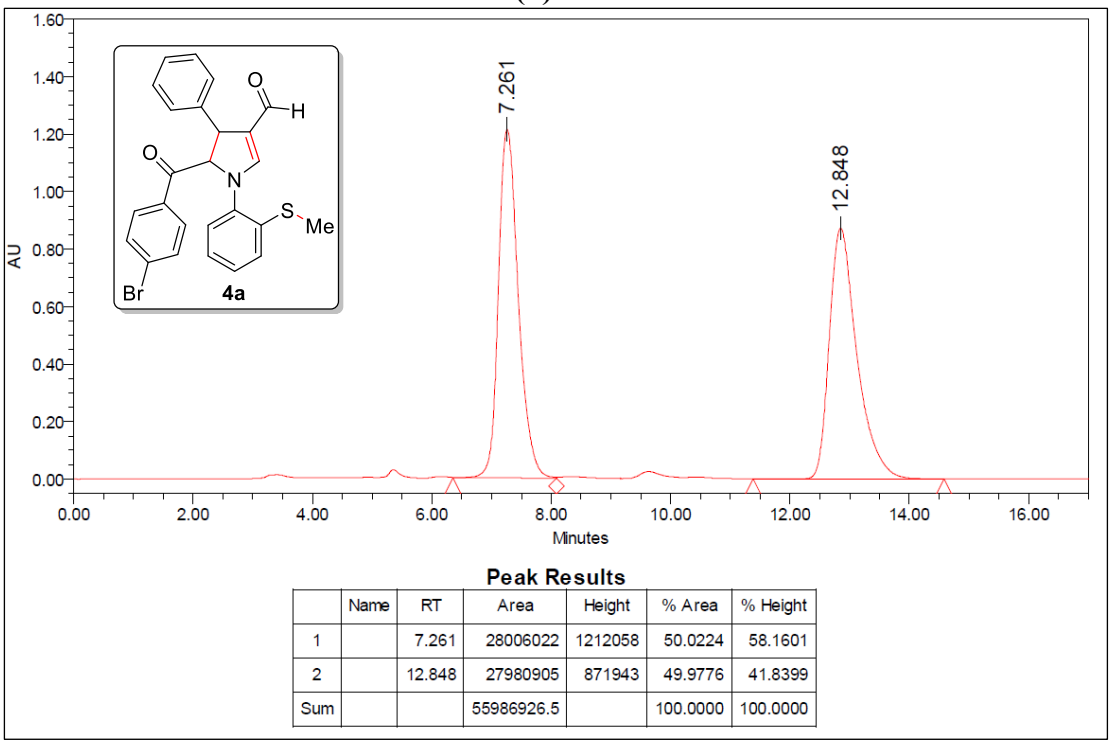

Peak Results

	Name	RT	Area	Height	% Area	% Height
1		7.261	28006022	1212058	50.0224	58.1601
2		12.848	27980905	871943	49.9776	41.8399
Sum			55986926.5		100.0000	100.0000

Optical active 4a

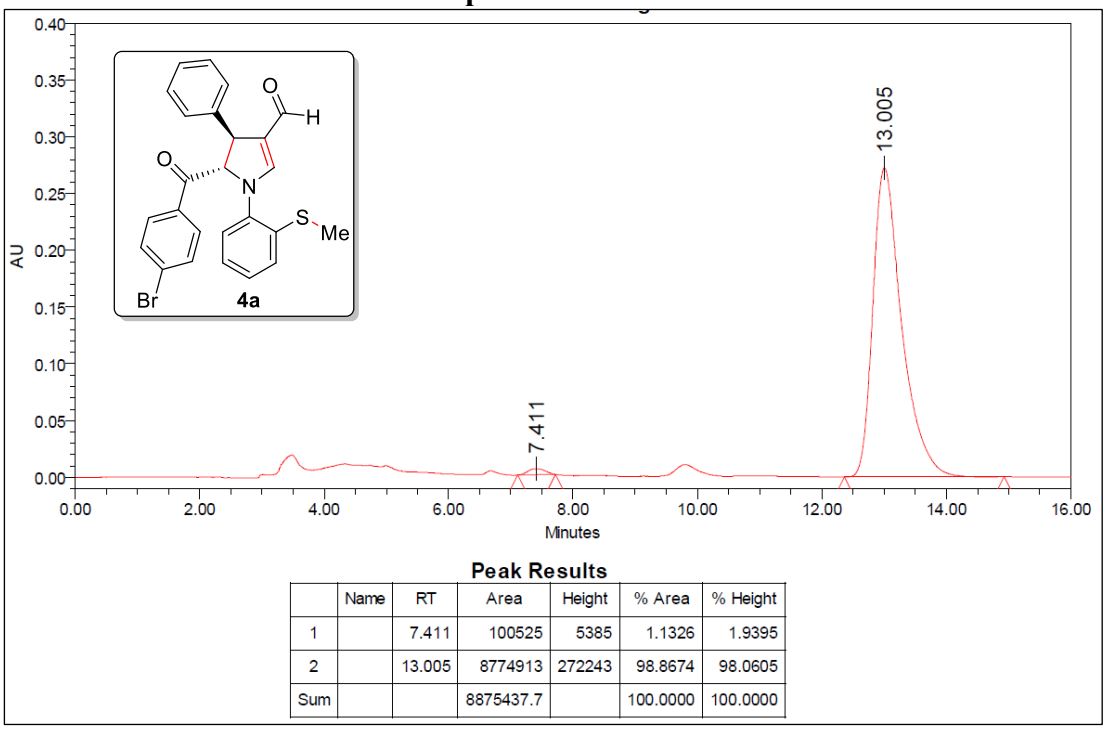

Peak Results

	Name	RT	Area	Height	% Area	% Height
1		7.411	100525	5385	1.1326	1.9395
2		13.005	8774913	272243	98.8674	98.0605
Sum			8875437.7		100.0000	100.0000

(±)-4b

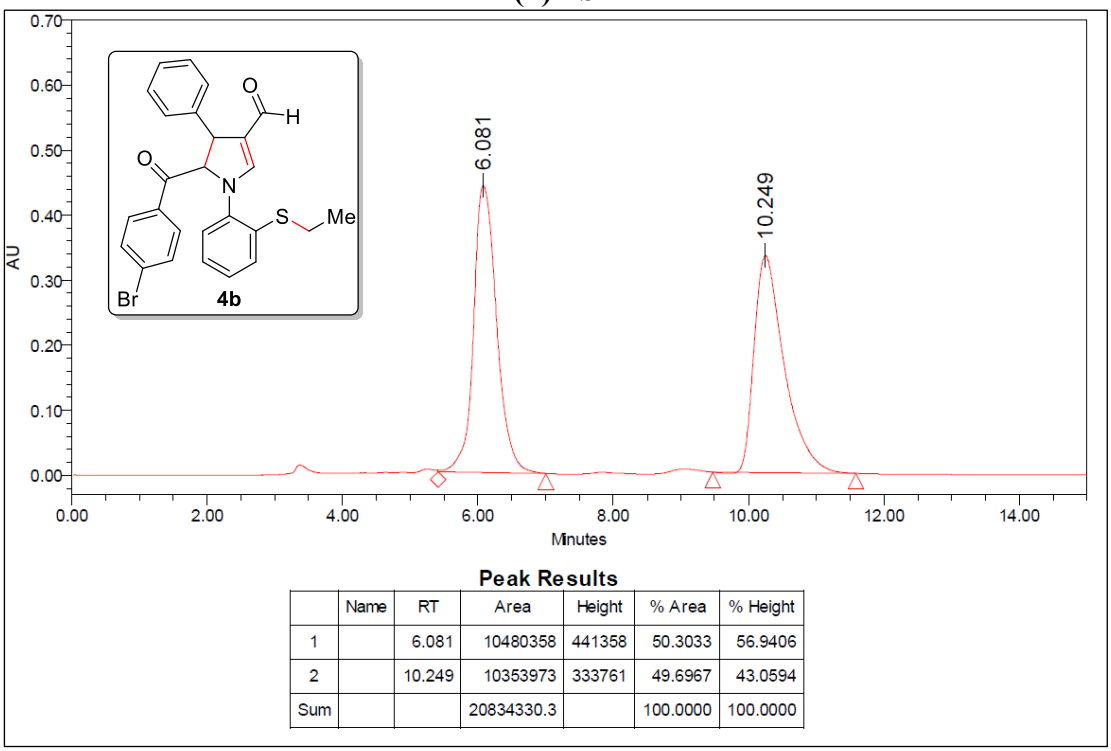

Peak Results

	Name	RT	Area	Height	% Area	% Height
1		6.081	10480358	441358	50.3033	56.9406
2		10.249	10353973	333761	49.6967	43.0594
Sum			20834330.3		100.0000	100.0000

Optical active 4b

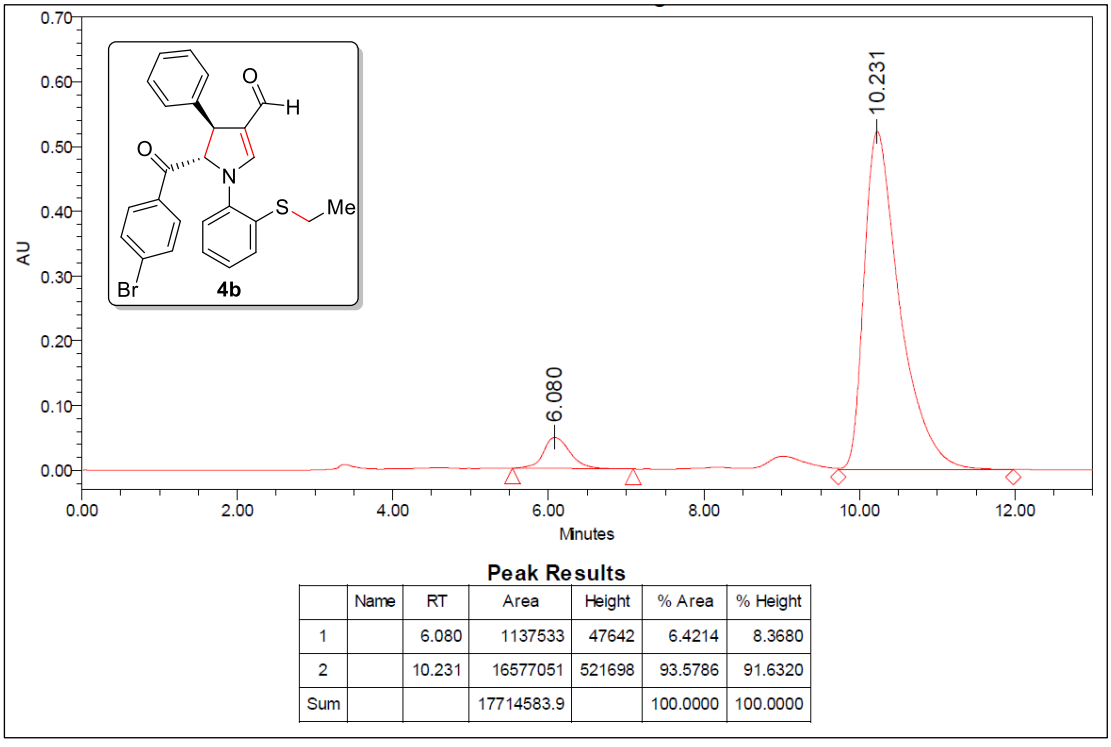

Peak Results

	Name	RT	Area	Height	% Area	% Height
1		6.080	1137533	47642	6.4214	8.3680
2		10.231	16577051	521698	93.5786	91.6320
Sum			17714583.9		100.0000	100.0000

(±)-4c

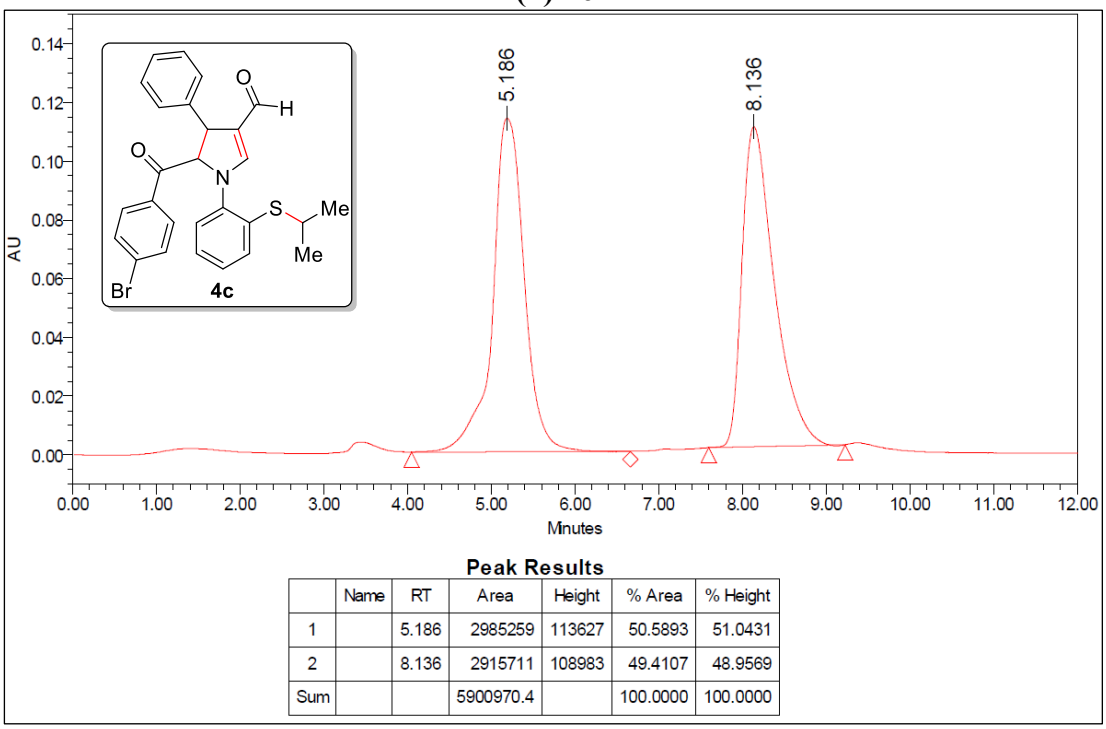

Peak Results

	Name	RT	Area	Height	% Area	% Height
1		5.186	2985259	113627	50.5893	51.0431
2		8.136	2915711	108983	49.4107	48.9569
Sum			5900970.4		100.0000	100.0000

Optical active 4c

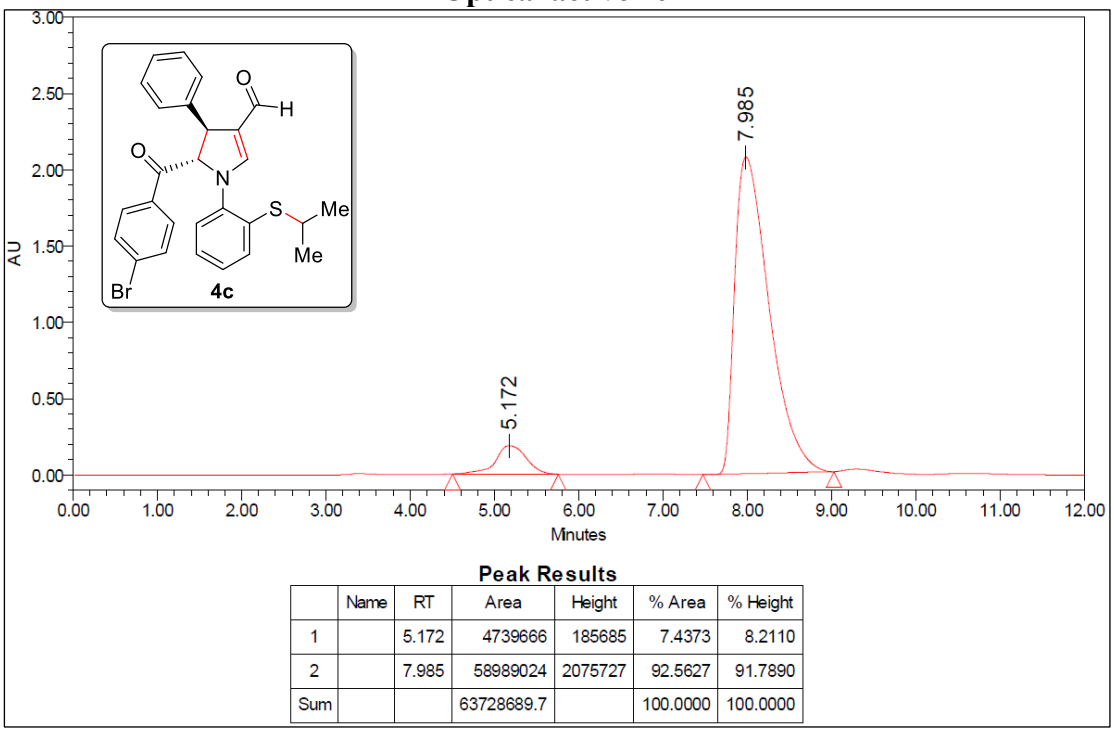

Peak Results

	Name	RT	Area	Height	% Area	% Height
1		5.172	4739666	185685	7.4373	8.2110
2		7.985	58989024	2075727	92.5627	91.7890
Sum			63728689.7		100.0000	100.0000

(±)-4d

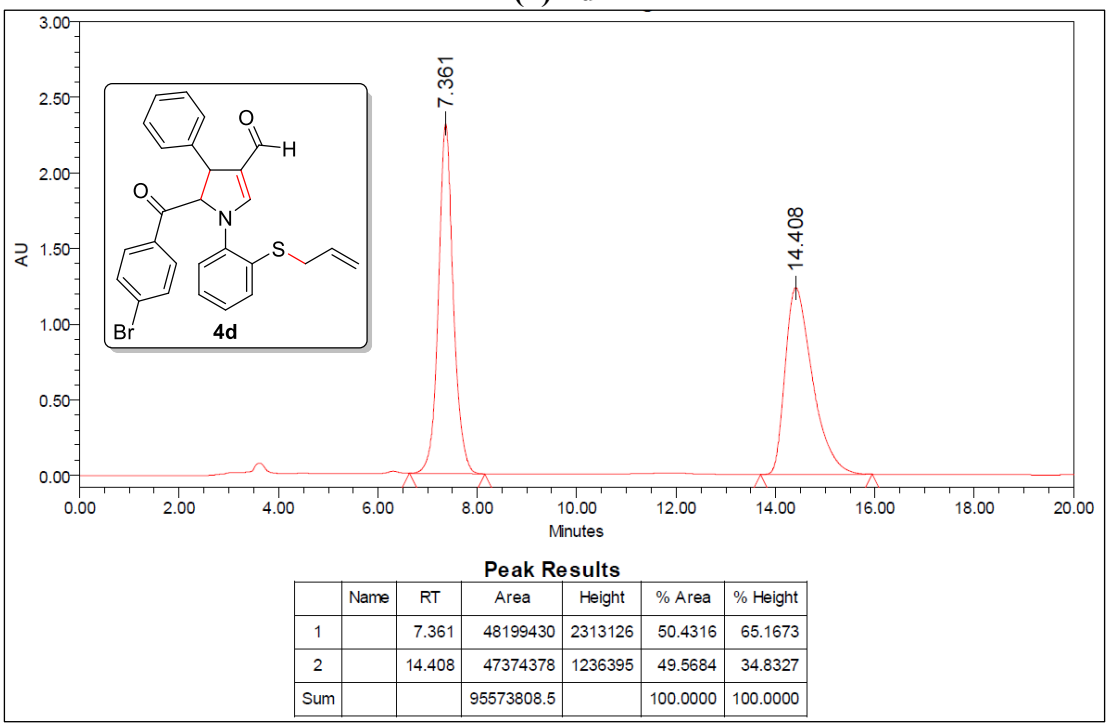

Peak Results

	Name	RT	Area	Height	% Area	% Height
1		7.361	48199430	2313126	50.4316	65.1673
2		14.408	47374378	1236395	49.5684	34.8327
Sum			95573808.5		100.0000	100.0000

Optical active 4d

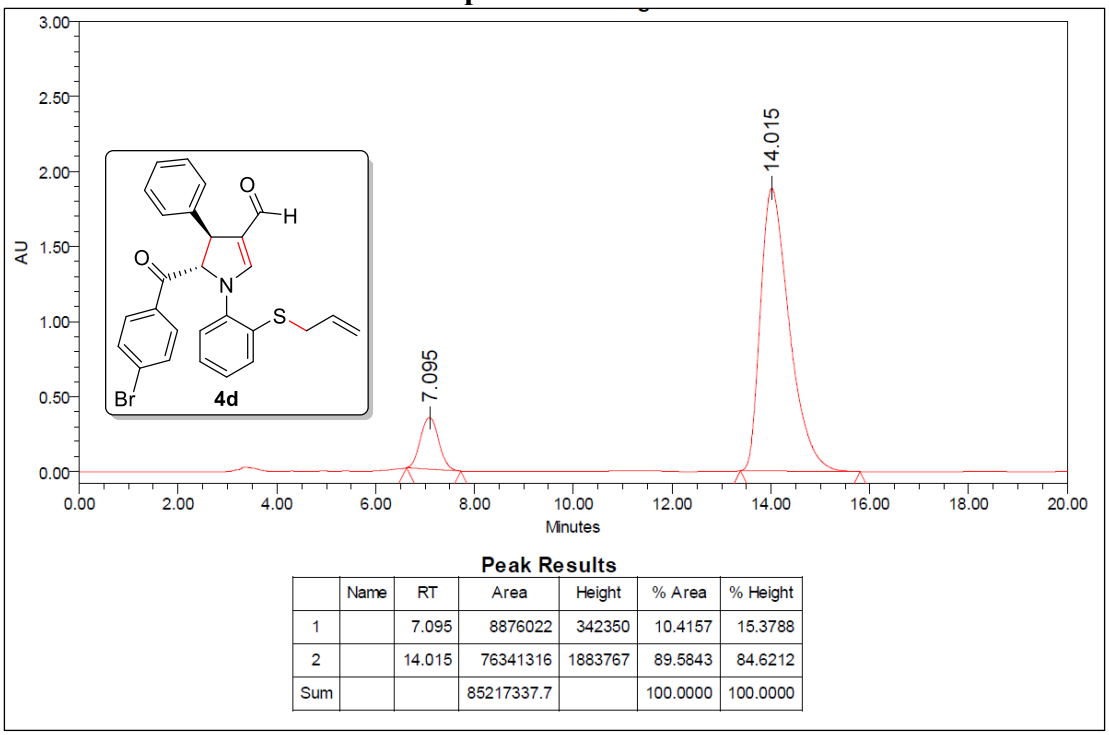

Peak Results

	Name	RT	Area	Height	% Area	% Height
1		7.095	8876022	342350	10.4157	15.3788
2		14.015	76341316	1883767	89.5843	84.6212
Sum			85217337.7		100.0000	100.0000

(±)-4e

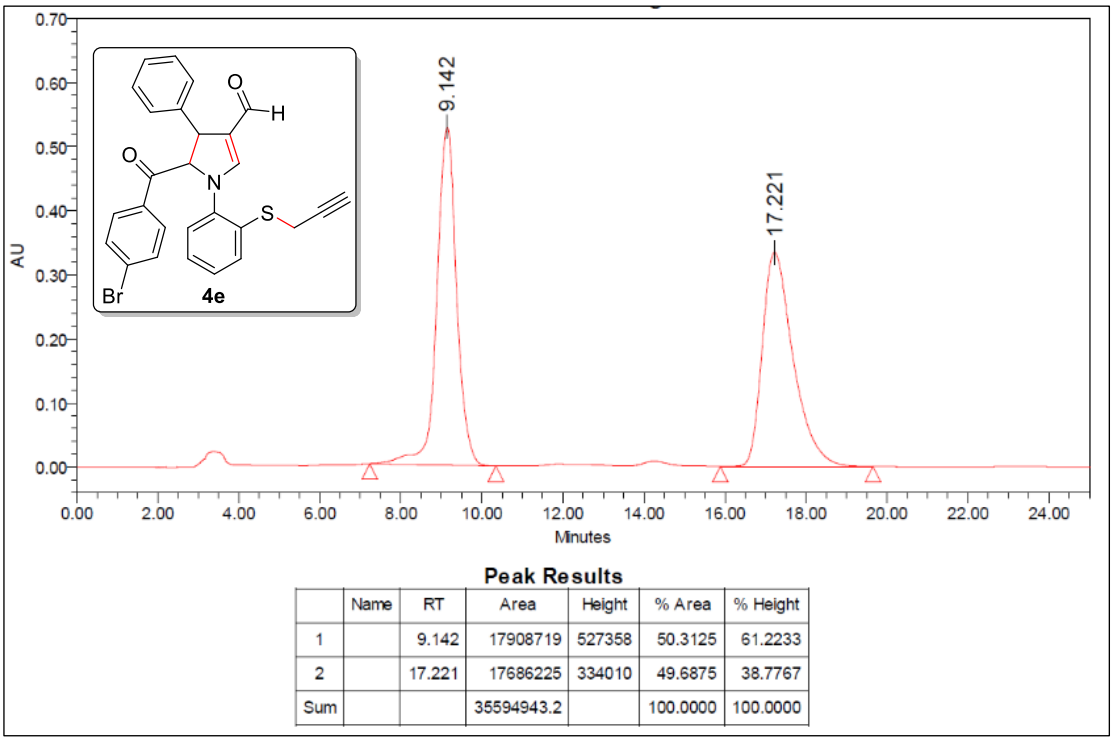

Peak Results

	Name	RT	Area	Height	% Area	% Height
1		9.142	17908719	527358	50.3125	61.2233
2		17.221	17686225	334010	49.6875	38.7767
Sum			35594943.2		100.0000	100.0000

Optical active 4e

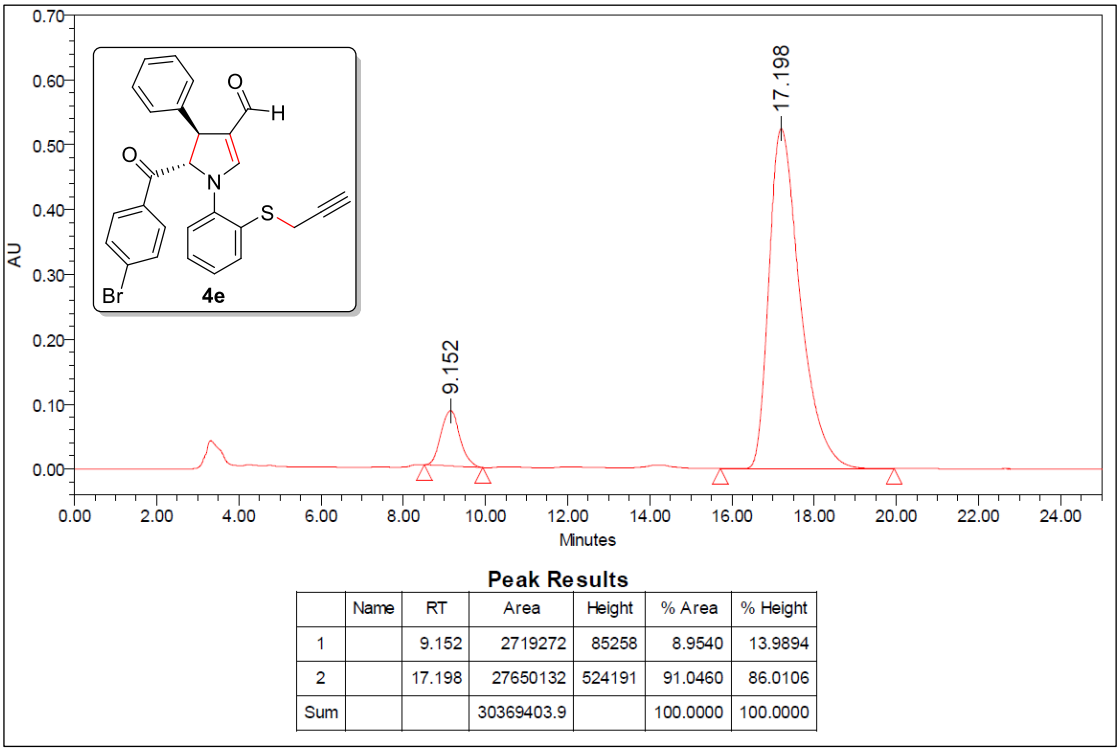

Peak Results

	Name	RT	Area	Height	% Area	% Height
1		9.152	2719272	85258	8.9540	13.9894
2		17.198	27650132	524191	91.0460	86.0106
Sum			30369403.9		100.0000	100.0000

(±)-4e

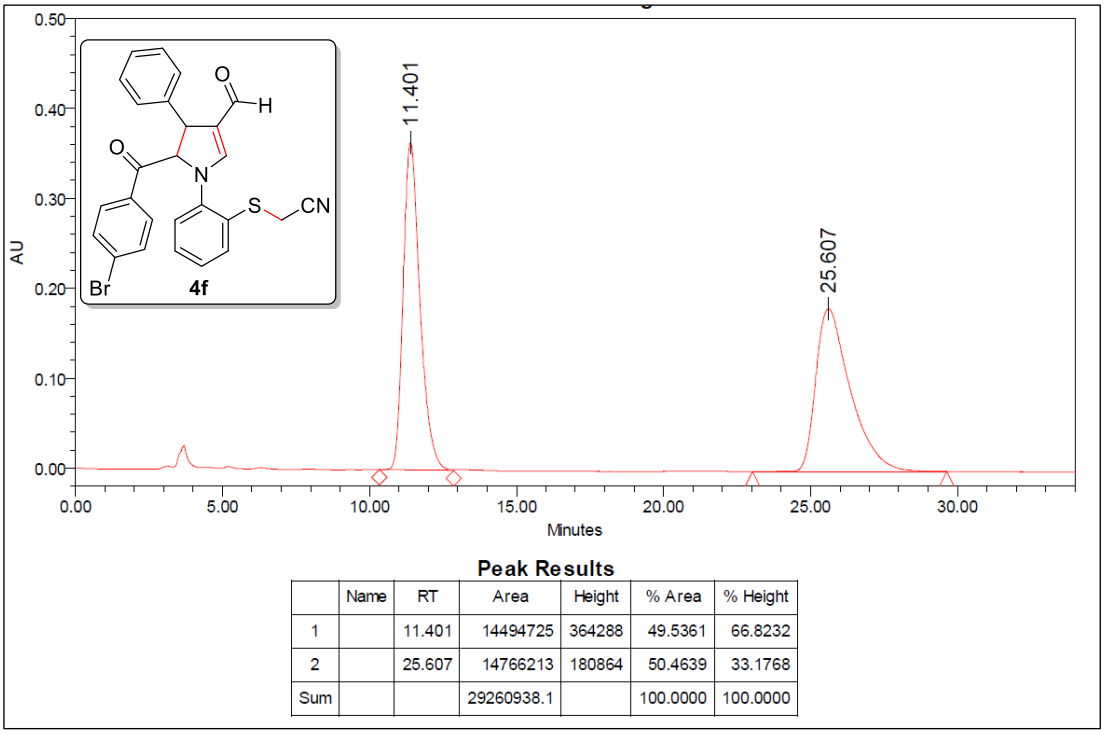

Peak Results

	Name	RT	Area	Height	% Area	% Height
1		11.401	14494725	364288	49.5361	66.8232
2		25.607	14766213	180864	50.4639	33.1768
Sum			29260938.1		100.0000	100.0000

Optical active 4f

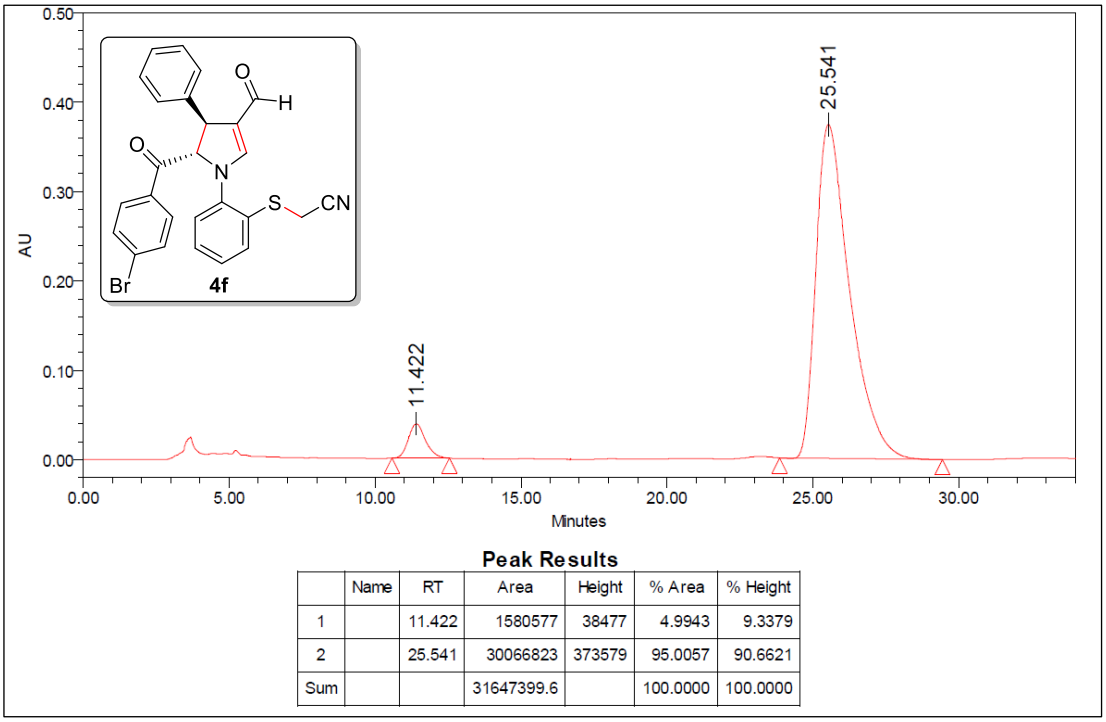

Peak Results

	Name	RT	Area	Height	% Area	% Height
1		11.422	1580577	38477	4.9943	9.3379
2		25.541	30066823	373579	95.0057	90.6621
Sum			31647399.6		100.0000	100.0000

(±)-4g

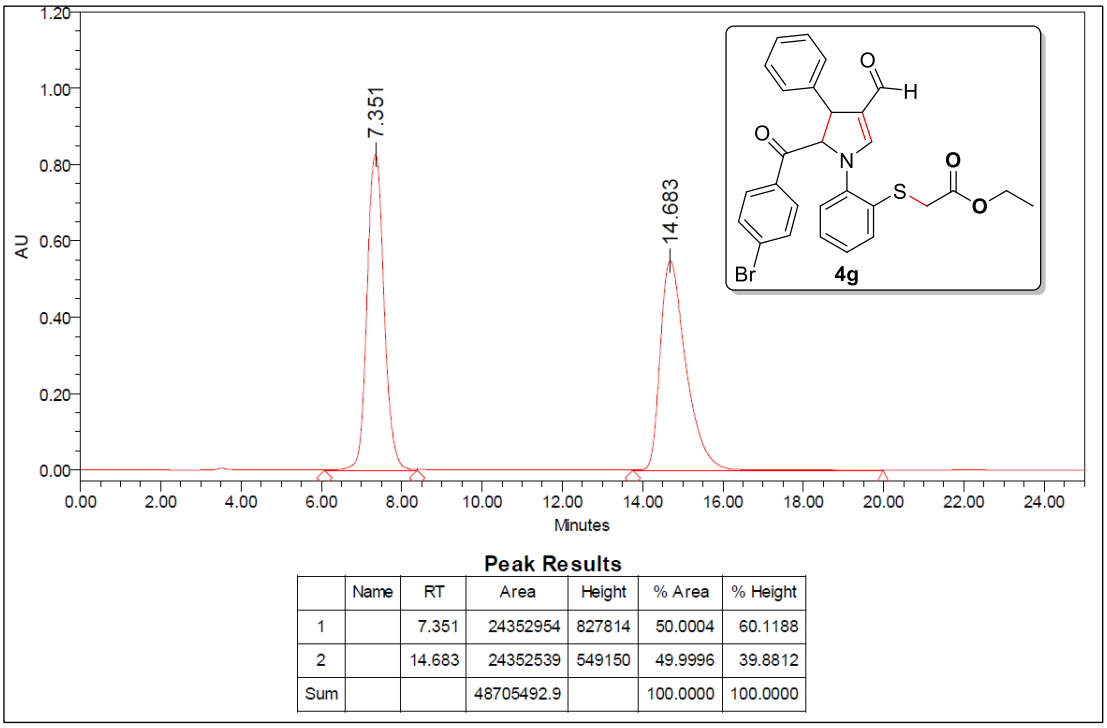

Peak Results

	Name	RT	Area	Height	% Area	% Height
1		7.351	24352954	827814	50.0004	60.1188
2		14.683	24352539	549150	49.9996	39.8812
Sum			48705492.9		100.0000	100.0000

Optical active 4g

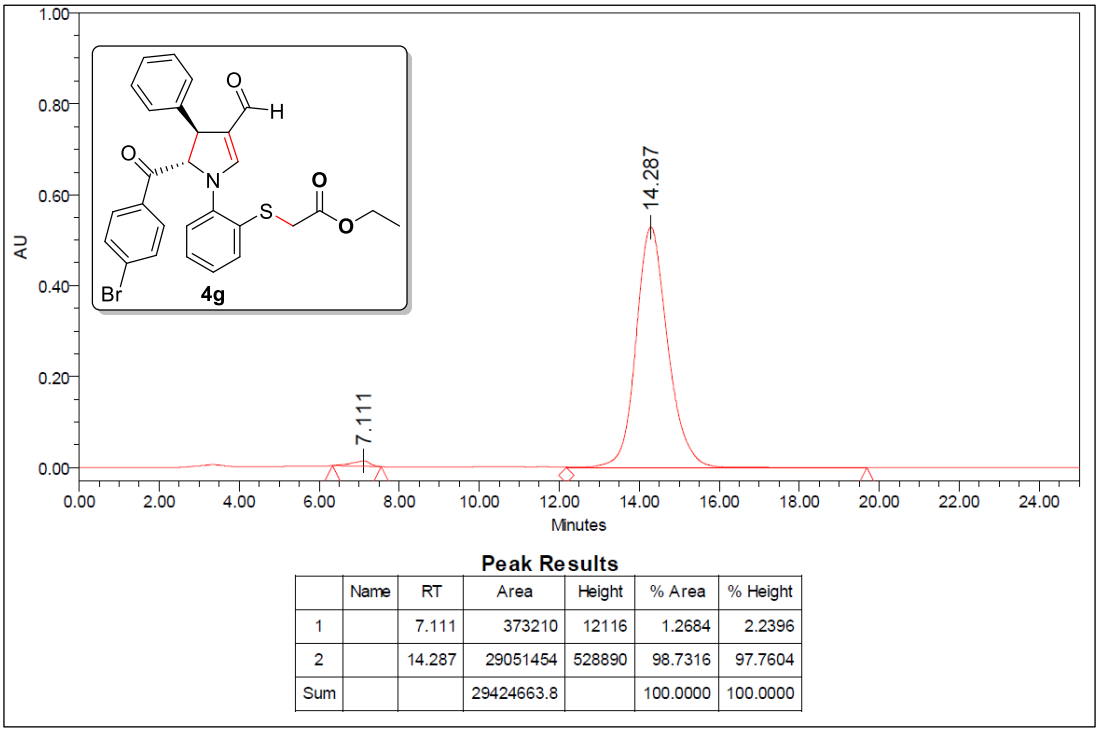

Peak Results

	Name	RT	Area	Height	% Area	% Height
1		7.111	373210	12116	1.2684	2.2396
2		14.287	29051454	528890	98.7316	97.7604
Sum			29424663.8		100.0000	100.0000

(±)-4h

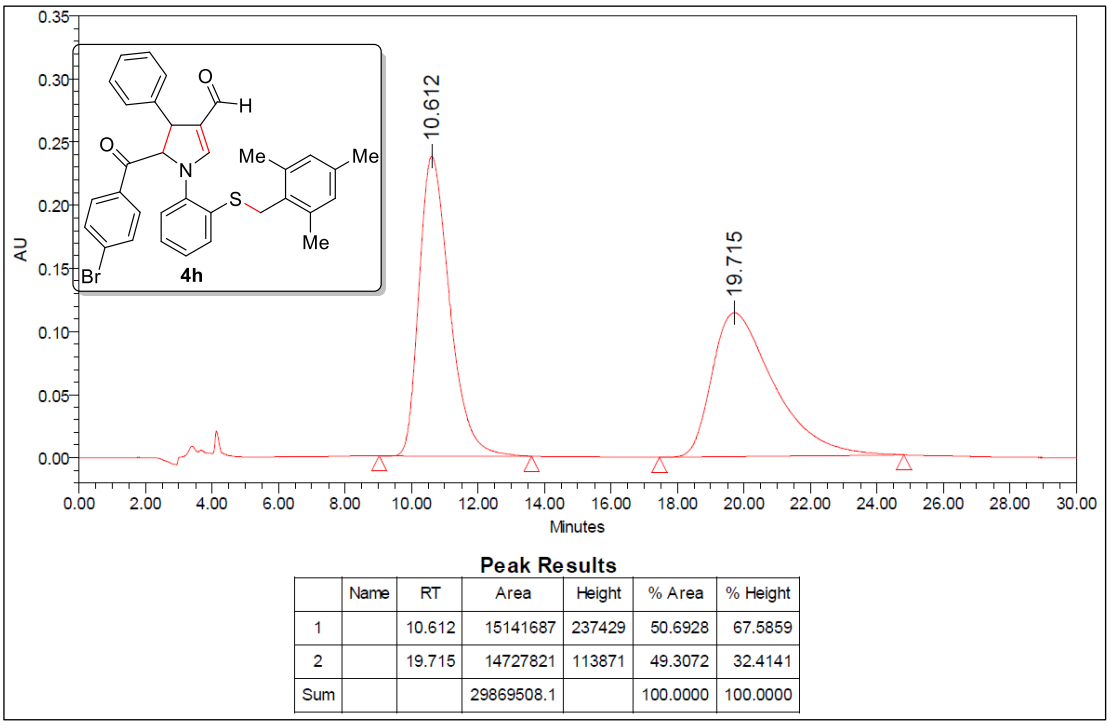

Peak Results

	Name	RT	Area	Height	% Area	% Height
1		10.612	15141687	237429	50.6928	67.5859
2		19.715	14727821	113871	49.3072	32.4141
Sum			29869508.1		100.0000	100.0000

Optical active 4h

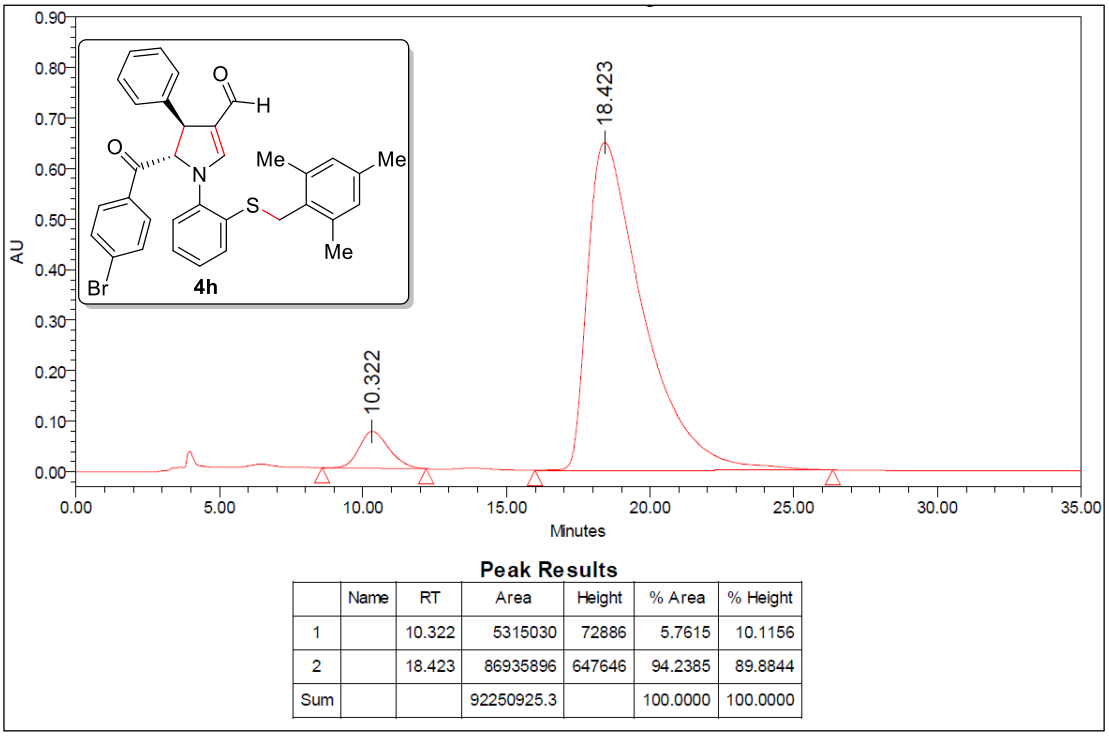

Peak Results

	Name	RT	Area	Height	% Area	% Height
1		10.322	5315030	72886	5.7615	10.1156
2		18.423	86935896	647646	94.2385	89.8844
Sum			92250925.3		100.0000	100.0000

(±)-4i

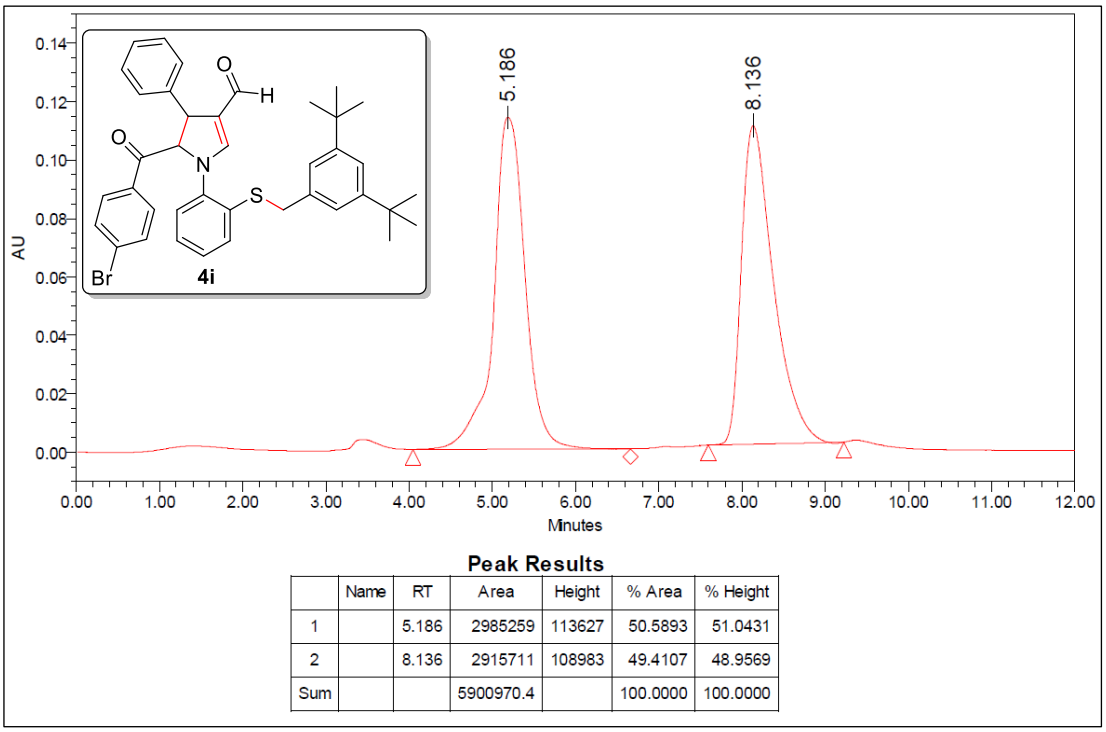

Peak Results

	Name	RT	Area	Height	% Area	% Height
1		5.186	2985259	113627	50.5893	51.0431
2		8.136	2915711	108983	49.4107	48.9569
Sum			5900970.4		100.0000	100.0000

Optical active 4i

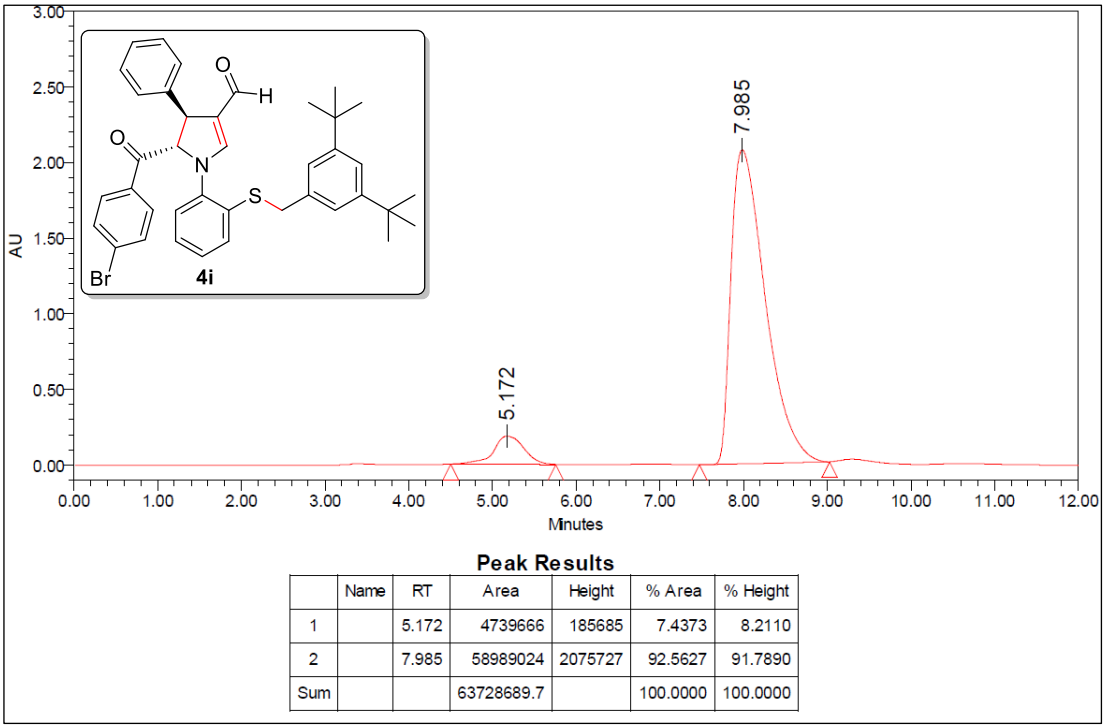

Peak Results

	Name	RT	Area	Height	% Area	% Height
1		5.172	4739666	185685	7.4373	8.2110
2		7.985	58989024	2075727	92.5627	91.7890
Sum			63728689.7		100.0000	100.0000

(±)-4j

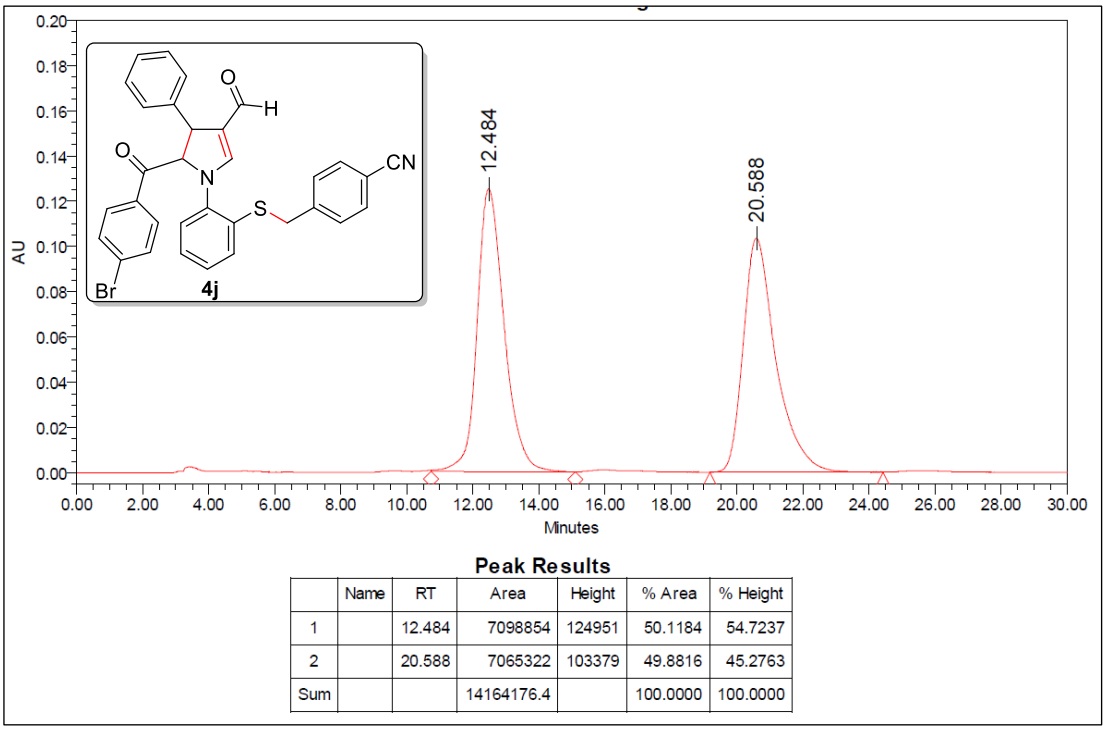

Peak Results

	Name	RT	Area	Height	% Area	% Height
1		12.484	7098854	124951	50.1184	54.7237
2		20.588	7065322	103379	49.8816	45.2763
Sum			14164176.4		100.0000	100.0000

Optical active 4j

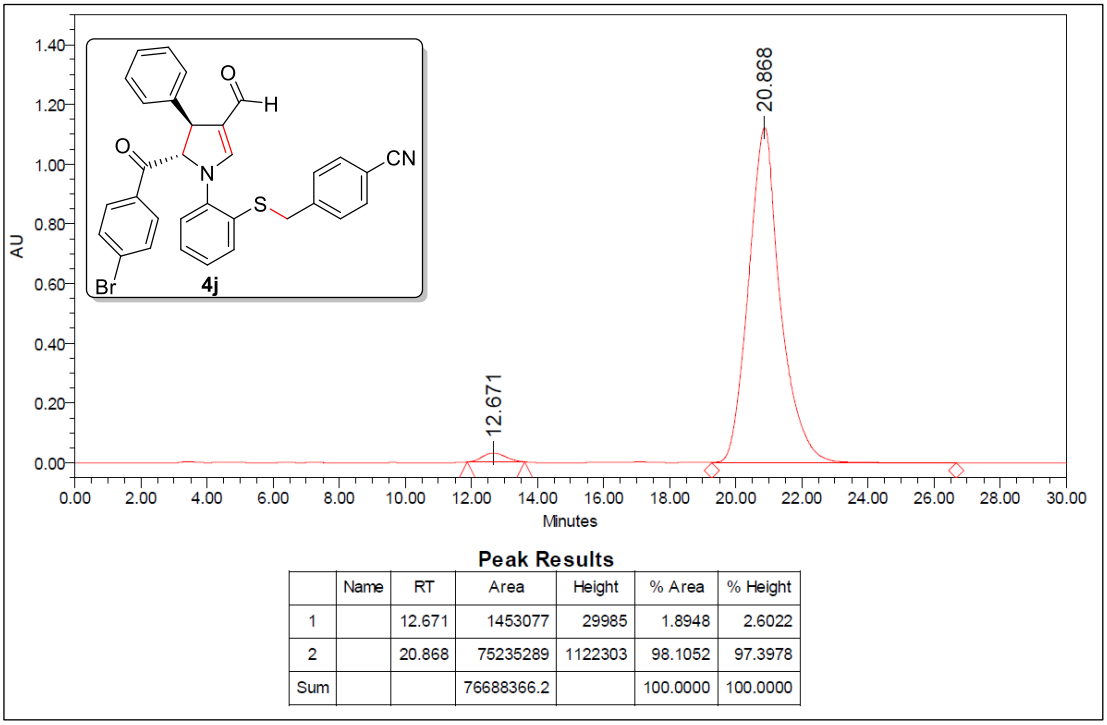

Peak Results

	Name	RT	Area	Height	% Area	% Height
1		12.671	1453077	29985	1.8948	2.6022
2		20.868	75235289	1122303	98.1052	97.3978
Sum			76688366.2		100.0000	100.0000

(±)-4k

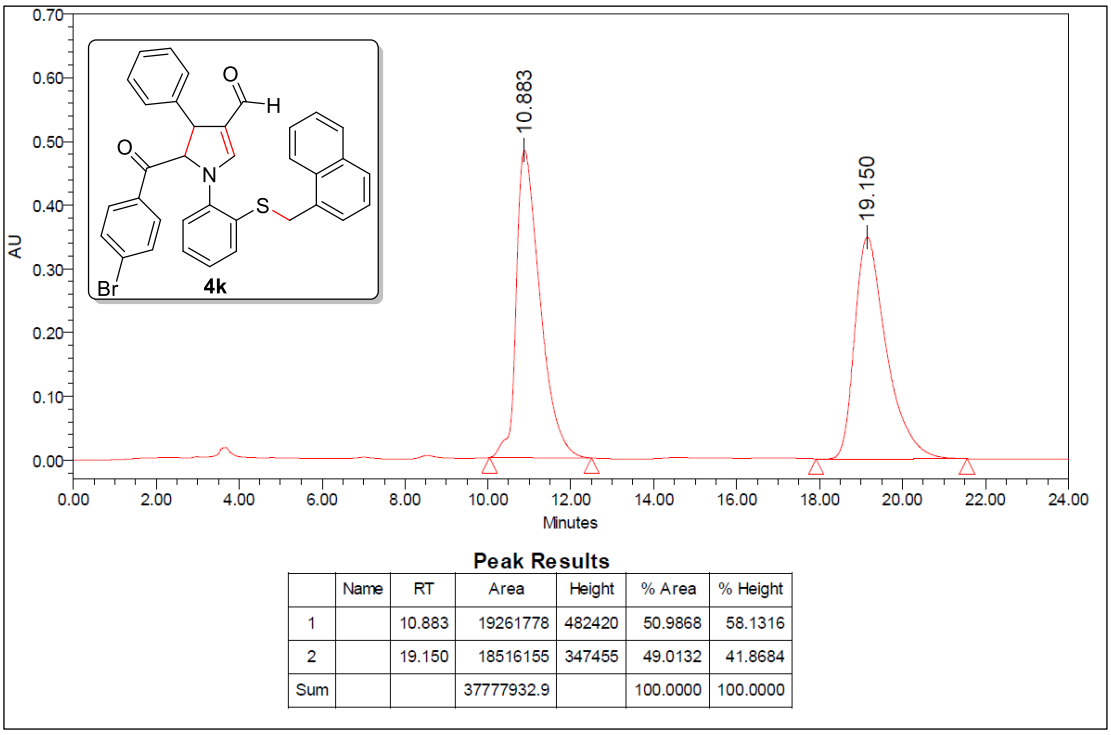

Peak Results

	Name	RT	Area	Height	% Area	% Height
1		10.883	19261778	482420	50.9868	58.1316
2		19.150	18516155	347455	49.0132	41.8684
Sum			37777932.9		100.0000	100.0000

Optical active 4k

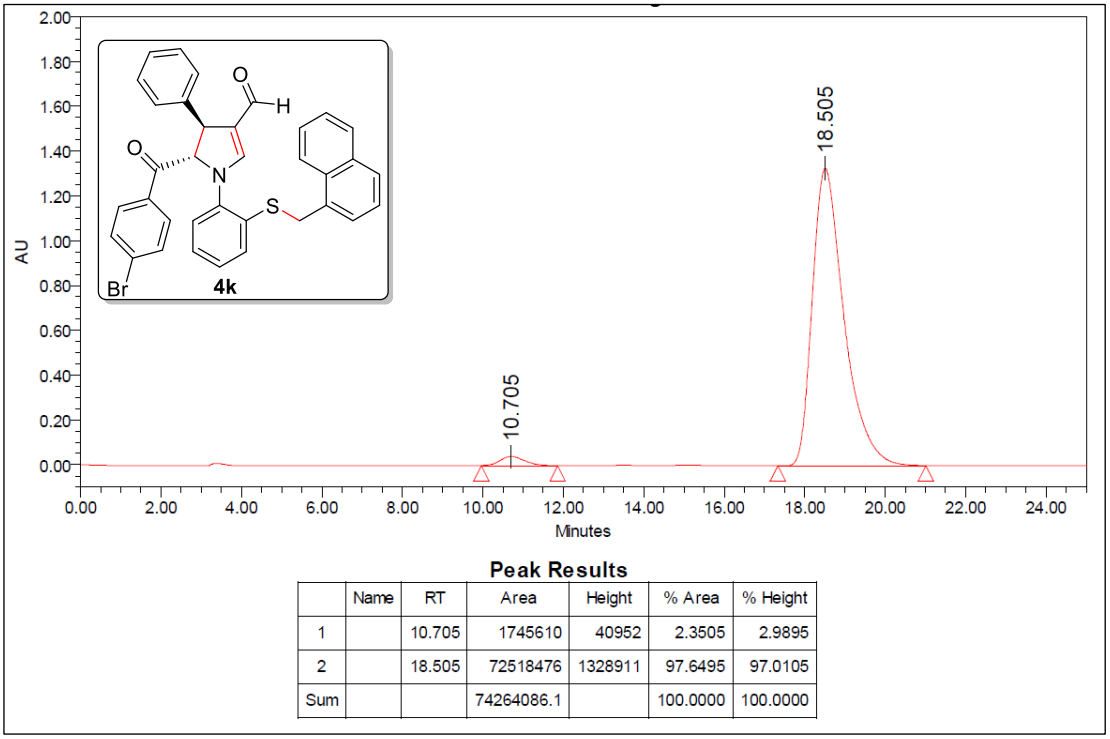

Peak Results

	Name	RT	Area	Height	% Area	% Height
1		10.705	1745610	40952	2.3505	2.9895
2		18.505	72518476	1328911	97.6495	97.0105
Sum			74264086.1		100.0000	100.0000

(±)-4l

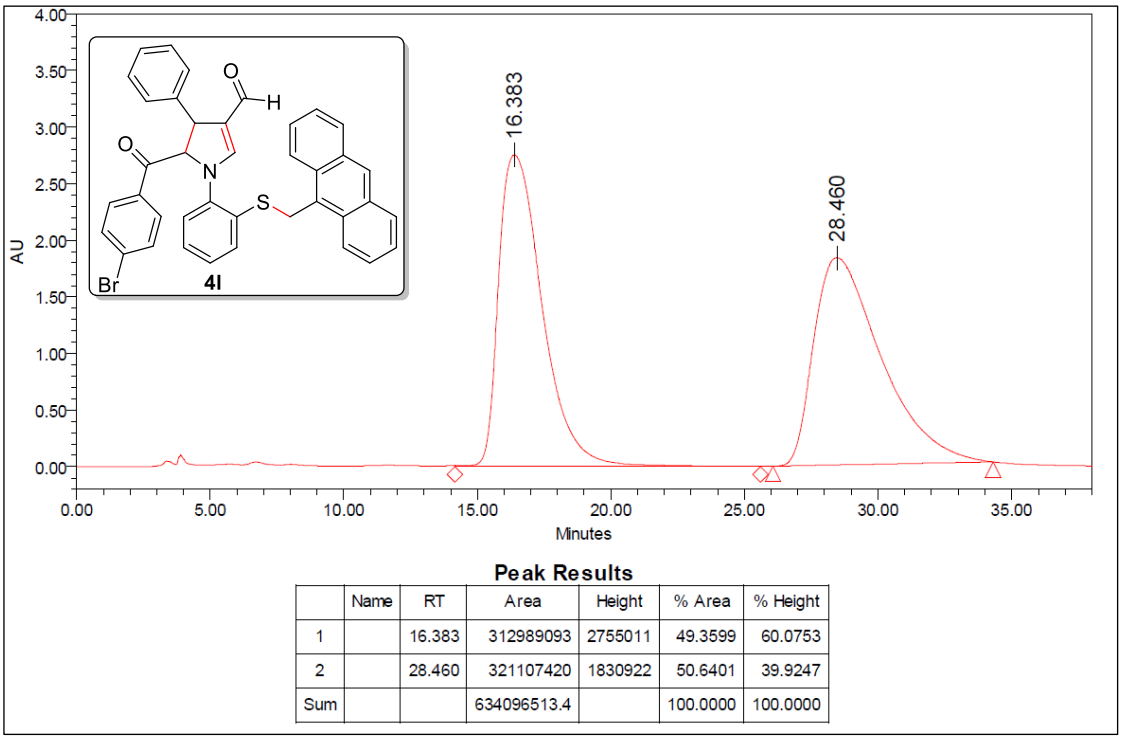

Peak Results

	Name	RT	Area	Height	% Area	% Height
1		16.383	312989093	2755011	49.3599	60.0753
2		28.460	321107420	1830922	50.6401	39.9247
Sum			634096513.4		100.0000	100.0000

Optical active 4l

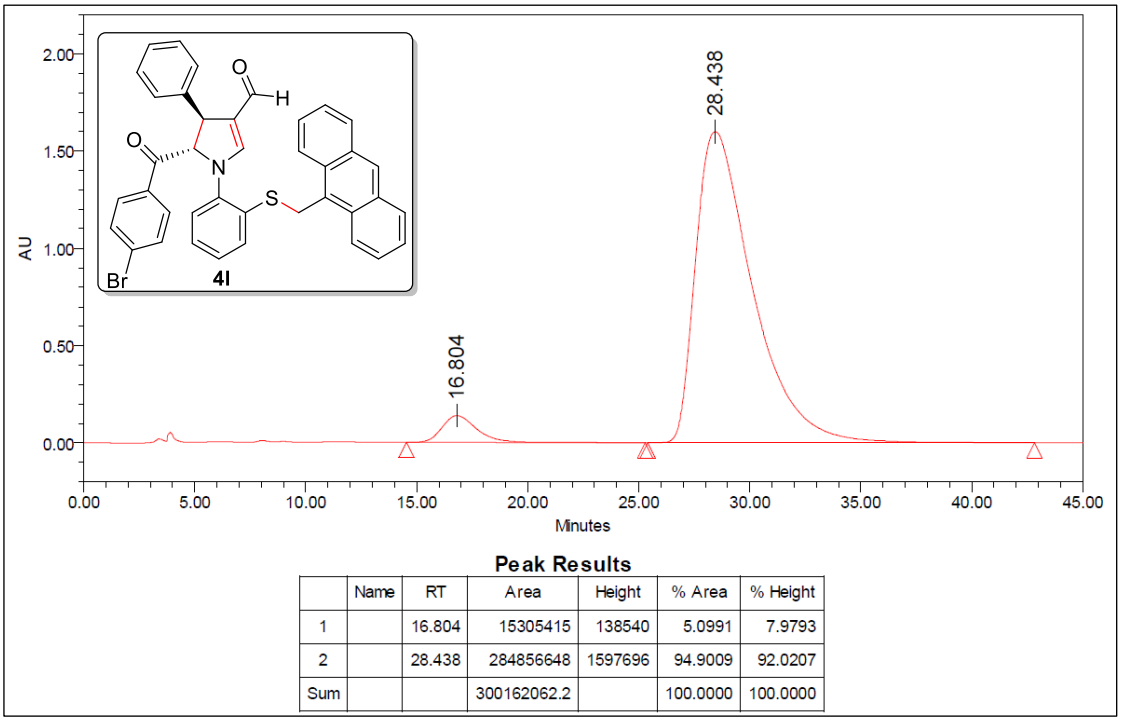

Peak Results

	Name	RT	Area	Height	% Area	% Height
1		16.804	15305415	138540	5.0991	7.9793
2		28.438	284856648	1597696	94.9009	92.0207
Sum			300162062.2		100.0000	100.0000

(±)-4m

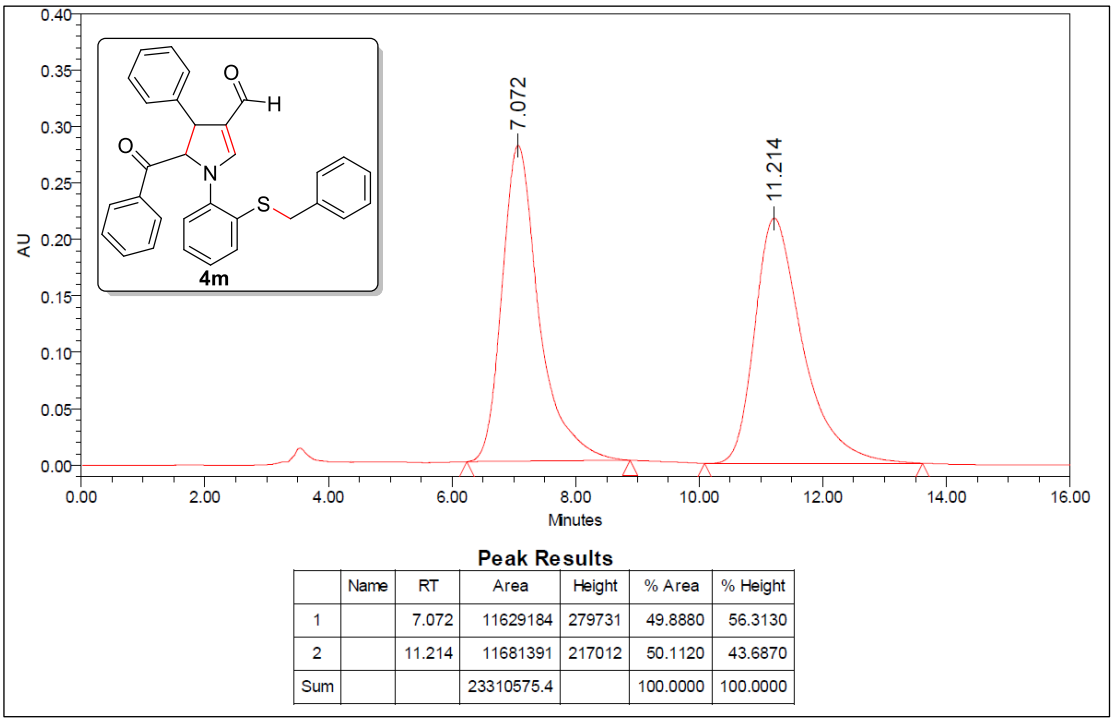

Peak Results

	Name	RT	Area	Height	% Area	% Height
1		7.072	11629184	279731	49.8880	56.3130
2		11.214	11681391	217012	50.1120	43.6870
Sum			23310575.4		100.0000	100.0000

Optical active 4m

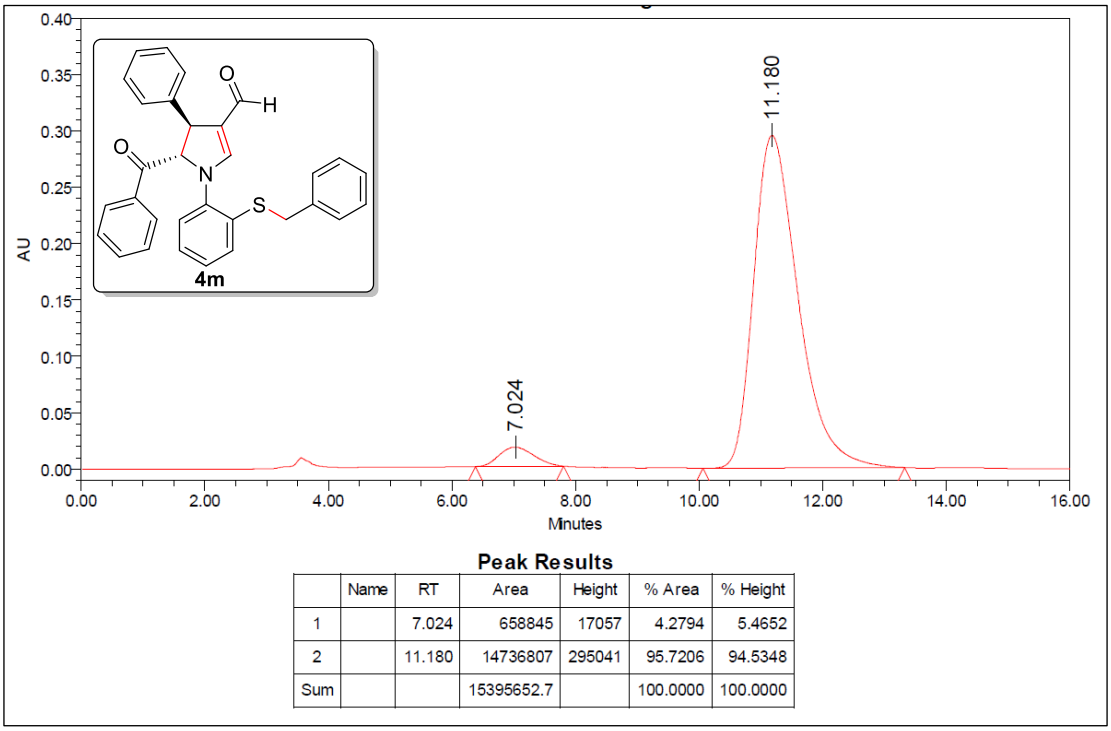

Peak Results

	Name	RT	Area	Height	% Area	% Height
1		7.024	658845	17057	4.2794	5.4652
2		11.180	14736807	295041	95.7206	94.5348
Sum			15395652.7		100.0000	100.0000

(±)-4n

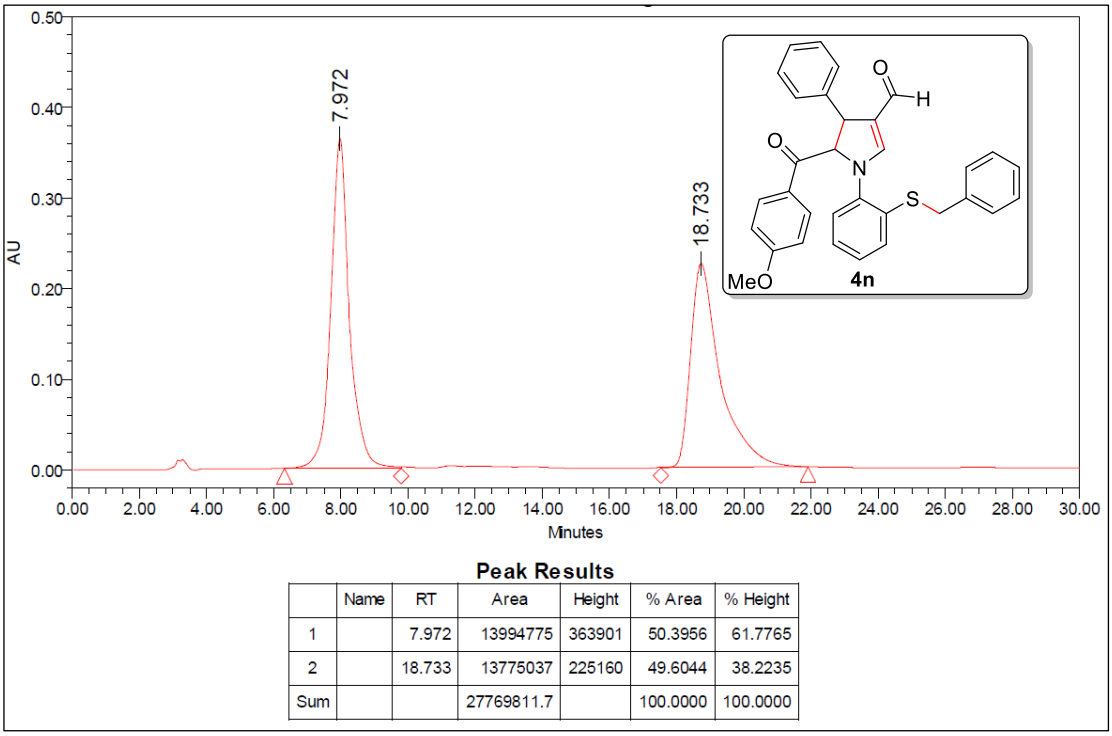

Peak Results

	Name	RT	Area	Height	% Area	% Height
1		7.972	13994775	363901	50.3956	61.7765
2		18.733	13775037	225160	49.6044	38.2235
Sum			27769811.7		100.0000	100.0000

Optical active 4n

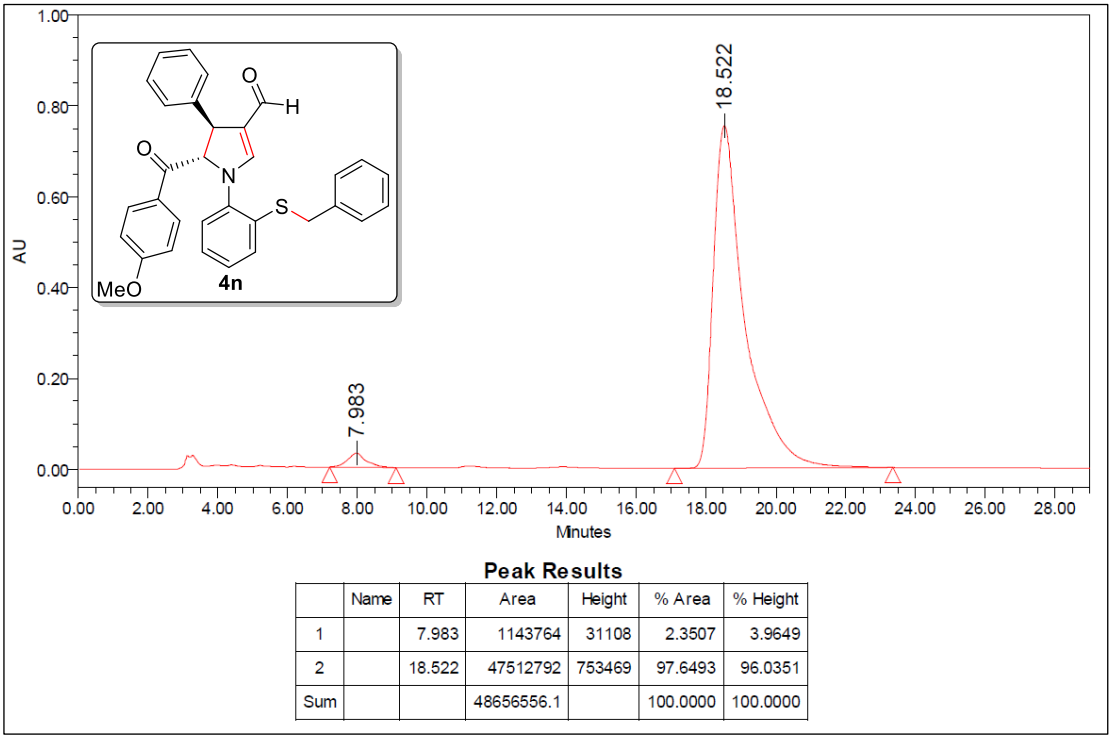

Peak Results

	Name	RT	Area	Height	% Area	% Height
1		7.983	1143764	31108	2.3507	3.9649
2		18.522	47512792	753469	97.6493	96.0351
Sum			48656556.1		100.0000	100.0000

(±)-4o

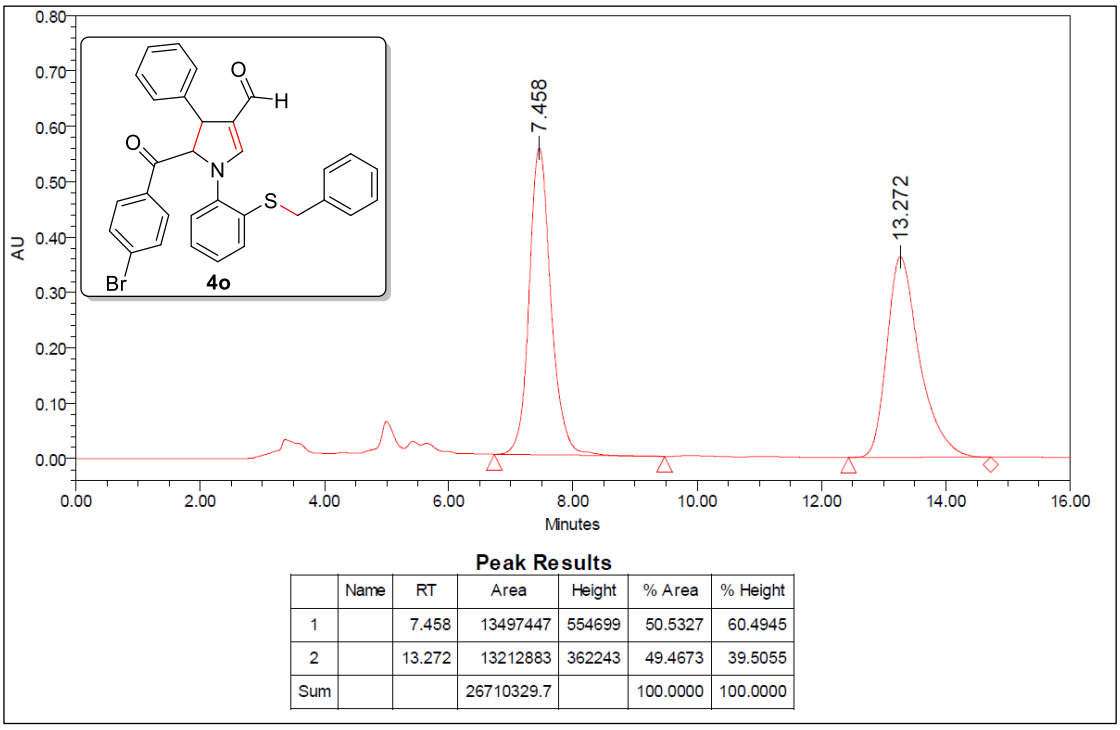

Peak Results

	Name	RT	Area	Height	% Area	% Height
1		7.458	13497447	554699	50.5327	60.4945
2		13.272	13212883	362243	49.4673	39.5055
Sum			26710329.7		100.0000	100.0000

Optical active 4o

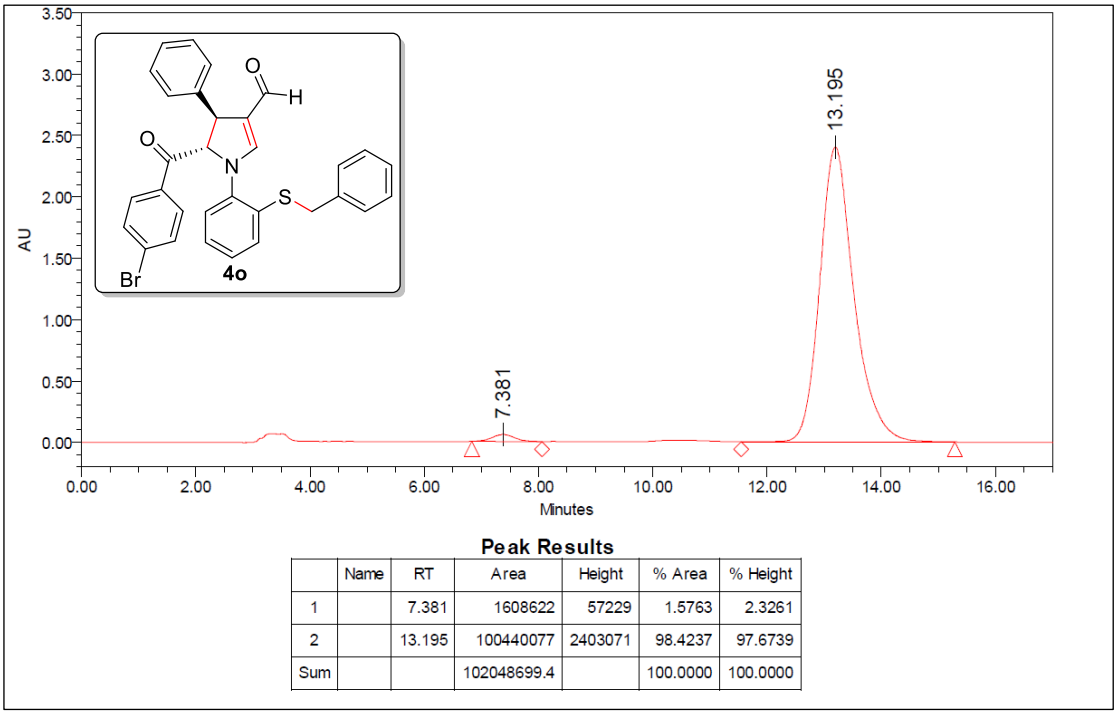

Peak Results

	Name	RT	Area	Height	% Area	% Height
1		7.381	1608622	57229	1.5763	2.3261
2		13.195	100440077	2403071	98.4237	97.6739
Sum			102048699.4		100.0000	100.0000

(±)-4p

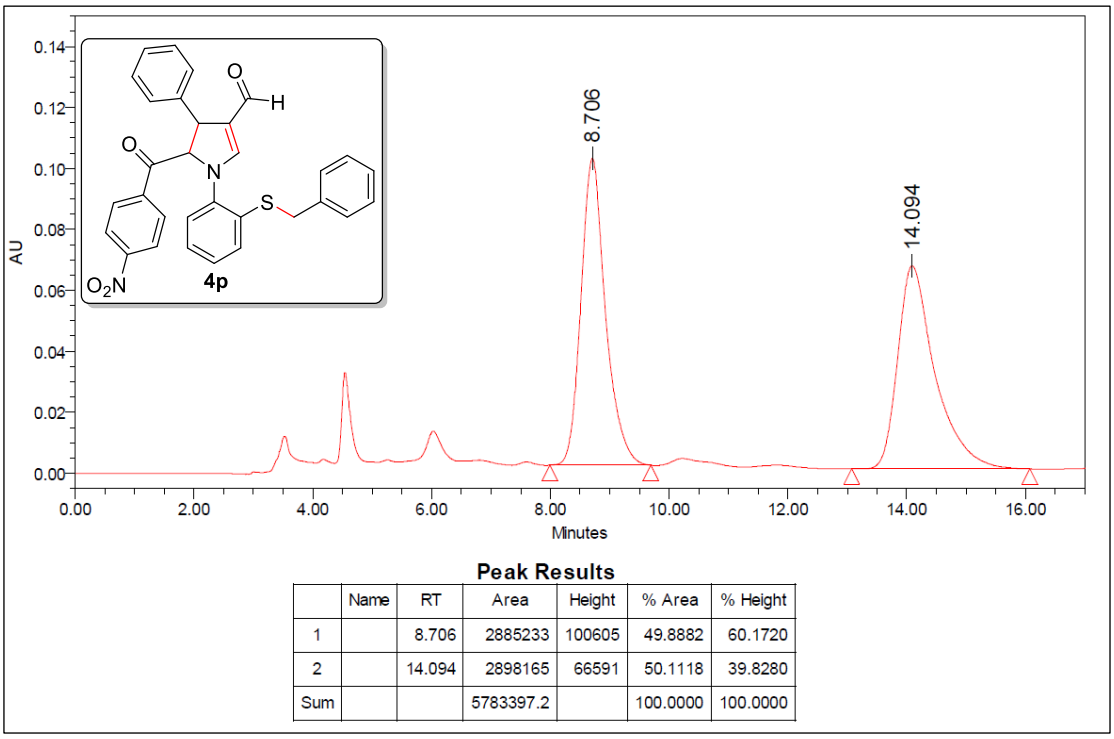

Peak Results

	Name	RT	Area	Height	% Area	% Height
1		8.706	2885233	100605	49.8882	60.1720
2		14.094	2898165	66591	50.1118	39.8280
Sum			5783397.2		100.0000	100.0000

Optical active 4p

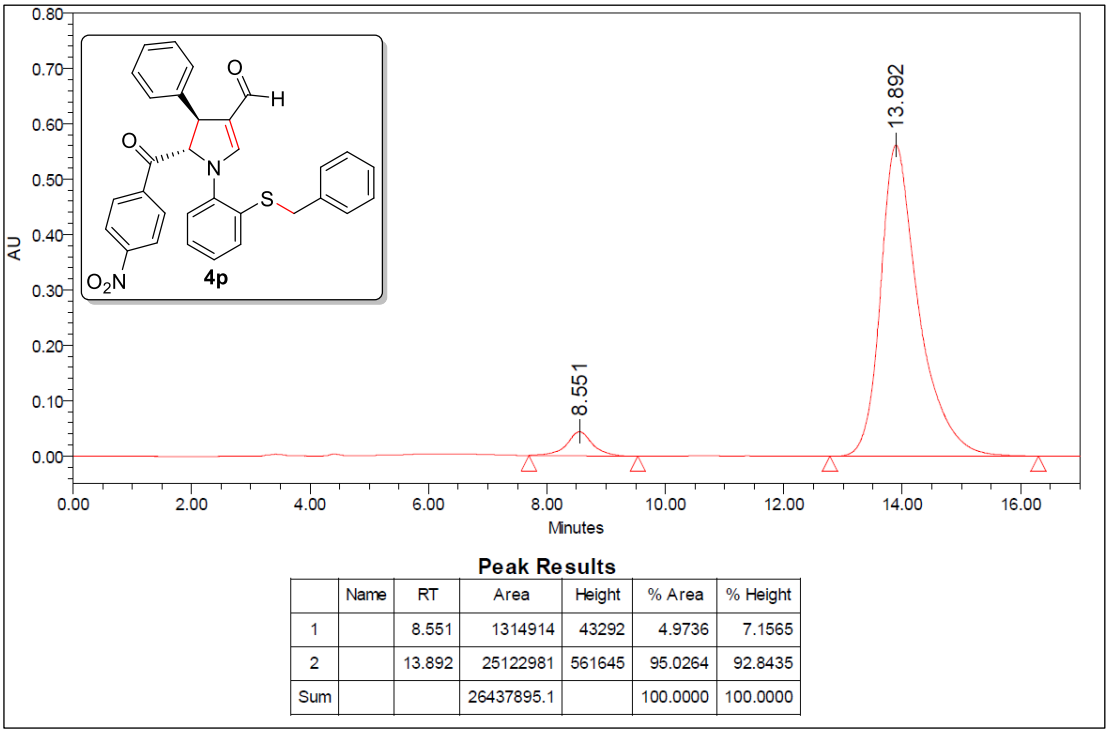

Peak Results

	Name	RT	Area	Height	% Area	% Height
1		8.551	1314914	43292	4.9736	7.1565
2		13.892	25122981	561645	95.0264	92.8435
Sum			26437895.1		100.0000	100.0000

(±)-4q

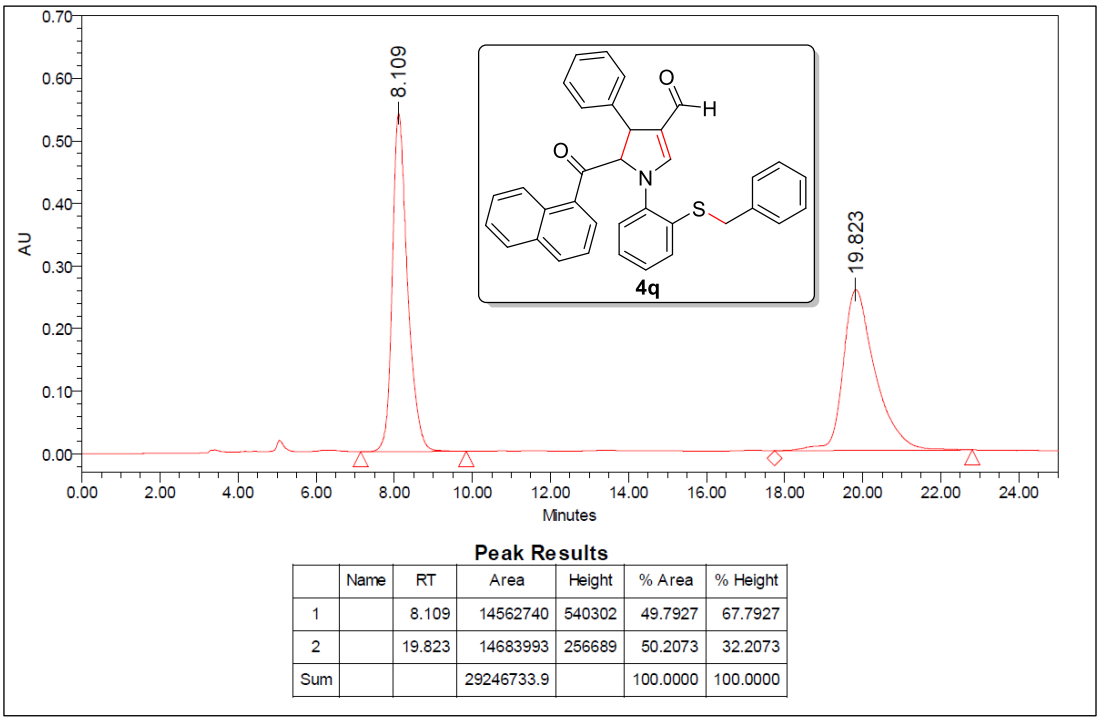

Peak Results

	Name	RT	Area	Height	% Area	% Height
1		8.109	14562740	540302	49.7927	67.7927
2		19.823	14683993	256689	50.2073	32.2073
Sum			29246733.9		100.0000	100.0000

Optical active 4q

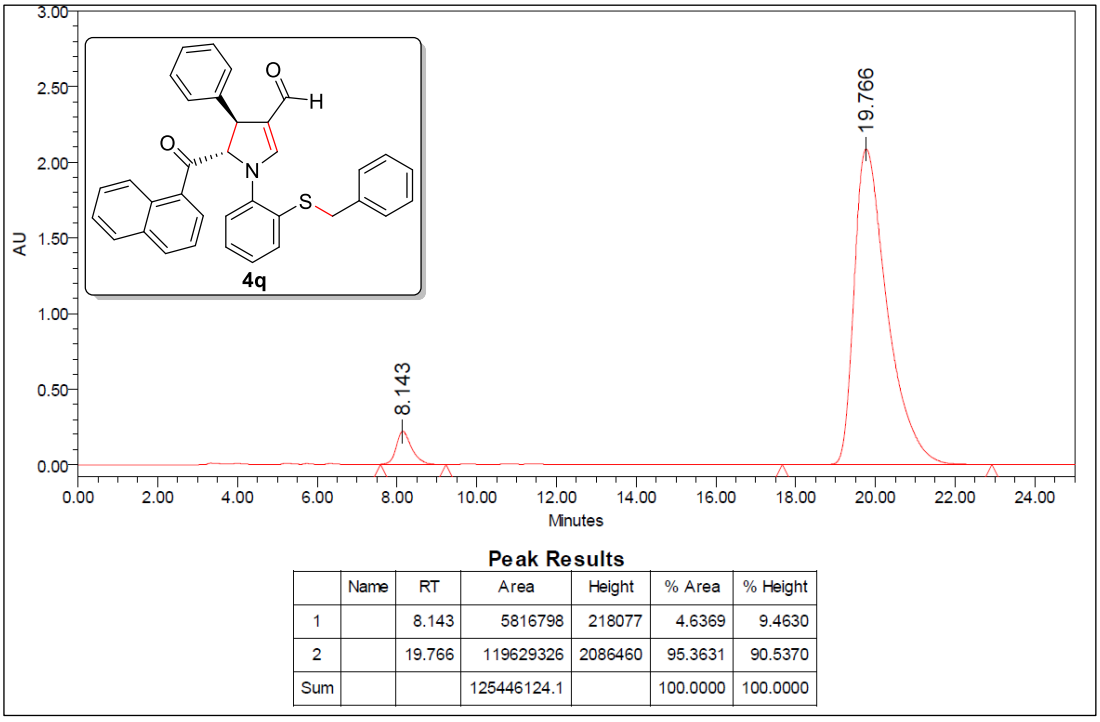

Peak Results

	Name	RT	Area	Height	% Area	% Height
1		8.143	5816798	218077	4.6369	9.4630
2		19.766	119629326	2086460	95.3631	90.5370
Sum			125446124.1		100.0000	100.0000

(±)-4r

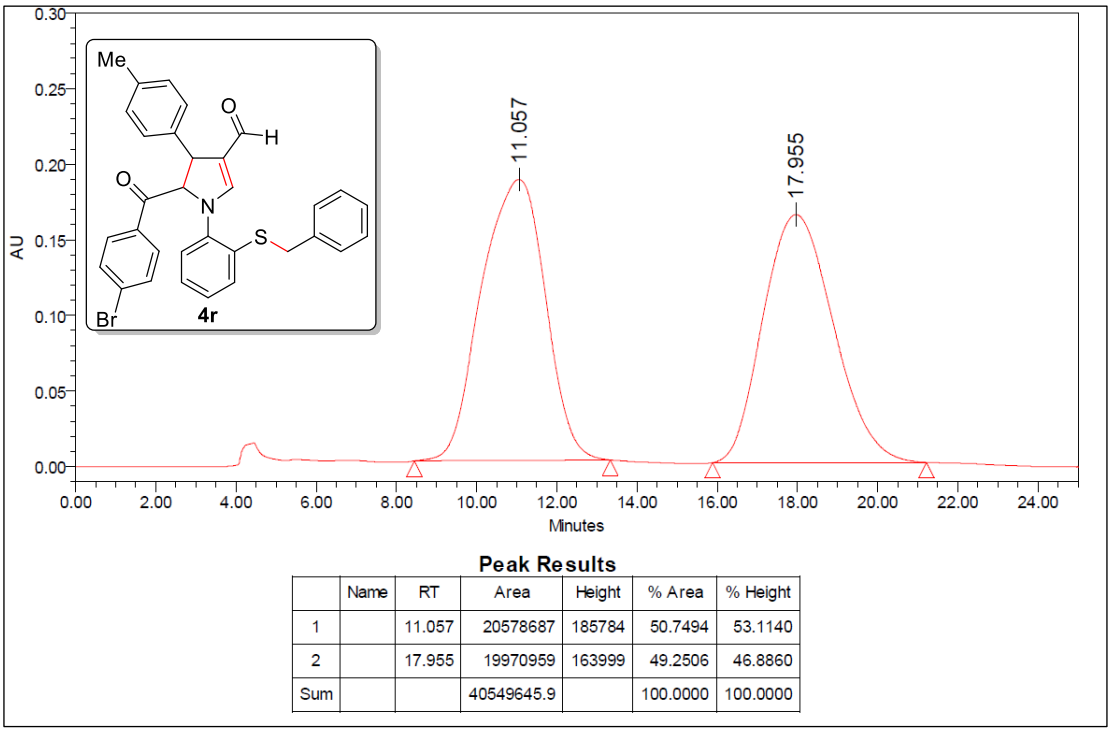

Peak Results

	Name	RT	Area	Height	% Area	% Height
1		11.057	20578687	185784	50.7494	53.1140
2		17.955	19970959	163999	49.2506	46.8860
Sum			40549645.9		100.0000	100.0000

Optical active 4r

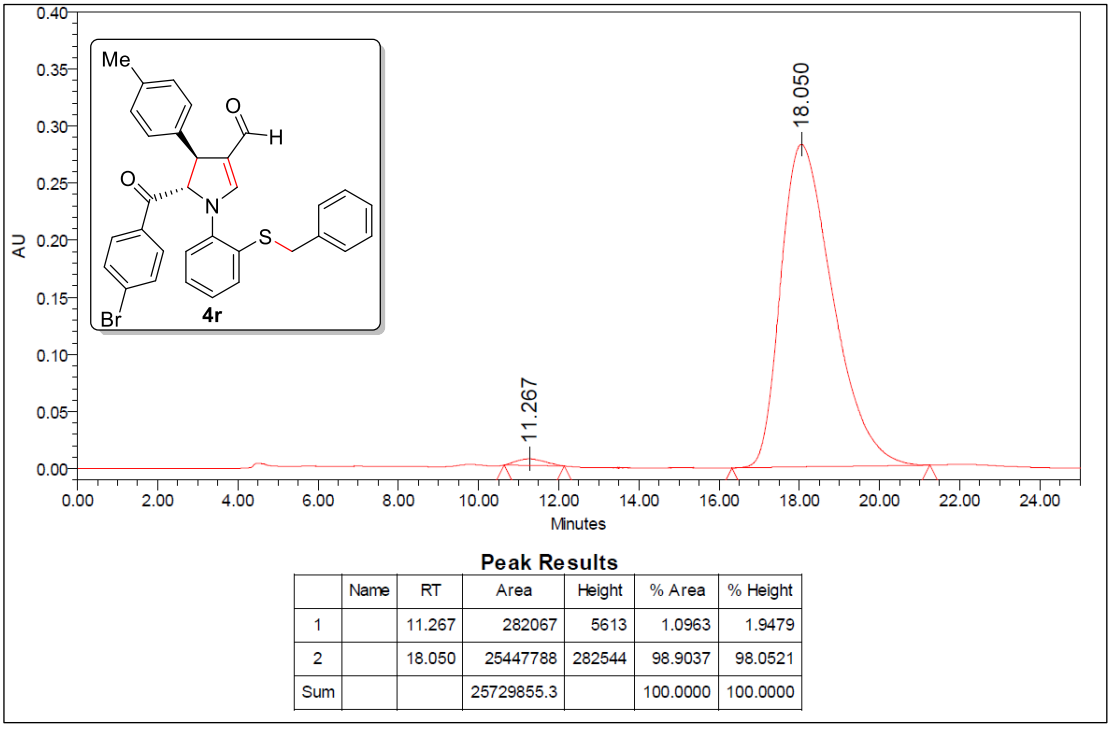

Peak Results

	Name	RT	Area	Height	% Area	% Height
1		11.267	282067	5613	1.0963	1.9479
2		18.050	25447788	282544	98.9037	98.0521
Sum			25729855.3		100.0000	100.0000

(±)-4s

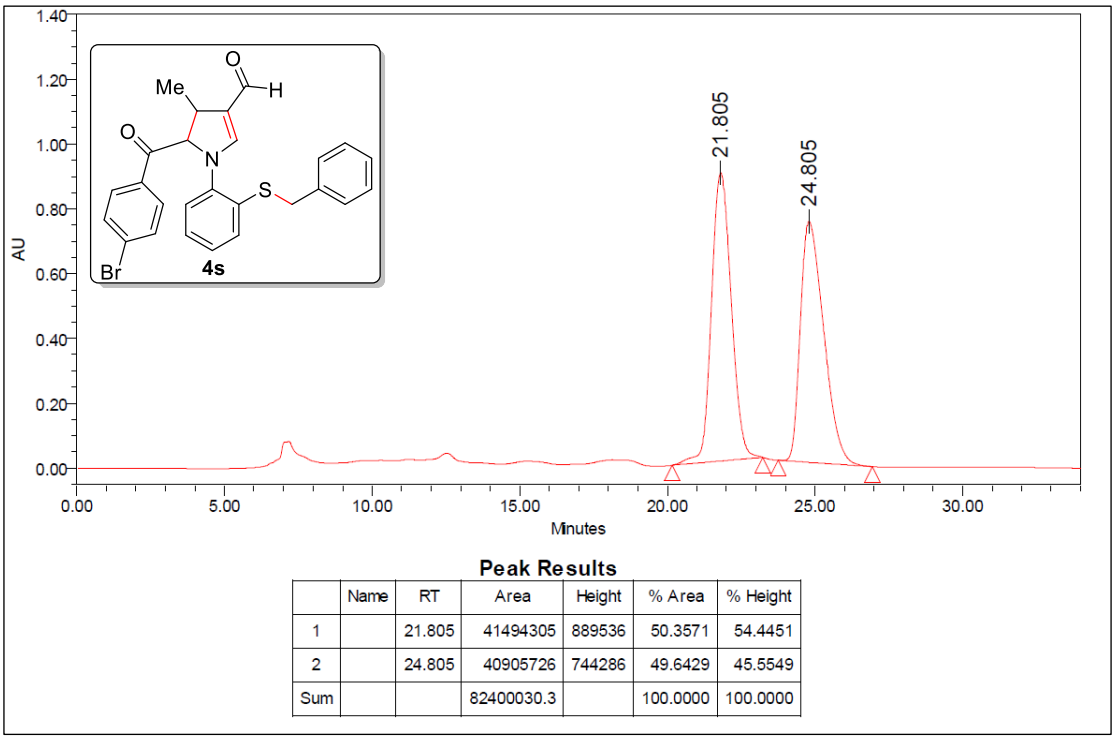

Peak Results

	Name	RT	Area	Height	% Area	% Height
1		21.805	41494305	889536	50.3571	54.4451
2		24.805	40905726	744286	49.6429	45.5549
Sum			82400030.3		100.0000	100.0000

Optical active 4s

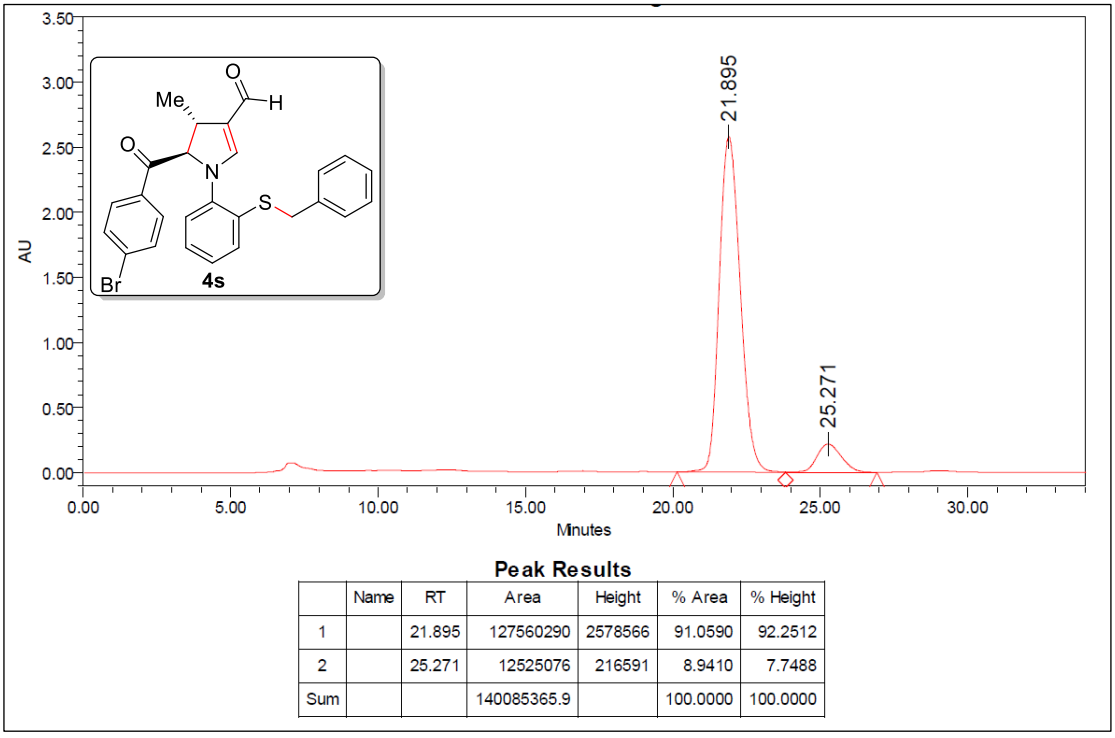

Peak Results

	Name	RT	Area	Height	% Area	% Height
1		21.895	127560290	2578566	91.0590	92.2512
2		25.271	12525076	216591	8.9410	7.7488
Sum			140085365.9		100.0000	100.0000

(±)-4t

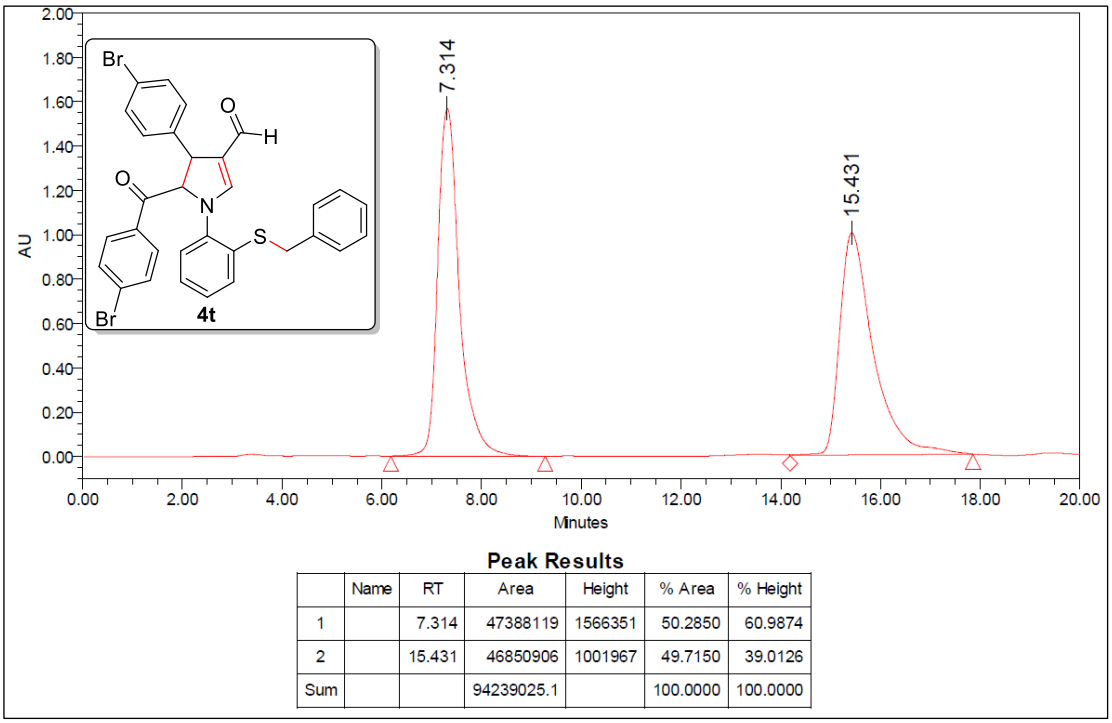

Peak Results

	Name	RT	Area	Height	% Area	% Height
1		7.314	47388119	1566351	50.2850	60.9874
2		15.431	46850906	1001967	49.7150	39.0126
Sum			94239025.1		100.0000	100.0000

Optical active 4t

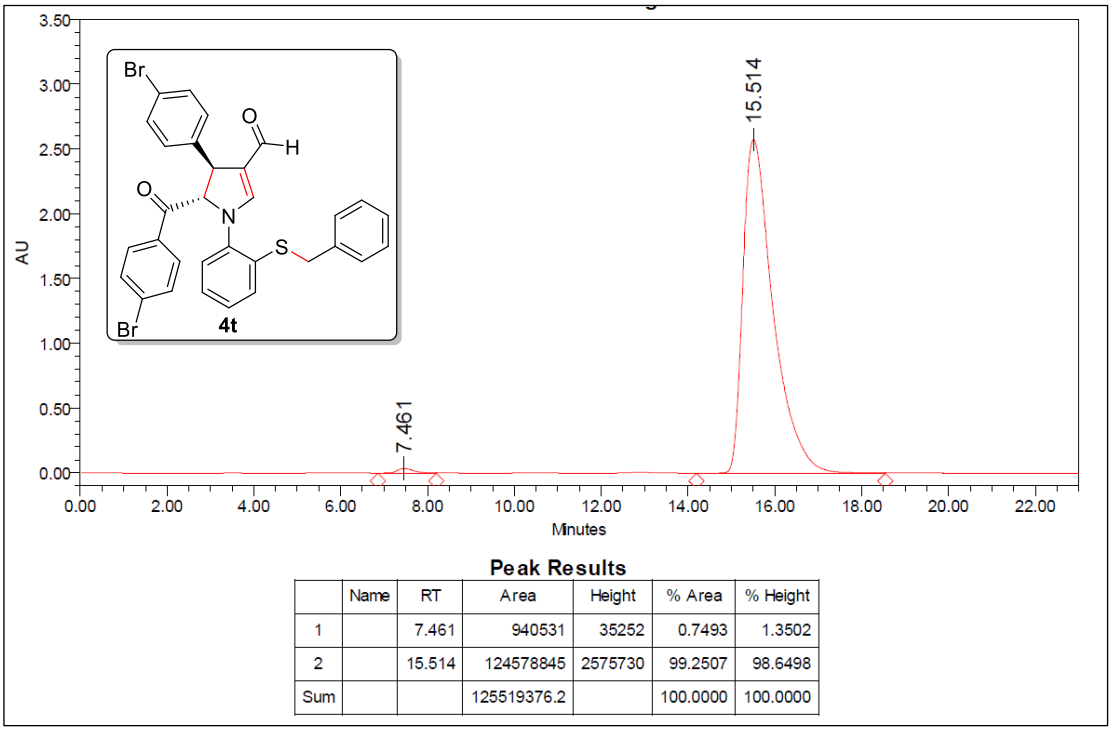

Peak Results

	Name	RT	Area	Height	% Area	% Height
1		7.461	940531	35252	0.7493	1.3502
2		15.514	124578845	2575730	99.2507	98.6498
Sum			125519376.2		100.0000	100.0000

(±)-4u

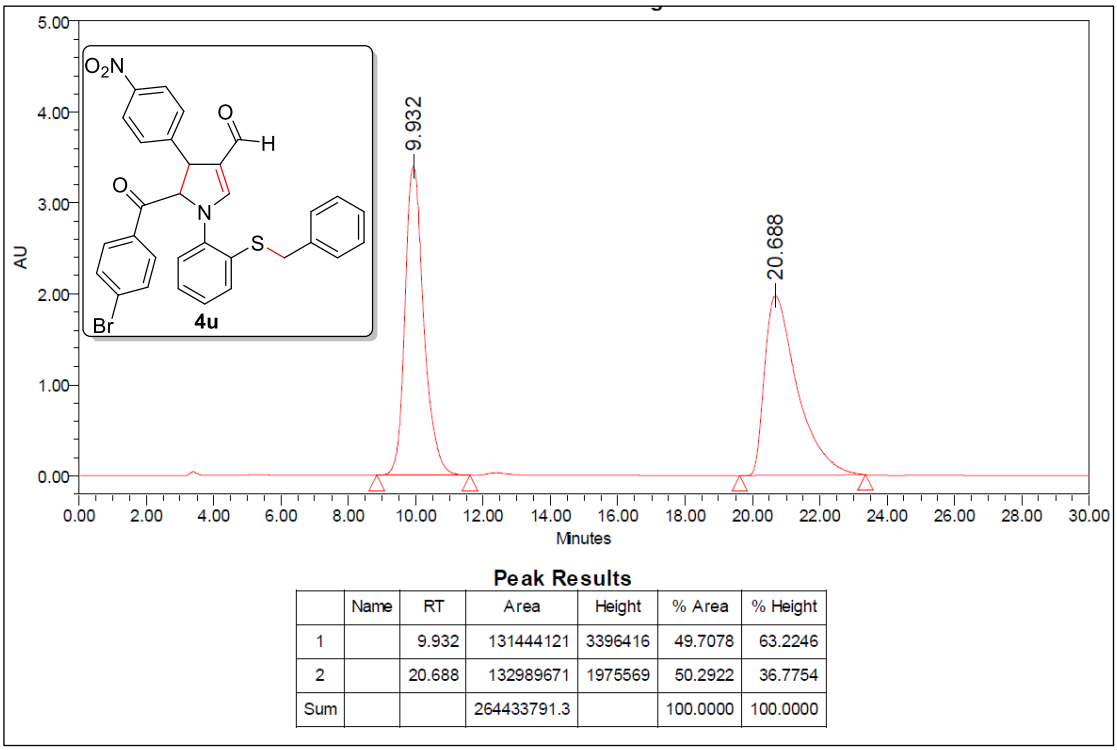

Peak Results

	Name	RT	Area	Height	% Area	% Height
1		9.932	131444121	3396416	49.7078	63.2246
2		20.688	132989671	1975569	50.2922	36.7754
Sum			264433791.3		100.0000	100.0000

Optical active 4u

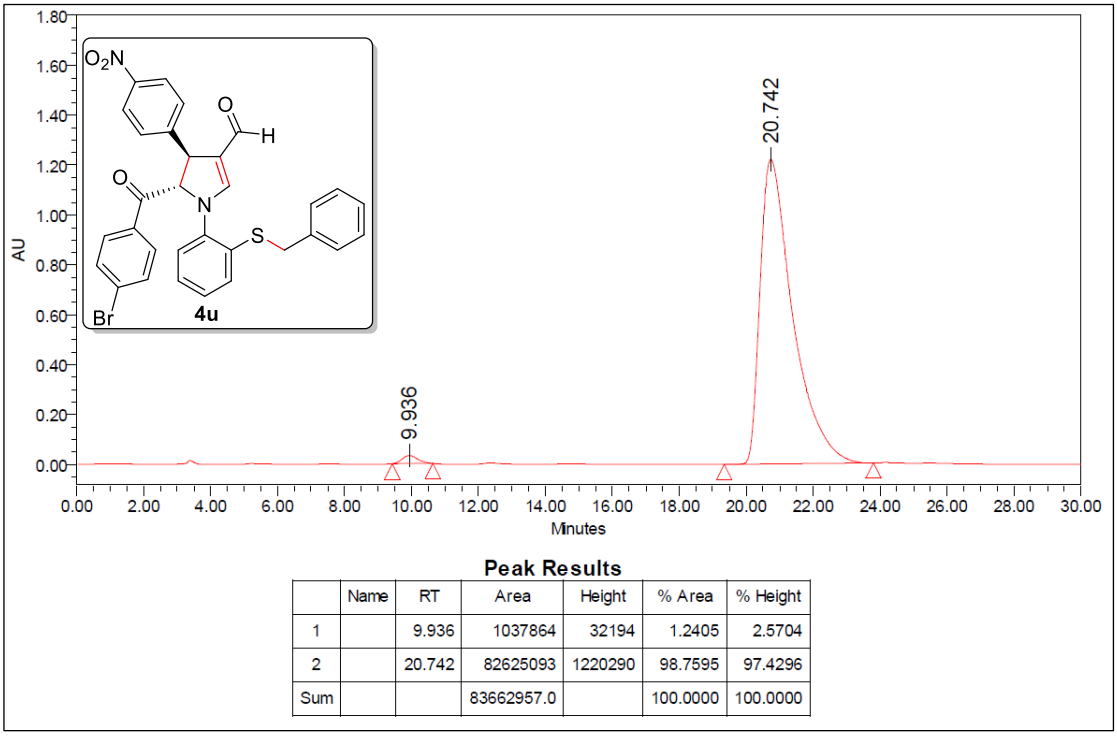

Peak Results

	Name	RT	Area	Height	% Area	% Height
1		9.936	1037864	32194	1.2405	2.5704
2		20.742	82625093	1220290	98.7595	97.4296
Sum			83662957.0		100.0000	100.0000

(±)-4v

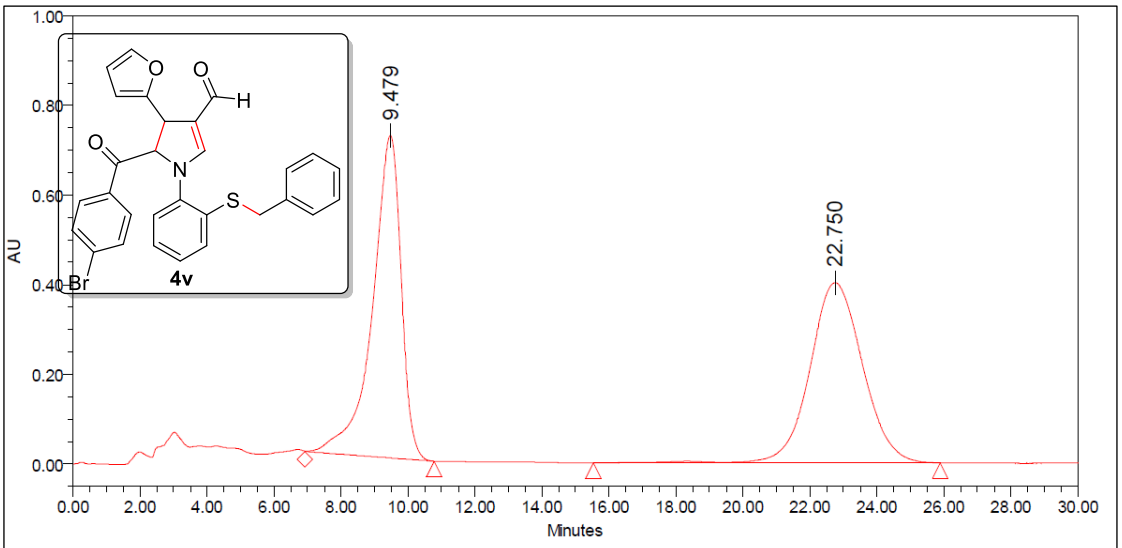

Peak Results

	Name	RT	Area	Height	% Area	% Height
1		9.479	42842885	719821	49.2657	64.1508
2		22.750	44119954	402256	50.7343	35.8492
Sum			86962838.5		100.0000	100.0000

Optical active 4v

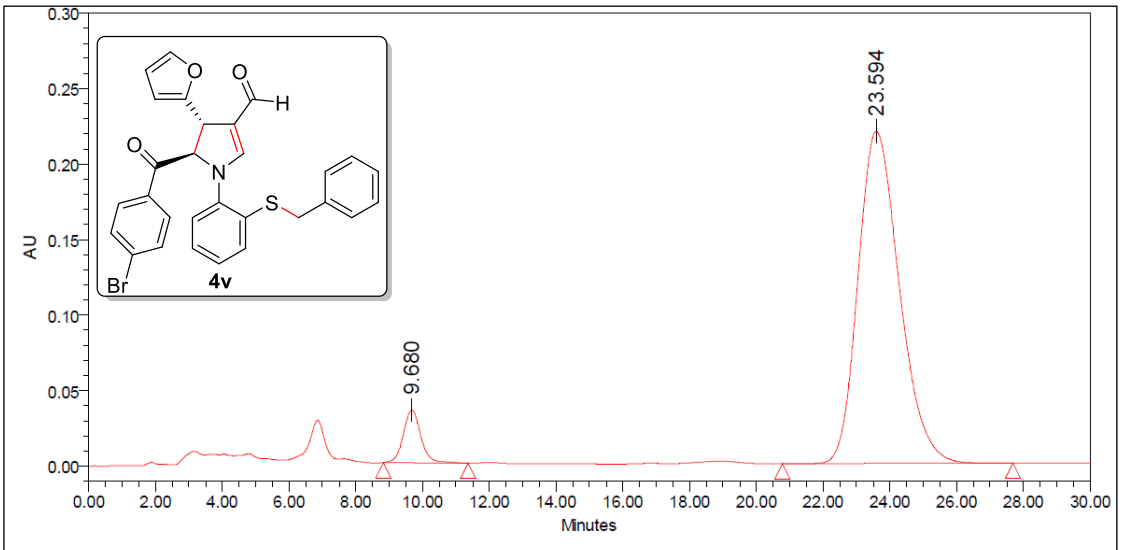

Peak Results

	Name	RT	Area	Height	% Area	% Height
1		9.680	1276292	35073	6.3309	13.7572
2		23.594	18883425	219873	93.6691	86.2428
Sum			20159717.5		100.0000	100.0000

(±)-5a

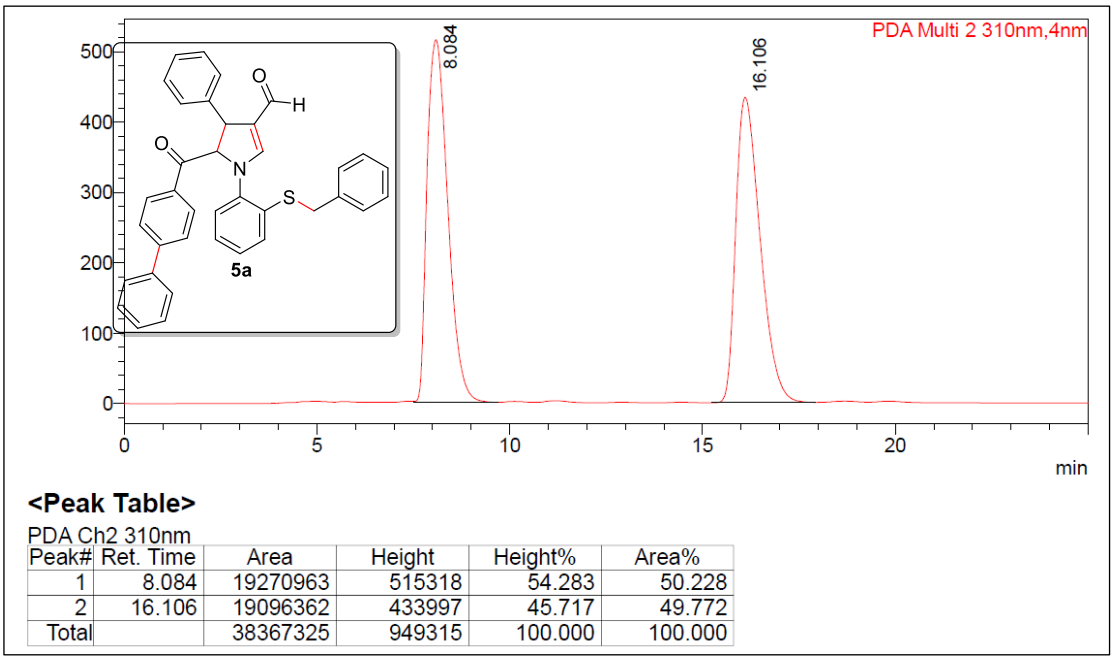

<Peak Table>

PDA Ch2 310nm

Peak#	Ret. Time	Area	Height	Height%	Area%
1	8.084	19270963	515318	54.283	50.228
2	16.106	19096362	433997	45.717	49.772
Total		38367325	949315	100.000	100.000

Optical active 5a

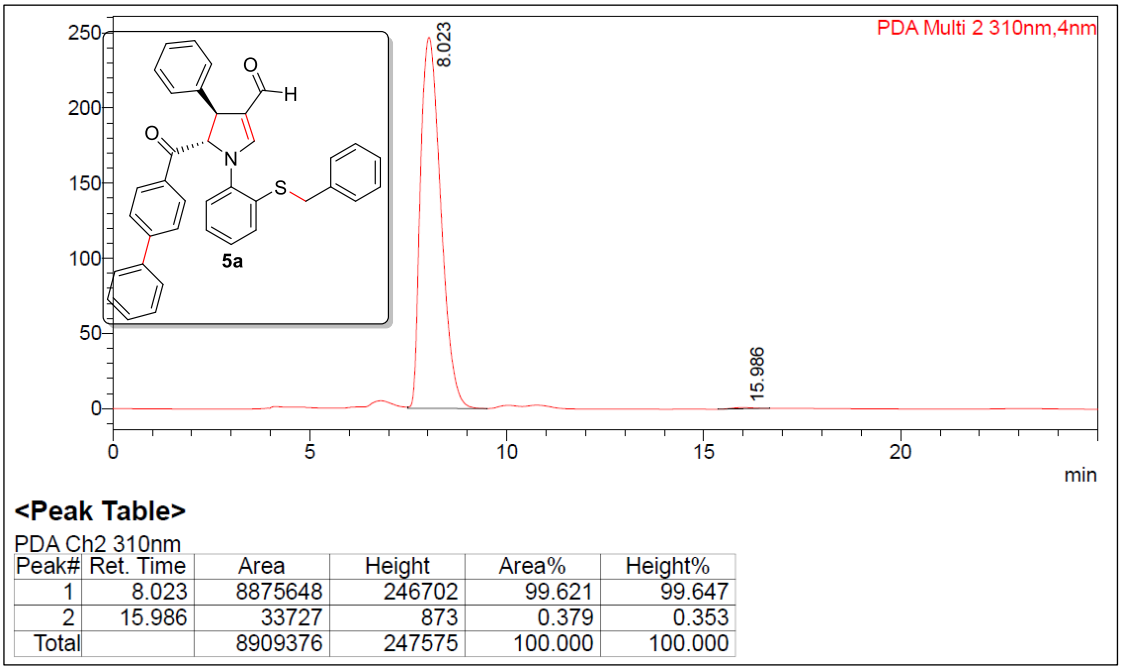

<Peak Table>

PDA Ch2 310nm

Peak#	Ret. Time	Area	Height	Area%	Height%
1	8.023	8875648	246702	99.621	99.647
2	15.986	33727	873	0.379	0.353
Total		8909376	247575	100.000	100.000

CHAPTER 4

SYNTHESIS OF TRISUBSTITUTED 1*H*-PYRROLE AND CHIRAL TRISUBSTITUTED 4,5-DIHYDRO-1*H*-PYRROLE

CHAPTER 4A

FORMAL DOMINO 1,3-DIPOLAR CYCLOADDITION/C-S AND C-N BOND-CLEAVAGE REACTION: SYNTHESIS OF TRISUBSTITUTED 1*H*-PYRROLE-3-CARBALDEHYDES

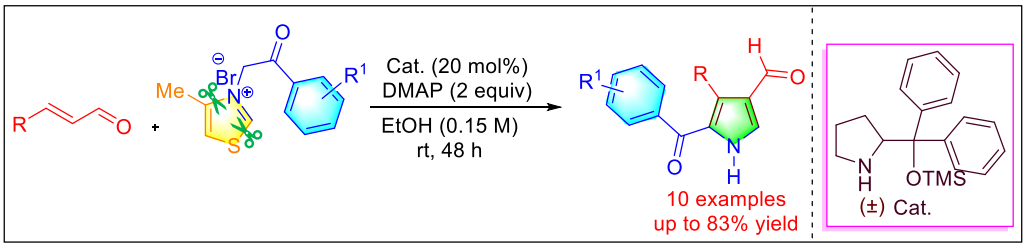

4.1 INTRODUCTION

4.1.1 Importance of 1*H*-Pyrroles and Poly-Substituted 1*H*-Pyrroles

1*H*-Pyrroles represent a fundamental class of heterocyclic compounds that have drawn significant attention from synthetic chemist owing to their broad applications in organic synthesis and medicinal chemistry.[217,218] 1*H*-Pyrroles are five-membered nitrogen-containing aromatic heterocycles. Due to their planar structure and electron-rich nature, they can be used as a versatile building block in organic synthesis.[219] Most of the unique properties such as basicity, nucleophilicity, and coordination ability possessed by 1*H*-pyrroles are valuable in various chemical transformations and molecular interactions.[220-223]

Poly-substituted 1*H*-pyrroles are known to attract many synthetic chemists because of their diverse use in organic synthesis, bioactive molecules, and catalysis.[224] The unique structural features owing to the construction of complex molecules and functional materials.[225] There are several chemical modifications which include electrophilic aromatic substitution,[226] nucleophilic addition,[227,228] and transition-metal-catalyzed reactions,[229] assist the introduction of substituents onto the pyrrole ring. To synthesize poly-substituted 1*H*-pyrroles, there are numerous synthetic methods have been reported in the literature. The traditional synthesis of pyrrole includes Hantzsch,[230] which involves the condensation of β-ketoesters or β-dicarbonyl compounds with primary amines and a suitable carbonyl compound. Another key method of pyrrole synthesis is named Paal-Knorr synthesis,[231] which offers a reaction between 1,4-dicarbonyl compounds and primary amines under acidic conditions. Numerous modern methodologies have emerged to access diverse poly-substituted 1*H*-pyrroles,[232] such as cycloaddition reactions,[233-235] transition-metal mediated cyclization reactions,[236] cyclopropane ring-opening reaction,[237] multicomponent and cascade reactions.[238-240]

Poly-substituted 1*H*-pyrroles serve as privileged structures in drug discovery due to their potential biological activities,[241] such as antitumor, antibacterial, antiviral, anti-inflammatory agents, anticancer drug veliparib[242, 243] and antibacterial agent selvamicin[244] (Figure 4.1).

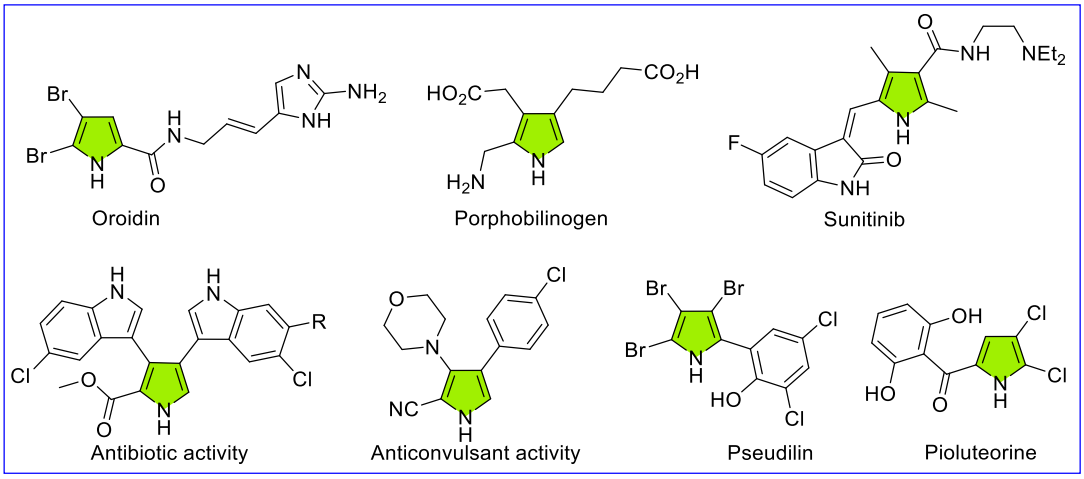

Figure 4.1. Biologically active poly-substituted-1*H*-pyrrole scaffolds

In materials science, the π-conjugated nature of poly-substituted 1*H*-pyrroles makes them attractive candidates for optoelectronic materials.[245] They have been incorporated into organic semiconductors, light-emitting diodes (LEDs), and photovoltaic devices, contributing to advancements in organic electronics.[246]

In molecular probes, functionalized poly-substituted 1*H*-pyrroles have been utilized as fluorescent probes and sensors for detecting various analytes, including metal ions, biomolecules, and environmental pollutants.[247,248] Their tunable optical properties and selective sensing capabilities make them valuable chemical biology and environmental monitoring tools. The transition-metal complexes based on poly-substituted 1*H*-pyrroles exhibit catalytic activity in various transformations, such as cross-coupling reactions, cycloadditions, and asymmetric synthesis. These catalysts offer advantages such as high catalytic efficiency, mild reaction conditions, and substrate tolerance.

1,3-Dipolar cycloaddition reaction is one of the most powerful methods for the construction of diverse heterocyclic compounds, mainly poly-substituted pyrroles.[108] This reaction enables the rapid assembly of complex molecular architectures with high efficiency and atom economy. By exploiting the reactivity of 1,3-dipoles and dipolarophiles, which involves the concerted, stereospecific formation of a cyclic product. In the context of pyrrole synthesis, commonly employed 1,3-dipoles include azomethine ylides and nitrile oxides, which undergo cycloaddition with electron-deficient alkenes or alkynes as dipolarophiles.[249] The reaction proceeds *via* a transition state characterized by the simultaneous formation of two new σ-bonds, resulting in the regio- and stereochemically-defined formation of pyrrole rings. A wide range of substituents can be introduced onto the pyrrole ring in a controlled manner by judicious selection of 1,3-dipoles and dipolarophiles. The regioselectivity and stereochemistry of the cycloaddition can be modulated through appropriate choice of reaction conditions and functional group compatibility, enabling the synthesis of complex poly-substituted pyrrole derivatives.[250-253]

4.2 LITERATURE BACKGROUNDS

4.2.1 Synthetic Approaches for Polysubstituted 1*H*-Pyrroles

A mild and efficient method for the synthesis of highly substituted pyrroles using four component reaction has been reported by Aziaian *et al.* in 2010. The reaction involved triphenyl phosphine, α-diketones, ammonium acetate, and dialkyl acetylenedicarboxylate at room temperature providing polysubstituted pyrroles with excellent yield (Scheme 4.1).[253]

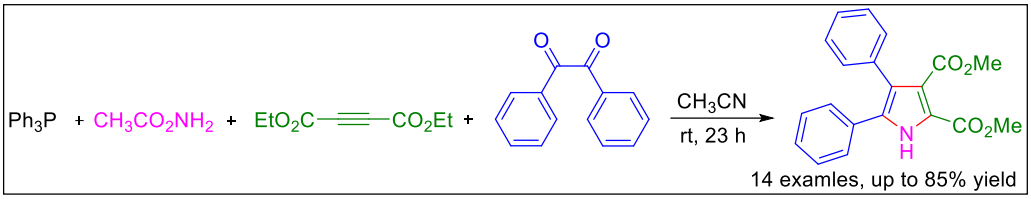

Scheme 4.1 Four-component reaction for the synthesis of polysubstituted 1*H*-pyrroles

In 2021, Kanova and co-workers accomplished a one-pot, two-step synthesis of 2-acetyl-1*H*-pyrroles from *N*-propargylic *β*-enaminone with zinc chloride in the presence of chloroform under reflux conditions. The reaction provided 2-methylene-2,3-dihydro-1,4-oxazipines *via* intramolecular cyclization. Further refluxing with zinc chloride in methanol *via* intramolecular ring-opening and ring-closing afforded the 2-acetyl-1*H*-pyrroles with excellent yields and high functional group tolerance (Scheme 4.2) [254]

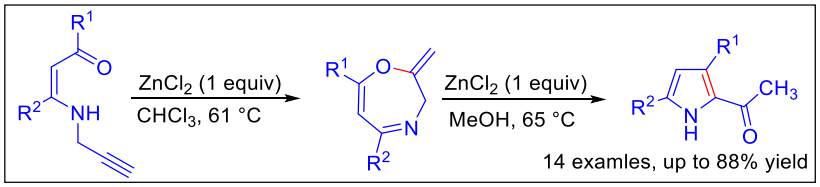

Scheme 4.2 One-pot intramolecular cyclization for the synthesis of 2-acetyl-1*H*-pyrroles

Wang *et al*. in 2023 described the synthesis of multi-substituted pyrroles *via* 1,3-dipolar cycloaddition of azomethine ylides with ynones in the presence of AgOAc as a catalyst and PPh_3 as a ligand. The reaction furnished the corresponding poly-substituted pyrroles in moderate to high yields (Scheme 4.3).[255]

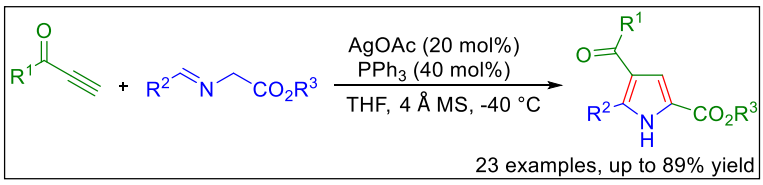

Scheme 4.3 Silver-catalyzed 1,3-dipolar cycloaddition for the synthesis of multi-substituted-1*H*-pyrroles

The synthesis of functionalized substituted pyrroles was achieved in 2010 by Robles and co-workers *via* Cu-catalyzed 1,3-dipolar cycloaddition of -iminoester azomethine ylide with sulfonyl dipolarophiles. This method was adopted to prepare 2,5-disubstituted and 2,3,5-and 2,4,5-trisubstituted pyrroles in good yields (Scheme 4.4).[256]

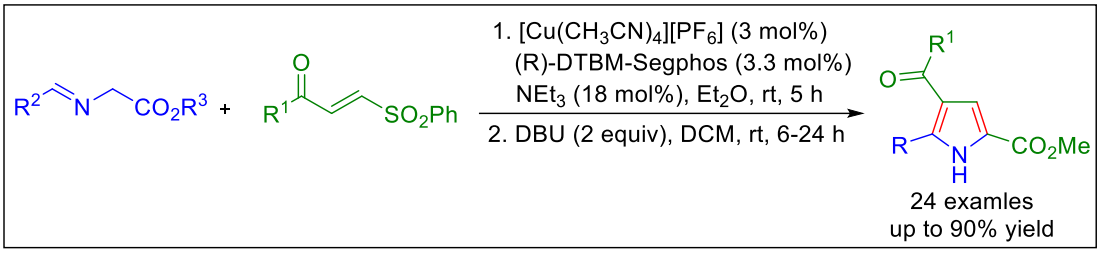

Scheme 4.4 Cu-catalysed 1,3-dipolar cycloaddition catalyzed for the synthesis of poly-substituted-1*H*-pyrroles

In 2010, Kim *et al*. furnished the regioselective synthesis of tetrasubstituted pyrroles in good yields through classic 1,3-dipolar cycloaddition of unsaturated benzofuran 3(2*H*)-one and azlactones azomethine ylide followed by spontaneous decarboxylation in the presence of silver acetate under microwave condition (Scheme 4.5).[257]

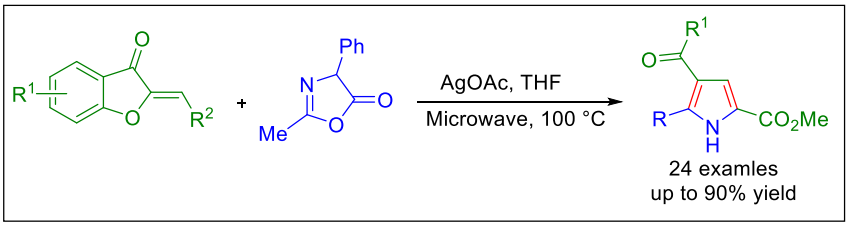

Scheme 4.5 Silver catalyzed 1,3-dipolar cycloaddition for the synthesis of tetrasubstituted-1*H*-pyrroles

The synthesis of poly-substituted pyrroles using silver-catalyzed 1,3 dipolar cycloaddition/benzyl peroxide mediated oxidative dehydrogenation/aromatization reaction sequence was developed by Liu and co-workers in 2017. This method provided the tetrasubstituted pyrroles in good to excellent yields (Scheme 4.6).[258]

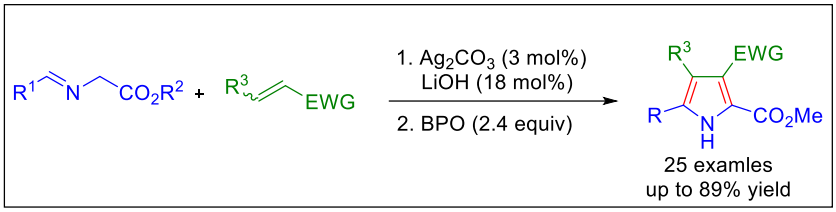

Scheme 4.6 Silver catalyzed 1,3-dipolar/oxidative dehydrogenation reaction for the synthesis of tetrasubstituted-1*H*-pyrroles

In 2023, Larkovich *et al.* developed the Barton-Zard reaction of β-fluoro-β-nitrostyrenes with ethyl α-isocyanoacetate for the synthesis of highly chemoselective formation of 4-fluoro trisubstituted pyrroles in good yields. In addition, 4-nitro trisubstituted pyrroles are formed as minor products as shown in Scheme 4.7.[259]

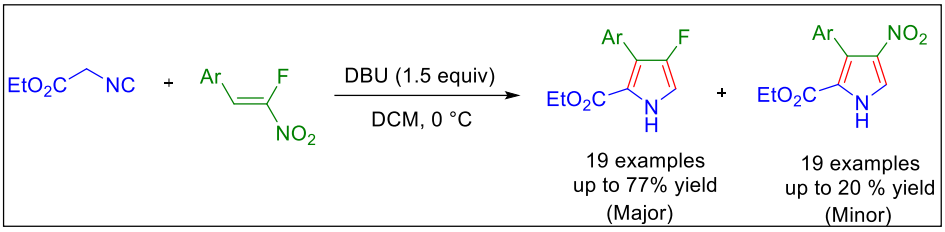

Scheme 4.7 Barton-Zard reaction for the synthesis of 4-fluoro trisubstituted 1*H*-pyrroles

An unprecedented dimerization of 2*H*-azirines *via* palladium/silver co-catalyzed divergent dimerization for the regioselective synthesis of tetrasubstituted pyrroles with moderate yields has been achieved in 2023 by Zhao *et al.* (Scheme 4.8).[260]

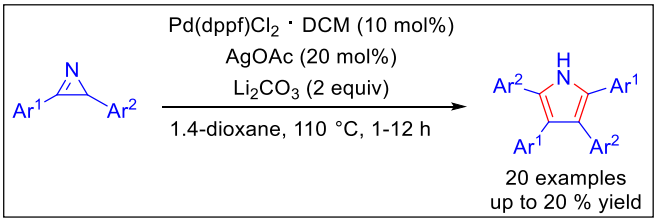

Scheme 4.8 Palladium/silver co-catalyzed dimerization reaction for the synthesis of tetrasubstituted 1*H*-pyrroles

In 2013, Chen and co-workers reported an aerobic synthesis of substituted pyrroles from *N*-allyl imines *via* palladium(II)-catalyzed/intramolecular C-H dehydrogenative cyclization sequence with excellent yields (Scheme 4.9).[261]

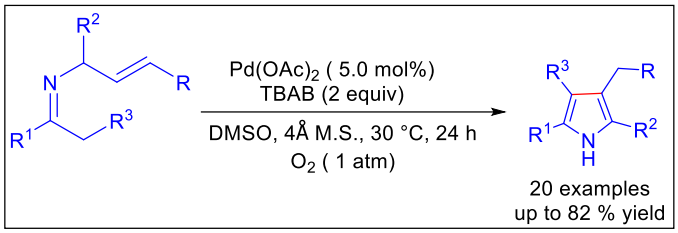

Scheme 4.9 Palladium (II)-catalyzed/intramolecular C-H dehydrogenative reaction for the synthesis of 1*H*-pyrroles

The first multicomponent synthesis of pyrrole was published in 1890 by Hantzsch and co-workers. The reaction between an equimolar mixture of chloroacetate and acetoacetic ester in concentrated aqueous ammonia under reflux conditions afforded the polysubstituted pyrrole (Scheme 4.10).[262]

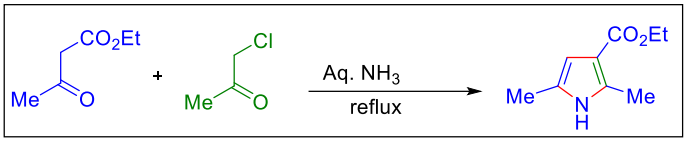

Scheme 4.10 Cycloisomerization reaction for synthesis of trisubstituted-1*H*-pyrroles

In 2014, Xin *et al.* reported an efficient and divergent one-pot synthesis of 3-alkyl-1*H*-pyrroles and 3-alkenyl-1*H*-pyrroles from readily accessible 2,4-pentadienenitriles with isocyanide. The reaction proceeded *via* [3+2] annulation in the presence of DBU (2.0 equiv) as a base with EtOH under reflux conditions afforded the 3-alkyl-1*H*-pyrroles. The synthesis of 3-alkenyl-1*H*-pyrrole has been achieved by DBU/EtOH at room temperature followed by the addition of DDQ under reflux conditions. Both methods provided the desired trisubstituted pyrroles in good yields (Scheme 4a.11).[263]

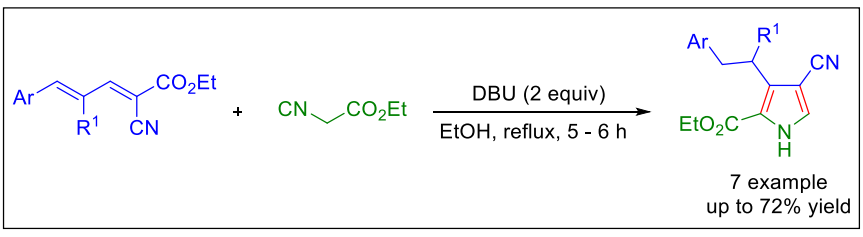

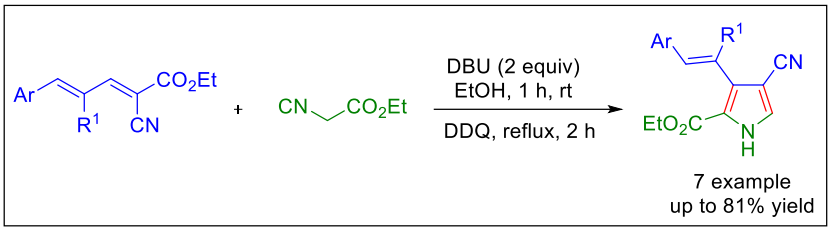

Scheme 4.11 One-pot annulation reaction for the synthesis of 3-alkyl-1*H*-pyrroles and 3-alkenyl-1*H*-pyrroles

The regioselective synthesis of 2,3,4 or 2,3,5-trisubstituted pyrroles *via* [3,3] or [1,3] sigmatropic rearrangement of *O*-vinyl oximes has been accomplished in 2011 by Wang and groups. The *O*-vinyl oximes were prepared by iridium-catalyzed isomerization of O-allyl oximes. When enolization was favored in this reaction, a [3,3]-sigmatropic rearrangement followed by a Pall-Knorr cyclization provided a 2,3,4-trisubstituted pyrroles. When the enolization was disfavored, a [1,3]-sigmatropic rearrangement occurred to provide the 2,3,5-trisubstituted pyrroles (Scheme 4.12).[264]

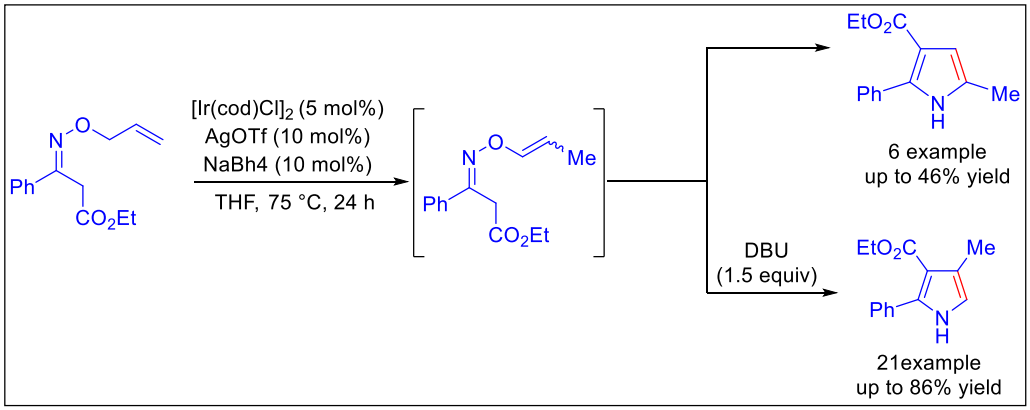

Scheme 4.12 Iridium-catalyzed isomerization/[3,3] or [1,3] sigmatropic rearrangement reaction for the synthesis of trisubstituted NH-pyrroles

In 2015, Cai and co-workers furnished the synthesis of 2-acylpyrroles *via* microwave-promoted iminyl radical cyclization with TEMPO, using alkynes as radical acceptors to provide the functionalized 2-acylpyrroles in good yields (Scheme 4.13).[265]

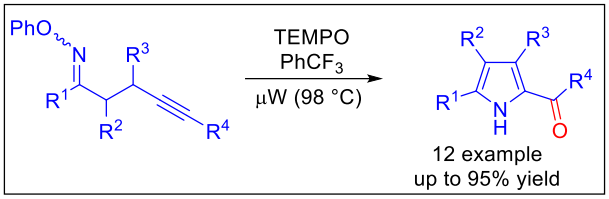

Scheme 4.13 Microwave-promoted radical cyclization reaction for the synthesis of 1*H*-2-acylpyrroles

A one-pot, three-component reaction for the synthesis of 2-amino-5-ketoaryl pyrroles has been reported in 2010 by Wang *et al*. The reaction between aminoacetophenone sulphonamides, heteroaromatic aldehydes, and malononitriles or cyanoacetic acid derivatives in a one-pot manner provided the tetrasubstituted pyrroles in good yields (Scheme 4.14).[266]

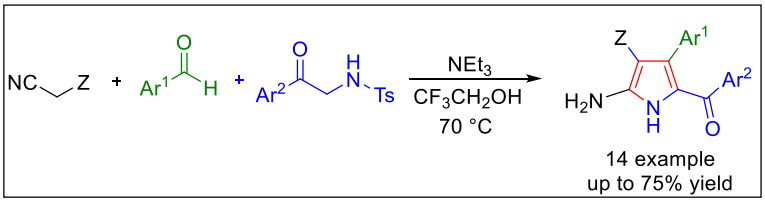

Scheme 4.14 One-pot, three-component reaction for the synthesis of tetrasubstituted 1*H*-pyrroles.

The first step is continuous flow synthesis of pyrrole-3-carboxylic acids directly from t-butyl acetoacetates, amine, and 2-bromoketones *via in-situ* hydrolysis of t-butyl esters generated by HBr as the byproduct. This protocol was used in the multistep synthesis of pyrrole-3-carboxyamides, including two CB1 inverse agonists, directly from commercially available starting materials in a single continuous process, has been reported in 2010 by Wang *et al.* (Scheme 4.15).[267]

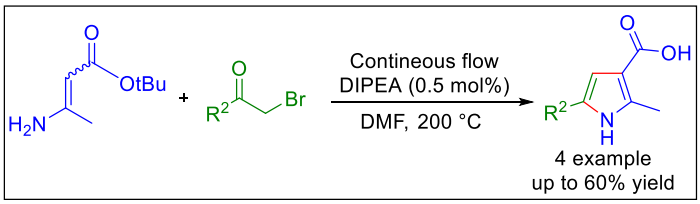

Scheme 4.15 One step, continuous flow synthesis of NH-pyrrole-3-carboxylic acids

In 2013, Tamaddon *et al.* developed a facile, three-component method for the regioselective synthesis of tetrasubstituted pyrroles from readily accessible 1,3-dicarbonyls, benzoin derivatives and ammonium acetates *via* a catalyst and solvent-free condition provided the desired products in good yields (Scheme 4.16).[268]

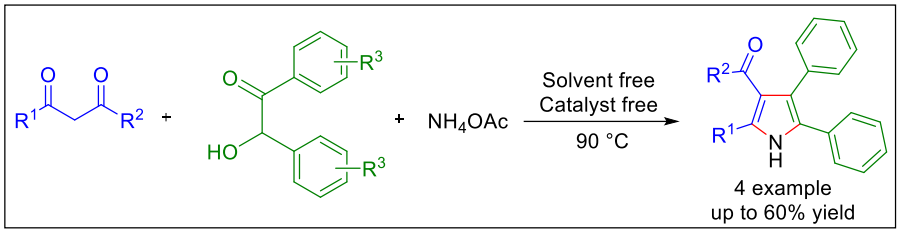

Scheme 4.16 Three-component reaction for the synthesis of tetrasubstituted 1*H*-pyrroles

In 2012, Chen and co-workers reported a facile synthesis of 2,3,4-trisubstituted pyrroles from tosylmethyl isocyanide (TOSMIC) and readily synthesized vinyl azides *via* Michael addition/intramolecular cyclization reaction sequence under mild reaction condition. The reaction afforded polysubstituted pyrroles in moderate to good yields (Scheme 4.17).[269]

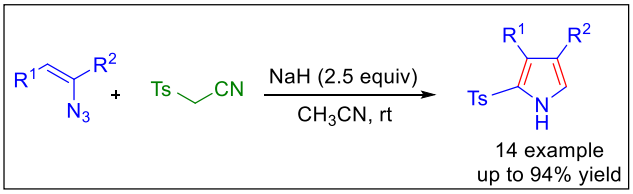

Scheme 4.17 Michael addition/intramolecular cyclization reaction for the synthesis of 2,3,4-trisubstituted NH-pyrroles

An iron-catalyzed addition and cyclization of the Blaise reaction intermediate obtained from phenyl nitrile and 2-bromoethylacetate in the presence of zinc as a catalyst followed by nitroolefins furnished highly functionalized NH-pyrroles in a tandem one-pot manner in 2013 by Zhao *et al*. This reaction afforded good functional group tolerance to achieve the substituted NH-pyrroles in good yields (Scheme 4.18).[270]

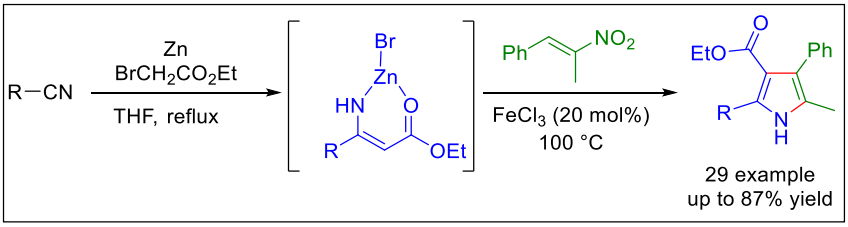

Scheme 4.18 Iron-catalyzed addition/cyclization reaction for the synthesis of highly functionalized 1*H*-pyrroles.

A copper-catalyzed three-component reaction for the synthesis of polysubstituted pyrroles from α-diazo ketones, nitroalkenes, and amines under aerobic conditions was described in 2011 by Hong and co-workers. This three-component reaction involves N-H insertion of carbene, a copper-catalyzed oxidative dehydrogenation of amines, and *in-situ* formation of azomethine ylides. The [3+2] cycloaddition of azomethine ylides with nitroalkene furnished polysubstituted pyrrolidines intermediate, which was further aerobic oxidation provided the polysubstituted pyrroles in good yields (Scheme 4.19).[271]

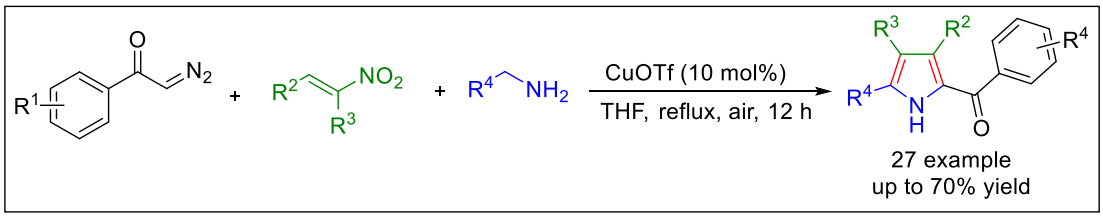

Scheme 4.19 Copper-catalyzed three-component reaction for the synthesis of polysubstituted 1*H*-pyrroles

The synthesis of tetrasubstituted pyrroles in excellent yields was accomplished in 2009 by Yavari *et al.* for the three-component condensation reaction of acid chlorides, dialkyl acetylene dicarboxylates, and amino acids in the presence of ionic liquid [RTILs] as a catalyst in aqueous media at room temperature (Scheme 4.20).[272]

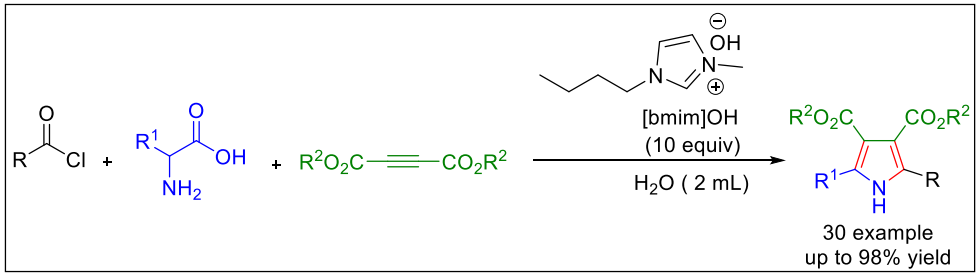

Scheme 4.20 Ionic liquid-catalyzed three-component reaction for the synthesis of polysubstituted NH-pyrroles

In 2010, Cadierno and co-workers developed the Ru-catalyzed one-pot, three-component reaction for the synthesis of functionalized ester or ketone groups at the C-3 position containing tetrasubstituted NH-pyrroles. The coupling of secondary propargylic alcohol with 1,3-dicarbonyl compounds and tert-butyl carbamate *via in-situ* deprotection of the corresponding pentasubstituted N-Boc, pyrroles using trifluoracetic acid as shown in Scheme 4.21.[273]

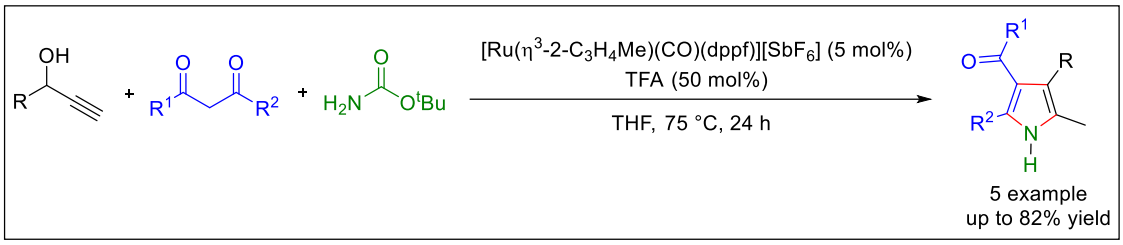

Scheme 4.21 Ru-catalyzed three-component reaction for the synthesis of tetrasubstituted NH-pyrroles

A silver-catalyzed three-component reaction towards the direct synthesis of multi-functionalized trisubstituted pyrroles was achieved in 2011 by Zeng *et al. via* unusual imidazole ring decomposition, 1,5-isomerization, and subsequent hydrolysis provided the polysubstituted pyrroles in good yields (Scheme 4.22).[274]

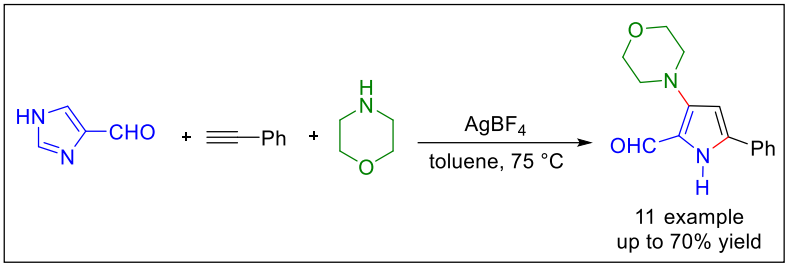

Scheme 4.22 Silver-catalyzed three-component reaction for the synthesis of trisubstituted NH-pyrroles

In 2010, Wang *et al.* developed a method to synthesize pyrrole derivatives, particularly penta-substituted pyrroles. The reaction involved the 1,3-dipolar cycloaddition, otherwise known as Huisgen pyrrole synthesis, the intermediate mesoionic 2-oxazilium-5-olates, which are also known as munchnones, reacted with acetylenic or olefinic dipolarophiles, followed by carbon dioxide CO_2 evolution and subsequent aromatization or tautomerization (Scheme 4.23).[275] The munchnones can be easily prepared by the acetic anhydride-induced dehydrative cyclization of *N*-alkyl-*N*-acyl-α-amino acids at high temperatures.

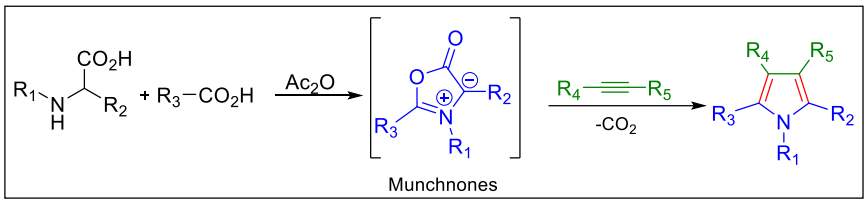

Scheme 4.23 Huisgen pyrrole synthesis *via* 1,3-dipolar cycloaddition

4.3 OBJECTIVE

- Inspired by literature reports, a new and domino methodology will be developed for the synthesis of trisubstituted-*1H*-pyrrole-3-carbaldehdes.
- This method will utilize readily available 4-methyl thiazolium salts and commercially available α,β-unsaturated aldehydes, using racemic diphenylprolinol trimethylsilyl ether as an organocatalyst (Scheme 4.24).

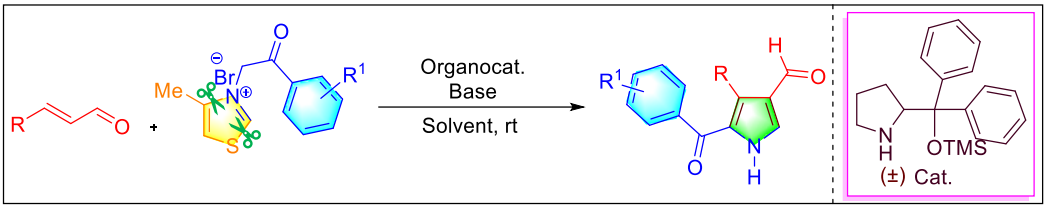

Scheme 4. 24 Formal domino 1,3-dipolar cycloaddition/ring-opening/*C*-*S* and *C*-*N* bond cleavage for synthesis of trisubstituted-1*H*-pyrrole-3-carbaldehydes.

- In this method, 4-methyl thiazolium salt will undergo a formal domino intermolecular 1,3-dipolar cycloaddition/intramolecular ring-opening/C-*S* and *C*-*N* bond cleavage in the presence of a base.

4.3.1 Hypothesis of Present Work

As described in the previous Chapter **2**, the synthesis of pyrrolo-thiazine-2-carbaldehydes **3** has been achieved by formal domino intermolecular 1,3-dipolar cycloaddition/intramolecular rearrangement reaction sequence of benzothiazolium azomethine **2** ylide and α,β-unsaturated aldehydes **1** with chiral organocatalyst. In Chapter **3**, the product formed from Chapter **2** will be reacted with alkyl and benzyl halides in the presence of a base to afford the *N*-phenyl thioether-tethered tetrasubstituted dihydropyrrole-3-carbaldehydes **6** *via* one-pot intermolecular 1,3-dipolar cycloaddition/intramolecular rearrangement followed by C-S bond formation/base-promoted intramolecular ring-opening reaction (Scheme 4.25). It is hypothesis that instead of benzothiazolium azomethine ylide **2**, use of 4-methyl thiazolium azomethine ylide **8** and α,β-unsaturated aldehydes **1** in the presence of asymmetric organocatalysts **5**, the reaction will expected to provide 4-methyl-pyrrolo[2,1-*c*][1,4]thiazine-7-carbaldehyde **9** as like in Chapter **2**.

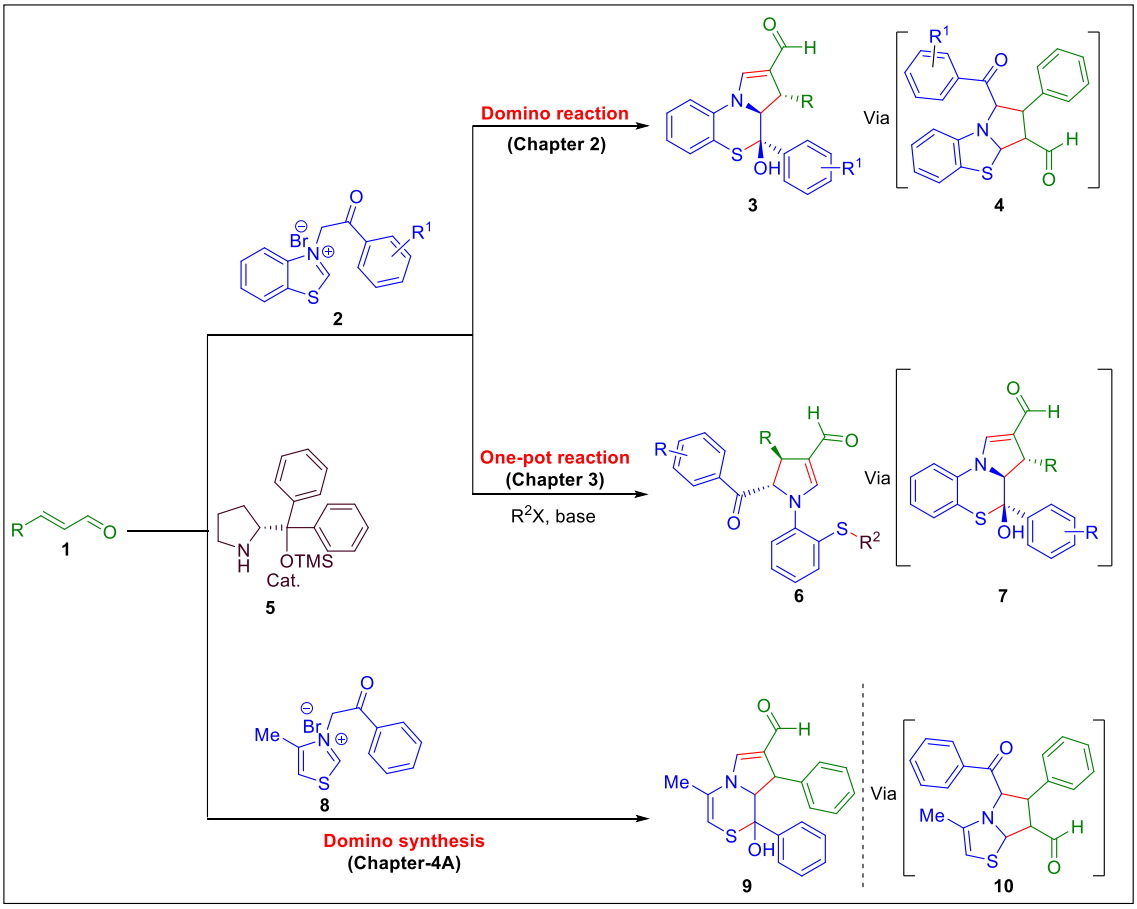

Scheme 4.25 Hypothesis of formal 1,3-dipolar cycloaddition/rearrangement

In contrast, the reaction furnished trisubstituted 1*H*-pyrrole-3-carbaldehyde **11**, which can be rationalized by a formal domino1,3-dipolar cycloaddition/C-S and C-N bond cleavage reaction sequence (Scheme 4.26).

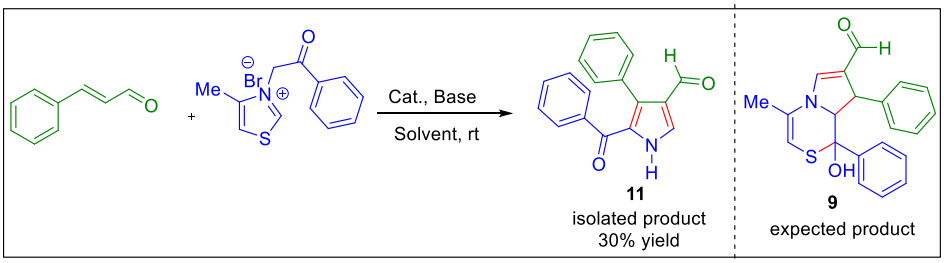

Scheme 4.26 Synthesis of trisubstituted-1*H*-pyrrole-3-carbaldeydes

A literature survey reveals that few reports are available for synthesizing poly-substituted pyrrole using thiazolium azomethine ylide.[108] As of now, there are no reports for the formal domino 1,3-dipolar cycloaddition of 4-methyl thiazolium salts

with α,β-unsaturated aldehydes to synthesize trisubstituted-1*H*-pyrroles-3-carbaldehydes using organocatalyst is highly warranted. Thus, a formal domino 1,3-dipolar cycloaddition method will be developed for the synthesis of trisubstituted 1*H*-pyrrole-3-carbaldehydes from readily available α,β-unsaturated aldehydes, 4-methyl thiazolium salts, and racemic diphenylprolinol trimethylsilyl ether as an organocatalyst (Scheme 4.24).

4.4 RESULTS AND DISCUSSION

Initially, the reaction was performed to synthesize the racemic product of **9** using 4-methyl thiazolium salt **8**, α,β-unsaturated aldehydes **1** in the presence of racemic proline as the organocatalyst and NEt_3 as a base in IPA at room temperature. After 48 h, the reaction provided an achiral product of trisubstituted 1*H*-pyrrole-3-carbaldehydes **11** albeit in 30% yield**,** instead of furnishing hypothesized product **9** (Scheme 4.27).

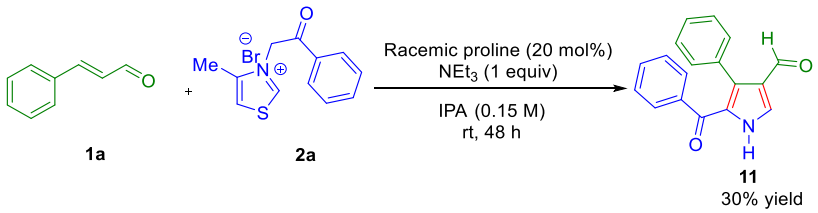

Scheme 4.27 Trail reaction for the synthesis of trisubstituted 1*H*-pyrrole **11**

4.4.1 Optimization Studies

Based on the preliminary result, to improve the yield of product **11**, an optimization of the reaction condition by modifying parameters such as catalysts, bases, and solvents was carried out, and the results are presented in Tables 4.1 – 4.3. First, several racemic secondary amine-based organic catalysts were examined in the reaction (Table 4.1, entries 1-4). The product yield was increased when the catalyst changed to **C2** (Table 4.1, entry 2). The catalyst was changed from **C2** to **C3**, and the

yield was enhanced to 40% (Table 4.1, entry 3). After that, the catalyst changed to **C4**, and the reaction yield was enhanced to 45% (Table 4.1, entry 4).

When the catalyst bulkiness was increased **C5**, the reaction yielded product **11** in 55% yield (Table 4.1 entry 5). When the chiral catalyst **C6** was used instead of racemic catalysts, the reaction gave a 47% yield of product **11** (Table 4.1, entry 6). Then, to improve the yield of the product **11,** the reaction was performed with several bases such as DBU, DBA, 2,6-lutidine, K_2CO_3, K_3PO_4, DBA, DABCO, DMAP (Table 4.2, entries 1-7).

Table 4.1 Catalyst Screening[a]

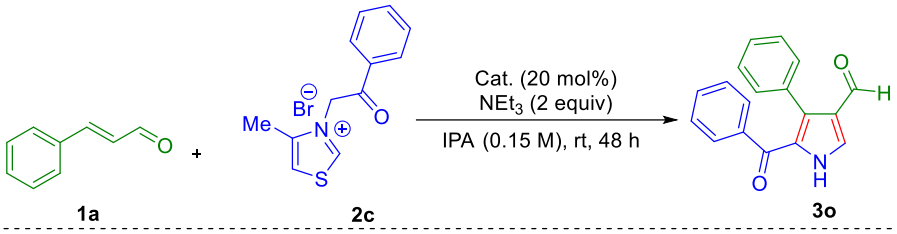

Entry	Base (equiv)	Catalyst	Yield (%) [b]
1	NEt_3 (2)	**C1**	30
2	NEt_3 (2)	**C2**	15
3	NEt_3 (2)	**C3**	40
4	NEt_3 (2)	**C4**	45
5	NEt_3 (2)	**C5**	55

[a]Reaction conditions: **1a** (0.3 mmol), **2a** (0.3 mmol), NEt_3 (2 equiv), catalyst **C1-C5** (20 mol%), and IPA (0.15 M) at 48 h. [b]Isolated yield.

Table 4.2 Base Screening[a]

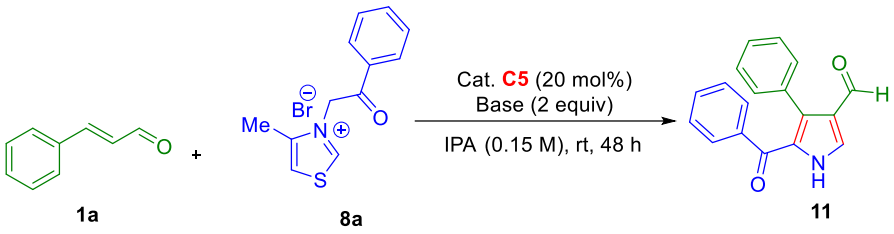

Entry	Base (equiv)	Catalyst	Yield (%) [b]
1	NEt_3 (2)	**C5**	55
2	DBU (2)	**C5**	15
3	DBA (2)	**C5**	22
4	2,6-lutidine (2)	**C5**	15
5	K_2CO_3 (2)	**C5**	20
6	K_3PO_4 (2)	**C5**	25
7	DBA (2)	**C5**	35
8	DABCO (2)	**C5**	45
9	DMAP (2)	**C5**	65

[a]Reaction conditions: **1a** (0.3 mmol), **2a** (0.3 mmol), base (2 equiv), catalyst **C5** (20 mol%), and IPA (0.15 M) at 48 h. [b]Isolated yield.

Among the bases used, the reaction gave **11a** in 65% yield (Table 4.2, entry 9). Then the rection was screened with several solvents (Table 4.2, entries 1-6). In this solvent screening, EtOH as a solvent furnished the product **11a** in 75% yield. When the quantity of DMAP was decreased from two equivalent to one equivalent, the yield of product **11a** was also decreased to 60% (entry 8). When the loading of the catalyst was decreased to 10 mol%, the yield was also reduced to 50% yield (entry 10). When

the reaction was performed without a catalyst, the yield of **11a** was reduced to 30% (entry 11).

Table 4.3 Solvent Screening[a]

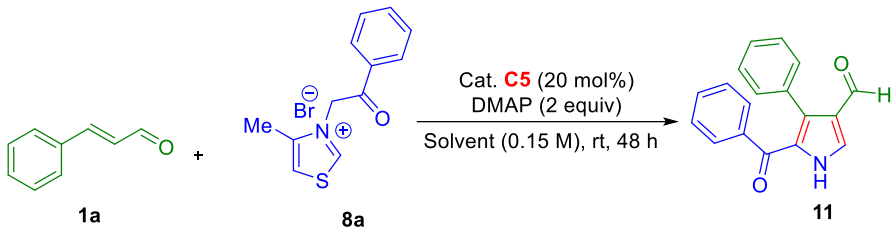

Entry	Base (equiv)	Catalyst	Solvent	Yield (%)[b]
1	DMAP (2)	**C5**	IPA	65
2	DMAP (2)	**C5**	toluene	41
3	DMAP (2)	**C5**	THF	40
4	DMAP (2)	**C5**	DCM	44
5	DMAP (2)	**C5**	DMSO	15
6	DMAP (2)	**C5**	HFIP	47
7	DMAP (2)	**C5**	Et_2O	30
8	DMAP (2)	**C5**	EtOH	75
9	DMAP (1)	**C5**	EtOH	60
10	DMAP (2)	**C5** (10 mol%)	EtOH	45
11	DMAP (2)	-	EtOH	30

[a]Reaction conditions: **1a** (0.3 mmol), **8a** (0.3 mmol), DMAP (2 equiv), catalyst **C5** (20 mol%), and solvent (0.15 M) at 48 h. [b]Isolated yield.

The structure of **11h** was unambiguously confirmed by single-crystal X-ray diffraction analysis (Figure 4.2).

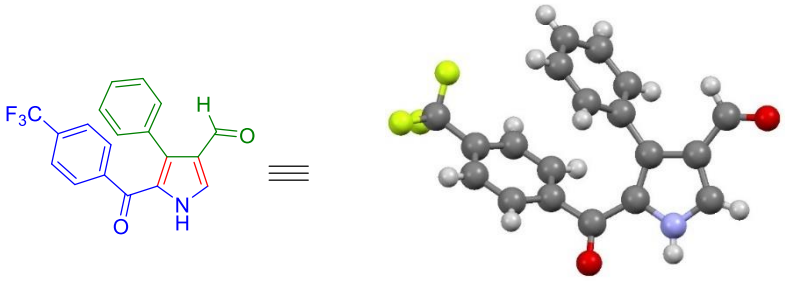

Figure 4.2 X-ray structure of compound **11h** (CCDC: 2354829) with 50% probability ellipsoids

4.5 SUBSTRATE SCOPES

From the optimization tables 4.1- 4.3 it is clearly understood that α,β-unsaturated aldehyde **1a** (1 equiv), 4-methylthiazolium salt **8a** (1 equiv), DMAP (2 equiv), and catalyst **C5** in EtOH (0.15 M) at room temperature for 48 h, was found to be an optimized reaction condition. With this optimized reaction condition, generality and functional group tolerance of the domino reactions were investigated with various 4-methyl thiazolium salts and α,β-unsaturated aldehydes having electron-donating, electron-withdrawing, halogens, and bulky substituents. All the reactions furnished the desired products **11a-11h** in good yields (Tables 4.4 and 4.4). The 4-methyl thiazolium salt **8b** having the election donating group at *ortho* position gave product **11b** a moderate yield of 54% compared to the unsubstituted product **11a**. It may be due to steric hindrance of ortho -OMe substitution on the phenyl ring. Whereas the halogen substitutes at *para* positions of 4-methyl thiazolium salts were delivering the products **11c-11e** in good yield (Table 4.4, entries 3-5). The electron-withdrawing groups such as -NO_2, -CN, -CF_3 at *para* positions of 4-methyl thiazolium salt gave the desired trisubstituted 1*H*-pyrrole products **11f-11h** in 78-83% yield (Table 4.4, entries 6-8). The bulky naphthyl group was well tolerated for this domino strategy, obtaining the product **11i** in 65% yield (Table 4.4, entry 9). The α,β-unsaturated

aldehydes containing electron-withdrawing group at *para* position deliver the trisubstituted pyrrole product **11j** in excellent yield **(**Table 4.4, entry 10).

Table 4.4 Substrate Scope of Trisubstituted 1*H*-Pyrroles [a,b]

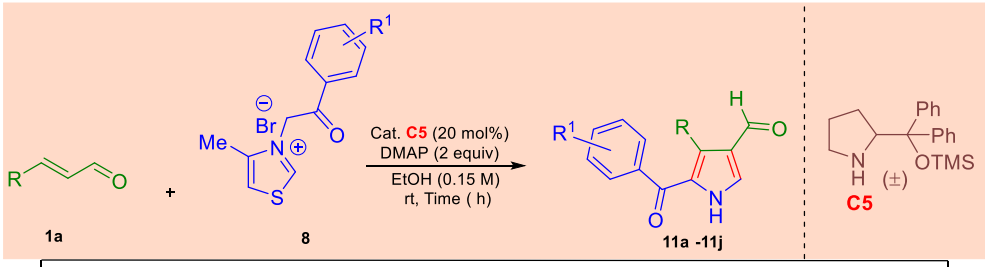

Entry	α,β-unsaturated aldehyde	Thiazolium salt	Product
1	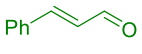	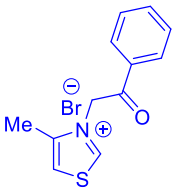	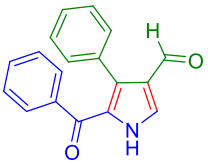 11a; 72%, 48 h
2	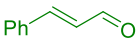	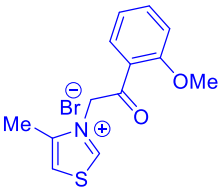	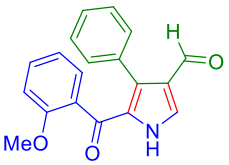 11b; 54%, 48 h
3	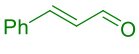	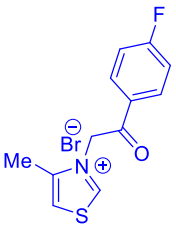	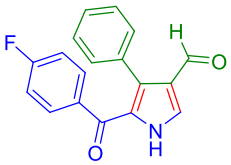 11c; 70%, 13 h
4	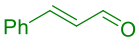	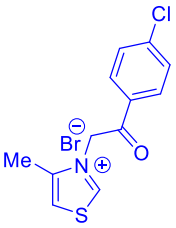	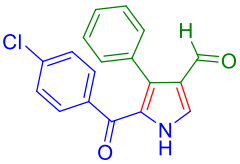 11d; 65%, 13 h
5	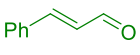	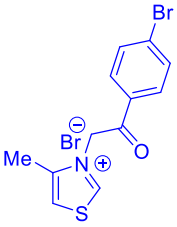	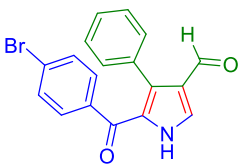 11e; 65%, 15 h

Entry	α,β-unsaturated aldehyde	Thiazolium salt	Product
6	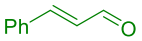	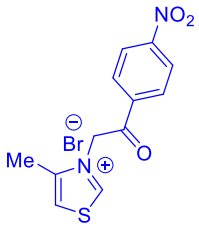	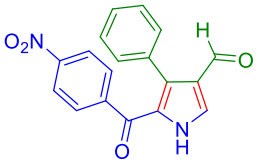 11f; 83%, 42 h
7	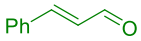	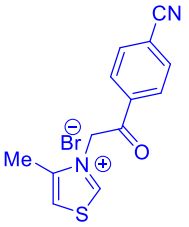	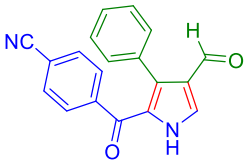 11g; 78%, 42 h
8	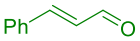	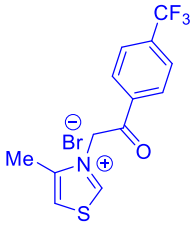	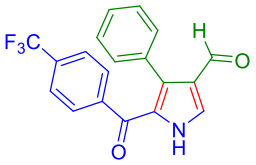 11h; 82%, 42 h
9	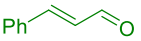	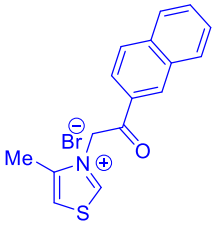	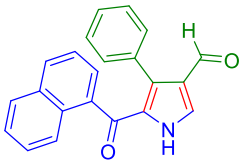 11i; 82%, 24 h
10	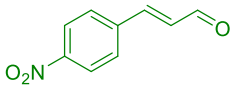	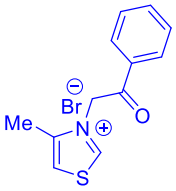	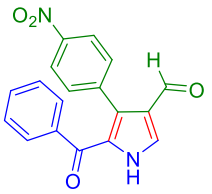 11j; 81%, 24 h

[a]Reaction conditions: **1a** (0.3 mmol), **8a** (0.3 mmol), DMAP (2 equiv), catalyst **C5** (20 mol%), and solvent (0.15 M). [b]Isolated yield.

4.6. CONTROL EXPERIMENTS

Control experiments were carried out to probe the reaction mechanism. When the reaction was carried out with **C4**, in the absence of DMAP base under room temperature, the failed to provide the expected product (Scheme 4.28a). The

background reaction occurs when the reaction was performed only with base, and the reaction afforded the product **11a** a 30% yield (Scheme 4.28b).

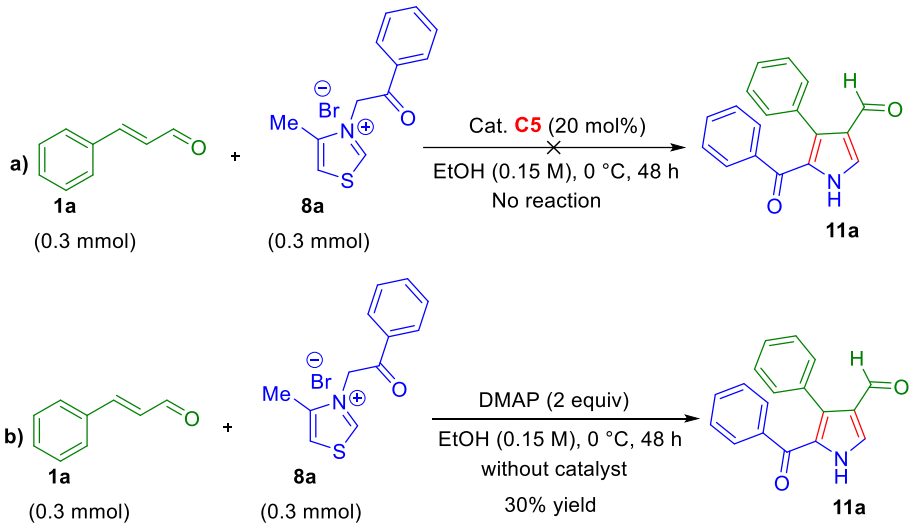

Scheme 4.28 Control experiments

4.7. GRAM SCALE SYNTHESIS

To check the scalability of the domino methodology, a gram-scale reaction was performed using cinnamaldehyde **1a** (3 mmol, 396 mg, 374 μL), benzothiazolium salt **8a** (3 mmol, 1.24 g), and DMAP (6 mmol 0.73 g) under the optimized reaction conditions. The reaction furnished the desired chiral product **11a** in 65% yield (0.62 g) as shown in Scheme 4.29.

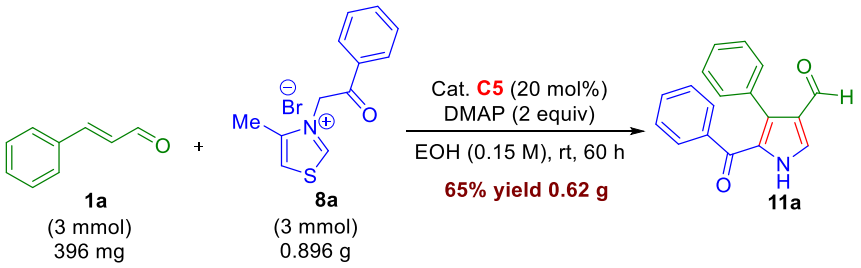

Scheme 4.29 Gram scale synthesis of **11a**

4.8 MECHANISTIC STUDY

The crude reaction mixture was analyzed by HRMS to find out the domino reaction pathway and to determine the byproduct formed during the reaction. After the reaction was completed, the smell of thiol was also noticed during the workup. HRMS analysis confirmed that the formed cleavage product was 1-mercaptopropan-2-one (Scheme 4.30). The calculated mass of the cleaved product was exactly matched with found mass (Figure 4.3).

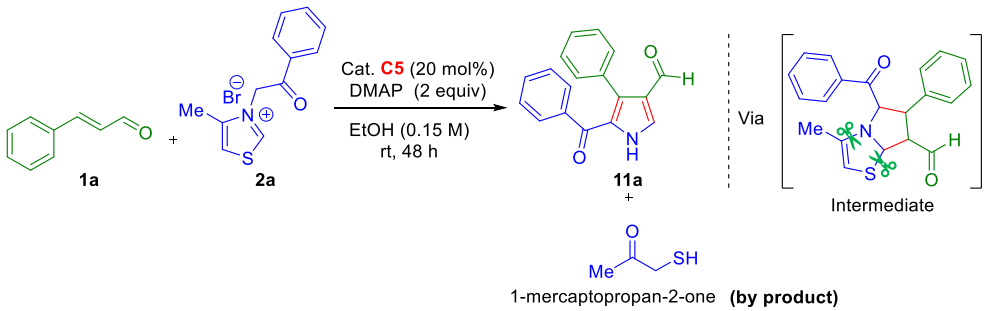

Scheme 4.30 HRMS analysis of crude reaction mixture

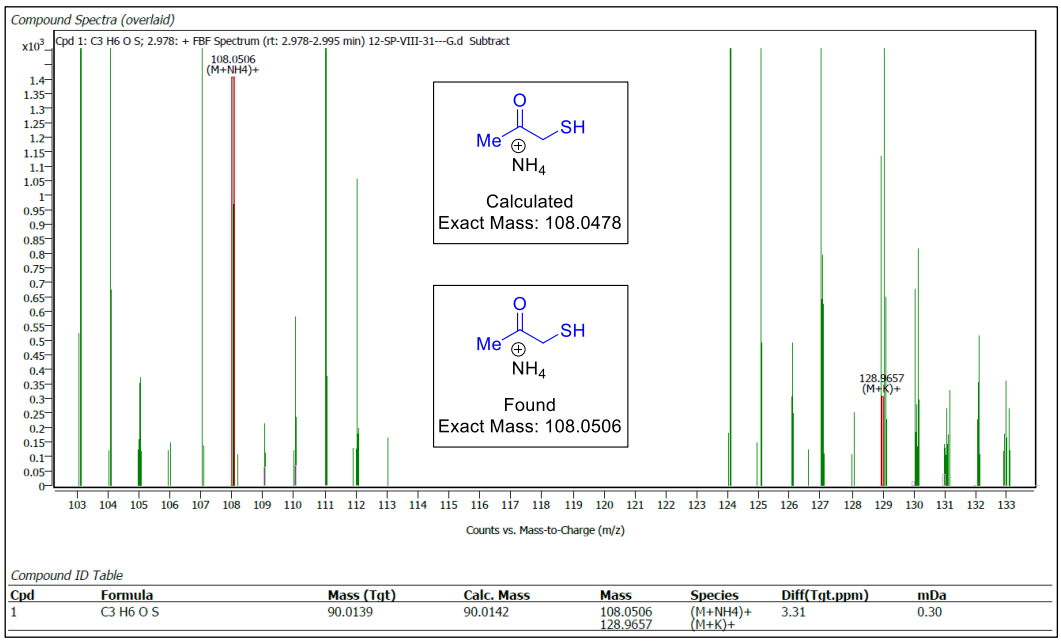

Figure 4.3 HRMS spectrum of 1-mercaptopropan-2-one

4.9 PLAUSIBLE REACTION MECHANISM

Based on the mechanistic study and previous study from Chapter **2**, a plausible mechanism has been proposed (Scheme 4. 31). Initially, a racemic secondary amine catalyst **C5** and cinnamaldehyde **1a** in the presence of *in-situ* formed HBr or protonated DMAP will generate iminium ion complex **I** by the elimination of water. Meanwhile, thiazolium salt **8a** will react with DMAP base to form 1,3-dipolar thiazolium ylide intermediate **III**. The ylide intermediate **III** can react further with iminium ion complex **I** to give Michael adduct intermediate **IV**. This intermediate **IV** will undergo dearomatization of thiazolium salt to produce 1,3-dipolar cycloadduct intermediate **V**. Hydrolysis of **V** will result in the regeneration of catalyst **I** for the next catalytic cycle. In this process, hydropyrrolo-thiazole intermediate **VI** and HBr will be generated. Intermediate **VI**, in the presence of DMAP base will produce the ring opening thiazloate anion intermediate **VII**. Then, the intermediate sulfur anion **VII** will be quenched by a proton to produce the intermediate **VIII**. This intermediate **VIII** will undergo enamine-imine tautomerism to furnish iminium ion intermediate **IX**. This iminium ion intermediate **IX** will react with *in-situ* generated water molecules to produce the intermediate **X**. In intermediate **X**, the nitrogen lone pair delocalized to produce the enolate of iminium ion intermediate **XI**, followed by protonation of enolate intermediate **XI** to produce intermediate **XII**. In intermediate **XII**, the C-N bond cleavage will take place to yield byproduct 1-mercaptopropan-2-one and intermediate **XIII**. The formation of byproduct 1-mercaptopropan-2-one was confirmed by HRMS and ^{1}H NMR analysis of crude reaction mixture. The enol ether intermediate **XIII** will converted to the final product trisubstituted 1H-pyrrole-3-carbaldehyde **11** *via* intermediates **XIV** and **XV**.

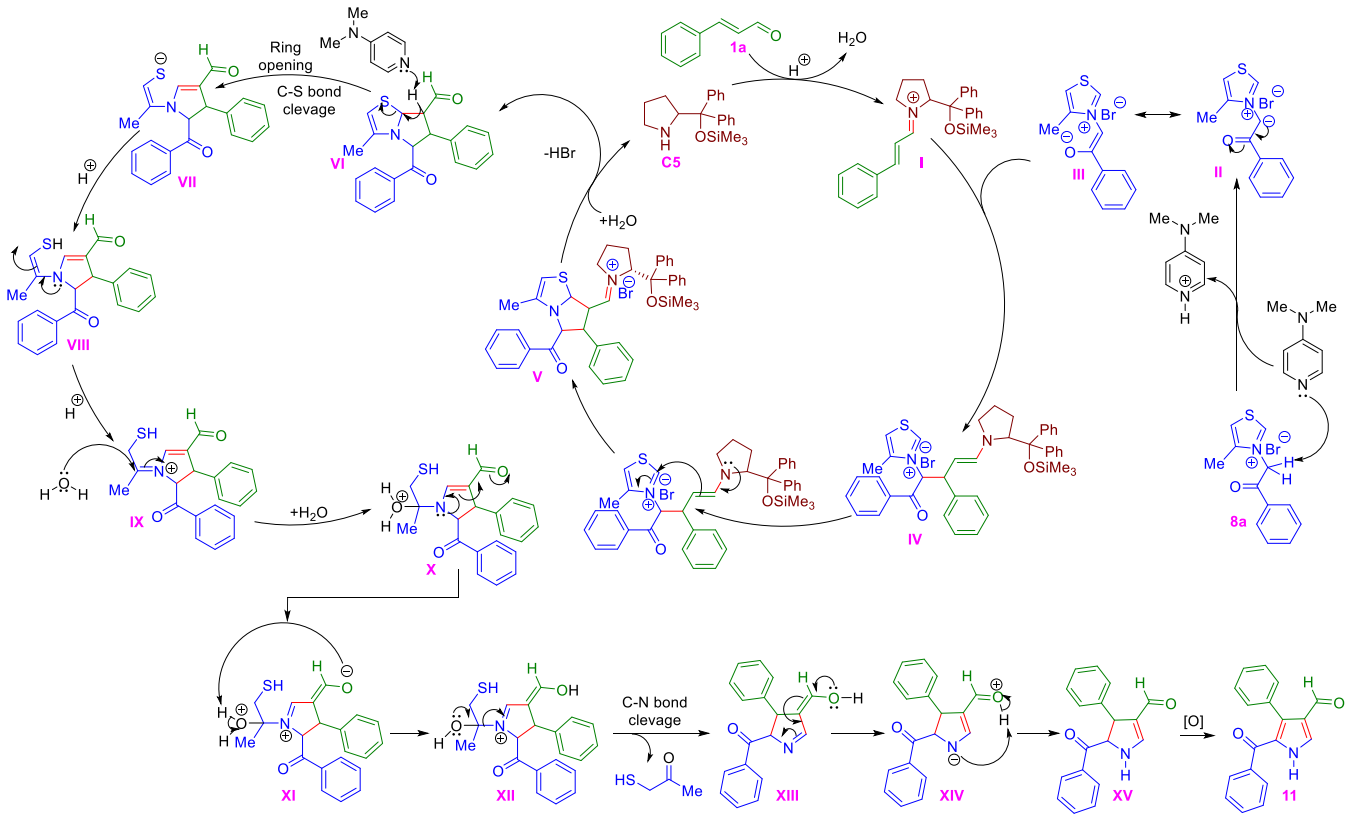

Scheme 4.31 Plausible reaction mechanism for the formation of trisubstituted-1*H*-pyrrole

4.10 CONCLUSION

- A novel method was developed for the synthesis of trisubstituted 1*H*-pyrrole-3-carbaldehydes. This method involved radially available α,β-unsaturated aldehydes, easily synthesizable 4-methyl thiazolium salts, and commercially available racemic amine organocatalysts.
- The reaction proceeded by domino reaction sequences like formal 1,3-dipolar cycloaddition/ring-opening/C-S and C-N bond cleavage provided the trisubstituted 1*H*-pyrrole-3-carbaldehydes in good to excellent yield.
- This method worked well and tolerated various functional groups.

- This is the first report on the synthesis of trisubstituted 1*H*-pyrrole-3-carbaldehyde derivatives using 4-methylthiazolium salts, α,β-unsaturated aldehyde, and racemic amine organocatalysts *via* a domino synthesis.

4.11 EXPERIMENTAL SECTION

4.11.1 General information

All reactions were carried out in oven-dried reaction tubes. 4-Methyl thiazole, phenacyl bromides, and cinnamaldehydes were purchased from Sigma-Aldrich, Spectrochem, BLD, Carbanio, and Avra Synthesis Pvt. Ltd. The racemic proline and DMAP were purchased from Spectrochem, Avra Synthesis Pvt. Ltd. and used directly as received. All the starting materials were synthesized according to the reported procedures. Reactions were monitored by thin-layer chromatography (TLC) using Merck silica gel 60 F_{254} precoated plates (0.25 mm) and visualized by UV fluorescence quenching using an appropriate mixture of ethyl acetate and hexanes as eluting solvent mixtures. Silica gel for column chromatography (particle size 100-200 mesh) was purchased from Avra Synthesis Pvt. Ltd. and used for column chromatography using hexanes and ethyl acetate mixture as eluent. Organic solutions were concentrated under reduced pressure on a Büchi, Heidolph rotary evaporator using a water bath. ^{1}H and ^{13}C NMR spectra were recorded on a Bruker 400 or 500 MHz instrument.^{1}H NMR is reported relative to residual $CDCl_3$ (δ 7.26 ppm) or DMSO-d_6 (δ 2.50 ppm). ^{13}C NMR is reported close to residual $CDCl_3$ (δ 77.16 ppm) or DMSO-d_6 (δ 39.52 ppm). Chemical shifts were recorded in parts per million (ppm). Multiplicities are as indicated: s (singlet,) d (doublet,) t (triplet,) q (quartet,) quint (quintet), sext (sextet), sept (septet) dd (doublet of doublet,) m (multiplet,) tt (triplet of triplet,) td (triplet of doublet). The coupling constant, *J*, is reported in Hertz.

Melting points were recorded on a Guna capillary melting point apparatus and were corrected with benzoic acid as a reference. FTIR spectra were recorded on a JASCO spectrometer and were reported in the frequency of absorption (cm^{-1}) using a dry KBr pellet. The polarimetry was recorded in P-2000 High Accuracy Digital Polarimeter - Jasco Inc. High-resolution mass spectra (HRMS) were recorded on Q-Tof Micro mass spectrometer. All the single crystal X-ray data was collected with a Bruker AXS (Kappa Apex 2) CCD diffractometer equipped with graphite monochromatic Mo (Kα) (λ = 0.7107 A) radiation source. The data were collected with 100% completeness for Θ up to 25º. ω and ϕ scans were employed to collect the data. The frame width for ω for was fixed to 0.5º for data collection. The crystal was solved by direct methods using Bruker SHELXS (Sheldrick, 1997). The Structure was refined using the Bruker SHELXTL (Version 6.12) software package.

4.11.2 Typical procedure for the domino synthesis of trisubstituted 1*H*-pyrrole-3-carbaldehyde

General procedure A: To a 20 mL oven-dried reaction tube with a magnetic stir bar under an open atmosphere, racemic catalyst **C4** (20 mg, 0.06 mmol), and cinnamaldehyde **1a** (38 µL, 0.3 mmol) were dissolved in (0.075 M) EtOH and closed with glass-stopper and stirred for 1 hour at room temperature. 4-Methy thiazolium salt **11a** (90 mg, 0.3 mmol), DMAP (73 mg, 0.6 mmol), and (0.75 M) EtOH were successively added to the reaction mixture. Reaction progress was monitored by TLC. After completely consuming both starting materials, the EtOH was evaporated from the reaction mixture by a rotary evaporator. Then, the reaction mixture was poured into water and extracted with EtOAc (3 x15 mL), and brine wash (1×10 mL) was given to the combined organic extractions and dried over anhydrous Na_2SO_4. Evaporation of

organic layer to provide the crude product. This crude product was purified by column chromatography on silica gel (eluent: Hexane/Ethyl acetate = 80/20) to yield the desired chiral product **11a** in 75% yield (Scheme 4.32).

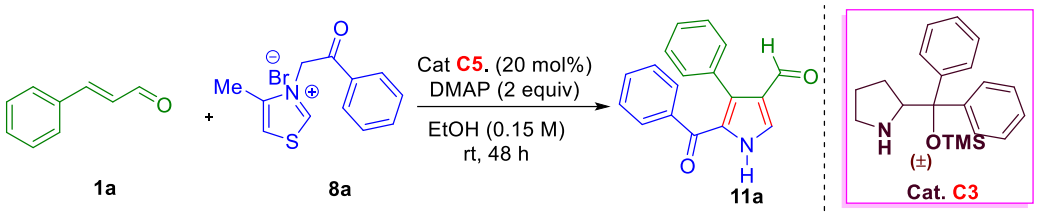

Scheme 4.32 Domino synthesis of trisubstituted 1*H*-pyrrole-3-carbaldehyde

4.12. ANALYTICAL AND SPECTRAL CHARACTERIZATION DATA

5-Benzoyl-4-phenyl-1*H*-pyrrole-3-carbaldehyde 11a; Prepared according to general procedure A using racemic diphenylprolinol trimethylsilyl ether **C4**. Purification of crude product was done by column chromatography using (hexane/ethyl acetate) mixture (80:20) to afford the title compound as pale yellow solid, (72% yield, 60 mg); R_f = 0.41 (20 % ethyl acetate in hexane); mp 102 – 104 °C; **^{1}H NMR (500 MHz, CDCl$_3$)** δ 10.34 (s, 1H), 9.73 (s, 1H), 7.82 (d, *J* = 3.4 Hz, 1H), 7.38 (d, *J* = 7.6 Hz, 2H), 7.24 (t, *J* = 7.5 Hz, 1H), 7.15 – 7.10 (m, 1H), 7.10 – 7.06 (m, 4H), 7.04 (t, *J* = 7.6 Hz, 2H); **^{13}C NMR (125 MHz, CDCl$_3$)** δ 187.7, 187.2, 137.1, 134.0, 131.9, 131.8, 131.2, 129.4, 129.1, 128.0, 127.8, 127.7, 127.3, 125.8; **FTIR (neat)** 3270, 1670, 1627, 1540, 1449, 1284, 738 cm^{-1}; **HRMS (ESI)** calculated for $C_{18}H_{14}NO_2$ $[M+H]^+$: 276.1019; found: 276.1013.

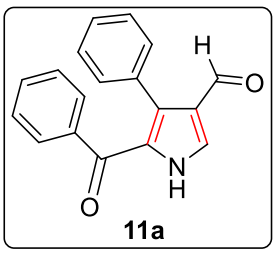

5-(2-Methoxybenzoyl)-4-phenyl-1*H*-pyrrole-3-carbaldehyde 11b; Prepared according to general procedure A using racemic diphenylprolinol trimethylsilyl ether **C4**. Purification of crude product was done by column chromatography using (hexane/ethyl acetate) mixture (80:20) to afford the title

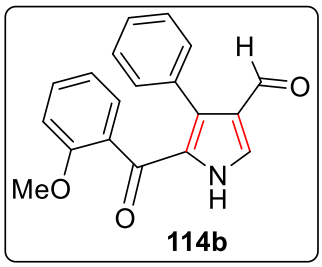

compound as pale yellow solid, (76% yield, 70 mg); R_f = 0.36 (30 % ethyl acetate in hexane); mp 140 – 142 °C; **^{1}H NMR (400 MHz, DMSO-d$_6$)** δ 12.82 (s, 1H), 9.66 (s, 1H), 7.92-7.87(m, 1H), 7.15-7.05 (m, 6H), 6.99 (d, *J* = 7.0 Hz, 1H), 6.89-6.83 (m, 2H), 3.59 (s, 3H); **^{13}C NMR (126 MHz, DMSO-d$_6$)** δ 186.7, 186.1, 158.4, 138.9, 132.2, 132.1, 130.8, 129.6, 129.2, 128.9, 127.4, 127.1, 124.2, 121.3, 118.1, 113.3, 55.0; **FTIR (neat)** 3263, 2924, 1675, 1626, 1538, 1452, 1287, 762 cm^{-1}; **HRMS (ESI)** calculated for $C_{19}H_{16}NO_3$ $[M+H]^+$: 306.1125; found: 306.1136.

5-(4-Fluorobenzoyl)-4-phenyl-1*H*-pyrrole-3-carbaldehyde 11c; Prepared according to general procedure C using racemic diphenylprolinol trimethylsilyl ether **C4**. Purification of crude product was done by column chromatography using (hexane/ethyl acetate) mixture (80:20) to afford the title compound as pale yellow solid (70% yield, 62 mg);

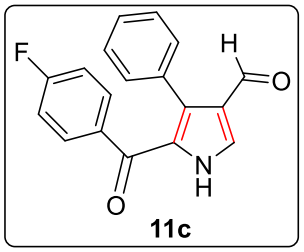

11c

R_f = 0.25 (20 % ethyl acetate in hexane); mp 152 – 154 °C; **^{1}H NMR (500 MHz, CDCl$_3$)** δ 10.36 (s, 1H), 9.74 (s, 1H), 7.83 (s, 1H), 7.44 – 7.38 (m, 2H), 7.21 – 7.17 (m, 1H), 7.13 (t, *J* = 7.5 Hz, 2H), 7.08 (d, *J* = 7.5 Hz, 2H), 6.71 (d, *J* = 8.5 Hz, 2H); **^{13}C NMR (125 MHz, CDCl$_3$)** δ 187.1, 186.3, 164.9 (d, *J* = 253.7 Hz), 134.0, 133.2 (d, *J* = 3.3 Hz), 131.8, 131.7, 131.2, 129.3, 128.2, 128.0, 127.5, 127.5, 125.7, 114.9 (d, *J* = 21.9 Hz); **^{19}F NMR (471 MHz, CDCl$_3$)** δ -106.50; **FTIR (neat)** 3403, 2256, 1666, 1025, 825, 764 cm^{-1}; **HRMS (ESI)** calculated for $C_{18}H_{13}FNO_2$ $[M+H]^+$: 294.0925; found: 294.0924.

5-(4-Chlorobenzoyl)-4-phenyl-1*H*-pyrrole-3-carbaldehyde 11d; Prepared according to general procedure C using racemic diphenylprolinol trimethylsilyl ether **C4**. Purification of crude product was done by column chromatography using

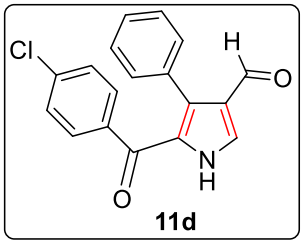

11d

(hexane/ethyl acetate) mixture (80:20) to afford the title compound as pale yellow solid (65% yield, 60 mg); R_f = 0.32 (20 % ethyl acetate in hexane); mp 148 – 150 °C; **^{1}H NMR (500 MHz, DMSO-d$_6$)** δ 12.87 (s, 1H), 9.66 (s, 1H), 7.94 – 7.90 (m, 1H), 7.39 – 7.33 (m, 2H), 7.19 – 7.13 (m, 3H), 7.13 – 7.09 (m, 4H); **^{13}C NMR (126 MHz, DMSO-d$_6$)** δ 185.9, 185.7, 136.3, 132.3, 132.0, 130.9, 130.6, 129.8, 129.3, 129.1, 127.6, 127.4, 127.1, 124.2; **FTIR (neat)** 3268, 2926, 2853, 1670, 1599, 1538, 1415, 1283, 768 cm^{-1}; **HRMS (ESI)** calculated for $C_{18}H_{13}ClNO_2$ $[M+H]^+$: 310.0629; found: 310.0621.

5-(4-Bromrobenzoyl)-4-phenyl-1*H*-pyrrole-3-carbaldehyde 11e; Prepared according to general procedure C using racemic diphenylprolinol trimethylsilyl ether **C4**. Purification of crude product was done by column chromatography using (hexane/ethyl acetate) mixture (80:20) to afford the title compound as yellow solid (71% yield, 75 mg); R_f = 0.35 (20 % ethyl acetate in hexane); mp 142 – 146 °C; **^{1}H NMR (500 MHz, DMSO-d$_6$)** δ 13.10 (s, 1H), 9.89 (s, 1H), 8.15 (s, 1H), 7.54 – 7.50 (m, 4H), 7.41 – 7.37 (m, 1H), 7.37 – 7.32 (m, 4H); **^{13}C NMR (126 MHz, DMSO-d$_6$)** δ 186.4, 186.4, 159.4, 137.1, 132.8, 132.5, 131.4, 131.2, 131.1, 130.3, 129.6, 128.0, 127.6, 125.8, 124.8; **FTIR (neat)** 3258, 2360, 1668, 1624, 1538, 1405, 1284, 764 cm^{-1}; **HRMS (ESI)** calculated for $C_{18}H_{13}BrNO_2$ $[M+H]^+$: 354.0124; found: 354.0118.

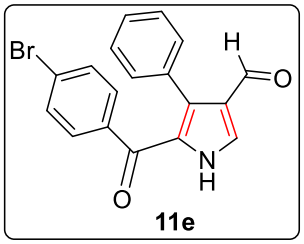

11e

5-(4-Nitrobenzoyl)-4-phenyl-1H-pyrrole-3-carbaldehyde 11f; Prepared according to general procedure C using racemic diphenylprolinol trimethylsilyl ether **C4**. Purification of crude product was done by column chromatography using (hexane/ethyl acetate) mixture (70:30) to afford the title compound as pale yellow solid, (83% yield,

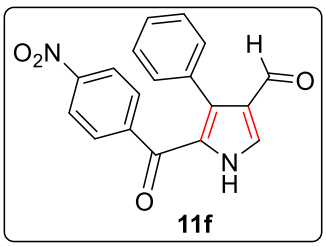

11f

81mg); R_f = 0. 38 (30 % ethyl acetate in hexane); mp 204 – 206 °C; **^{1}H NMR (500 MHz, $CDCl_3$)** δ 10.31 (s, 1H), 9.73 (s, 1H), 7.82 (d, *J* = 3.5 Hz, 1H), 7.32 – 7.29 (m, 2H), 7.23 – 7.17 (m, 1H), 7.15 – 7.11 (m, 2H), 7.09 – 7.05 (m, 2H), 7.05 – 6.97 (m, 2H); **^{13}C NMR (125 MHz, $CDCl_3$)** δ 187.0, 186.4, 138.2, 135.4, 134.1, 131.6, 131.2, 130.5, 129.3, 128.2, 128.1, 128.0, 127.6, 125.8; **FTIR (neat)** 3230, 2925, 2340, 1682, 1680, 1601, 1348, 1288, 702 cm^{-1}; **HRMS (ESI)** calculated for $C_{18}H_{13}N_2O_4$ $[M+H]^+$: 321.0870; found: 321.0906.

4-(4-Formyl-3-phenyl-1*H*-pyrrole-2-carbonyl)benzonitrile 11g; Prepared according to general procedure C using racemic diphenylprolinol trimethylsilyl ether **C4**. Purification of crude product was done by column chromatography using (hexane/ethyl acetate) mixture (70:30) to afford the title compound as brown solid, (78% yield, 70 mg); R_f = 0.33 (30 % ethyl acetate in hexane); mp 138 – 140 °C; **^{1}H NMR (500 MHz, $CDCl_3$)** δ 10.44 (s, 1H), 9.71 (s, 1H), 7.86 (s, 1H), 7.41 (d, *J* = 8.0 Hz, 2H), 7.31 (d, *J* = 8.0 Hz, 2H), 7.20 (t, *J* = 7.5 Hz, 1H), 7.11 (t, *J* = 7.5 Hz, 2H), 7.04 (d, *J* = 7.5 Hz, 2H); **^{13}C NMR (125 MHz, $CDCl_3$)** δ 186.9, 185.9, 141.0, 134.9, 131.4, 131.2, 131.1, 129.3, 128.9, 128.4, 128.4, 128.2, 125.9, 118.1, 114.8; **FTIR (neat)** 3390, 2954, 2360, 1678, 1633, 1538, 1410, 1278, 767 cm^{-1}; **HRMS (ESI)** calculated for $C_{19}H_{13}N_2O_2$ $[M+H]^+$: 301.0972; found: 301.0948.

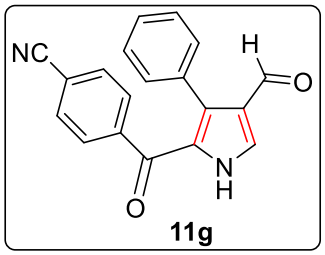

11g

4-Phenyl-5-(4-(trifluoromethyl)benzoyl)-1*H*-pyrrole-3-carbaldehyde 11h; Prepared according to general procedure C using racemic diphenylprolinol trimethylsilyl ether **C4**. Purification of crude product was done by column chromatography using (hexane/ethyl acetate) mixture (80:20) to afford the title compound as yellow solid,

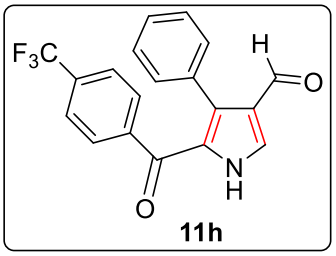

11h

(82% yield, 85 mg); R_f = 0.30 (30 % ethyl acetate in hexane); mp 136 – 138 °C; **^{1}H NMR (500 MHz, $CDCl_3$)** δ 10.24 (s, 1H), 9.72 (s, 1H), 7.85 (s, 1H), 7.42 (d, *J* = 8.0 Hz, 2H), 7.27 (d, *J* = 8.0 Hz, 2H) 7.15 (t, *J* = 7.5 Hz, 1H), 7.08 (t, *J* = 7.5 Hz, 2H), 7.02 (d, *J* = 7.5 Hz, 2H); **^{13}C NMR (125 MHz, $CDCl_3$)** δ 186.9, 186.4, 140.3, 134.8, 133.0 (q, *J* = 32.6 Hz), 131.3 131.1, 129.1, 128.2, 128.1, 127.9, 127.1, 126.0, 124.6 (q, *J* = 3.6 Hz), 123.0 (q, *J* = 270 Hz); **^{19}F NMR (471 MHz, $CDCl_3$)** δ -63.4; **FTIR (neat)** 3224, 1665, 1618, 1511, 1413, 1329, 772cm^{-1}; **HRMS (ESI)** calculated for $C_{19}H_{13}F_3NO_2$ $[M+H]^+$: 344.0893; found: 344.0901.

5-(2-Naphthoyl)-4-phenyl-1*H*-pyrrole-3-carbaldehyde 11i; Prepared according to general procedure C using racemic diphenylprolinol trimethylsilyl ether **C4**. Purification of crude product was done by column chromatography using (hexane/ethyl acetate) mixture (80:20) to afford the title compound as pale yellow solid (81% yield, 80 mg); R_f = 0.36 (20 % ethyl acetate in hexane); mp 172– 174 °C; **^{1}H NMR (500 MHz, $CDCl_3$)** δ 10.37 (s, 1H), 9.75 (s, 1H), 7.95-7.80 (m, 2H), 7.71 (d, *J* = 8.0 Hz, 1H), 7.60-7.55 (m, 3H), 7.51-7.45 (m, 1H), 7.45-7.35 (m, 1H), 7.16-7.10 (m, 2H), 7.00-6.93 (m, 1H), 6.92-6.85 (m, 1H); **^{13}C NMR (126 MHz, $CDCl_3$)** δ 187.5, 187.3, 134.9, 134.0, 131.9, 131.4, 131.1, 129.6, 129.2, 128.1, 128.1, 127.7, 127.6, 127.2, 126.4, 125.9, 124.9; **FTIR (neat)** 3268, 3055, 2961, 1671, 1619, 1539, 1400, 1287, 703 cm^{-1}; **HRMS (ESI)** calculated for $C_{22}H_{15}NO_2$ $[M+H]^+$: 326.1176; found: 326.1164.

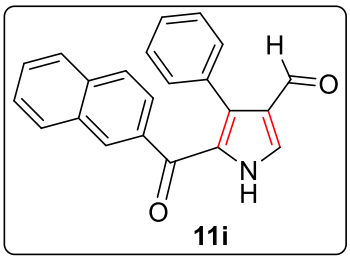

11i

5-Benzoyl-4-(4-nitrophenyl)-1*H*-pyrrole-3-carbaldehyde 11j; Prepare according to general procedure C using racemic diphenylprolinol trimethylsilyl ether **C4**. Purification of crude product was done by column chromatography using (hexane/ethyl acetate) mixture (70:30) to afford the title compound as orange solid, (80% yield, 77 mg); R_f = 0.36 (30 % ethyl acetate in hexane); mp 198 – 200 °C; **^{1}H NMR (500 MHz, $CDCl_3$)** δ 10.21 (s, 1H), 9.72 (s, 1H), 7.92-7.80 (m, 2H), 7.46 (d, *J* = 8.0 Hz, 2H), 7.19-7.13 (m, 1H), 7.12-7.07 (m, 2H), 7.04 (d, *J* = 7.5 Hz, 2H); **^{13}C NMR (125 MHz, $CDCl_3$)** δ 186.8, 186.2, 138.0, 135.3, 134.0, 131.5, 131.0, 130.4, 129.1, 128.0, 127.9, 127.8, 127.4, 125.7; **FTIR (neat)** 3240, 2926, 2360, 1712, 1601, 1525, 1348, 1286, 698 cm^{-1}; **HRMS (ESI)** calculated for $C_{18}H_{11}ClN_2O_4$ [M+]: 354.0407; found: 354.0429.

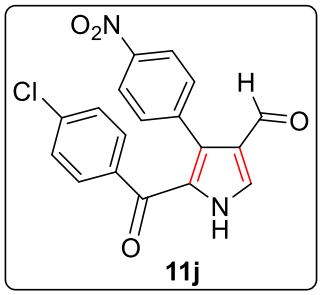

11j

4.13. X-RAY CRYSTALLOGRAPHY DATA

Figure 4.4 X-ray crystallographic data for compound 11h

All the single crystals X-ray data was collected with a Bruker AXS (Kappa Apex 2) CCD diffractometer equipped with graphite monochromatic Mo (Kα) (λ = 0.7107 A) radiation source. The data were collected with 100% completeness for Θ up to 25º. ω and ϕ scans were employed to collect the data. The frame width for ω for was fixed to 0.5º for data collection. The crystals were solved by direct methods using Bruker SHELXS (Sheldrick, 1997). The Structure was refined using the Bruker SHELXTL (Version 6.12) software package.

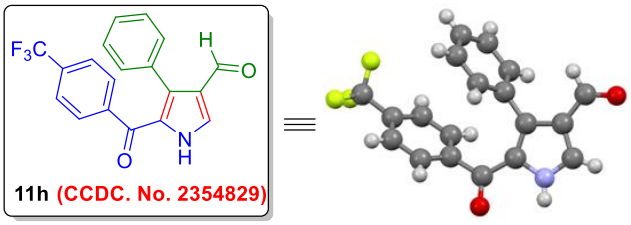

The purified compound **11h** was dissolved in acetonitrile 0.1 M and placed in a dark cabinet for slow evaporation. Crystals were collected after a few days for X-ray analysis. Thermal ellipsoids are shown at the 50% probability level.

Table 4.5. Crystal data and structure refinement for 11h (CCDC No. 2354829)

Identification code	198	
Empirical formula	$C_{19}H_{12}F_3NO_2$	
Formula weight	343.30	
Temperature	296(2) K	
Wavelength	0.71073 Å	
Crystal system	Monoclinic	
Space group	$P2_1$	
Unit cell dimensions	a = 7.4749(4) Å	α = 90°
	b = 9.2492(5) Å	β = 94.679(3)°
	c = 11.6066(8) Å	γ = 90°
Volume	799.77(8) $Å^3$	
Z	2	
Density (calculated)	1.426 g cm^{-3}	
Absorption coefficient	0.116 mm^{-1}	
F(000)	352	

Crystal size	0.180 x 0.160 x 0.120 mm^3
Theta range for data collection	2.734 to 24.999°
Index ranges	-8<=h<=8, -10<=k<=10, -13<=l<=11
Reflections collected	5036
Independent reflections	2750 [R(int) = 0.0164]
Completeness to theta = 24.999°	99.9 %
Refinement method	Full-matrix least-squares on F^2
Data / restraints / parameters	2750 / 1 / 235
Goodness-of-fit on F^2	1.539
Final R indices [I>2sigma(I)]	R1 = 0.0329, wR2 = 0.0828
R indices (all data)	R1 = 0.0369, wR2 = 0.0851
Absolute structure parameter	0.2(3)
Extinction coefficient	0.032(6)
Largest diff. peak and hole	0.187 and -0.132 e.$Å^{-3}$

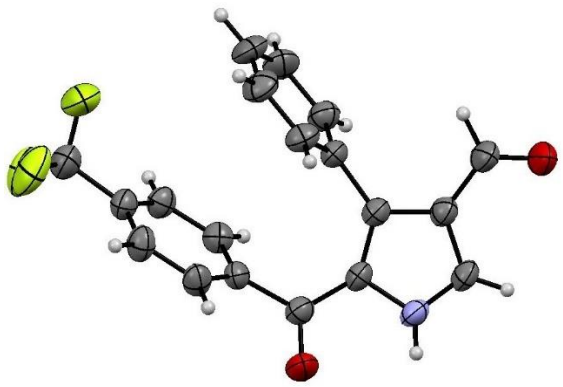

Figure caption: ORTEP diagram of compound **11h** (198) displacement ellipsoids are drawn at the 50% probability level, and H atoms are shown as small spheres of arbitrary radius.

4.14 ^{1}H, ^{13}C, and ^{19}F NMR SPECTRA

(5-Benzoyl-4-phenyl-1*H*-pyrrole-3-carbaldehyde 11a

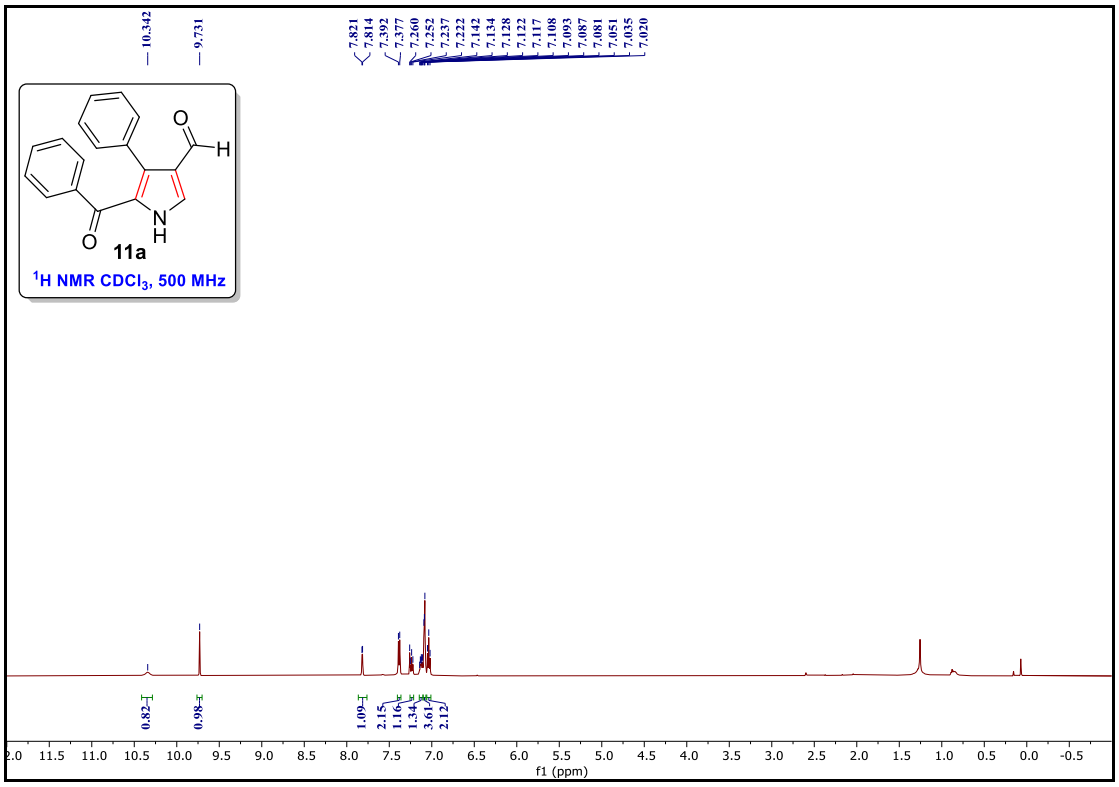

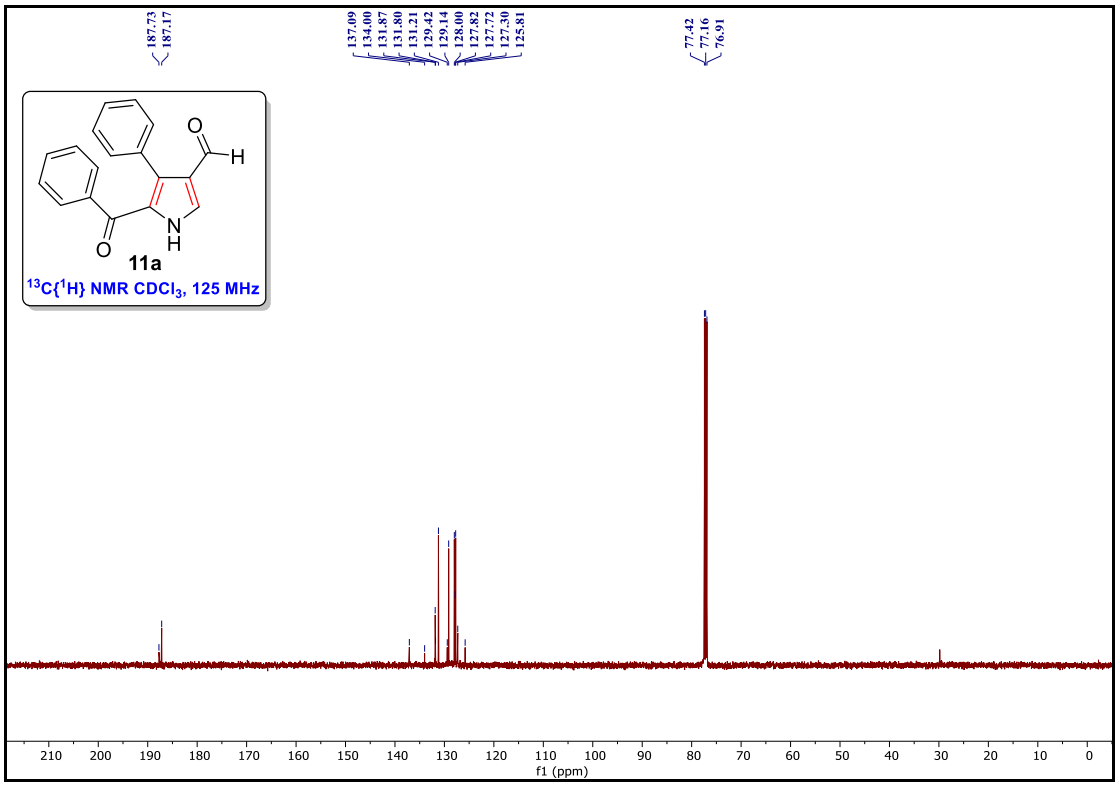

5-(2-Methoxybenzoyl)-4-phenyl-1*H*-pyrrole-3-carbaldehyde 11b

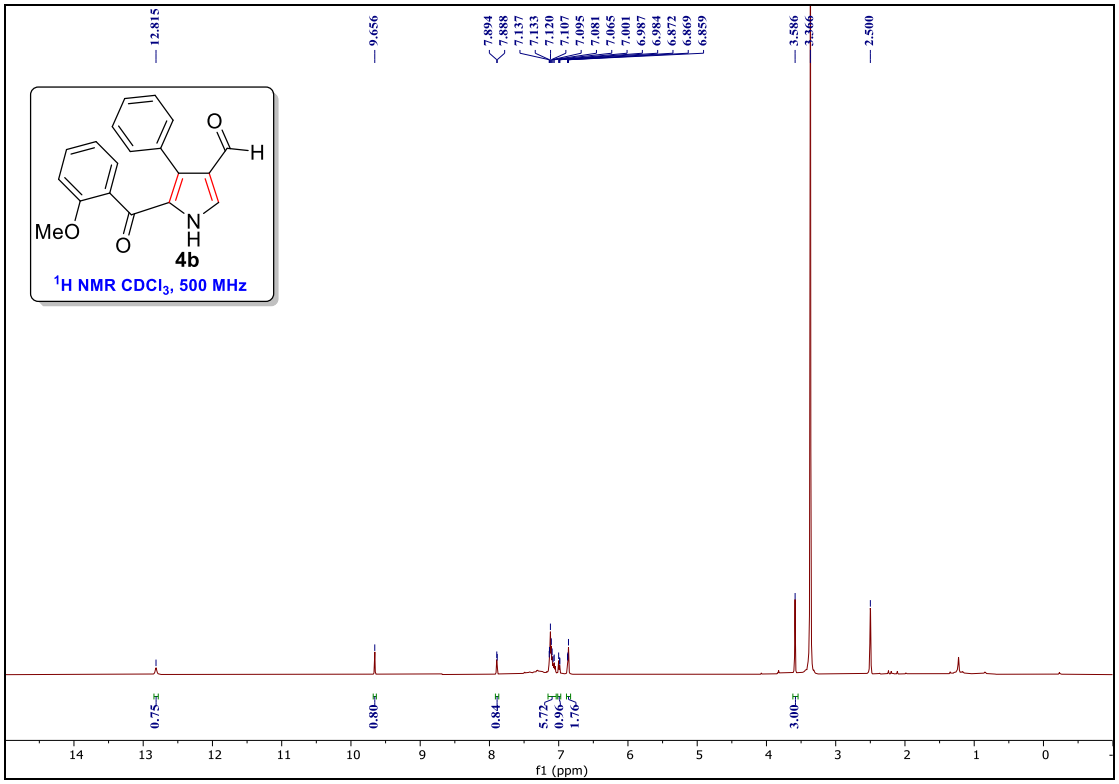

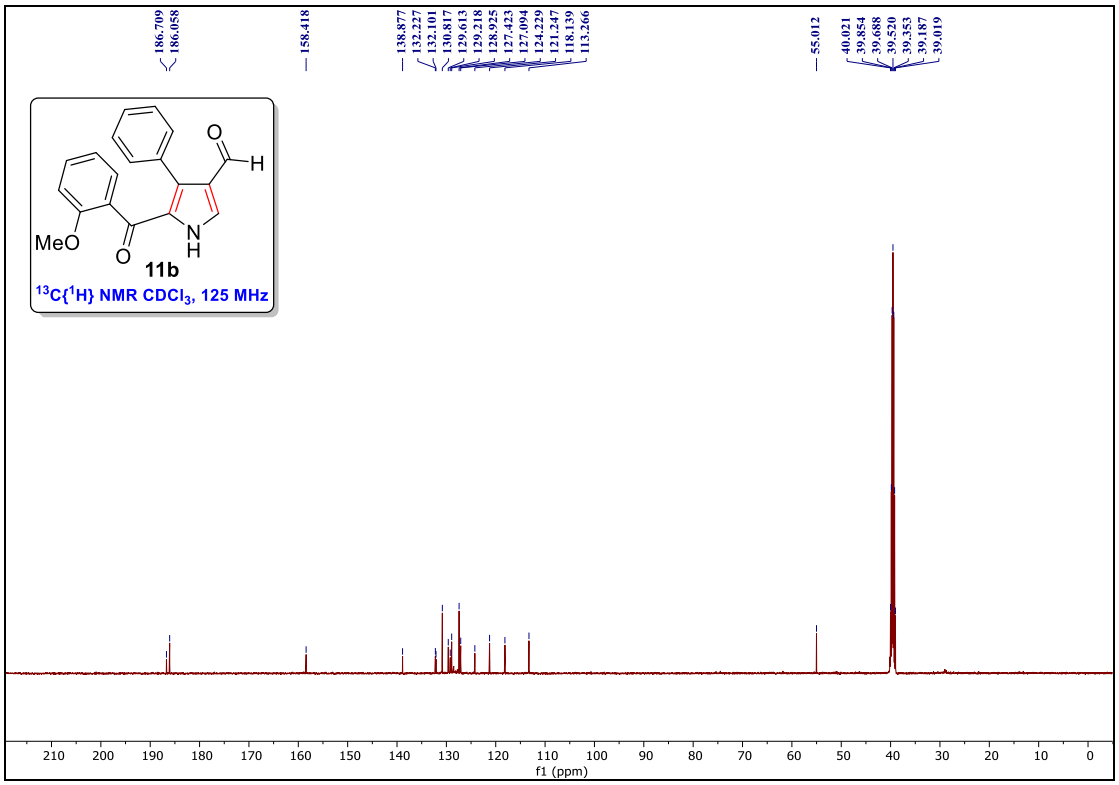

5-(4-Chlorobenzoyl)-4-phenyl-1*H*-pyrrole-3-carbaldehyde 11c

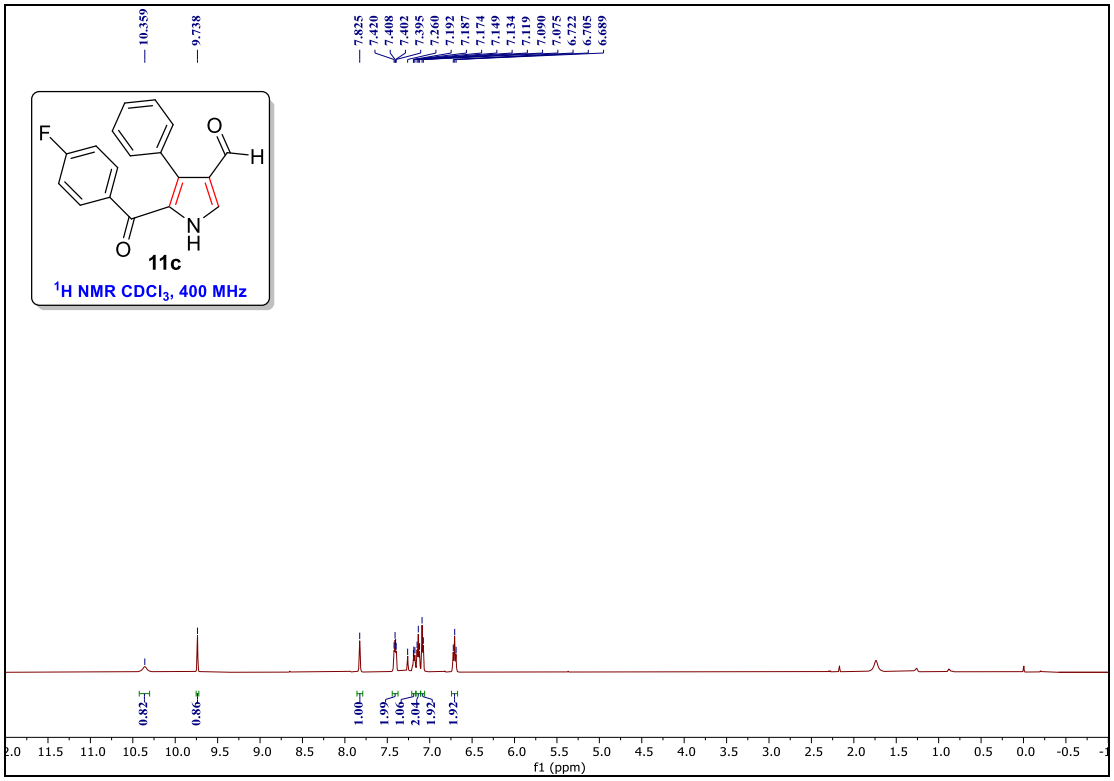

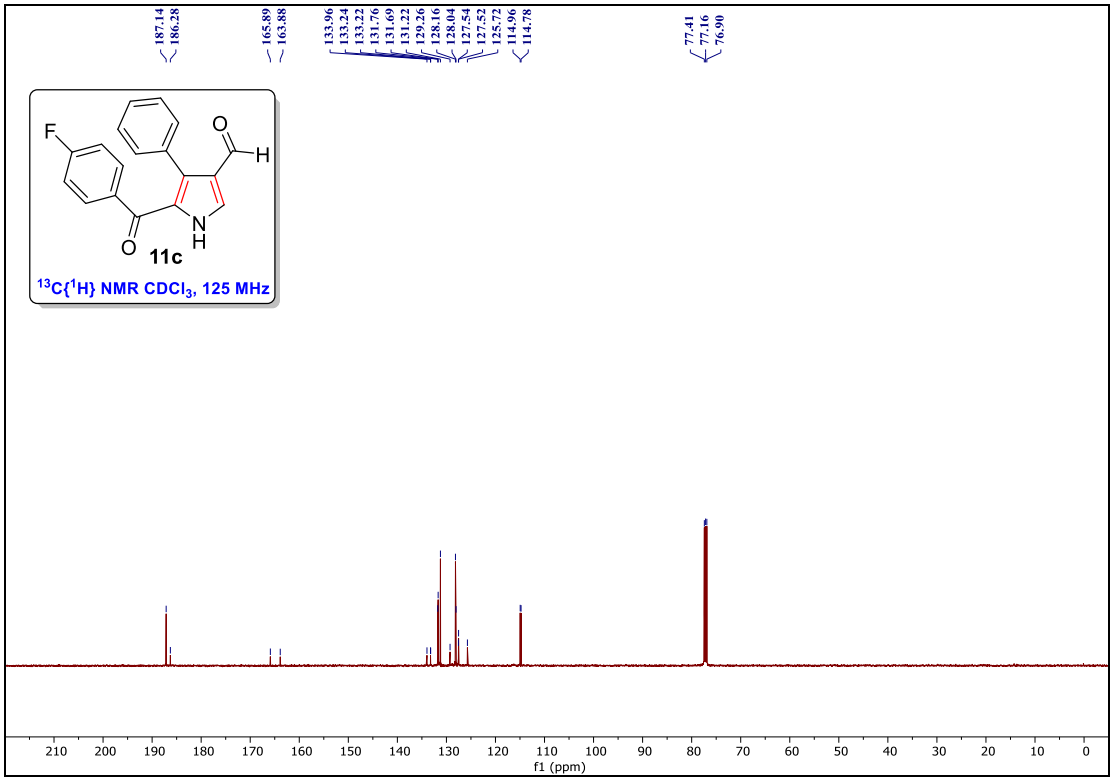

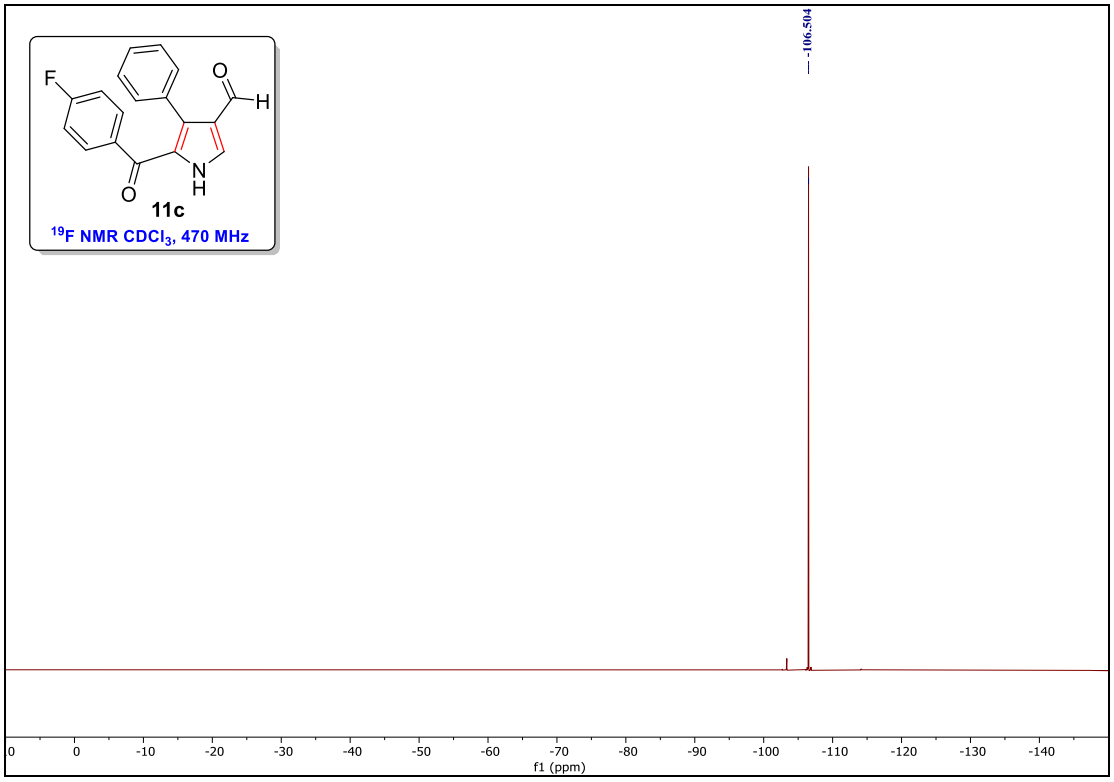
F
O
H
N
H
O
11c
^{19}F NMR CDCl$_3$, 470 MHz
-106.504
0
0
-10
-20
-30
-40
-50
-60
-70
-80
-90
-100
-110
-120
-130
-140
f1 (ppm)

5-(4-Chlorobenzoyl)-4-phenyl-1*H*-pyrrole-3-carbaldehyde 11d

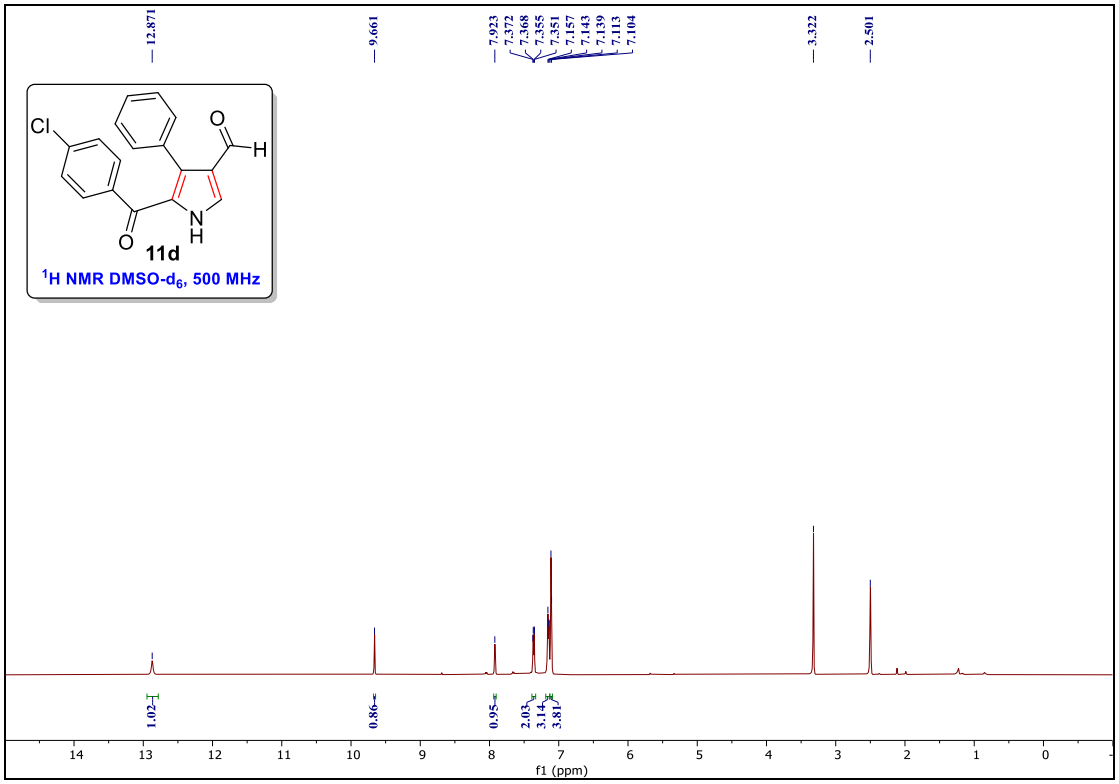

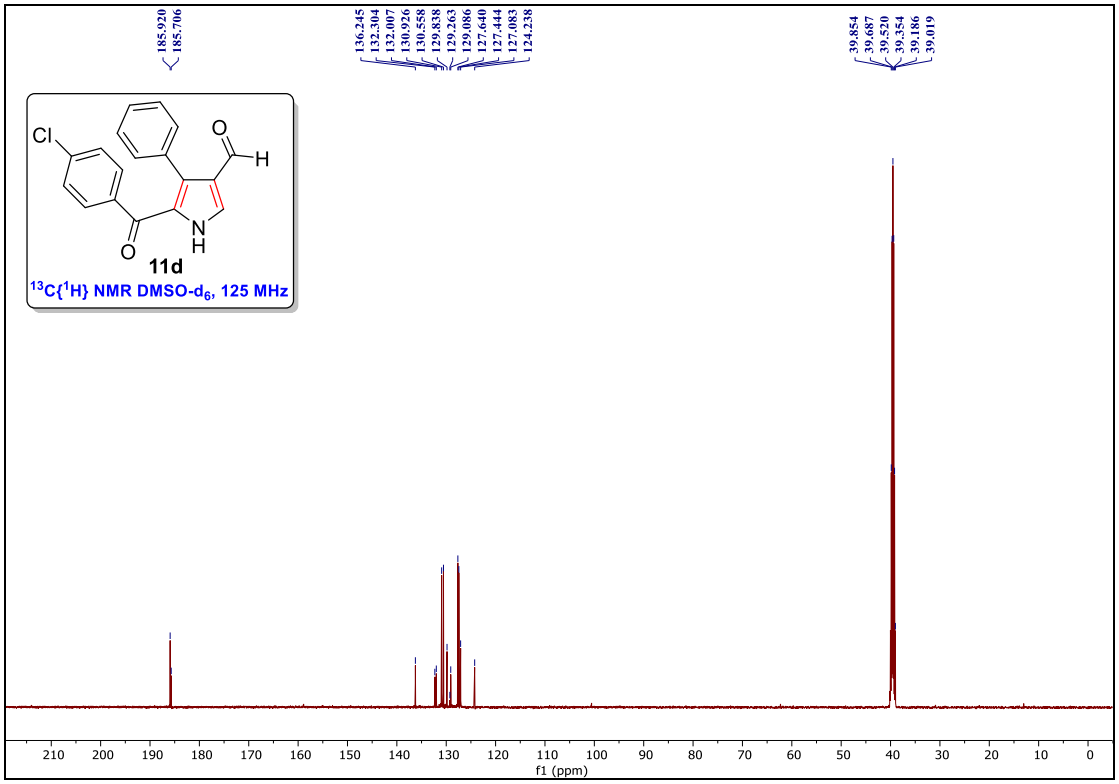

5-(4-Bromobenzoyl)-4-phenyl-1*H*-pyrrole-3-carbaldehyde 11e

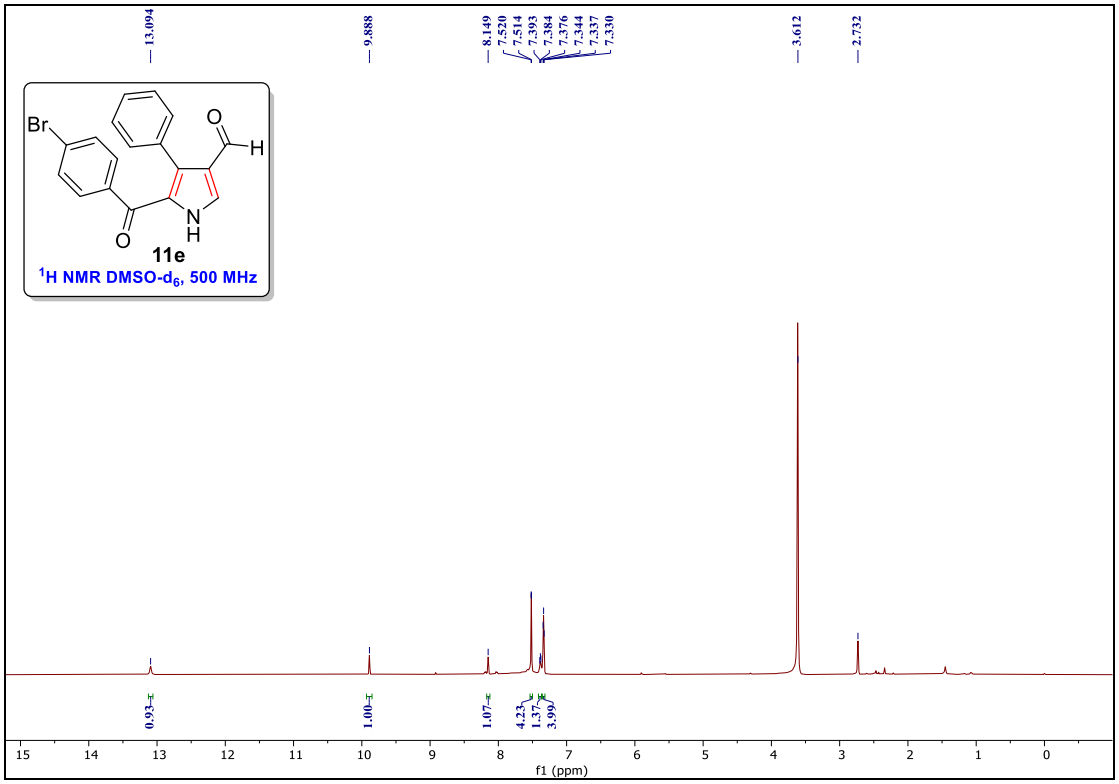

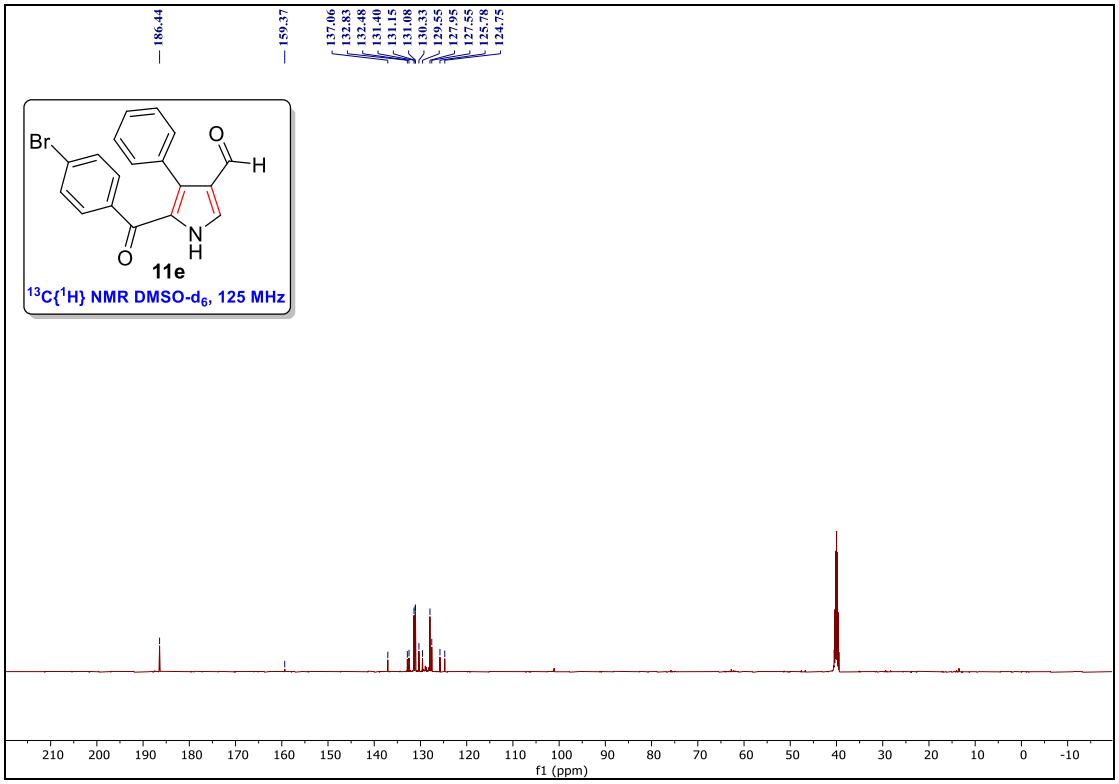

5-(4-Nitrobenzoyl)-4-phenyl-1*H*-pyrrole-3-carbaldehyde 11f

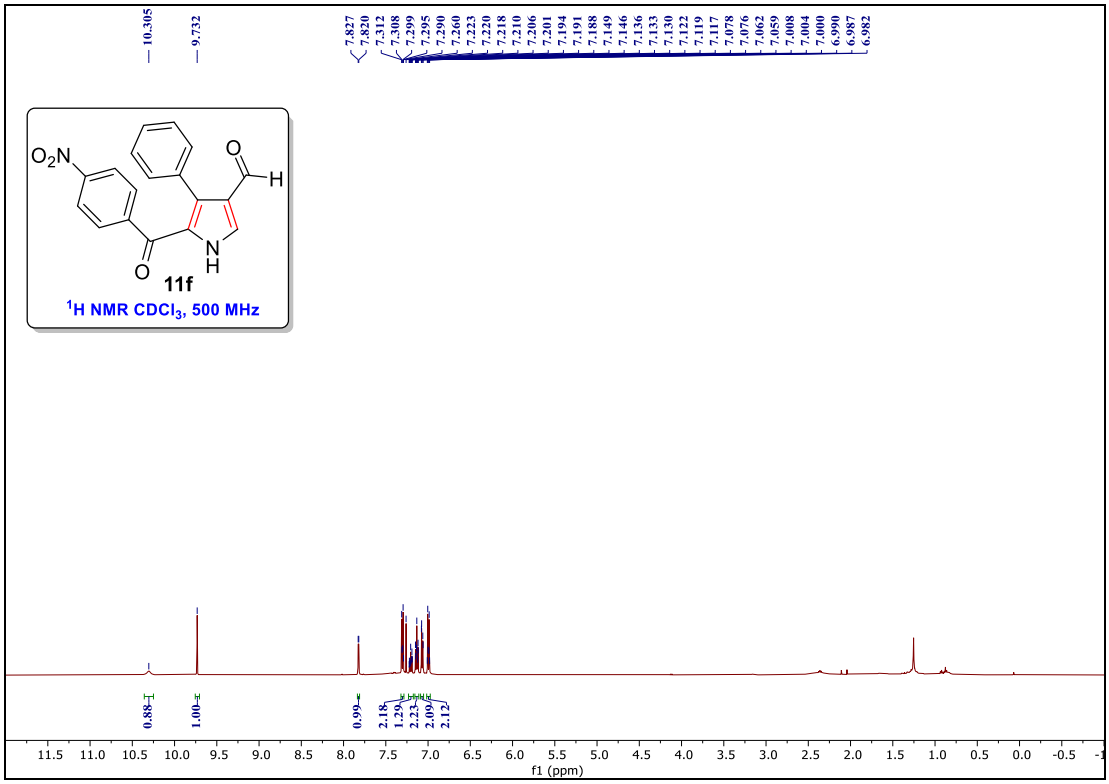

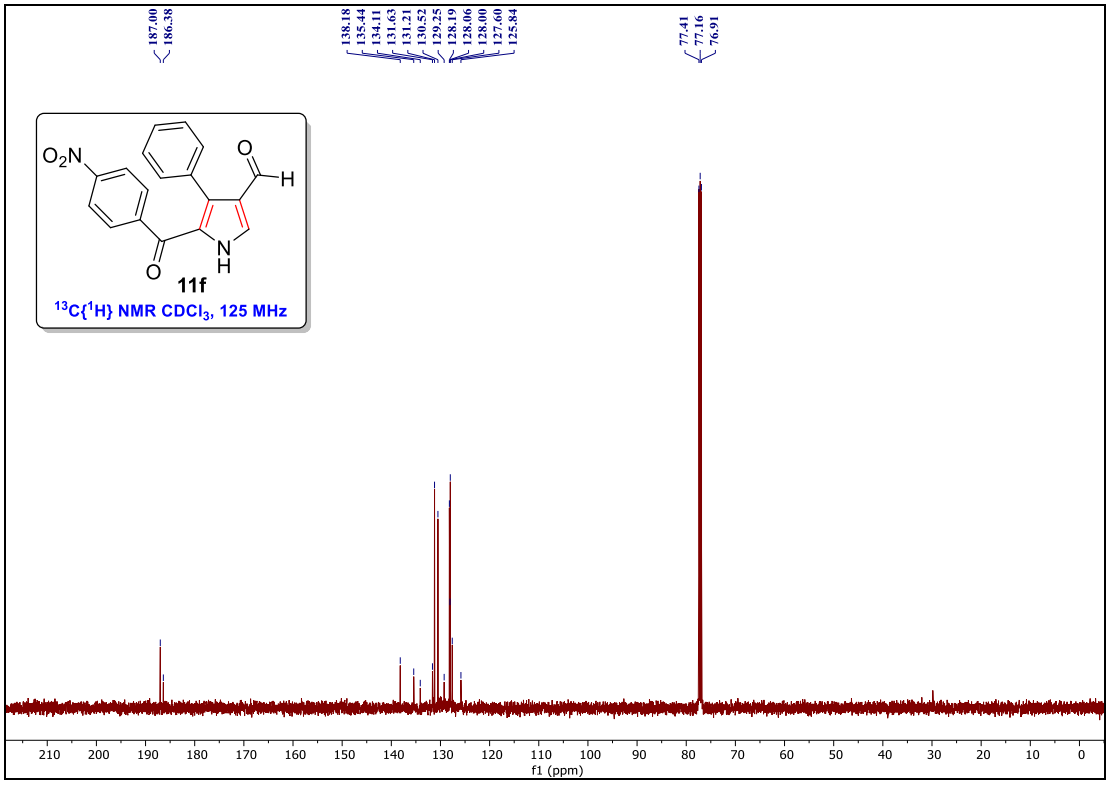

4-(4-Formyl-3-phenyl-1*H*-pyrrole-2-carbonyl)benzonitrile 11g

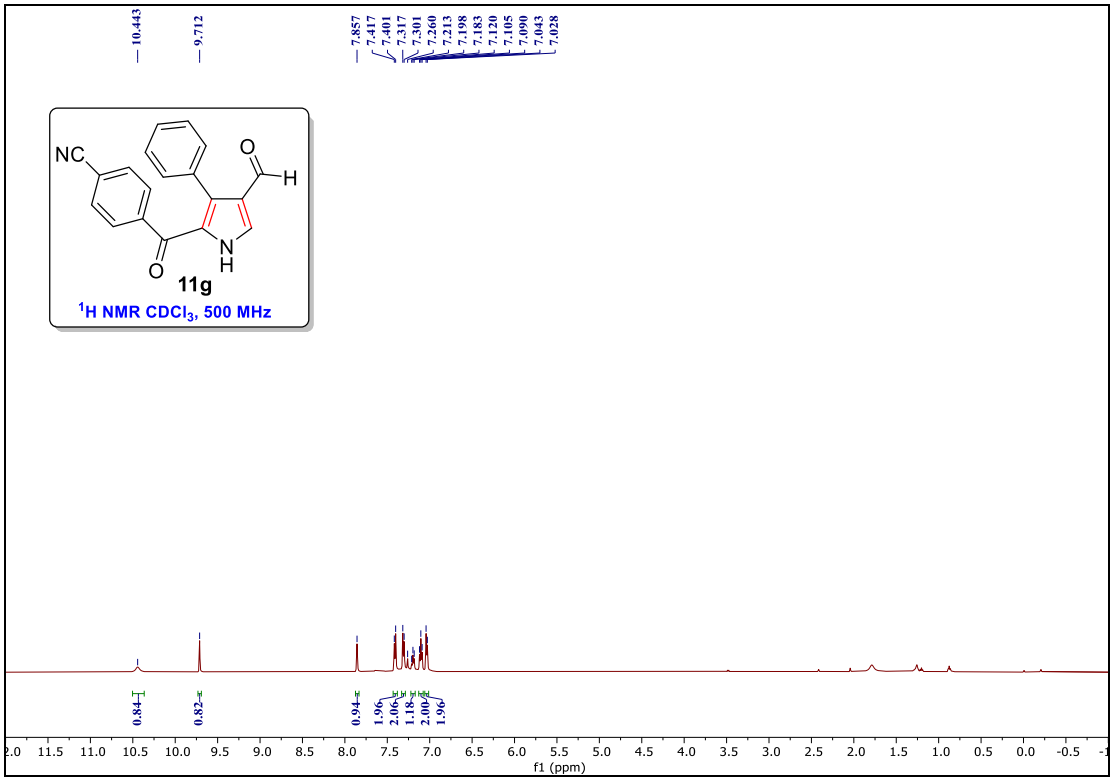

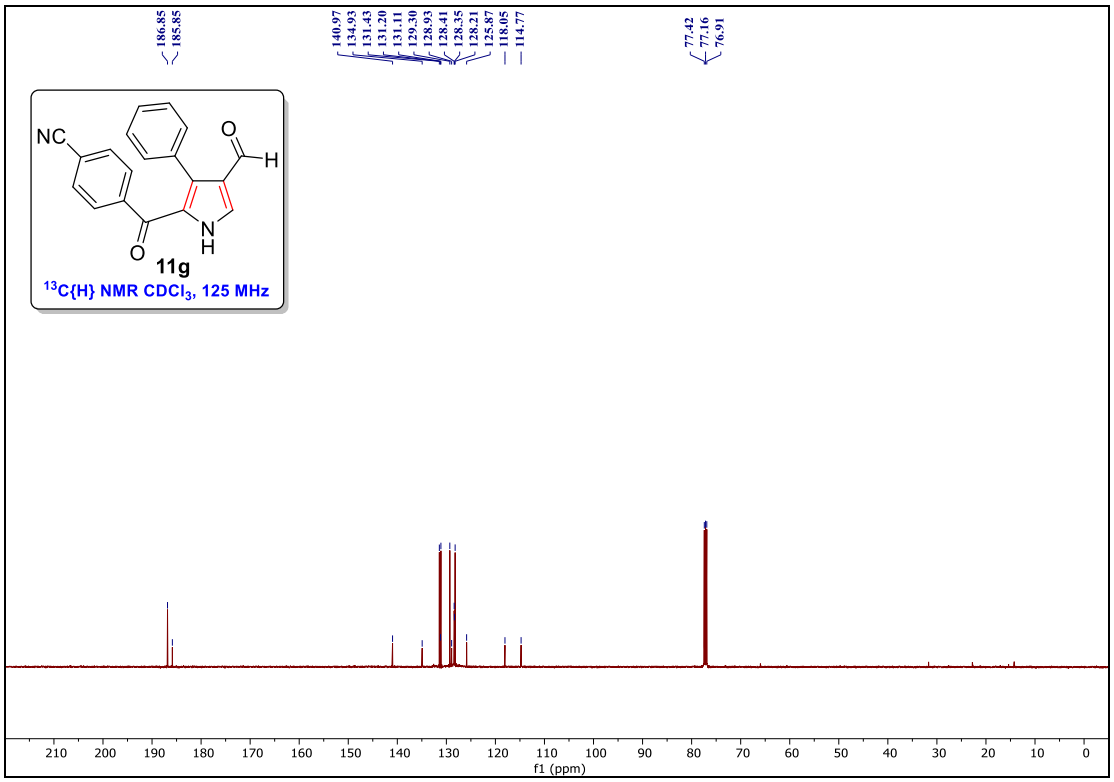

4-Phenyl-5-(4-(trifluoromethyl)benzoyl)-1*H*-pyrrole-3-carbaldehyde 11h

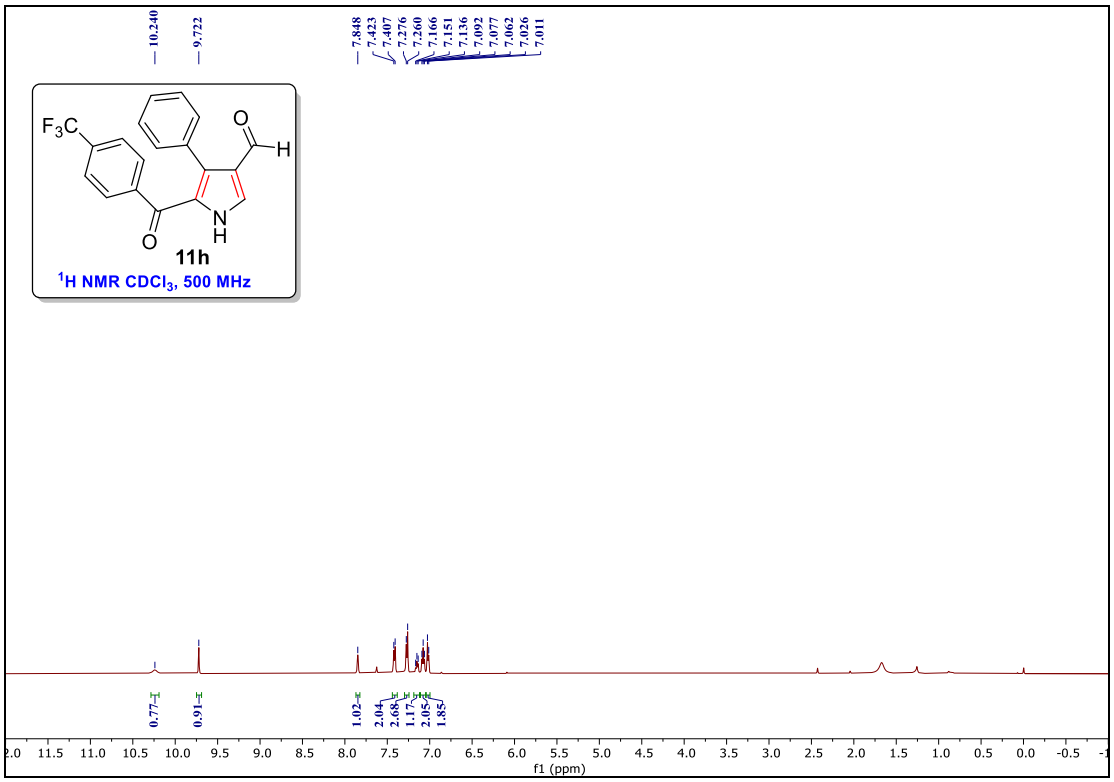

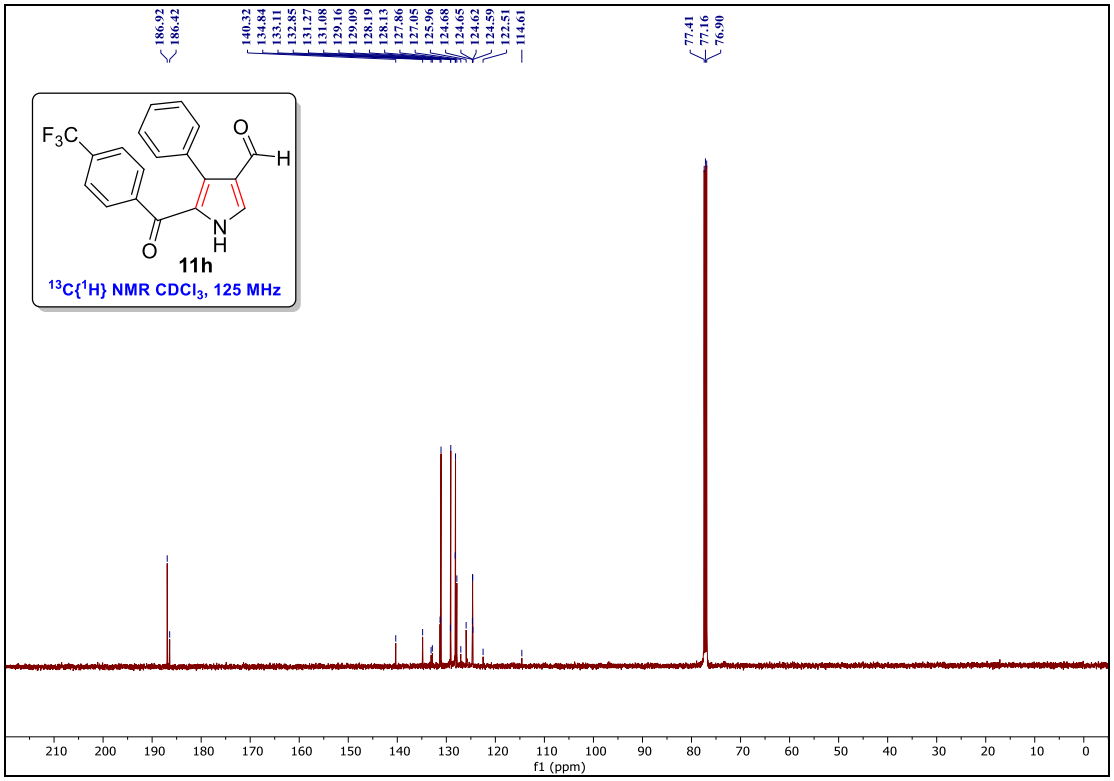

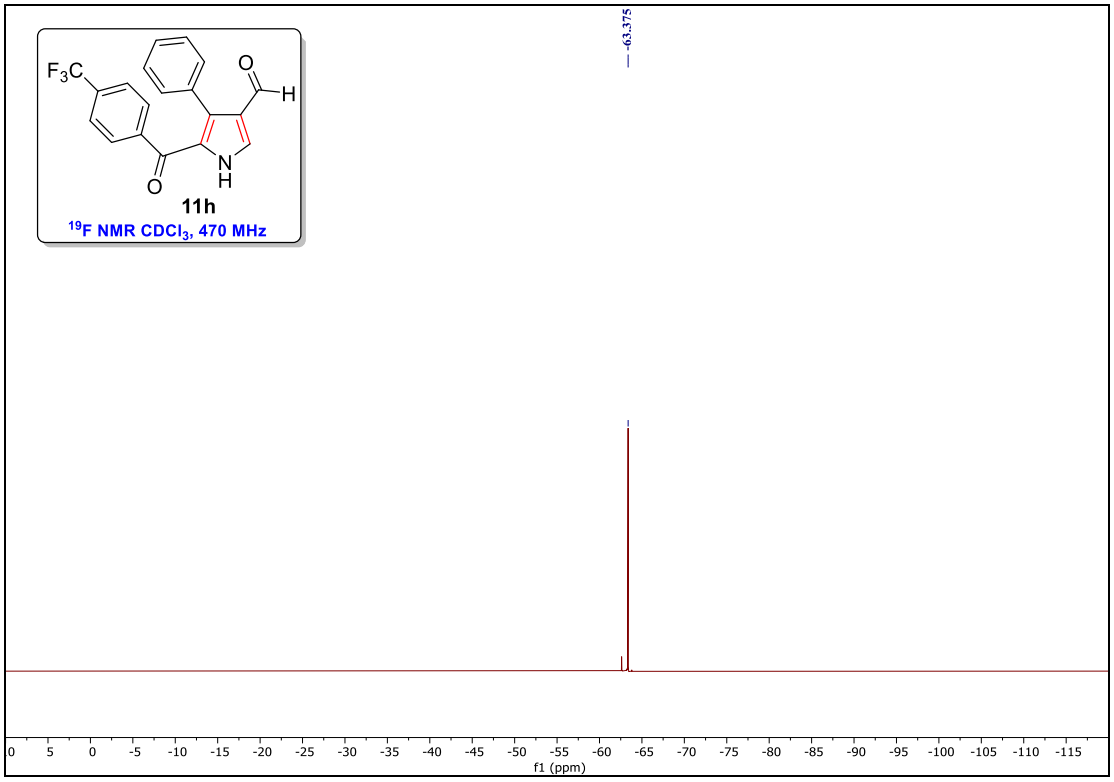
F3C
O
H
N
H
O
11h
19F NMR CDCl3, 470 MHz
-63.375
0 5 0 -5 -10 -15 -20 -25 -30 -35 -40 -45 -50 -55 -60 -65 -70 -75 -80 -85 -90 -95 -100 -105 -110 -115
f1 (ppm)

5-(2-Naphthoyl)-4-phenyl-1*H*-pyrrole-3-carbaldehyde 11i

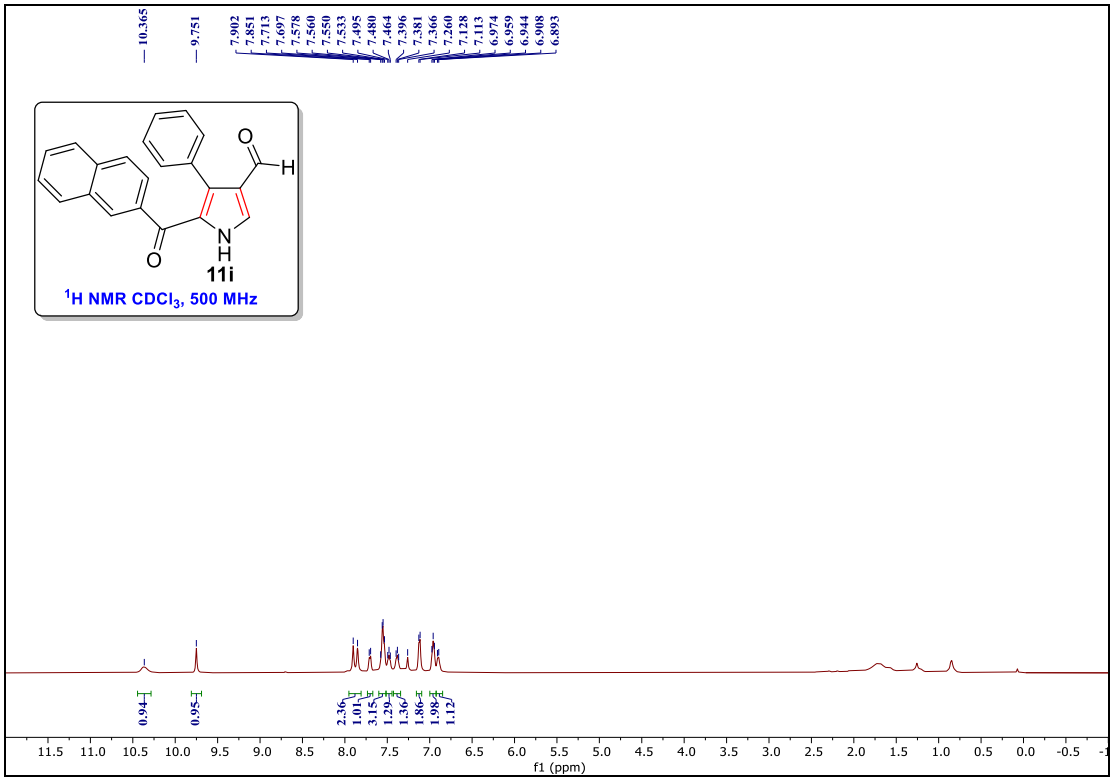

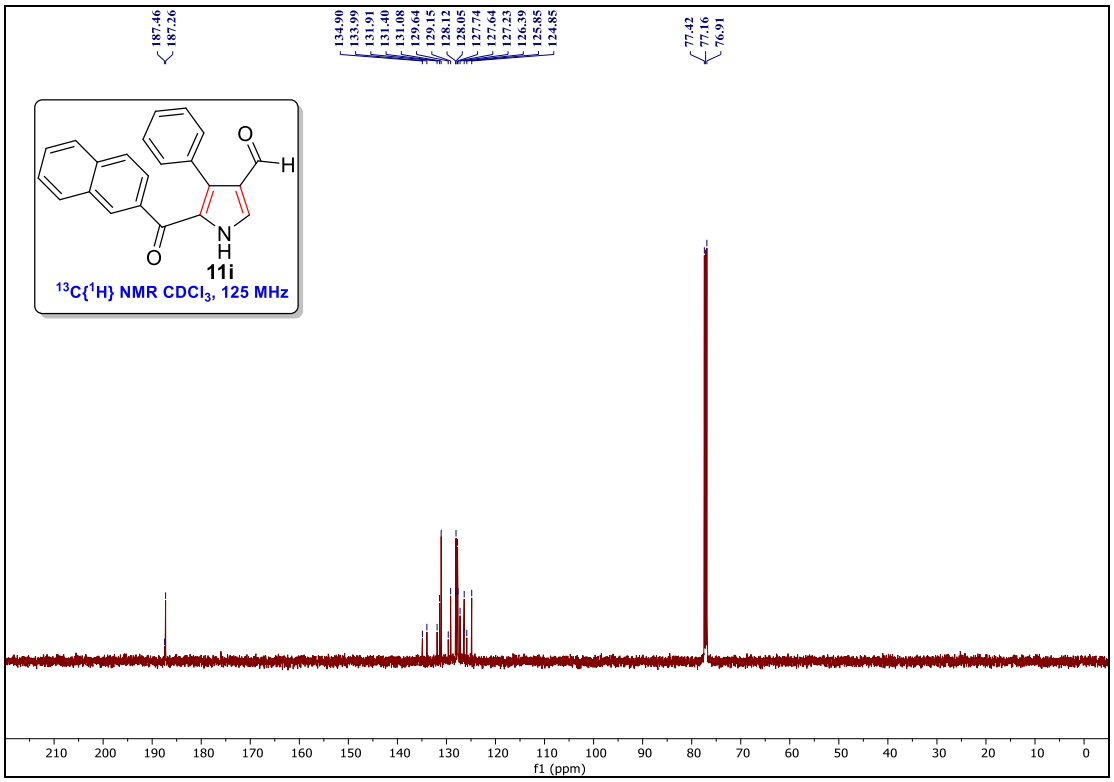

5-Benzoyl-4-(4-nitrophenyl)-1*H*-pyrrole-3-carbaldehyde 11j

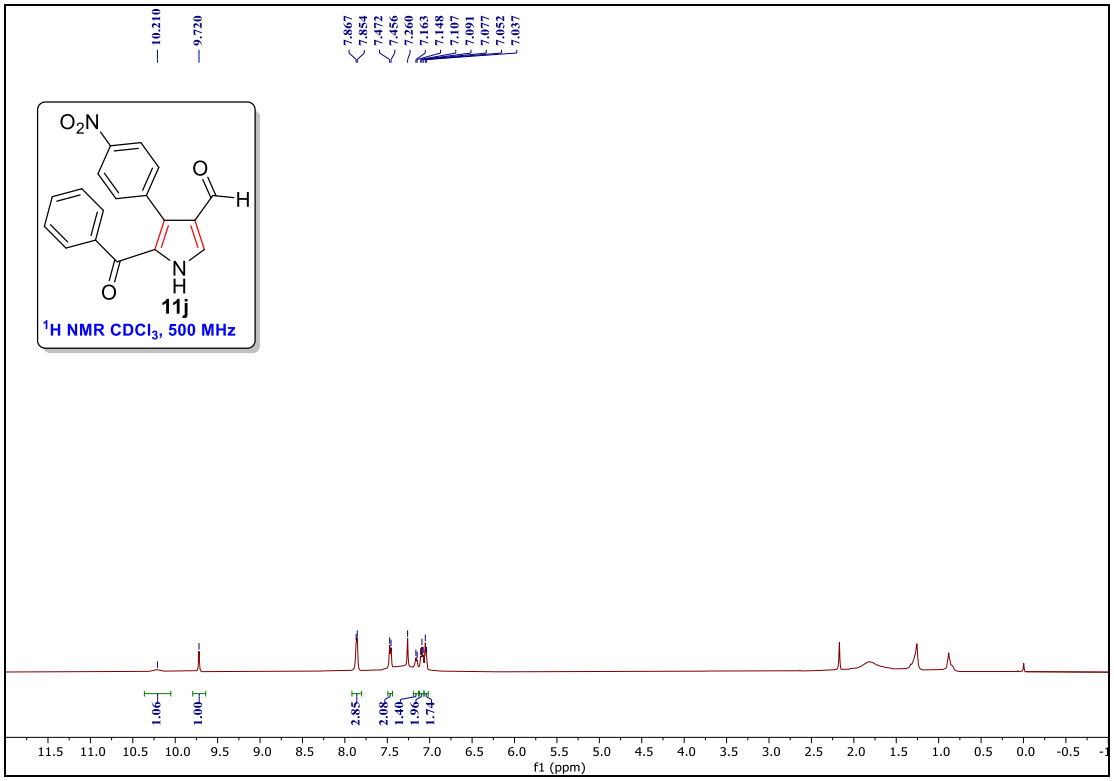

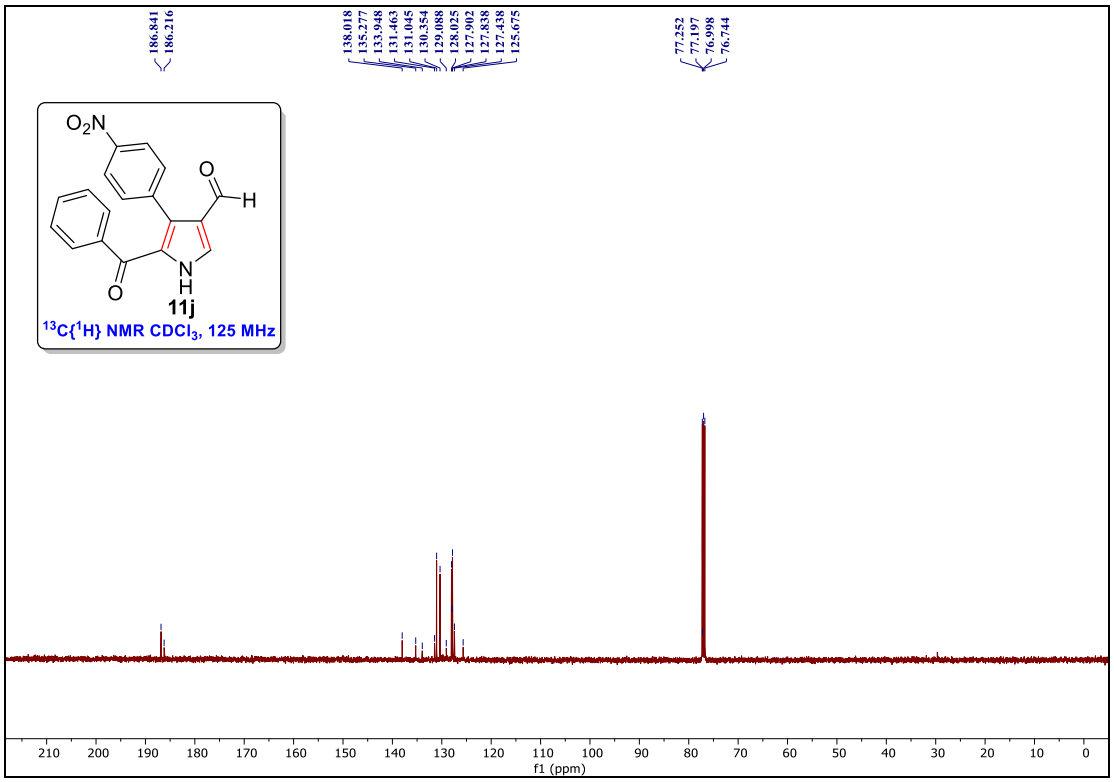

CHAPTER 4B

ASYMMETRIC SYNTHESIS OF TRISUBSTITUTED 4,5-DIHYDRO-1*H*-PYRROLE-3-CARBALDEHYDES THROUGH FORMAL DOMINO 1,3-DIPOLAR CYCLOADDITION/C-S AND C-N BOND-CLEAVAGE

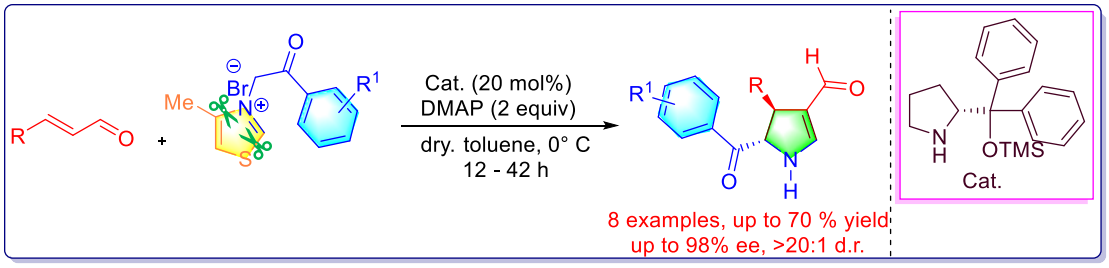

4.15 INTRODUCTION

4.15.1 Importance of Dihydro-1*H*-pyrroles

Dihydro-1*H*-pyrroles represent a class of *N*-heterocyclic compounds. These structures are entirely distinct from their aromatic pyrrole counterparts and possess unique chemical properties and versatile reactivity, making them valuable tools in organic synthesis and drug discovery. The structural motif of dihydropyrroles involves a saturated ring system, which alters their electronic structure and reactivity compared to aromatic pyrroles. This modification affects their interactions with other molecules, influencing their utility in various applications.[177] Synthetic methods for dihydro1*H*-pyrroles encompass diverse strategies, including the condensation of primary amines with α,β-unsaturated carbonyl compounds[178] followed by reduction to yield the saturated dihydro pyrrole ring.[276] It can also be achieved through functional group manipulation, enabling the introduction of diverse substituents to fine-tune their properties for specific applications.[179`]

Dihydro-1*H*-pyrroles have gained attention in medicinal chemistry due to their potential scaffolds for drug design. The dihydro-1*H*-pyrroles derivatives have shown promising pharmacological activities in preclinical studies, including antimicrobial, anticancer, and neuroprotective properties. Their saturated nature can impart improved metabolic stability and bioavailability compared to aromatic pyrroles, enhancing their suitability for drug development.[277, 278] Their reactivity towards electrophiles, nucleophiles, and transition metal catalysts enables the construction of complex molecular architectures with high efficiency and selectivity.[279] They can serve as versatile intermediates in organic synthesis to afford structurally diverse compounds and a key building blocks in the synthesis of natural products, pharmaceuticals, and functional materials.[280]

1,3-Dipolar cycloaddition reactions offer versatile routes to access poly-substituted pyrroles with diverse substitution patterns.[281] A wide range of substituents can be introduced into the pyrrole ring in a controlled manner by judicious selection of 1,3-dipoles and dipolarophiles. However, synthesizing dihydropyrroles using 1,3-dipolar cycloaddition is still challenging, and only a few methods have been reported in the literature.[108, 283-284] The regioselectivity and stereochemistry of the cycloaddition can be modulated through appropriate choice of reaction conditions and functional group compatibility, enabling the synthesis of complex poly-substituted dihydropyrrole derivatives. Particularly, azomethine ylides are versatile reactive intermediates for the synthesis of five-membered containing highly substituted pyrrolidines *via* 1,3-dipolar cycloaddition with various dipolarophiles.[285] Very few reports in the literature use azomethine ylides for the synthesis of substituted-dihydro-1*H*-pyrroles.[282-284, 286-287]

4.16 LITERATURE BACKGROUND

4.16.1 Synthesis of Dihydro-1*H*-pyrroles

In 2011, Shi and co-workers reported a chiral phosphoric acid catalyzed three-component, organocatalytic, asymmetric 1,3-dipolar cycloaddition reactions of aldehydes, aminoester, and alkyl ynones for the synthesis of synthetically and biologically important new chiral 2,5-dihydropyrrole derivatives in high yields with excellent enantio- and diastereoselectivity (Scheme 4.33).[282]

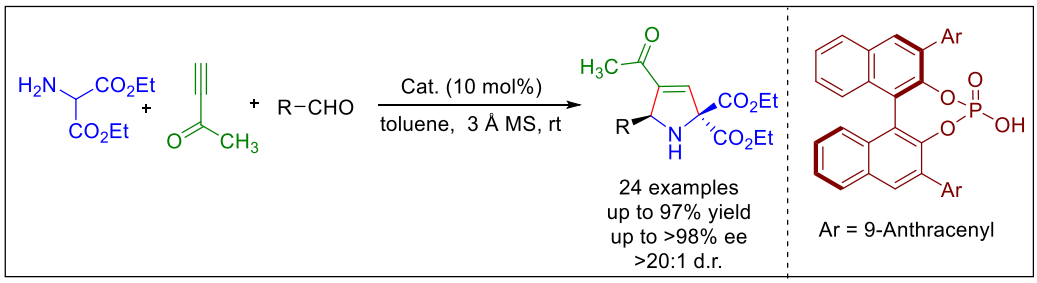

Scheme 4.33 Enantioselective three-component reaction for the synthesis of alkyl ketone substituted 2,5-dihydro-1*H*-pyrroles

The same research group in 2012 developed a chiral phosphoric acid organocatalyst for three components, asymmetric 1,3-dipolar cycloaddition reactions using arylglycine ester, aryl ynones, and aldehyde for the synthesis of synthetically and biologically important both the diastereomers of 2,5-dihydropyrrole scaffolds with multiple chiral centers including one quaternary stereogenic center in high yields with excellent enantioselectivity (Scheme 4.34).[283]

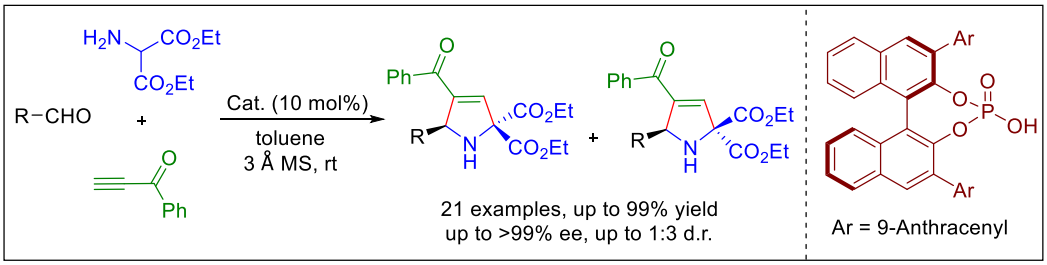

Scheme 4.34 Enantioselective, three-component reaction for the synthesis of aryl ketone substituted 2,5-dihydro1*H*-pyrroles

A first catalytic asymmetric 1,3-dipolar cycloaddition of alkynes, *N*-protected isatin, and aminoester using chiral phosphoric acid as an organocatalyst was developed for the synthesis of spirofused dihydropyrroles. In 2013, Shi *et al.* achieved synthetically and pharmaceutically important spiro-oxindole-based 2,5-dihydropyrrole scaffolds with quaternary chiral center in high yields with excellent enantio- and diastereoselectivity (Scheme 4.35).[284]

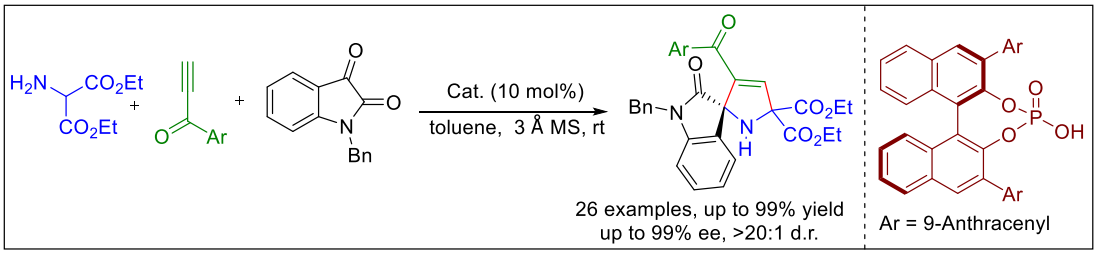

Scheme 4.35 Enantioselective, three-component reaction for the synthesis of spiro-oxindole based 2,5-dihydro1*H*-pyrroles

In 2019, Zhanguo *et al.* accomplished the synthesis of 4,5-dihydro-1*H*-pyrrole derivatives starting from nitro-nitriles, which can be synthesized from nitro-alkene reaction with malononitrile. The nitro group of nitro-nitriles was reduced *via* Fe/HCl system in methanol at room temperature to provide amine. The amino group reacted with the nitrile group through intramolecular nucleophilic addition/and rearrangement reaction to furnish the 4,5-dihydropyrroles in good yields (Scheme 4.36).[286]

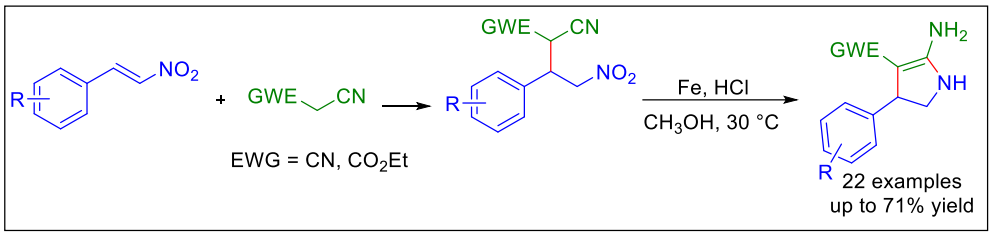

Scheme 4.36 Intramolecular nucleophilic addition/rearrangement reaction for the synthesis of 4,5-dihydro1*H*-pyrroles

A new method for the synthesis of 4,5-dihydro-1*H*-pyrrole derivatives was achieved in 2009 by Panek and co-workers *via* Lewis acid-promoted annulations of enantioenriched allenylsilanes with *in-situ* generated iminium ions derived from tert-butyl carbamate and methylcarbamate. This method afforded the 4,5-dihydro-1*H*-pyrrols good yields (Scheme 4.37).[287]

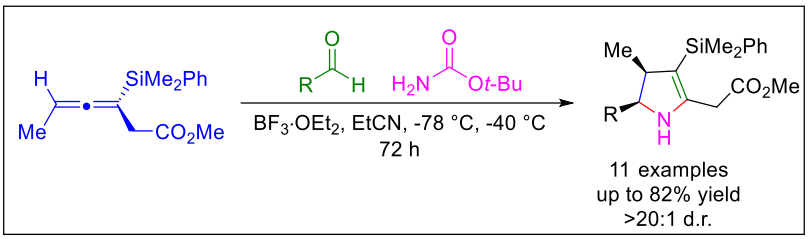

Scheme 4.37 Lewis acid promoted annulation reaction for the synthesis of 4,5-dihydro1*H*-pyrroles

4.17 OBJECTIVE

- A new domino methodology will be developed for the synthesis of enantioenriched trisubstituted 4,5-dihydro-*1H*-pyrrole-3-carbaldehydes.

- This method will utilize an easily available 4-methyl thiazolium salts, commercially available α,β-unsaturated aldehydes, using chiral (*R*)-diphenylprolinol trimethylsilyl ether as an organocatalyst (Scheme 4.38).
- In this domino process, the 4-methyl thiazolium salt will undergo a formal domino, intermolecular 1,3-dipolar cycloaddition/intramolecular ring-opening/C-S and C-N bond cleavage reaction sequence in the presence of base.

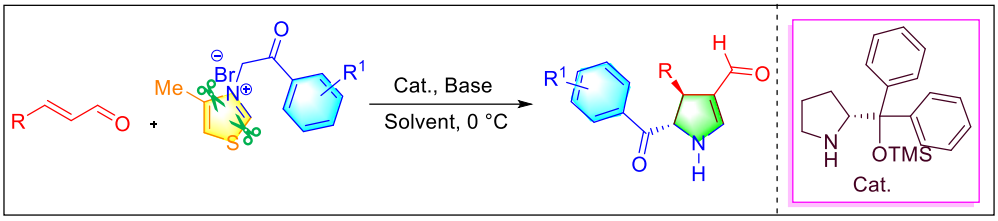

Scheme 4.38 Domino 1,3-dipolar cycloaddition/ring-opening/C-S and C-N bond cleavage reaction for the synthesis of chiral trisubstituted dihydro-1*H*-pyrrole-3-carbaldehydes

4.17.1 Hypothesis of Present Work

As described in Chapter **4**, the 4-methyl thiazolium azomethine ylide **8** reacted with α,β-unsaturated aldehydes **1** in the presence of an organocatalyst at "room temperature" to afford trisubstituted 1*H*-pyrrole-3-carbaldehydes **11**. The reaction proceeded by formal domino intermolecular 1,3-dipolar cycloaddition/intramolecular ring-opening/unprecedented C-S and C-N bond cleavage reaction sequence (Scheme 4.39 a). In this reaction, the reaction mechanism is expected to be through the formation of 4,5-dihydro-1*H*-pyrrole intermediate **12**, which was already confirmed by HRMS (Chapter **4)**. To consider the valuable importance of enantioenriched dihydropyrroles, the asymmetric synthesis of dihydropyrroles using enantiopure organocatalysts under the same strategies is more warranted.

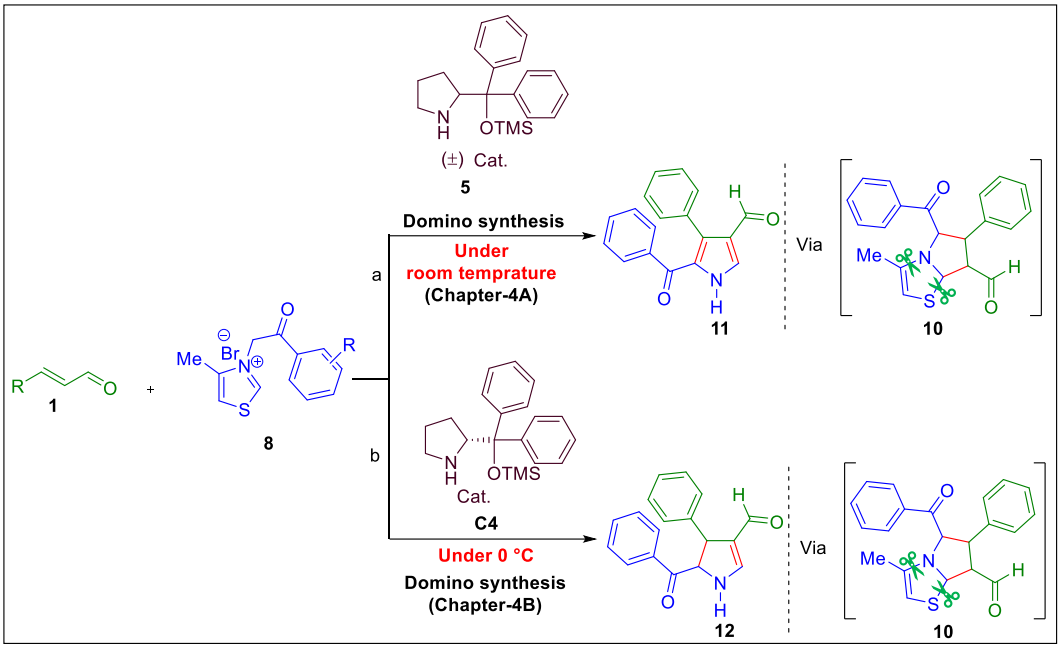

Scheme 4.39 Formal domino 1,3-dipolar cycloaddition reactions strategies for the synthesis of chiral dihydropyrroles

Therefore, it is hypothesized that chiral dihydropyrroles can be synthesized when the same reaction is performed at low temperature with a chiral organocalyst, thereby making it possible to stop the reaction at the dihydropyrrole intermediate stage (Scheme 4.39 b). It is important to mention that this reaction gives only achiral product **4** at room temperature. By lowering the reaction temperature, it will be possible to obtain the target chiral molecule **12**.

With this hypothesis, the domino reaction will be carried out by reacting the cinnamaldehyde **1a** (1 equiv), 4-methyl thiazolium salt **2a** (1 equiv), and (*L*)-proline **C1** (20 mol%) as a chiral catalyst, NEt_3 (1 equiv) as a base, EtOH as a solvent under 0 °C. After 24 h, the reaction resulted in the formation of two spots. By analyzing two different spots, it was observed that one product is the expected 4,5-dihydro1*H*-pyrroles **6** (36% yield), and the other one is the trisubstituted 1*H*-pyrrole **4** (35% yield). It is important to mention that the enantiomeric excess of newly formed dihydropyrroles **6** is 30% with >20:1 d.r. (Scheme 4.40). Thus, the synthesis of 4,5-dihydro-1*H*-pyrroels

7 was achieved successfully in an enantioselective manner by lowering the reaction temperature to 0 °C.

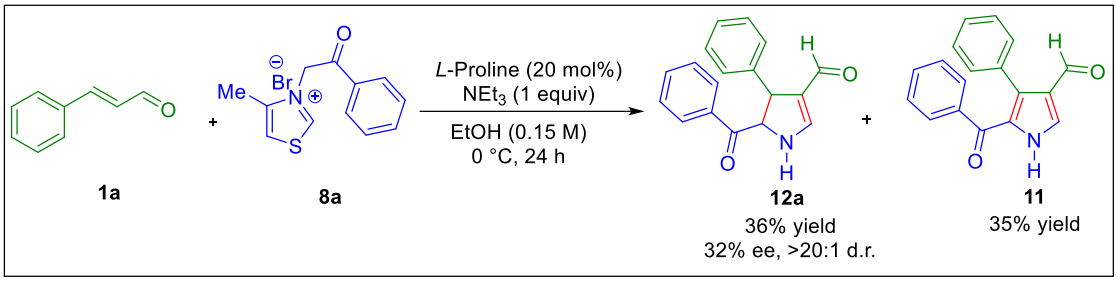

Scheme 4.40 Formal domino 1,3-dipolar cycloaddition/ring-opening/*C*-*S* and *C*-*N* bond cleavage reaction for the synthesis of chiral trisubstituted-1H-pyrrole-3-carbaldeydes

4. 18. RESULT AND DISCUSSION

With the above preliminary result, the optimization of the domino reaction with selective formation of only chiral product **7a** over the achiral product **4** by varying parameters such as chiral catalysts, bases, and solvents were carried out and the results are summarized in Tables 4.1, 4.2, and 4.3. The initial focus was to increase the enantiomeric excess of the chiral product **7**, thus, the reaction condition was screened with different chiral proline-derived catalysts (Table 4.5, entries 1-6).

4.18.1 Reaction Optimization

Table 4.6: Catalyst Screening[a]

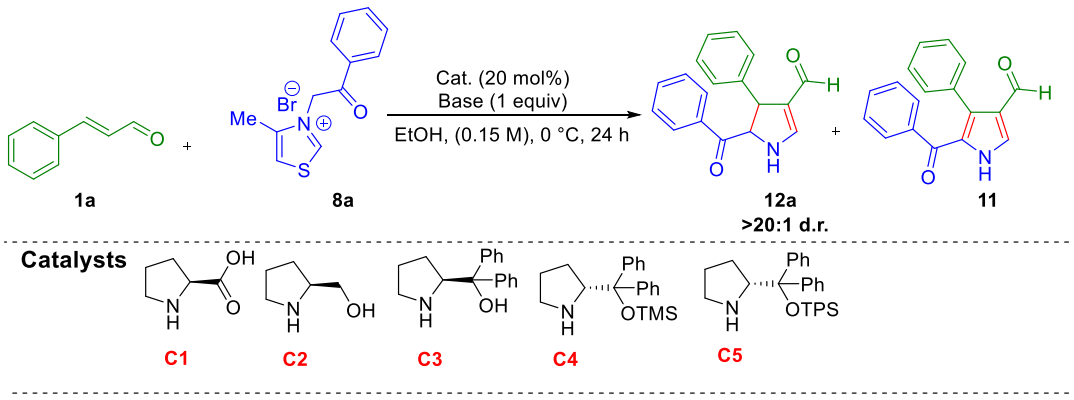

Entry	Base (equiv)	Catalyst	Yield of 12a (%) [b]	ee of 12a (%) [c]	Yield of 4 (%) [e]
1	NEt_3	**C1**	36	32	35
2	NEt_3	**C2**	37	10	10
3	NEt_3	**C3**	35	15	15
4	NEt_3	**C4**	40	16	20
5	NEt_3	**C5**	30	12	25
6	DMAP	**C4**	50	65	25

Table 4.7: Base Screening[a]

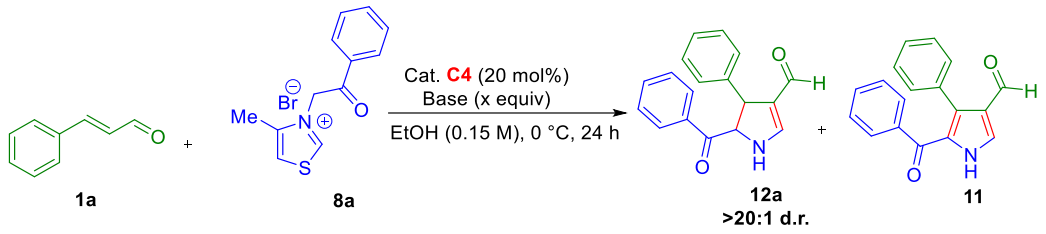

Entry	Base (equiv)	Catalyst	Yield of 12a (%) [b]	ee of 12a (%) [c]	Yield of 4 (%) [e]
1	DMAP (1)	**C4**	50	65	25
2	DIPEA (1)	**C4**	40	20	5
3	DIA (1)	**C3**	28	85	20
4	DEA (1)	**C4**	10	28	12
5	K_2CO_3 (1)	**C5**	47	32	15
6	DABCO (1)	**C4**	24	70	8
7	DMAP (2)	**C4**	48	85	12

[a]Reaction conditions: **1a** (0.3 mmol), **2a** (0.3 mmol), base (1-2 equiv), catalyst **C4** (20 mol%), and EtOH (0.15 M) at 0 °C for 24 h. [b,e] Isolated yield. [c]Ee was determined by using a chiralcel HPLC chiral column. [d]D.r. was determined by ^1H NMR using a crude reaction mixture.

The product yield was increased when the catalyst was changed to **C2** (entry 2). Upon increasing the bulkiness of the catalysts **C3,** yield was slightly improved, but no difference in enantioselectivity (entry 3). Next, with chiral ligand **C3** to **C4** change, there was no change in the yield and asymmetric induction. There was no change in the yield and enantiomeric excess when the chiral ligand was changed from **C4** to **C5**. The best reaction condition was obtained with catalyst **C4** and DMAP as a base, and it provided a 50% yield of product **7a** with 62% enantiomeric excess (entry 6). To improve the yield and enantiomeric excess of the product, the reaction was screened with several bases (Table 4.6, entries 1-6) such as DMAP, DIPEA, DIA, DEA, K_2CO_3, and DABCO. Among them, DMAP (2 equiv) was the best choice as it afforded 48% yield with 85% enantiomeric excess (entry 6). Then, the reaction was performed with several solvents like EtOH, MeOH, IPA, HIPF, DCM, toluene, THF, dry toluene, and dry THF (Table 4.7, entries 1-8). Dry toluene furnished the product **12a** with a maximum yield of 60 % with 96% enantiomeric excess. When the quantity of DMAP was decreased from two to one equivalent, product **12a** was obtained in 45% yield with 90% ee (Table 4.7, entry 9). When the catalyst loading was decreased to 10 mol%, this reaction afforded product 12a with a 40% yield and 60% ee (entry 10).

Table 4.8: Solvent Screening[a]

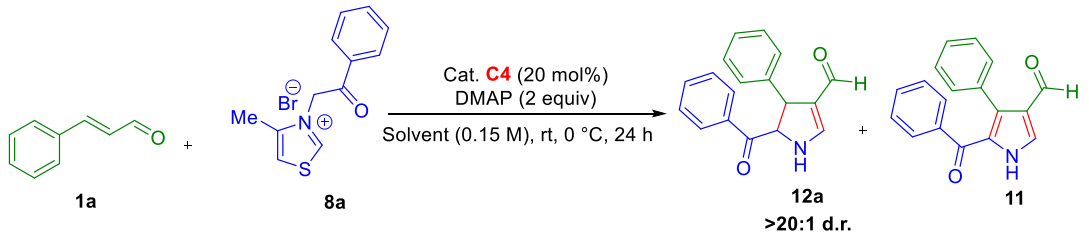

Entry	Base (equiv)	Catalyst	Solvent	Yield of 12a (%) [b]	ee of 12a (%)[c]	Yield of 4 (%)[e]
1	DMAP (2)	**C4**	EtOH	48	85	12
2	DMAP (2)	**C1**	MeOH	48	48	12
2	DMAP (2)	**C2**	IPA	36	60	20
3	DMAP (2)	**C3**	HFIP	10	0	15
4	DMAP (2)	**C4**	DCM	10	40	30
5	DMAP (2)	**C5**	1,2-DCE	10	40	20
6	DMAP (2)	**C4**	THF	30	96	30
7	DMAP (2)	**C4**	toluene	25	94	20
8	DMAP (2)	**C4**	dry toluene	60	96	9
9	DMAP (2)	**C4**	dry THF	45	96	15
10	DMAP (2)	**C4**	EtOH	40	16	20
11	DMAP (1)	**C4**	dry toluene	45	90	25
12[e]	DMAP (2)	**C4**	dry toluene	40	60	20

[a]Reaction conditions: **1a** (0.3 mmol), **2a** (0.3 mmol), DMAP (2 equiv), catalyst **C4** (20 mol%), and solvent (0.15 M) at 24 h. [b,e] Isolated yield. [c]Ee was determined by using a chiralcel HPLC chiral column. [d]D.r. was determined by ^{1}H NMR using a crude reaction mixture. [e] Reaction was performed with chiral catalyst **C4** with (10 mol%).

4.19 SUBSTRATE SCOPES

From the optimizing reaction conditions, the best condition was found to be the usage of the chiral catalyst **C4** (20 mol%), α,β-unsaturated aldehyde **1a** (1 equiv), 4-methylthiazolium salt **8a** (1 equiv), and DMAP (2 equiv) in dry toluene (0.15 M) at 0 °C at 24 h.

Table 4.9 Substrate Scope of Trisubstituted Chiral Dihydro-1*H*-pyrrole-3-carbaldehydes[a,b]

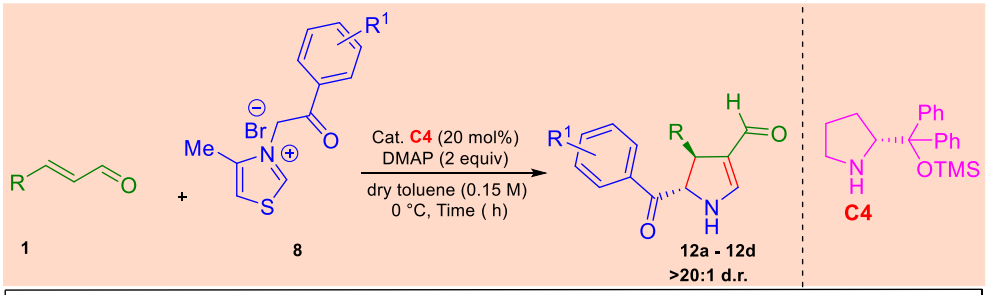

Entry	α,β-Unsaturated aldehyde	Thiazolium salt	Product
1	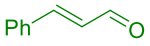	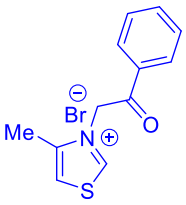	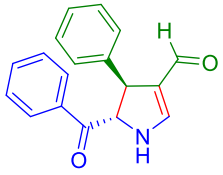 12a; 60, 96% ee, 24 h
2	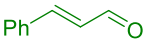	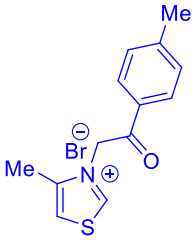	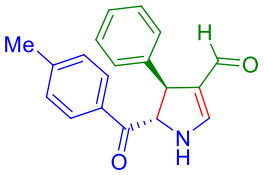 12b; 70, 82% ee, 24 h
3	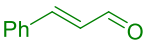	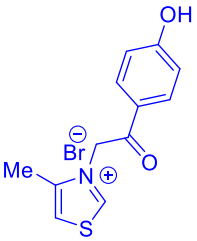	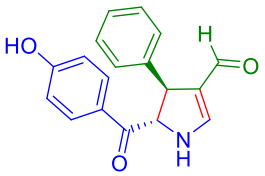 12c; 50, 88% ee, 24 h
4	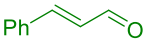	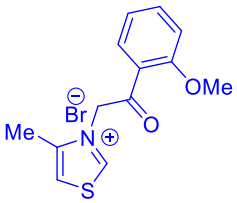	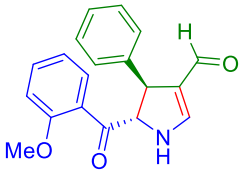 12d; 50, 96% ee, 24 h
5	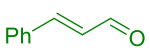	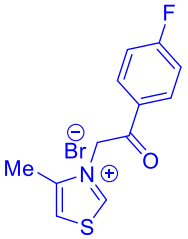	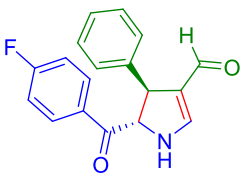 12e; 60%, 98% ee, 17 h

Entry	α,β-Unsaturated aldehydes	Thiazolium salt	Product
6	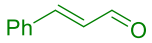	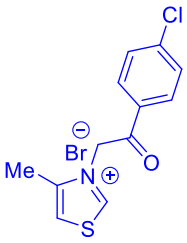	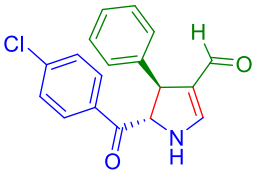 12f; 65%, 96% ee, 124 h
7	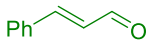	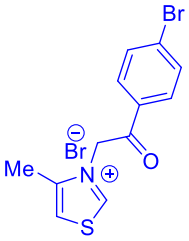	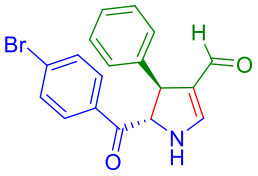 12g; 69%, 98% ee, 24 h
8	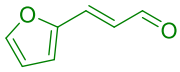	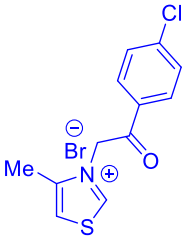	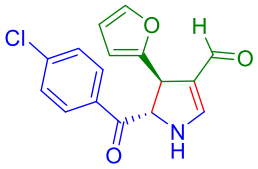 12h; 57%, 64% ee, 24 h

[a]Reaction conditions: **1a**, **1b** (0.3 mmol), **2e – 2h** (0.3 mmol), DMAP (2 equiv), **C4** (20 mol%), dry toluene (0.15 M). [b]Isolated yield. [c]Ee was determined by using a chiralcel chiral HPLC column. [d]D.r. ratio was determined by ^{1}H NMR using a crude reaction mixture. In all cases, the aromatized product **4** was obtained in minor quantity.

With these optimized reaction conditions, the functional group tolerance of the domino reaction was investigated with various 4-methyl thiazolium salts **8** such as electron-donating, electron-withdrawing, halogens containing, and bulky substituents containing 4-methyl thiazolium salts to furnish the desired products **12a-12i** in good yields with high enantio- and diastereoselectivity (Table 4.9). The 4-methyl thiazolium salt-bearing electron-donating groups at the *ortho*, *meta*, and *para* positions (**12a-12g)** exhibited good reactivity and provided moderate to good yields with 80-98% ee. Halogen substitution at the *para* position accomplished the desired product **12h-12i** in 98% yield with moderate yield (Table 4.9). An electron-withdrawing substitution such as -NO_2, -CN, and -CF_3 groups failed to deliver the desired chiral products and instead

gave only aromatized products exclusively. Instead of a phenyl ring at the 3-position, the α,β-unsaturated aldehydes bearing furan ring afforded the desired chiral product in good yield with moderate enantioselectivity (Table 4.9).

4.20. GRAM SCALE SYNTHESIS

To check the scalability of the domino methodology, a gram-scale reaction was performed using chiral catalyst **C4,** cinnamaldehyde **1a** (3 mmol, 396 mg, 374 μL), 4-methylthiazolium salt **2a** (3 mmol, 1.24 g), and DMAP (6 mmol 0.73 g) using the optimized reaction conditions. The reaction furnished the desired chiral product **7a** in 66% yield (0.65 g) (Scheme 4.41).

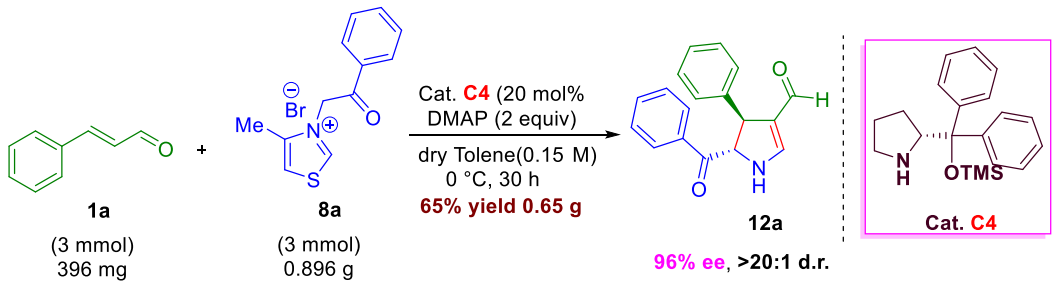

Scheme 4.41 Gram scale synthesis of **12a**

4.21 CONTROL EXPERIMENTS

Several control experiments were carried out to probe the reaction mechanism. When cinnamaldehyde **1a** was reacted with thiazolium salt **2a** with catalyst **C4** at room temperature, only the aromatized product **4** was observed (Scheme 4.42-i). It indicates that the above reaction delivers the chiral dihydropyrrole product only at 0 °C. When the reaction was performed under the standard condition without a DMAP base, the reaction did not proceed. This result confirms that the base is essential for product formation (Scheme 4.42-ii). When the reaction was carried out only with base, this reaction produced a 30% yield of racemic product (Scheme 4.42-iii). This result shows

that the reaction can happen only with base (background reaction) without the need for the chiral catalyst.

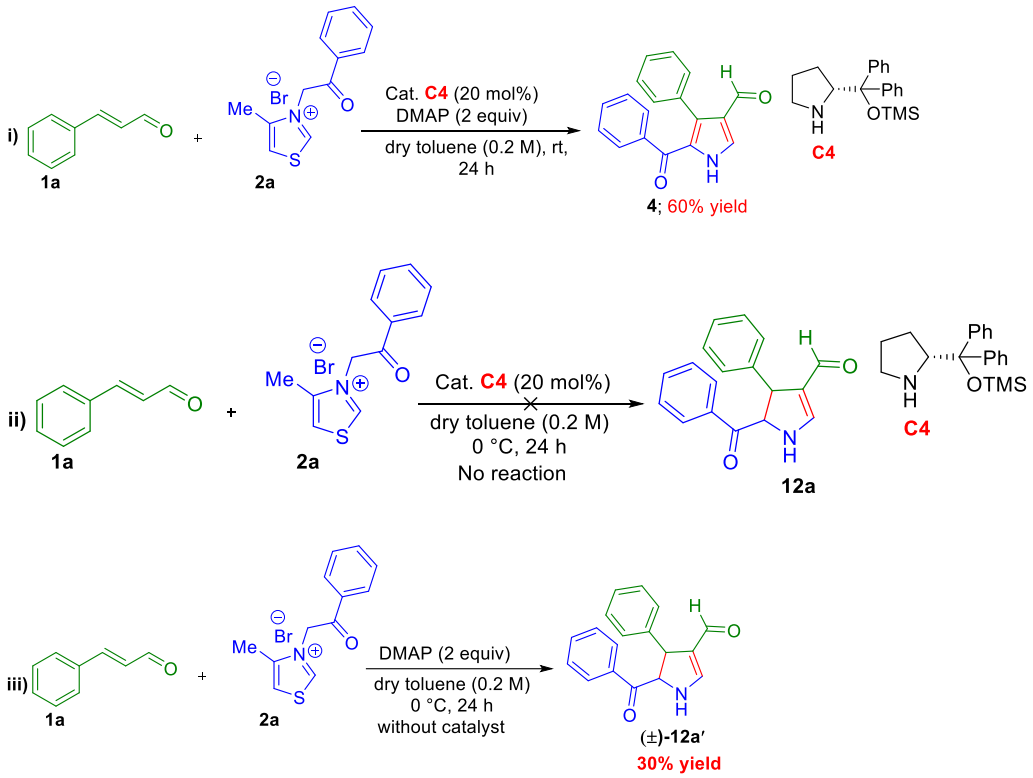

Scheme 4.42 Control experiments

4.22 PLAUSIBLE REACTION MECHANISM

Based on control experiments and a previous study from Chapter **4**, a plausible reaction mechanism has been proposed (Scheme 4. 42). First, the chiral secondary amine catalyst **C4** and cinnamaldehyde **1a** in the presence of *in-situ* produced HBr or protonated DMAP will generate iminium ion complex **I** by elimination of water. Meanwhile, the thiazolium salt **8a** will react with DMAP to form 1,3-dipolar thiazolium salt ylide intermediate **III**. The ylide intermediate **III** will react with chiral iminium ion complex **I** in a 1,4-addition reaction *via Si*-face (favorable transition state (Figure 4.5 a) to give Michael adduct intermediate **IV** which is the first chiral induction step of the entire catalytic cycle. This intermediate **IV** will undergo dearomatatiozation of

thiazolium salt to produce 1,3-dipolar cycloadduct intermediate **V**. Hydrolysis of **V** with water will result in the regeneration of chiral catalyst **C4** for the next catalytic cycle. In this process, hydropyrrolo-thiazole intermediate **VI** and HBr will be generated**.** Intermediate **VI**, in the presence of base will produce the ring opening thiolate anion intermediate **VII**.

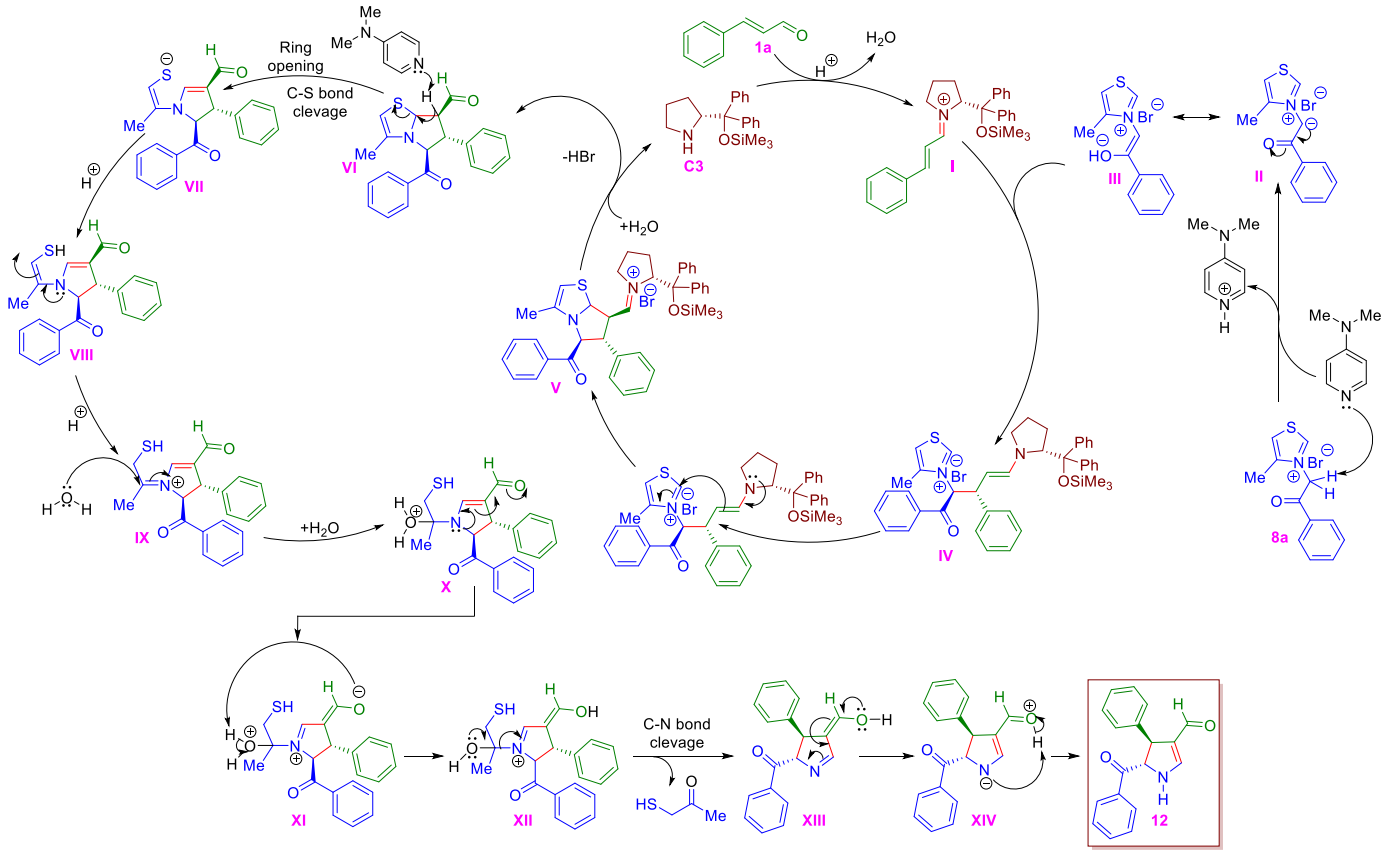

Scheme 4.43 Plausible reaction mechanism for the formation of chiral trisubstituted 4,5-dihydro-1*H*-pyrrole

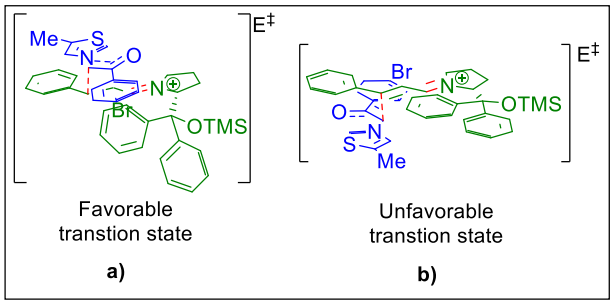

Figure 4.5 Favorable and unfavorable transition state

Then, the intermediate sulfur anion **VII** will be quenched by a proton to produce the intermediate **VIII.** This intermediate **VIII** will undergo enamine imine tautomerism, and the double bond will be protonated to produce the iminium ion intermediate **IX** using nitrogen atom lone pair electrons. This iminium ion intermediate **IX** will react with *in-situ* generated water molecules to produce the intermediate **X**. In intermediate **X, the** nitrogen lone pair will be delocalized to produce the enolate of iminium ion intermediate **XI,** followed by protonation of enolate **XI** to produce the intermediate **XII**. In intermediate **XII**, the *C-N* bond cleavage will take place to yield byproduct 1-mercaptopropan-2-one and intermediate **XIII**. The formation of byproduct 1-mercaptopropan-2-one was confirmed by HRMS and ^{1}H NMR analysis of crude reaction mixture. The enol ether intermediate **XIII** will be converted to the final product trisubstituted 4,5-dihydro-1*H*-pyrrole-3-caldehyde **12** *via* intermediate **XIV**.

4.23 CONCLUSION

- In conclusion, a novel domino method has been developed for the asymmetric synthesis of trisubstituted 1*H*-pyrrole-3-carbaldehydes.
- This approach uses radially available α,β-unsaturated aldehydes, and 4-methyl thiazolium salts in the presence of chiral proline-derived organocatalysts.
- The reaction proceeded *via* formal 1,3-dipolar cycloaddition/ring-opening/*C-S* and *C-N* bond cleavage reaction sequence to provide the enantioenriched trisubstituted 1*H*-pyrrole-3-carbaldehydes in moderate to good yields with excellent enantio- and diastereoselectivity.
- This approach worked well for various functional groups.

- This is the first report for the synthesis of enantioenriched trisubstituted 1*H*-pyrrole-3-carbaldehyde derivatives using 4-methylthiazolium salts and α,β-unsaturated aldehyde *via* a domino synthesis.

4.24 EXPERIMENTAL SECTION

4.24.1 General information

All reactions were carried out in oven-dried reaction tubes. 4-methyl thiazole, phenacyl bromides, and cinnamaldehydes were purchased from Sigma-Aldrich, Spectrochem, BLD, Carbanio, and Avra Synthesis Pvt. Ltd. The racemic proline and DMAP were purchased from Spectrochem, Avra Synthesis Pvt. Ltd. and used directly as received. All the starting materials were synthesized according to the reported procedures. Reactions were monitored by thin-layer chromatography (TLC) using Merck silica gel 60 F_{254} precoated plates (0.25 mm) and visualized by UV fluorescence quenching using an appropriate mixture of ethyl acetate and hexanes as eluting solvent mixtures. Silica gel for column chromatography (particle size 100-200 mesh) was purchased from Avra Synthesis Pvt. Ltd. and used for column chromatography using hexanes and ethyl acetate mixture as eluent. Organic solutions were concentrated under reduced pressure on a Büchi, Heidolph rotary evaporator using a water bath. ^{1}H and ^{13}C NMR spectra were recorded on a Bruker 400 or 500 MHz instrument.^{1}H NMR is reported relative to residual $CDCl_3$ (δ 7.26 ppm) or DMSO-d_6 (δ 2.50 ppm). ^{13}C NMR is reported close to residual $CDCl_3$ (δ 77.16 ppm) or DMSO-d_6 (δ 39.52 ppm). Chemical shifts were recorded in parts per million (ppm). Multiplicities are as indicated: s (singlet,) d (doublet,) t (triplet,) q (quartet,) quint (quintet), sext (sextet), sept (septet) dd (doublet of doublet,) m (multiplet,) tt (triplet of triplet,) td (triplet of doublet). The coupling constant, *J*, is reported in Hertz.

Melting points were recorded on a Guna capillary melting point apparatus and were corrected with benzoic acid as a reference. FTIR spectra were recorded on a JASCO spectrometer and were reported in the frequency of absorption (cm^{-1}) using a dry KBr pellet. The polarimetry was recorded in P-2000 High Accuracy Digital Polarimeter - Jasco Inc. High-resolution mass spectra (HRMS) were recorded on Q-Tof Micro mass spectrometer. All the single crystal X-ray data was collected with a Bruker AXS (Kappa Apex 2) CCD diffractometer equipped with graphite monochromatic Mo (Kα) (λ = 0.7107 A) radiation source. The data were collected with 100% completeness for Θ up to 25º. ω and ϕ scans were employed to collect the data. The frame width for ω for was fixed to 0.5º for data collection. The crystal was solved by direct methods using Bruker SHELXS (Sheldrick, 1997). The Structure was refined using the Bruker SHELXTL (Version 6.12) software package. HPLC spectra were recorded on a Waters Alliance 2695 HPLC System using the CHIRALCEL-OD-H, AD-H, and CHIRALPACK-AI columns.

4.24.2 Typical Procedure for the Domino Synthesis of Racemic Trisubstituted Dihydro-1*H*-pyrrole-3-carbaldehyde

General procedure A: To a 20 mL oven-dried reaction tube with a magnetic stir bar under an open atmosphere racemic proline catalyst **C1** (20 mg, 0.06 mmol), and cinnamaldehyde **1a** (38 µL, 0.3 mmol) were dissolved in dry. toluene (0.075 M) and stirring for 1 hour at room temperature. 4-Methy thiazolium salt **2a** (90 mg, 0.3 mmol), DMAP (73 mg, 0.6 mmol), and (0.75 M) dry. toluene was successively added to the reaction mixture. The reaction progress was monitored by TLC. After complete consumption of both starting materials, toluene was evaporated from the reaction mixture. After evaporation of toluene, the reaction mixture was poured into water and

extracted with EtOAc (3 x15 mL), washed with brine (1×10 mL), and the combined organic extractions were dried over anhydrous Na_2SO_4. Evaporation of organic layer to give the crude product. This crude product was purified by column chromatography on silica gel (eluent: hexane/ethyl acetate = 80/20) to get the desired racemic product **7a'** (Scheme 4.44).

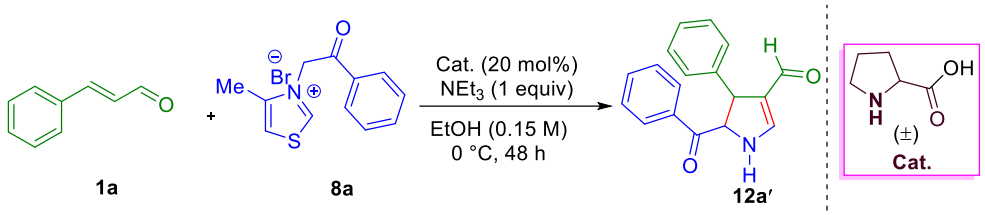

Scheme 4.44 Synthesis of racemic trisubstituted dihydro-1*H*-pyrrole-3-carbaldehyde

4.24.3 Typical Procedure for the Asymmetric Domino Synthesis of Chiral Trisubstituted Dihydro-1*H*-pyrrole-3-carbaldehyde

General procedure B: To a 20 mL oven-dried reaction tube with a magnetic stir bar under an open atmosphere chiral catalyst **C4** (20 mg, 0.06 mmol), and cinnamaldehyde **1a** (38 µL, 0.3 mmol) were dissolved in dry. toluene (0.075 M) and stirring for 1 hour at room temperature. 4-Methy thiazolium salt **2a** (90 mg, 0.3 mmol), DMAP (73 mg, 0.6 mmol), and (0.75 M) dry toluene was successively added to the reaction mixture. The reaction progress was monitored by TLC. After complete consumption of both starting materials, toluene was evaporated from the reaction mixture. After evaporation of toluene, the reaction mixture was poured into water and extracted with EtOAc (3 x15 mL), washed with brine (1×10 mL), and the combined organic extractions were dried over anhydrous Na_2SO_4. Evaporation of organic layer to give the crude product. This crude product was purified by column chromatography on silica gel (eluent: hexane/ethyl acetate = 80/20) to get the desired chiral product **7a** in 75% yield with 96% enantioselectivity (Scheme 4.45).

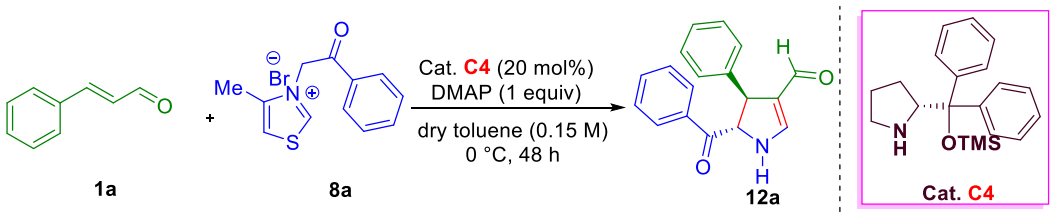

Scheme 4.45 Enantioselective synthesis of trisubstituted dihydro-1*H*-pyrrole-3-carbaldehyde

4.25. ANALYTICAL AND SPECTRAL CHARACTERIZATION DATA

(4*S*,5*S*)-5-Benzoyl-4-phenyl-4,5-dihydro-1*H*-pyrrole-3-carbaldehyde 12a;

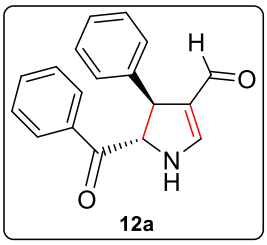

Prepared according to general procedure C using (*R*)-diphenylprolinol trimethylsilyl ether **C4**. Purification of crude product was done by column chromatography using (hexane/ethyl acetate) mixture (50:50) to afford the title compound as orange semi solid, (60% yield, 50 mg); R_f = 0.34 (50 % ethyl acetate in hexane); mp = 86 – 88 °C; **^{1}H NMR (500 MHz, DMSO-d$_6$)** δ 9.12 (s, 1H), 8.16 (s, 1H), 7.87 (s, 1H), 7.81 (d, *J* = 7.5 Hz, 2H), 7.68 (t, *J* = 7.5 Hz, 1H), 7.52 (t, *J* = 7.5 Hz, 2H), 7.32 (t, *J* = 7.5 Hz, 2H), 7.27 – 7.21 (m, 1H), 7.14 (d, *J* = 7.5 Hz, 2H), 5.40 (d, *J* = 4.5 Hz, 1H), 4.01 (d, *J* = 4.5 Hz, 1H); **^{13}C NMR (125 MHz, CDCl$_3$)** δ 196.0, 180.4, 157.8, 143.2, 133.8, 128.9, 128.7, 128.5, 127.1, 126.8, 118.7, 72.0, 48.0; **FTIR (neat)** 3359, 3062, 2925, 2853, 1692, 1577, 1453, 1234, 702 cm^{-1}; **HRMS (ESI)** calculated for $C_{18}H_{16}NO_2$ $[M+H]^+$: 278.1176; found: 278.1170. **HPLC** condition: HPLC Chiralcel AD-H, hexane/i-PrOH = 70:30 v/v, flow rate = 1.0 mL/min, λ = 310 nm, 25 °C, t_R (major) = 5.18, t_R (minor) = 9.90 min, 96% *ee*, $[\alpha]_D^{20}$ = +318.00 (c 0.5, CH_3CN).

(4*S*,5*S*)-5-(4-Methylbenzoyl)-4-phenyl-4,5-dihydro-1*H*-pyrrole-3-carbaldehyde

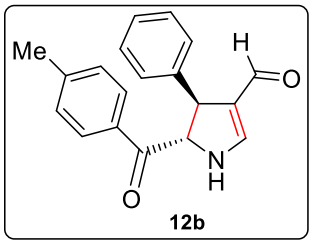

12b

12b; Prepared according to general procedure C using (*R*)-diphenylprolinol trimethylsilyl ether **C4**. Purification of crude product was done by column chromatography using (hexane/ethyl acetate) mixture (50:50) to afford the title compound as orange viscous liquid, (70% yield, 61 mg); R_f = 0.36 (50 % ethyl acetate in hexane); **^{1}H NMR (400 MHz, CDCl$_3$)** δ 9.29 (s, 1H), 7.69 (d, *J* = 7.6 Hz, 2H), 7.47 (s, 1H), 7.42 – 7.29 (m, 5H), 7.28 – 7.22 (m, 3H), 5.53 (s, 1H), 5.22 (s, 1H), 4.30 (s, 1H), 2.43 (s, 3H); **^{13}C NMR (100 MHz, CDCl$_3$)** δ 196.3, 182.9, 155.4, 145.4, 142.7, 130.7, 129.7, 129.3, 129.1, 127.6, 127.5, 122.5, 73.3, 49.3, 21.9; **FTIR (neat)** 3387, 3065, 2925, 2860, 1685, 1606, 1584, 1460, 1238, 758 cm^{-1}; **HRMS (ESI)** calculated for $C_{19}H_{18}NO_2$ $[M+H]^+$: 292.1332; found: 292.1331. **HPLC** condition: HPLC Chiralcel AD-H, hexane/i-PrOH = 70:30 v/v, flow rate = 1.0 mL/min, λ = 300 nm, 25 °C, t_R (major) = 16.60, t_R (minor) = 20.36 min, 82% *ee*, $[\alpha]_D^{20}$ = +277.77 (c 0.1, CH_3CN).

(4*S*,5*S*)-5-(4-Hydroxybenzoyl)-4-phenyl-4,5-dihydro-1*H*-pyrrole-3-carbaldehyde

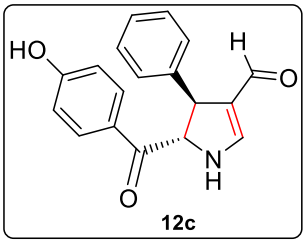

12c

12c; Prepared according to general procedure C using (*R*)-diphenylprolinol trimethylsilyl ether **C4**. Purification of crude product was done by column chromatography using (hexane/ethyl acetate) mixture (40:60) to afford the title compound as orange solid, (50% yield, 44 mg); R_f = 0.22 (60 % ethyl acetate in hexane); mp = 78 – 80 °C; **^{1}H NMR (500 MHz, CDCl$_3$)** 10.60 (s, 1H), 9.07 (s, 1H), 8.13 (d, *J* = 3.5 Hz, 1H), 7.85 (d, *J* = 3.5 Hz, 1H), 7.67 (d, *J* = 9.0 Hz, 2H), 7.32 (t, *J* = 8.0 Hz, 2H), 7.24 (t, *J* = 7.5 Hz, 1H), 7.15 (d, *J* = 8.5 Hz, 2H), 6.83 (d, *J* = 8.5 Hz, 2H), 5.27 (d, *J* = 4.0 Hz, 1H), 3.98 (d, *J* = 4.0 Hz, 1H); **^{13}C NMR (125 MHz, CDCl$_3$)** δ 194.4, 180.9, 163.1, 158.5, 143.8, 131.8, 129.0, 127.6, 127.2, 125.4, 119.2, 116.0, 72.1, 48.8; **FTIR (neat)** 3437, 2922,

2859, 1738, 1656, 1580, 1460, 1238, 703 cm^{-1}; **HRMS (ESI)** calculated for $C_{18}H_{16}NO_3$ $[M+H]^+$: 294.1125; found: 294.1114. **HPLC** condition: HPLC Chiralpak IB, hexane/i-PrOH = 70:30 v/v, flow rate = 1.0 mL/min, λ = 300 nm, 25 °C, t_R (major) = 14.38, t_R (minor) = 10.61 min, 88% *ee*, $[\alpha]_D^{20}$ = +159.62 (c 0.3, CH_3CN).

(4*S*,5*S*)-5-(2-Methoxybenzoyl)-4-phenyl-4,5-dihydro-1*H*-pyrrole-3-carbaldehyde

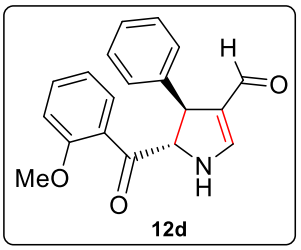

12d

12d; Prepared according to general procedure C using (*R*)-diphenylprolinol trimethylsilyl ether **C4**. Purification of crude product was done by column chromatography using (hexane/ethyl acetate) mixture (40:60) to afford the title compound as pale yellow solid, (54% yield, 50 mg); R_f = 0.41 (60% ethyl acetate in hexane); mp = 56 – 58 °C; **^{1}H NMR (500 MHz, DMSO-d$_6$)** δ 9.10 (s, 1H), 8.17 (d, *J* = 3.0 Hz, 1H), 7.87 (d, *J* = 3.5 Hz, 1H), 7.43 (d, *J* = 8.0 Hz, 1H), 7.37 (d, *J* = 7.5 Hz, 1H), 7.34 – 7.28 (m, 3H), 7.26 – 7.22 (m, 2H), 7.18 – 7.12 (m, 2H), 5.41 (d, *J* = 4.5 Hz, 1H), 4.00 (d, *J* = 4.0 Hz, 1H), 3.70 (s, 3H); **^{13}C NMR (125 MHz, DMSO-d$_6$)** δ 195.8, 180.4, 159.4, 157.9, 143.2, 135.2, 130.1, 128.5, 127.2, 126.8, 121.1, 120.2, 118.6, 113.1, 72.1, 55.2, 48.1; **FTIR (neat)** 3432, 3065, 2925, 2852, 1690, 1579, 1462, 1263, 726 cm^{-1}; **HRMS (ESI)** calculated for $C_{19}H_{18}NO_3$ $[M+H]^+$: 308.1281; found: 308.1277. **HPLC** condition: HPLC Chiralpak IB, hexane/i-PrOH = 70:30 v/v, flow rate = 1.0 mL/min, λ = 300 nm, 25 °C, t_R (major) = 22.40, t_R (minor) = 18.55 min, 96% *ee*, $[\alpha]_D^{20}$ = +261.10 (c 0.5, CH_3CN).

(4*S*,5*S*)-5-(4-Fluorobenzoyl)-4-phenyl-4,5-dihydro-1*H*-pyrrole-3-carbaldehyde

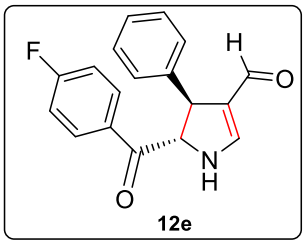

12e

12e; Prepared according to general procedure C using (*R*)-diphenylprolinol trimethylsilyl ether **C4**. Purification of crude product was done by column chromatography using

(hexane/ethyl acetate) mixture (50:50) to afford the title compound as orange brown viscous liquid, (60% yield, 53 mg); R_f = 0.33 (50 % ethyl acetate in hexane); **^{1}H NMR (500 MHz, $CDCl_3$)** 9.31 (s, 1H), 7.86 – 7.80 (m, 2H), 7.46 (s, 1H), 7.37 (t, *J* = 7.4 Hz, 2H), 7.34 – 7.28 (m, 3H), 7.13 (t, *J* = 8.5 Hz, 2H), 5.43 (s, 1H), 5.21 (d, *J* = 4.0 Hz, 1H), 4.29 (d, *J* = 4.0 Hz, 1H); **^{13}C NMR (125 MHz, $CDCl_3$)** δ 195.0, 182.9, 166.5 (d, *J* = 257.0 Hz), 155.0, 142.5, 131.9 (d, *J* = 9.5 Hz), 129.6 (d, *J* = 3.4 Hz), 129.3, 127.7, 127.4, 122.6, 116.4 (d, *J* = 22.0 Hz), 73.2, 49.3; **FTIR (neat)** 3408, 3065, 2925, 2853, 1687, 1597, 1509, 1460, 1233, 805 cm^{-1}; **HRMS (ESI)** calculated for $C_{18}H_{15}FNO_2$ $[M+H]^+$: 296.1081; found: 296.1081. **HPLC** condition: HPLC Chiralcel AD-H, hexane/i-PrOH = 70:30 v/v, flow rate = 1.0 mL/min, λ = 320 nm, 25 °C, t_R (major) = 5.28, t_R (minor) = 7.30 min, 98% *ee*, $[\alpha]_D^{20}$ = +105.46 (c 1.0, CH_3CN).

(4*S*,5*S*)-5-(4-Chlorobenzoyl)-4-phenyl-4,5-dihydro-1*H*-pyrrole-3-carbaldehyde

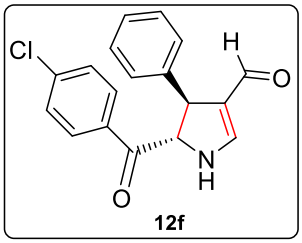

12f

12f; Prepared according to general procedure C using (*R*)-diphenylprolinol trimethylsilyl ether **C4**. Purification of crude product was done by column chromatography using (hexane/ethyl acetate) mixture (60:40) to afford the title compound as pale yellow viscous liquid, (65% yield, 60 mg); R_f = 0.27 (40 % ethyl acetate in hexane); mp = **^{1}H NMR (500 MHz, $CDCl_3$)** δ 9.32 (s, 1H), 7.76 – 7.72 (m, 2H), 7.47 – 7.42 (m, 3H), 7.39 – 7.34 (m, 2H), 7.33 – 7.29 (m, 3H), 5.39 (s, 1H), 5.20 (d, *J* = 4.1 Hz, 1H), 4.28 (d, *J* = 4.0 Hz, 1H); **^{13}C NMR (125 MHz, $CDCl_3$)** δ 195.4, 182.8, 154.9, 142.4, 141.0, 131.5, 130.5, 129.5, 129.3, 127.8, 127.4, 122.6, 73.3, 49.3; **FTIR (neat)** 3394, 2926, 2851, 1692, 1580, 1464, 1231, 838 cm^{-1}; **HRMS (ESI)** calculated for $C_{18}H_{14}ClNO_2$ [M+]: 311.0713; found: 311.0747. **HPLC** condition: HPLC Chiralcel AD-H, hexane/i-PrOH = 70:30 v/v, flow rate = 1.0 mL/min, λ = 301 nm, 25 °C, t_R (major) = 6.17, t_R (minor) = 7.80 min, 96% *ee*, $[\alpha]_D^{20}$ = +70.00 (c 0.1, CH_3CN).

(4*S*,5*S*)-5-(4-Bromobenzoyl)-4-phenyl-4,5-dihydro-1*H*-pyrrole-3-carbaldehyde

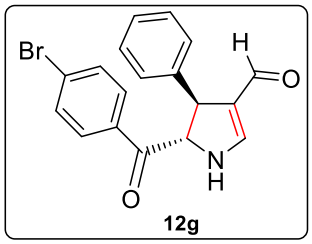

12g

12g; Prepared according to general procedure C using (*R*)-diphenylprolinol trimethylsilyl ether **C4**. Purification of crude product was done by column chromatography using (hexane/ethyl acetate) mixture (50:50) to afford the title compound as yellow viscous liquid, (69% yield, 73 mg); R_f = 0.34 (50 % ethyl acetate in hexane); **^{1}H NMR (400 MHz, DMSO-d$_6$)** δ 9.11 (s, 1H), 8.16 (s, 1H), 7.87 (s, 1H), 7.79 – 7.71 (m, 4H), 7.32 (d, *J* = 7.6 Hz, 2H), 7.25 (d, *J* = 7.5 Hz, 1H), 7.14 (d, *J* = 7.6 Hz, 2H), 5.38 (d, *J* = 4.0 Hz, 1H), 4.01 (s, 1H); **^{13}C NMR (126 MHz, CDCl$_3$)** δ 201.2, 185.6, 163.0, 148.4, 139.0, 134.1, 133.9, 133.7, 132.3, 132.0, 123.9, 77.2, 53.2; **FTIR (neat)** 3431, 2925, 2852, 1695, 1625, 1577, 1223, 837 cm^{-1}; **HRMS (ESI)** calculated for $C_{18}H_{14}BrNO_2$ [M+]: 355.0208; found: 355.0209. **HPLC** condition: HPLC Chiralcel AD-H, hexane/i-PrOH = 70:30 v/v, flow rate = 1.0 mL/min, λ = 300 nm, 25 °C, t_R (major) = 6.81, t_R (minor) = 8.50 min, 98% *ee*, $[\alpha]_D^{20}$ = +134.00 (c 0.5, CH_3CN).

(4*S*,5*S*)-5-(4-Chlorobenzoyl)-4-(furan-2-yl)-4,5-dihydro-1*H*-pyrrole-3-carbaldehyde

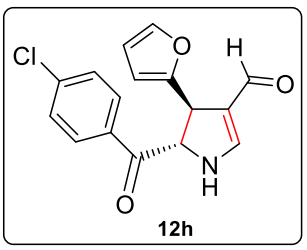

12h

12h; Prepared according to general procedure C using (*R*)-diphenylprolinol trimethylsilyl ether **C4**. Purification of crude product was done by column chromatography using (hexane/ethyl acetate) mixture (40:60) to afford the title compound as brown viscous liquid, (57% yield, 51 mg); R_f = 0.36 (60 % ethyl acetate in hexane); **^{1}H NMR (500 MHz, DMSO-d$_6$)** δ 9.14 (s, 1H), 8.19 (d, *J* = 3.5 Hz, 1H), 7.95 (d, *J* = 8.5 Hz, 2H), 7.83 (d, *J* = 3.0 Hz, 1H), 7.65 (d, *J* = 8.0 Hz, 2H), 7.58 (d, *J* = 2.0 Hz, 1H), 6.38 (t, *J* = 2.5 Hz, 1H), 6.07 (d, *J* = 3.0 Hz, 1H), 5.51 (d, *J* = 4.0 Hz, 1H), 4.20 (d, *J* = 4.5 Hz, 1H); **^{13}C NMR (126 MHz, DMSO-d$_6$)** δ 195.1, 180.9, 158.6, 155.0, 142.5, 139.3, 132.9, 131.1, 129.5, 115.3, 111.0, 106.6, 69.5, 41.5; **FTIR (neat)** 3378,

2926, 2854, 1692, 1580, 1470, 1231, 734, cm^{-1}; **HRMS (ESI)** calculated for $C_{16}H_{13}ClNO_3$ $[M+H]^+$: 302.0578; found: 302.0603. **HPLC** condition: HPLC Chiralcel AD-H, hexane/i-PrOH = 80:20 v/v, flow rate = 1.0 mL/min, λ = 300 nm, 25 °C, t_R (major) = 9.16, t_R (minor) = 13.52 min, 64% *ee*, $[\alpha]_D^{20}$ = +139.00 (c 0.5, CH_3CN).

4.26 ^{1}H, ^{13}C and ^{19}F NMR SPECTRA

(4*S*,5*S*)-5-benzoyl-4-phenyl-4,5-dihydro-1*H*-pyrrole-3-carbaldehyde 12a

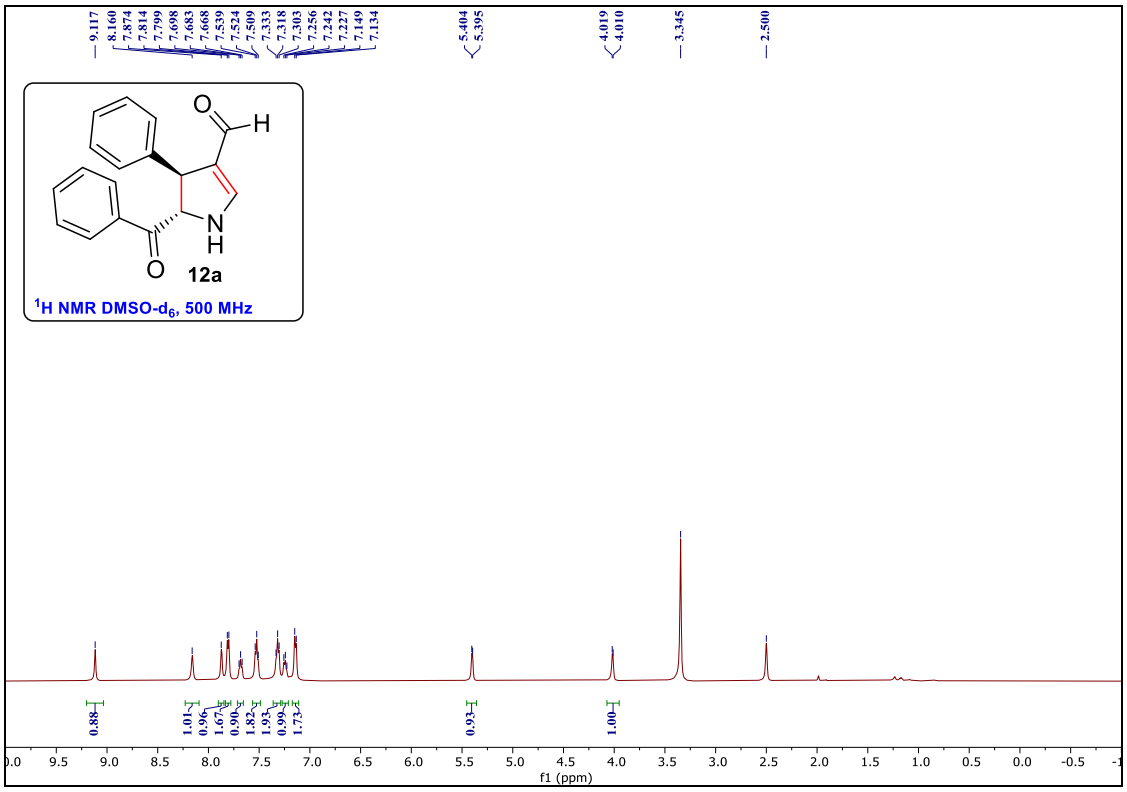

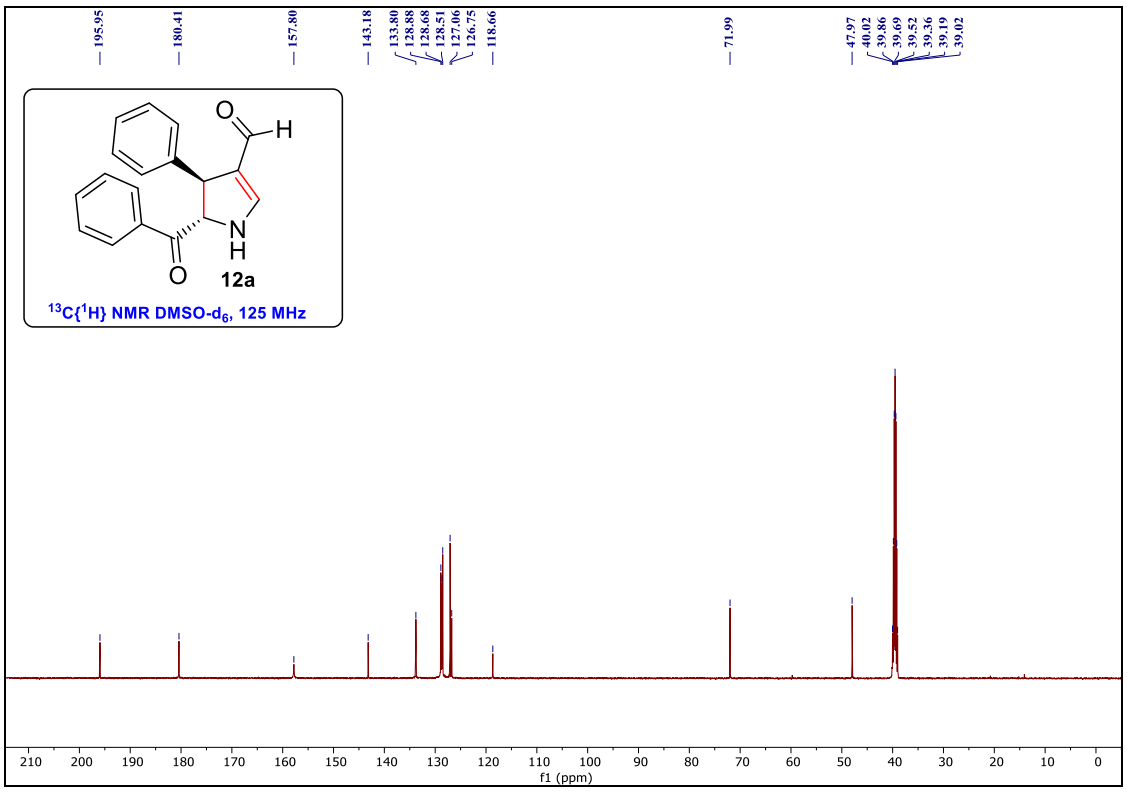

(4*S*,5*S*)-5-(4-Methylbenzoyl)-4-phenyl-4,5-dihydro-1*H*-pyrrole-3-carbaldehyde 12b

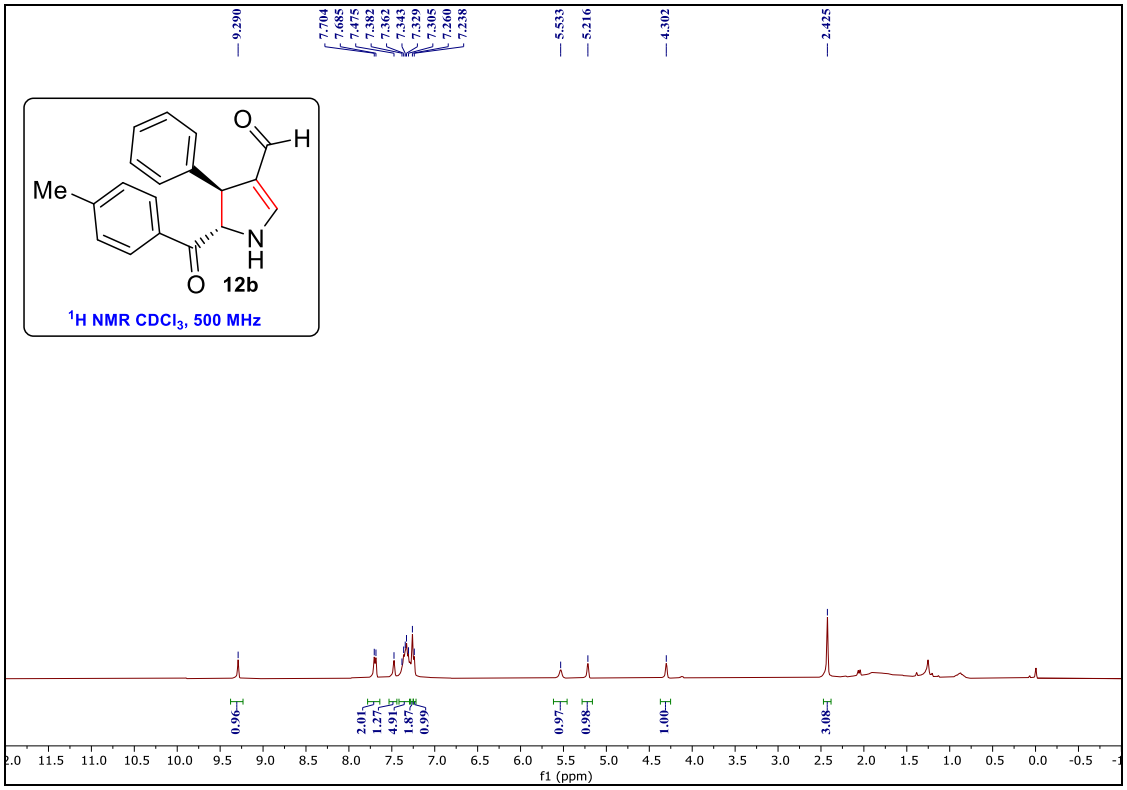

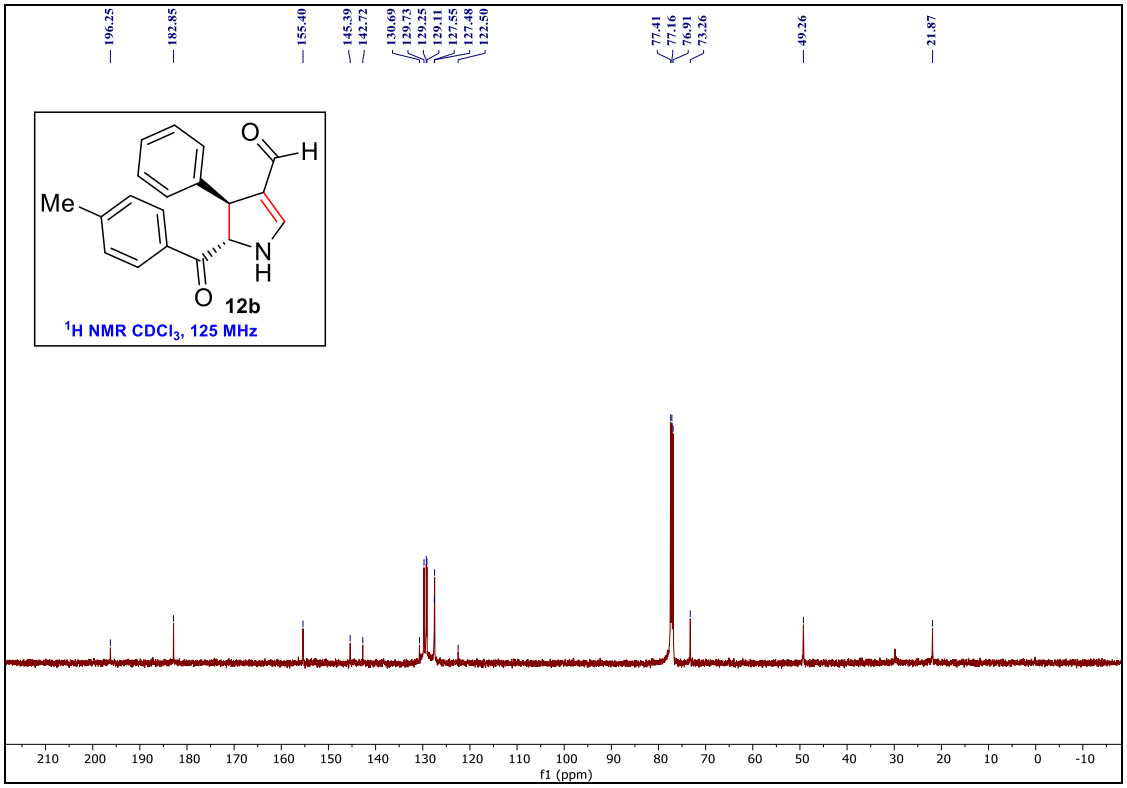

(4*S*,5*S*)-5-(4-Hydroxybenzoyl)-4-phenyl-4,5-dihydro-1*H*-pyrrole-3-carbaldehyde 12c

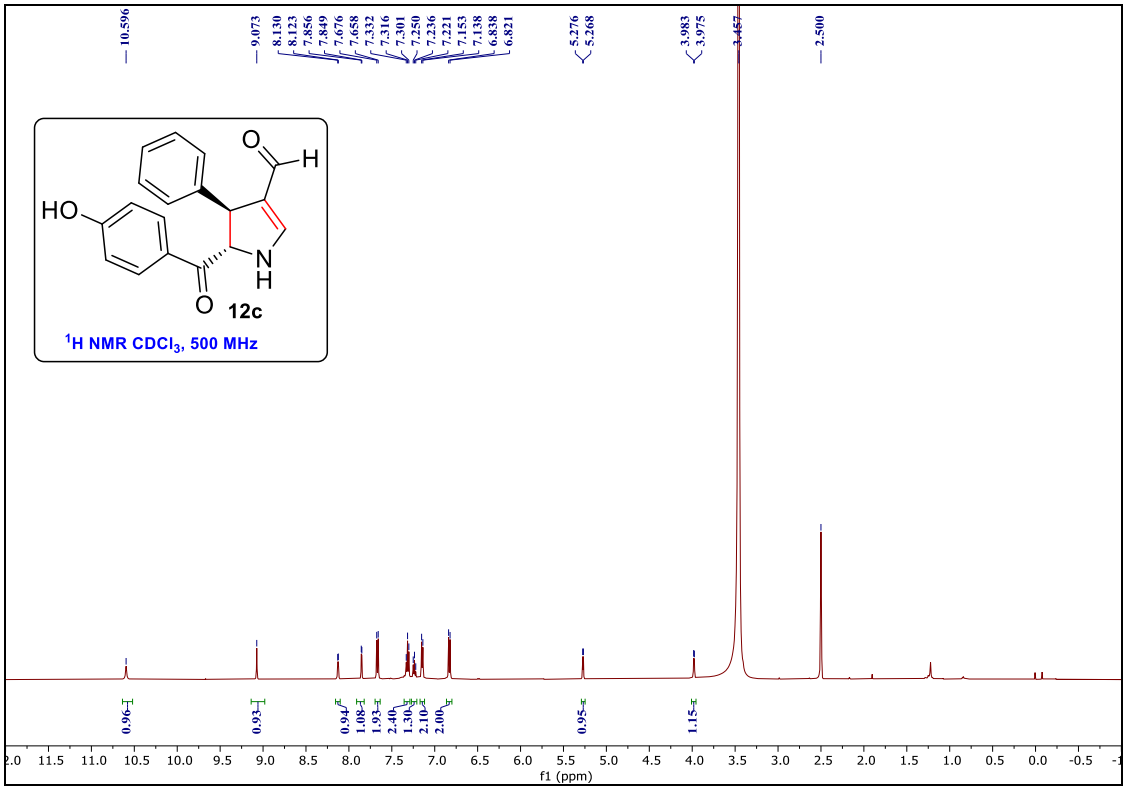

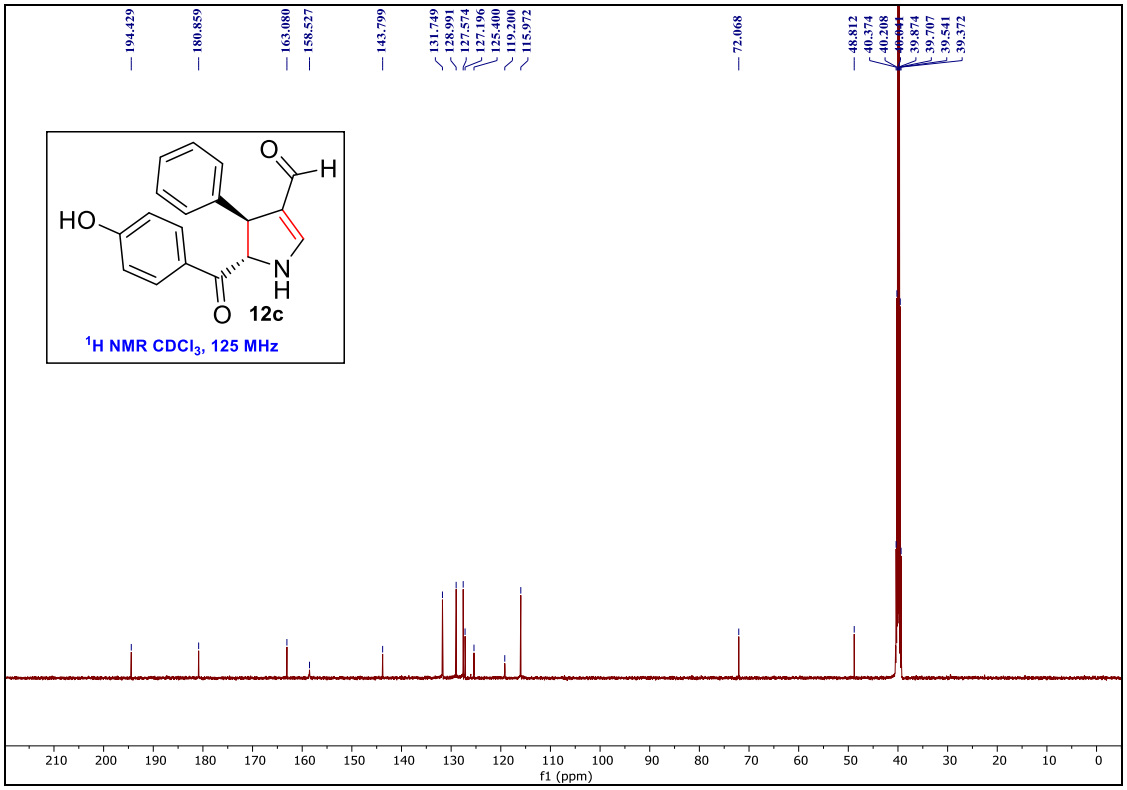

(4*S*,5*S*)-5-(2-Methoxybenzoyl)-4-phenyl-4,5-dihydro-1*H*-pyrrole-3-carbaldehyde 12d

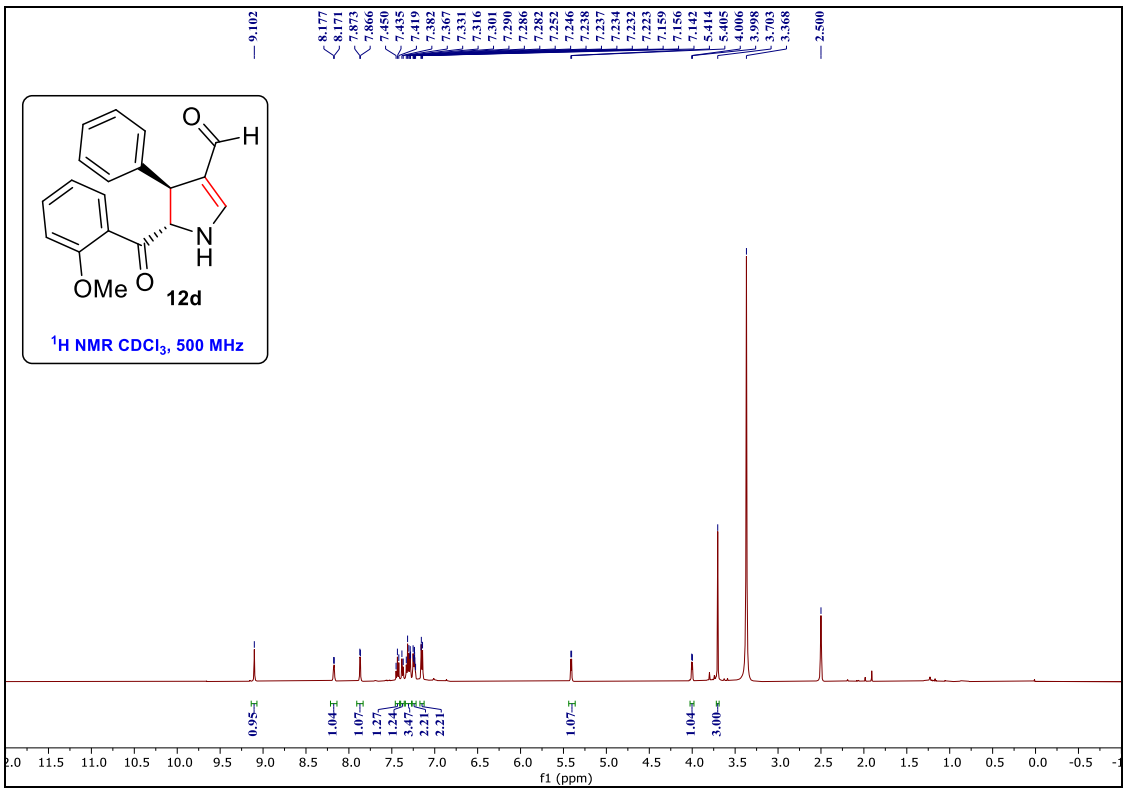

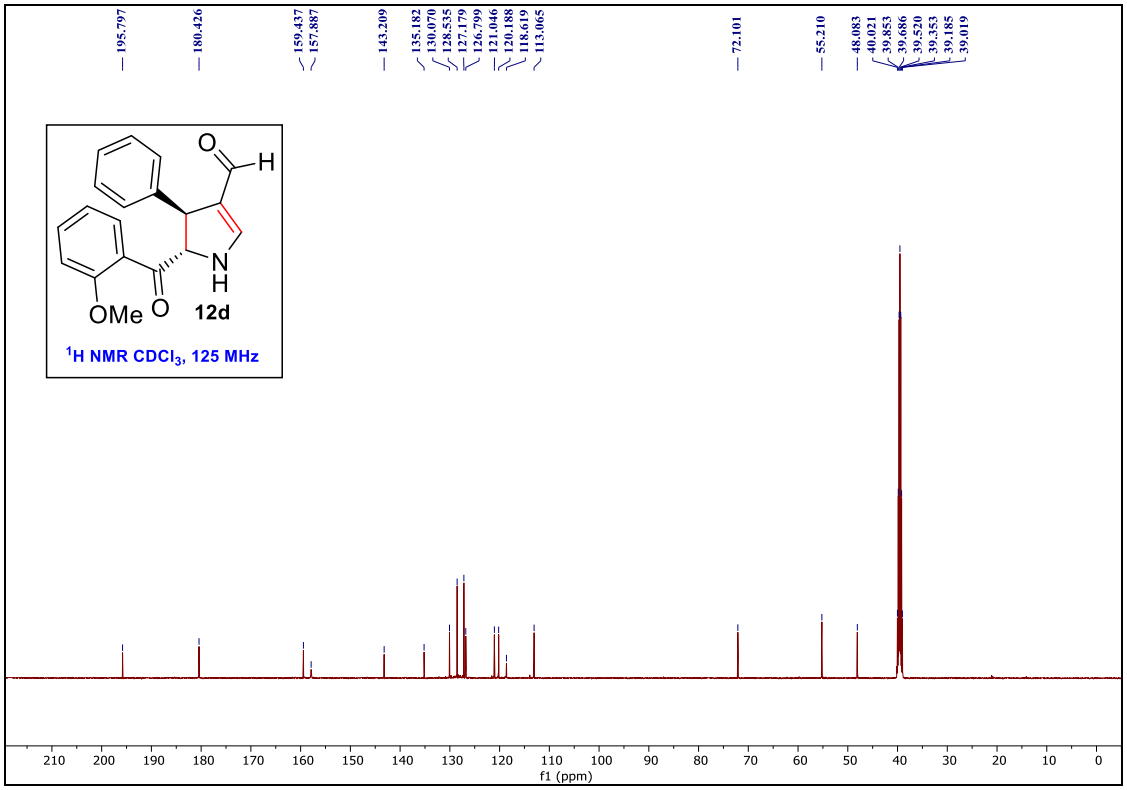

(4*S*,5*S*)-5-(4-Fluorobenzoyl)-4-phenyl-4,5-dihydro-1*H*-pyrrole-3-carbaldehyde 12e

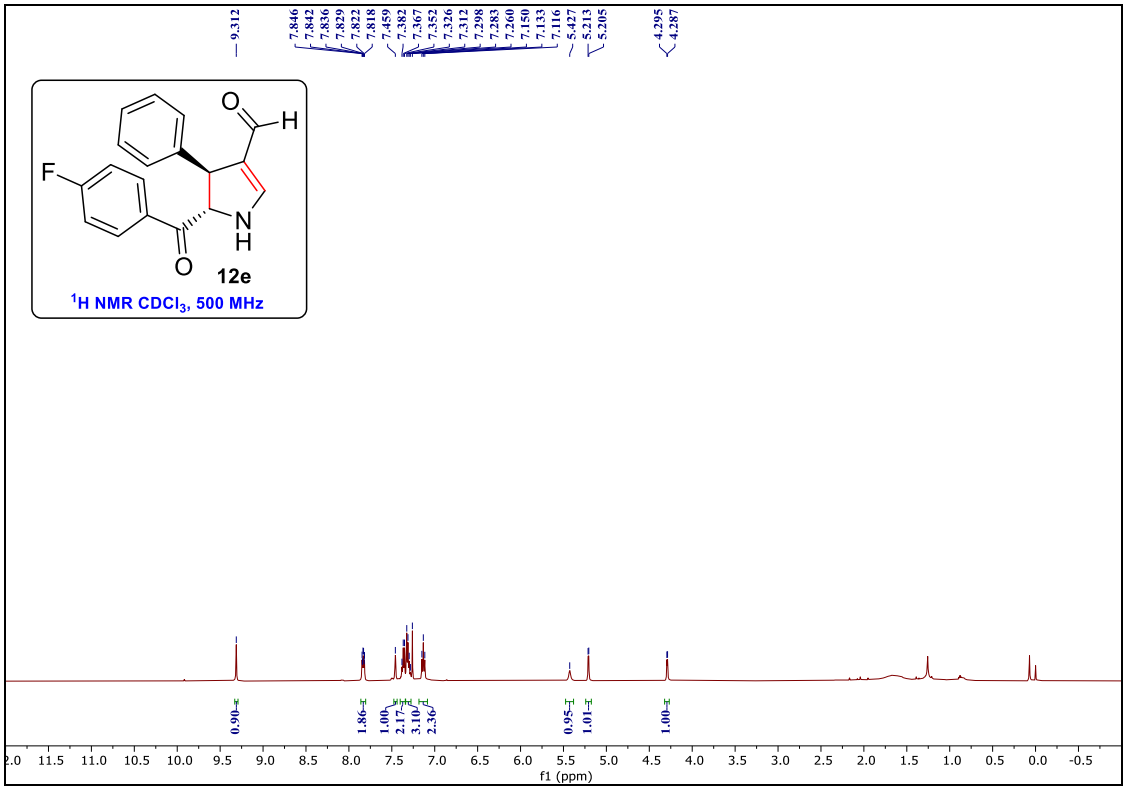

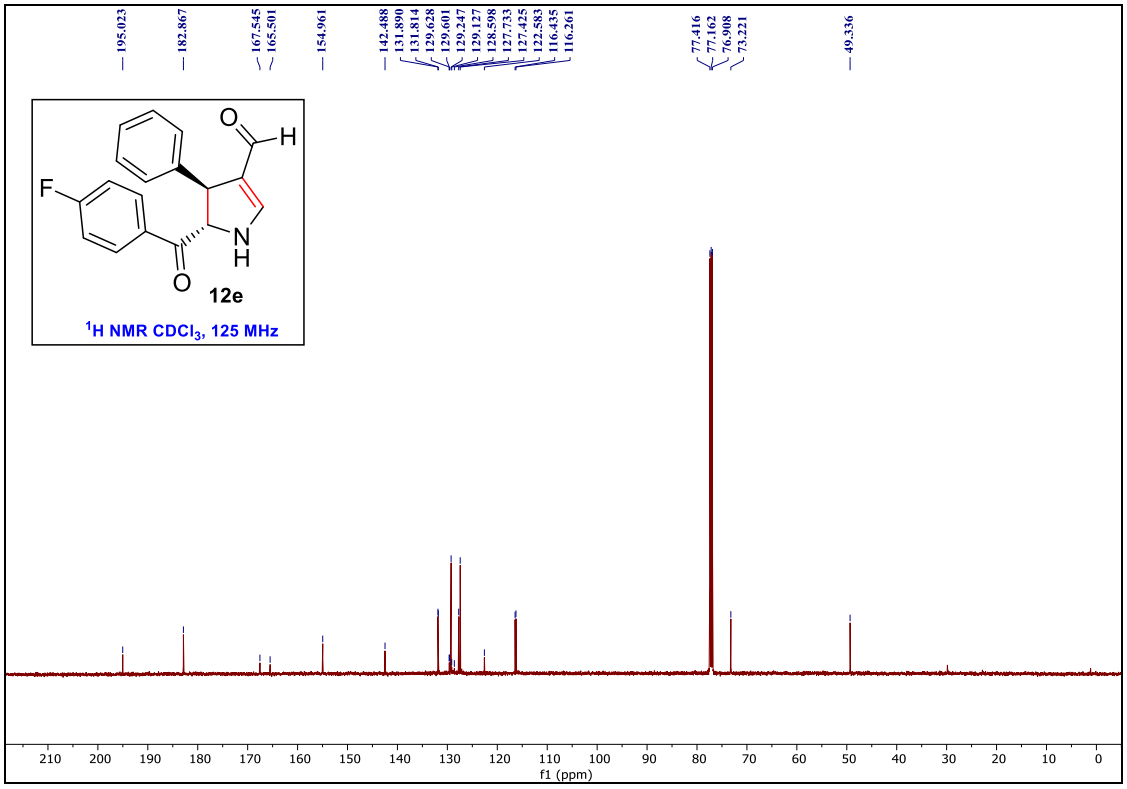

(4*S*,5*S*)-5-(4-Chlorobenzoyl)-4-phenyl-4,5-dihydro-1*H*-pyrrole-3-carbaldehyde 12f

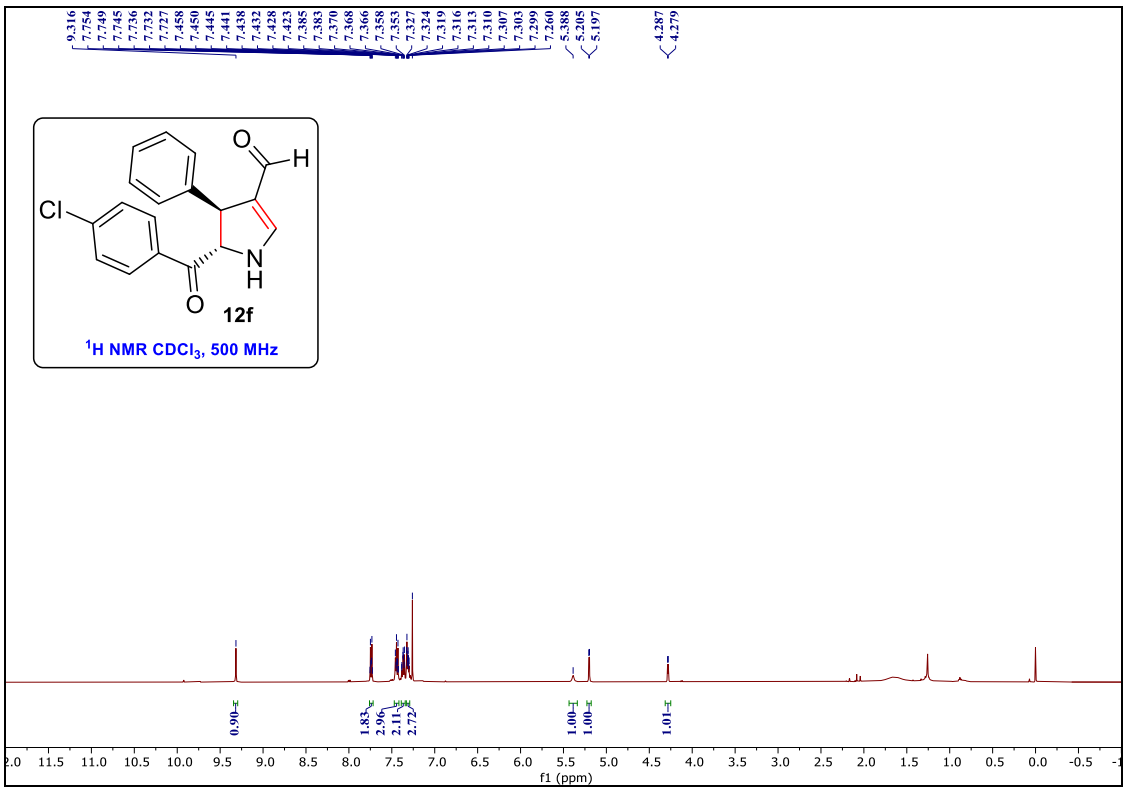

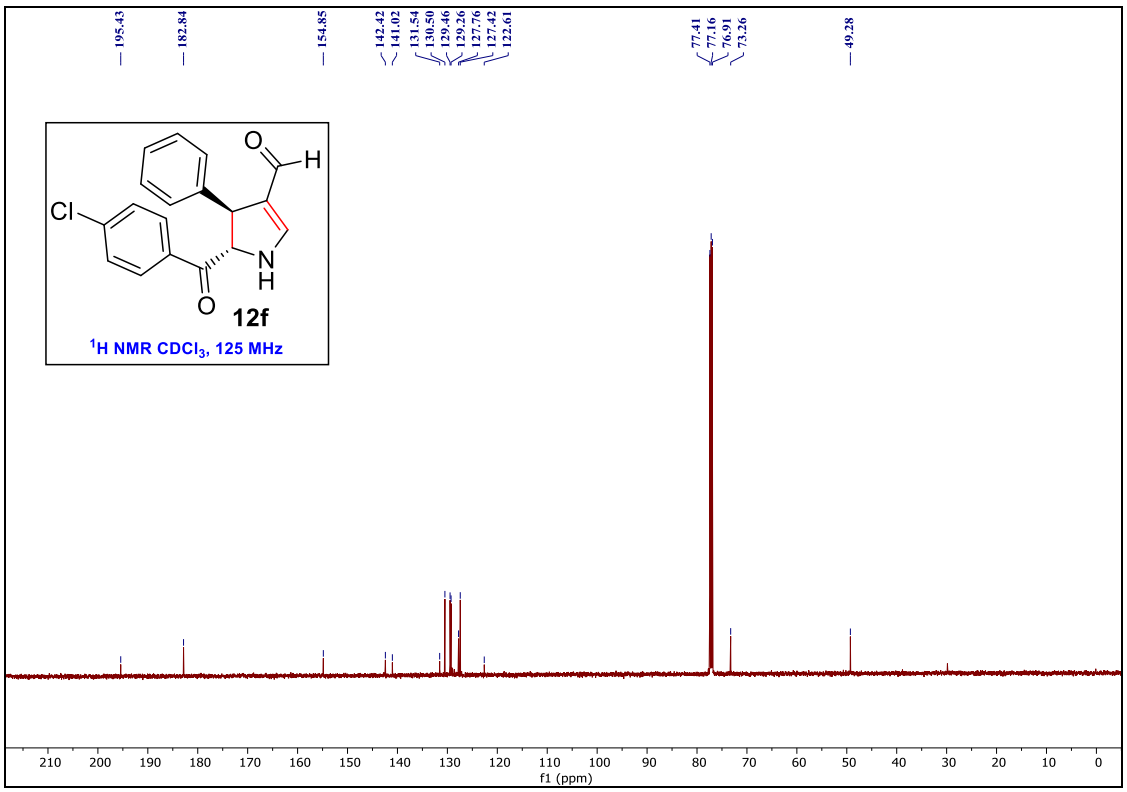

(4*S*,5*S*)-5-(4-bromobenzoyl)-4-phenyl-4,5-dihydro-1*H*-pyrrole-3-carbaldehyde 12g

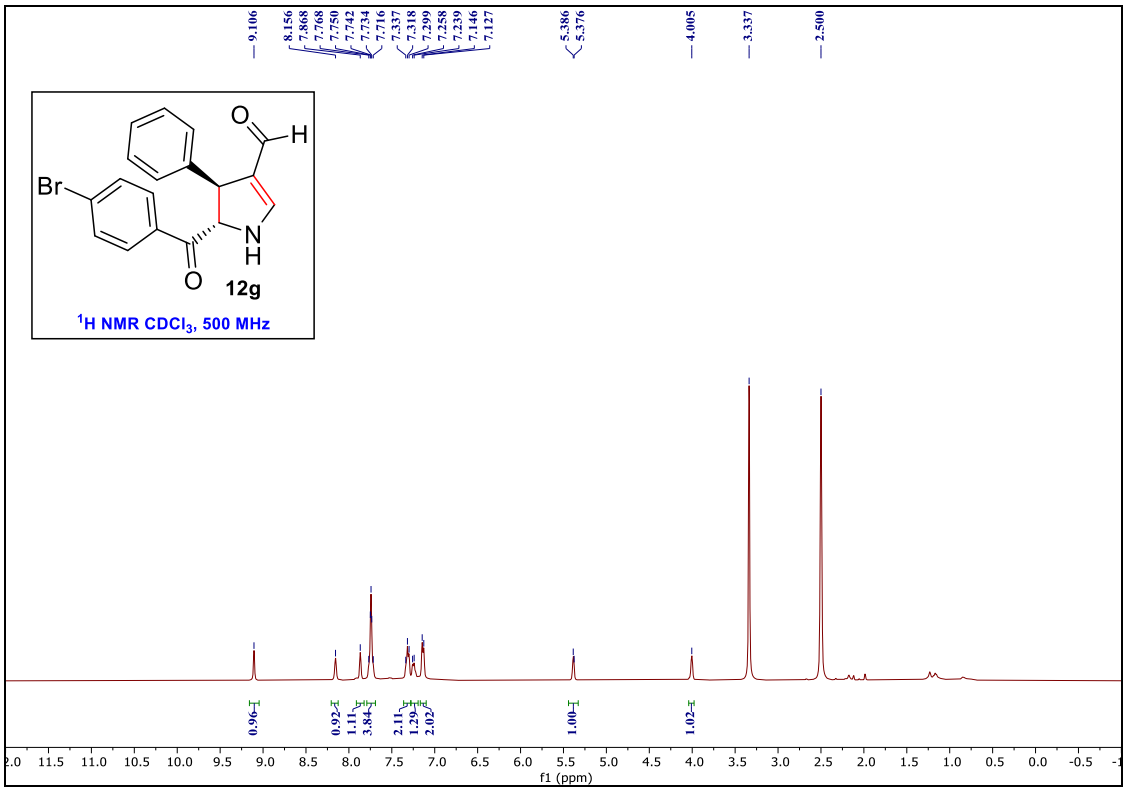

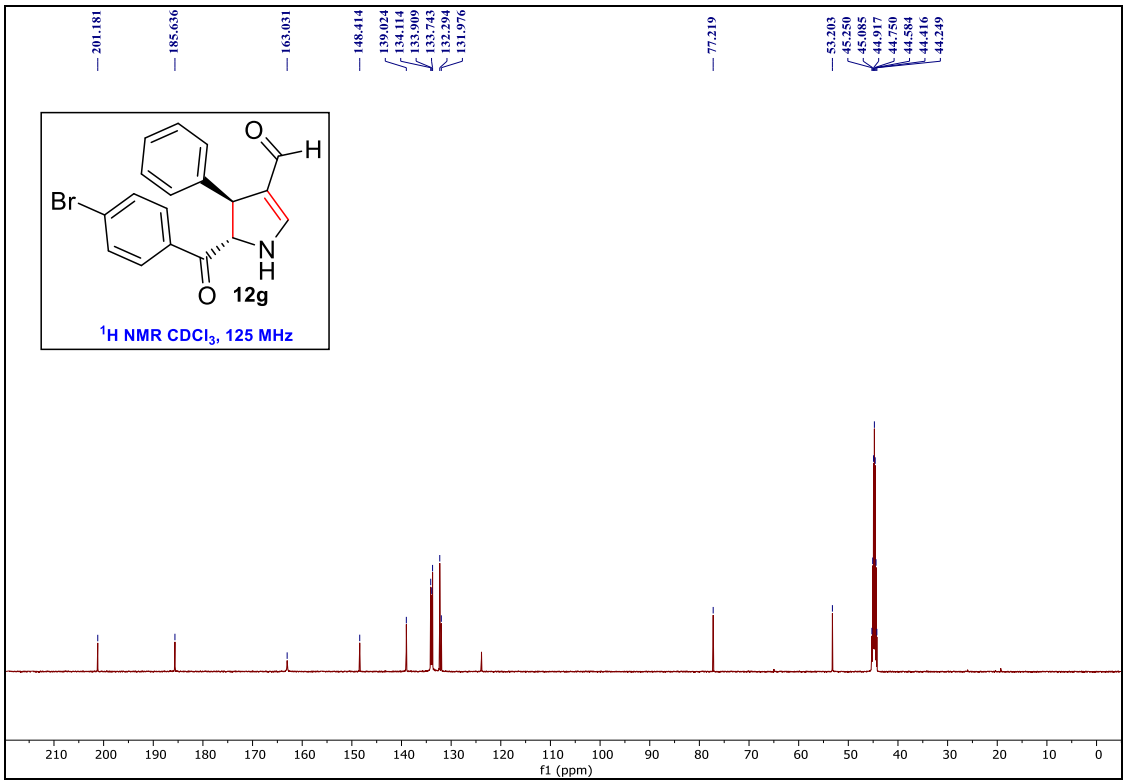

(4*S*,5*S*)-5-(4-chlorobenzoyl)-4-(furan-2-yl)-4,5-dihydro-1*H*-pyrrole-3-carbaldehyde 12h

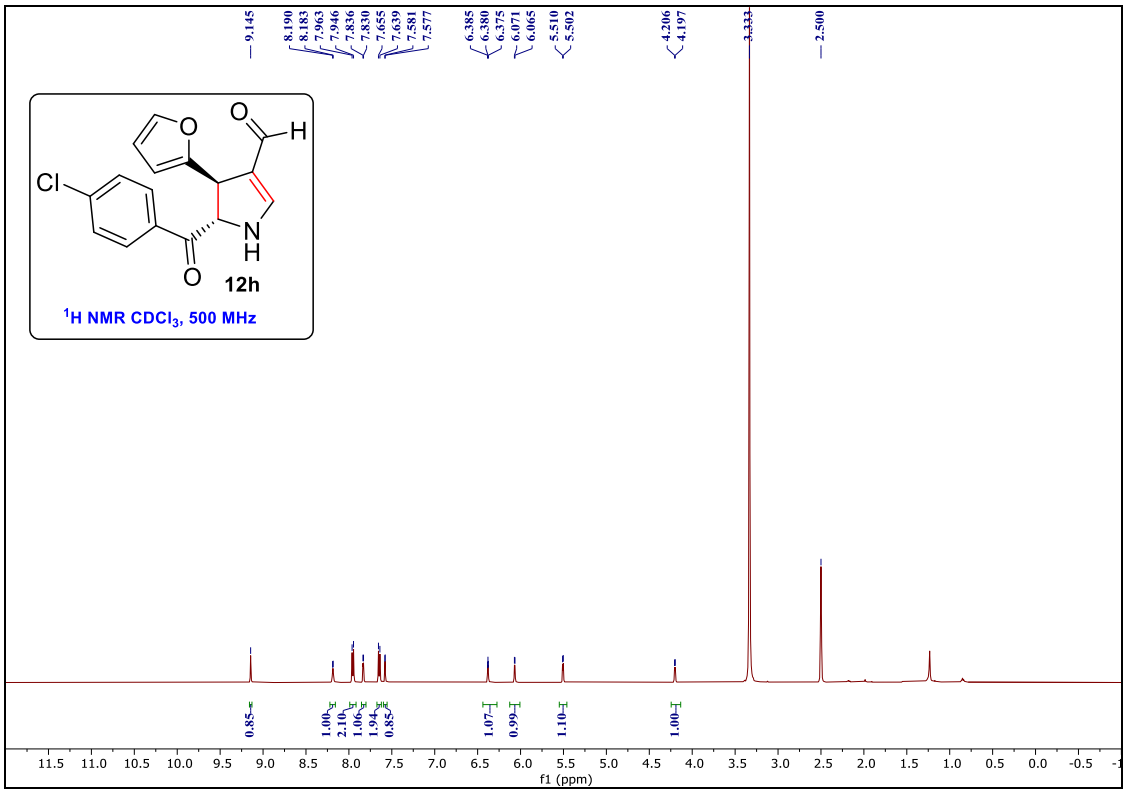

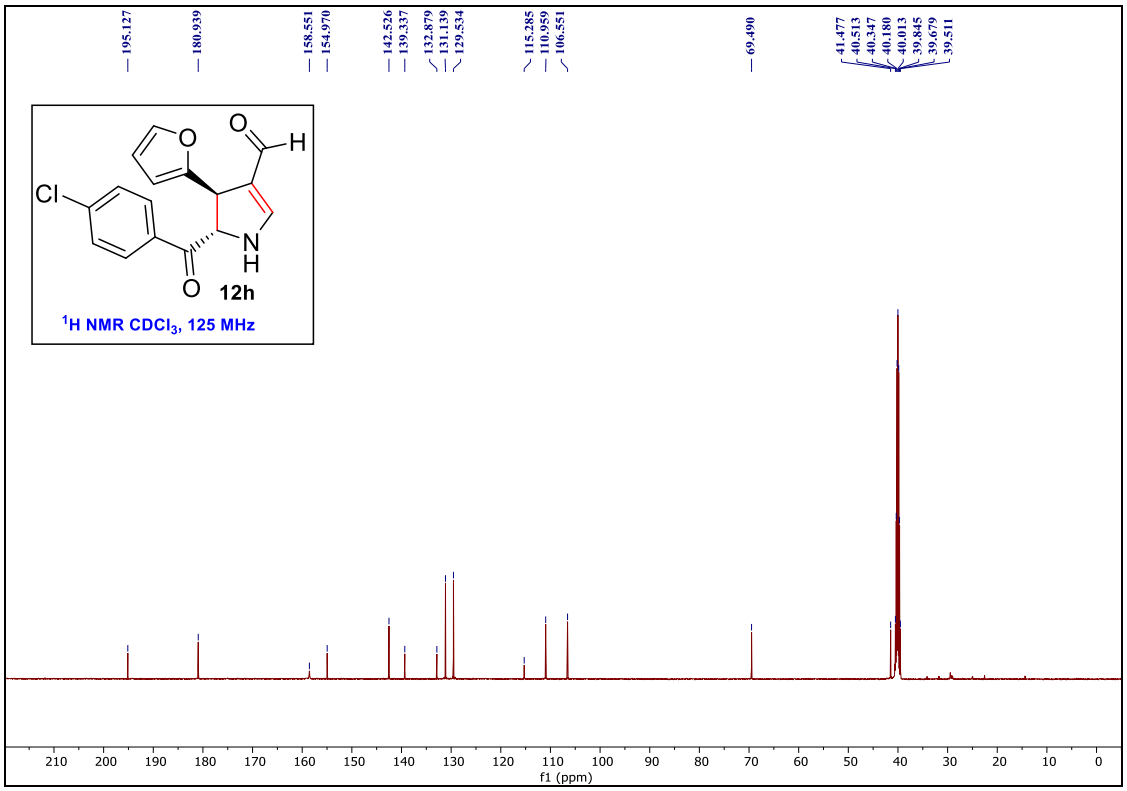

4.27 HPLC CHROMATOGRAMS

(±)-12a

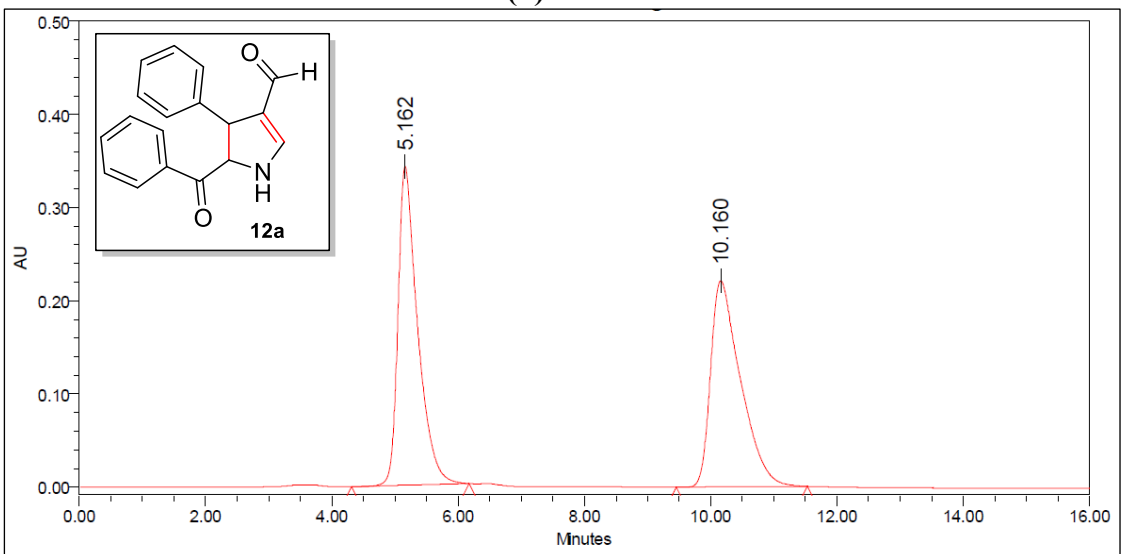

Peak Results

	Name	RT	Area	Height	% Area	% Height
1		5.162	7378055	342444	50.3258	60.7387
2		10.160	7282525	221355	49.6742	39.2613
Sum			14660580.0		100.0000	100.0000

Optical active 12a

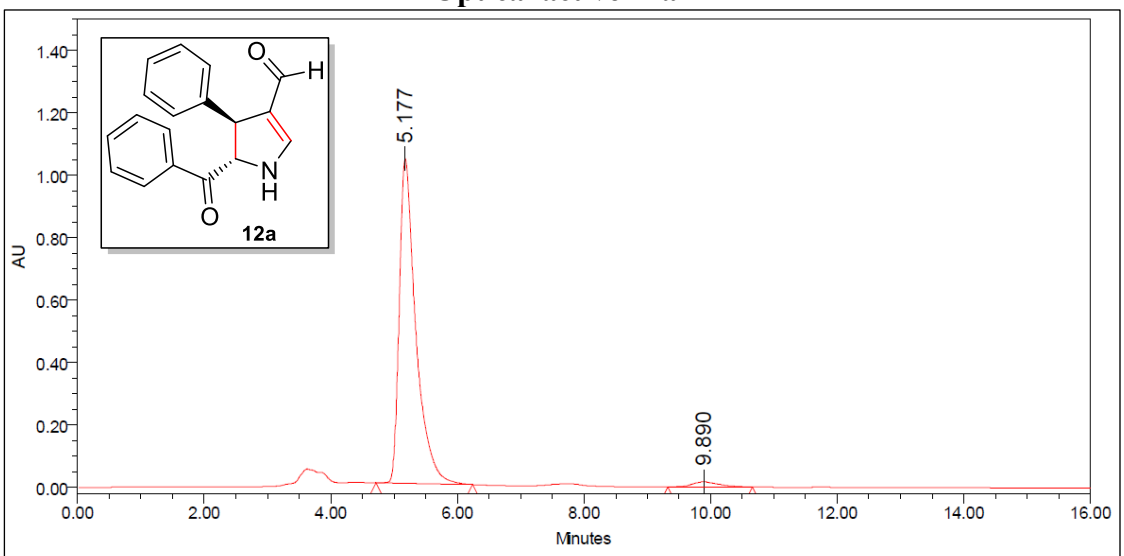

Peak Results

	Name	RT	Area	Height	% Area	% Height
1		5.177	18824400	1041320	97.5836	98.4659
2		9.890	466137	16223	2.4164	1.5341
Sum			19290537.8		100.0000	100.0000

(±)-12b

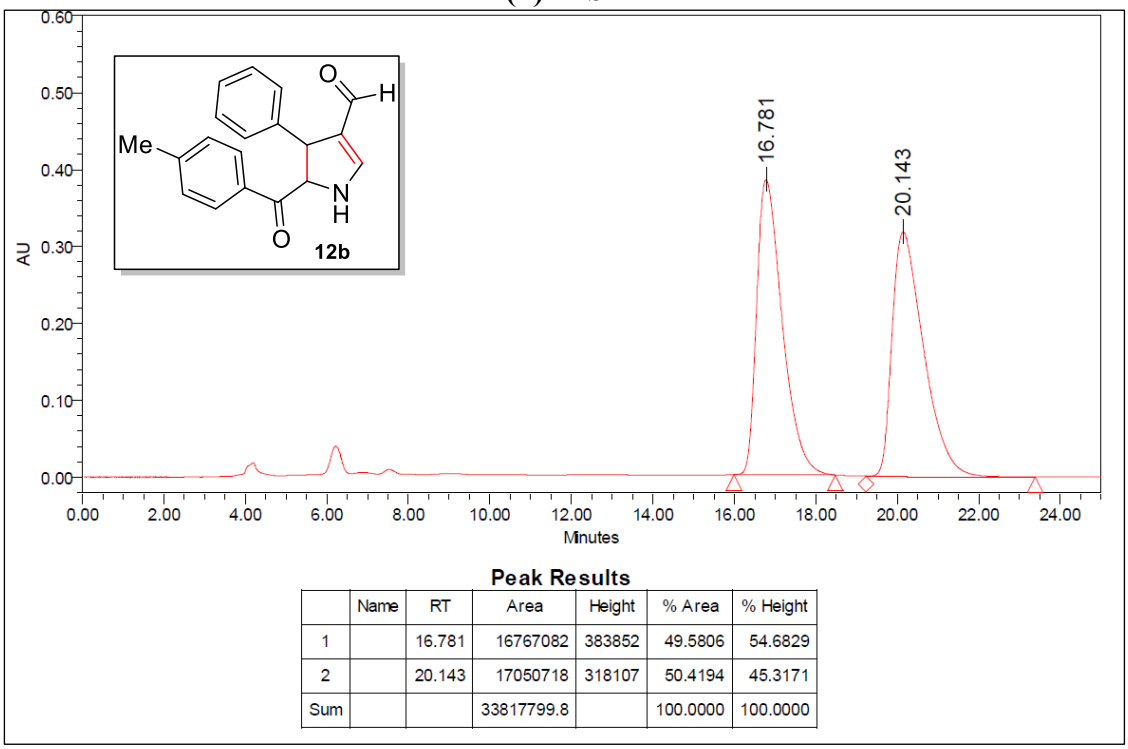

Peak Results

	Name	RT	Area	Height	% Area	% Height
1		16.781	16767082	383852	49.5806	54.6829
2		20.143	17050718	318107	50.4194	45.3171
Sum			33817799.8		100.0000	100.0000

Optical active 12b

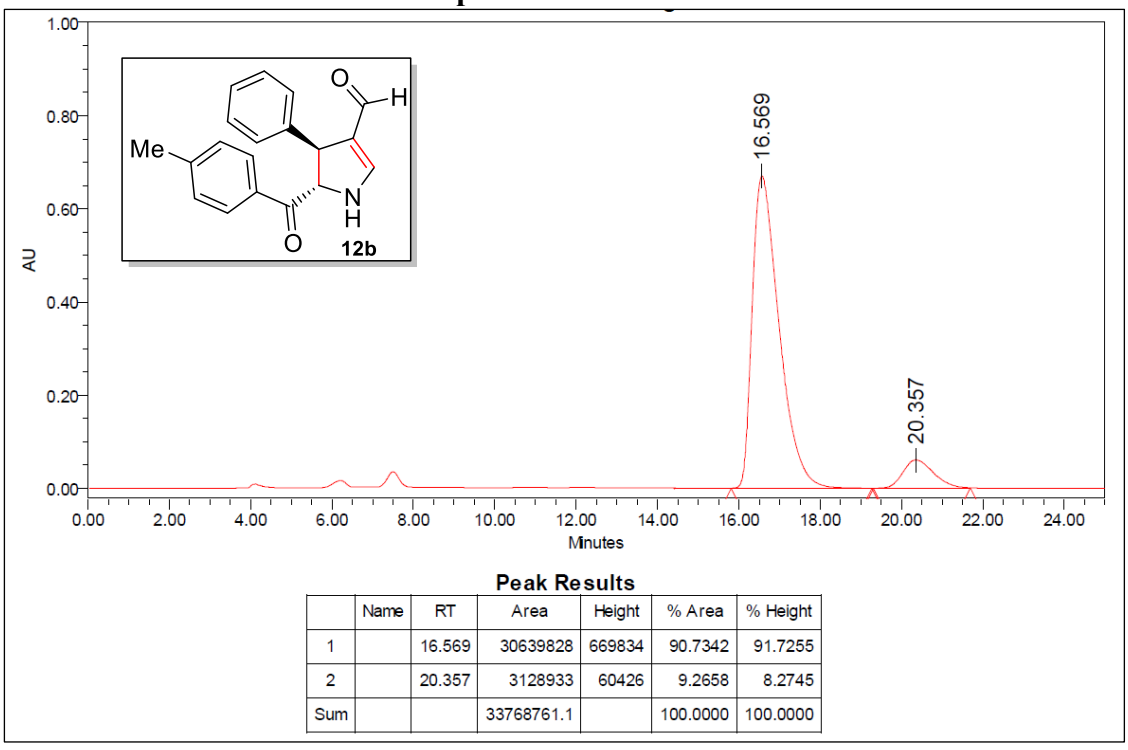

Peak Results

	Name	RT	Area	Height	% Area	% Height
1		16.569	30639828	669834	90.7342	91.7255
2		20.357	3128933	60426	9.2658	8.2745
Sum			33768761.1		100.0000	100.0000

(±)-12c

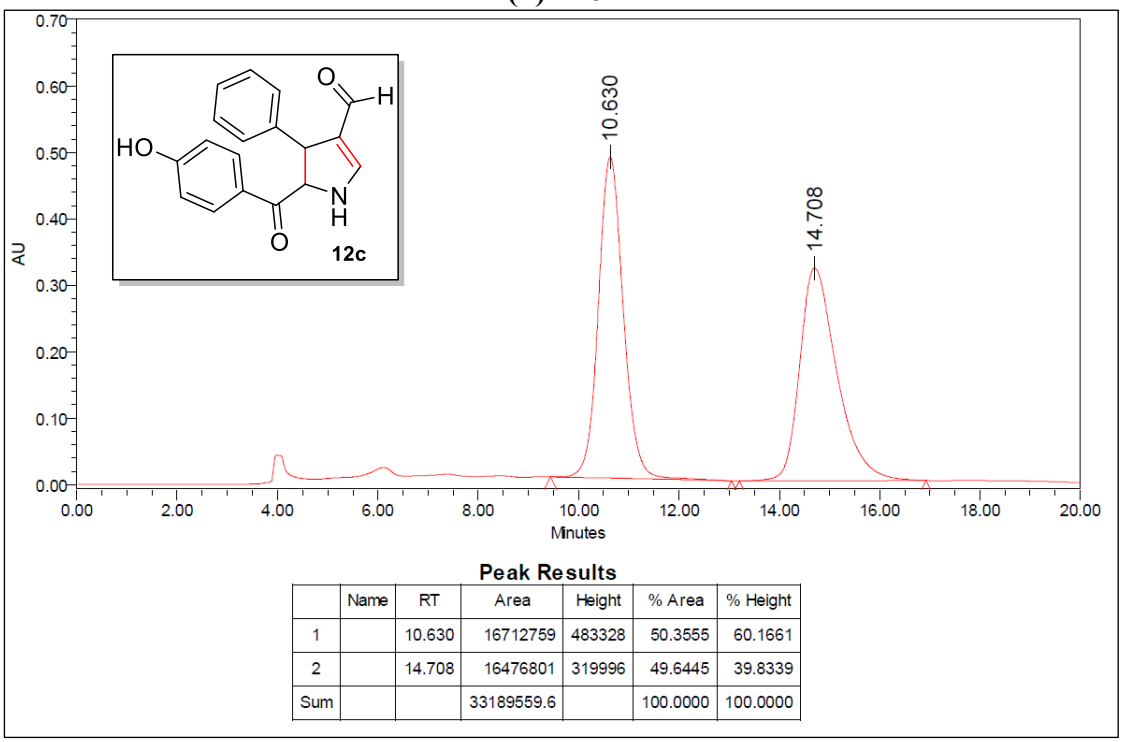

Peak Results

	Name	RT	Area	Height	% Area	% Height
1		10.630	16712759	483328	50.3555	60.1661
2		14.708	16476801	319996	49.6445	39.8339
Sum			33189559.6		100.0000	100.0000

Optical active 12c

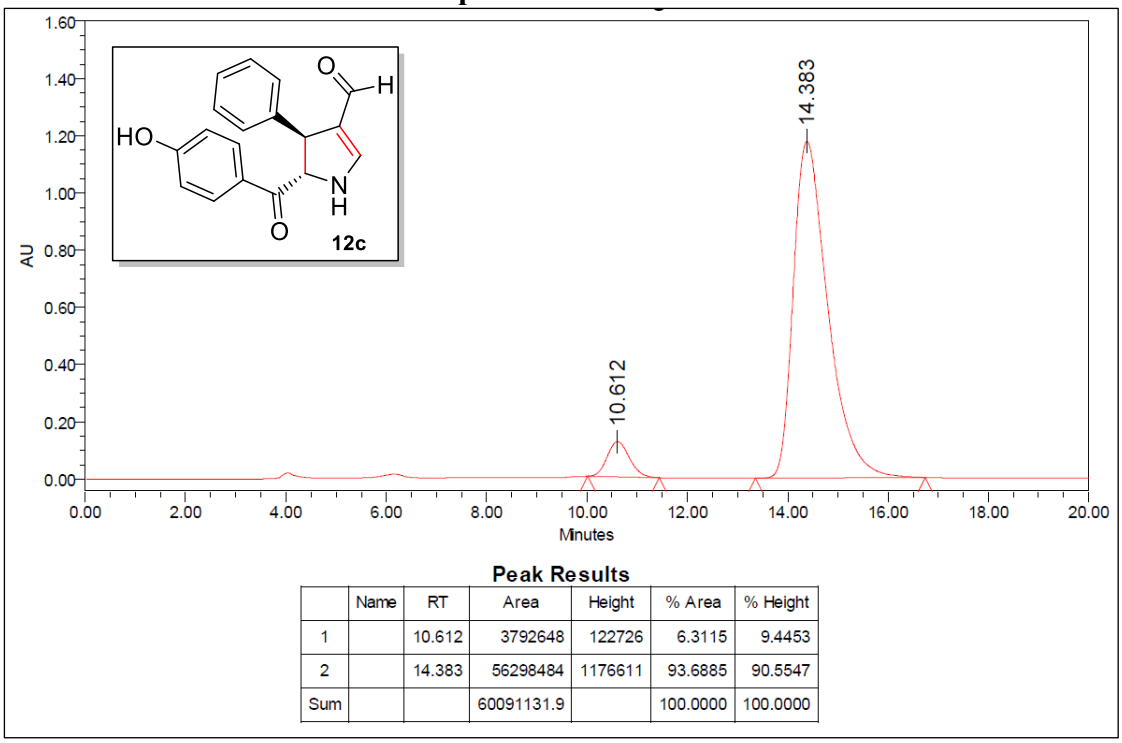

Peak Results

	Name	RT	Area	Height	% Area	% Height
1		10.612	3792648	122726	6.3115	9.4453
2		14.383	56298484	1176611	93.6885	90.5547
Sum			60091131.9		100.0000	100.0000

(±)-12c

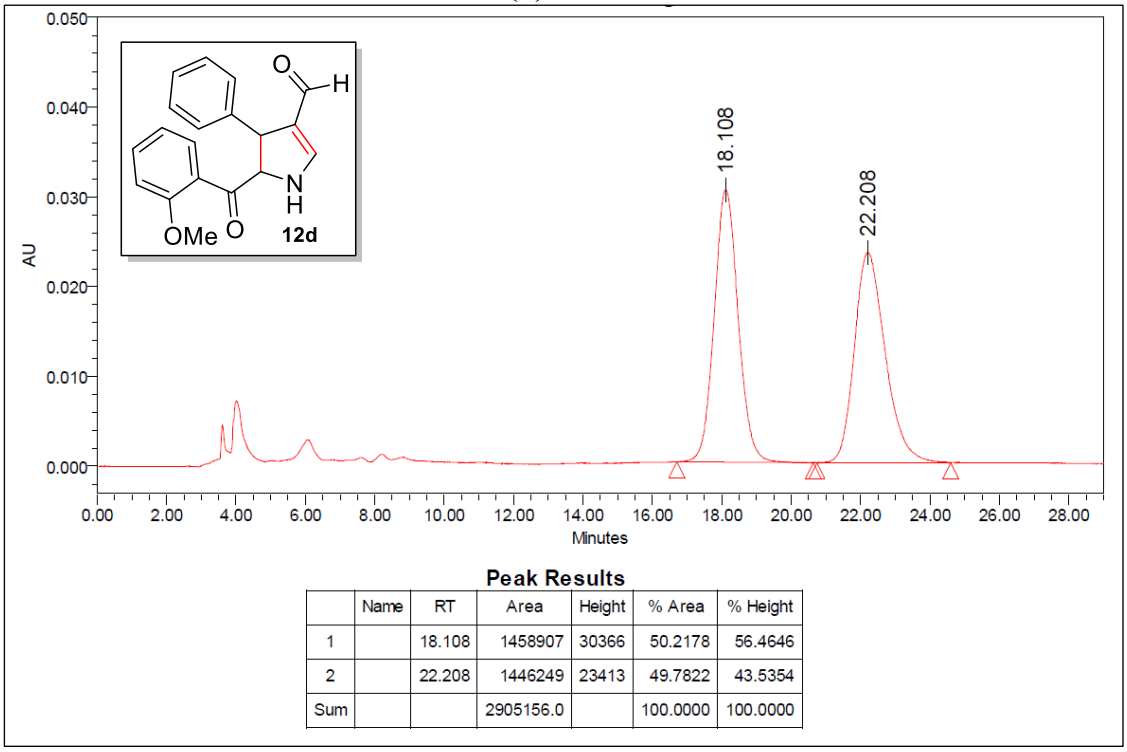

Peak Results

	Name	RT	Area	Height	% Area	% Height
1		18.108	1458907	30366	50.2178	56.4646
2		22.208	1446249	23413	49.7822	43.5354
Sum			2905156.0		100.0000	100.0000

Optical active 12d

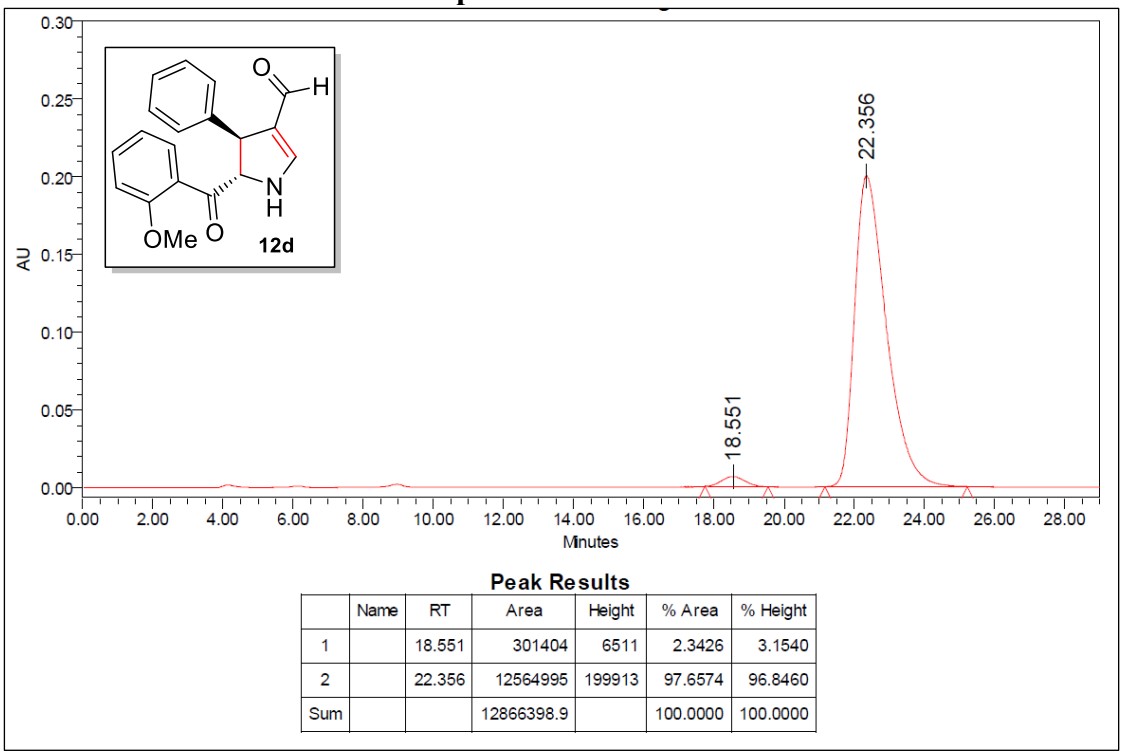

Peak Results

	Name	RT	Area	Height	% Area	% Height
1		18.551	301404	6511	2.3426	3.1540
2		22.356	12564995	199913	97.6574	96.8460
Sum			12866398.9		100.0000	100.0000

(±)-12e

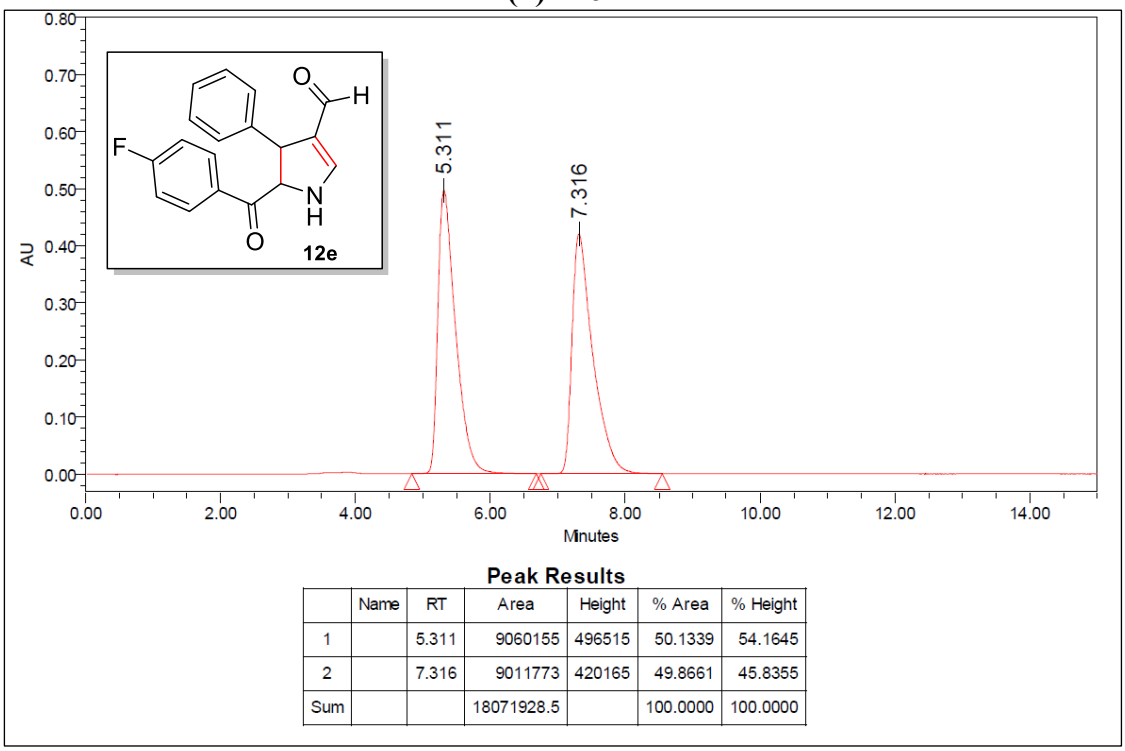

Peak Results

	Name	RT	Area	Height	% Area	% Height
1		5.311	9060155	496515	50.1339	54.1645
2		7.316	9011773	420165	49.8661	45.8355
Sum			18071928.5		100.0000	100.0000

Optical active 12e

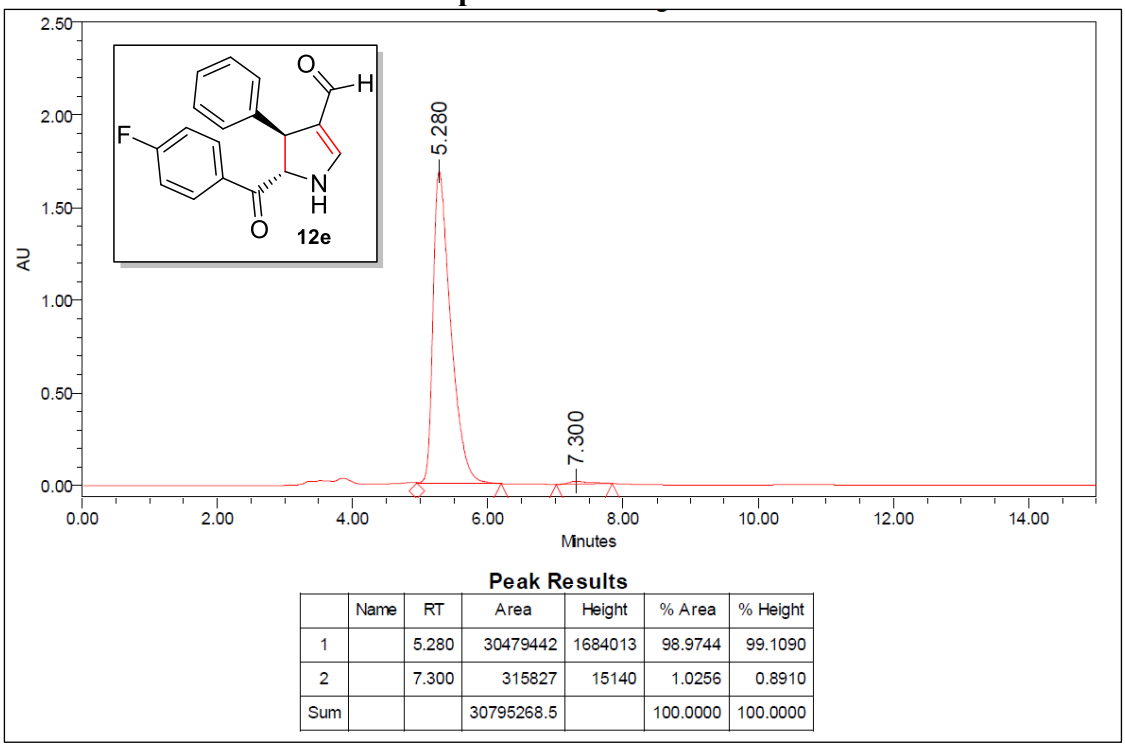

Peak Results

	Name	RT	Area	Height	% Area	% Height
1		5.280	30479442	1684013	98.9744	99.1090
2		7.300	315827	15140	1.0256	0.8910
Sum			30795268.5		100.0000	100.0000

(±)-12f

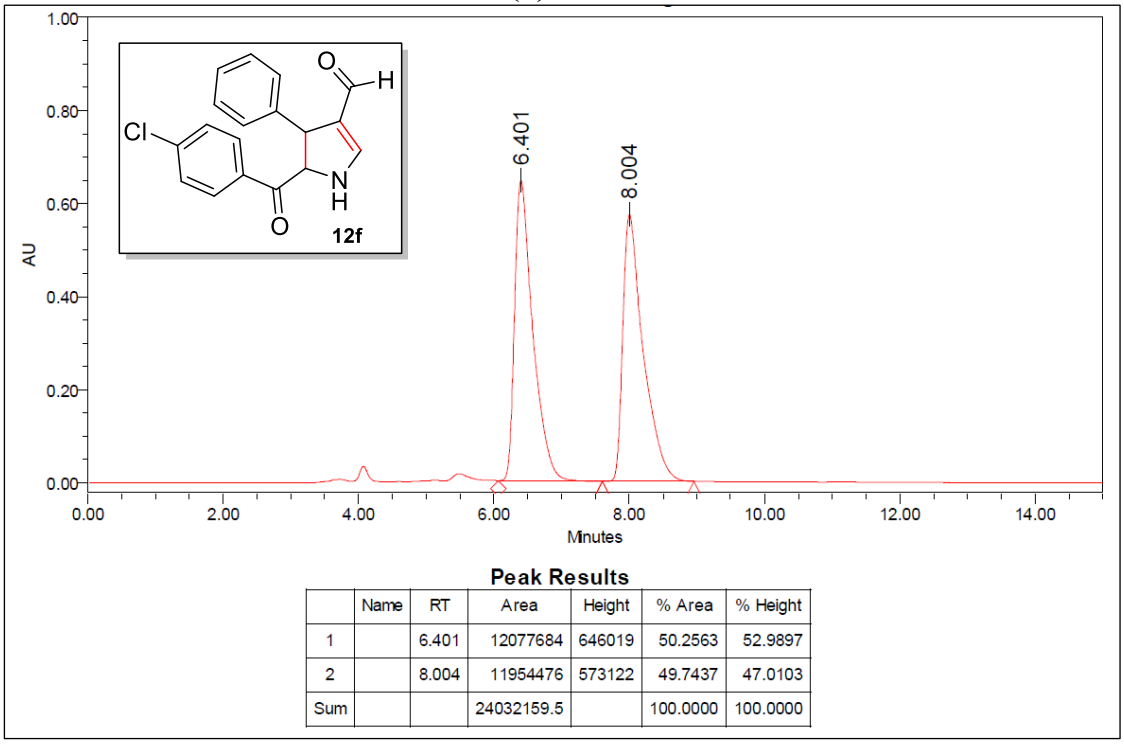

Peak Results

	Name	RT	Area	Height	% Area	% Height
1		6.401	12077684	646019	50.2563	52.9897
2		8.004	11954476	573122	49.7437	47.0103
Sum			24032159.5		100.0000	100.0000

Optical active 12f

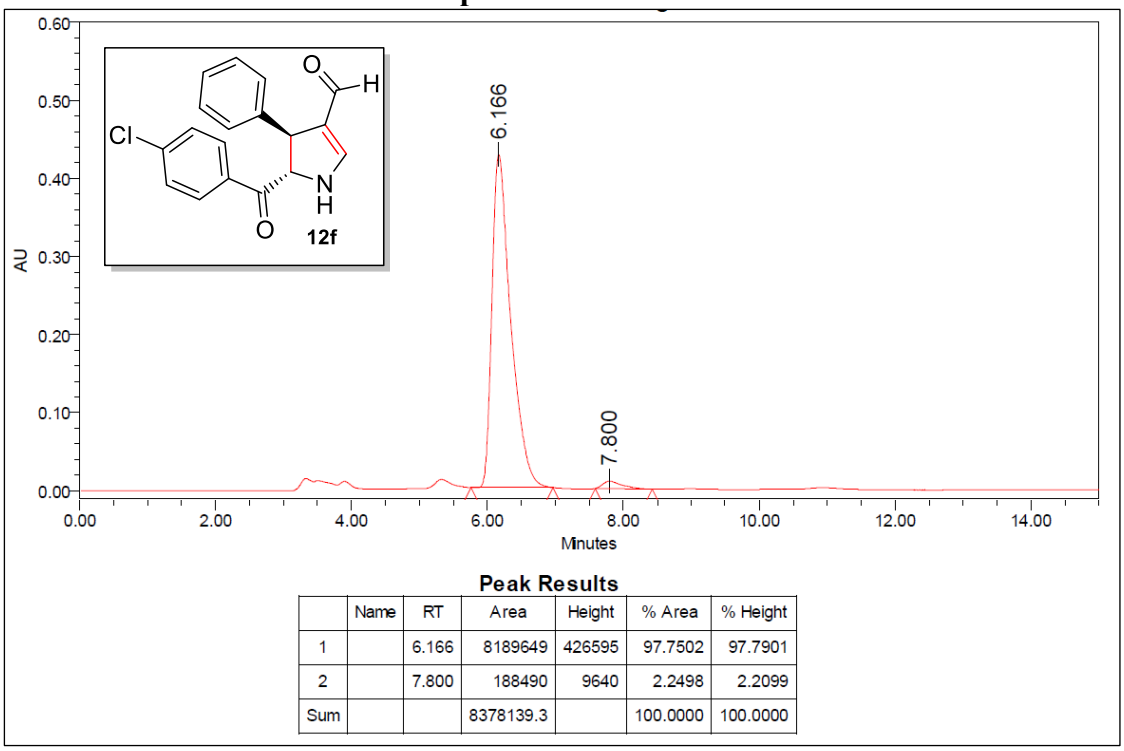

Peak Results

	Name	RT	Area	Height	% Area	% Height
1		6.166	8189649	426595	97.7502	97.7901
2		7.800	188490	9640	2.2498	2.2099
Sum			8378139.3		100.0000	100.0000

(±)-12g

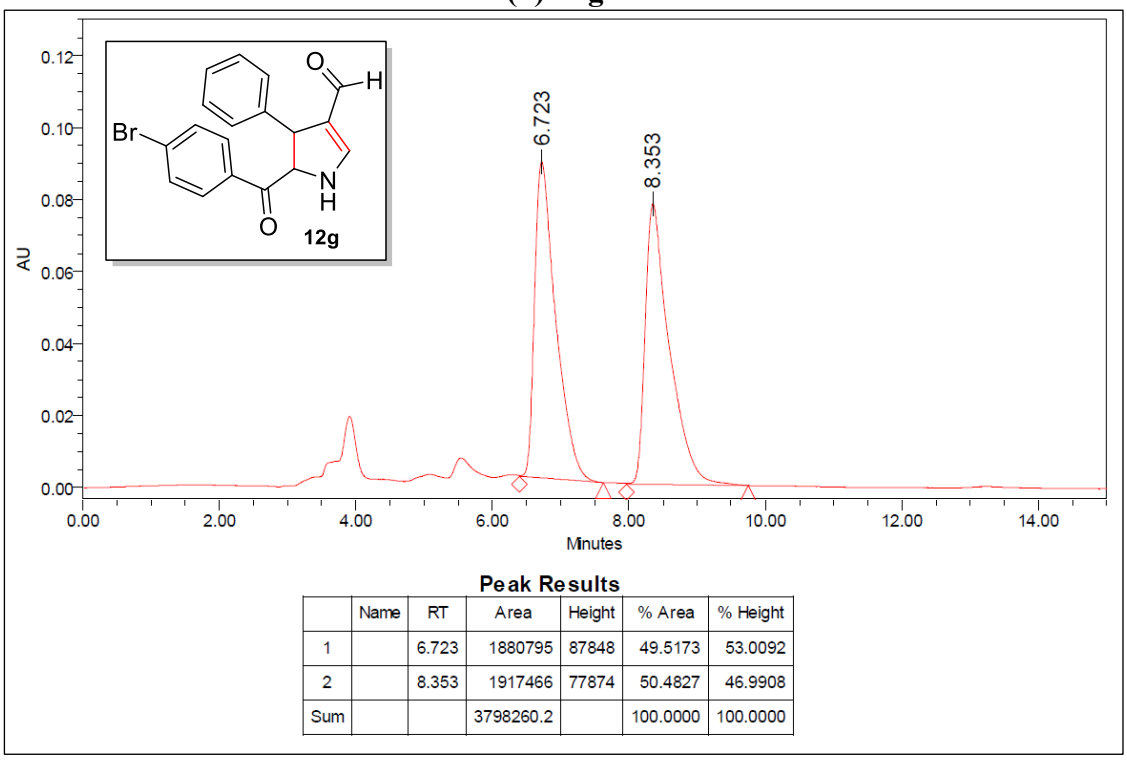

Peak Results

	Name	RT	Area	Height	% Area	% Height
1		6.723	1880795	87848	49.5173	53.0092
2		8.353	1917466	77874	50.4827	46.9908
Sum			3798260.2		100.0000	100.0000

Optical active 12g

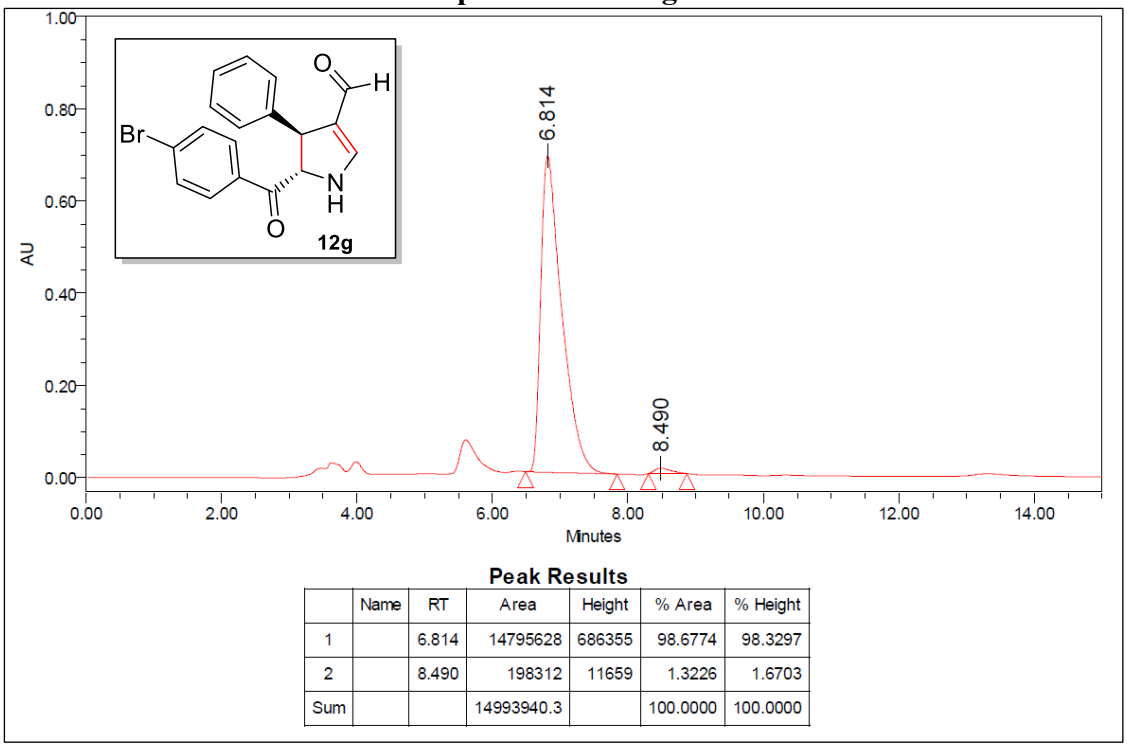

Peak Results

	Name	RT	Area	Height	% Area	% Height
1		6.814	14795628	686355	98.6774	98.3297
2		8.490	198312	11659	1.3226	1.6703
Sum			14993940.3		100.0000	100.0000

(±)-12h

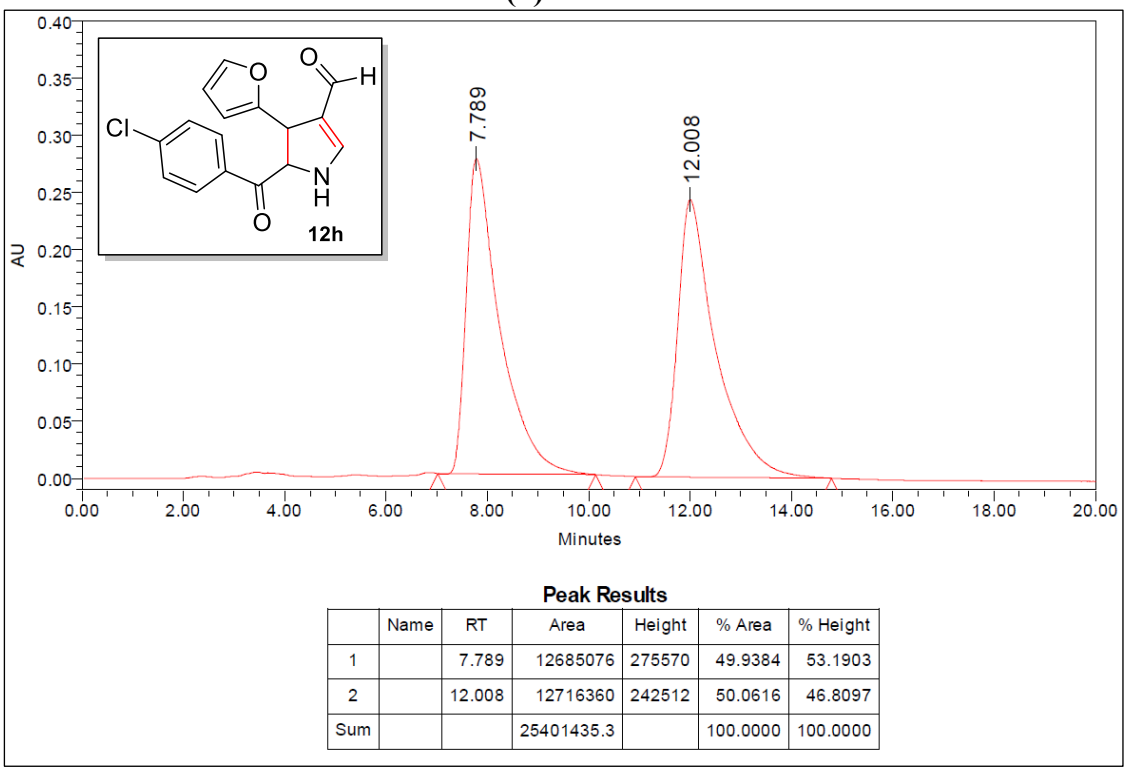

Peak Results

	Name	RT	Area	Height	% Area	% Height
1		7.789	12685076	275570	49.9384	53.1903
2		12.008	12716360	242512	50.0616	46.8097
Sum			25401435.3		100.0000	100.0000

Optical active 12h

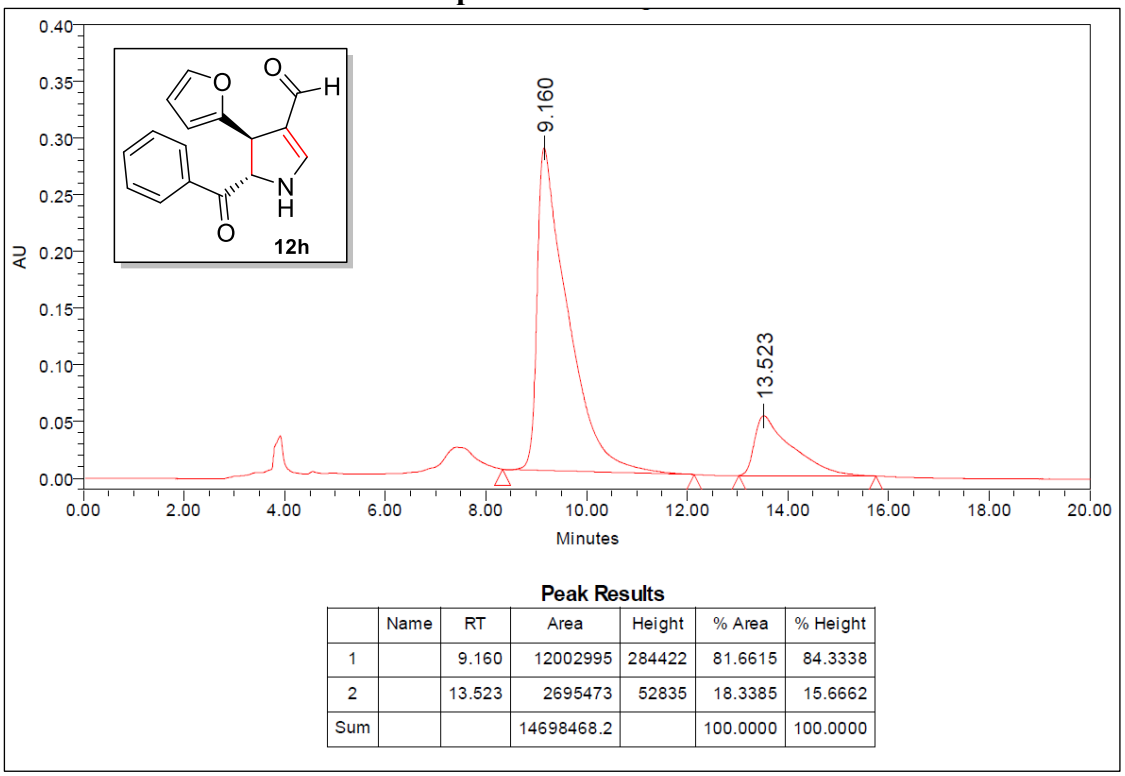

Peak Results

	Name	RT	Area	Height	% Area	% Height
1		9.160	12002995	284422	81.6615	84.3338
2		13.523	2695473	52835	18.3385	15.6662
Sum			14698468.2		100.0000	100.0000

CHAPTER 5

SUMMARY AND CONCLUSION

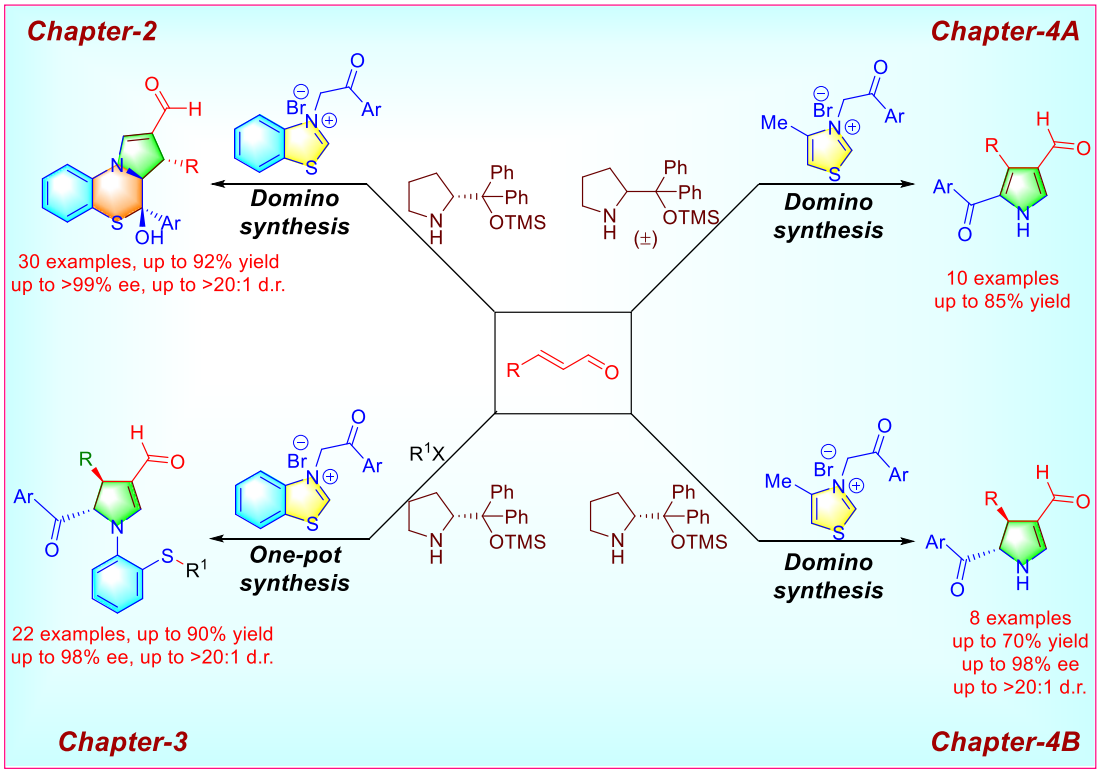

5.1 SUMMARY

This thesis has been divided into four Chapters based on the development of organocatalytic asymmetric methodologies that led to the synthesis of diverse chiral *N*, *S*- containing heterocycles using thiazolium and benzothiazolium azomethine ylides and α,β-unsaturated aldehydes *via* 1,3-dipolar cycloaddition/rearrangement/ring-opening/ring-cleavage reaction sequences. Chapter 1 is the introduction Chapter, which is further divided into two parts. The first part briefly introduces asymmetric synthesis, organocatalysts, proline chiral catalyst modification, and its applications. The second part briefly discusses ylides, azomethine ylides, classifications, and their application in asymmetric 1,3-dipolar cycloadditions. Chapters 2 and 3 discuss the development of chiral domino and one-pot methodologies for the synthesis of pyrrolo-thiazine-2-carbaldehydes and *N*-phenyl thioether-tethered tetrasubstituted dihydropyrrole-3-carbaldehydes by the using (*R*)-diphenylprolinol trimethyl silyl ether as an asymmetric organocatalysts. Chapter 4 is divided into two parts; Chapter 4A deals with the development of achiral domino methodology using racemic diphenylprolinol trimethyl silyl ether as a catalyst for the synthesis of novel trisubstituted 1*H*-pyrrole-3-carbaldehydes. Chapter 4B deals with the extension chiral version of Chapter 4A. It deals with developing a chiral domino methodology for synthesizing trisubstituted chiral 4,5-dihydro-1*H*-pyrrole-3-carbaldehydes using (*R*)-diphenylprolinol trimethyl silyl ether.

5.1.1 Organocatalyzed Enantio- and Diastereoselective Synthesis of Pyrrolo-thiazine-2-carbaldehydes via Formal Domino 1,3-Dipolar Cycloaddition/Rearrangement

The pyrrolo-thiazines are biologically active heterocyclic compounds due to their significance in pharmaceutical, medicinal, and biological compounds. Considering the

various utilities of these pyrrolro-thiazine derivatives, numerous efforts have been made to synthesize these moieties. The conventional methods for synthesizing these compounds in the racemic form are base-mediated and metal-catalyzed reactions. Using expensive metal precursors and isolating trace metal impurities in the final product is very difficult. To overcome these difficulties, methods for the synthesis of pyrrolo-thiazine compounds will need to be developed. Hence, a new protocol was developed for the synthesis of racemic and achiral pyrrolo-thiazine compounds directly *via* base-promoted 1,3-dipolar cycloaddition with thiazolium and benzothiazolium azomethine ylides with alkenes and alkynes.

The second Chapter of the thesis deals with the synthesis of enantioenriched pyrrolo-thiazines-2-carbaldehydes and its derivatives using commercially available α,β-unsaturated aldehydes, and easily synthesizable benzothiazolium salts utilizing environmentally friendly chiral amino organocatalysts. Initially, the optimization of reaction conditions with different parameters such as various chiral ligands, bases, solvents, and additives produced a maximum of >99% ee, and up to >20:1 d.r. with good yield. The optimized reaction condition was applied to a wide range of benzothiazolium salts and α,β-unsaturated aldehydes containing electron-donating, electron-withdrawing, bulky aryl, and heterocyclic groups tolerated under the optimized reaction conditions to achieve the excellent yield and enantio- and diastereoselectivity (Scheme 5.1). A DFT study was performed to understand the reaction mechanism. The molecular docking and fluorescent studies were performed to show the synthetic application of synthesized chiral products.

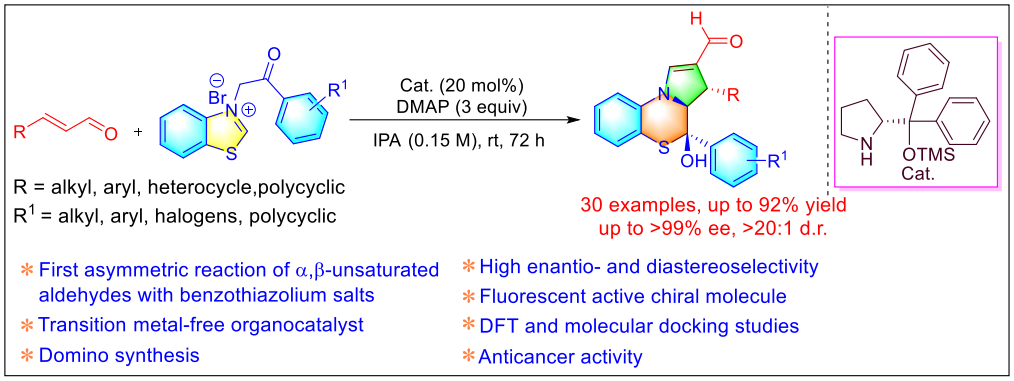

Scheme 5.1 Asymmetric domino synthesis of pyrrolo-thiazine-2-carbaldehydes

5.1.2 One-pot Enantioselective Synthesis of *N*-Phenyl Thioether-tethered Tetrasubstituted 4,5-Dihydropyrrole-3-carbaldehydes

Polysubstituted dihydropyrrole moiety is a central structural motif in various heterocyclic compounds that exhibit pharmacological and biological activities such as anti-cancer, anti-viral, and anti-microbial agents. The dihydropyrrole framework has been discovered to be abundant in natural products and synthetically bioactive compounds. Several approaches have been explored in the literature for synthesizing poly-substituted dihydropyrroles, including dipolar cycloaddition, metal-mediated cyclization, ring-opening, multicomponent, and cascade reactions. While significant efforts have been directed toward the synthesis of 2,3- and 2,5-dihydropyrroles, the synthesis of 4,5-dihydropyrroles remains an attempt. Thus, developing an efficient method for synthesizing highly substituted chiral dihydropyrroles from readily available starting materials is highly warranted.

Chapter 3 discloses an efficient enantioselective one-pot method for the synthesis of *N*-phenyl thioether-tethered tetrasubstituted 4,5-dihydropyrrole-3-carbaldehydes *via* 1,3-dipolar cycloaddition of benzothiazolium salts and α,β-unsaturated aldehydes utilizing an (*R*)-diphenylprolinol trimethyl silyl ether as a catalyst. Optimization of reaction conditions with different parameters like various chiral ligands, bases, solvents, and

additives to produce the maximum >96% ee with up to >20:1 d.r. in good yields. The optimized reaction condition was applied to a wide range of benzothiazolium salts and α,β-unsaturated aldehydes, like alkyl and aryl halides containing electron-donating, electron-withdrawing, bulky aryl, alkyl, and heterocyclic groups. All the reactions were well tolerated to produce a wide range of chiral tetrasubstituted 4,5-dihydropyrrole-3-carbaldehydes (Scheme 5.2).

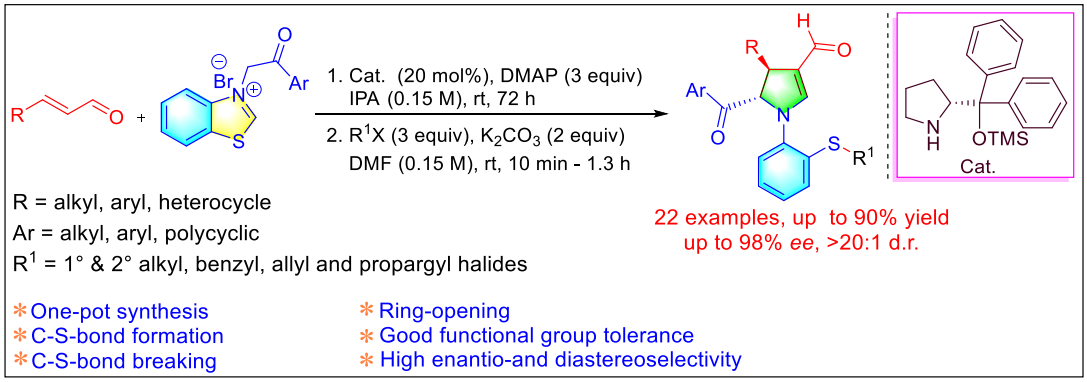

Scheme 5.2 Asymmetric one-pot synthesis of N-phenyl thioether-tethered tetrasubstituted 4,5-dihydropyrrole-3-carbaldehydes

5.1.3 Formal Domino 1,3-Dipolar Cycloaddition/C-S and C-N Bond Cleavage Reaction: Synthesis of Trisubstituted 1*H*-pyrrole-3-carbaldehydes

Polysubstituted 1*H*-pyrroles have been found in various pharmaceutical chemicals, biologically active molecules, and natural products. For the synthesis of polysubstituted pyrroles, enormous work has been done such as multi-component, metal-mediated cyclization, dipolar cycloaddition, ring-opening, nucleophile and electrophilic substitution of simple pyrrole, and cascade reactions. Among them, the dipolar cycloaddition of various azomethine ylides with alkyne has been well explored. However, using thiazolium azomethine ylide to synthesize polysubstituted pyrroles using α,β-unsaturated aldehydes utilizing the organocatalysts is yet to be developed. Chapter 4A deals with the development of a catalytic domino approach to producing trisubstituted 1*H*-pyrroles *via* 1,3-dipolar cycloaddition/ring-opening/C-S and C-N

bond cleavage reaction sequence from readily available α,β-unsaturated aldehydes, and 4-metylthaozolium salt utilizing a racemic diphenylprolinol trimethyl silyl ether as a catalyst under room temperature has been devised (Scheme 5.3).

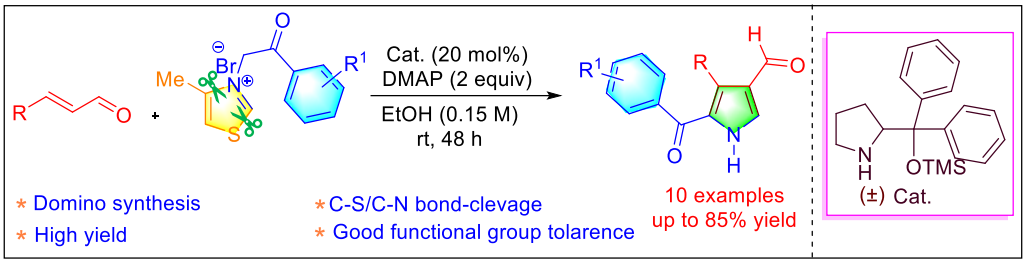

Scheme 5.3 Formal domino synthesis of trisubstituted 1*H*-pyrrole-3-carbaldehydes

5.1.4 Asymmetric Domino Synthesis of Trisubstituted 4,5-Dihydro-1*H*-pyrrole-3-carbaldehydes Through Formal Domino 1,3-Dipolar Cycloaddition/C-S and C-N Bond Cleavage

Polysubstituted chiral dihydro-1*H*-pyrroles can be found in various pharmaceutical chemicals, biologically active molecules, and natural products. Furthermore, these compounds are components of various biologically significant motifs in medicinal chemistry. Chapter 4B deals with the catalytic asymmetric domino approach to enantioselective synthesis of trisubstituted 4,5-dihydro-1*H*-pyrroles *via* changing the reaction condition from room temperature to low-temperature 1,3-dipolar cycloaddition/ring-opening/C-S and C-N bond cleavage reaction sequence from readily available α,β-unsaturated aldehydes, and 4-metylthaozolium salt utilizing a chiral (*R*)-diphenylprolinol trimethyl silyl ether as a catalyst has been devised (Scheme 5.4).

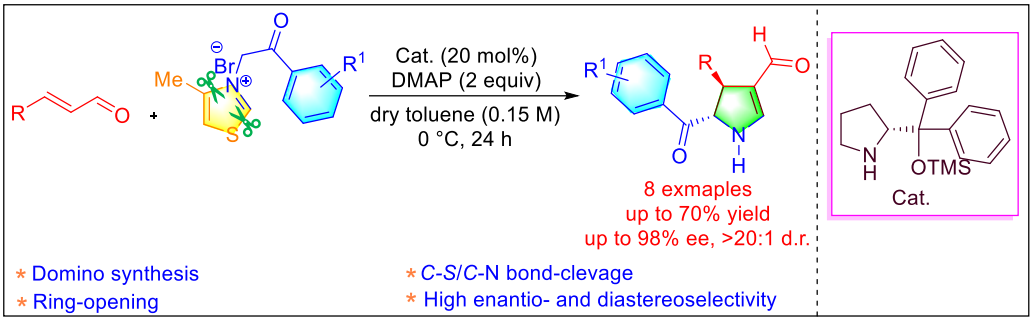

Scheme 5.4 Asymmetric domino synthesis of trisubstituted 4,5-dihydro-1*H*-pyrrole-3-carbaldehydes

5.2 CONCLUSION

- The first proline-derived organocatalytic asymmetric formal domino intermolecular 1,3-cycloaddition/intramolecular rearrangement of α,β-unsaturated aldehydes, and benzothiazolium salt for the synthesis of pyrrolo[1,2-*d*][1,4]thiazine-2-carbaldehydes is developed in good to excellent yield with high enantio- and diastereoselective (up to >99% ee and >20:1 d.r.). This domino approach yielded fluorescent emissive chiral compounds with three contiguous stereogenic centers and one chiral quaternary carbon center in a single step, with high enantioselectivity. This approach works well with a wide range of functional groups, notably aliphatic α,β-unsaturated aldehydes. DFT study helped to understand the stability of the reaction intermediates. It showed that the formation of hydropyrrolo-thiazine intermediates is the rate-determining step in the whole catalytic cycle, which is responsible for the formation of pyrrolo[1,2-*d*][1,4]thiazine-2-carbaldehydes. To showcase the applications of chiral products, the in-silico investigation indicated that it shows anticancer activity, and a fluorescent study was performed to confirm the fluorescence nature of chiral compounds.

- An easy and efficient one-pot methodology for the enantio- and diastereoselective synthesis of diverse *N*-phenyl thioether-tethered chiral tetrasubstituted 4,5-dihydropyrroles via 1,3-dipolar cycloaddition of benzothiazolium salt and α,β-unsaturated aldehydes utilizing an (*R*)-diphenylprolinol trimethyl silyl ether as a catalyst. This enantioselective reaction goes *via* a one-pot formal 1,3-dipolar intermolecular cycloaddition/intramolecular rearrangement followed by an intermolecular C-S bond formation/base-promoted intramolecular ring-opening reaction to achieve the good to excellent yield with high enantio- and diastereoselectivity (up to 96% ee and >20:1 d.r.). This newly developed reaction works well with various functional groups, notably aliphatic α,β-unsaturated aldehydes. It is important to mention that this is the first report for the synthesis of enantioenriched tetrasubstituted dihydropyrrole-3-carbaldehyde derivatives using benzothiazolium salts and α,β-unsaturated aldehyde using a one-pot methodology.

- A new methodology was developed towards the formal domino 1,3-dipolar cycloaddition of 4-methyl thiazolium slat with α,β-unsaturated aldehyde for the synthesis of trisubstituted 1*H*-pyrroles utilizing a racemic diphenylprolinol trimethyl silyl ether as a catalyst under room temperature. This domino reaction goes through the initial 1,3-dipolar cycloaddition of 4-methyl thiazolium salt and α,β-unsaturated aldehyde to produce the hydropyrrolo-thiazine as an intermediate. Further, base promoted ring-opening/enamine tautomerism/iminium ion hydrolysis to cleavage C-S and C-N bond to produce the desired trisubstituted pyrrole in good to excellent yields. The mechanistic

study confirms that 1-mercaptopropan-2-one is a by-product formed during the reaction confirmed by HRMS and ^{1}H NMR. A wide range of substrate scope with decent functional group tolerance was demonstrated.

- An efficient asymmetric protocol was established for the synthesis of enantioenriched trisubstituted dihydro-1*H*-pyrroles via formal domino 1,3-dipolar cycloaddition of 4-methyl thiazolium slat with α,β-unsaturated aldehyde to synthesis of utilizing an (*R*)-diphenylprolinol trimethyl silyl ether as an chiral organocatalyst under 0 °C. This domino reaction goes through 1,3-dipolar cycloaddition of 4-methyl thiazolium salt and α,β-unsaturated aldehyde to produce the chiral hydropyrrolo-thiazine as an intermediate. Further, base promoted ring-opening/enamine tautomerism/iminium ion hydrolysis to cleavage of C-S and C-N bond to produce the desired trisubstituted pyrrole in good yield with excellent yield with enantio-and diastereoselectivity (up to 98% ee and >20:1 d.r.). The mechanistic study confirms that 1-mercaptopropan-2-one is a by-product formed during the reaction confirmed by HRMS and ^{1}H NMR. A wide range of substrate scope with decent functional group tolerance was demonstrated.

REFERENCES

1. **Kondepudi, D** Chapter 1 - Chiral Asymmetry in Nature. In P. L. Polavarapu (Ed.), *Chiral Analysis (Second Edition)* (pp. 3-28). Elsevier 2018.

2. **Chalk, S., and L. McEwen** (2017) The IUPAC Gold Book. *An Exemplar for IUPAC Asset Digitization*, **39**, 25-30.

3. **Shallenberger, R. S.** Taste Chemistry Principles. In R. S. Shallenberger (Ed.), *Taste Chemistry* (pp. 47-109). Springer US 1993.

4. **Kim, J. H., and A. R. Scialli** (2011) Thalidomide: The Tragedy of Birth Defects and the Effective Treatment of Disease. *Toxicological Sciences*, **122**, 1-6.

5. **Tokunaga, E., T. Yamamoto, E. Ito, and N. Shibata** (2018) Understanding the Thalidomide Chirality in Biological Processes by the Self-disproportionation of Enantiomers. *Sci. Rep.* **8**, 17131.

6. **Nguyen, L. A., H. He, and C. Pham-Huy** (2006) Chiral drugs: an overview. *Int. J Biomed. Sci*. **2**, 85-100.

7. **Chhabra, N., M. L. Aseri, and D. Padmanabhan** (2013) A review of drug isomerism and its significance. *Int. J. Appl. Basic. Med. Res*. **3**, 16-18.

8. **Shimazawa, R., N. Nagai, S. Toyoshima, and H. Okuda** (2008) Present state of new chiral drug development and review in Japan. *Journal of health science*, **54**, 23-29.

9. **Fogassy, E., M. Nógrádi, D. Kozma, G. Egri, E. Pálovics and V. Kiss (**2006) Optical resolution methods *Org. Biomol. Chem.* **4**, 3011-3030.

10. **Koskinen, A. M. P., and R. Atta-ur** (1994) Asymmetric Synthesis of Natural Products. *Nat. Prod. Lett.* **4**, 79-79.

11. **Read J.** (1952) Alexander McKenzie Obit. *Not. Fell. R. Soc*.**8**, 206–228.

12. **Pellissier, H.** (2003) Dynamic kinetic resolution. *Tetrahedron*, **59**, 8291-8327.

13. **Alfaro Blasco, M., and H. Gröger** (2014) Enzymatic resolution of racemates with a 'remote' stereogenic center as an efficient tool in drug, flavour, and vitamin synthesis. *Bioorg. Med. Chem.* **22**, 5539-5546.

14. **Akiyama, T., and I. Ojima** *Catalytic asymmetric synthesis*. John Wiley & Sons 2022.

15. **Gawley, R. E., and J**. **Aubé** *Principles of asymmetric synthesis*. Elsevier **2012**.

16. **Paek, S.-M., M. Jeong, J. Jo, Y. M. Heo, Y. T. Han, and H. Yun** (2016) Recent Advances in Substrate-Controlled Asymmetric Induction Derived from Chiral Pool α-Amino Acids for Natural Product Synthesis. *Molecules*, **21**, 951.

17. **Gröger, H.** Enzyme-catalyzed asymmetric synthesis. *Catalytic Asymmetric Synthesis*, *3*, **2010**.

18. **Hall, M.** (2021) Enzymatic strategies for asymmetric synthesis *RSC Chem. Biol.* 2, 958-989.

19. **Diaz-Muñoz, G., I. L. Miranda, S. K. Sartori, D. C. de Rezende, and Alves M. Nogueira Diaz** (2019) Use of chiral auxiliaries in the asymmetric synthesis of biologically active compounds: A review. *Chirality*, **31**, 776-812.

20. **Kukor, A. J., and J. E. Hein** Crystallization: A Tool for Asymmetric Synthesis and Isolation. In *Reference Module in Chemistry, Molecular Sciences and Chemical Engineering*. Elsevier 2022.

21. **Caprio, V., and J. M. Williams** *Catalysis in asymmetric synthesis* (Vol. 3). John Wiley & Sons 2009.

22. **Masel, R. I** *Chemical Kinetics and Catalysis*. New York: Wiley-Interscience 2001.

23. **Cigan, E., B. Eggbauer, J. H. Schrittwieser, and W. Kroutil** (2021) The role of biocatalysis in the asymmetric synthesis of alkaloids – an update *RSC Adv*, **11**, 28223-28270.

24. **Bosnich, B., & M. D. Fryzuk** (1981). Asymmetric synthesis mediated by transition metal complexes. *Topics in Stereochemistry: Topics in Inorganic and Organometallic Stereochemistry*, **12**, 119-154.

25. **García Mancheño, O., and M. Waser** (2023) Recent Developments and Trends in Asymmetric Organocatalysis. *Eur. J. Org. Chem.* **26**, e202200950.

26. **Oliveira, V. d. G., M. F. d. C.Cardoso, and L. d. S. M. Forezi,** (2018) Organocatalysis: A brief overview on its evolution and applications. *Catalysts*, **8**, 605.

27. **MacMillan, D. W. C.** (2008) The advent and development of organocatalysis. *Nature*. **455**, 304-308.

28. **Hall, M.** (2021) Enzymatic strategies for asymmetric synthesis. *RSC Chem. Biol*, **2**, 958-989.

29. **Fox, R. J., S. C. Davis, E. C. Mundorff, L. M. Newman, V. Gavrilovic, S. K. Ma, L. M. Chung, C. Ching, S. Tam, S. Muley, J. Grate, J. Gruber, J. C. Whitman, R. A. Sheldon, and G. W. Huisman** (2007) Improving catalytic function by ProSAR-driven enzyme evolution. *Nat. Biotechnol.* **25**, 338-344.

30. **Ma, S. K., J. Gruber, C. Davis, L. Newman, D. Gray, A. Wang, J. Grate, G. W. Huisman, and R. A. Sheldon (**2010) A green-by-design biocatalytic process for atorvastatin intermediate *Green Chem.* **12**, 81-86.

31. **Bai, Y.-Q., X.-W. Wang, B. Wu, X.-Q. Wang, R.-Z. Liao, M. Li, and Y.-G. Zhou** (2023) Design and Synthesis of Planar-Chiral Oxazole–Pyridine N,N-Ligands: Application in Palladium-Catalyzed Asymmetric Acetoxylative Cyclization. *ACS Catal*. **13**, 9829-9838.

32. **List, B.** (2007) Introduction: Organocatalysis. *Chem. Rev.* **107**, 413-5415.

33. **List, B., and J. A. A. Grimm** (2019) Carbonyl Catalysis: Acetaldehyde-Catalyzed Synthesis of Oxamide by Hydrolysis of Cyanogen. *Synfacts*, **15**, 1432.

34. **Bredig, G., P.S. Fiske (1912)** Durch Katalysatoren bewirkte Asymmetrische Synthese. *Biochem. Z.* **687**, 7–23.

35. **Hajos, Z. G., and D. R. Parrish** (1974) Asymmetric synthesis of bicyclic intermediates of natural product chemistry. *J. Org. Chem.* **39**, 1615-1621.

36. Hashimoto, T., and K. Maruoka (2007) Recent Development and Application of Chiral Phase-Transfer Catalysts. *Chem. Rev.* **107**, 5656-5682.

37. **Hayashi, Y.** Asymmetric Enamine, and Iminium Ion Catalysis. In *Catalytic Asymmetric Synthesis* (pp. 1-28), 2022.

38. **Narasaka, K. (1991)** Chiral Lewis Acids in Catalytic Asymmetric Reactions. *Synthesis*, **1**, 1-11.

39. **Denmark, S. E., and G. L. Beutner** (2008) Lewis Base Catalysis in Organic Synthesis. *Angew. Chem. Int., Ed. 47*, 1560-1638.

40. **Denmark, S. E., R. A. Stavenger, X. Su, K. T. Wong, and Y. Nishigaichi** (1998) Asymmetric catalysis with chiral Lewis bases. *Pure Appl. Chem.***70**, 1469-1476.

41. **Kampen, D., C. M. Reisinger, and B. List** (2009) Chiral Brønsted Acids for Asymmetric Organocatalysis. In B. List (Ed.), *Asymmetric Organocatalysis* (pp. 1-37). Springer Berlin Heidelberg.

42. **Akiyama, T., J. Itoh, and K. Fuchibe** (2006) Recent progress in chiral Brønsted acid catalysis. *Adv. Syn. Catal*. **348**, 999-1010.

43. **Palomo, C., M. Oiarbide, and R. López** (2009) Asymmetric organocatalysis by chiral Brønsted bases: implications and applications *Chem. Soc. Rev.* **38**, 632-653.

44. **Ting, A., J. M. Goss, N. T. McDougal, and S. E. Schaus** Brønsted Base Catalysts. In B. List (Ed.), *Asymmetric Organocatalysis* (pp. 201-232). Springer Berlin Heidelberg, 2009.

45. **Paull, D. H., C. J. Abraham, M. T. Scerba, E. Alden-Danforth, and T. Lectka** (2008) Bifunctional asymmetric catalysis: cooperative Lewis acid/base systems. *Acc. Chem. Res*. **41**, 655-663.

46. **Holland, M. C., and R. Gilmour,** (2015) Deconstructing covalent organocatalysis. *Angew. Chem. Int., Ed.* **54**, 3862-3871.

47. **Phillips, A. M., M. H. G. Prechtl, and A. J. L. Pombeiro** (2021) Non-Covalent Interactions in Enantioselective Organocatalysis: Theoretical and Mechanistic Studies of Reactions Mediated by Dual H-Bond Donors, Bifunctional Squaramides, Thioureas and Related Catalysts. *Catalysts*, **11**, 569.

48. **Gambhir, D., S. Singh, and R. P. Singh** (2023) Enamine/Iminium-based Dual Organocatalytic Systems for Asymmetric Catalysis and Synthesis. *Chem. Asian J.* **18**, e202300627.

49. **Guo, H., Y. C. Fan, Z. Sun, Y. Wu, and O. Kwon** (2018) Phosphine Organocatalysis. *Chem. Rev.* **118**, 10049-10293.

50. **Ni, H., W.-L. Chan, and Y. Lu** (2018) Phosphine-Catalyzed Asymmetric Organic Reactions. *Chem. Rev.* **118**, 9344-9411.

51. **Sućˇ, J., I. Dokli, and M. Gredičak,** (2016) Chiral Brønsted acid-catalysed enantioselective synthesis of isoindolinone-derived N(acyl),S-acetals. *Chem. Commun.* **52**, 2071-2074.

52. **Yin, Q., Y. Shi, J. Wang, and X. Zhang** (2020) Direct catalytic asymmetric synthesis of α-chiral primary amines. *Chem. Soc. Rev.* **49**, 6141-6153.

53. **Sulzer-Mossé, S., and A. Alexakis,** (2007) Chiral amines as organocatalysts for asymmetric conjugate addition to nitroolefins and vinyl sulfonesviaenamine activation *Chem. Commun.* **30**, 3123-3135.

54. **Kamanna, K.** (2022) Organocatalysts based on natural and modified amino acids for asymmetric reactions. **7**, 429-467.

55. **Singh G, and E. Yeboah** (2016) Recent applications of Cinchona alkaloid-based catalysts in asymmetric addition reactions. *Rep. Org. Chem*. 6, 47-75.

56. **Mandalapu, D.** (2015) L-Proline and D-Proline (Chiral Amino Acid Catalysts). *Synlett*, **26**, 707-708.

57. **Thorat, R. B., N. S. Mali, S. S. Wavhal, S. D. Bhagat, M. R. Borade, A. Chapolikar, A. Gandhi, and P. Shinde** (2023) L-Proline: A Versatile Organo-Catalyst in Organic Chemistry. *Comb. Chem. High. T. Scr.* **26**, 1108-1140.

58. **Schneider, J. F., C. L. Ladd, and S. Bräse** Proline as an asymmetric organocatalysts 2015.

59. **Palomo, C., M., Oiarbide, and J. M. García** (2004) Current progress in the asymmetric aldol addition reaction. *Chem. Soc. Rev.* **33**, 65-75.

60. **Bui, T., and C. F. Barbas** (2000) A Proline-catalyzed Asymmetric Robinson Annulation Reaction. *Tetrahedron Lett.* **41**, 6951-6954.

61. **Pasuparthy, S. D., and B. Maiti** (2022) Enantioselective Organocatalytic Michael Addition Reactions Catalyzed by Proline/Prolinol/Supported Proline based Organocatalysts: An Overview. *ChemistrySelect*, **7**, e202104261.

62. **Enders, D., and A. Seki** (2002) Proline-catalyzed Enantioselective Michael Additions of Ketones to Nitrostyrene. *Synlett*, **1**, 0026-0028.

63. **Yang, J. W., M., Stadler, and B. List** (2007) Proline-Catalyzed Mannich Reaction of Aldehydes with N-Boc-Imines. *Angew. Chem. Int., Ed.* **46**, 609-611.

64. **Utsumi, N., H. Zhang, F. Tanaka, and C. F. Barbas Iii** (2007) A Way to Highly Enantiomerically Enriched aza-Morita–Baylis–Hillman–Type Products. *Angew. Chem. Int., Ed.* **46**, 1878-1880.

65. **Kumaragurubaran, N., K. Juhl, W. Zhuang, A. Bøgevig, and K. A. Jørgensen** (2002) Direct L-Proline-Catalyzed Asymmetric α-Amination of Ketones. *J. Am. Chem. Soc.***124**, 6254-6255.

66. **List, B.** (2002) Direct Catalytic Asymmetric α-Amination of Aldehydes. *J. Am. Chem. Soc.* **124**, 5656-5657.

67. **Bøgevig, A., H. Sundén, and A. Córdova** (2004) Direct Catalytic Enantioselective α-Aminoxylation of Ketones: A Stereoselective Synthesis of α-Hydroxy and α,α′-Dihydroxy Ketones. *Angew. Chem. Int., Ed.* **43**, 1109-1112.

68. **Shaikh, R. R., A. Mazzanti, M. Petrini, G. Bartoli, and P. Melchiorre** (2008) Proline-Catalyzed Asymmetric Formal α-Alkylation of Aldehydes via Vinylogous Iminium Ion Intermediates Generated from Arylsulfonyl Indoles. *Angew. Chem. Int., Ed* **47**, 8707-8710.

69. **Steiner, D. D., N. Mase, and C. F Barbas Iii** (2005) Direct Asymmetric α-Fluorination of Aldehydes. *Angew. Chem. Int., Ed.* **44**, 3706-3710.

70. **Moyano, A., ad R. Rios** (2011) Asymmetric Organocatalytic Cyclization and Cycloaddition Reactions. *Chem. Rev.* **111**, 4703-4832.

71. **Hong, B.-C., M.-F. Wu, H.-C. Tseng, and J.-H. Liao** (2006) Enantioselective Organocatalytic Formal [3 + 3]-Cycloaddition of α,β-Unsaturated Aldehydes and Application to the Asymmetric Synthesis of (−)-Isopulegol Hydrate and (−)-Cubebaol. *Org. Lett.* **8**, 2217-2220.

72. **Wróblewska, A**. (2012) (S)-α,α-Diphenylprolinol Trimethylsilyl Ether. *Synlett*, **23**, 953-954.

73. **Donslund, B. S., T. K. Johansen, P. H. Poulsen, K. S. Halskov, and K. A. Jørgensen** (2015) The Diarylprolinol Silyl Ethers: Ten Years After. *Angew. Chem. Int., Ed*. **54**, 13860-13874.

74. **Duan, G.-J., J.-B. Ling, W.-P. Wang, Y.-C. Luo, and P.-F. Xu** (2013) Organocatalytic Formal [2+2] Cycloaddition Initiated by Vinylogous Friedel–Crafts Alkylation: Enantioselective Synthesis of Substituted Cyclobutane Derivatives. *Chem. Commun.* **49**, 4625-4627.

75. **Nielsen, A. J., H. A. Jenkins, and J. McNulty** (2016) Asymmetric Organocatalytic Stepwise [2+ 2] Entry to Tetra-Substituted Heterodimeric and Homochiral Cyclobutanes. *Chem. Eur. J.* **22**, 9111-9115.

76. **Halskov, K. S., L. Næsborg, F. Tur, and K. A. Jørgensen** (2016) Asymmetric [3 + 2] Cycloaddition of Vinylcyclopropanes and α,β-Unsaturated Aldehydes by Synergistic Palladium and Organocatalysis. *Org. Lett.* **18**, 2220-2223.

77. **Gotoh, H., and Y. Hayashi** (2007) Diarylprolinol silyl ether as catalyst of an exo-selective, enantioselective Diels− Alder reaction. *Org. Lett.* **9**, 2859-2862.

78. **Enders, D., C., Joie, and K**. **Deckers** (2013) Organocatalytic Asymmetric Synthesis of Tetracyclic Pyridocarbazole Derivatives by Using a Diels–Alder/aza-Michael/Aldol Condensation Domino Reaction. *Chem. Eur. J.* **19**, 10818-10821.

79. **Riaño, I., U. Uria, L. Carrillo, E. Reyes, and J. L. Vicario** (2015) 4-Alkenyl-5H-1,2,3-Oxathiazole 2,2-Dioxides in Catalytic and Enantioselective [4 + 2] Cycloaddition Through Iminium Activation. Straightforward Access to the Trans-Decaline Framework and to Densely Functionalized Cyclohexenes. *Org. Chem. Front.* **2**, 206-210.

80. **Meazza, M. and R. Rios (**2016) Synergistic Catalysis: Enantioselective Ring Expansion of Vinyl Cyclopropanes Combining Four Catalytic Cycles for the Synthesis of Highly Substituted Spirocyclopentanes Bearing up to Four Stereocenters. *Chem. Eur. J.* **22**, 9923-9928.

81. **McNaught, A. D., and A.** Wilkinson *Compendium of chemical terminology* (Vol. 1669). Blackwell Science Oxford, 1997.

82. **Escolano, C., M. D. Duque, S. Vázquez** (2007) "Nitrile Ylides: Generation, Properties and Synthetic Applications". *Cur. Org. Chem.* **11**, 741–772.

83. **Oleg I. K.** C,P-Carbon-Substituted Phosphorus Ylides. In *Phosphorus Ylides* (pp. 9-156), 1999.

84. **Caiuby, C. A. D., L. G. Furniel, and A. C. B. Burtoloso** (2022). Asymmetric transformations from sulfoxonium ylides *Chem. Sci.* **13**, 1192-1209.

85. **Maercker, A.** (2004) The wittig reaction. *Org. React*. **14**, 270-490.

86. **Kumar, M., I. Sadaf, J. Pamidighantam, Anamika, and S. Kumar** (2024) Recent advance: Sulfur ylides in organic synthesis. *J. Heterocycl. Chem.* **61**, 29-70.

87. **Bumgardner, C. L.** (1963) Sommelet-Hauser Rearrangement of Allylbenzyldimethylammonium Bromide and Cyclopropylcarbinylbenzyldimethylammonium Bromide. Evidence for Carbanion Stabilization by the Cyclopropane Ring. *J. Am. Chem. Soc.* **85**, 73-78.

88. **Baidilov, D.** (2020) On the Mechanism of the Stevens Rearrangement. *Synthesis*, *52*, 21-26.

89. **Harwood, L. M., and R. J. Vickers** Azomethine Ylides. In *Synthetic Applications of 1,3-Dipolar Cycloaddition Chemistry Toward Heterocycles and Natural Products* (pp. 169-252), 2002.

90. **Kobayashi, S., and K. A. Jørgensen** *Cycloaddition reactions in organic synthesis*. John Wiley & Sons. 2002.

91. **Breugst, M. and H.-U. Reissig** (2020) The Huisgen Reaction: Milestones of the 1,3-Dipolar Cycloaddition. *Angew. Chem. Int., Ed.* **59**, 12293-12307.

92. **Tsuge, O., and S. Kanemasa** (1989) Recent advances in azomethine ylide chemistry. *Adv. Heterocycl. Cem*. **45**, 231-349.

93. **Adrio, J., and J. C. Carretero** (2019) Stereochemical diversity in pyrrolidine synthesis by catalytic asymmetric 1,3-dipolar cycloaddition of azomethine ylides *Chem. Commun*. **55**, 11979-11991.

94. **Gomes, P. J. S., C. M. Nunes, A. A. C. C. Pais, T. M. V. D. Pinho e Melo, and L. G. Arnaut** (2006) 1,3-Dipolar cycloaddition of azomethine ylides generated from aziridines in supercritical carbon dioxide. *Tetrahedron Letters*, **47**, 5475-5479.

95. **Novikov, M. S., A. F. Khlebnikov, E. S. Sidorina, and R. R. Kostikov** (2000) 1,3-Dipolar cycloaddition of azomethine ylides derived from imines and difluorocarbene to alkynes: a new active Pb-mediated approach to 2-fluoropyrrole derivatives. *J. Chem. Soc. Perkin Trans.1.* **2**, 231-237.

96. **Díez-Barra, E., C. Pardo, J. Elguero, and J. Arriau** (1983) 1,3-Dipolar cycloaddition of azolium dicyanomethylides. *J. Chem. Soc. Perkin Trans.* **2**, 1317-1320.

97. **Dubey, S., A. Pal, S. Roy, S. Sasmal, A. Tamrakar, R. Jana, and T. Das** (2023) Recent advances in the (3+2) cycloaddition of azomethine ylide. *New. J. Chem*. **47**, 8997-9034.

98. **Huisgen, R.** (2002) Mechanism of 1, 3-dipolar cycloadditions. Reply. *J. Org. Chem.* **33**, 2291-2297.

99. **Carmen N., and J. M. Sansano** (2003) Current Organic Chemistry **7**, 1105-1150.

100. **Touimi Benjelloun, A., G. Morel, and E. Marchand** (2000) 5-aminothiazolium salts as potential cyclic azomethine ylides: Base-induced cycloaddition reactions with aryl, alkyl, and benzoyl isothiocyanates. *Heteroatom Chemistry*, **11**, 16-26.

101. **Moldoveanu, C., G. Zbancioc, D. Mantu, D. Maftei, and I. Mangalagiu,** (2016) The Cycloaddition of the Benzimidazolium Ylides with Alkynes: New Mechanistic Insights. *PLoS One*, **11**, e0156129.

102. **Allgäuer, D. S., P. Mayer, and H. Mayr** (2013) Nucleophilicity Parameters of Pyridinium Ylides and Their Use in Mechanistic Analyses. *J. Am. Chem. Soc.* **135**, 15216-15224.

103. **Das, S.** (2022) Recent Applications of Quinolinium Salts in the Synthesis of Annulated Heterocycles. *SynOpen*, **06**, 86-109.

104. **Das, S. (**2022) Stereoselective Synthesis of Fused-, Spiro- and Bridged Heterocycles via Cyclization of Isoquinolinium Salts: a Recent Update. *Org. Biomol. Chem.* **20**, 1838−1868.

105. **Nájera, C., J. M. Sansano, and M. Yus** (2015). 1,3-Dipolar cycloadditions of azomethine imines. *Org. Biomol. Chem.* **13**, 8596-8636.

106. **Ding, B.-D., J. Sun, W. Jiang, G. Jin, and C.-G. Yan** (2020) Formation of N,S-Containing Polycycles via Base Promoted Dimerization of N-Phenacyl and N-Benzylbenzothiazolium Bromides. *ChemistrySelect*, **5**, 1092-1096.

107. **Singh, H., D. j. Singh, and S. Kumar** (1992) Aqueous base induced selective transformations of 3-(2-oxoalkyl) thiazolium cations. *Tetrahedron*, **48**, 4545-4550.

108. **Iwamura, T., M. Kobayashi, T. Ichikawa, H. Shimizu, and T. Kataoka** (1996) Reinvestigation of reactions of thiazolium and benzothiazolium N-phenacylides with electron-deficient acetylenes. *J. Chem. Soc. Perkin Trans. 1.* **7**, 629-635.

109. **Zhang, X., X. Liu, J. Zhang, D. Zhang, L. Lin, and X. Feng** (2018) Enantioselective [3 + 2] cycloaddition and rearrangement of thiazolium salts to synthesize thiazole and 1,4-thiazine derivatives. *Org. Chem. Front.* **5**, 2126-2131.

110. **Khalafi-Nezhad, A., F. Panahi, R. Yousefi, Y. Gholamalipour, and S. Sarrafi** (2014) An efficient procedure for the synthesis of phenacyl and benzyl azolium salts using fluorous alcohols. *J. Iran. Chem. Soc.***11**, 1189-1196.

111. **Matralis, A. N., and A. P. Kourounakis** (2014) Design of Novel Potent Antihyperlipidemic Agents with Antioxidant/Anti-inflammatory Properties: Exploiting Phenothiazi's Strong Antioxidant Activity. *J. Med. Chem.* **57**, 2568−2581.

112. **Jin, G., J. Sun, R.-Y. Yang, and C.-G. Yan** (2017) Stepwise cycloaddition reaction of N-phenacylbenzothiazolium bromides and nitroalkenes for tetrahydro-, dihydro- and benzo[d]pyrrolo[2,1-b]thiazoles. *Sci. Rep.* **7**, 46470.

113. **Tsuge, O., S. Kanemasa, and S. Takenaka** (1985) Stereochemical Study on 1,3-Dipolar Cycloaddition Reactions of Heteroaromatic N-Ylides with Symmetrically Substituted cis and trans Olefins. *Bull. Chem. Soc. Jap.* **58**, 3137-3157.

114. **Berry, C. R., C. A. Zificsak, A. C. Gibbs, and D. J. Hlasta** (2007) Cycloaddition Reactions of Thiazolium Azomethine Ylides: Application to Pyrrolo[2,1-b]thiazoles. *Org. Lett.* **9**, 4099-4102.

115. **Motornov, V. A., A. A. Tabolin, and S. L. Ioffe** (2022) Oxidative [3+2]-Annulation of Nitroalkenes and Azolium Ylides in the Presence of Cu(II): Efficient Synthesis of [5,5]-Annulated N-Fused Heterocycles. *New. J. Chem.* **46**, 4134-4141.

116. **García Ruano, J. L., A. Fraile, M. R. Martín, G. González, and C. Fajardo** (2008) Pyrrolo[2,1-b]thiazole Derivatives by Asymmetric 1,3-Dipolar Reactions of Thiazolium Azomethine Ylides to Activated Vinyl Sulfoxides. *J. Org. Chem*. **73**, 8484-8490.

117. **Tsuge, O., H. Shimoharada, and M. Noguchi** (1981). Novel Reactions of Benzothiazolium N-Phenacylide with Methylenecyclopropenes. *Chem. Lett.* **10**, 199-1202.

118. **Shen, G. L., J. Sun, and C. G. Yan** (2015) Diastereoselective synthesis of spiro[benzo[d]pyrrolo[2,1-b]thiazole-3,3′-indolines] via cycloaddition reaction of N-phenacylbenzothiazolium bromides and 3-methyleneoxindoles. *Org. Biomol. Chem.* **13**, 10929–10938.

119. **Jiang, W., J. Sun, and C. G. Yan** (2017). Diastereoselective synthesis of benzo[D] chromeno[3′,4′:3,4]pyrrolo[2,1- b] thiazoles via cycloaddition reaction of benzothiazolium salts with 3-nitrochromenes. *RSC Adv.* **7**, 42387–42392.

120. **Adrio, J., and J. C. Carretero** (2014) Recent advances in the catalytic asymmetric 1,3-dipolar cycloaddition of azomethine ylides *Chem. Commun.* **50**, 12434-12446.

121. **Kumar, S. V., and P. J. Guiry** (2023) Catalytic Enantioselective [3+2] Cycloaddition of N-Metalated Azomethine Ylides. *Chem. Eur. J.* **29**, e202300296.

122. **Das, T., P. Saha, and V. K. Singh,** (2015). Silver(I)–Ferrophox Catalyzed Enantioselective Desymmetrization of Cyclopentenedione: Synthesis of Highly Substituted Bicyclic Pyrrolidines. *Org. Lett.* **17**, 5088-5091.

123. **Chen, X.-H., Q. Wei, S.-W. Luo, H. Xiao, and L.-Z. Gong** (2009) Organocatalytic Synthesis of Spiro[pyrrolidin-3,3′-oxindoles] with High Enantiopurity and Structural Diversity. *J. Am. Chem. Soc.* **131**, 13819-13825.

124. **Antonchick, A. P., C. Gerding-Reimers, M. Catarinella, M. Schürmann, H. Preut, S. Ziegler, D. Rauh, and H. Waldmann** (2010) Highly enantioselective synthesis and cellular evaluation of spirooxindoles inspired by natural products. *Nat. Chem.* **2**, 735-740.

125. **Lim, A. D., J. A. Codelli, and S. E. Reisman** (2013) Catalytic asymmetric synthesis of highly substituted pyrrolizidines. *Chem. Sci.* **4**, 650-654.

126. **Takayama, H., Z.-J. Jia, L. Kremer, J. O. Bauer, C. Strohmann, S. Ziegler, A. P. Antonchick, and H. Waldmann** (2013) Discovery of Inhibitors of the Wnt and Hedgehog Signaling Pathways through the Catalytic Enantioselective Synthesis of an Iridoid-Inspired Compound Collection. *Angew. Chem. Int., Ed.* **52***,* 12404-12408.

127. **Narayan, R., J. O. Bauer, C. Strohmann, A. P. Antonchick, and H. Waldmann,** (2013) Catalytic Enantioselective Synthesis of Functionalized Tropanes Reveals Novel Inhibitors of Hedgehog Signaling. *Angew. Chem. Int. Ed.* **52**, 12892-12896.

128. **Liu, K., H.-L. Teng, L. Yao, H.-Y. Tao, and C.-J. Wang** (2013) Silver-Catalyzed Enantioselective Desymmetrization: Facile Access to Spirolactone-Pyrrolidines Containing a Spiro Quaternary Stereogenic Center. *Org. Lett.* **15**, 2250-2253.

129. **Li, J., Lian, X., X. Liu, L. Lin, and X. Feng** (2013) Nickel(II)-Catalyzed Enantioselective 1,3-Dipolar Cycloaddition of Azomethine Imines with Alkylidene Malonates. *Chem. Eur. J.* **19**, 5134-5140.

130. **Hashimoto, T., M. Omote, and K**. **Maruoka** (2011) Asymmetric Inverse-Electron-Demand 1,3-Dipolar Cycloaddition of C,N-Cyclic Azomethine Imines: An Umpolung Strategy. *Angew. Chem. Int., Ed.* **50**, 3489-3492.

131. **Zhang, D., Z. Su, Q. He, Z. Wu, Y. Zhou, C. Pan, X. Liu, and X. Feng** (2020) Diversified Transformations of Tetrahydroindolizines to Construct Chiral 3-Arylindolizines and Dicarbofunctionalized 1,5-Diketones. *J. Am. Chem. Soc.* **142**, 15975-15985.

132. **Ibrahem, I., R. Rios, J. Vesely, and A. Córdova** (2007) Organocatalytic asymmetric multi-component [C+NC+CC] synthesis of highly functionalized pyrrolidine derivatives. *Tetrahedron Lett.* **48**, 6252-6257.

133. **Lamhauge, J. N., D. A. McLeod, C. L. Barløse, G. A. Oliver, L. Viborg, T. Warburg, and K. Anker Jørgensen** (2023) Enantioselective Synthesis of Tropane Scaffolds by an Organocatalyzed 1,3-Dipolar Cycloaddition of 3-Oxidopyridinium Betaines and Dienamines. *Chem. Eur. J.* **29**, e202301830.

134. **Suga, H., T. Arikawa, K. Itoh, Y. Okumura, A. Kakehi, and M. Shiro** *Asymmetric 1, 3-dipolar cycloaddition reactions of azomethine imines with acrolein catalyzed by l-proline and its derivatives* Shinshu University Library 2010.

135. **Vicario, J. L., S. Reboredo, D. Badia, L. Carrillo** (2007) Organocatalytic Enantioselective [3 + 2] Cycloaddition of Azomethine Ylides and *α,β*-Unsaturated Aldehydes. *Angew. Chem., Int. Ed.* **46**, 5168−5170.

136. **Chen, X.-P., K.-Q. Hou, F. Zhou, A. S. C. Chan, and X.-F. Xiong** (2021) Organocatalytic Asymmetric Synthesis of Benzothiazolopyrimidines via [4 + 2] Cyclization of 2-Benzothiazolimines and Aldehydes. *J. Org. Chem.* **86**, 1667-1675.

137. **Ma, M., Y. Zhu, Q. Sun, X. Li, J. Su, L. Zhao, Y. Zhao, S. Qiu, W. Yan, K. Wang, and R. Wang** (2015) The asymmetric synthesis of CF3-containing spiro[pyrrolidin-3,2′-oxindole] through the organocatalytic 1,3-dipolar cycloaddition reaction. *Chem. Commun.* **51***,* 8789-8792.

138. **Chow, S. S., M. Nevalainen, C. A. Evans, and C. W. Johannes** (2007) A new organocatalyst for 1,3-dipolar cycloadditions of nitrones to α,β-unsaturated aldehydes. *Tetrahedron Lett.* **48**, 277-280.

139. **Rios, R., Ibrahem, I., J. Vesely, G.-L. Zhao, and A. Córdova** (2007) A simple one-pot, three-component, catalytic, highly enantioselective isoxazolidine synthesis *Tetrahedron Lett.* **48**, 5701-5705.

140. **Vesely, J., R. Rios, I. Ibrahem, G.-L. Zhao, L. Eriksson, and A. Córdova** (2008) One-Pot Catalytic Asymmetric Cascade Synthesis of Cycloheptane Derivatives. *Chem. Eur. J.* **14**, 2693-2698.

141. **Poulsen, P. H., S. Vergura, A. Monleón, D. K. B. Jørgensen, and K. A. Jørgensen** (2016) Controlling Asymmetric Remote and Cascade 1,3-Dipolar Cycloaddition Reactions by Organocatalysis. *J. Am. Chem. Soc.* **138**, 6412-6415.

142. **Li, W., J. Wei, Q. Jia, Z. Du, K. Zhang, and J. Wang** (2014) Asymmetric Synthesis of Tetrahydroquinolines through a [3+2] Cycloaddition Controlled by Dienamine Catalysis. *Chem. Euro. J.* **20**, 6592-6596.

143. **Li, W., Q. Jia, Z. Du, K. Zhang, and J. Wang** (2014) Amine-Catalyzed Enantioselective 1,3-Dipolar Cycloadditions of Aldehydes to C,N-Cyclic Azomethine Imines. *Chem. Eur. J.* **20**, 4559-4562.

144. **Badshah, S. L.** and **Naeem, A.** (2016) Bioactive thiazine and benzothiazine derivatives: Green synthesis methods and their medicinal importance. *Molecules* **21**, 1054.

145. **Matralis, A. N.** and **A. P. Kourounakis** (2014) Design of novel potent antihyperlipidemic agents with antioxidant/anti- inflammatory properties: Exploiting phenothiazine's strong antioxidant activity. *J. Med. Chem*. **57**, 2568–2581.

146. **Campiani, G., A. Garofalo, I. Fiorini, M. Botta, V. Nacci, A. Tafi, A. Chiarini, R. Budriesi, G. Bruni, and M. R. Romeo** (1995) Pyrrolo[2,l-c][l,4]benzothiazines: Synthesis, Structure-Activity Relationships, Molecular Modeling Studies, and Cardiovascular Activity1. *J. Med. Chem* **38**, 4393-4410.

147. **Trapanil, G., M. Francol, A. Latrofal, G. Genchi, G. Siro Brigiani, M. Mazzoccoli, M. Persichella, M. Serra, G. Biggie, G. Lisol,** and **D. Farmaco-Chirnico** (1994) Synthesis and anticonvulsant activity of some 1,2,3,3a-tetrahydropyrrolo[2,1-b]benzothiazol-~-ones and pyrrolo[2,M]thiazole analogues. *Eur. J. Med. Chem.* **29**, 109-204.

148. **Corelli, F., F. Manetti, A. Tafi, G. Campiani, V. Nacci, and M. Botta** (1997) Diltiazem-like Calcium Entry Blockers: A Hypothesis of the Receptor-Binding Site Based on a Comparative Molecular Field Analysis Model. *Med. Chem.* **40**, 125–131.

149. **Matralis, A. N** and **A. P. Kourounakis** (2014). Design of novel potent antihyperlipidemic agents with antioxidant/anti- inflammatory properties: Exploiting phenothiazine's strong antioxidant activity. *J. Med. Chem*. **57**, 2568–2581.

150. **Budriesi, R., B. Cosimelli, P. Ioan, C. Z. Lanza, D. Spinelli, and A. Chiarini** (2002) Cardiovascular characterization of [1,4]thiazino[3,4-c][1,2,4]oxadiazol-1-one derivatives: Selective myocardial calcium channel modulators. *J. Med. Chem.* **45**, 3475–3481.

151. **Gao, L** and **R. I Hollingsworth** (2005) Design and evaluation of dihydroxytetrahydro-1H-pyrrolo[2,1-c]-[1,4]benzothiazines as conformationally restricted transition-state inhibitors of β-ribosidases. *J. Org. Chem*. **70**, 9013–9016.

152. **Li, C. S., Y. Ding, B. J. Yang, G. Miklossy, H. Q. Yin, L. A. Walker, J. Turkson, and S. Cao** (2015). A New Metabolite with a Unique 4-Pyranone-γ-Lactam-1,4-Thiazine Moiety from a Hawaiian-Plant Associated Fungus. *Org. Lett*. **17**, 3556–3559.

153. **Danton, F., M. Othman, A. M. Lawson, J. Moncol, A. Ghinet, B. Rigo, and A. Daïch** (2019) Phenyliodine(III) Diacetate/I 2 -Mediated Domino Approach for Pyrrolo[1,4]Thiazines and 1,4-Thiazines by a One-Pot Morin Rearrangement of N,S-Acetals. *Chem. Eur. J*. **25**, 6113–6118.

154. **Kadam, V., T. S. Choudhare,** and **D. Netankar** (2023). Four Components One-Pot Synthesis of New Thiazoles and Their Biological Screening for Anti-Tuberculosis Activity. *Iran. J. Chem. Chem. Eng.* **42**, 2840-2847.

155. **Liu, X., H. Zheng, Y. Xia, L. Lin,** and **X. Feng** (2017) Asymmetric Cycloaddition and Cyclization Reactions Catalyzed by Chiral N,N′-Dioxide-Metal Complexes. *Acc. Chem. Res.* **50**, 2621–2631.

156. **Coldham, I. and R. Hufton** (2005). Intramolecular dipolar cycloaddition reactions of azomethine ylides. *Chem. Rev.* **105**, 2765–2809.

157. **Funt, L. D., M. S**. **Novikov, and A. F. Khlebnikov** (2020) New applications of pyridinium ylides toward heterocyclic synthesis. *Tetrahedron* **76**, 131415.

158. **Chandra Sahoo, S., M. Joshi, and S. Chandra Pan** (2017) Diastereoselective Desymmetrization of Prochiral Cyclopentenediones via Cycloaddition Reaction with N-Phenacylbenzothiazolium Bromides. *J. Org. Chem.* **82**, 12763–12770.

159. **Sahoo, S. C. and S. C. Pan** (2019) Synthesis of N-Formyl-2-benzoyl Benzothiazolines, 2-Substituted Benzothiazoles, and Symmetrical Disulfides from N-Phenacylbenzothiazolium Bromides. *Org. Lett*. **21**, 6208–6212.

160. **Jiang, W., J. Sun, and C. G. Yan** (2017) Diastereoselective synthesis of benzo[D] chromeno[3′,4′:3,4]pyrrolo[2,1- b] thiazoles via cycloaddition reaction of benzothiazolium salts with 3-nitrochromenes. *RSC Adv.* **7**, 42387–42392.

161. **Shen, G. L., J. Sun**, **and C. G. Yan** (2015) Diastereoselective synthesis of spiro[benzo[d]pyrrolo[2,1-b]thiazole-3,3′-indolines] via cycloaddition reaction of N-phenacylbenzothiazolium bromides and 3-methyleneoxindoles. *Org. Biomol. Chem*. **13**, 10929–10938.

162. **Zeng, Q., D. Ren, Y. Huang, Fu, and X. Li** (2018) Diastereoselective synthesis of spiro[pyrrolo[2,1-b][1,3] benzothiazole-3,5′-[1,3]thiazolo[3,2-b][1,2,4]triazol]-6′-ones via cycloaddition reaction of benzothiazolium salts. *J. Chem. Res*. **42**, 371–373.

163. **Zeng, Q., D. Ren, Y. Huang, Fu, and X. Li** (2018) Synthesis of spiro[pyrrolo[2,1-b][1,3]benzothiazole-3,2′-[1,3]thiazolo[3,2-a] pyrimidine] via cycloaddition reactions. **42,** 260-262.

164. **Wang, Z. H., T. Zhang, L. W. Shen, X. Yang, Y. P. Zhang, Y. You, J. Q Zhao, and W. C. Yuan** (2023) Diverse Synthesis of Fused Polyheterocyclic Compounds via [3 + 2] Cycloaddition of In Situ-Generated Heteroaromatic N-Ylides and Electron-Deficient Olefins. *Molecules*, **28**, 4410.

165. **Vicario, J. L., S. Reboredo, D. Badía**, and **L. Carrillo** (2007) Organocatalytic enantioselective [3+2] cycloaddition of azomethine ylides and α,β-unsaturated aldehydes. *Angew. Chem. Int. Ed.* **46**, 5168–5170.

166. **Iratxe, Ugarriza., Uria Uxue, Reyes. Efraím, Luisa, Carrillo, and L. Vicario Jose** (2015) Organocatalytic Enantioselective [3+2] Cycloaddition of Azomethine Ylides and Acrolein **2**, 26-36.

167. **Frisch, M. J., G. W. Trucks, H. B. Schlegel, G. E. Scuseria, M. A. Robb, J. R. Cheeseman, G. Scalmani, V. Barone, G. A. Petersson, H. Nakatsuji, X. Li, M. Caricato, A. V. Marenich, J. Bloino, B. G. Janesko, R. Gomperts, B. Mennucci, H. P. Hratchian, J. V. Ortiz, A. F. Izmaylov, J. L. Sonnenberg, D. Williams-Young, F. Ding, F. Lipparini, F. Egidi, J. Goings, B. Peng, A. Petrone, T. Henderson, D. Ranasinghe, V. G. Zakrzewski, J. Gao, N. Rega, G. Zheng, W. Liang, M. Hada, M. Ehara, K. Toyota, R. Fukuda, J. Hasegawa, M. Ishida, T. Nakajima, Y. Honda, O. Kitao, H. Nakai, T. Vreven, K. Throssell, J. A. Montgomery, Jr., J. E. Peralta, F. Ogliaro, M. J. Bearpark, J. J. Heyd, E. N. Brothers, K. N. Kudin, V. N. Staroverov, T. A. Keith, R. Kobayashi, J. Normand, K. Raghavachari, A. P. Rendell, J. C. Burant, S. S. Iyengar, J. Tomasi, M. Cossi, J. M. Millam, M. Klene, C. Adamo, R. Cammi, J. W. Ochterski, R. L. Martin, K. Morokuma, O. Farkas, J. B. Foresman, and D. J. Fox** Gaussian 16, Revision C.01. *Gaussian, Inc., Wallingford CT* Gaussian, Inc., Wallingford CT 2016.

168. **Zhao, Y, and D. G. Truhlar** (2008) The M06 suite of density functionals for main group thermochemistry, thermochemical kinetics, noncovalent interactions, excited states, and transition elements: two new functionals and systematic testing of four M06-class functionals and 12 other functionals. *Theor. Chem. Account.* **120**, 215-241.

169. **Dunning Jr, T. H,** and **P. J. Hay** *in Modern Theoretical Chemistry*, Ed. H. F. Schaefer III, Vol. 3 Plenum, (pp 1–28) New York, 1977.

170. **Ditchfield, R., W. J Hehre, and J. A. Pople** (1971) Self-Consistent Molecular-Orbital Methods. IX. An Extended Gaussian-Type Basis for Molecular-Orbital Studies of Organic Molecules. *J. Chem. Phys.* **54,** 724-728.

171. **Tian, W., C. Chen, X. Lei, J. Zhao, and J. Liang** (2018) CASTp 3.0: computed atlas of surface topography of proteins. *Nucleic acids Res.* **46**, W363-W367.

172. **Yang, J., A. Roy, and Y. Zhang** (2013) Protein–ligand binding site recognition using complementary binding-specific substructure comparison and sequence profile alignment. *Bioinformatics* **29**, 2588-2595.

173. **Friesner, R. A., R. B. Murphy, M. P. Repasky, L. L. Frye, J. R. Greenwood, T. A. Halgren, P. C. Sanschagrin, and D. T. Mainz** (2006) Extra precision glide: Docking and scoring incorporating a model of hydrophobic enclosure for protein−ligand complexes. *J. Med. Chem.* **49**, 6177-6196.

174. Schrodinger Release 2023-1: Glide, Schrödinger, LLC, New York, NY, 2021.

175. BIOVIA, Dassault Systèmes, BIOVIA Workbook, Release 2020; BIVIA Pipeline Pilot, Release, San Diego, 2020.

176. **Battistuzzi, G., S. Cacchi, and G. Fabrizi** (2003) An Efficient Palladium-Catalyzed Synthesis of Cinnamaldehydes from Acrolein Diethyl Acetal and Aryl Iodides and Bromides. *Org. Lett.* **5**, 777-780.

177. **Zhang, G., Y. Zhang, X. Jiang, W. Yan, and R. Wang** (2011) Highly Enanti-oselective Synthesis of Multisubstituted Polyfunctional Dihydro-pyrrole via an Organocatalytic Tandem Michael/Cyclization Se-quence. *Org. Lett.* **13**, 3806-3809.

178. **Wang, D., Y. Fan, P. Yu, and L. Désaubry** (2020). Recent advances in the synthesis of 2,3-dihydropyrroles *Chem. Commun.* **56**, 5584-5592.

179. **Barluenga, J., F. J. Fañanás, R. Sanz, and J. M. Ignacio** (2003). Synthesis of Pyrrole Derivatives through Functionalization of 3,4-Bis (lithiomethyl) dihydropyrroles. *Eur. J. Org. Chem.* **4**, 771-783.

180. **Sweeney, J. B**., **Doulcet, J., and B. Thapa** (2018). Synthesis of 3-Substituted Pyrrolidines via Palladium-Catalyzed Hydroarylation. *iScience*, **9**, 328-336.

181. **Castellano, S., H. D. G. Fiji, S. S. Kinderman, M. Watanabe, P. de Leon, F. Tamanoi, and O. Kwon** (2007) Small-Molecule Inhibitors of Protein Geranylgeranyltransferase Type I. *J. Am. Chem. Soc.* **129**, 5843-5845.

182. **Cox, C. D., P. J. Coleman, M. J. Breslin, D. B. Whitman, R. M. Garbaccio, M. E. Fraley, C. A. Buser, E. S. Walsh, K. Hamilton, and M. D. Schaber** (2008) Kinesin Spindle Protein (KSP) Inhibitors. 9. Discovery of (2S)-4-(2,5-Difluorophenyl)-N-[(3R,4S)-3-fluoro-1-methylpiperidin-4-yl]-2-(hydroxymethyl)-N-methyl-2-phenyl-2,5-dihydro-1H-pyrrole-1-carboxamide (MK-0731) for the Treatment of Taxane-Refractory Cancer. *J. Med. Chem.* **51**, 4239-4252.

183. **Shi, F., G. J. Xing, W. Tan, R. Y. Zhu, and S. Tu** (2013) Enantioselective construction of 2,5-dihydropyrrole skeleton with quaternary stereogenic center via catalytic asymmetric 1,3-dipolar cycloaddition involving α-arylglycine esters. *Org. Biomol. Chem.* **11**, 1482-1489.

184. **Medran, N. S., A. La-Venia, and S. A. Testero** (2007) Metal-mediated synthesis of pyrrolines. *RSC Adv.* **9**, 6804-6844.

185. **Yang, Q., H. Alper, and W. J. Xiao** (2007) Efficient Method for the Synthesis of Chiral Pyrrolidine Derivatives via Ring-Closing Enyne Metathesis Reaction. *Org. Lett.* **9**, 769-771.

186. **Kolos, N. N., S. A. Karpan, I. V. Omelchenko, N. Y. V. Chechina, and F. G. Yaremenko** (2019) One-pot diastereoselective synthesis of functionalized 4,5-dihydropyrroles by reactions of arylglyoxals, β-dicarbonyl compounds, and aromatic amines. *Chem. Heterocycl. Compd.* **55**, 827-833.

187. **Wang, D., Y. Fan, P. Yu, and L. Désaubry** (2020) Recent advances in the synthesis of 2,3-dihydropyrroles. *Chem. Commun.* **56**, 5584-5592.

188. **Kim, J. M., K. Y. Lee, S. Lee, and J. N Kim** (2004) Ring-closing metathesis toward the synthesis of 2,5-dihydrofuran and 2,5-dihydropyrrole skeletons from Baylis–Hillman adducts. *Tetrahedron Letters* **45**, 2805-2808.

189. **Walag, A. M. P., O. Ahmed, J. Jeevanandam, M. Akram, B. C. Ephraim-Emmanuel, C. Egbuna, P. Semwal, M. Iqbal, S. Hassan, and J. O. Uba** Health Benefits of Organosulfur Compounds. In C. Egbuna & G. Dable Tupas (Eds.), *Functional Foods and Nutraceuticals: Bioactive Components, Formulations, and Innovations* Springer International Publishing. (pp 445-472), 2020.

190. **Williams, J. M., K. M. J. Brands, R. T. Skerlj, R. B. Jobson, G. Marchesini, K. M. Conrad, B. Pipik, K. A. Savary, F. R. Tsay, and P. G. Houghton** (2005) Practical Synthesis of the New Carbapenem Antibiotic Ertapenem Sodium. *J. Org. Chem.* **70**, 7479-7487.

191. **Inaba, T., A. G. Birchler, Y. Yamada, S. Sagawa, K. Yokota, K. Ando, and I. A Uchida** (1998) Practical Synthesis of Nelfinavir, an HIV-Protease Inhibitor, Using a Novel Chiral C4 Building Block: (5R,6S)-2,2-Dimethyl-5-hydroxy-1,3-dioxepan-6-ylammonium Acetate. *J. Org. Chem.* **63**, 7582-7583.

192. **Kahan, F. M., H. Kropp, J. G. Sundelof, and J. Birnbaum (1983)** Thienamycin: development of imipenen-cilastatin. *J. Antimicrob. Chemother*. **12***,* 1-35.

193. **Zhang, R., H. Ding, X. Pu, Z. Qian, and Y. Xiao** (2020) Recent Advances in the Synthesis of Sulfides, Sulfoxides and Sulfones via C-S Bond Construction from Non-Halide Substrates. *Catalysts* **10**, 1339.

194. **Ai, H. J., J. Rabeah, A. Brückner, and X.F. Wu,** (2021) Rhodium-catalyzed carbonylative coupling of alkyl halides with thiols: a radical process faster than easier nucleophilic substitution. *Chem. Commun.* **57**, 1466-1469.

195. **Lee, C. F., Y. C. Liu, and S. S. Badsara** (2014) Transition-Metal-Catalyzed C-S Bond Coupling Reaction. *Chem. Asian. J.* **9**, 706-722.

196. **Zhao, W., P. Xie, Z. Bian, A. Zhou, H. Ge, M. Zhang, Y. Ding, and L**. **Zheng** (2015) Ammonium Iodide Induced Nonradical Regioselective Sulfenylation of Flavones via a C–H Functionalization Process. *J. Org. Chem.* **80**, 9167-9175.

197. **Ahmad, S., A. F. Zahoor, S. A. R. Naqvi, and M. Akash (2018)** Recent trends in ring opening of epoxides with sulfur nucleophiles. *Molecular Diversity* **22**, 91-205.

198. **Chen, Z., M. S. Nasr, M. Kazemi, and M. A Mohammadi** (2020) Mini-Review: Achievements in the Thiolysis of Epoxides. *Mini-Rev. Org. Chem.* **17**, 352-362.

199. **Sureshkumar, D., S. M. Koutha, and S. Chandrasekaran** (2005) Chemistry of Tetrathiomolybdate: Aziridine Ring Opening Reactions and Facile Synthesis of Interesting Sulfur Heterocycles. *J. Am. Chem. Soc.* **127**, 12760-12761.

200. **Zhu, Y., C. Zhai, Y. Yue, L. Yang, and W. Hu** (2009). One-pot three-component tandem reaction of diazo compounds with anilines and unsaturated ketoesters: a novel synthesis of 2,3-dihydropyrrole derivatives *Chem. Commun.* 11, 1362-1364.

201. **Tong, G., H. Xu, W. Fan, B. Jiang, S. Wang, and S. Tu** (2013). A Highly Diastereoselective Three-component Domino Reaction in Water Yielding Poly-substituted 4,5-Dihydropyrroles. *Chin. J. Chem.* **31**, 1039-1044.

202. **Pandidurai, S., V. S. Kumar Choutipalli, V. Subramanian, and G. Sekar** (2024) Organocatalyzed Enantio- and Diastereoselective Formal Domino 1,3-Dipolar Cycloaddition/Rearrangement: Synthesis of Chiral Pyrrolo-thiazine-2-carbaldehydes. *Org. Lett.* **26***,* 2971-2975.

203. **Shaikh A. C, and O. Kwon** (2019) Phosphine-Catalyzed [3 + 2] Annulation: Synthesis of Ethyl 5-(*tert*-Butyl)-2-phenyl-1-tosyl-3-pyrroline-3-carboxylate *Organic Synth*. **96**, 214–231.

204. **Zhu, X. F., C. E. Henry, and O. Kwon** (2005). A highly diastereoselective synthesis of 3-carbethoxy-2,5-disubstituted-3-pyrrolines by phosphine catalysis. *Tetrahedron*, **61**, 6276-6282.

205. **Li, L., X. Wu, and J. Zhang** (2011). Lewis acid-catalyzed formal [3+2] cycloadditions of N-tosyl aziridines with electron-rich alkenesvia selective carbon–carbon bond cleavage. *Chem. Commun* **47**, 5049-5051.

206. **Ghorai, M. K., and D. P. Tiwari** (2013). Enantioselective Synthesis of 4,5-Dihydropyrroles via Domino Ring-Opening Cyclization (DROC) of N-Activated Aziridines with Malononitrile. *J. Org. Chem.* **78**, 2617-2625.

207. **Miura, T., T. Tanaka, K. Hiraga, S. G. Stewart, and M. Murakami** (2013) Stereoselective Synthesis of 2,3-Dihydropyrroles from Terminal Alkynes, Azides, and α,β-Unsaturated Aldehydes via N-Sulfonyl-1,2,3-triazoles. *J. Am. Chem. Soc.* **135**, 13652-13655.

208. **Martin, M. C., D. V. Patil, and S. France** (2014) Functionalized 4-Carboxy- and 4-Keto-2,3-dihydropyrroles via Ni(II)-Catalyzed Nucleophilic Amine Ring-Opening Cyclizations of Cyclopropanes. *J. Org. Chem.* **79**, 3030-3039.

209. **Anaraki-Ardakani, H., A. Hassanabadi, A. Fazilnia, A. Tabarzad, and T. Heidari-Rakati** (2014) A Facile Route to the Synthesis of 2,5-Dihydropyrrole Derivatives. *J. Chem. Res.* **38**, 9-11.

210. **Li, Y., H. Xu, M. Xing, F. Huang, J. Jia, and J. Gao** (2015) Iodine-Promoted Construction of Polysubstituted 2,3-Dihydropyrroles from Chalcones and β-Enamine Ketones (Esters). *Org. Lett.* **17**, 3690-3693.

211. **Chen, J., J. Li, J. Wang, H. Li, W. Wang, and Y. Guo** (2015) Phosphine-Catalyzed Aza-MBH Reactions of Vinylpyridines: Efficient and Rapid Access to 2,3,5-Triarylsubstituted 3-Pyrrolines. *Org. Lett.* **17**, 2214-2217.

212. **Xiang, J., H. Xie, Z. Li, Q. Dang, and X**. **Bai** (2015) Stereoselective Synthesis of 3-Carboxy-4,5-dihydropyrroles via an Intramolecular Iminium Ion Cyclization Reaction. *Org. Lett.* **7**, 3818-3821.

213. **Guđmundsson, A., K. P. J. Gustafson, B. K. Mai, V. Hobiger, F. Himo, and J. E. Bäckvall** (2019) Diastereoselective Synthesis of N-Protected 2,3-Dihydropyrroles via Iron-Catalyzed Cycloisomerization of α-Allenic Sulfonamides. *ACS Cat.* **9**, 1733-1737.

214. **Kolos, N. N., S. A. Karpan, I. V. Omelchenko, N. y. V. Chechina, & F. G. Yaremenko** (2019) One-pot diastereoselective synthesis of functionalized 4,5-dihydropyrroles by reactions of arylglyoxals, β-dicarbonyl compounds, and aromatic amines. *Chem. Heterocycl. Compd* **55**, 827-833.

215. **Iddum, S., D. Y. Yang, and T. J. Liou** (2021) Diastereoselective Synthesis of Polysubstituted Pyrrolidines/Dihydropyrroles: Photochemical Properties of Polysubstituted Pyrroles. *Asian J. Org. Chem* **10**, 2663-2669.

216. **Yang, Q., H. Alper, and W.J. Xiao** (2007) Efficient Method for the Synthesis of Chiral Pyrrolidine Derivatives via Ring-Closing Enyne Metathesis Reaction. *Org. Lett.* **9**, 769-771.

217. **Bhardwaj, V., D. Gumber, V. Abbot, S. Dhiman, and P. Sharma** (2015) Pyrrole: a resourceful small molecule in key medicinal hetero-aromatics *RSC Adv*. **5**, 15233-15266.

218. **Ahmad, S., O. Alam, M. J. Naim, M. Shaquiquzzaman, M. M. Alam and M. Iqbal** (2018) Pyrrole: An insight into recent pharmacological advances with structure activity relationship. *Eur. J. Med. Chem.* **157**, 527-561.

219. **Baltazzi, E. and L. I. Krimen** (1963) Recent Advances in the Chemistry of Pyrrole. *Chem. rev.* **63**, 511-556.

220. **Naqvi, N., and Q. Fernando** (1960) The Basic Strength of Pyrrole. *J. Org. Chem.* **25**, 551-554.

221. **Nigst, T. A., M. Westermaier, A. R. Ofial, and H. Mayr** (2008) Nucleophilic Reactivities of Pyrroles. *Eur. J. Org. Chem.* 14, 2369-2374.

222. **Koide, T., Ono, T., H. Shimakoshi, and Y. Hisaeda** (2022) Functions of bioinspired pyrrole cobalt complexes–recently developed catalytic systems of vitamin B12 related complexes and porphycene complexes. *Coord. Chem. Rev.* **470**, 214690.

223. **R. A. Jones., and G. P. Bean.** CHAPTER 4 - Electrophilic Substitution of the Pyrrole Ring. (Eds.), *Organic Chemistry: A Series of Monographs* (Vol. 34, pp. 115-207), Academic Press 1977.

224. **Ghosh, H., and A. Jana** (2023) Recent Advances in the Green Synthesis of Poly Functionalized Pyrroles. *Prog. Chem. Biochem. Res.* 60-71.

225. **Thwin, M., B. Mahmoudi, O. A. Ivaschuk, and Q. A Yousif** (2019) An efficient and recyclable nanocatalyst for the green and rapid synthesis of biologically active polysubstituted pyrroles and 1, 2, 4, 5-tetrasubstituted imidazole derivatives. *RSC Adv.* **9**, 15966-15975.

226. **Hunjan, M. K., S. Panday, A. Gupta, J. Bhaumik, P. Das, and J. K Laha** (2021) Recent Advances in Functionalization of Pyrroles and their Translational Potential. *Chem Rec* **21**, 715-780.

227. **Berini, C., F. N. Minassian, J. N. Pelloux-Léon, Y. Denis, Vallée, and C. Philouze** (2008) Efficient stereoselective nucleophilic addition of pyrroles to chiral nitrones. *Org. Biomole. Chem*. **6**, 2574-2586.

228. **Rakowski, D. B. M.,** (1998) The activation of η5-pyrrole complexes toward nucleophilic attack. *Coord. Chem. Rev.* **174**, 191-205.

229. **Akhmetova, V. R., E. M. M. N. S. Bikbulatova, N. F. Akhmadiev, R. V. Galimzyanova, A. G. Kunakova, and Ibragimov** (2018) Transition metal-catalyzed C,C- and C,N-cycloaminomethylation reactions of pyrrole and indole. *Chem. Heterocyl. Comp.* **54***,* 520-527.

230. **Roomi, M., and S. MacDonald** (1970) The Hantzsch pyrrole synthesis. *Cana. J. Chem*. **48**, 1689-1697.

231. **Banik, B. K., I. Banik, M. Renteria, and S. K. Dasgupta** (2005) A straightforward highly efficient Paal–Knorr synthesis of pyrroles. *Tetrahedron Lett.* **46**, 2643-2645.

232. **Diana, T., V. Stanislava, P. Lily, and G. Maya** (2018) Synthesis of Pyrrole and Substituted Pyrroles (Review). *J. Chem. Tech. Metall.* **53**, 451-464.

233. **Ma, Z., Z. Ma, and D. Zhang** (2018) Synthesis of Multi-Substituted Pyrrole Derivatives Through [3+2] Cycloaddition with Tosylmethyl Isocyanides (TosMICs) and Electron-Deficient Compounds. *Molecules*, **23**, 2666.

234. **Kondoh, A., A. Iino, S. Ishikawa, T. Aoki, and M**. **Terada** (2018) Efficient Synthesis of Polysubstituted Pyrroles Based on [3+2] Cycloaddition Strategy Utilizing [1,2]-Phospha-Brook Rearrangement under Brønsted Base Catalysis. *Chem. Eur. J.* **24**, 15246-15253.

235. **Shi, Z., W. Mao, Z. Yang, S. Sun, C. H. Tung, and Z. Xu** (2023) Au-catalyzed neighboring hydroxymethyl group directed cycloaddition of alkyne with diazadienes: Synthesis of polysubstituted pyrroles. *Chin. Chem. Lett.* **34**, 107488.

236. **Wang, Z.-P., Y. He, and P. L. Shao** (2018) Transition-metal-free synthesis of polysubstituted pyrrole derivatives via cyclization of methyl isocyanoacetate with aurone analogues. *Org. Biomole. Chem.* **16**, 5422-5426.

237. **Fu, Q., and C. G. Yan** (2011) Efficient synthesis of polysubstituted pyrrole-3-carbonitriles via reactions of 1,1-dicyano-2,3-diarylcyclopropanes with aromatic imines. *Tetrahedron Lett.* **52**, 4497-4500.

238. **Javahershenas, R., F. M. Arlan, R. H. Prager, and J. Khalafy** (2020) Recent advances in the synthesis of pyrroles via multicomponent reactions using arylglyoxals. *Arkivoc*, **1**, 117-152.

239. **Nazeri, M. T., and A. Shaabani** (2021) Synthesis of polysubstituted pyrroles via isocyanide-based multicomponent reactions as an efficient synthesis tool *N. J. Chem.* **45**, 21967-22011.

240. **Hwu, J. R., A. Roy, A. Panja, W. C. Huang, Y. C. K. Hu, T. Tan, C. C. Lin, K. C. Hwang, M.-H. Hsu, and S. C. Tsay** (2020) Domino Reaction for the Synthesis of Polysubstituted Pyrroles and Lamellarin R. *J. Org. Chem*. **85**, 9835-9843.

241. **Pourtaher, H., A. Hasaninejad, and A. Iraji** (2022) Design, synthesis, in silico and biological evaluations of novel polysubstituted pyrroles as selective acetylcholinesterase inhibitors against Alzheimer's disease. *Sci. Rep*. **12**, 15236.

242. **Boussios, S., P. Karihtala, M. Moschetta, C. Abson, A. Karathanasi, N. Zakynthinakis-Kyriakou, J. E. Ryan, M. Sheriff, E. Rassy, and N. Pavlidis** (2020) Veliparib in ovarian cancer: a new synthetically lethal therapeutic approach. *Invest. New Drugs.* **38**, 181-193.

243. **Khajuria, R., S. Dham, and K. K Kapoor** (2016) Active methylenes in the synthesis of a pyrrole motif: An imperative structural unit of pharmaceuticals, natural products, and optoelectronic materials. *RSC Adv.* **6**, 37039-37066.

244. **Van Arnam, E. B., A. C. Ruzzini, C. S. Sit, H. Horn, A. A. Pinto-Tomás, C. R. Currie, and J. Clardy** (2016) Selvamicin, an atypical antifungal polyene from two alternative genomic contexts. *Proc. Natl. Acad. Sci. U S A*, **113**, 12940-12945.

245. **Díaz, J. L., A. Dobarro, B. Villacampa, and D. Velasco** (2001). Structure and Optical Properties of 2,3,7,9-Polysubstituted Carbazole Derivatives. Experimental and Theoretical Studies. *Chem. Mat.***13**, 2528-2536.

246. **Bulumulla, C., R. Gunawardhana, P. L. Gamage, J. T. Miller, R. N. Kularatne, M. C. Biewer, and M. C. Stefan** (2020) Pyrrole-Containing Semiconducting Materials: Synthesis and Applications in Organic Photovoltaics and Organic Field-Effect Transistors. *ACS Appl. Mater. Interfaces*. **12**, 32209-32232.

247. **Chen, D., Y. Shan, J. Li, J. You, X. Sun, and G. Qiu** (2019) External Reductant-Free Palladium-Catalyzed Reductive Insertion of Isocyanide: Synthesis of Polysubstituted Pyrroles and Its Applications as a Cysteine Probe. *Org. Lett.* **21**, 4044-4048.

248. **Murakami, Y., Y. Matsuda, and K. Sakata** (1971) Transition metal complexes of pyrrole pigments. IV. Electronic and vibrational spectra of cobalt(II), nickel(II),

and copper(II) complexes of some substituted dipyrromethenes. *Inorg. Chem.* **10**, 1728-1734.

249. **Yan, R.-L., J. Luo, C. X. Wang, C. W. Ma, G.-S. Huang, and Y. M. Liang** (2010) Cu (I)-Catalyzed Synthesis of Polysubstituted Pyrroles from Dialkyl Ethylenedicarboxylates and β-Enamino Ketones or Esters in the Presence of O2. *Org. Chem.* **75***, 5395–5397.*

250. **Amblard, F., J. H. Cho, and R. F. Schinazi** (2009) Cu(I)-Catalyzed Huisgen Azide−Alkyne 1,3-Dipolar Cycloaddition Reaction in Nucleoside, Nucleotide, and Oligonucleotide Chemistry. *Chem. rev.* **109**, 4207-4220.

251. **Lopchuk, J. M., M. Song, B. Butler, and G. W. Gribble** (2015) Synthesis of Heteroaryl-Substituted Pyrroles via the 1,3-Dipolar Cycloaddition of Unsymmetrical Münchnones and Nitrovinylheterocycles. *Synthesis*, **47**, 2776-2780.

252. **Leeper, F. J., and J. M. Kelly** (2013) Synthesis of 3, 4-disubstituted pyrroles. A review. *Org. Prep. Proced. Int*. **45**, 171-210.

253. **Azizian, J., J. Hosseini, M. Mohammadi, and F. Sheikholeslami** (2010) Efficient route for the synthesis of highly substituted pyrroles. S*ynth. Commun.* **40**, 3472-3479.

254. **Kanova, N., B. A. Dundar, Y. Kelgokmen, and M. Zora** (2021) One-Pot Synthesis of 2-Acetyl-1H-pyrroles from N-Propargylic β-Enaminones via Intermediacy of 1,4-Oxazepines. *J. Org. Chem.* **86**, 6289-6304.

255. **Wang, Z., Y. Shi, X. Luo, D. M. Han, and W. P. Deng** (2013) Direct synthesis of pyrroles via 1,3-dipolar cycloaddition of azomethine ylides with ynones *New. J. Chem.* **37**, 1742-1745.

256. **Robles-Machín, R., A. López-Pérez, M. González-Esguevillas, J. Adrio, and J. C. Carretero** (2010) Pyrrole and oligopyrrole synthesis by 1,3-dipolar cycloaddition of azomethine ylides with sulfonyl dipolarophiles. *Chem. Eur. J.* **16**, 9864-9873.

257. **Kim, Y., J. Kim, and S. B. Park** (2009) Regioselective Synthesis of Tetrasubstituted Pyrroles by 1,3-Dipolar Cycloaddition and Spontaneous Decarboxylation. *Org. Lett.* **11**, 17-20.

258. **Liu, Y., H. Hu, X. Wang, S. Zhi, Y. Kan, and C. Wang** (2017) Synthesis of Pyrrole via a Silver-Catalyzed 1,3-Dipolar Cycloaddition/Oxidative Dehydrogenative Aromatization Tandem Reaction. *J. Org. Chem.* **82**, 4194-4202.

259. **Larkovich, R. V., V. E. Shambalova, S. A. Ponomarev, A. S. Aldoshin, K. A. Lyssenko, M. S. Nechaev, and V. G. Nenajdenko** (2023) Barton–Zard Reaction of β-Fluoro-β-nitrostyrenes─a Selective Route to Functionalized 4-Fluoropyrroles. *J. Org. Chem.* **88**, 10122-10136.

260. **Zhao, Y., R. Li, Q. Zhao, J. Yao, and M. Miao** (2023) Palladium/Silver Cocatalyzed Divergent Dimerization of 2H-Azirines for Regioselective Synthesis of Tetrasubstituted Pyrroles and Pyrimidines. *Org. Lett.* **25**, 3978-3983.

261. **Chen, Z., B. Lu, Z. Ding, K. Gao, and N. Yoshikai** (2013) α-Palladation of Imines as Entry to Dehydrogenative Heck Reaction: Aerobic Oxidative Cyclization of N-Allylimines to Pyrroles. *Org. Lett.* **15**, 1966-1969.
262. **Li, J. J.** Hantzsch pyrrole synthesis. *Name Reactions: A Collection of Detailed Reaction Mechanisms* (pp. 283-284). Springer Berlin Heidelberg 2006.

263. **Xin, X., X. Liu, D. Zhang, R. Zhang, Y. Liang, F. Han, and D. Dong** (2014) Divergent synthesis of 2,3-dihydro-1H-pyrroles, 3-alkyl-1H-pyrroles and 3-alkenyl-1H-pyrroles from 2,4-pentadienenitriles and isocyanides *Org. Biomol. Chem.* **12**, 5477-5483.

264. **Wang, H.-Y., D. S. Mueller, R. M. Sachwani, R. Kapadia, H. N. Londino, and L. L. Anderson** (2011) Regioselective Synthesis of 2,3,4- or 2,3,5-Trisubstituted Pyrroles via [3,3] or [1,3] Rearrangements of O-Vinyl Oximes. *J. Org. Chem.* **76**, 3203-3221.

265. **Cai, Y., A. Jalan, A. R. Kubosumi, & S. L. Castle** (2015) Microwave-Promoted Tin-Free Iminyl Radical Cyclization with TEMPO Trapping: A Practical Synthesis of 2-Acylpyrroles. *Org. Lett.* **17**, 488-491.

266. **Wang, K., and A. Dömling** (2010) Design of a Versatile Multicomponent Reaction Leading to 2-amino-5-ketoaryl pyrroles. *Chem. Biol. Drug. Des*. **75**, 277-283.

267. **Herath, A., and N. D. P. Cosford** (2010) One-Step Continuous Flow Synthesis of Highly Substituted Pyrrole-3-carboxylic Acid Derivatives via in Situ Hydrolysis of tert-Butyl Esters. *Org. Lett.* **12**, 5182-5185.

268. **Tamaddon, F., and F. Amirpoor** (2013) Improved Catalyst-Free Synthesis of Pyrrole Derivatives in Aqueous Media. *Synlett*. **24**, 1791 - 1794.

269. **Chen, W., J. Shao, Z. Li, M. A. Giulianotti, and Y. Yu** (2011) Synthesis of 2,3,4-trisubstituted pyrroles via a facile reaction of vinyl azides and tosylmethyl isocyanide. *Can. J. Chem.* **90**, 214-221.

270. **Zhao, M. N., H. Liang, Z. H. Ren, and Z. H. Guan (2013)** Iron-Catalyzed Tandem One-Pot Addition and Cyclization of the Blaise Reaction Intermediate and Nitroolefins: Synthesis of Substituted NH-Pyrroles from Nitriles. *Adv. Syn. Catal. V.* **355**, 221-226.

271. **Hong, D., Y. Zhu, Y. Li, X. Lin, P. Lu, and Y. Wang** (2011) Three-Component Synthesis of Polysubstituted Pyrroles from α-Diazoketones, Nitroalkenes, and Amines. *Org. Lett.* **13**, 4668-4671.

272. **Yavari, I., and E. Kowsari** (2009) Efficient and green synthesis of tetrasubstituted pyrroles promoted by task-specific basic ionic liquids as catalyst in aqueous media. *Mol. Div.* **13**, 519-528.

273. **Cadierno, V., J. Gimeno, and N. Nebra** (2010) One-pot three-component synthesis of tetrasubstituted N—H pyrroles from secondary propargylic alcohols, 1,3-dicarbonyl compounds and tert-butyl carbamate. *J. Heterocylic. Chem.* **47**, 233-236.

274. **Zeng, J., Y. Bai, S. Cai, J. Ma, and X. W. Liu** (2011) Direct synthesis of pyrroles via a silver-promoted three-component reaction involving unusual imidazole ring opening *Chem. Commun.* **47**, 12855-12857.

275. **Wang, Z.** Huisgen Pyrrole Synthesis: *Comprehensive Organic Name Reactions and Reagents. (*pp.1504-1507), 2010.

276. **Majhail, M. K., P. M., Ylioja, and M. C. Willis** (2016) Direct Synthesis of Highly Substituted Pyrroles and Dihydropyrroles Using Linear Selective Hydroacylation Reactions. *Chemistry*, **22***,* 7879-7884.

277. **Niknam, K., M. Bavadi, S. Mojikhalifeh and O. Shahraki** (2018) A clean synthesis of 2,5-dihydro-1H-pyrrole-2-carboxylates under catalyst-free and solvent-free conditions: cytotoxicity and molecular docking studies. *J. Iran. Chem. Soc.* **15**, 1613-1623.

278. **Kuznietsova, H., N. Dziubenko, I. Byelinska, V. Hurmach, A. Bychko, O. Lynchak, D. Milokhov, O. Khilya, and V. Rybalchenko** (2020) Pyrrole derivatives as potential anti-cancer therapeutics: synthesis, mechanisms of action, safety. *J. Drug Target*. **28**, 547-563.

279. **Wang, D., Y. Fan, P. Yu, and L. Désaubry (2020)** Recent advances in the synthesis of 2,3-dihydropyrroles. *Chem. Commun.* **56**, 5584-5592.

280. **Olivier, W. J., J. A. Smith, and A. C. Bissember** (2022) Synthesis of Pyrrolidine- and γ-Lactam-Containing Natural Products and Related Compounds from Pyrrole Scaffolds. *Chem. Rec.* **22**, e202100277.

281. **Xuan, D. D** (2020) Recent Progress in the Synthesis of Pyrroles. *Curr. Org. Chem*. **24**, 622-657.

282. **Shi, F., Z. L. Tao, J. Yu, and S. J. Tu** (2011) Highly enantioselective synthesis of biologically important 2, 5-dihydropyrroles via phosphoric acid-catalyzed three-component reactions and evaluation of their cytotoxicity. *Tetrahedron: Asymmetry* **22**, 2056-2064.

283. **Shi, F., G.-J. Xing, W. Tan, R.-Y. Zhu, and S. Tu** (2013) Enantioselective construction of 2,5-dihydropyrrole skeleton with quaternary stereogenic center via catalytic asymmetric 1,3-dipolar cycloaddition involving α-arylglycine esters *Org. Biomol. Chem.* **11**, 1482-1489.

284. **Shi, F., R. Y. Zhu, X. Liang, and S. J. Tu** (2013) Catalytic Asymmetric 1, 3-Dipolar Cycloadditions of Alkynes with Isatin-Derived Azomethine Ylides:

Enantioselective Synthesis of Spiro [indoline-3, 2′-pyrrole] Derivatives. *Adv. Syn. Catal.* **355**, 2447-2458.

285. **Narayan, R., M. Potowski, Z.-J. Jia, A. P. Antonchick, and H. Waldmann** (2014) Catalytic Enantioselective 1,3-Dipolar Cycloadditions of Azomethine Ylides for Biology-Oriented Synthesis. *Acc. Chem. Res.* **47**, 1296-1310.

286. **Wen Ting, K. M., and Chen Zhanguo** (2019) Synthesis of 4, 5-Dihydropyrrole from γ-Nitro-nitrile. *Chin. Org. Chem*. **39**, 3162-3168.

287. **Brawn, R. A., and J. S. Panek** (2009) Annulations of Enantioenriched Allenylsilanes with in Situ Generated Iminium Ions: Stereoselective Synthesis of Diverse Heterocycles. *Org. Lett.* **11***,* 473-476.

CURRICULUM VITAE

1. **NAME** : PANDIDURAI S

2. **DATE OF BIRTH** : 2 June 1995

3. **EDUCATIONAL QUALIFICATIONS**

Bachelor of Science **2012– 2015**

Institution : Presidency College (Autonomous), Chennai

Specialization : Chemistry

Master of Science **2015 – 2017**

Institution : Bharathidasan University, Tiruchirappalli

Specialization : Chemistry

Doctor of Philosophy **2018 – 2024**

Institution : Indian Institution of Technology Madras, Chennai

Research area : Asymmetric Organic Synthesis and Catalysis

Registration Date : 09th July 2018

DOCTORAL COMMITTEE

CHAIRPERSON:	**Prof. Md. Mahiuddin Baidya** Professor Department of Chemistry
GUIDE:	**Prof. G. Sekar** Professor Department of Chemistry
MEMBERS:	**Prof. S. Baskaran** G. Aravamudan Chair Professor Department of Chemistry
	Prof. P. Venkatakrishnan Professor Department of Chemistry
	Prof. M. Michael Gromiha Professor Department of Biotechnology